frontiers | Research Topics

Gene therapy for hearing loss: From mechanism to clinic

Edited by
Zuhong He, Wenwen Liu, Yu Sun and Qingyin Zheng

Published in
Frontiers in Molecular Neuroscience
Frontiers in Neuroscience

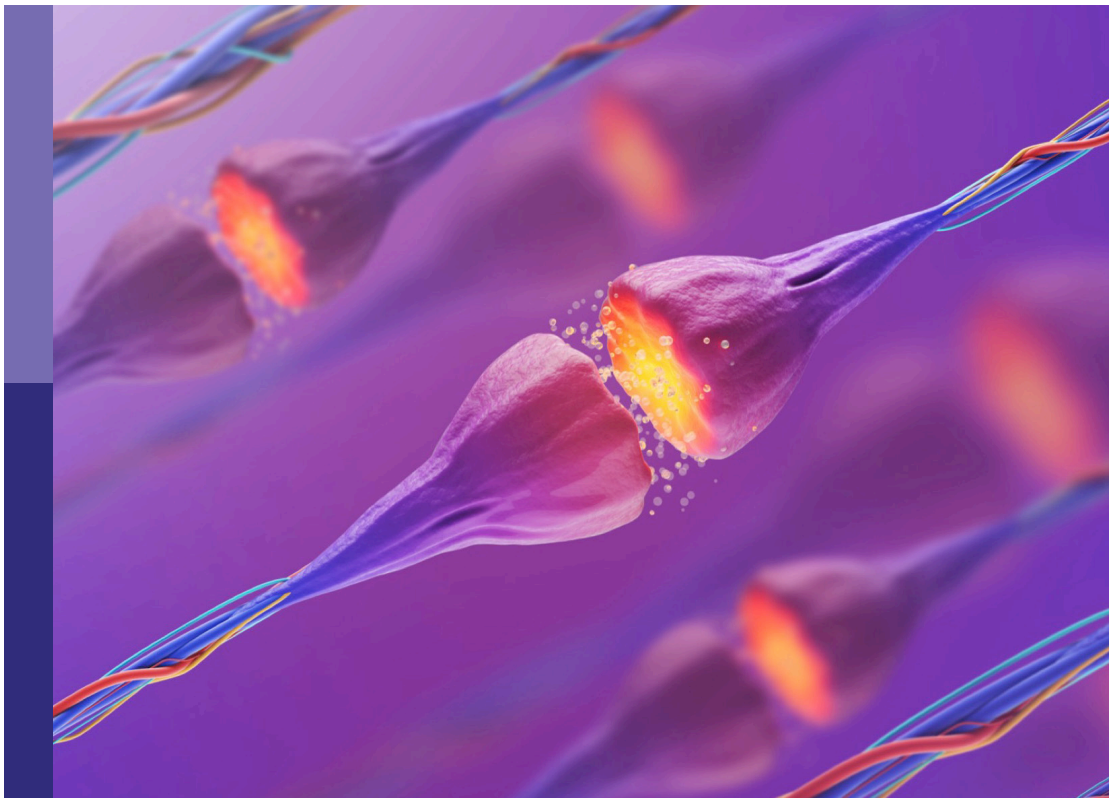

ISSN 1664-8714
ISBN 978-2-8325-3099-3
DOI 10.3389/978-2-8325-3099-3

About Frontiers

Frontiers is more than just an open access publisher of scholarly articles: it is a pioneering approach to the world of academia, radically improving the way scholarly research is managed. The grand vision of Frontiers is a world where all people have an equal opportunity to seek, share and generate knowledge. Frontiers provides immediate and permanent online open access to all its publications, but this alone is not enough to realize our grand goals.

Frontiers journal series

The Frontiers journal series is a multi-tier and interdisciplinary set of open-access, online journals, promising a paradigm shift from the current review, selection and dissemination processes in academic publishing. All Frontiers journals are driven by researchers for researchers; therefore, they constitute a service to the scholarly community. At the same time, the *Frontiers journal series* operates on a revolutionary invention, the tiered publishing system, initially addressing specific communities of scholars, and gradually climbing up to broader public understanding, thus serving the interests of the lay society, too.

Dedication to quality

Each Frontiers article is a landmark of the highest quality, thanks to genuinely collaborative interactions between authors and review editors, who include some of the world's best academicians. Research must be certified by peers before entering a stream of knowledge that may eventually reach the public - and shape society; therefore, Frontiers only applies the most rigorous and unbiased reviews. Frontiers revolutionizes research publishing by freely delivering the most outstanding research, evaluated with no bias from both the academic and social point of view. By applying the most advanced information technologies, Frontiers is catapulting scholarly publishing into a new generation.

What are Frontiers Research Topics?

Frontiers Research Topics are very popular trademarks of the *Frontiers journals series*: they are collections of at least ten articles, all centered on a particular subject. With their unique mix of varied contributions from Original Research to Review Articles, Frontiers Research Topics unify the most influential researchers, the latest key findings and historical advances in a hot research area.

Find out more on how to host your own Frontiers Research Topic or contribute to one as an author by contacting the Frontiers editorial office: frontiersin.org/about/contact

Gene therapy for hearing loss: From mechanism to clinic

Topic editors

Zuhong He — Wuhan University, China
Wenwen Liu — Shandong University, China
Yu Sun — Huazhong University of Science and Technology, China
Qingyin Zheng — Case Western Reserve University, United States

Citation

He, Z., Liu, W., Sun, Y., Zheng, Q., eds. (2023). *Gene therapy for hearing loss: From mechanism to clinic*. Lausanne: Frontiers Media SA.
doi: 10.3389/978-2-8325-3099-3

Table of contents

frontiers | Frontiers in Neuroscience

TYPE Editorial
PUBLISHED 12 July 2023
DOI 10.3389/fnins.2023.1235627

OPEN ACCESS

EDITED AND REVIEWED BY
Isabelle Peretz,
Montreal University, Canada

*CORRESPONDENCE
Zuhong He
✉ hezuhong@163.com

RECEIVED 06 June 2023
ACCEPTED 03 July 2023
PUBLISHED 12 July 2023

CITATION
Zou S, Liu W, Sun Y, Zheng Q and He Z (2023) Editorial: Gene therapy for hearing loss: from mechanism to clinic.
Front. Neurosci. 17:1235627.
doi: 10.3389/fnins.2023.1235627

Editorial: Gene therapy for hearing loss: from mechanism to clinic

Shengyu Zou[1], Wenwen Liu[2], Yu Sun[3], Qingyin Zheng[4] and Zuhong He[1]*

[1]Department of Otorhinolaryngology-Head and Neck Surgery, Zhongnan Hospital of Wuhan University, Wuhan, China, [2]Department of Otolaryngology-Head and Neck Surgery, Shandong Provincial ENT Hospital, Shandong University, Jinan, China, [3]Department of Otorhinolaryngology, Union Hospital, Tongji Medical College, Huazhong University of Science and Technology, Wuhan, China, [4]Department of Otolaryngology-Head & Neck Surgery, Case Western Reserve University, Cleveland, OH, United States

KEYWORDS

sensorineural hearing loss, hair cell, auditory nerve, hearing regeneration, gene therapy

Editorial on the Research Topic
Gene therapy for hearing loss: from mechanism to clinic

As the most prevalent sensory disorder, hearing loss causes patients a great deal of hardship and leads to a number of psychological and mental disorders. Such as the elderly individuals with presbycusis will causing social isolation, depressive symptoms and mild cognitive impairment. In addition, the cochlear hair cell loss and the degradation of auditory cortex are typical pathological alterations that lead to presbycusis. As pathological changes occur during the process of hearing loss, cognitive abilities and sound perception can be affected by lesions in the cochlea, auditory nerve, or auditory center. The common factors that can cause sensorineural hearing loss include genetic factors, medicines, infections, diseases, trauma, age, and the environment. With in-depth investigation of the pathophysiology of hearing disorders and enhancement of diagnosis and treatment technologies, gene therapy in hearing regeneration is gradually attracting our interest and is a future exploration direction. Gene therapy is a novel approach to preventing hair cell death, promoting hair cell regeneration and regulating the expression of genes associated with deafness. Remarkable advances have been made in gene therapy for hearing loss, but there are still many obstacles to overcome. New technologies and material applications will help us better understand the process of hearing loss and optimize the impact of gene therapy to restore auditory function. This Frontiers Research Topic entitled "*Gene therapy for hearing loss: from mechanism to clinic*" encompasses 11 manuscripts on the topic of gene therapy for sensorineural hearing loss, inner ear development regulation and clinical surgery treatment.

In the cochlea, inner ear cells are in charge of receiving acoustic signals and transmitting auditory information to the brain. Ribbon synapses can facilitate the conveying of signals to the appropriate spiral ganglion neurons by inner ear cells. However, hidden hearing loss (HHL) caused by ribbon synapse loss is usually ignored, and the mechanisms underlying ribbon synapse loss are largely unknown. Hou et al. conducted a series of experiments using an FGF22 knockout mouse model ($Fgf22^{-/-}$) to explore the relationship between the *Fgf22* gene and synaptic defects in HHL. The authors found that $Fgf22^{-/-}$ mice had lower wave I amplitudes at 8 and 16 kHz than $Fgf22^{+/+}$ mice. However, the numbers of inner hair cells and ribbon synapses in $Fgf22^{-/-}$ mice was not significantly different from those in $Fgf22^{+/+}$ mice. The authors found that FGF22 deletion may cause calcium channels to be

more easily activated and cause Ca^{2+}-triggered exocytosis in response to stimuli. The real-time PCR results showed that the synaptic vesicle-related proteins SNAP-25 and Gipc3 were significantly decreased in *Fgf22*$^{-/-}$ mice, which may affect the function of IHC ribbon synapses and induce HHL.

Endoplasmic reticulum (ER) stress is well-investigated in aminoglycoside-induced hearing loss, and ER stress inhibition exhibits a protective effect on aminoglycoside-induced ototoxicity. Wu et al. devoted much work to the protective role of pitavastatin (PTV), a new-generation lipophilic statin, on neomycin-induced hair cell loss. In *in-vitro* experiments, PTV protected not only HEI-OC1 cells but also cochlear explant cultures from hair cell damage caused by neomycin. In a mouse model, pretreatment with intraperitoneal injection of PTV prevented neomycin-induced hearing loss and hair cell damage. The authors further explored the mechanism underlying the protective effect of PTV and found that PTV could inhibit neomycin-induced apoptosis and ES under neomycin stimulation. In addition, PTV could inhibit PERK/eIF2α/ATF4 signaling to attenuate ER stress and inhibit the Rho/ROCK signaling pathway to protect against neomycin-induced ototoxicity.

Chen P. et al. reviewed the pathological mechanisms of connexin-26 (Cx26)-related hearing loss. Members of the Cx family play important roles in the cochlea, as these proteins can form gap junctions, which maintain the balance of ion and substance exchange between cells. The authors summarized two types of Cx26 transgenic mice, congenital deafness and late-onset progressive deafness model mice, and described the different pathological changes of these two models. Cxs are crucial for gap junction (GJ) combination, and Cx26 mutation disrupts the GJ system, which maintains stable endocochlear potential. The authors further explored the hypothesis that Cx26 deficiency causes cochlear potassium recycling dysfunction and put forth his own perspective. Furthermore, the authors discussed the crucial regulatory functions of Cx26 in the Ca^{2+} signaling pathway throughout the development of the inner ear. GJs play an important role in energy supply and glucose transport in the inner ear during development and hair cell (HC) survival. Mutations in Cx26 cause energy supply limitations and lead to Corti development disorder, OHC function decline and hearing failure.

Fei et al. introduced semicircular canal occlusion (SCO) to the treatment of vertigo in clinical and related basic research. SCO was initially applied to treat benign paroxysmal positional vertigo (BPPV). Later, semicircular canal fistula and Meniere's disease were also treated with SCO. The vertigo of most patients with Meniere's disease is controlled vertigo after SCO. The efficiency and safety of TSCO in the ear with endolymphatic hydrops were confirmed in animal models. Some patients with refractory BVVP who undergo posterior SCO show complete resolution of positional vertigo after long-term follow-up. However, some patients experience short-term hearing loss, which can recover within 6 months. Superior SCO is an ideal operation for treating superior semicircular canal dehiscence syndrome and has a low incidence of complications. Although the vertigo of most patients who undergo SCO is alleviated, there are still a few reports of hearing deterioration after SCO. Hence, further exploration is needed to determine the effect of SCO on hearing and vestibular function.

Adeno-associated virus (AAV) is a widely used vector for gene therapy in animal models and clinical trials. However, due to its packaging capacity, AAV cannot deliver a large gene or multiple genes. Therefore, a procedure for the cotransduction of dual-AAV vectors has been developed to solve these problems. Chen Z.-R. et al. tested the efficiency and safety profiles of cotransduced dual-AAV vectors in the vestibular sensory epithelium of mice. First, mixtures of dual-AAV-ie vectors with CGA or CMV promoters were injected into the adult and neonatal mouse inner ear. Compared with adult mice, the cotransduction rates in the striolar and extrastriolar region hair cells were significantly higher in neonatal mice. After diphtheria toxin administration to damage the utricle HCs, the authors found that the cotransduction rate increased in striolar and extrastriolar region HCs compared with those of control adult mice. Three months after dual-AAV-ie vector transduction, mouse auditory and vestibular functions were tested, and no significant effects were observed. The cotransduction efficiency was also maintained for 3 months in adult mice. This study provided a feasible safety profile for future gene therapies through the cotransduction of dual-AAV vectors into the vestibule.

G protein-coupled receptors (GPCRs) are the largest superfamily of mammalian cell surface receptors, and some of them are related to hearing disorders. Ma et al. reviewed 53 GPCRs expressed in the cochlea and offered a new GPCR-based medication development strategy for hearing loss therapy. In the manuscript, class A, class B2, class C and class F GPCRs in the cochlea and their functions are described. With the development of structural analysis, researchers have designed several GPCR structure-oriented drugs that target the complicated structure of GPCRs. With the exploration of cochlear gene therapy and GPCR-related gene therapy drugs that are applied in the treatment of other organ diseases, it is hoped that inner ear-oriented GPCR-related drugs will emerge in the near future.

Cochlear ribbon synapse maturation in postnatal mice requires morphological and functional modifications. Song et al. observed IHC ribbon synapse changes from P1-P28, and the data showed that the number of synapses undergoing pruning was accompanied by the activation and migration of macrophages. The expression of CX3CR1 was significantly associated with macrophage activation, and the expression level was increased at P7 and gradually decreased thereafter. Moreover, consecutive injection of a CX3CR1 inhibitor for 7 days after P7 showed that synapse pruning was affected, with impaired hearing in adulthood. Spiral neurons secreted CX3CL1 to recruit migrating macrophages at postnatal day 7. Exogenous supplementation with CX3CL1 activated synapse pruning and reduced the number of IHC ribbon synapses, and hearing was also impaired at P28. These results indicate that ribbon synaptic remodeling by macrophages via the CX3CL1/CX3CR1 axis occurs postnatally in mice prior to the onset of hearing and that this remodeling is essential for the development of hearing.

As a transient cellular cluster structure, Kölliker's organ (KO) plays a crucial role in cochlear development and degenerates during cochlear maturation. Chen J. et al. reviewed the morphological changes, biological functions and potential mechanisms for HC regeneration in KO. The structure of KO-SCs folds, cell gaps widen, and columnar cell numbers decrease and are replaced by cuboidal-like cells during maturation. The rhythmic morphological

changes may be triggered by the intracellular Ca^{2+} concentration and contractile protein activation. Spontaneous ATP and Ca^{2+} release from KO-SCs is crucial for cochlear development, and KO-SCs secrete glycoproteins for tectorial membrane formation. Chen J. et al. also described the regulatory role of the apoptosis pathway, thyroid hormone signaling and autophagy in KO-SC programmed degeneration. Through the regulation of a variety of transcription factors and signaling pathways, KO-SCs can be a source of progenitor cells for hair cell regeneration in the early postnatal period, providing opportunities for the treatment of hearing disorders in the future.

Meng et al. compared the changes in vestibular function and hearing after different semicircular canal surgery techniques were performed for labyrinthine fistula treatment. In Group 1, the labyrinthine fistula was only partially covered with simple fascia when dexamethasone injection was administered. In Group 2, the labyrinthine fistula was capped with a "sandwich" composed of fascia, bone meal, and fascia. After surgery, several Group 1 patients experienced vertigo symptoms. The patients in Group 2 with type II labyrinthine fistulas showed short-term vertigo symptoms after surgery but no occurrences of vertigo during a long-term follow-up. For the patients with type I labyrinthine fistulas, there was no significant difference between bone conduction (BC) and air conduction (AC) thresholds or the A-B gap after surgery. However, for patients with type II labyrinthine fistulas, the recovery of the A-B gap in Group 2 was poorer than that in Group 1, but there was a significant recovery in hearing compared to preoperative hearing.

Mu et al. explored FOXG1-related epigenetic modifications that affect HC survival in cisplatin treatment. The expression of FOXG1 and the autophagy pathway were initially activated in both *in vivo* and *in vitro* models after cisplatin administration, and the expression decreased at high doses of cisplatin treatment. Subsequently, the authors found that the inhibition of FOXG1 and the autophagy pathway might be regulated by H3K9 methylation. Pretreatment with BIX01294, a G9a inhibitor that could transiently and reversibly inhibit H3K9me2 activity, reverse the inhibition of FOXG1 and autophagy and alleviate the HC damage and hearing loss induced by cisplatin. Interestingly, the authors also found that FOXG1 and H3K9me2 could affect the activation of the autophagy pathway by regulating autophagy-related miRNAs and affecting the ROS levels and apoptosis ratio changes in OC1 cells after cisplatin treatment.

Sun et al. provided a review of recent research progress in the role and regulation of autophagy and ferroptosis in the inner ear. As an important physiological process for metabolic waste degradation and reuse, autophagy plays a key role in maintaining normal cellular functions. In the auditory system, autophagy activation mostly promotes HC survival, such as in aging, ototoxic drug use and noise-related hearing loss. The autophagy pathway is regulated by many factors and signals, and this pathway needs to be further explored for deafness prevention. The authors also described ferroptosis regulation mechanisms in the auditory system and demonstrated that the prevention of ferroptosis activation had a protective effect on HCs during ototoxic drug exposure and aging-induced auditory cortex degeneration. Ferritinophagy, autophagy-induced ferroptosis, has recently attracted much attention from many researchers. Ferritinophagy is a kind of selective autophagy process that is mediated by NCOA4. NCOA4 induces the binding of autophagosomes and ferritin, and free Fe^{2+} increases with the degradation of ferritin and induces ferroptosis in cells. More studies are needed to clarify the mechanisms of ferritinophagy in the auditory system.

For this Research Topic, research on inner ear hair cell protection, ribbon synapses and organ of Corti development regulation and clinical middle ear surgery was collected. The content of this Research Topic includes recent research progress in the auditory system and the latest inner ear gene therapy methods and thus could provide a reference for further exploration of auditory disorders.

Author contributions

SZ and ZH participated in writing the manuscript. ZH, SZ, WL, YS, and QZ participated in reviewing the manuscript. All authors contributed to the article and approved the submitted version.

Funding

This work was financially supported by the National Natural Science Foundation of China (Nos. 82222017 and 82271183).

Conflict of interest

The authors declare that the research was conducted in the absence of any commercial or financial relationships that could be construed as a potential conflict of interest.

Publisher's note

frontiers | Frontiers in Molecular Neuroscience

TYPE Original Research
PUBLISHED 28 July 2022
DOI 10.3389/fnmol.2022.922665

OPEN ACCESS

EDITED BY
Zuhong He,
Wuhan University, China

REVIEWED BY
Zheng-De Du,
Capital Medical University, China
Tao Yang,
Shanghai Jiao Tong University, China
Jing-Yi Jeng,
The University of Sheffield,
United Kingdom
Philippe Vincent,
The Johns Hopkins Hospital,
United States

*CORRESPONDENCE
Jiarui Chen
drchenjiarui@163.com
Jun Yang
yangjun@xinhuamed.com.cn
Shuna Li
lishuna@xinhuamed.com.cn

†These authors have contributed equally to this work

SPECIALTY SECTION
This article was submitted to Methods and Model Organisms, a section of the journal Frontiers in Molecular Neuroscience

RECEIVED 18 April 2022
ACCEPTED 04 July 2022
PUBLISHED 28 July 2022

CITATION
Hou S, Zhang J, Wu Y, Junmin C, Yuyu H, He B, Yang Y, Hong Y, Chen J, Yang J and Li S (2022) FGF22 deletion causes hidden hearing loss by affecting the function of inner hair cell ribbon synapses.
Front. Mol. Neurosci. 15:922665.
doi: 10.3389/fnmol.2022.922665

FGF22 deletion causes hidden hearing loss by affecting the function of inner hair cell ribbon synapses

Shule Hou[1,2,3†], Jifang Zhang[1,2,3†], Yan Wu[1,2,3†], Chen Junmin[1,2,3], Huang Yuyu[1,2,3], Baihui He[1,2,3], Yan Yang[4], Yuren Hong[5], Jiarui Chen[6*], Jun Yang[1,2,3*] and Shuna Li[1,2,3*]

[1]Department of Otorhinolaryngology-Head and Neck Surgery, Xinhua Hospital, School of Medicine, Shanghai Jiao Tong University, Shanghai, China, [2]Ear Institute, School of Medicine, Shanghai Jiao Tong University, Shanghai, China, [3]Shanghai Key Laboratory of Translational Medicine on Ear and Nose Diseases, Shanghai, China, [4]Liaoning Medical Device Test Institute, Shenyang, China, [5]Laboratory of Electron Microscope Center, Shanghai Medical College, Fudan University, Shanghai, China, [6]Department of Otorhinolaryngology-Head and Neck Surgery, Shanghai Children's Hospital, Shanghai Jiao Tong University, Shanghai, China

Ribbon synapses are important structures in transmitting auditory signals from the inner hair cells (IHCs) to their corresponding spiral ganglion neurons (SGNs). Over the last few decades, deafness has been primarily attributed to the deterioration of cochlear hair cells rather than ribbon synapses. Hearing dysfunction that cannot be detected by the hearing threshold is defined as hidden hearing loss (HHL). The relationship between ribbon synapses and FGF22 deletion remains unknown. In this study, we used a 6-week-old FGF22 knockout mice model (*Fgf22*$^{-/-}$) and mainly focused on alteration in ribbon synapses by applying the auditory brainstem response (ABR) test, the immunofluorescence staining, the patch-clamp recording, and quantitative real-time PCR. In *Fgf22*$^{-/-}$ mice, we found the decreased amplitude of ABR wave I, the reduced vesicles of ribbon synapses, and the decreased efficiency of exocytosis, which was suggested by a decrease in the capacitance change. Quantitative real-time PCR revealed that *Fgf22*$^{-/-}$ led to dysfunction in ribbon synapses by downregulating SNAP-25 and Gipc3 and upregulating MEF2D expression, which was important for the maintenance of ribbon synapses' function. Our research concluded that FGF22 deletion caused HHL by affecting the function of IHC ribbon synapses and may offer a novel therapeutic target to meet an ever-growing demand for deafness treatment.

KEYWORDS

FGF22, ribbon synapse, hidden hearing loss, SNAP-25, Gipc3, MEF2D

Introduction

The mammalian cochlea consists of outer hair cells (OHCs) and inner hair cells (IHCs). OHCs amplify sound, thereby increasing the hearing sensitivity of the mammalian inner ear. In contrast, IHCs are responsible for capturing acoustic signals and delivering auditory information to the central nervous system. In mammals, the loss of hair cells cannot be spontaneously replaced, but the functional alteration can be rescued before hair cell loss (Jan et al., 2013; Li et al., 2016; Ni et al., 2016; Waqas et al., 2016; Wu et al., 2016; Chen et al., 2017).

Ribbon synapses are important structures in transmitting auditory signals from the IHCs to their corresponding spiral ganglion neurons (SGNs). Ribbon synapses, which are located at the base of the IHCs, contain presynaptic RIBEYE and postsynaptic glutamate receptors. For the signals to be transmitted accurately, the presynaptic active domain needs to quickly and precisely release glutamate-filled synaptic vesicles (SVs) (Nouvian et al., 2006).

The fibroblast growth factor (FGF) family comprises 22 structurally related molecules that can be grouped into seven subfamilies based on their similarities and fibroblast growth factor receptor (FGFR) binding (Itoh and Ornitz, 2004). For example, FGFs 7, 10, and 22 are similar in sequence, and they all activate FGFR2b (Zhang et al., 2006).

Numerous phenotypic similarities in FGF signaling between mice and humans have been illustrated in the branching morphogenesis of the lung epithelium (Goto et al., 2014), heart development (Itoh et al., 2016), skeletal growth (Teven et al., 2014), muscle regeneration (Yablonka-Reuveni et al., 2015), angiogenesis and lymphangiogenesis (Yu P. et al., 2017), kidney development (Carev et al., 2008), neurogenesis and neurodegeneration (Woodbury and Ikezu, 2014), craniofacial suture ossification (Prochazkova et al., 2018), and ear development (Raft and Groves, 2015). Due to conserved developmental functions and genome accessibility, the mouse is a superb model to study the mechanisms of FGF signaling *in vivo*. Consequently, many experiments concerning FGFs in the auditory system have been performed in mice as well as in other animals. Previously, FGF signaling was reported to play an important role in otic placode specification (Wright et al., 2015), cochlear development (Ebeid and Huh, 2017), neuromast hair cell regeneration (Lee et al., 2016), inner ear hair cell differentiation (Leger and Brand, 2002; Haque et al., 2016; Ratzan et al., 2020), and middle ear formation (Lysaght et al., 2014).

FGF22, a member of the FGF family, plays an intermediary role in synapse reconstruction (Jacobi et al., 2015) and axon rehabilitation (Zhu et al., 2020). As a presynaptic organizer originating from a postsynaptic cell in mammals, FGF22 is vital for excitatory synapse formation in the hippocampus (Umemori et al., 2004; Terauchi et al., 2015). It also contributes to neural growth in the dentate gyrus (Terauchi et al., 2017). We previously demonstrated that FGF22 could protect against hearing loss resulting from gentamycin ototoxicity and generate ribbon synapses by suppressing myocyte enhancer factor 2D (MEF2D) (Li et al., 2020). However, how ribbon synapses are related to FGF22 deletion remains unclear.

In this study, an FGF22 knockout mice model ($Fgf22^{-/-}$) was utilized. Wild-type mice ($Fgf22^{+/+}$) served as controls. Hearing thresholds were unchanged, but a decrease in wave I amplitude and synaptic defects was found, suggesting that Fgf22−/− mice suffer from hidden hearing loss (HHL). A set of experiments, such as the ABR test, the immunofluorescence staining, and the patch-clamp recording, were performed. Then, we measured the gene expression of synaptosome-associated protein 25 (SNAP-25), GIPC PDZ domain-containing family member 3 (Gipc3), and MEF2D. In brief, we tried to clarify the relationship between FGF22 and HHL.

Materials and methods

Animals

All animal experiments were in accordance with the guidelines approved by the experimental animal care institution of Shanghai Jiao Tong University School of Medicine. The approval number is XHEC-F-2021-065.

In the study, the mice (C57BL/6 background, 6-week-old) were obtained from the Harvard Children's Hospital (Terauchi et al., 2010). Then $Fgf22^{-/-}$ mice were derived from a heterozygous mating scheme. Wild-type littermates of the same age were used as controls. The mice were housed in the group on a schedule of 12 h of light and 12 h of darkness, and they had free access to food and water. We inspected the ears of the mice, and those with infections in the external auditory canal and middle ear were excluded.

Genotyping

Deoxyribonucleic acid (DNA) was extracted from mice tails using a TIANamp Genomic DNA Kit. Polymerase chain reaction (PCR) was then performed to determine the

Abbreviations: IHCs, inner hair cells; SGNs, spiral ganglion neurons; HHL, hidden hearing loss; $Fgf22^{-/-}$, FGF22 knockout mice model; OHCs, outer hair cells; FGF, fibroblast growth factor; FGFR, fibroblast growth factor receptor; SNAP-25, synaptosome-associated protein 25; Gipc3, GIPC PDZ domain-containing family member 3; MEF2D, myocyte enhancer factor 2D; DNA, deoxyribonucleic acid; PCR, polymerase chain reaction; ABR, auditory brainstem response; SPLs, sound pressure levels; PFA, paraformaldehyde; CtBP2, C-terminal binding protein-2; GluR2, glutamate receptor 2; TEM, transmission electron microscopy; AN, auditory nerve; V_{half}, half-activation voltage; VGCCs, voltage –gated Ca^{2+} channels; EDTA, ethylene diamine tetraacetic acid; SVs, synaptic vesicles.

presence of *Fgf22* alleles; i.e., wild-type, *Fgf22* homozygous, and *Fgf22* heterozygous.

The primer sequences used for FGF22 genotyping are as follows: *Fgf22* GS (E) (5′-TGCCTGACCATCTACTCCTGTCTCC-3′), *Fgf22* GS (T, E) (5′-GAACCTACAGTCCACAGAGTAGACC-3′), and Neo (T) (5′-GGGCCAGCTCATTCCTCCCACTCAT-3′). After amplification, whole products were separated using 1% agarose gel electrophoresis. GeneRed (TIANGEN, China) was used to stain the gel, and the stained gel was viewed under ultraviolet light.

Auditory brainstem response testing

Mice (n = 12) were weighed and anesthetized with intraperitoneal injections of 150 mg/kg ketamine and 6 mg/kg xylazine. ABR recordings were carried out in a soundproof chamber by placing the electrodes subcutaneously, and the TDT RZ6 system was used for testing. The recording electrode was placed at the vertex of the head, while the stimulating electrode was inserted into one mastoid process. The ground electrode was inserted into the contralateral thigh. The sensing resistance was <1 kΩ.

The ABR test was carried out using BiosigRZ software. The sound stimulation output at 4–32 KHz was presented at a rate of 20 pips per second, lasted for 3 ms, and was overlaid 400 times. The sound was delivered to the ears *via* a loudspeaker placed 10 cm from the pinna. The stimulating intensities ranged from 10 to 90 dB sound pressure levels (SPLs). The hearing threshold, defined as the lowest stimuli level triggering a replicable response, was measured using decrements from high to low intensity in steps of 5 dB SPL. Additionally, the ABR wave I amplitudes and peak latencies were identified manually (Song et al., 2006).

Tissue preparation

Mice (n = 12) were quickly decapitated after anesthesia with 150 mg/kg ketamine and 6 mg/kg xylazine intraperitoneally. The temporal bones were taken off and immersed in fresh 4% paraformaldehyde (PFA). The walls of the auditory sac and footplates of the stapes were cleared. Then, the round and oval windows were opened, and a hole was drilled into the cochlea apex from where 4% PFA solution was perfused. After fixation, the basal membrane (middle turn) was gently separated from the cochlea for whole-mount staining.

Immunofluorescence staining

For immunofluorescence staining, we used antibodies against rhodamine-phalloidin (1:200, Yeasen, #40734ES75), C-terminal binding protein-2 (CtBP2, 1:400, mouse IgG1, BD Bioscience, #612044[1]), glutamate receptor 2 (GluR2, 1:200, mouse IgG2a, Millipore, Cat #mab397[2]), and 4′, 6-diamidino-2-phenylindole (1:1,000, Sigma, United States, #D9542).

Whole-mount organs of Corti were permeabilized with 0.1% Triton X-100 for 40 min and then blocked with 10% normal goat serum for 30 min at 37°C. Subsequently, the tissue was incubated with the primary antibodies overnight at 4°C. After rinsing, the samples were incubated with their specific secondary antibodies: 1:500 of goat anti-mouse IgG1 (Invitrogen, Alexa Flour™ 568-conjugated, ref#A21134, RRID: AB_2535766) and goat anti-mouse IgG2a (Invitrogen, Alexa Flour™ 647-conjugated, ref#A21241, RRID: AB_2535810) at 37°C for 2 h. The samples were imaged using a laser confocal microscope (Leica SP8, Germany).

3D reconstruction using a laser confocal microscope

Whole-mount organs of Corti were imaged using a 60× water-immersion objective coupled to a laser confocal microscope (Zeiss LSM 880, Germany). The presynaptic (CtBP2) and postsynaptic structures (GluR2) were detected in the red and green channels, respectively. Each orange fluorescent dot (i.e., red and green merge) indicated one ribbon synapse. Continuous scans were carried out from top to bottom with a step size of 0.5 μm. After each layer was scanned, the signals from each layer were obtained, and then ribbon synapses were quantified *via* signal superposition.

Transmission electron microscopy

Ribbon-attached vesicles were counted using transmission electron micrographs of complete serial sections encompassing the ribbon synapses.

The cochleae (n = 6) were fixed in 2.5% glutaraldehyde/0.1 M phosphate buffer and decalcified by immersion in a 10% ethylene diamine tetraacetic acid (EDTA) solution. Afterward, the specimens were postfixed in a 1% osmium acid solution for 2 h at room temperature. Following postfixation, the specimens were rinsed three times for 5 min each with 0.1 M butylene succinate. Next, the sections were dehydrated using gradients of ethanol and acetone solution. For embedment, the specimens were immersed in a 1:1 solution of acetone and Epon 812 for 2–4 h, followed by a 2:1 acetone:Epon 812 solution overnight. Then, they were immersed in Epon 812 for 5–8 h. The samples were subsequently inserted, while

1 www.bdbiosciences.com

2 www.millipore.com

immersed in Epon 812, into an embedment plate in a 37°C incubator overnight; afterward, they were polymerized in a 60°C incubator for 36 h. Using an ultramicrotome, semithin sections (2.0 μm) were sliced serially to the central axis plane and collected onto glass slides. The sections were unfolded and dried on a 95°C heating plate; afterward, they were stained with a 1% toluidine blue for a few seconds. The standard plane of the cochlear axis was located under the microscope. Additionally, ultrathin sections (50–60 nm) were sliced using an ultramicrotome. The sections were stained with 2% uranyl acetate saturated alcohol solution for 15 min. After the first stain was completed, the tissues were stained with lead citrate for 15 min. Finally, the dual-stained sections were dewatered at room temperature overnight. IHC ribbon synapses were imaged using a transmission electron microscope (Philips CM-120) for analysis.

Patch-clamp recording

The IHCs were oriented for the patch-clamp experiment using the AXON patch-clamp system. Recording pipettes were pulled from borosilicate glass (World Precision Instruments) to a resistance of 4–6 MΩ. The bath solution contained 130 mM sodium chloride, 1 mM magnesium chloride, 2.8 mM potassium chloride, 10 mM calcium chloride, 10 mM amphoteric HEPES buffer, and 10 mM D-glucose, pH adjusted to 7.20 with NaOH, and osmolarity adjusted to 300 mOsm with D-glucose. To increase the calcium current and capacitance jumps, 10 mM calcium chloride was added. The electrode liquid consisted of 135 mM Cs-methanesulfonate, 10 mM cesium chloride, 10 mM tetraethylammonium chloride, 10 mM amphoteric HEPES buffer, 2 mM calcium chelator EGTA, 0.5 mM Na-GTP, and 3 mM Mg-ATP, pH adjusted to 7.20 with CsOH and osmolarity adjusted to 290 mOsm with D-glucose. The jClamp software was used to acquire and analyze all data. Recordings were performed at room temperature (∼24°C). Cells were held at −80 mV (unless otherwise indicated). Traces were recorded immediately after the cell membrane was broken through at a giga-ohm (GΩ) seal, and the series resistance (Rs) and membrane capacitance (Cm) were corrected. Liquid junction potential (−9.3 mV) was corrected offline. Data with a leakage current of less than 30 pA were included in the statistics.

The current-voltage relationship, which displays how Ca^{2+} currents react to the voltage ramp, was quantified using a point-by-point calculation. The curve-fitting equation was as follows:

$$I(V) = (V - V_{rev}) \times \frac{G_{max}}{1\exp(-(V - V_{half})/k)}$$

In the above equation, V_{rev} refers to the reversal membrane potential.

A constant double-sinusoidal wave (390.6 and 781.2 Hz, 20 mV) superposed on the holding potential (−80 mV) was used to record membrane capacitance at different depolarization times of 10, 30, 50, 100, and 200 ms. The membrane capacitance change (ΔC_m) is the difference between the average capacitance before and after depolarization. The area from the beginning of the Ca^{2+} current to the end of the Ca^{2+} tail current was integrated using the Patchmaster software to obtain the calcium influx charge (Q_{Ca}). The ratio of the capacitance change to the Ca^{2+} current charge ($\Delta C_m/Q_{Ca}$) was used to quantify the efficiency of Ca^{2+} in triggering exocytosis.

Quantitative real-time PCR

Freshly separated inner ears were collected from 6-week-old *Fgf22*$^{+/+}$ ($n = 6$) and *Fgf22*$^{-/-}$ ($n = 6$) mice. The apical-basal membrane was micro-dissected rapidly, and the samples were stored at −80°C until further treatment. All of the ribonucleic acids were extracted to synthesize the complementary DNA, which then acted as a template for the amplification. The PCR amplification was conducted using the primers which are listed in **Table 1**.

The real-time PCR procedures were conducted as follows: 48°C for 30 min then 95°C for 5 min, followed by 40 cycles consisting of 94°C for 15 s, 60°C for 30 s, and 72° for 30 s. The reactions were replicated three times. The $2^{-\Delta Ct}$ method was employed to quantify messenger ribonucleic acid (mRNA) levels of the above-mentioned genes.

Statistical analysis

Data in **Figures 1**, **5–7** were analyzed by one-way analysis of variance using Graphpad Prism 8. Data in **Figures 2–4** were analyzed by a two-tailed *t*-test using Excel 2019. A *P*-value of <0.05 indicates statistical significance. Statistical data were normally distributed and equal variances were assumed.

Results

The wave I amplitude decreased in *Fgf22*$^{-/-}$ mice

Hidden hearing loss manifests as decreased wave I amplitude with normal hearing thresholds. We used the ABR to assess the hearing thresholds, amplitudes, and latencies of *Fgf22*$^{-/-}$ mice. The wave I amplitude of *Fgf22*$^{-/-}$ mice at 8 and 16 KHz was presented for the well-representative characteristics in hearing conditions, and it was significantly reduced compared to *Fgf22*$^{+/+}$ mice (**Figure 1A**), while no significant difference in wave I latency or hearing threshold was observed between the two groups (**Figures 1B,C**).

TABLE 1 Primers for quantitative real-time PCR.

Gene	Forward	Reverse
SNAP-25	5′-CGGATCCATGGCCGAGGACGCAGACAT-3′	5′-TTAACCACTTCCCAGCATCTT-3′
Gipc3	5′-AGGATCGAGGGCTTCACCAAT-3′	5′-GCAACTTTTGCATGTCCACTTT-3′
MEF2D	5′-CGTTGGGAATGGCTATGTC-3′	5′-GAGGCCCTGGCTGAGTAA-3′
β-*actin*	5′-AAGGACTCCTATAGTGGGTGACGA-3′	5′-ATCTTCTCCATGTCGTCCCAG TTG-3′

β-actin was used as a reference.

The number of inner hair cells was unchanged in *Fgf22*$^{-/-}$ mice

The basal membranes obtained from *FGF22*$^{-/-}$ mice were processed, and the isolated hair cells were immunostained with phalloidin (red). The images showed that no difference was found in the IHCs between *Fgf22*$^{-/-}$ and *Fgf22*$^{+/+}$ mice (27.60 ± 1.855 in *FGF22*$^{-/-}$ mice vs. 26.40 ± 1.497 in *FGF22*$^{+/+}$ mice; Figure 2). Most hearing impairments are closely associated with hair cell loss. And from this result, it does not appear to be the cause of this model mouse.

The number of ribbon synapses in *Fgf22*$^{-/-}$ mice kept intact

Our previous study suggested that FGF22 could preserve hearing by maintaining the number of ribbon synapses. The IHC ribbon synapses in *Fgf22*$^{-/-}$ and *Fgf22*$^{+/+}$ mice were clearly labeled by the double immunofluorescence staining. Antibodies against CtBP2 (red) and GluR2 (green) were used, respectively, to label presynaptic ribbons and postsynaptic glutamate receptors (Figure 3A). Juxtaposed puncta were identified as ribbon synapses and were quantified using 3D reconstruction. *Fgf22*$^{+/+}$ and *Fgf22*$^{-/-}$ mice did not significantly differ in their number of IHCs ribbon synapses (17.00 ± 0.8944 in *Fgf22*$^{+/+}$ mice vs. 17.50 ± 1.376 in *Fgf22*$^{-/-}$ mice; Figure 3B).

Ribbon synapse synaptic vesicles was reduced in *Fgf22*$^{-/-}$ mice

To quantify the number of vesicles per IHC ribbon synapse, sections of the IHCs from different *Fgf22*$^{-/-}$ mice were imaged using TEM and subsequently compared with sections from *Fgf22*$^{+/+}$ mice (n = 6 animals/genotype; Figure 4A). The number of ribbon SVs was significantly reduced in *Fgf22*$^{-/-}$ mice than in *Fgf22*$^{+/+}$ mice (11.40 ± 2.074 in *Fgf22*$^{-/-}$ mice vs. 19.00 ± 1.581 in *Fgf22*$^{+/+}$ mice; $P < 0.01$; Figure 4B).

Alterations in Ca^{2+} current and exocytosis in *Fgf22*$^{-/-}$ mice

To examine the role of FGF22 on ribbon synapses, we investigated the electrophysiological characteristics of Ca^{2+} currents using patch-clamp analysis (Figure 5A). The number of recorded IHCs was 15 in *Fgf 22*$^{+/+}$ mice and 12 in *Fgf 22*$^{-/-}$ mice. Neither the Ca^{2+} current amplitude (I_{Ca}) nor the slope factor (k) of voltage-dependent calcium channels differed between *Fgf22*$^{-/-}$ IHCs and those from wild-types (Figures 5B,C). A more negative half activation voltage (V_{half}) was found in *Fgf22*$^{-/-}$ IHCs, which indicated that the calcium channel was more easily activated in response to stimulus (Figure 5D).

To quantify exocytosis, a depolarizing pulse of 0 mV was applied to induce Ca^{2+} currents (Figure 6A). The stimulation durations ranged from 10 to 200 ms. During depolarization, we recorded capacitance changes (ΔC_m) as well as changes in Ca^{2+} influx (Q_{Ca}). For depolarization stimulations of 50, 100, and 200 ms, neither ΔC_m nor Q_{Ca} differed between *Fgf22*$^{-/-}$ IHCs and those from wild-types. However, for depolarization stimulation durations of 10 and 30 ms, ΔC_m was significantly reduced in *Fgf22*$^{-/-}$ IHCs, while no differences in Q_{Ca} were found between *Fgf22*$^{-/-}$ and *Fgf22*$^{+/+}$ IHCs (Figures 6B,C).

Afterward, we calculated the ratio of capacitance change to Ca^{2+} current charge ($\Delta C_m/Q_{Ca}$) to quantify the efficiency of calcium-evoked exocytosis (Figure 6D). For depolarization stimulation durations of 10 and 100 ms, the $\Delta C_m/Q_{Ca}$ in *FGF22*$^{-/-}$ IHCs was significantly reduced compared to *Fgf22*$^{+/+}$ IHCs. Meanwhile, $\Delta C_m/Q_{Ca}$ was not altered for other stimulation durations (i.e., 30, 50, and 200 ms). These findings indicate that the decrease in ΔC_m for short stimuli results in the reduced efficiency of Ca^{2+}-triggered exocytosis while Ca^{2+} currents remain.

Modulation of SNAP-25, Gipc3, and MEF2D in *Fgf22*$^{-/-}$ mice

SNAP-25 is essential for Ca^{2+}-induced SV fusion and neurotransmitter release. Gipc3 (GAIP interacting protein, C terminus 3). Defects of the human GIPC3 gene cause human deafness and Gipc3 disruption in mice leads to audiogenic seizures and progressive hearing loss. MEF2D belongs to the myocyte-specific enhancer-binding factor 2 family and plays an important role in human development and physiological function. To investigate how FGF22 affected ribbon synapses, we used quantitative real-time PCR to compare mRNA expression levels of SNAP-25, Gipc3, and MEF2D between

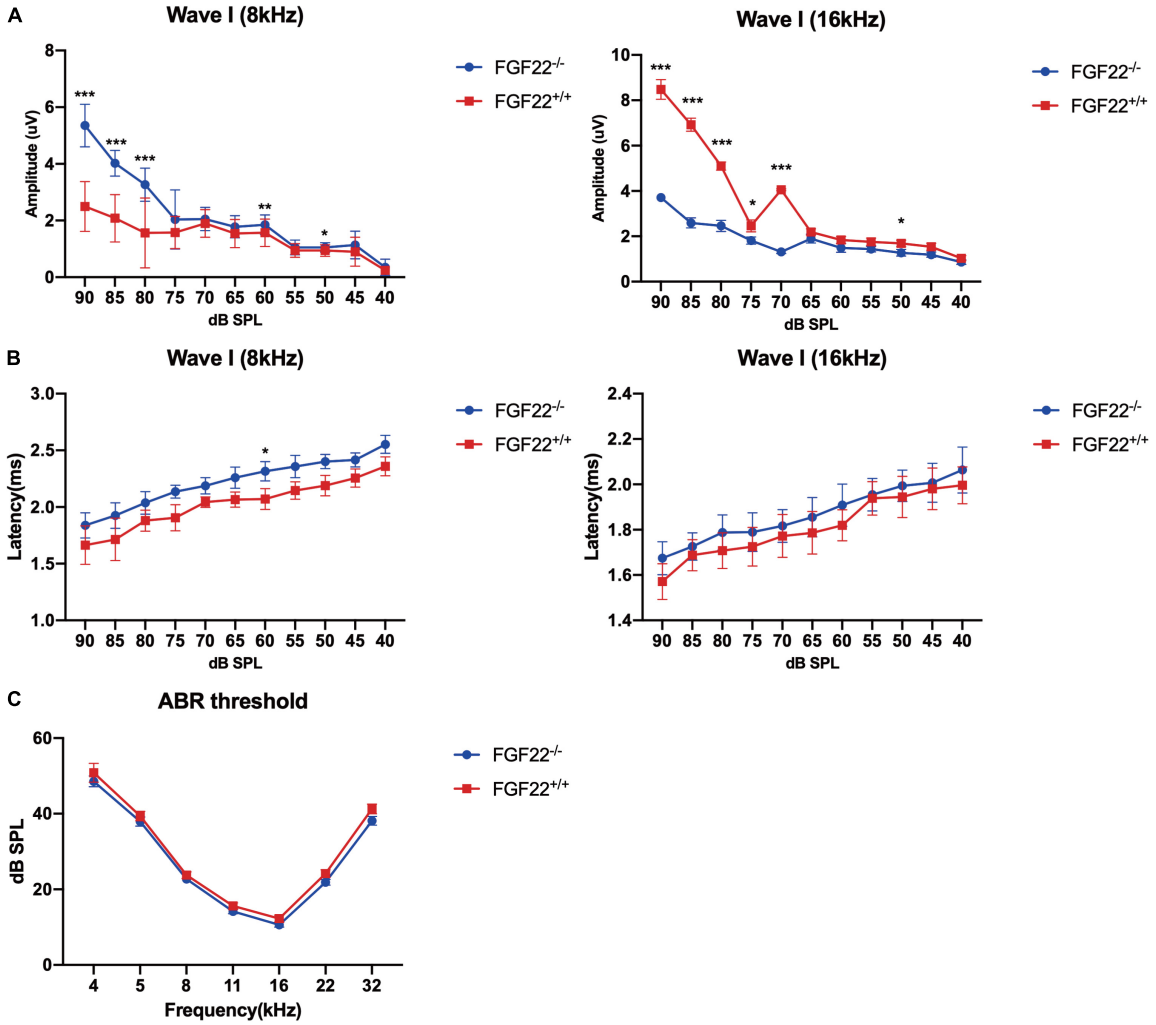

FIGURE 1
Auditory function parameters in the *Fgf22*$^{+/+}$ and *Fgf22*$^{-/-}$ groups. **(A)** Mean amplitudes of the ABR wave I in the *Fgf22*$^{+/+}$ and *Fgf22*$^{-/-}$ groups at 8 and 16 kHz. **(B)** Mean latency values of the ABR wave I in the *Fgf22*$^{+/+}$ and *Fgf22*$^{-/-}$ groups at 8 and 16 kHz. **(C)** Mean values of the ABR threshold in the *Fgf22*$^{+/+}$ and *Fgf22*$^{-/-}$ groups at 8 and 16 kHz. Data are expressed as the mean ± SD, statistical significance was assessed with two-way ANOVA followed by Bonferroni *post hoc* test, *$P < 0.05$, **$P < 0.01$, ***$P < 0.001$.

Fgf22$^{-/-}$ and *Fgf22*$^{+/+}$ mice. *Fgf22*$^{-/-}$ mice displayed downregulation of SNAP-25 and Gipc3 and upregulation of MEF2D (**Figure 7**).

Discussion

The main function of the IHC in the inner ear focuses on transducing sound waves into electric signals (Wang et al., 2017; Zhu et al., 2018; Qi et al., 2019, 2020; He et al., 2020). Deafness could be caused by genetic factors, infectious diseases, aging, ototoxic drugs, and noise exposure and is primarily attributed to the deterioration of cochlear hair cells (Zhu et al., 2018; Gao et al., 2019; Wagner and Shin, 2019; Zhang Y. et al., 2019; Qian et al., 2020; Zhang et al., 2020b; Zhou et al., 2020). Recently, much effort has been made to regenerate hair cells (White, 2020). Although the neonatal cochlea has limited hair cell regeneration ability, this regeneration ability decreases rapidly with increased age (Wang et al., 2015; Lu et al., 2017; He et al., 2019; Tan et al., 2019; Zhang S. et al., 2019; Zhang et al., 2020a,c). Many previous studies have reported that hair cell loss is mainly caused by oxidative damage (Liu et al., 2016; Li H. et al., 2018; Ding et al., 2020; Zhong et al., 2020; Zhou et al., 2020), which eventually induces apoptosis of hair cells (Sun et al., 2014; He et al., 2016; Yu X. et al., 2017; Li A. et al., 2018; Zhang Y. et al., 2019). Besides hair cells, the auditory nerve (AN) has been demonstrated to be involved in deafness, with pathogenic factors including noise, ototoxic drugs, and aging (Guo et al., 2016, 2019, 2020;

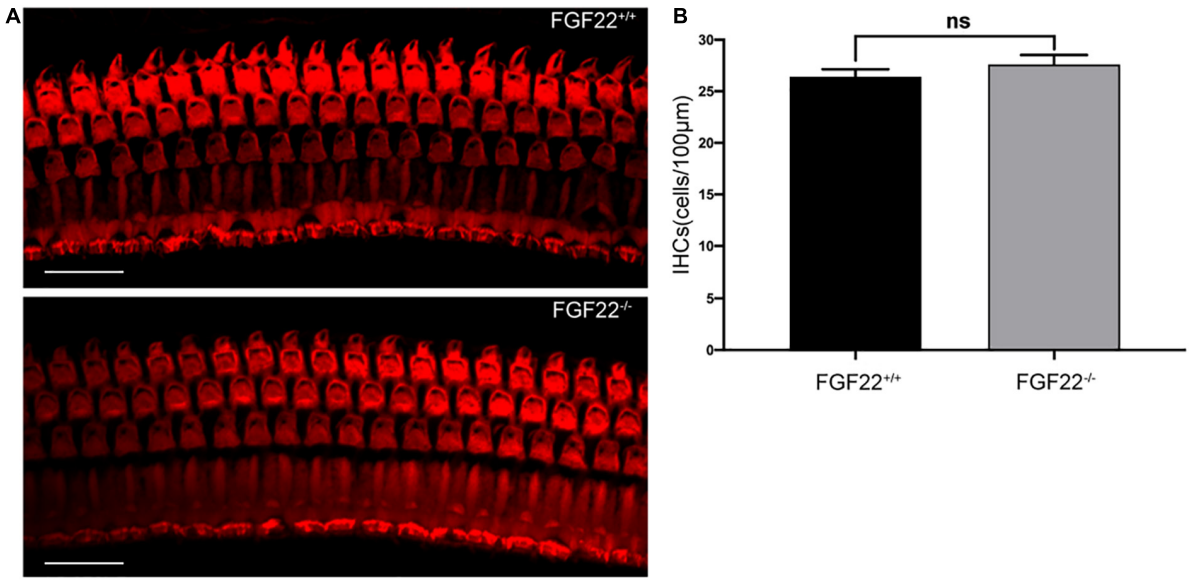

FIGURE 2
Whole-mount of the cochlea hair cells in *Fgf22*$^{+/+}$ and *Fgf22*$^{-/-}$ groups. **(A)** Isolated cochlea hair cells were immunostained with phalloidin (red). Scale bars: 20 μm. **(B)** The bar chart showed no difference in the hair cells between the *Fgf22*$^{+/+}$ and *Fgf22*$^{-/-}$ groups.

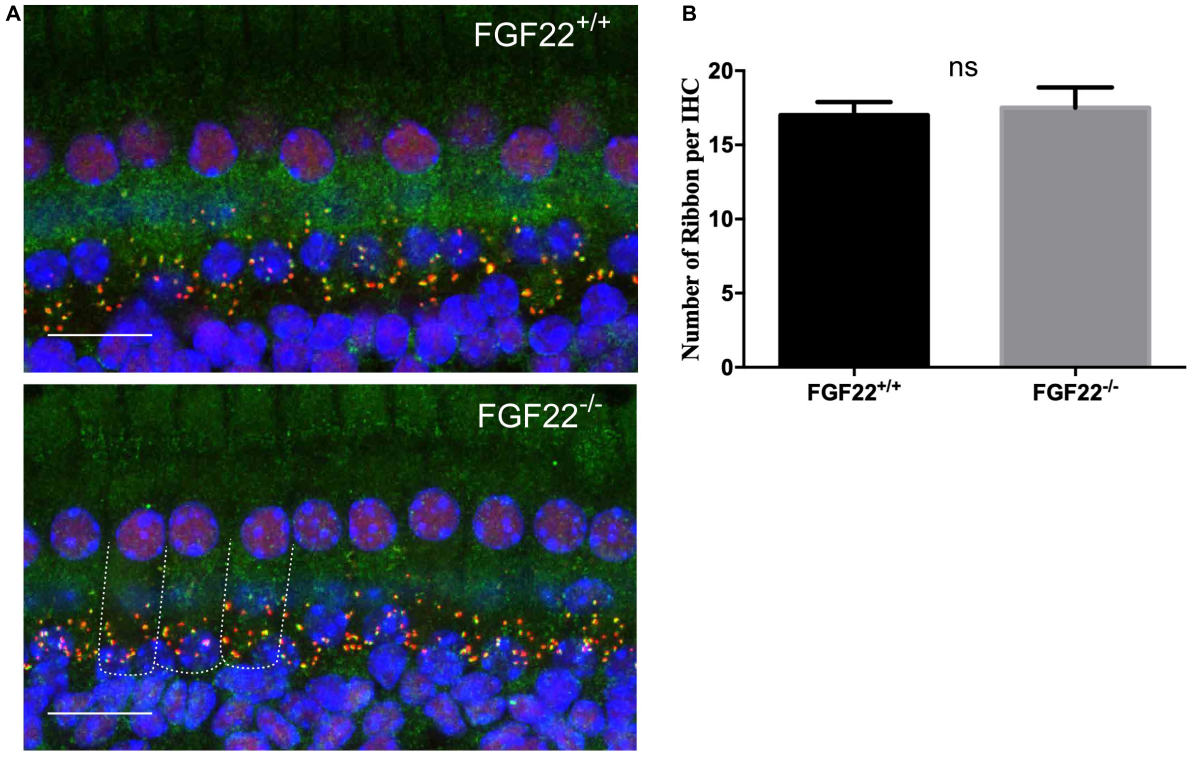

FIGURE 3
The number of synaptic ribbons in *Fgf22*$^{+/+}$ and *Fgf22*$^{-/-}$ mice. **(A)** Representative cochlear whole-mount preparation (n = 6, middle turn) images of CtBP2-labeled presynaptic ribbons (red) and GluR2-labeled postsynaptic glutamate receptors (green) from the *Fgf22*$^{+/+}$ and *Fgf22*$^{-/-}$ groups showing the overlapped puncta (yellow). Scale bars: 20 μm. **(B)** The bar chart showed the number of synaptic ribbons per IHC, which was similar in the *Fgf22*$^{+/+}$ and *Fgf22*$^{-/-}$ groups.

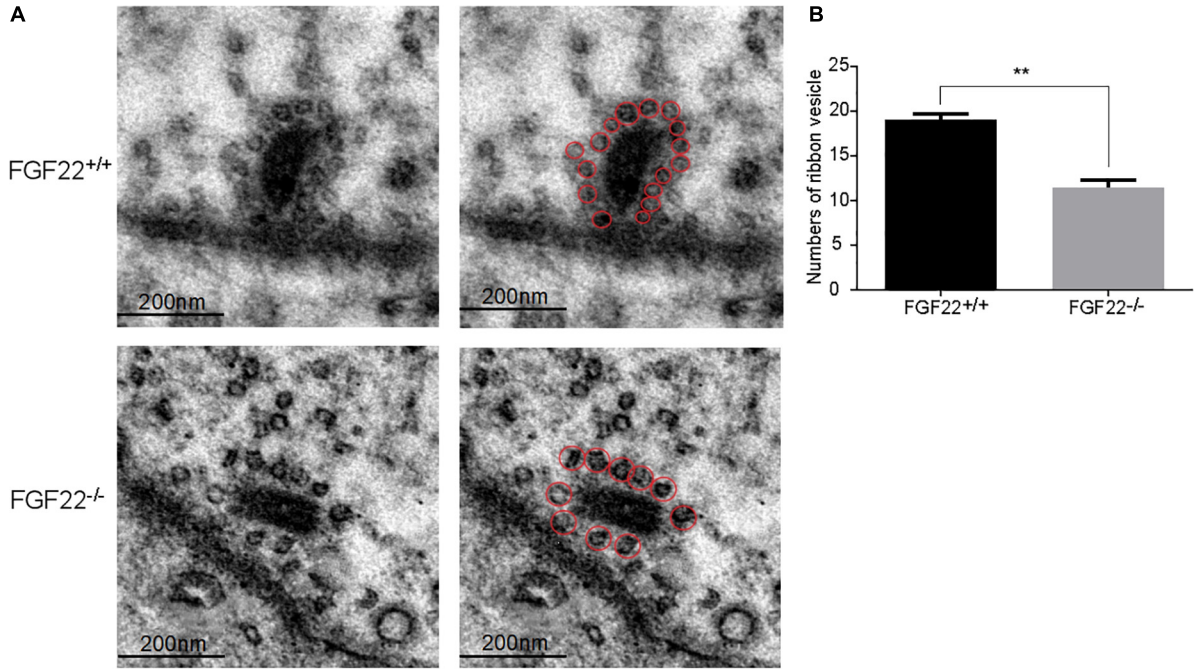

FIGURE 4
The number of synaptic vesicles in the *Fgf22*$^{+/+}$ and *Fgf22*$^{-/-}$ groups. **(A)** Representative images of synaptic vesicles in the *Fgf22*$^{+/+}$ and *Fgf22*$^{-/-}$ groups under a transmission electron microscopy (TEM). Scale bars: 200 nm. **(B)** The number of ribbon SVs was significantly reduced in *Fgf22*$^{-/-}$ mice than in *Fgf22*$^{+/+}$ mice. $^{**}P < 0.01$ vs. the *Fgf22*$^{-/-}$ group.

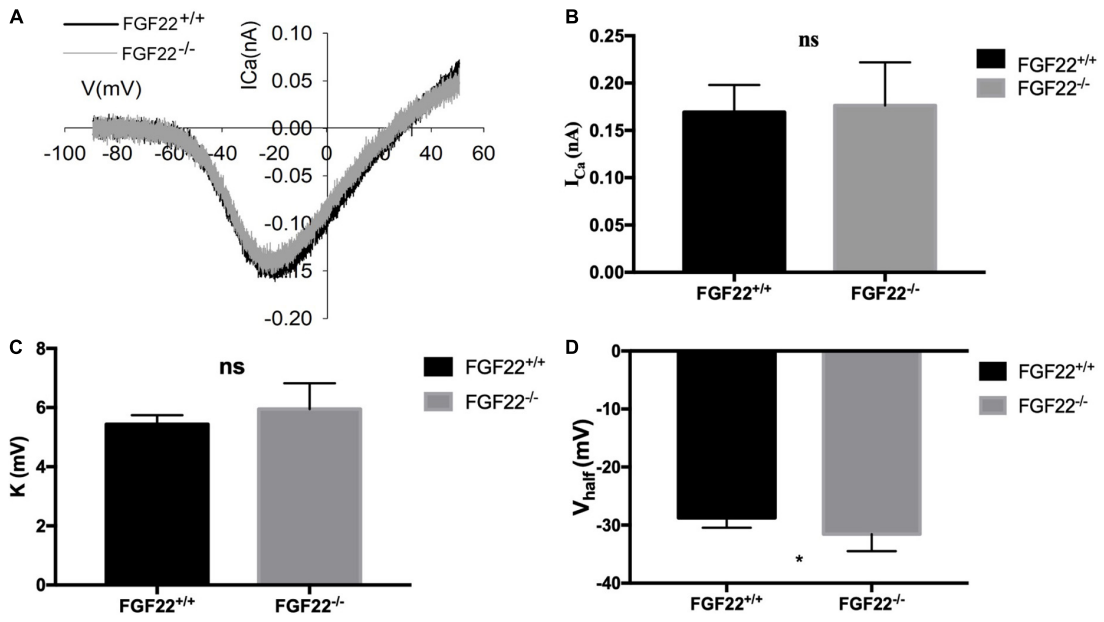

FIGURE 5
Changes in Ca^{2+} current in IHCs of the *Fgf22*$^{+/+}$ and *Fgf22*$^{-/-}$ groups. **(A)** Representative curves of the Ca^{2+} current in IHCs of the *Fgf22*$^{+/+}$ (black) and *Fgf22*$^{-/-}$ (gray) groups. The current response was induced by a voltage ramp from −80 to 60 mV and then the leak was subtracted. **(B,C)** No significance was found in the Ca^{2+} current amplitude (I_{Ca}) and the slope factor (k) between the *Fgf22*$^{+/+}$ and *Fgf22*$^{-/-}$ groups. **(D)** IHCs from the *Fgf22*$^{-/-}$ mice (−31.55 mV) have a more negative half-activation voltage (V_{half}) than Fgf22$^{+/+}$ mice (−28.76 mV). $^{*}P = 0.0301$, which indicates significant differences with $P < 0.05$. Statistical significance was assessed with a two-way ANOVA followed by Bonferroni *post hoc* test.

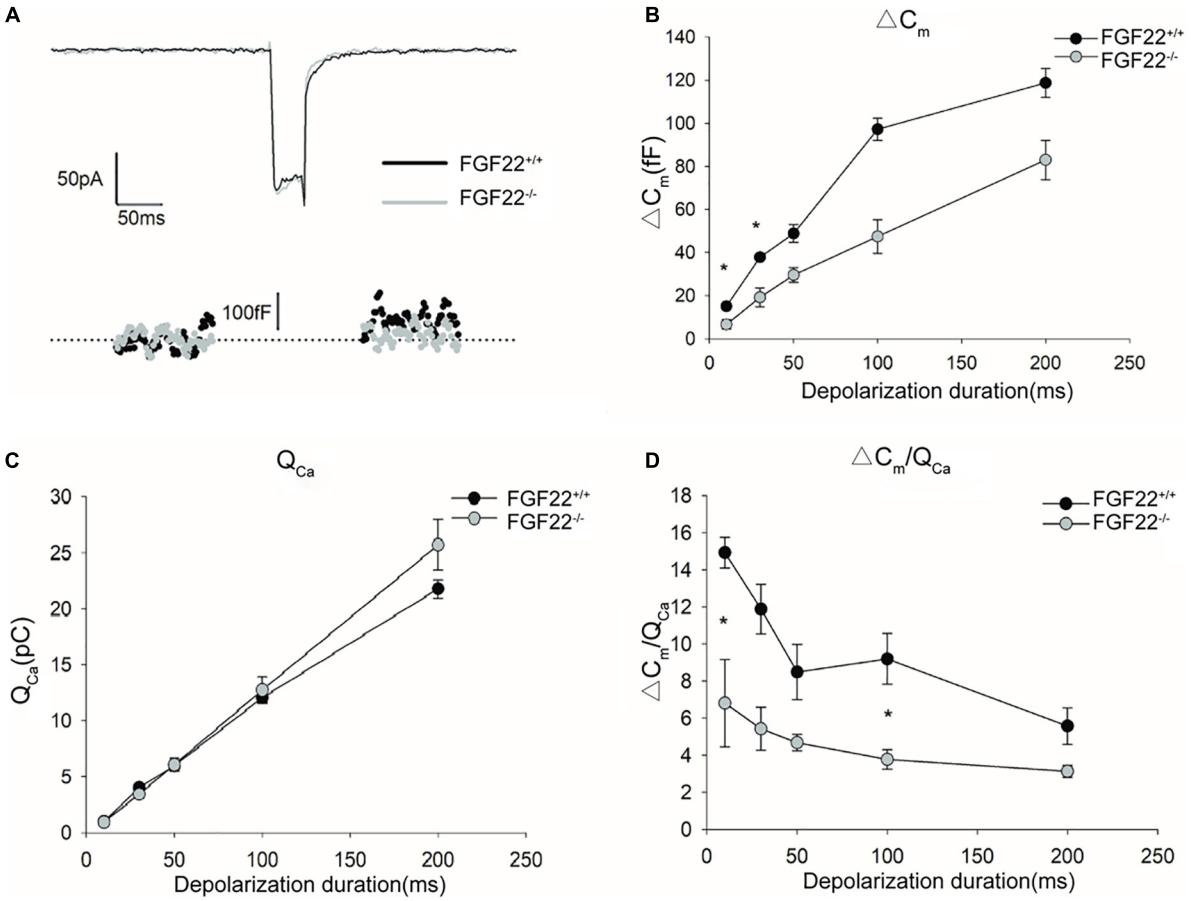

FIGURE 6
Changes in exocytosis in IHCs between the *Fgf22*$^{+/+}$ and *Fgf22*$^{-/-}$ groups. **(A)** Representative Ca^{2+} currents (I_{Ca}) and the resulting capacitance jumps (ΔC_m) recorded from IHCs between the *Fgf22*$^{+/+}$ (black) and *Fgf22*$^{-/-}$ (gray) groups. **(B,C)** ΔC_m and the Ca^{2+} charge (Q_{Ca}) evoked by stimulations of different durations, from 10 to 200 ms. ΔC_m for stimulation of 10 and 30 ms was significantly reduced in the *Fgf22*$^{-/-}$ group, *P = 0.0301, and P = 0.0251 < 0.05, respectively. **(D)** The Ca^{2+} efficiency of triggering exocytosis, assessed based on the ratio of $\Delta C_m/Q_{Ca}$, was reduced significantly for stimulation of 10 and 100 ms in the *Fgf22*$^{-/-}$ group. Data are expressed as the mean ± SD. *Indicates significant differences with P = 0.0476, and P = 0.0201 < 0.05, respectively.

Sun et al., 2016; Yan et al., 2018; Liu W. et al., 2019; Kohrman et al., 2020). Hearing dysfunction that cannot be detected by the hearing threshold is defined as HHL (Schaette and McAlpine, 2011). The relationship between ribbon synapses and FGF22 deletion remains indistinct. We previously demonstrated that FGF22 could be expressed in IHCs and gentamycin-induced hearing impairments occurred through ribbon synapse damage. Moreover, FGF22 infusion into the cochlea protected hearing by maintaining the number of ribbon synapses (Li et al., 2020). Here, we used 6-week-old mice with mature hearing.

We performed the ABR test in both *Fgf22*$^{-/-}$ and *Fgf22*$^{+/+}$ mice and found that the wave I amplitude was significantly decreased in *Fgf22*$^{-/-}$ mice. The shift in wave I amplitude indicated impairment in sound-elicited discharges from the acoustic afferent nerve (Liu H. et al., 2019). However, wave I latency and hearing threshold were similar between the two groups of mice. The unaltered latency of wave I meant the unchanged traveling wave velocity in the basilar membrane of the cochlea, which may prove that the bundles of hair cells were unaffected (Popov and Supin, 2001), i.e., FGF22 deficiency-induced HHL. However, from the immunofluorescence staining, we found that the number of hair cells remained unchanged in *Fgf22*$^{-/-}$ mice, as did the number of ribbon synapses.

Auditory signals are dynamically encoded at synapses and precisely transmitted from IHCs to SGNs (Wichmann and Moser, 2015). As part of the audio encoding, SVs containing neurotransmitters are released, which are continuously tethered at the active zones (Jeng et al., 2020). Vesicles are tightly coupled with calcium channels, which promote the rapid and sustained release of neurotransmitters. As the number of hair cells and ribbon synapses were kept intact, SVs were further studied and quantified using TEM. *Fgf22*$^{-/-}$ IHCs exhibited

reduced SVs, implying that FGF22 deficiency might led to a decline in vesicle formation. Besides, other explanations for such a decrease could be an impairment of vesicular replenishment, smaller ribbons, and a deficit in vesicular docking. We also assessed the biophysical characteristics of Ca^{2+} in IHCs. For basic properties of Ca^{2+} channels, a more negative half-activation voltage (V_{half}) was presented in $Fgf22^{-/-}$ mice, which revealed increasing excitability of Ca^{2+} channels in $Fgf22^{-/-}$ mice. Considering the relevance between SVs and voltage-gated Ca^{2+} channels (VGCCs), we speculate that the conformation change triggers the rapid activation and deactivation of the Ca^{2+} channels, which influences the fusion of SVs (Atlas, 2013; Ghelani and Sigrist, 2018). Then, we applied a depolarizing pulse and different stimulus durations to measure calcium influx charge quantity (Q_{Ca}), increments in membrane capacitance (ΔC_m), and $\Delta C_m/Q_{Ca}$. IHC depolarization triggered the fusion of vesicles with the cell membrane, which increased the cell membrane area and, accordingly, membrane capacitance. In $Fgf22^{-/-}$ IHCs, the significantly decreased ΔC_m after short stimulation reflected the attenuated release of SVs. Due to unchanged Q_{Ca}, the change in ΔC_m was not caused by differences in Ca^{2+} influx. Notably, $\Delta C_m/Q_{Ca}$ was significantly decreased in $Fgf22^{-/-}$ IHCs, which indicated that the reduction likely reflected a reduced efficiency in Ca^{2+}-triggered exocytosis.

Altogether, we found the decreased wave I amplitude of ABR, the receding presynaptic SVs, the reduced ΔC_m, and $\Delta C_m/Q_{Ca}$, so we speculate that the reduction in neurotransmitter release by SVs was accompanied by weaker acoustic afferent fiber discharges and, accordingly, HHL.

To determine how *Fgf22* knockout reduces the amount of SVs, we performed real-time PCR to quantify the expression levels of SNAP-25 and Gipc3, important proteins for SVs. We found a significant decrease in SNAP-25 and Gipc3 mRNA levels. As a homologous protein of the SNAP protein family, SNAP-25 is essential for the fusion of Ca^{2+}-induced SVs and neurotransmitter release (Najera et al., 2019). In SNAP-25 knockout neurons, rapid SV release is barely observed (Washbourne et al., 2002). Exocytosis at the hair cell ribbon synapse appears to function without neuronal SNARE proteins, according to Nouvian et al. (2011). However, we discovered that SNAP-25 and Gipc3 mRNA levels were significantly lower in $Fgf22^{-/-}$ mice. Unknown mechanisms that are more sophisticated may exist. Previous studies have demonstrated that the Gipc3 allelomorph disrupts the configuration of the hair bundle (Charizopoulou et al., 2011). Moreover, Gipc3 mutations induce non-syndromic sensorineural hearing loss in humans (Katoh, 2013), and Gipc3 disruption enhances Ca^{2+} influx and exocytosis in IHCs, reverses the spatial gradient of maximal Ca^{2+} influx in IHCs, and increases the maximal firing rate of SGNs at sound onset (Ohn et al., 2016). While in this study, the decrease in Gipc3 expression was induced by the lack of

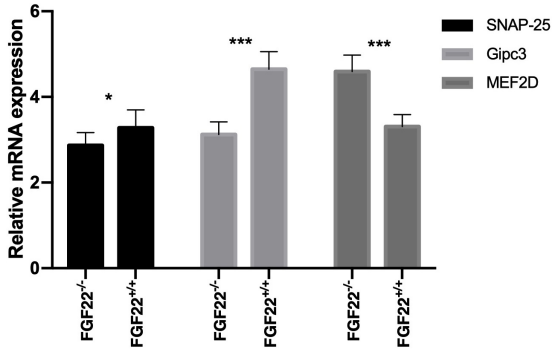

FIGURE 7
Quantitative real-time PCR analysis in the Corti's organ of the $Fgf22^{+/+}$ and $Fgf22^{-/-}$ groups. $Fgf22^{-/-}$ mice displayed downregulation of SNAP-25 and Gipc3 and upregulation of MEF2D. Data are expressed as the mean ± SD, and statistical significance was assessed with a two-way ANOVA followed by Bonferroni *post hoc* test, $*P < 0.05$, $***P < 0.001$.

Fgf22, it did not affect the Ca^{2+} current, only slightly shifting the Vhalf of the Ca^{2+} currents toward more hyperpolarized potentials and reducing exocytosis. We hypothesized that the absence of Fgf22 might have changed the expression of some proteins that affected calcium channel regulation, such as CtBP 2, though the expression level of calcium channel proteins was not thought to be impacted. The Gipc family may be involved in regulating vesicular trafficking (De Vries et al., 1998), and Gipc1 has been reported to be expressed in SVs at the presynaptic axon terminals of hippocampal neurons (Yano et al., 2006). Notably, we had reported that FGF22 triggered Ca^{2+} influx and activated calcineurin to downregulate MEF2D. Moreover, the transduction of cultured mouse cells with AAV-shFGF22 activated MEF2D and reduced the number of ribbon synapses (Li et al., 2020). MEF2D belongs to the myocyte-specific enhancer-binding factor 2 family and plays an important role in human development and physiological function. Here, we found that FGF22 knockout increased MEF2D expression and decreased the number of tethered SVs to the ribbon (**Figure 4**). Thus, we speculate that FGF signaling may antagonize the bone morphogenetic protein pathway to downregulate MEF2D (Cho et al., 2014). In addition, the myocyte enhancer factor 2 family may be associated with the WNT pathway (Snyder et al., 2013). These signaling pathways may regulate SV formation and release together. Regardless, the complex interplay between SNAP-25, Gipc3, and MEF2D needs to be further elucidated.

This study has some limitations. In this study, 6-week-old mice were used, and elder mice are under investigation. To sum up, despite this limitation, the mechanisms described above may offer novel therapeutic strategies to meet an ever-growing demand for deafness treatment.

Conclusion

Our study lays the foundation for further elucidating the molecular mechanism of IHC ribbon synapses in HHL and provides a more in-depth understanding and potential clues to the pathophysiology of HHL from the regulatory genes. FGF22 deletion caused HHL by affecting the function of IHC ribbon synapses, which may offer a new idea and therapeutic target for hearing development in HHL.

Data availability statement

The raw data supporting the conclusions of this article will be made available by the authors, without undue reservation.

Ethics statement

The animal study was reviewed and approved by No. XHEC-F-2021-065. Written informed consent was obtained from the owners for the participation of their animals in this study.

Author contributions

SH: study conception, data quality control, and wrote the manuscript. JZ: study conception, drafted the manuscript, and graphic abstract. YW: study conception, immunohistochemical staining, and drafted the manuscript. CJ: western blot and real-time PCR. HY: qPCR experiments. BH and YH: collection of cochlear samples for TEM experiments. YY: collection of cochlear samples for H&E experiments. JC: study conception. JY: data quality control and wrote the manuscript. SL: study conception, data quality control, and data analysis. All authors contributed to the article and approved the submitted version.

Funding

This work was supported by the National Natural Science Foundation of China (81600799, 81873698, 82000977, and 82171135), Shanghai Sailing Program (20YF1428900), and Shanghai Natural Science Foundation (21ZR1452800).

Conflict of interest

The authors declare that the research was conducted in the absence of any commercial or financial relationships that could be construed as a potential conflict of interest.

The reviewer, TY, declared a shared affiliation with several of the authors SH, JZ, YW, CJ, HY, BH, JY, and SL to the handling editor at the time of review.

Publisher's note

Supplementary material

The Supplementary Material for this article can be found online at: https://www.frontiersin.org/articles/10.3389/fnmol.2022.922665/full#supplementary-material

References

Atlas, D. (2013). The voltage-gated calcium channel functions as the molecular switch of synaptic transmission. *Annu. Rev. Biochem.* 82, 607–635.

Carev, D., Saraga, M., and Saraga-Babic, M. (2008). Involvement of FGF and BMP family proteins and VEGF in early human kidney development. *Histol. Histopathol.* 23, 853–862. doi: 10.14670/HH-23.853

Charizopoulou, N., Lelli, A., Schraders, M., Ray, K., Hildebrand, M. S., Ramesh, A., et al. (2011). Gipc3 mutations associated with audiogenic seizures and sensorineural hearing loss in mouse and human. *Nat. Commun.* 2:201. doi: 10.1038/ncomms1200

Chen, Y., Lu, X., Guo, L., Ni, W., Zhang, Y., Zhao, L., et al. (2017). Hedgehog signaling promotes the proliferation and subsequent hair cell formation of progenitor cells in the neonatal mouse cochlea. *Front. Mol. Neurosci.* 10:426. doi: 10.3389/fnmol.2017.00426

Cho, A., Tang, Y., Davila, J., Deng, S., Chen, L., Miller, E., et al. (2014). Calcineurin signaling regulates neural induction through antagonizing the BMP pathway. *Neuron* 82, 109–124. doi: 10.1016/j.neuron.2014.02.015

Kohrman, D. C., Wan, G., Cassinotti, L., and Corfas, G. (2020). Hidden hearing loss: a disorder with multiple etiologies and mechanisms. *Cold Spring Harb. Perspect. Med.* 10:a035493. doi: 10.1101/cshperspect.a035493

De Vries, L., Lou, X., Zhao, G., Zheng, B., and Farquhar, M. G. (1998). GIPC, a PDZ domain containing protein, interacts specifically with the C terminus of RGS-GAIP. *Proc. Natl. Acad. Sci. U.S.A.* 95, 12340–12345. doi: 10.1073/pnas.95.21.12340

Ding, Y., Meng, W., Kong, W., He, Z., and Chai, R. (2020). The role of FoxG1 in the inner ear. *Front. Cell Dev. Biol.* 8:614954. doi: 10.3389/fcell.2020.614954

Ebeid, M., and Huh, S. H. (2017). FGF signaling: diverse roles during cochlear development. *BMB Rep.* 50, 487–495.

Gao, S., Cheng, C., Wang, M., Jiang, P., Zhang, L., Wang, Y., et al. (2019). Blebbistatin inhibits neomycin-induced apoptosis in hair cell-like HEI-OC-1 cells and in cochlear hair cells. *Front. Cell Neurosci.* 13:590. doi: 10.3389/fncel.2019.00590

Ghelani, T., and Sigrist, S. J. (2018). Coupling the structural and functional assembly of synaptic release sites. *Front. Neuroanat.* 12:81. doi: 10.3389/fnana.2018.00081

Goto, A., Yamazaki, N., and Nogawa, H. (2014). Characterization of FGF family growth factors concerning branching morphogenesis of mouse lung epithelium. *Zoolog Sci.* 31, 267–273. doi: 10.2108/zs130252

Guo, R. X. M., Zhao, W., Zhou, S., Hu, Y., Liao, M., Wang, S., et al. (2020). 2D Ti3C2TxMXene couples electrical stimulation to promote proliferation and neural differentiation of neural stem cells. *Acta Biomater.* 139, 105–117. doi: 10.1016/j.actbio.2020.12.035

Guo, R., Ma, X., Liao, M., Liu, Y., Hu, Y., Qian, X., et al. (2019). Development and application of cochlear implant-based electric-acoustic stimulation of spiral ganglion neurons. *ACS Biomater. Sci. Eng.* 5, 6735–6741. doi: 10.1021/acsbiomaterials.9b01265

Guo, R., Zhang, S., Xiao, M., Qian, F., He, Z., Li, D., et al. (2016). Accelerating bioelectric functional development of neural stem cells by graphene coupling: implications for neural interfacing with conductive materials. *Biomaterials* 106, 193–204. doi: 10.1016/j.biomaterials.2016.08.019

Haque, K., Pandey, A. K., Zheng, H. W., Riazuddin, S., Sha, S. H., and Puligilla, C. (2016). MEKK4 signaling regulates sensory cell development and function in the mouse inner ear. *J. Neurosci.* 36, 1347–1361. doi: 10.1523/JNEUROSCI.1853-15.2016

He, Z. H., Zou, S. Y., Li, M., Liao, F. L., Wu, X., Sun, H. Y., et al. (2020). The nuclear transcription factor FoxG1 affects the sensitivity of mimetic aging hair cells to inflammation by regulating autophagy pathways. *Redox Biol.* 28, 101364. doi: 10.1016/j.redox.2019.101364

He, Z., Fang, Q., Li, H., Shao, B., Zhang, Y., Zhang, Y., et al. (2019). The role of FOXG1 in the postnatal development and survival of mouse cochlear hair cells. *Neuropharmacology* 144, 43–57.

He, Z., Sun, S., Waqas, M., Zhang, X., Qian, F., Cheng, C., et al. (2016). Reduced TRMU expression increases the sensitivity of hair-cell-like HEI-OC-1 cells to neomycin damage in vitro. *Sci. Rep.* 6:29621. doi: 10.1038/srep29621

Itoh, N., and Ornitz, D. M. (2004). Evolution of the Fgf and Fgfr gene families. *Trends Genet.* 20, 563–569.

Itoh, N., Ohta, H., Nakayama, Y., and Konishi, M. (2016). Roles of FGF signals in heart development, health and disease. *Front. Cell Dev. Biol.* 4:110. doi: 10.3389/fcell.2016.00110

Jacobi, A., Loy, K., Schmalz, A. M., Hellsten, M., Umemori, H., Kerschensteiner, M., et al. (2015). FGF22 signaling regulates synapse formation during post-injury remodeling of the spinal cord. *EMBO J.* 34, 1231–1243. doi: 10.15252/embj.201490578

Jan, T. A., Chai, R., Sayyid, Z. N., van Amerongen, R., Xia, A., Wang, T., et al. (2013). Tympanic border cells are Wnt-responsive and can act as progenitors for postnatal mouse cochlear cells. *Development* 140, 1196–1206. doi: 10.1242/dev.087528

Jeng, J. Y., Ceriani, F., Olt, J., Brown, S. D. M., Holley, M. C., Bowl, M. R., et al. (2020). Pathophysiological changes in inner hair cell ribbon synapses in the ageing mammalian cochlea. *J. Physiol.* 598, 4339–4355. doi: 10.1113/JP280018

Katoh, M. (2013). Functional proteomics, human genetics and cancer biology of GIPC family members. *Exp. Mol. Med.* 45:e26. doi: 10.1038/emm.2013.49

Lee, S. G., Huang, M., Obholzer, N. D., Sun, S., Li, W., Petrillo, M., et al. (2016). Myc and Fgf are required for zebrafish neuromast hair cell regeneration. *PLoS One* 11:e0157768. doi: 10.1371/journal.pone.0157768

Leger, S., and Brand, M. (2002). Fgf8 and Fgf3 are required for zebrafish ear placode induction, maintenance and inner ear patterning. *Mech. Dev.* 119, 91–108. doi: 10.1016/s0925-4773(02)00343-x

Li, A., You, D., Li, W., Cui, Y., He, Y., Li, W., et al. (2018). Novel compounds protect auditory hair cells against gentamycin-induced apoptosis by maintaining the expression level of H3K4me2. *Drug Deliv.* 25, 1033–1043. doi: 10.1080/10717544.2018.1461277

Li, H., Song, Y., He, Z., Chen, X., Wu, X., Li, X., et al. (2018). Meclofenamic acid reduces reactive oxygen species accumulation and apoptosis, inhibits excessive autophagy, and protects hair cell-like HEI-OC1 cells from cisplatin-induced damage. *Front. Cell Neurosci.* 12:139. doi: 10.3389/fncel.2018.00139

Li, S., He, J., Liu, Y., and Yang, J. (2020). FGF22 promotes generation of ribbon synapses through downregulating MEF2D. *Aging* 12, 6456–6466. doi: 10.18632/aging.103042

Li, W., You, D., Chen, Y., Chai, R., and Li, H. (2016). Regeneration of hair cells in the mammalian vestibular system. *Front. Med.* 10:143–151. doi: 10.1007/s11684-016-0451-1

Liu, H., Lu, J., Wang, Z., Song, L., Wang, X., Li, G. L., et al. (2019). Functional alteration of ribbon synapses in inner hair cells by noise exposure causing hidden hearing loss. *Neurosci. Lett.* 707:134268.

Liu, L., Chen, Y., Qi, J., Zhang, Y., He, Y., Ni, W., et al. (2016). Wnt activation protects against neomycin-induced hair cell damage in the mouse cochlea. *Cell Death Dis.* 7:e2136.

Liu, W., Xu, X., Fan, Z., Sun, G., Han, Y., Zhang, D., et al. (2019). Wnt signaling activates TP53-induced glycolysis and apoptosis regulator and protects against cisplatin-induced spiral ganglion neuron damage in the mouse cochlea. *Antioxid. Redox Signal.* 30, 1389–1410. doi: 10.1089/ars.2017.7288

Lu, X., Sun, S., Qi, J., Li, W., Liu, L., Zhang, Y., et al. (2017). Bmi1 regulates the proliferation of cochlear supporting cells via the canonical Wnt signaling pathway. *Mol. Neurobiol.* 54, 1326–1339. doi: 10.1007/s12035-016-9686-8

Lysaght, A. C., Yuan, Q., Fan, Y., Kalwani, N., Caruso, P., Cunnane, M., et al. (2014). FGF23 deficiency leads to mixed hearing loss and middle ear malformation in mice. *PLoS One* 9:e107681. doi: 10.1371/journal.pone.0107681

Najera, K., Fagan, B. M., and Thompson, P. M. (2019). SNAP-25 in major psychiatric disorders: a review. *Neuroscience* 420, 79–85.

Ni, W., Zeng, S., Li, W., Chen, Y., Zhang, S., Tang, M., et al. (2016). Wnt activation followed by Notch inhibition promotes mitotic hair cell regeneration in the postnatal mouse cochlea. *Oncotarget* 7, 66754–66768. doi: 10.18632/oncotarget.11479

Nouvian, R., Beutner, D., Parsons, T. D., and Moser, T. (2006). Structure and function of the hair cell ribbon synapse. *J. Membr. Biol.* 209, 153–165.

Nouvian, R., Neef, J., Bulankina, A. V., Reisinger, E., Pangršič, T., Frank, T., et al. (2011). Exocytosis at the hair cell ribbon synapse apparently operates without neuronal SNARE proteins. *Nat. Neurosci.* 14, 411–413. doi: 10.1038/nn.2774

Ohn, T. L., Rutherford, M. A., Jing, Z., Jung, S., Duque-Afonso, C. J., Hoch, G., et al. (2016). Hair cells use active zones with different voltage dependence of Ca2+ influx to decompose sounds into complementary neural codes. *Proc. Natl. Acad. Sci. U.S.A.* 113, E4716–E4725. doi: 10.1073/pnas.1605737113

Popov, V. V., and Supin, A. Y. (2001). Contribution of various frequency bands to ABR in dolphins. *Hear. Res.* 151, 250–260.

Prochazkova, M., Prochazka, J., Marangoni, P., and Klein, O. D. (2018). Bones, glands, ears and more: the multiple roles of FGF10 in craniofacial development. *Front. Genet.* 9:542. doi: 10.3389/fgene.2018.0054

Qi, J., Liu, Y., Chu, C., Chen, X., Zhu, W., Shu, Y., et al. (2019). A cytoskeleton structure revealed by super-resolution fluorescence imaging in inner ear hair cells. *Cell Discov.* 5:12. doi: 10.1038/s41421-018-0076-4

Qi, J., Zhang, L., Tan, F., Liu, Y., Chu, C., Zhu, W., et al. (2020). Espin distribution as revealed by super-resolution microscopy of stereocilia. *Am. J. Transl. Res.* 12, 130–141.

Qian, F., Wang, X., Yin, Z., Xie, G., Yuan, H., Liu, D., et al. (2020). The slc4a2b gene is required for hair cell development in zebrafish. *Aging* 12, 18804–18821. doi: 10.18632/aging.103840

Raft, S., and Groves, A. K. (2015). Segregating neural and mechanosensory fates in the developing ear: patterning, signaling, and transcriptional control. *Cell Tissue Res.* 359, 315–332. doi: 10.1007/s00441-014-1917-6

Ratzan, E. M., Moon, A. M., and Deans, M. R. (2020). Fgf8 genetic labeling reveals the early specification of vestibular hair cell type in mouse utricle. *Development* 147:dev192849. doi: 10.1242/dev.192849

Schaette, R., and McAlpine, D. (2011). Tinnitus with a normal audiogram: physiological evidence for hidden hearing loss and computational model. *J. Neurosci.* 31, 13452–13457. doi: 10.1523/JNEUROSCI.2156-11.2011

Snyder, C. M., Rice, A. L., Estrella, N. L., Held, A., Kandarian, S. C., and Naya, F. J. (2013). MEF2A regulates the Gtl2-Dio3 microRNA mega-cluster to modulate WNT signaling in skeletal muscle regeneration. *Development* 140, 31–42. doi: 10.1242/dev.081851

Song, L., McGee, J., and Walsh, E. J. (2006). Frequency- and level-dependent changes in auditory brainstem responses (ABRS) in developing mice. *J. Acoust. Soc. Am.* 119, 2242–2257. doi: 10.1121/1.2180533

Sun, G., Liu, W., Fan, Z., Zhang, D., Han, Y., Xu, L., et al. (2016). The three-dimensional culture system with matrigel and neurotrophic factors preserves the structure and function of spiral ganglion neuron in vitro. *Neural Plast.* 2016:4280407. doi: 10.1155/2016/4280407

Sun, S., Sun, M., Zhang, Y., Cheng, C., Waqas, M., Yu, H., et al. (2014). In vivo overexpression of X-linked inhibitor of apoptosis protein protects against neomycin-induced hair cell loss in the apical turn of the cochlea during the ototoxic-sensitive period. *Front. Cell Neurosci.* 8:248. doi: 10.3389/fncel.2014.00248

Tan, F., Chu, C., Qi, J., Li, W., You, D., Li, K., et al. (2019). AAV-ie enables safe and efficient gene transfer to inner ear cells. *Nat. Commun.* 10:3733.

Terauchi, A., Gavin, E., Wilson, J., and Umemori, H. (2017). Selective inactivation of fibroblast growth factor 22 (FGF22) in CA3 pyramidal neurons impairs local synaptogenesis and affective behavior without affecting dentate neurogenesis. *Front. Synaptic Neurosci.* 9:17. doi: 10.3389/fnsyn.2017.00017

Terauchi, A., Johnson-Venkatesh, E. M., Toth, A. B., Javed, D., Sutton, M. A., and Umemori, H. (2010). Distinct FGFs promote differentiation of excitatory and inhibitory synapses. *Nature* 465, 783–787. doi: 10.1038/nature09041

Terauchi, A., Timmons, K. M., Kikuma, K., Pechmann, Y., Kneussel, M., and Umemori, H. (2015). Selective synaptic targeting of the excitatory and inhibitory presynaptic organizers FGF22 and FGF7. *J. Cell Sci.* 128, 281–292. doi: 10.1242/jcs.158337

Teven, C. M., Farina, E. M., Rivas, J., and Reid, R. R. (2014). Fibroblast growth factor (FGF) signaling in development and skeletal diseases. *Genes Dis.* 1, 199–213.

Umemori, H., Linhoff, M. W., Ornitz, D. M., and Sanes, J. R. (2004). FGF22 and its close relatives are presynaptic organizing molecules in the mammalian brain. *Cell* 118, 257–270. doi: 10.1016/j.cell.2004.06.025

Wagner, E. L., and Shin, J. B. (2019). Mechanisms of hair cell damage and repair. *Trends Neurosci.* 42, 414–424.

Wang, T., Chai, R., Kim, G. S., Pham, N., Jansson, L., Nguyen, D. H., et al. (2015). Lgr5+ cells regenerate hair cells via proliferation and direct transdifferentiation in damaged neonatal mouse utricle. *Nat. Commun.* 6:6613. doi: 10.1038/ncomms7613

Wang, Y., Li, J., Yao, X., Li, W., Du, H., Tang, M., et al. (2017). Loss of CIB2 causes profound hearing loss and abolishes mechanoelectrical transduction in mice. *Front. Mol. Neurosci.* 10:401. doi: 10.3389/fnmol.2017.00401

Waqas, M., Guo, L., Zhang, S., Chen, Y., Zhang, X., Wang, L., et al. (2016). Characterization of Lgr5+ progenitor cell transcriptomes in the apical and basal turns of the mouse cochlea. *Oncotarget* 7, 41123–41141. doi: 10.18632/oncotarget.8636

Washbourne, P., Thompson, P. M., Carta, M., Costa, E. T., Mathews, J. R., Lopez-Bendito, G., et al. (2002). Genetic ablation of the t-SNARE SNAP-25 distinguishes mechanisms of neuroexocytosis. *Nat. Neurosci.* 5, 19–26. doi: 10.1038/nn783

White, P. M. (2020). Perspectives on human hearing loss, cochlear regeneration, and the potential for hearing restoration therapies. *Brain Sci* 10:756.

Wichmann, C., and Moser, T. (2015). Relating structure and function of inner hair cell ribbon synapses. *Cell Tissue Res.* 361, 95–114.

Woodbury, M. E., and Ikezu, T. (2014). Fibroblast growth factor-2 signaling in neurogenesis and neurodegeneration. *J. Neuroimmune Pharmacol.* 9, 92–101.

Wright, K. D., Mahoney Rogers, A. A., Zhang, J., and Shim, K. (2015). Cooperative and independent functions of FGF and Wnt signaling during early inner ear development. *BMC Dev Biol.* 15:33. doi: 10.1186/s12861-015-0083-8

Wu, J., Li, W., Lin, C., Chen, Y., Cheng, C., Sun, S., et al. (2016). Co-regulation of the Notch and Wnt signaling pathways promotes supporting cell proliferation and hair cell regeneration in mouse utricles. *Sci. Rep.* 6:29418. doi: 10.1038/srep29418

Yablonka-Reuveni, Z., Danoviz, M. E., Phelps, M., and Stuelsatz, P. (2015). Myogenic-specific ablation of Fgfr1 impairs FGF2-mediated proliferation of satellite cells at the myofiber niche but does not abolish the capacity for muscle regeneration. *Front. Aging Neurosci.* 7:85. doi: 10.3389/fnagi.2015.00085

Yan, W., Liu, W., Qi, J., Fang, Q., Fan, Z., Sun, G., et al. (2018). Three-dimensional culture system with matrigel promotes purified spiral ganglion neuron survival and function in vitro. *Mol. Neurobiol.* 55, 2070–2084. doi: 10.1007/s12035-017-0471-0

Yano, H., Ninan, I., Zhang, H., Milner, T. A., Arancio, O., and Chao, M. V. (2006). BDNF-mediated neurotransmission relies upon a myosin VI motor complex. *Nat. Neurosci.* 9, 1009–1018. doi: 10.1038/nn1730

Yu, P., Wilhelm, K., Dubrac, A., Tung, J. K., Alves, T. C., Fang, J. S., et al. (2017). FGF-dependent metabolic control of vascular development. *Nature* 545, 224–228.

Yu, X., Liu, W., Fan, Z., Qian, F., Zhang, D., Han, Y., et al. (2017). c-Myb knockdown increases the neomycin-induced damage to hair-cell-like HEI-OC1 cells in vitro. *Sci. Rep.* 7:41094. doi: 10.1038/srep41094

Zhang, S., Liu, D., Dong, Y., Zhang, Z., Zhang, Y., Zhou, H., et al. (2019). Frizzled-9+ supporting cells are progenitors for the generation of hair cells in the postnatal mouse cochlea. *Front. Mol. Neurosci.* 12:184. doi: 10.3389/fnmol.2019.00184

Zhang, S., Qiang, R., Dong, Y., Zhang, Y., Chen, Y., Zhou, H., et al. (2020a). Hair cell regeneration from inner ear progenitors in the mammalian cochlea. *Am. J. Stem Cells* 9, 25–35.

Zhang, S., Zhang, Y., Dong, Y., Guo, L., Zhang, Z., Shao, B., et al. (2020b). Knockdown of Foxg1 in supporting cells increases the trans-differentiation of supporting cells into hair cells in the neonatal mouse cochlea. *Cell Mol. Life Sci.* 77, 1401–1419.

Zhang, X., Ibrahimi, O. A., Olsen, S. K., Umemori, H., Mohammadi, M., and Ornitz, D. M. (2006). Receptor specificity of the fibroblast growth factor family. The complete mammalian FGF family. *J. Biol. Chem.* 281, 15694–15700.

Zhang, Y., Li, W., He, Z., Wang, Y., Shao, B., Cheng, C., et al. (2019). Pre-treatment with fasudil prevents neomycin-induced hair cell damage by reducing the accumulation of reactive oxygen species. *Front. Mol. Neurosci.* 12:264. doi: 10.3389/fnmol.2019.00264

Zhang, Y., Zhang, S., Zhang, Z., Dong, Y., Ma, X., Qiang, R., et al. (2020c). Knockdown of Foxg1 in Sox9+ supporting cells increases the trans-differentiation of supporting cells into hair cells in the neonatal mouse utricle. *Aging* 12, 19834–19851. doi: 10.18632/aging.104009

Zhong, Z., Fu, X., Li, H., Chen, J., Wang, M., Gao, S., et al. (2020). Citicoline protects auditory hair cells against neomycin-induced damage. *Front. Cell Dev. Biol.* 8:712. doi: 10.3389/fcell.2020.00712

Zhou, H., Qian, X., Xu, N., Zhang, S., Zhu, G., Zhang, Y., et al. (2020). Disruption of Atg7-dependent autophagy causes electromotility disturbances, outer hair cell loss, and deafness in mice. *Cell Death Dis.* 11:913. doi: 10.1038/s41419-020-03110-8

Zhu, C., Cheng, C., Wang, Y., Muhammad, W., Liu, S., Zhu, W., et al. (2018). Loss of ARHGEF6 causes hair cell stereocilia deficits and hearing loss in mice. *Front. Mol. Neurosci.* 11:362. doi: 10.3389/fnmol.2018.00362

Zhu, S., Chen, M., Chen, M., Ye, J., Ying, Y., Wu, Q., et al. (2020). Fibroblast growth factor 22 inhibits ER stress-induced apoptosis and improves recovery of spinal cord injury. *Front. Pharmacol.* 11:18. doi: 10.3389/fphar.2020.00018

frontiers | Frontiers in Molecular Neuroscience

TYPE Original Research
PUBLISHED 03 August 2022
DOI 10.3389/fnmol.2022.963083

OPEN ACCESS

EDITED BY
Yu Sun,
Huazhong University of Science and Technology, China

REVIEWED BY
Yan Chen,
Fudan University, China
Yaodong Dong,
ShengJing Hospital of China Medical University, China
Yunfeng Wang,
Fudan University, China

*CORRESPONDENCE
Yafeng Yu
yfyu1024@163.com
Yong Cui
entcui@126.com
Shuangba He
hesb@njtrh.org
Renjie Chai
renjiec@seu.edu.cn

†These authors have contributed equally to this work

SPECIALTY SECTION
This article was submitted to Methods and Model Organisms, a section of the journal Frontiers in Molecular Neuroscience

RECEIVED 07 June 2022
ACCEPTED 13 July 2022
PUBLISHED 03 August 2022

CITATION
Wu Y, Meng W, Guan M, Zhao X, Zhang C, Fang Q, Zhang Y, Sun Z, Cai M, Huang D, Yang X, Yu Y, Cui Y, He S and Chai R (2022) Pitavastatin protects against neomycin-induced ototoxicity through inhibition of endoplasmic reticulum stress. *Front. Mol. Neurosci.* 15:963083. doi: 10.3389/fnmol.2022.963083

Pitavastatin protects against neomycin-induced ototoxicity through inhibition of endoplasmic reticulum stress

Yunhao Wu[1†], Wei Meng[2†], Ming Guan[3†], Xiaolong Zhao[4†], Chen Zhang[5], Qiaojun Fang[1], Yuhua Zhang[1], Zihui Sun[2], Mingjing Cai[2], Dongdong Huang[2], Xuechun Yang[6], Yafeng Yu[7]*, Yong Cui[6,8,9]*, Shuangba He[2]* and Renjie Chai[1,4,10,11,12]*

[1]State Key Laboratory of Bioelectronics, Jiangsu Province High-Tech Key Laboratory for Bio-Medical Research, Department of Otolaryngology Head and Neck Surgery, School of Life Sciences and Technology, Zhongda Hospital, Advanced Institute for Life and Health, Southeast University, Nanjing, China, [2]Department of Otorhinolaryngology Head and Neck Surgery, School of Medicine, Nanjing Tongren Hospital, Southeast University, Nanjing, China, [3]Department of Otolaryngology, Affiliated Hangzhou First People's Hospital, Zhejiang University School of Medicine, Hangzhou, China, [4]Department of Otolaryngology Head and Neck Surgery, Sichuan Provincial People's Hospital, University of Electronic Science and Technology of China, Chengdu, China, [5]Beijing Key Laboratory of Neural Regeneration and Repair, Department of Neurobiology, Advanced Innovation Center for Human Brain Protection, School of Basic Medical Sciences, Capital Medical University, Beijing, China, [6]Department of Otolaryngology-Head and Neck Surgery, Guangdong Provincial People's Hospital, Guangdong Academy of Medical Sciences, Guangzhou, China, [7]Department of Otolaryngology, First Affiliated Hospital of Soochow University, Suzhou, China, [8]The Second School of Clinical Medicine, South Medical University, Guangzhou, China, [9]School of Medicine, South China University of Technology, Guangzhou, China, [10]Co-Innovation Center of Neuroregeneration, Nantong University, Nantong, China, [11]Institute for Stem Cell and Regeneration, Chinese Academy of Sciences, Beijing, China, [12]Beijing Key Laboratory of Neural Regeneration and Repair, Capital Medical University, Beijing, China

Irreversible injury to inner ear hair cells induced by aminoglycoside antibiotics contributes to the formation of sensorineural hearing loss. Pitavastatin (PTV), a 3-hydroxy-3-methylglutaryl coenzyme A reductase inhibitor, has been reported to exert neuroprotective effects. However, its role in aminoglycoside-induced hearing loss remains unknown. The objectives of this study were to investigate the beneficial effects, as well as the mechanism of action of PTV against neomycin-induced ototoxicity. We found that PTV remarkably reduced hair cell loss in mouse cochlear explants and promoted auditory HEI-OC1 cells survival after neomycin stimulation. We also observed that the auditory brainstem response threshold that was increased by neomycin was significantly reduced by pretreatment with PTV in mice. Furthermore, neomycin-induced endoplasmic reticulum stress in hair cells was attenuated by PTV treatment through inhibition of PERK/eIF2α/ATF4

signaling. Additionally, we found that PTV suppressed the RhoA/ROCK/JNK signal pathway, which was activated by neomycin stimulation in HEI-OC1 cells. Collectively, our results showed that PTV might serve as a promising therapeutic agent against aminoglycoside-induced ototoxicity.

KEYWORDS

pitavastatin, neomycin, hearing loss, hair cell, endoplasmic reticulum stress

Introduction

Aminoglycosides are extensively used for serious infections in clinical therapeutics, but the side effect of permanent hearing impairment limits their application. It has been reported that sensory hair cells in the inner ear are the main targets of aminoglycosides (Zhanel et al., 2012). Aminoglycosides enter inner ear compartments which are filled with endolymph by passing through the blood–labyrinth barrier, and they enter hair cells *via* interacting with several cation channels, resulting in the reactive oxygen species accumulation and cell apoptosis (Alharazneh et al., 2011; Stepanyan et al., 2011; Kros and Steyger, 2019). Although in-depth studies have been performed to elucidate the mechanisms responsible for aminoglycoside-induced ototoxicity, most therapeutic strategies to improve outcomes have been frustrated up to now.

The endoplasmic reticulum (ER), which is an intracellular vesicle-like structure that participates in the process of protein folding, plays a critical role in maintaining normal cellular function and homeostasis (Wang and Kaufman, 2016). ER stress occurs when unfolded or misfolded proteins accumulate, leading to an impairment of ER function and perturbation of ER homeostasis (Fernández et al., 2015; Oakes and Papa, 2015; So, 2018). Prolonged ER stress responses can trigger cellular apoptosis and thus play a pivotal role in the pathological process of numerous diseases, including cardiovascular diseases, neurodegenerative diseases, cancer, and metabolic diseases (Urra et al., 2016; Brown et al., 2020; Ghemrawi and Khair, 2020; Radwan et al., 2020). The relationship between ER stress and hearing loss has been investigated for several decades, and aminoglycoside antibiotics have been demonstrated for the induction of hair cell apoptosis accompanied by ER stress. Also, ER stress inhibition exhibits attenuation for aminoglycoside-induced cochlear hair cell death (Jia et al., 2018), thus highlighting the need for further investigation on the relationship between ER stress and aminoglycoside-induced ototoxicity.

Statins that act as antilipemic agents by preventing cholesterol biosynthesis are the inhibitors of 3-hydroxy-3-methylglutaryl coenzyme A (HMG-CoA) reductase. Statins are not only applied for the therapeutics of cardiovascular diseases, but also for the treatment of neurological disorders (Oesterle et al., 2017; Sanz-Cuesta and Saver, 2021), and lots of studies have suggested that statins have potential protective effects against sensorineural hearing loss (Brand et al., 2011; Park et al., 2012; Fernandez et al., 2020; Whitlon, 2022). Pitavastatin (PTV) is a new-generation lipophilic statin that has been reported to exert anti-oxidative, anti-inflammatory, anti-neoplastic, and neuroprotective effects (Kaneyuki et al., 2007; Gbelcová et al., 2017; Cui et al., 2018; Li and Liu, 2022), but the role of PTV in aminoglycoside-induced ototoxicity remains unknown.

In the current research, we studied the protective properties and potential mechanisms of PTV on neomycin-triggered hearing loss by constructing *in vivo* and *in vitro* models. The ultimate goal was to assist in the discovery and development of therapeutic drugs for preventing aminoglycoside-triggered sensorineural hearing loss.

Materials and methods

Cell viability assay

HEI-OC1 cells were inoculated into 96-well plates (2×10^5 cells/ml) overnight. Then, the cells were incubated with PTV at different concentrations (0.001, 0.005, 0.01, 0.05, 0.1, and 0.5 μm) for 24 h and challenged with neomycin for the next 24 h. Then, CCK-8 solution (1:10 dilution in DMEM) was given to the cells for 30-min incubation at 37°C. The absorbance value was measured by a Thermo Scientific microplate reader at 450 nm.

In vivo experiments

SPF C57BL/6 mice were purchased from Gempharmatech Co., Ltd. (Nanjing, China). After being allowed to acclimate for 3 days, mice of P28 were intraperitoneal injected PTV (Aladdin, P129617) with a dose of 3 mg/kg. After 2 h, neomycin (Sigma, N6386) at 100 mg/kg was injected intraperitoneally, and then after 30 min, mice were given a single dose of furosemide (Sigma, BP547) at 200 mg/kg by intraperitoneal injection. The measurement of auditory brainstem response (ABR) and counting of cochlear hair cells were performed 2 days later.

Whole-organ explants culture

The cochleae of P3 wild-type mice were dissected from the inner ear and immersed in bioclean HBSS (Multicell, 311512011) using a stereo microscope. The spiral ganglion, spiral ligament, and stria vascularis of cochleae were removed, and the cochlear basilar membranes were put in dishes that were smeared with Corning® Cell-Tak™ and then cultured with DMEM-F12 medium added with ampicillin (Beyotime, ST008), N2 Supplement (Stemcell, 07152), and SM1 neuronal supplement (Stemcell, 05711) for 12 h in an incubator at 37°C, 5% CO_2. About 0.01 μm PTV was given to the samples for 12 h, and then, 0.5 mm neomycin with 0.01 μm PTV was given together to the cochleae for another 12 h.

Auditory brainstem response audiometry

Hearing thresholds of mice were assessed by ABR. ABR experiment was carried out in an acoustic space, and the variation in brain electrical activity in mice in answer to different sounds was recorded by electrodes. After being anesthetized, the mice were kept on a preheating pad (37°C), and the ABR responses were recorded at different frequencies on a Tucker-Davis Technology System III system (Tucker Davies Technologies, Gainesville, FL, United States).

Immunofluorescence

The tissue or cell samples fixed with 4% paraformaldehyde were permeabilized with 1% Triton X-100. After blocking with QuickBlock™ buffer (Beyotime, P0260) for 1 h, and the primary antibodies against myosin 7a (Abcam, ab150386, 1:200 dilution), cleaved caspase-3 (Abcam, ab32042, 1:150 dilution), GRP78 (Proteintech, 11587-1-AP, 1:200 dilution), and CHOP (Proteintech, 15204-1-AP, 1:200 dilution) were added to the samples at 4°C overnight. Next day after washing three times with phosphate-buffered saline (PBS), the samples were incubated with corresponding secondary antibodies for 1 h at room temperature then washed three times with PBS and incubated with ECL solution and imaged using confocal laser scanning microscope (Zeiss, Germany).

Flow cytometry

The effect of PTV on neomycin-triggered apoptosis of HEI-OC1 cells was evaluated by an Annexin-V/PI kit (BD, 556419). Briefly, cells were harvested by digestion and centrifugation. Precooling PBS was used to wash the cells three times, and after being suspended by the binding buffer, cells were incubated with 5 μl Annexin V-FITC and 5 μl PI for 20 min at room temperature. The apoptosis was subsequently assayed by flow cytometry (MACSQuant, Germany).

Terminal deoxynucleotidyl transferase dUTP nick end labeling staining

A terminal deoxynucleotidyl transferase dUTP nick end labeling (TUNEL) BrightGreen apoptosis detection kit (Vazyme, A112-01) was used to determine the apoptosis of HEI-OC1 cells and cochlear explants. Briefly, the samples were fixed and permeabilized, then equilibrated with 1 × Equilibration Buffer for 30 min at room temperature. After incubating with the label solution at 37°C for 1 h, the samples were washed by PBS for 2 times and imaged by a confocal laser scanning microscope.

Western blot

The total protein of cell samples was extracted using RIPA lysis buffer (Beyotime, P0013C) containing phenylmethanesulfonyl fluoride (1 mm). After quantification by a BCA kit (Beyotime, P0012S), the sodium dodecyl sulfate–polyacrylamide gel electrophoresis (SDS-PAGE) sample loading buffer (Beyotime, P0015) was added to the total protein lysate, and the mixed buffer was boiled at 100°C for 5 min. Total proteins (40 μg) of each group were added to the gels and separated through electrophoresis and then transferred to polyvinylidene fluoride (PVDF) membranes. After being blocked in 5% BSA-PBST for 2 h, the immunoblots were immersed in 5% BSA-PBST, which contained primary antibodies overnight at 4°C. Next day, the bands were washed three times with 0.05% tween-PBS (PBST) and then combined with the corresponding HRP conjugated secondary antibodies and detected by an ECL kit (Vazyme, E411-04) and analyzed by ImageJ software.

Statistical analysis

All data are analyzed by GraphPad Prism 9 software and are presented as the mean ± standard deviation (SD). Statistical significance was calculated with one-way analysis of variance (ANOVA) followed by Dunnett's test when comparing more than two groups. A p-value < 0.05 indicated a statistically significant difference.

Results

Pitavastatin protects against neomycin-induced hair cell damage

To confirm whether PTV has a beneficial effect on neomycin-triggered hair cell injury, auditory HEI-OC1 cells

were administrated with different doses of PTV (0.001, 0.005, 0.01, 0.05, 0.1, and 0.5 μm) prior to neomycin (2 mm) treatment. PTV showed significant attenuation of cell injury triggered by neomycin at doses of 0.01–0.5 μm, and PTV at 0.01 μm exhibited the best protective effect, so premedication of 0.01 μm PTV for 24 h was chosen as the best administration scheme (Figure 1A). We also measured the influence of PTV on whole-organ cochlear explant cultures from P3 mice after neomycin treatment. Immunostaining results indicated that neomycin treatment resulted in an obvious missing of hair cells in cochleae in the middle and basal turns and that PTV pretreatment distinctly prevented neomycin-stimulated inner ear hair cell loss (Figures 1B–E). The above results disclose that PTV has effective protection against neomycin-triggered hair cell injury.

Pitavastatin alleviates neomycin-triggered hearing loss *in vivo*

Next, we investigated the protective property of PTV on neomycin-triggered hearing loss by establishing an acute neomycin-induced ototoxicity model according to the previous study (He et al., 2020). C57BL/6 mice (P28) were intraperitoneally injected with 3 mg/kg PTV, and after 2 h, mice were given an intraperitoneal injection of 100 mg/kg neomycin in conjunction with 200 mg/kg furosemide (Figure 2A). ABR measurements were employed to determine the auditory function of mice, and the results suggested that neomycin treatment led to an obvious elevation of ABR thresholds, whereas PTV administration strongly attenuated this effect (Figure 2B). By counting cochlear hair cells, we found a massive loss of cochlear hair cells in the neomycin plus furosemide group, whereas PTV had an apparent promotion for hair cell survival (Figures 2C,D). Collectively, the data reveal that PTV attenuates neomycin-triggered hearing loss *in vivo*.

Pitavastatin attenuates neomycin-triggered apoptosis in HEI-OC1 cells

To explore the protective effects of PTV against neomycin-induced HEI-OC1 cell damage, TUNEL and cleaved caspase-3 (cleaved CASP-3) dying were conducted to detect apoptosis. We observed that neomycin stimulation for 24 h dramatically

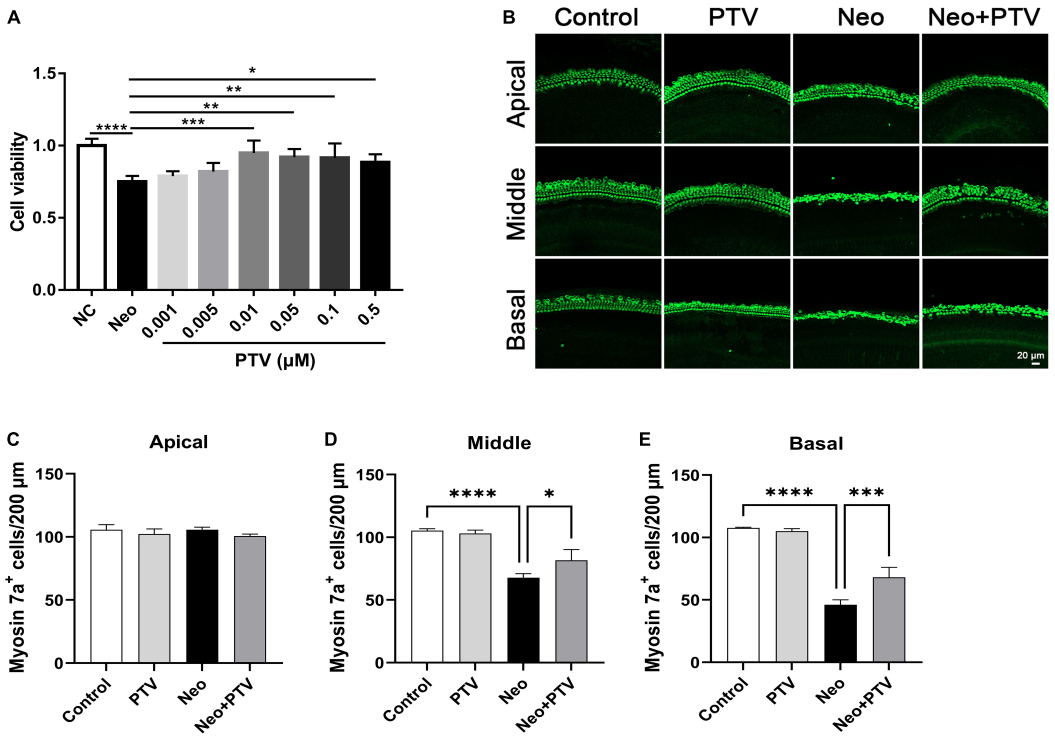

FIGURE 1
PTV attenuates neomycin-induced HEI-OC1 cell damage and missing of hair cells in cochlear explants *in vitro*. **(A)** The CCK8 method was used to determine the protective effect of PTV (0.001, 0.005, 0.01, 0.05, 0.1, and 0.5 μm) on neomycin-induced HEI-OC1 cell injury ($n = 6$). **(B)** Immunostaining of hair cells in cochlear explants in the apical, middle, and basal turns with anti-myosin 7a antibody. Scale bars = 20 μm. **(C–E)** Counting of the amount of hair cells per 200 μm in inner ear in the apical, middle and basal turns ($n = 3$). *$p < 0.05$, **$p < 0.01$, ***$p < 0.001$, ****$p < 0.0001$.

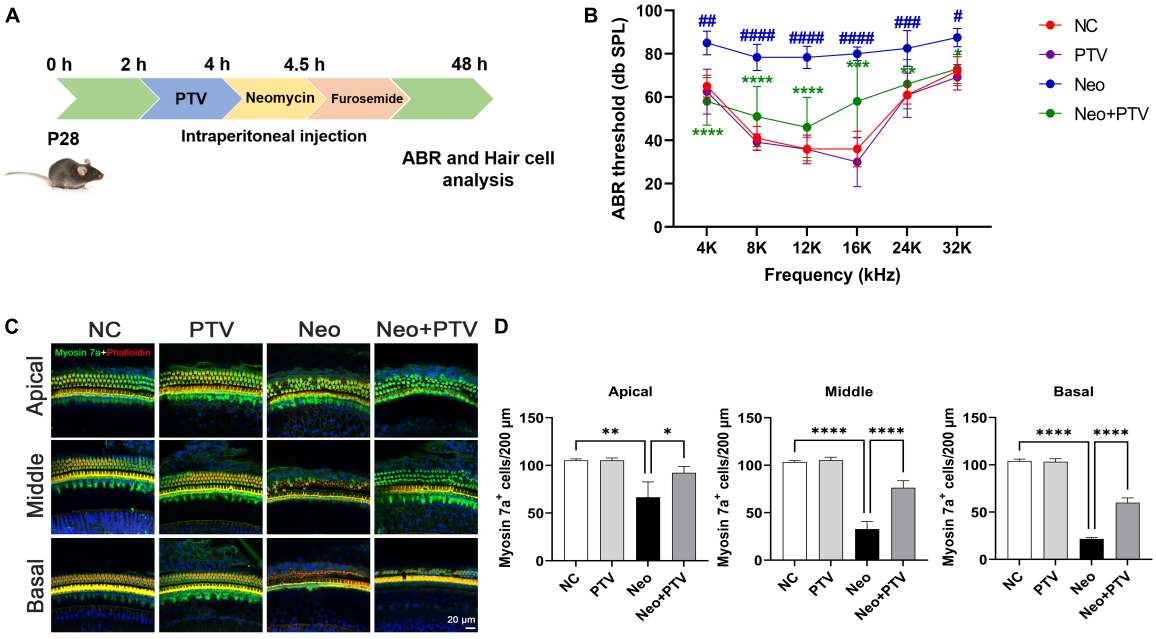

FIGURE 2
PTV promotes auditory function recovery and prevents neomycin-triggered hair cell loss *in vivo*. **(A)** Procedure of the experiments *in vivo*. **(B)** Auditory function of mice was detected using ABR method (n = 6). **(C)** Immunofluorescence of mouse cochlear hair cells stained with myosin 7a and phalloidin in the apical, middle, and basal turns. Scale bars = 20 μm. **(D)** Counting of the amount of cochlear hair cells per 200 μm in mice (n = 3). $^{\#}p < 0.05$, $^{\#\#}p < 0.01$, $^{\#\#\#}p < 0.001$, $^{\#\#\#\#}p < 0.0001$ vs. NC group; $^{*}p < 0.05$, $^{**}p < 0.01$, $^{****}p < 0.0001$ vs. Neo group.

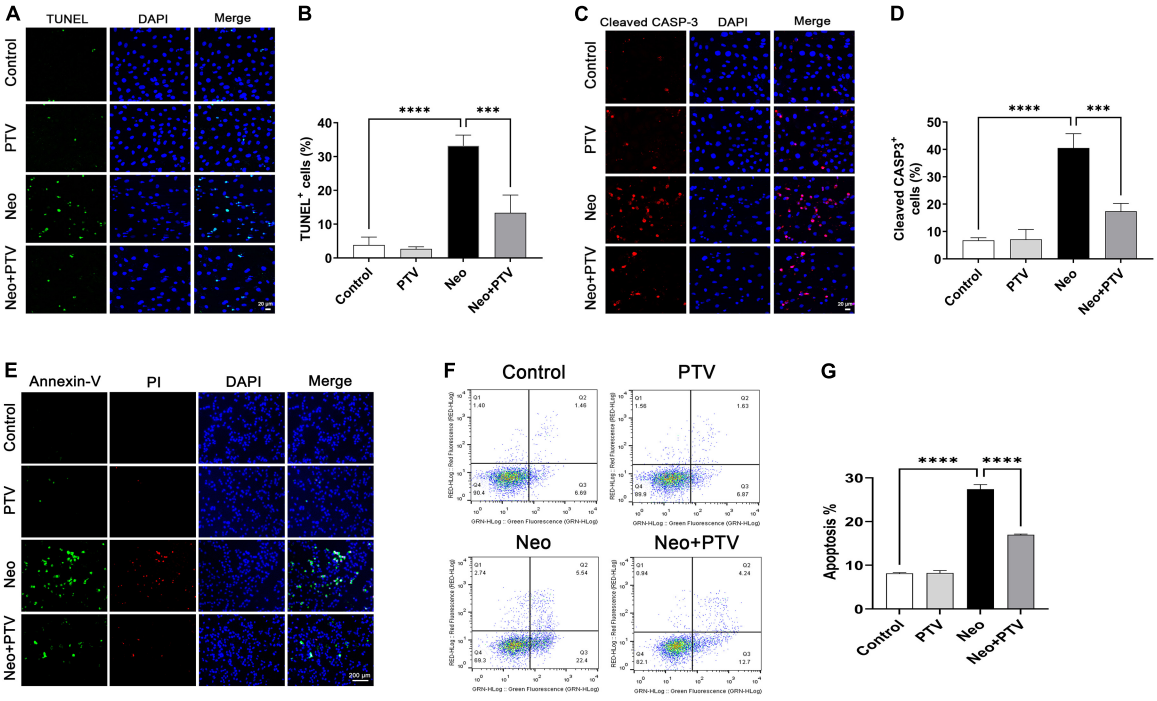

FIGURE 3
Effects of PTV on neomycin-triggered HEI-OC1 cell apoptosis. **(A,C)** TUNEL staining and cleaved CASP-3 immunostaining of HEI-OC1 cells. Scale bars = 20 μm. **(B,D)** Statistics of the proportions of TUNEL or cleaved CASP-3 highlighted HEI-OC1 cells in **(A,C)** (n = 3). **(E)** Annexin-V/PI staining in PTV and neomycin treatment HEI-OC1 cells. Scale bars = 200 μm. **(F)** Apoptosis detection of HEI-OC1 cells by flow cytometry. **(G)** Statistics of the proportions of apoptotic HEI-OC1 cells in different groups (n = 3). $^{***}p < 0.001$, $^{****}p < 0.0001$.

increased the count of TUNEL and cleaved CASP-3-positive cells, whereas PTV group exhibited an effective improvement (Figures 3A–D). Annexin V-FITC/PI kit was employed to further confirm the benefit of PTV on the apoptosis triggered by neomycin, and immunostaining and flow-cytometric assays exhibited that neomycin significantly induced cell apoptosis, whereas PTV administration showed a notable attenuation in the apoptosis of HEI-OC1 cells (Figures 3E–G). Our results indicate that PTV attenuates HEI-OC1 cell apoptosis induced by neomycin.

Pitavastatin reduces apoptosis of cochlear hair cells after neomycin treatment

We further explored the impact of PTV on neomycin-triggered apoptosis of hair cells in cochlear explant cultures. After being dissected from P3 mice, the cochlear explants were cultured at 37°C and 5% CO_2 for 12 h and then pretreated with 0.01 μm PTV for 12 h followed by neomycin (0.5 mm) treatment together with PTV for another 12 h. Using TUNEL and cleaved CASP-3 staining, we found that the amount of TUNEL-positive hair cells that were marked by myosin 7a and the amount of cleaved CASP-3 staining hair cells in model group were prominently higher than the control group, whereas PTV administration clearly decreased the amount of apoptotic hair cells, which is in accordance with the results discussed above in HEI-OC1 cells (Figures 4A–D). Collectively, the data demonstrate that PTV suppresses the apoptotic cascade under aminoglycosides stimulation.

Pitavastatin inhibits neomycin-induced endoplasmic reticulum stress in cochlear hair cells

It has been reported that ER stress plays a pivotal role in aminoglycoside-induced hair cell apoptosis (Jia et al., 2018), so we next determined the expression of ER stress-relevant proteins

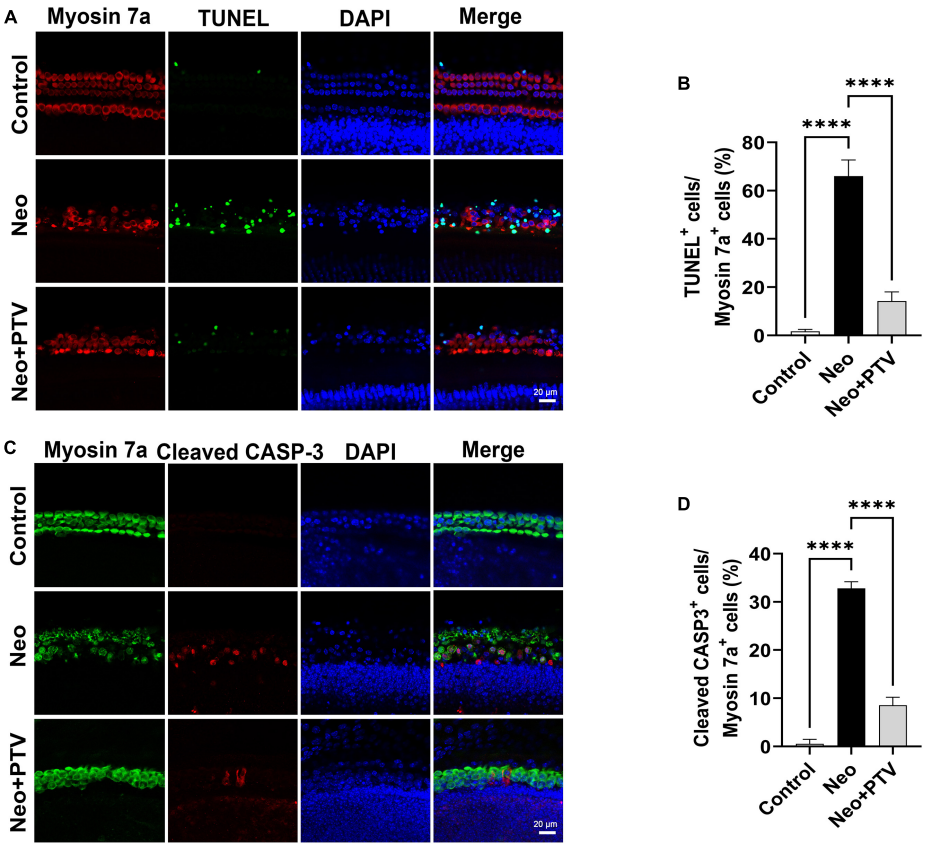

FIGURE 4
Effects of PTV on apoptosis of cochlear hair cell in whole-organ explants induced by neomycin. **(A)** Immunostaining with TUNEL and myosin 7a labeling in the middle turns in cochlear explants. Scale bars = 20 μm. **(B)** Statistics of the proportions of TUNEL highlighted hair cells in **(A)**. **(C)** Immunostaining with cleaved CASP-3 and myosin 7a in the middle turns in cochlear explants. Scale bars = 20 μm. **(D)** Statistics of the proportions of cleaved CASP-3 highlighted hair cells in **(C)**. ****$p < 0.0001$.

GRP78 and CHOP after neomycin stimulation. We discovered that the level of GRP78 together with CHOP was remarkably higher than the control group after neomycin treatment. PTV administration could inhibit ER stress by suppressing the elevated expression of GRP78 and CHOP induced by neomycin (**Figures 5A–D**), and this further indicates that PTV can ameliorate neomycin-induced ER stress.

Pitavastatin suppresses neomycin-induced endoplasmic reticulum stress by inhibiting PERK/eIF2α/ATF4 signaling in HEI-OC1 cells

To explore the molecular mechanism by which PTV inhibits neomycin-triggered ER stress, we examined the three classical signal pathways (PERK signaling, IRE1α signaling, and ATF6 signaling) that are involved in ER stress. First, by immunostaining, we confirmed that PTV could prevent the high expression of GRP78 and CHOP induced by neomycin in HEI-OC1 cells (**Figures 6A–D**). Next, western blot analysis revealed that the expression levels of p-PERK, p-eIF2α, ATF4, GRP78, and CHOP were markedly increased after neomycin stimulation in cells, which was strongly inhibited by PTV treatment (**Figures 6E–J**). Also, there was no obvious change in IRE1α or ATF6 expression after PTV and neomycin treatment (**Figures 6K,L**). Together, the results above suggest that PTV attenuates neomycin-induced ER stress mainly by restricting PERK/eIF2α/ATF4 signaling in HEI-OC1 cells.

Pitavastatin significantly inhibits the RhoA/ROCK signaling pathway activated by neomycin

Previous research has shown that PTV exerts its neuroprotective effects mainly through the inhibition of Rho/ROCK signaling pathway (Hamano et al., 2012). PTV is a competitive inhibitor of the HMG-CoA reductases that activate

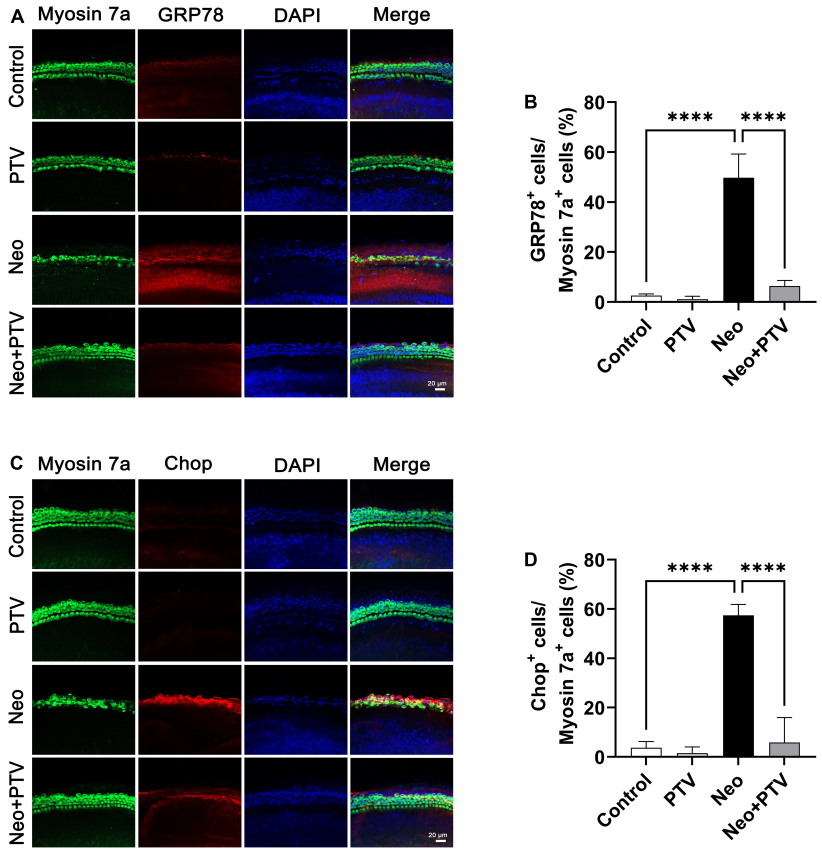

FIGURE 5
Impacts of PTV on neomycin-triggered ER stress in cochlear hair cells. **(A)** Immunostaining with myosin 7a and GRP78 in middle turns in cochlear explants. Scale bars = 20 μm. **(B)** Statistics of the proportions of GRP78 highlighted hair cells in **(A)**. **(C)** Immunostaining with myosin 7a and CHOP in middle turns in cochlear explants. Scale bars = 20 μm. **(D)** Statistics of the proportions of CHOP highlighted hair cells in **(C)**. ****$p < 0.0001$.

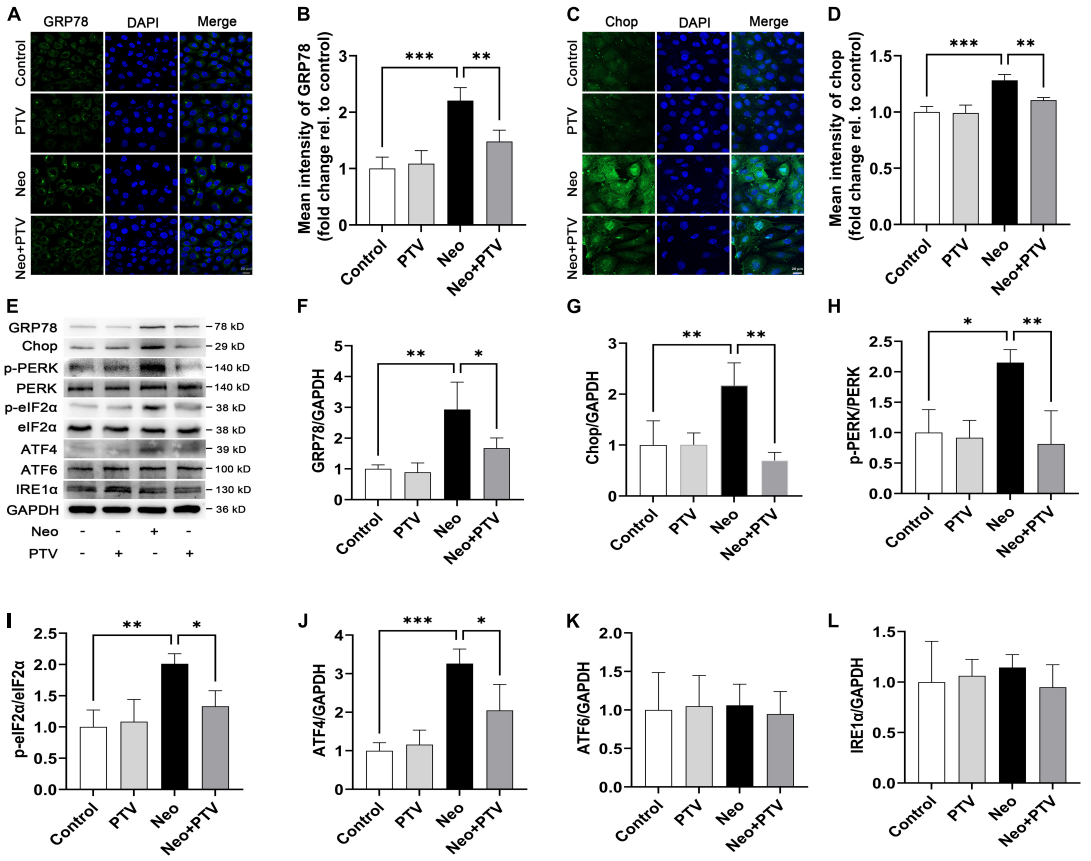

FIGURE 6
PTV alleviates neomycin-induced ER stress by inhibiting PERK/eIF2α/ATF4 signaling. **(A,C)** Immunofluorescence of HEI-OC1 cells with anti-GRP78 and anti-CHOP antibodies. Scale bars = 20 μm. **(B,D)** Statistics of the mean intensity of GRP78 and CHOP in HEI-OC1 cells in **(A,C)**. **(E)** Western blot analysis of GRP78, CHOP, p-PERK, PERK, p-eIF2α, eIF2α, ATF4, ATF6, IRE1α, and GAPDH in HEI-OC1 cells with PTV pretreatment followed by neomycin exposure. **(F–L)** Quantification of the protein expression in **(E)** with ImageJ ($n = 3$). $^{*}p < 0.05$, $^{**}p < 0.01$, $^{***}p < 0.001$.

the Rho/ROCK signaling pathway, but whether PTV protects against neomycin-induced ototoxicity through the inhibition of the Rho/ROCK signaling pathway remains unclear. In this study, we also tested the change of Rho/ROCK signaling after PTV administration and neomycin treatment in HEI-OC1 cells. Western blot results showed that the expression levels of the key factors in Rho signaling, including RhoA, ROCK, and JNK, were prominently upregulated after neomycin stimulation, whereas PTV pretreatment strongly downregulated the elevated expression of RhoA, ROCK, and JNK induced by neomycin (**Figures 7A–D**). These data suggest that PTV protects against neomycin-induced ototoxicity by inhibiting the Rho/ROCK signaling pathway.

Discussion

Aminoglycoside antibiotics are used to treat gram-negative bacterial infections, but their application is restricted by the severe side effects of ototoxicity and vestibular toxicity. Aminoglycosides can accumulate in cochlear hair cells and are hard to metabolize, which may lead to irreversible damage of cochlear hair cells and result in permanent hearing loss. In the present study, we show that the HMG-CoA reductase inhibitor PTV could efficiently attenuate neomycin-triggered ototoxicity. By *in vitro* and *in vivo* studies, we demonstrated that PTV protected against neomycin-induced apoptosis of cochlear hair cells, and the protective effect might be in connection with the inhibition of ER stress. We further confirmed that PTV exerted anti-apoptotic effects and suppressed PERK/eIF2α/ATF4 signaling-mediated ER stress by inhibiting Rho/ROCK signaling.

PTV is a novel synthetic lipophilic statin with greater safety, tolerability, and fewer adverse effects compared with conventional statins and is commonly used for the treatment of hypercholesteremia (Hoy, 2017; Chan et al., 2019; Adams et al., 2020). Previous research showed that PTV exhibited efficient neuroprotective effects independent of its antilipemic effect (Kozuki et al., 2011; Kurata et al., 2011a,b). However, there is no investigation in regard to the beneficial effect of

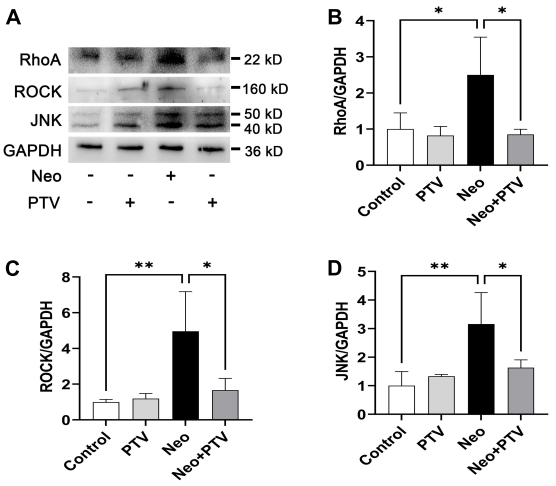

FIGURE 7
PTV inhibits neomycin-triggered activation of the Rho/ROCK signaling pathway. **(A)** Western blot analysis of RhoA, ROCK, JNK, and GAPDH in HEI-OC1 cells with PTV pretreatment followed by neomycin exposure. **(B–D)** Quantification of the protein expression in **(A)** with ImageJ ($n = 3$). $^{*}p < 0.05$, $^{**}p < 0.01$.

PTV on aminoglycoside-triggered hearing loss. In this study, by establishing an acute neomycin-induced ototoxicity model, we observed that PTV could effectively mitigate neomycin-triggered hearing loss *in vivo* (**Figure 2**). We also found that PTV protected against auditory HEI-OC1 cell and cochlear explant injury triggered by neomycin *in vitro* (**Figure 1**). These results suggested that PTV might be a promising agent for the prevention of aminoglycoside-triggered ototoxicity.

Apoptosis of hair cells leading to hearing loss is the key factor in the "ototoxicity" of aminoglycosides (Wu et al., 2021). Using TUNEL staining, we found that the proportions of TUNEL/myosin 7a double-positive cells in cochlear explants were remarkably increased after neomycin treatment, confirming that neomycin may cause cochlear hair cell death through apoptosis. In addition, there was very less TUNEL staining observed in the PTV pretreatment group (**Figures 4A,B**). Cleaved CASP-3 is considered a universal marker of apoptosis due to its critical role in the pathogenesis of cell apoptosis (Wang et al., 2021). In our study, we also found that PTV could significantly reduce the increased numbers and proportions of apoptotic hair cells induced by neomycin (**Figures 4C,D**), which is consistent with our *in vitro* results in HEI-OC1 cells (**Figure 3**). Collectively, these results demonstrate that PTV exerts its beneficial effect on neomycin-triggered hair cell injury by inhibiting the occurrence of apoptosis.

It is well documented that ER stress is triggered by the disruption of homeostasis in the ER and results in the activation of the unfolded protein response (UPR) (Lu et al., 2014; Fu et al., 2021). When the unfolded or misfolded proteins in the ER accumulate and exceed a tolerable threshold, the function of ER may be lost and be difficult to restore leading to cellular dysfunction and apoptosis (Gorman et al., 2012; Verfaillie et al., 2013; Hu et al., 2019). There are three classical signal pathways involved in UPR, including PERK signaling, IRE1 signaling, and transcription factor ATF6 signaling (Walter and Ron, 2011). GRP78, which is a type of peptide-binding protein that prevents the aggravation of protein folding, has been reported to be a key regulator of ER stress and UPR activation (Adams et al., 2019). Changes in the microenvironment due to physiological processes or to pathological conditions, such as hypoxia, viral, or bacterial infections and drugs, can induce ER stress, thus causing GRP78 to separate from the sensors (PERK, IRE1, and ATF6) and further activate downstream signaling (Hollien and Weissman, 2006; Díaz-Bulnes et al., 2020; Kapadia et al., 2021; Mazel-Sanchez et al., 2021). It was observed that neomycin treatment significantly increased the expression levels of GRP78 and CHOP in cochlear hair cells, which indicated that neomycin could activate ER stress (**Figure 5**). We also found that PTV pretreatment effectively alleviated neomycin-induced ER stress through inhibition of the PERK/eIF2α/ATF4 signaling pathway (**Figure 6**). These results manifest that PTV is able to suppress neomycin-induced hair cell apoptosis by inhibiting ER stress *via* mediation of the PERK/eIF2α/ATF4 signaling pathway.

As an HMG-CoA reductase inhibitor, PTV has been reported to exert its neuroprotective effect *via* the inhibition of Rho/ROCK signaling (Hamano et al., 2012, 2020). It has also been reported that ROCK inhibitor has neuroprotective and regenerative effects on synaptic pathways by promoting synapse formation in cochlear hair cells (Koizumi et al., 2020). By western blot assays, we confirmed that PTV could decrease the elevated expression of RhoA, ROCK, and JNK induced by neomycin (**Figure 7**). Thus, PTV appears to attenuate neomycin-induced ototoxicity by inactivation of Rho/ROCK signaling.

Conclusion

In summary, we show that PTV can ameliorate neomycin-triggered cochlear hair cell injury and hearing loss by inhibiting RhoA/ROCK signaling and can suppress ER stress by blocking the PERK/eIF2α/ATF4 pathway. The findings indicate that PTV may serve as a promising agent for the prevention of aminoglycoside-induced ototoxicity.

Data availability statement

The original contributions presented in the study are included in the article/**Supplementary material**, further inquiries can be directed to the corresponding author/s.

Ethics statement

The animal study was reviewed and approved by the Animal Care and Use Committee of Southeast University.

Author contributions

YW, RC, SH, and XZ designed the whole experiments. YW, YY, WM, and MG conducted the most part of the experiments and analyzed the data. CZ, QF, and YZ conducted part of the *in vitro* experiments. DH, MC, and ZS conducted part of the *in vivo* experiments. XY and YC drafted the manuscript. All authors contributed to the article and approved the submitted version.

Funding

The present research was supported by the grants from the National Basic Research Program of China (grant no. 2017YFA0105201), the National Key R&D Program of China (grant nos. 2017YFA0105201, 2021YFA1101300, and 2020YFA0112503), the Strategic Priority Research Program of the Chinese Academy of Science (XDA16010303), the National Natural Science Foundation of China (grant nos. 82171153, 82101228, 82101206, 82030029, 81970882, and 92149304), the Natural Science Foundation of Jiangsu Province (grant nos. BK20211012 and BE2019711), the Nanjing Medical Science and Technique Development Foundation (grant no. QRX17033), the Natural Science Foundation of Zhejiang Province (grant no. LY20H130003), the Hangzhou Science and Technology Development Plan Project (grant no. 20201203B205), the Science and Technology Department of Sichuan Province (grant no. 2021YFS0371), the Shenzhen Fundamental Research Program (grant nos. JCYJ20190814093401920 and JCYJ20210324125608022), the Open Research Fund of State Key Laboratory of Genetic Engineering, Fudan University (grant no. SKLGE-2109), the Guangdong Basic and Applied Basic Research Foundation (grant no. 2021A1515220179), and the Fundamental Research Funds for the Central Universities (grant no. 2242022R20068).

Conflict of interest

The authors declare that the research was conducted in the absence of any commercial or financial relationships that could be construed as a potential conflict of interest.

Publisher's note

All claims expressed in this article are solely those of the authors and do not necessarily represent those of their affiliated organizations, or those of the publisher, the editors and the reviewers. Any product that may be evaluated in this article, or claim that may be made by its manufacturer, is not guaranteed or endorsed by the publisher.

Supplementary material

The Supplementary Material for this article can be found online at: https://www.frontiersin.org/articles/10.3389/fnmol.2022.963083/full#supplementary-material

References

Adams, C. J., Kopp, M. C., Larburu, N., Nowak, P. R., and Ali, M. M. U. (2019). Structure and molecular mechanism of ER stress signaling by the unfolded protein response signal activator IRE1. *Front. Mol. Biosci.* 6:11. doi: 10.3389/fmolb.2019.00011

Adams, S. P., Alaeiilkhchi, N., and Wright, J. M. (2020). Pitavastatin for lowering lipids. *Cochrane. Data. Syst. Rev.* 6:CD012735. doi: 10.1002/14651858.CD012735.pub2

Alharazneh, A., Luk, L., Huth, M., Monfared, A., Steyger, P. S., Cheng, A. G., et al. (2011). Functional hair cell mechanotransducer channels are required for aminoglycoside ototoxicity. *PLoS One* 6:e22347. doi: 10.1371/journal.pone.0022347

Brand, Y., Setz, C., Levano, S., Listyo, A., Chavez, E., Pak, K., et al. (2011). Simvastatin protects auditory hair cells from gentamicin-induced toxicity and activates Akt signaling in vitro. *BMC Neurosci.* 12:114. doi: 10.1186/1471-2202-12-114

Brown, M., Dainty, S., Strudwick, N., Mihai, A. D., Watson, J. N., Dendooven, R., et al. (2020). Endoplasmic reticulum stress causes insulin resistance by inhibiting delivery of newly synthesized insulin receptors to the cell surface. *Mol. Biol. Cell* 31, 2597–2629. doi: 10.1091/mbc.E18-01-0013

Chan, P., Shao, L., Tomlinson, B., Zhang, Y., and Liu, Z. M. (2019). An evaluation of pitavastatin for the treatment of hypercholesterolemia. *Exp. Opin. Pharmacother* 20, 103–113. doi: 10.1080/14656566.2018.1544243

Cui, X., Fu, Z., Wang, M., Nan, X., and Zhang, B. (2018). Pitavastatin treatment induces neuroprotection through the BDNF-TrkB signalling pathway in cultured cerebral neurons after oxygen-glucose deprivation. *Neurol. Res.* 40, 391–397. doi: 10.1080/01616412.2018.1447318

Díaz-Bulnes, P., Saiz, M. L., López-Larrea, C., and Rodríguez, R. M. (2020). Crosstalk between hypoxia and ER stress response: A key regulator of macrophage polarization. *Front. Immunol.* 10:2951. doi: 10.3389/fimmu.2019.02951

Fernández, A., Ordóñez, R., Reiter, R. J., González-Gallego, J., and Mauriz, J. L. (2015). Melatonin and endoplasmic reticulum stress: relation to autophagy and apoptosis. *J. Pineal. Res.* 59, 292–307. doi: 10.1111/jpi.12264

Fernandez, K., Spielbauer, K. K., Rusheen, A., Wang, L., Baker, T. G., Eyles, S., et al. (2020). Lovastatin protects against cisplatin-induced hearing loss in mice. *Hear. Res.* 389:107905. doi: 10.1016/j.heares.2020.107905

Fu, X., Cui, J., Meng, X., Jiang, P., Zheng, Q., Zhao, W., et al. (2021). Endoplasmic reticulum stress, cell death and tumor: Association between

endoplasmic reticulum stress and the apoptosis pathway in tumors. *Oncol. Rep*. 45, 801–808. doi: 10.3892/or.2021.7933

Gbelcová, H., Rimpelová, S., Ruml, T., Fenclová, M., Kosek, V., Hajšlová, J., et al. (2017). Variability in statin-induced changes in gene expression profiles of pancreatic cancer. *Sci. Rep*. 7:44219. doi: 10.1038/srep44219

Ghemrawi, R., and Khair, M. (2020). Endoplasmic reticulum stress and unfolded protein response in neurodegenerative diseases. *Int. J. Mol. Sci*. 21:6127. doi: 10.3390/ijms21176127

Gorman, A. M., Healy, S. J., Jäger, R., and Samali, A. (2012). Stress management at the ER: regulators of ER stress-induced apoptosis. *Pharmacol. Ther*. 134, 306–316. doi: 10.1016/j.pharmthera.2012.02.003

Hamano, T., Shirafuji, N., Yen, S. H., Yoshida, H., Kanaan, N. M., Hayashi, K., et al. (2020). Rho-kinase ROCK inhibitors reduce oligomeric tau protein. *Neurobiol. Aging* 89, 41–54. doi: 10.1016/j.neurobiolaging.2019.12.009

Hamano, T., Yen, S. H., Gendron, T., Ko, L. W., and Kuriyama, M. (2012). Pitavastatin decreases tau levels via the inactivation of Rho/ROCK. *Neurobiol. Aging* 33, 2306–2320. doi: 10.1016/j.neurobiolaging.2011.10.020

He, Y., Li, W., Zheng, Z., Zhao, L., Li, W., Wang, Y., et al. (2020). Inhibition of Protein arginine methyltransferase 6 reduces reactive oxygen species production and attenuates aminoglycoside- and cisplatin-induced hair cell death. *Theranostics* 10, 133–150. doi: 10.7150/thno.37362

Hollien, J., and Weissman, J. S. (2006). Decay of endoplasmic reticulum-localized mRNAs during the unfolded protein response. *Science* 313, 104–107. doi: 10.1126/science.1129631

Hoy, S. M. (2017). Pitavastatin: A review in hypercholesterolemia. *Am. J. Cardiovasc. Drugs* 17, 157–168. doi: 10.1007/s40256-017-0213-8

Hu, H., Tian, M., Ding, C., and Yu, S. (2019). The C/EBP homologous protein (CHOP) Transcription factor functions in endoplasmic reticulum stress-induced apoptosis and microbial infection. *Front. Immunol*. 9:3083. doi: 10.3389/fimmu.2018.03083

Jia, Z., He, Q., Shan, C., and Li, F. (2018). Tauroursodeoxycholic acid attenuates gentamicin-induced cochlear hair cell death in vitro. *Toxicol. Lett*. 294, 20–26. doi: 10.1016/j.toxlet.2018.05.007

Kaneyuki, U., Ueda, S., Yamagishi, S., Kato, S., Fujimura, T., Shibata, R., et al. (2007). Pitavastatin inhibits lysophosphatidic acid-induced proliferation and monocyte chemoattractant protein-1 expression in aortic smooth muscle cells by suppressing Rac-1-mediated reactive oxygen species generation. *Vascul. Pharmacol*. 46, 286–292. doi: 10.1016/j.vph.2006.11.002

Kapadia, P., Bikkina, P., Landicho, M. A., Parekh, S., Haas, M. J., and Mooradian, A. D. (2021). Effect of anti-hyperglycemic drugs on endoplasmic reticulum (ER) stress in human coronary artery endothelial cells. *Eur. J. Pharmacol*. 907:174249. doi: 10.1016/j.ejphar.2021.174249

Koizumi, Y., Ito, T., Mizutari, K., and Kakehata, S. (2020). Regenerative effect of a rock inhibitor, Y-27632, on excitotoxic trauma in an organotypic culture of the cochlea. *Front. Cell Neurosci*. 14:572434. doi: 10.3389/fncel.2020.572434

Kozuki, M., Kurata, T., Miyazaki, K., Morimoto, N., Ohta, Y., Ikeda, Y., et al. (2011). Atorvastatin and pitavastatin protect cerebellar Purkinje cells in AD model mice and preserve the cytokines MCP-1 and TNF-α. *Brain Res*. 1388, 32–38. doi: 10.1016/j.brainres.2011.03.024

Kros, C. J., and Steyger, P. S. (2019). Aminoglycoside- and cisplatin-induced ototoxicity: Mechanisms and otoprotective strategies. *Cold Spring Harb. Perspect. Med*. 9:a033548. doi: 10.1101/cshperspect.a033548

Kurata, T., Miyazaki, K., Kozuki, M., Morimoto, N., Ohta, Y., Ikeda, Y., et al. (2011a). Progressive neurovascular disturbances in the cerebral cortex of Alzheimer's disease-model mice: protection by atorvastatin and pitavastatin. *Neuroscience* 197, 358–368. doi: 10.1016/j.neuroscience.2011.09.030

Kurata, T., Miyazaki, K., Kozuki, M., Panin, V. L., Morimoto, N., Ohta, Y., et al. (2011b). Atorvastatin and pitavastatin improve cognitive function and reduce senile plaque and phosphorylated tau in aged APP mice. *Brain Res*. 1371, 161–170. doi: 10.1016/j.brainres.2010.11.067

Li, M., and Liu, X. (2022). Pitavastatin maintains MAPK7 expression and alleviates angiotensin II-induced vascular endothelial cell inflammation and injury. *Exp. Ther. Med*. 23:132. doi: 10.3892/etm.2021.11055

Lu, M., Lawrence, D. A., Marsters, S., Acosta-Alvear, D., Kimmig, P., Mendez, A. S., et al. (2014). Opposing unfolded-protein-response signals converge on death receptor 5 to control apoptosis. *Science* 345, 98–101. doi: 10.1126/science.1254312

Mazel-Sanchez, B., Iwaszkiewicz, J., Bonifacio, J. P. P., Silva, F., Niu, C., Strohmeier, S., et al. (2021). Influenza A viruses balance ER stress with host protein synthesis shutoff. *Proc. Natl. Acad. Sci. U. S. A*. 118:e2024681118. doi: 10.1073/pnas.2024681118

Oakes, S. A., and Papa, F. R. (2015). The role of endoplasmic reticulum stress in human pathology. *Annu. Rev. Pathol*. 10, 173–194. doi: 10.1146/annurev-pathol-012513-104649

Oesterle, A., Laufs, U., and Liao, J. K. (2017). Pleiotropic effects of statins on the cardiovascular system. *Circ. Res*. 120, 229–243. doi: 10.1161/CIRCRESAHA.116.308537

Park, J. S., Kim, S. W., Park, K., Choung, Y. H., Jou, I., and Park, S. M. (2012). Pravastatin attenuates noise-induced cochlear injury in mice. *Neuroscience* 208, 123–132. doi: 10.1016/j.neuroscience.2012.02.010

Radwan, E., Bakr, M. H., Taha, S., Sayed, S. A., Farrag, A. A., and Ali, M. (2020). Inhibition of endoplasmic reticulum stress ameliorates cardiovascular injury in a rat model of metabolic syndrome. *J. Mol. Cell Cardiol*. 143, 15–25. doi: 10.1016/j.yjmcc.2020.04.020

Sanz-Cuesta, B. E., and Saver, J. L. (2021). Lipid-Lowering therapy and hemorrhagic stroke risk: Comparative meta-analysis of statins and PCSK9 inhibitors. *Stroke* 52, 3142–3150. doi: 10.1161/STROKEAHA.121.034576

So, J. S. (2018). Roles of endoplasmic reticulum stress in immune responses. *Mol. Cells* 41, 705–716. doi: 10.14348/molcells.2018.0241

Stepanyan, R. S., Indzhykulian, A. A., Vélez-Ortega, A. C., Boger, E. T., Steyger, P. S., Friedman, T. B., et al. (2011). TRPA1-mediated accumulation of aminoglycosides in mouse cochlear outer hair cells. *J. Assoc. Res. Otolaryngol*. 12, 729–740. doi: 10.1007/s10162-011-0288-x

Urra, H., Dufey, E., Avril, T., Chevet, E., and Hetz, C. (2016). Endoplasmic reticulum stress and the hallmarks of cancer. *Trends Cancer* 2, 252–262.

Verfaillie, T., Garg, A. D., and Agostinis, P. (2013). Targeting ER stress induced apoptosis and inflammation in cancer. *Cancer Lett*. 332, 249–264. doi: 10.1016/j.canlet.2010.07.016

Walter, P., and Ron, D. (2011). The unfolded protein response: from stress pathway to homeostatic regulation. *Science* 334, 1081–1086. doi: 10.1126/science.1209038

Wang, M., and Kaufman, R. J. (2016). Protein misfolding in the endoplasmic reticulum as a conduit to human disease. *Nature* 529, 326–335. doi: 10.1038/nature17041

Wang, X., Liu, K., Gong, H., Li, D., Chu, W., Zhao, D., et al. (2021). Death by histone deacetylase inhibitor quisinostat in tongue squamous cell carcinoma via apoptosis, pyroptosis, and ferroptosis. *Toxicol. Appl. Pharmacol*. 410:115363. doi: 10.1016/j.taap.2020.115363

Whitlon, D. S. (2022). Statins and hearing. *Hear. Res*. 424:108453. doi: 10.1016/j.heares.2022.108453

Wu, P., Wu, X., Zhang, C., Chen, X., Huang, Y., and Li, H. (2021). Hair cell protection from ototoxic drugs. *Neural. Plast*. 2021:4909237. doi: 10.1155/2021/4909237

Zhanel, G. G., Lawson, C. D., Zelenitsky, S., Findlay, B., Schweizer, F., Adam, H., et al. (2012). Comparison of the next-generation aminoglycoside plazomicin to gentamicin, tobramycin and amikacin. *Expert Rev. Anti Infect. Ther*. 10, 459–473. doi: 10.1586/eri.12.25

frontiers | Frontiers in Neuroscience

TYPE Systematic Review
PUBLISHED 19 August 2022
DOI 10.3389/fnins.2022.977323

OPEN ACCESS

EDITED BY
Zuhong He,
Wuhan University, China

REVIEWED BY
Pedro L. Mangabeira-Albernaz,
Hospital Israelita Albert Einstein, Brazil
Xiaofei Li,
Shandong Provincial ENT Hospital, China

*CORRESPONDENCE
Meng Wei
mengw@njtrh.org
He Shuangba
hesb@njtrh.org

†These authors share first authorship

SPECIALTY SECTION
This article was submitted to Auditory Cognitive Neuroscience, a section of the journal Frontiers in Neuroscience

RECEIVED 24 June 2022
ACCEPTED 28 July 2022
PUBLISHED 19 August 2022

CITATION
Fei S, Guangfei L, Jie M, Yiling G, Mingjing C, Qingxiang Z, Wei M and Shuangba H (2022) Development of semicircular canal occlusion. *Front. Neurosci.* 16:977323. doi: 10.3389/fnins.2022.977323

Development of semicircular canal occlusion

Su Fei[1†], Li Guangfei[1†], Meng Jie[1†], Gao Yiling[2], Cai Mingjing[1], Zhang Qingxiang[1], Meng Wei[1*] and He Shuangba[1*]

[1]Department of Otorhinolaryngology Head and Neck Surgery, School of Medicine, Nanjing Tongren Hospital, Southeast University, Nanjing, China, [2]Department of Pharmacy, School of Medicine, Nanjing Tongren Hospital, Southeast University, Nanjing, China

Surgical treatment of vertigo is performed with in-depth study of inner ear diseases. Achieving an effective control of vertigo symptoms while reducing damage to hearing and reducing surgical complications is the principle followed by scholars studying surgical modalities. Semicircular canal occlusion is aimed at treatment of partial peripheral vertigo disease and has attracted the attention of scholars because of the above advantages. This article provides a review of the origins of semicircular canal occlusion, related basic research, clinical applications, and the effects of surgery on vestibular and hearing function.

KEYWORDS

benign paroxysmal positional vertigo, Meniere's disease, labyrinthine fistula, semicircular canal occlusion, superior semicircular canal dehiscence syndrome

Introduction

Vertigo is a challenging and common disease entity. For a long time, no advancement in the diagnosis and treatment has been observed, and guidelines for treatment and diagnosis are not standardized, leading to inaccuracies. Medical treatment is often administered as a symptomatic treatment of vertebrobasilar insufficiency in clinics. In recent years, research on vertigo has made an important breakthrough, which has become the focus of multi-disciplinary attention. Presently, the direction of development of diagnosis and treatment technology is standardized and specialized. This is manifested in the diagnosis, treatment, daily management, and rehabilitation of vertigo. Clinicians pay close attention to the surgical treatment of especially some vertigo disorders.

Through the study of an animal model and the evaluation of postoperative effect of a large number of clinical cases, indications, perioperative treatment, surgery matters needing attention, postoperative vestibular rehabilitation, and follow-up of semicircular canal occlusion have gradually been standardized. The postoperative effect is also gradually emerging. This paper summarizes relevant studies by experts to facilitate clinical application.

Origin of semicircular canal occlusion

Semicircular canal occlusion was first initiated by Parnes and McClure (1990) in 1990 to treat benign paroxysmal positional vertigo (BPPV). The first routine treatment for vertigo is comprehensive drug therapy, with the main purpose of regulating autonomic nerve function and improving inner ear microcirculation. However, for recurrent and increasing intractable vertigo, clinicians consider surgical intervention, with unilateral semicircular canal occlusion becoming a research hotspot due to the decreased risk of trauma and good hearing protection; furthermore, the curative effect has been affirmed.

Minor et al. (1998) and Minor (2000) first reported findings related to symptomatic superior semicircular canal fistula in 1998. Five cases of surgical treatment *via* the middle cranial fossa approach through packing or surface covering the semicircular canal fistula have been reported. Brantberg et al. (2001) promoted filling of the superior semicircular canal through the mastoid approach to avoid the complications of craniotomy and temporal lobe injury. However, the transmastoid superior semicircular canal occlusion was widely criticized when it was first used because semicircular canal fistula is not fully demonstrated, and labyrinthine opening can easily lead to sensorineural hearing loss, tinnitus, and postoperative vertigo. In addition, the material and technology of semicircular canal occlusion also limited the application of this technology.

However, a number of subsequent studies have confirmed that in the case of BPPV or superior semicircular canal fistula, transmastoid semicircular canal occlusion can effectively relieve vertigo and preserve hearing. Thereafter, some scholars explored the application of triple semicircular canal occlusion (TSCO) in the treatment of Meniere's disease. Gentine et al. (2008) reported that 11 patients with Meniere's disease were treated with horizontal semicircular canal occlusion, and nine cases of vertigo were controlled. Yin et al. (2008) reported that TSCO was used to treat three patients with recurrent vertigo after endolymphatic sac decompression or drainage. Vertigo was controlled effectively.

Basic research on semicircular canal occlusion

The animal model of semicircular canal occlusion has been used to study vestibular function compensation. Unilateral labyrinthectomy in albino rats and TSCO in guinea pigs are recognized as vestibular compensatory animal models. As the largest vestibular nucleus, some electrophysiological data show that the medial vestibular nucleus may be one of the important areas of vestibular nerve compensation after semicircular canal occlusion. One study (Zhang et al., 2015) used guinea pigs to establish a model for unilateral horizontal semicircular canal occlusion to simulate the clinical semicircular canal occlusion operation. Then, the level of serotonin in medial vestibular nucleus was monitored by *in vivo* microdialysis combined with high- performance liquid chromatography and electrochemical detection. It was found that unilateral horizontal semicircular canal occlusion could increase the level of serotonin in the medial vestibular nucleus. It is suggested that serotonin and central compensation may play an important role in the compensatory process of residual vestibular function. Concurrently, the animal model of vestibular compensation with unilateral horizontal semicircular canal was successfully established.

Yin et al. (2006) verified the effectiveness and safety of TSCO in the ear with endolymphatic hydrops. They used the endolymphatic sac closure method to establish endolymphatic hydrops model in 20 guinea pigs. Among them, 12 animals underwent TSCO 120 days after operation, and eight were sacrificed for morphological observation to determine the existence of an endolymphatic fluid. The auditory and vestibular functions of the subjects were detected prior to the occurrence of endolymphatic hydrops to 1 month after TSCO, and the success of endolymphatic hydrops and semicircular canal occlusion was confirmed by morphological observation. Finally, it was concluded that TSCO effectively eliminated the response of semicircular canals to rotation and caloric test. It was safe in the ear with endolymphatic hydrops, and simultaneously, the static compensation for imbalance was fast and complete. It was suggested that TSCO was also an effective method to control rotational vertigo in ears with endolymphatic hydrops.

Application of semicircular canal occlusion in treatment of BPPV

BPPV, also known as otolithic vertigo, is an idiopathic paroxysmal vestibular organ disease with nystagmus and transient paroxysmal vertigo caused by head position change. It is self-limited and the most common form of peripheral vestibular vertigo (Bhattacharyya et al., 2017). Adler (1897) first described this disease in 1897. In 1921, Bárány (1920) reported a patient with sudden vertigo nystagmus in the right recumbent position. The symptoms disappeared after 30 s. Barany believes that this phenomenon is caused by damage to otolith. In 1952, Dix and Hallpike (1952) introduced the term BPPV, expounded the disease systematically, and put forward the gold standard Dix-Hallpike test for the diagnosis of the disease. With the deepening of scholars' understanding of the disease, different treatments have emerged. Treatment methods are otolith manual reduction, otolith machine reduction, vestibular rehabilitation training, and surgery. Among them, for patients with refractory BPPV after manual reduction, surgical treatment can be used.

Currently, surgical treatment for BPPV mainly includes posterior ampullary neurotomy and semicircular canal occlusion (Zhang and Fan, 2014; Kalmanson et al., 2021). The former was first proposed by Gacek (1974) and Gacek (1984) to treat BPPV by cutting off the posterior ampullary nerve that innervates the posterior semicircular canal. The operation may lead to serious complications such as sensorineural deafness, cerebrospinal fluid leakage, and facial paralysis. Posterior semicircular canal occlusion was first proposed by Parnes and McClure (1990). Its purpose is to make the crest physiologically fixed by closing the liquid space between the crest top and the site of obstruction. Presently, a posterior semicircular canal occlusion is most widely used in the treatment of BPPV, and its curative effect has been affirmed.

Walsh et al. (1999) performed posterior semicircular canal occlusion in 13 patients with refractory BPPV, with special emphasis on their long-term follow-up. The mean follow-up was 66 months (range, 29–119 months). All patients reported complete and immediate resolution of their positional vertigo, which has been maintained in the long term. Most patients, however, reported some postoperative transient unsteadiness which lasted up to 4 weeks. All patients developed a transient mild conductive hearing loss postoperatively, which usually resolved within 4 weeks. Five patients developed a transient mild sensorineural hearing loss at high frequency which resolved in all cases within 6 months. There were no reports of sensorineural hearing loss nor tinnitus in the long term. Parnes (1996) reported that positional vertigo was completely relieved after posterior semicircular canal occlusion, and most patients had temporary mixed hearing loss after surgery, and their hearing later returned to the preoperative level. The efficacy of this surgical method in the treatment of refractory BPPV has been affirmed; temporary vertigo or hearing loss may occur after surgery and gradually disappear after surgery (Uetsuka et al., 2012).

Application of semicircular canal occlusion in the treatment of Meniere's disease

Meniere's disease is a clinical condition defined by spontaneous vertigo attacks (each lasting 20 min to 12 h) with documented low to midfrequency sensorineural hearing loss in the affected ear before, during or after one of the episodes of vertigo. It also presents with fluctuating aural symptoms (hearing loss, tinnitus, or ear fullness) in the affected ear (Basura et al., 2020). Its incidence varies from 3.5 to 513 per 100,000 persons (Zhang et al., 2019) and is most common between the ages of 40 and 60 years (Basura et al., 2020).

Although Meniere's disease is caused by a variety of factors, such as microcirculatory disorders, viral infections, allergies, autoimmune reactions, and genetic factors, most scholars believe that the pathological basis of Meniere's disease is that when the inner ear endolymph accumulates, vertigo occurs when the potassium-rich endolymph leaks into sodium-rich perilymph. In 1938, Hallpike and Cairns (1938) confirmed the role of endolymphatic hydrops in Meniere's disease through the study of animal models. Although there is currently no cure, more than 85% of patients with Meniere's disease are helped by either changes in lifestyle and medical treatment, or minimally invasive surgical procedures such as intratympanic steroid therapy, intratympanic gentamicin therapy, and endolymphatic sac surgery (Sajjadi and Paparella, 2008). In addition, the surgical treatment of Meniere's disease is a research hotspot in recent years.

The surgical treatment of Meniere's disease has a history of more than 100 years, with Frazier first transecting the eighth cerebral nerve through the posterior fossa approach to treat Meniere's disease in 1908. The traditional surgical treatment of Meniere's disease mainly includes endolymphatic sac surgery, vestibular neurotomy, and labyrinthectomy. In recent years, progress has been made in the surgical treatment of Meniere's disease, such as the application of semicircular canal occlusion, development of endolymphatic aqueduct obstruction, clinical application of vestibular implantation, and application of cochlear implant with labyrinthine surgery (Cowan et al., 2020).

Surgical treatment includes endolymphatic sac surgery, TSCO, vestibular neurotomy, and labyrinthectomy, etc (Editorial Board of Chinese Journal of Otorhinolaryngology Head Neck Surgery; Society of Otorhinolaryngology Head Neck Surgery Chinese Medical Association, 2017). The indications are patients with frequent and severe vertigo and ineffective conservative treatment for more than 6 months. And the semicircular canal occlusion is a new surgical treatment. The short-term control rate of vertigo was 100% and the long-term control rate was 95%. It is an ideal surgical treatment, with a very small number of patients having their hearing affected (Jiang et al., 2022). In the Editorial Board of Chinese Journal of Otorhinolaryngology Head Neck Surgery; Society of Otorhinolaryngology Head Neck Surgery Chinese Medical Association (2017), patients with Meniere's disease are divided into four stages, and patients whose hearing level is worse than 70dB are Classified into forth stage. The guideline alse suggests that semicircular canal occlusion is applicable to patients diagnosed stage IV Meniere's disease. Hence, patients with hearing loss above 70 dB should be selected (Editorial Board of Chinese Journal of Otorhinolaryngology Head Neck Surgery; Society of Otorhinolaryngology Head Neck Surgery Chinese Medical Association, 2017), and triple semicircular canals should be blocked concurrently, with the aim to block the movement of lymph in the semicircular canal so as to eliminate vertigo caused by postural changes.

Zhang et al. (2016) conducted semicircular canal occlusion in more than 200 patients with Meniere's disease. The efficacy of semicircular canal occlusion in the treatment of Meniere's disease was studied. The vertigo control rate at short-term

follow-up was 100%: 49 patients were followed up for more than 3 years, the total effective rate of vertigo control was 100%, and about 30% of the patients had hearing loss. This shows that semicircular canal occlusion is effective in the treatment of intractable Meniere's disease. The principle is that after the semicircular canal is blocked, the endolymphatic flow is blocked and the rotational vertigo caused by the displacement of the ampullary crest is eliminated. Although the application of this procedure is limited in some patients with a low cranial plate or mastoid sclerosis, semicircular canal occlusion may still be the first choice for most patients with intractable Meniere's disease (with severe hearing loss).

TABLE 1 Fistula staging.

Stage I: Pre-fistula (blue line)
Stage II: Small fistula 2 mm
Stage III: Fistula 2–4 mm
Stage IV: Invasion of one (a) or more (b) semicircular canal/s
Stage V:
(a) Invasion of the vestibule
(b) Invasion of the vestibule and cochlea
Stage VI:
(a) Fistula limited to the stapes footplate
(b) Promontorial fistula

Application of semicircular canal occlusion in treatment of labyrinthine fistula caused by middle ear cholesteatoma

Labyrinthine fistula is a complication of otitis media, with a reported incidence ranging from 4 to 15% (Ostri and Bak-Pedersen, 1989; Dornhoffer and Milewski, 1995; Copeland and Buchman, 2003; Stephenson and Saliba, 2011; Prasad et al., 2013). It is mostly caused by cholesteatoma invading the labyrinthine bone and can also be observed in ulcerative otitis media and mastoiditis, occasionally after middle ear mastoid surgery or trauma. Due to the damage of the bone wall connected to the cochlea, the endosteum is in direct contact with the cholesteatoma and causes damage to the endosteum and results in perilymph overflowing to the mastoid cavity of the middle ear; labyrinthine fistula can not only cause vertigo (Villari et al., 2021), but also lead to sensorineural hearing loss (Jang and Merchant, 1997). Fistula often occurs in the horizontal semicircular canal and can also be seen in the superior semicircular canal, posterior semicircular canal, and promontory (Bo et al., 2016). The mechanisms leading to bone wall destruction include: (1) localized osteitis caused by chronic infection; (2) non-inflammatory osteolysis mainly caused by cholesteatoma compression and chemicals such as collagenase produced by cholesteatoma matrix. Except for bone resorption, there are common pathological changes, such as fibrous tissue hyperplasia and new bone formation in the fistula (Ostri and Bak-Pedersen, 1989).

At present, there are many classification criteria for labyrinthine fistula, including Dornhofer's (1995) fistula, which are widely used at present and can be divided into three types (Dornhoffer and Milewski, 1995):

Type I: The labyrinthine bone is absorbed but the membranous labyrinth is intact.

Type II: The bone labyrinth and membranous labyrinth are destroyed at the same time to form a fistula, and the depth of the fistula is $<1 \times 2$ of the semicircular canal diameter.

Type III: The bone labyrinth and membranous labyrinth are destroyed at the same time to form a fistula. The depth is $>1 \times 2$ of the semicircular canal diameter until amputation.

Quaranta et al. (2009) provides the latest classification, in which labyrinthine fistula can be divided into six stages according to CT and intraoperative findings.

The staging system considers the size and depth of the fistula (Prasad et al., 2013) (see Table 1).

A labyrinthine fistula is usually difficult to diagnose preoperatively. Fistula test and CT of the temporal bone are commonly used to diagnose labyrinthine fistula, but they are not reliable when the test result is negative, and the most reliable method requires careful exploration during surgery. Simultaneously, with the development of diagnostic technology, HIT and semicircular canal multi-planar reconstruction (s-MPR) can be used appropriately to increase the positive rate of preoperative diagnosis. Indeed, the findings of intraoperative exploration is an important basis for diagnosis (D'Albora et al., 2017).

Yamauchi et al. (2014) first reported in 2014 the "underwater" endoscopic labyrinthine fistula closure technique. Thangavelu et al. (2022) reported the effect of "underwater technology" on postoperative hearing in patients with cholesteatoma complicated with labyrinthine fistula. The "underwater technique" for the removal of cholesteatoma in labyrinthine surgery is a feasible choice to maintain the function of the inner ear and promote the complete removal of cholesteatoma. There is no significant difference in bone conduction threshold before and after the operation. Sensory improvement in 20% of patients was more than 10 dB, and no patients had worsened postoperative sensorineural hearing loss. Some patients had temporary vertigo after the operation, but they eventually recovered. Pace et al. (2022) reported that the hearing of patients with cholesteatoma can be preserved using the "underwater technique" for labyrinthine fistula. Therefore,

for patients with destruction of bone labyrinth and membranous labyrinth, it is safe to use the appropriate fascia packing method during operation. Moreover, the operative method is simple, easy, and time-efficient; has fewer complications, and there is no obvious interference to hearing; thus, it is widely applied clinically. Labyrinthine fistula is a common complication of middle ear cholesteatoma; thus, the possibility of labyrinthine fistula should be greatly considered. During the operation, the fistula area should be completely removed and repaired to prevent the disease from worsening (Gersdorff et al., 2000).

Application of semicircular canal occlusion in treatment of superior semicircular canal dehiscence syndrome

Superior semicircular canal dehiscence syndrome (SCDS) is a vestibular disorder caused by a pathologic third window into the labyrinth, resulted from a bone defect above the superior semicircular canal, which leads to a series of auditory and vestibular function syndromes (Steenerson et al., 2020). Its typical clinical manifestations are vertigo and auditory hypersensitivity caused by strong sound stimulation.

In 1998, Minor et al. (1998) first reported eight cases of SCDS, and since then, many cases of SCDS have been reported (Steenerson et al., 2020; de Wolf et al., 2021; Kontorinis and Gaggini, 2021; Nieto et al., 2021; Ellsperman et al., 2022). The incidence of SCDS is low and its pathogenesis is unknown, and it may be related to head trauma, infection, and pathological changes in the middle ear or adjacent structures (Rosowski et al., 2004; Ward et al., 2017; Mau et al., 2018). Its diagnosis needs to involve clinical manifestations, auditory function examination, vestibular function examination, and imaging examination.

The surgical treatment of SCDS includes the management of the superior semicircular canal and round window, and the operation related to the superior semicircular canal is performed earlier and is more mature. There are relatively few reports of round window surgery, which is a new surgical method, and its long-term effects remain to be observed. Surgical approaches include the middle cranial fossa approach, mastoid approach, external auditory canal approach, and endoscope-assisted surgical approach (Creighton Jr et al., 2021). The above surgical method needs to be realized by different surgical approaches, among which the middle cranial fossa approach and mastoid approach are reported more frequently, the postoperative results are stable, and each has its own advantages (Gersdorff et al., 2022). The external auditory canal approach is often combined with round window surgery, which has the advantage of less trauma. And the modified middle cranial fossa approach combined with ear endoscopy avoids the greater trauma caused by the traditional middle fossa craniotomy and the disadvantage of being unable to observe the dehiscence directly (Tugrul et al., 2022).

Management of superior semicircular canal includes occlusion, capping, and covering. Occlusion of the superior semicircular canal is the most frequently reported operation, which can be achieved by the middle cranial fossa approach and mastoid approach (Allsopp et al., 2020), and there is no difference in the postoperative effect. Semicircular canal occlusion was first reported by Minor et al. (1998). The surgical procedure mainly includes enlarging the dehiscence and filling the lumen of the superior semicircular canal with fascia, bone cement, and other materials. Resurfacing covers the dehiscence of the superior semicircular canal with autogenous tissues such as cartilage and fascia without blocking the superior semicircular canal. Capping is an improvement to the covering technique and uses hydroxyapatite cement instead of its own tissue to cover the dehiscence of the superior semicircular canal; hence, there is no risk of absorption and migration. The success rate of capping is similar to that of occlusion, and it is advantageous in that it cures the Tullio phenomenon and hyperacusis (Vlastarakos et al., 2009; Kaski et al., 2012; Mueller et al., 2014; Smith et al., 2022).

According to the summary of clinical cases, in the superior semicircular canal-related surgery, the postoperative effect of occlusion has been affirmed by scholars worldwide (Hassannia et al., 2019), and the postoperative effects of other surgical methods are still controversial. Superior semicircular canal occlusion is an ideal surgical method for the treatment of superior semicircular canal dehiscence syndrome with a low incidence of complications.

Effect of semicircular canal occlusion on hearing and vestibular function

The preservation of cochlear function after semicircular canal occlusion is key to its popularization and application (Lin et al., 2021), and experimental studies and clinical applications show that there is a separation system between the superior labyrinth (vestibular labyrinth) and inferior labyrinth (auditory labyrinth), i.e., the membrana limitans and utricle-endolymphatic valve (Smith et al., 2022). The vestibular labyrinth is comprised of the semicircular canals (detecting angular acceleration) and otolith organs (utricle and saccule, which detect linear acceleration and head tilt relative to gravity). Lying just inferior to the utricle is the membranous membrana limitans (ML). Acting as a keystone to vestibular geometry, the ML provides support for the utricular macula and acts as a structural boundary between the superior (pars superior) and inferior (pars inferior) portions of the vestibular labyrinth. The utricle-endolymphatic valve is a living valve-like structure located at the entrance of the utricle in the anterior and

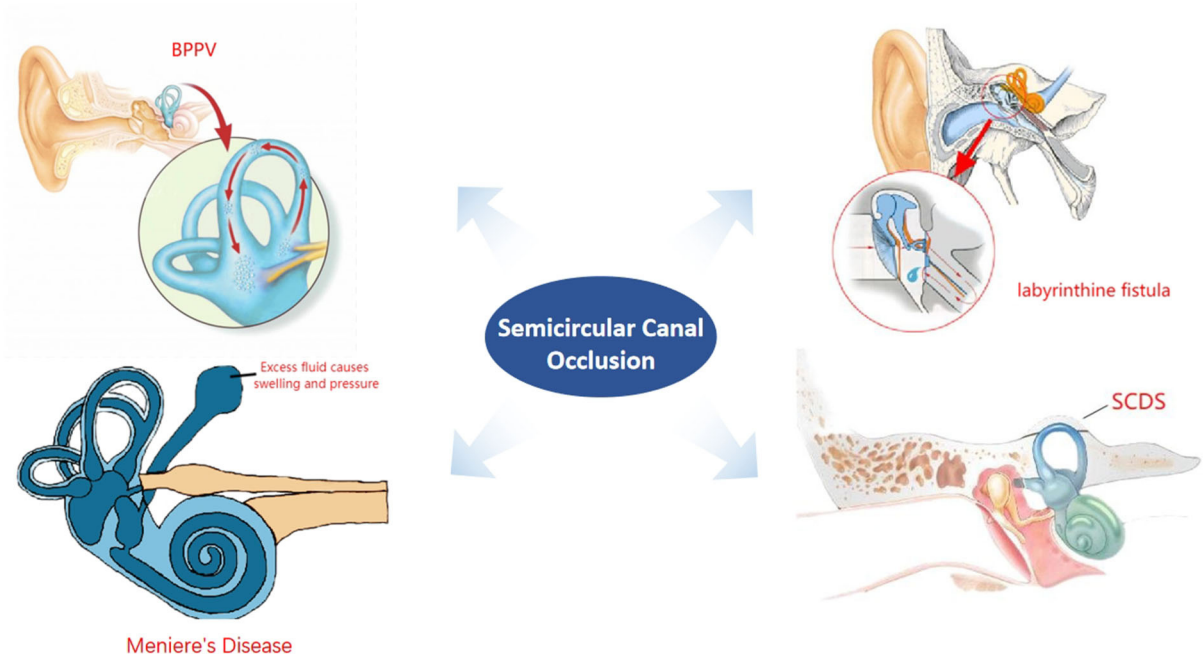

FIGURE 1
Development of semicircular canal occlusion.

inferior walls of the utricle. It is passively closed when the lymphatic pressure in the upper and lower labyrinth changes, which can prevent excessive endolymphatic loss caused by secondary labyrinthine destruction. The relative independence of the internal and external lymphatic system between the superior and inferior labyrinth provides an anatomical basis for semicircular canal occlusion to preserve hearing. In addition, the collapse and adhesion of the membranous semicircular canal caused by inflammation separate the fistula from the adjacent tissue and limit the spread of inflammation to the downward labyrinth. Animal experiments and clinical observations showed that single and multiple semicircular canal occlusion did not affect the function of the cochlea and other vestibular terminal organs other than the blocked semicircular canal.

Stultiens et al. (2021) performed vestibular function examination and hearing test before superior semicircular canal or posterior semicircular canal filling and 1 week, 2 months, and 6 months after the operation. Testing included caloric irrigation test, video Head Impulse Test (vHIT), cervical and ocular Vestibular Evoked Myogenic Potentials (VEMPs) and audiometry. Concurrently, the following oculomotor muscle movement tests were performed to rule out central lesions: smooth pursuit, saccade, optokinetic nystagmus, spontaneous nystagmus, and gaze evoked nystagmus. The results showed that the ipsilateral caloric test decreased in all patients, and the vHIT vestibulo-ocular refexes (VOR) gain decreased in six patients with unilateral semicircular canal. Six months after the operation, the thermal response of six patients recovered to 60% of the preoperative value. The bilateral unblocked semicircular canal vHIT VOR of five of six patients returned to 85% of the preoperative value. Four VEMP reactions in the neck and eyes were preserved in six patients. The results of the hearing function test were similar to those of the vestibular function test; during the 1-week follow-up after the operation, the bone conduction hearing of three of six patients deteriorated, and the 10 dB was even lower than that before the operation. Although one patient sustained a 15- dB injury at 8 Hz, it recovered within 6 months after the operation, and the vestibular function and hearing of patients after semicircular canal occlusion decreased significantly in a short period of time after semicircular canal occlusion.

Yin et al. (2006) concluded that TSCO controls vertigo, is easy to perform, and could be used as an alternative procedure for the treatment of Meniere's disease in selected patients who complain mainly of intractable vertigo. Three patients with Meniere's disease who underwent unsuccessful endolymphatic sac decompression or mastoid shunt was then selected to undergo TSCO.Vertigo control and vestibular and auditory function were measured. The early vestibular symptoms caused by surgery resolved quickly and no hearing deterioration occurred after surgery.

Chen et al. (2010) investigated the safety and efficacy of semicircular canal occlusion for surgical treatment of labyrinthine fistula caused by cholesteatoma. Twenty-two

patients with labyrinthine fistula who were treated surgically were enrolled in the study. All patients were treated by completely removing the cholesteatoma matrix followed by semicircular canal occlusion. With a follow-up of at least 6 months, there was no recurrent cholesteatoma in any of the patients. Vertigo disappeared in all the patients. Most patients presented no hearing deteriorate and four of them demonstrated hearing improvement. No patient presented with surgery-related deafness postoperatively.

Although the vestibular function and hearing of most patients recovered continuously during the follow-up period (Gill et al., 2021; Zhang et al., 2021; Kontorinis and Thachil, 2022), some patients still had persistent impairment of their inner ear function. The limitation of this study is that there are few samples, and the changes of biomechanical properties of the inner ear may also include perilymph leakage and postoperative local inflammation caused by tissue injury. This study cannot rule out the influence of related factors. However, with further development of basic scientific research and clinical follow-up monitoring related to semicircular canal occlusion, related research on the effect of semicircular canal occlusion on vestibular function and hearing will be more accurate.

Summary

Semicircular canal occlusion is a surgical method that has been highlighted in recent years and has a good effect after surgical treatment of refractory BPPV, intractable Meniere's disease, superior semicircular canal dehiscence syndrome, and middle ear cholesteatoma complicated with labyrinthine fistula. The symptoms of postoperative vertigo can be effectively controlled, the postoperative hearing loss is less, and other serious complications are minimized. These advantages have been recognized by scholars. However, there are still some reports that the hearing of patients after semicircular canal occlusion deteriorates over time (see Figure 1).

The degree of recovery and duration of postoperative vertigo vary from patient to patient, and the exact cause of the decline in inner ear function after semicircular canal surgery is not completely clear; therefore, effective control of the influence of semicircular canal occlusion on vestibular and cochlear organs is an important direction for future research.

Data availability statement

The original contributions presented in the study are included in the article/supplementary material, further inquiries can be directed to the corresponding authors.

Author contributions

SF, HS, and MW contributed to study concept. LG contributed to critical revision of the literature. SF and MJ contributed to literature search and drafting of the article. GY contributed to revising english translation and some medical terminology. CM contributed to guiding the submission process. ZQ contributed to English grammar and writing modifications. MW contributed to critical revision. MW and HS contributed to research direction guidance. All authors contributed to the article and approved the submitted version.

Funding

This work was supported by the National Natural Science Foundation of China (No. 82171153), the Natural Science Foundation of Jiangsu Province (No. BK20211012), Nanjing Medical Science and Technique Development Foundation (No. QRX17033).

Conflict of interest

The authors declare that the research was conducted in the absence of any commercial or financial relationships that could be construed as a potential conflict of interest.

Publisher's note

All claims expressed in this article are solely those of the authors and do not necessarily represent those of their affiliated organizations, or those of the publisher, the editors and the reviewers. Any product that may be evaluated in this article, or claim that may be made by its manufacturer, is not guaranteed or endorsed by the publisher.

References

Adler. (1897). Ueber den einseitigen Drehschwindel". *Deutsche Zeitschrift für Nervenheilkunde* 11, 358–375. doi: 10.1007/BF01669801

Allsopp, T., Kim, A. H., Robbins, A. M., Page, J. C., and Dornhoffer, J. L. (2020). Quality of life outcomes after transmastoid plugging of superior semicircular canal dehiscence. *Am. J. Otolaryngol.* 41, 102287. doi: 10.1016/j.amjoto.2019.102287

Bárány, E. (1920). Diagnose yon Krankheitserscheinungen im Bereiche des Otolithenapparates. *Acta Oto-Laryngol.* 2, 434–437. doi: 10.3109/00016482009123103

Basura, G. J., Adams, M. E., Monfared, A., Schwartz, S. R., Antonelli, P. J., Burkard, R., et al. (2020). Clinical practice guideline: Ménière's disease. *Otolaryngol. Head Neck Surg.* 162 (2_suppl), S1–S55. doi: 10.1177/0194599820909439

Bhattacharyya, N., Gubbels, S. P., Schwartz, S. R., Edlow, J. A., El-Kashlan, H., Fife, T., et al. (2017). Clinical practice guideline: benign paroxysmal positional vertigo (Update). *Otolaryngol. Head Neck Surg.* 156 (3_suppl), S1–S47. doi: 10.1177/0194599816689667

Bo, Y., Yang, Y., Xiaodong, C., Xi, W., Keyong, T., Yu, Z., et al. (2016). A retrospective study on post-operative hearing of middle ear cholesteatoma patients with labyrinthine fistula. *Acta Otolaryngol.* 136, 8–11. doi: 10.3109/00016489.2015.1087650

Brantberg, K., Bergenius, J., Mendel, L., Witt, H., Tribukait, A., and Ygge, J. (2001). Symptoms, findings and treatment in patients with dehiscence of the superior semicircular canal. *Acta Otolaryngol.* 121, 68–75. doi: 10.1080/000164801300006308

Chen, Z., Dongzhen, W.u Y., Shi, H., Zhou, H., Wang, J., et al. (2010). Surgical treatment of labyrinthine fistula caused by cholesteatoma with semicircular canal occlusion. *Acta Otolaryngol.* 130, 75–78. doi: 10.3109/00016480902875083

Copeland, B. J., and Buchman, C. A. (2003). Management of labyrinthine fistulae in chronic ear surgery. *Am. J. Otolaryngol.* 24, 51–60. doi: 10.1053/ajot.2003.10

Cowan, B., Oska, S., Arianpour, K., Svider, P. F., Bojrab, D. 2nd, and Hong, R. S. (2020). A systematic review of cochlear implantation in temporal bone fractures and the significance of otic capsule involvement. *Otol. Neurotol.* 41, 1309–1315. doi: 10.1097/MAO.0000000000002779

Creighton Jr, F. X., Zhang, L., Ward, B., and Carey, J. P. (2021). Hearing outcomes for an underwater endoscopic technique for transmastoid repair of superior semicircular canal dehiscence. *Otol. Neurotol.* 42, e1691–e1697. doi: 10.1097/MAO.0000000000003238

D'Albora, R., Silveira, L., Carmona, S., and Perez-Fernandez, N. (2017). Diagnostic bedside vestibuloocular reflex evaluation in the setting of a false negative fistula test in cholesteatoma of the middle ear. *Case Rep. Otolaryngol.* 2017, 2919463. doi: 10.1155/2017/2919463

de Wolf, M. J. F., Dawe, N., Jervis, S., Kumar, R., Dalton, C. L., Lindley, K., et al. (2021). Transmastoid occlusion surgery for superior semicircular canal dehiscence syndrome improves patient-reported quality-of-life measures and corrects cVEMP thresholds and amplitudes. *Otol. Neurotol.* 42, 1534–1543. doi: 10.1097/MAO.0000000000003329

Dix, M. R., and Hallpike, C. S. (1952). The pathology symptomatology and diagnosis of certain common disorders of the vestibular system. *Proc. R. Soc. Med.* 45, 341–354. doi: 10.1177/003591575204500604

Dornhoffer, J. L., and Milewski, C. (1995). Management of the open labyrinth. *Otolaryngol. Head Neck Surg.* 112, 410–414. doi: 10.1016/S0194-5998(95)70275-X

Editorial Board of Chinese Journal of Otorhinolaryngology Head and Neck Surgery; Society of Otorhinolaryngology Head and Neck Surgery Chinese Medical Association (2017). Guideline of diagnosis and treatment of Meniere disease (2017). *Zhonghua Er Bi Yan Hou Tou Jing Wai Ke Za Zhi.* 52, 167–172. Chinese. doi: 10.3760/cma.j.issn.1673-0860.2017.03.002

Ellsperman, S. E., Telian, S. A., Kileny, P. R., and Welch, C. M. (2022). Intraoperative electrocochleography correlates to outcomes in transmastoid and middle cranial fossa superior semicircular canal dehiscence repair. *Otol. Neurotol.* 43, 120–127. doi: 10.1097/MAO.0000000000003350

Gacek, R. R. (1974). Transection of the posterior ampullary nerve for the relief of benign paroxysmal positional vertigo. *Ann. Otol. Rhinol. Laryngol.* 83, 596–605. doi: 10.1177/000348947408300504

Gacek, R. R. (1984). Cupulolithiasis and posterior ampullary nerve transection. *Ann. Otol. Rhinol. Laryngol. Suppl.* 112, 25–30. doi: 10.1177/00034894840930S405

Gentine, A., Martin, E., Schultz, P., Debry, C., and Charpiot, A. (2008). Lateral semicircular canal plugging: a simple and effective surgical treatment against incapacitating Menière's disease. *Rev. Laryngol. Otol. Rhinol. (Bord).* 129, 11–16. doi: 10.1001/archderm.1988.01670050120041

Gersdorff, G., Blaivie, C., de Foer, B., Deggouj, N., Wyckmans, F., and Somers, T. (2022). Evaluation of the transmastoid plugging approach for superior semicircular canal dehiscences: a retrospective series of 30 ears. *Eur. Arch. Otorhinolaryngol.* doi: 10.1007/s00405-022-07316-8. [Epub ahead of print].

Gersdorff, M. C., Nouwen, J., Decat, M., Degols, J. C., and Bosch, P. (2000). Labyrinthine fistula after cholesteatomatous chronic otitis media. *Am. J. Otol.* 21, 32–35. doi: 10.1016/S0196-0709(00)80072-1

Gill, C., Muzaffar, J., Kumar, R., and Irving, R. (2021).Triple Canal occlusion for the treatment of intractable Menière's disease. *Otol. Neurotol.* 42, 116–120. doi: 10.1097/MAO.0000000000002841

Hallpike, C. S., and Cairns, H. (1938). Observations on the pathology of Ménière's syndrome: (Section of Otology). *Proc. R. Soc. Med.* 31, 1317–1336. doi: 10.1177/003591573803101112

Hassannia, F., Douglas-Jones, P., and Rutka, J. A. (2019). Gauging the effectiveness of canal occlusion surgery: how I do it. *J. Laryngol. Otol.* 133, 1012–1016. doi: 10.1017/S0022215119002032

Jang, C. H., and Merchant, S. N. (1997). Histopathology of labyrinthine fistulae in chronic otitis media with clinical implications. *Am. J. Otol.* 18, 15–25.

Jiang, Y., Xu, M., Yao, Q., Li, Z., Wu, Y., Chen, Z., et al. (2022). Changes of vestibular symptoms in menière's disease after triple semicircular canal occlusion: a long-term follow-up study. *Front. Neurol.* 13, 797699. doi: 10.3389/fneur.2022.797699

Kalmanson, O. A., Aasen, D. M., Gubbels, S. P., and Foster, C. A. (2021). Reversible canalith jam of the horizontal semicircular canal mimicking cupulolithiasis. *Ann. Otol. Rhinol. Laryngol.* 130, 1213–1219. doi: 10.1177/00034894211007245

Kaski, D., Davies, R., Luxon, L., Bronstein, A. M., and Rudge, P. (2012). The Tullio phenomenon: a neurologically neglected presentation. *J. Neurol.* 259, 4–21. doi: 10.1007/s00415-011-6130-x

Kontorinis, G., and Gaggini, M. (2021). Transmastoid superior semicircular canal plugging: a prospective analysis of surgical outcomes. *Otol. Neurotol.* 42, 1216–1222. doi: 10.1097/MAO.0000000000003191

Kontorinis, G., and Thachil, G. (2022). Triple semicircular canal occlusion: a surgical perspective with short- and long-term outcomes. *J. Laryngol. Otol.* 136, 125–128. doi: 10.1017/S002221512100387X

Lin, K. F., Bojrab, D. I. 2nd, Fritz, C. G., Vandieren, A., and Babu, S. C. (2021). Hearing outcomes after surgical manipulation of the membranous labyrinth during superior semicircular canal dehiscence plugging or posterior semicircular canal occlusion. *Otol. Neurotol.* 42, 806–814. doi: 10.1097/MAO.0000000000003100

Mau, C., Kamal, N., Badeti, S., Reddy, R., Ying, Y. M., Jyung, R. W., et al. (2018). Superior semicircular canal dehiscence: diagnosis and management. *J. Clin. Neurosci.* 48, 58–65. doi: 10.1016/j.jocn.2017.11.019

Minor, L. B. (2000). Superior canal dehiscence syndrome. *Am. J. Otol.* 21, 9–19. doi: 10.1016/S0196-0709(00)80068-X

Minor, L. B., Solomon, D., Zinreich, J. S., and Zee, D. S. (1998). Sound- and/or pressure-induced vertigo due to bone dehiscence of the superior semicircular canal. *Arch. Otolaryngol. Head Neck Surg.* 124, 249–258. doi: 10.1001/archotol.124.3.249

Mueller, S. A., Vibert, D., Haeusler, R., Raabe, A., and Caversaccio, M. (2014). Surgical capping of superior semicircular canal dehiscence. *Eur. Arch. Otorhinolaryngol.* 271, 1369–1374. doi: 10.1007/s00405-013-2533-x

Nieto, P., Gallois, Y., and Marx, M. (2021). Concomitant treatment of superior semicircular canal and tegmen dehiscence by transmastoid approach (with video). *Eur. Ann. Otorhinolaryngol. Head Neck. Dis.* 138 (Suppl 3), 77–78. doi: 10.1016/j.anorl.2021.07.001

Ostri, B., and Bak-Pedersen, K. (1989). Surgical management of labyrinthine fistulae in chronic otitis media with cholesteatoma by a one-stage closed technique. *ORL J. Otorhinolaryngol. Relat. Spec.* 51, 295–299. doi: 10.1159/000276077

Pace, A., Milani, A., Messineo, D., Rossetti, V., Cocuzza, S., Maniaci, A., et al. (2022). Labyrinthine fistula in cholesteatoma patients: outcomes of partial labyrinthectomy with "Underwater Technique" to preserve hearing. *Front. Neurol.* 13, 804915. doi: 10.3389/fneur.2022.804915

Parnes, L. S. (1996). Update on posterior canal occlusion for benign paroxysmal positional vertigo. *Otolaryngol. Clin. North Am.* 29, 333–342. doi: 10.1016/S0030-6665(20)30396-0

Parnes, L. S., and McClure, J. A. (1990). Posterior semicircular canal occlusion for intractable benign paroxysmal positional vertigo. *Ann. Otol. Rhinol. Laryngol.* 99 (5 Pt 1), 330–334. doi: 10.1177/000348949009900502

Prasad, S. C., Shin, S. H., Russo, A., Di Trapani, G., and Sanna, M. (2013). Current trends in the management of the complications of chronic otitis media with cholesteatoma. *Curr. Opin. Otolaryngol. Head Neck Surg.* 21, 446–454. doi: 10.1097/MOO.0b013e3283646467

Quaranta, N., Liuzzi, C., Zizzi, S., Dicorato, A., and Quaranta, A. (2009). Surgical treatment of labyrinthine fistula in cholesteatoma surgery. *Otolaryngol. Head Neck Surg.* 140, 406–411. doi: 10.1016/j.otohns.2008.11.028

Rosowski, J. J., Songer, J. E., Nakajima, H. H., Brinsko, K. M., and Merchant, S. N. (2004). Clinical, experimental, and theoretical investigations of the effect of superior semicircular canal dehiscence on hearing mechanisms. *Otol. Neurotol.* 25, 323–332. doi: 10.1097/00129492-200405000-00021

Sajjadi, H., and Paparella, M. M. (2008). Meniere's disease. *Lancet.* 372, 406–414. doi: 10.1016/S0140-6736(08)61161-7

Smith, C. M., Curthoys, I. S., Mukherjee, P., Wong, C., and Laitman, J. T. (2022). Three-dimensional visualization of the human membranous labyrinth: The

membrana limitans and its role in vestibular form. *Anat. Rec. (Hoboken)* 305, 1037–1050. doi: 10.1002/ar.24675

Steenerson, K. K., Crane, B. T., and Minor, L. B. (2020). Superior Semicircular Canal Dehiscence Syndrome. *Semin. Neurol.* 40, 151–159. doi: 10.1055/s-0039-3402738

Stephenson, M. F., and Saliba, I. (2011). Prognostic indicators of hearing after complete resection of cholesteatoma causing a labyrinthine fistula. *Eur. Arch. Otorhinolaryngol.* 268, 1705–1711. doi: 10.1007/s00405-011-1545-7

Stultiens, J. J. A., Guinand, N., Van Rompaey, V., Pérez Fornos, A., Kunst, H. P. M., Kingma, H., et al. (2021). The resilience of the inner ear-vestibular and audiometric impact of transmastoid semicircular canal plugging. *J. Neurol.* doi: 10.1007/s00415-021-10693-5. [Epub ahead of print].

Thangavelu, K., Weiß, R., Mueller-Mazzotta, J., Schulze, M., Stuck, B. A., and Reimann, K. (2022). Post-operative hearing among patients with labyrinthine fistula as a complication of cholesteatoma using "under water technique". *Eur. Arch. Otorhinolaryngol.* 279, 3355–3362. doi: 10.1007/s00405-021-07058-z

Tugrul, S., Yenigun, A., Kulaksiz, Y., Dogan, R., Aksoy, F., and Ozturan, O. (2022). Superior semicircular canal dehiscence repair with small middle fossa craniotomy using an oto-microscopic and co-endoscopic assisted approach. *J. Laryngol. Otol.* 136, 559–561. doi: 10.1017/S0022215121004308

Uetsuka, S., Kitahara, T., Horii, A., Imai, T., Uno, A., Okazaki, S., et al. (2012). Transient low-tone air-bone gaps during convalescence immediately after canal plugging surgery for BPPV. *Auris Nasus Larynx*. 39, 356–360. doi: 10.1016/j.anl.2011.06.005

Villari, D., Federici, G., Russo, P., Manto, A. L., and Bonali, M. (2021). Transcanal endoscopic management of lateral semicircular canal fistula: preliminary experience. *Eur. Arch. Otorhinolaryngol.* 278, 5099–5103. doi: 10.1007/s00405-021-07095-8

Vlastarakos, P. V., Proikas, K., Tavoulari, E., Kikidis, D., Maragoudakis, P., and Nikolopoulos, T. P. (2009). Efficacy assessment and complications of surgical management for superior semicircular canal dehiscence: a meta-analysis of published interventional studies. *Eur. Arch. Otorhinolaryngol.* 266, 177–186. doi: 10.1007/s00405-008-0840-4

Walsh, R. M., Bath, A. P., Cullen, J. R., and Rutka, J. A. (1999). Long-term results of posterior semicircular canal occlusion for intractable benign paroxysmal positional vertigo. *Clin. Otolaryngol. Allied. Sci.* 24, 316–323. doi: 10.1046/j.1365-2273.1999.00266.x

Ward, B. K., Carey, J. P., and Minor, L. B. (2017). Superior canal dehiscence syndrome: lessons from the first 20 years. *Front. Neurol.* 8, 177. doi: 10.3389/fneur.2017.00177

Yamauchi, D., Yamazaki, M., Ohta, J., Kadowaki, S., Nomura, K., Hidaka, H., et al. (2014). Closure technique for labyrinthine fistula by "underwater" endoscopic ear surgery. *Laryngoscope* 124, 2616–2618. doi: 10.1002/lary.24785

Yin, S., Chen, Z., Yu, D., Wu, Y., Shi, H., Zhou, H., et al. (2008). Triple semicircular canal occlusion for the treatment of Ménière's disease. *Acta Otolaryngol.* 128, 739–743. doi: 10.1080/00016480701730000

Yin, S., Yu, D., Li, M., and Wang, J. (2006). Triple semicircular canal occlusion in guinea pigs with endolymphatic hydrops. *Otol. Neurotol.* 27, 78–85. doi: 10.1097/01.mao.0000170535.42023.96

Zhang, D., and Fan, Z. (2014). Surgical procedures of vertigo disease. *J Clin Otorhinolaryngol Head Neck Surg*. 28, 1-5. Chinese. doi: 10.13201/j.issn.1001-1781.2016.01.002

Zhang, D., Fan, Z., Han, Y., Lv, Y., Li, Y., and Wang, H. (2016). Various approaches in semicircular canal plugging for treatment of intractable Meniere's disease. *Chin. J Otol.* 14, 446–450. Chinese. doi: 10.3969/j.issn.1672-2922.2016.04.002

Zhang, D., Lv, Y., Han, Y., Sun, G., Li, Y., Li, X., et al. (2019). Revision surgery after triple semicircular canal plugging and morphologic changes of vestibular organ. *Sci Rep*. 9, 19397. doi: 10.1038/s41598-019-55810-7

Zhang, K., Li, Q., Xu, J., Liu, J., Ke, J., Kang, W., et al. (2015). Unilateral horizontal semicircular canal occlusion induces serotonin increase in medial vestibular nuclei: a study using microdialysis in vivo coupled with HPLC-ECD. *Analyst*. 140, 3846–3851. doi: 10.1039/C5AN00110B

Zhang, Y., Cheng, Y., Chen, Z., Chen, F., and Zhang, Q. (2021). Case report: preservation of otolithic function after triple semicircular canal occlusion in a patient with intractable Ménière disease. *Front. Neurol.* 12, 713275. doi: 10.3389/fneur.2021.713275

frontiers | Frontiers in Molecular Neuroscience

TYPE Review
PUBLISHED 15 September 2022
DOI 10.3389/fnmol.2022.976388

OPEN ACCESS

EDITED BY
Zuhong He,
Wuhan University, China

REVIEWED BY
Kai Xu,
Huazhong University of Science and Technology, China
Esperanza Bas Infante,
University of Miami, United States

*CORRESPONDENCE
Shule Hou
houshule8562@xinhuamed.com.cn
Jun Yang
yangjun@xinhuamed.com.cn

†These authors have contributed equally to this work

SPECIALTY SECTION
This article was submitted to Methods and Model Organisms, a section of the journal Frontiers in Molecular Neuroscience

RECEIVED 23 June 2022
ACCEPTED 11 August 2022
PUBLISHED 15 September 2022

CITATION
Chen P, Wu W, Zhang J, Chen J, Li Y, Sun L, Hou S and Yang J (2022) Pathological mechanisms of connexin26-related hearing loss: Potassium recycling, ATP-calcium signaling, or energy supply? *Front. Mol. Neurosci.* 15:976388. doi: 10.3389/fnmol.2022.976388

Pathological mechanisms of connexin26-related hearing loss: Potassium recycling, ATP-calcium signaling, or energy supply?

Penghui Chen[1,2,3†], Wenjin Wu[1,2,3†], Jifang Zhang[1,2,3†], Junmin Chen[1,2,3], Yue Li[1,2,3], Lianhua Sun[1,2,3], Shule Hou[1,2,3*] and Jun Yang[1,2,3*]

[1]Department of Otorhinolaryngology-Head and Neck Surgery, Xinhua Hospital, Shanghai Jiao Tong University School of Medicine, Shanghai, China, [2]Ear Institute, Shanghai Jiaotong University School of Medicine, Shanghai, China, [3]Shanghai Key Laboratory of Translational Medicine on Ear and Nose Diseases, Shanghai, China

Hereditary deafness is one of the most common human birth defects. *GJB2* gene mutation is the most genetic etiology. Gap junction protein 26 (connexin26, Cx26) encoded by the *GJB2* gene, which is responsible for intercellular substance transfer and signal communication, plays a critical role in hearing acquisition and maintenance. The auditory character of different Connexin26 transgenic mice models can be classified into two types: profound congenital deafness and late-onset progressive hearing loss. Recent studies demonstrated that there are pathological changes including endocochlear potential reduction, active cochlear amplification impairment, cochlear developmental disorders, and so on, in connexin26 deficiency mice. Here, this review summarizes three main hypotheses to explain pathological mechanisms of connexin26-related hearing loss: potassium recycling disruption, adenosine-triphosphate-calcium signaling propagation disruption, and energy supply dysfunction. Elucidating pathological mechanisms underlying connexin26-related hearing loss can help develop new protective and therapeutic strategies for this common deafness. It is worthy of further study on the detailed cellular and molecular upstream mechanisms to modify connexin (channel) function.

KEYWORDS

connexin, cochlea, gap junction, hearing loss, mechanism

Introduction

Up to now, 21 human genes and 20 mouse genes encoding connexin (Cx) have been identified, of which 19 are considered homologous pairs (Söhl and Willecke, 2003). All Cxs are considered to share the same topology, with cytoplasmic amino and carboxyl terminals, and four transmembrane domains are connected by two extracellular rings and one cytoplasmic ring (Beyer and Berthoud, 2018). In the cochlea, there are varieties of Cxs including Cx26, Cx29, Cx30, Cx31, Cx32, Cx43, and Cx45, which are named according to their molecular weight size (Lautermann et al., 1998; Ahmad et al., 2003; Buniello et al., 2004). Different connexins have distinct distribution and expression characteristics during the development of cochlea (Forge, 1984). Cx26 and Cx30 are the prevailing Cxs in the developing and mature rodent cochlea (Tsutsui et al., 1976; Kikuchi et al., 1995; Zhao and Yu, 2006). Six connexins can combine into one single junctional hemichannel, and two hemichannels between two adjacent cells form a gap junction (GJ) (Sáez and Leybaert, 2014). The GJ which is composed of the same connexin protein is known as homomeric gap junction, while the GJ which is composed of heteromeric connexin is also known as heterotrimeric gap junction (Kumar and Gilula, 1996). GJ channels and hemichannels generally allow the passage of ions (K+), some second messengers [adenosine-triphosphate (ATP) and inositol-1,4,5-trisphosphate (IP3)],(Niessen et al., 2000; Beltramello et al., 2005; Bedner et al., 2006; Hernandez et al., 2007) and metabolites (glycolytic intermediates, vitamins, amino acids, and nucleotides) (Zou et al., 2005; Chang et al., 2008; Kanaporis et al., 2008) of molecular weight less than 1.4 kDa molecular weight or diameter less than 1.5 nm (Leybaert et al., 2017). The hemichannel is mainly maintained in a closed state, and its opening and closing are mainly regulated by (1) extracellular Ca^{2+} and Mg^{2+} concentrations (Verselis and Srinivas, 2008; Bennett et al., 2016), (2) membrane potential (Verselis et al., 1994), and (3) post-translational modifications of proteins (e.g., phosphorylation) (Moreno, 2005; Aasen et al., 2018).

Mammalian cochlear inter-cellular connections are divided into two main cellular network systems, namely the epithelial gap junction system (E-sys) and the connective tissue gap junction system (C-sys) (Kikuchi et al., 1995). In mammals, the E-sys forms around embryo day 19 (E19) and is well developed by postnatal day5 (P5). E-sys is located in supporting cells around the organ of Corti, the bordering epithelial cells of the inner sulcus and outer sulcus, the interdental cells of the spiral limbus, and the root cells (Jagger and Forge, 2013) that extend their process into the spiral ligament. C-sys develops around P0 and is further divided into two systems, (1) fibrocytes of the spiral limbus; (2) fibroblasts, basal cells, and intermediate cells of the *stria vascularis* (SVs), fibroblasts of the suprastrial region, mesenchymal cells of the vestibular scala, and dark cells (Kikuchi et al., 2000).

The maintenance of normal function of the inner ear depends on the homeostasis of three fluid environments—the perilymph fluid (cerebrospinal fluid), the endolymphatic fluid, and the intracellular fluid. Furthermore, the maintenance of the fluid environment homeostasis depends on the cellular network system of substance exchange and signaling transmission which is formed by intercellular GJ channels and extracellular hemichannels.

Gap junction protein 26 (connexin26, Cx26) encodes by the *GJB2* gene. *GJB2* mutations cause about 50% of non-syndromic hearing loss. There are more than 340 mutations of *GJB2* (Mammano, 2019), including missense mutation, nonsense mutation, frameshift mutation, insertion mutation, deletion mutation, and so on. Most *GJB2* mutations cause recessive non-syndromic deafness (DFNB1A, OMIM: 220290). *GJB2* mutations affect the following: (1) the protein expression level (Thönnissen et al., 2002); (2) their transport to the plasma membrane; (3) their channel biological characteristics (voltage gated, chemical gated, and channel permeability) (Gerido et al., 2007).

Cx26 is the most common and harmful deafness gene. Cx26 is responsible for intercellular substance transfer and signal communication and plays a critical role in hearing acquisition and maintenance. Cx26 mutations can not only cause congenital deafness but also cause delayed deafness. The deafness mechanism caused by Cx26 mutation is not clear. Mouse models are widely used in hearing and deafness mechanism research (Leibovici et al., 2008). Benefit from the development of transgenic technologies such as the Cre-loxP system and the establishment of the Cx26 conditional knockout mouse model has promoted the study of the mechanism of Cx26 mutation deafness (Gridley and Murray, 2022). This paper reviews the research progress of congenital deafness and delayed deafness caused by Cx26 mutation in recent years and tries to find the underlying pathological mechanisms of connexin26-related hearing loss.

Mouse models of connexin 26 deficiency

Given the complex phenotype and mutation in Cx26-related hearing loss, it is difficult to explore the underlying pathogenesis mechanism. More and more Cx26 transgenic mice have been used to study pathogenesis mechanisms. We summarized and classified Cx26 transgenic mice into two major types based on the deafness phenotype: profound

congenital deafness model mice and late-onset progressive deafness model mice. Profound congenital deafness model mice include $Gjb2^{loxP/loxP}$; Otog-Cre, $Gjb2^{loxP/loxP}$; Sox10-Cre, $Gjb2^{loxP/loxP}$; Pax2-Cre, $Gjb2^{loxP/loxP}$; Foxg1-Cre, $Gjb2^{loxP/loxP}$; Rosa26-Cre, $Gjb2^{loxP/loxP}$; Prox1-CreERT2, and $Gjb2^{loxP/loxP}$; Rosa26cre-ER injected with tamoxifen at E19 or P1 (Sun et al., 2009; Wang et al., 2009; Chang et al., 2015). The common pathological changes of these mice are the failure of the opening of the tunnel of Corti at P6, serious hair cell loss from the middle turn after P14, and the secondary loss of spiral ganglion neurons (Cohen-Salmon et al., 2002; Sun et al., 2009; Wang et al., 2009). Obviously, in Cx26 deficiency mice, the sensory epithelial cell injury precedes hearing loss. The failure of the tunnel of Corti to open is a landmark event (Lin et al., 2013). Since the tunnel of Corti and Nuel's space are not developed, perilymph failed to infiltrate around the outer hair cell body, resulting in an effective K^+ potential difference (endocochlear potential, EP), and cochlear amplifier function fail to form (Wang et al., 2009). Researchers found that the reduction of microtubules in inner and outer column cells is likely the reason that the tunnel of Corti failed to open (Lin et al., 2013; Xie et al., 2019). Cx26 plays a crucial role in the early development of the cochlea. The developmental disorder of supporting cells may be the main mechanism of congenital profound deafness caused by Cx26 deficiency.

Cx26 model mice that present late-onset progressive deafness mainly include p.V37I homozygous mutant mice, $Cx26^{\pm}$ mice, and $Gjb2^{loxP/loxP}$; Rosa26cre ER mice which received injection with tamoxifen at P5, P8, and later (Zhu et al., 2015; Chen et al., 2016; Lin et al., 2019). All these mice acquire normal hearing function and show normal cochlear development without hair cell loss at P30 (Chang et al., 2015). However, with aging, progressive hearing loss first started only at high frequency and gradually extended to full frequencies (Chang et al., 2015; Xie et al., 2019). It is like the phenotype of DFNA3 or DFNB1. The common pathophysiological alterations of these model mice are the active cochlear amplification impairment which showed that distortion product otoacoustic emission (DPOAE) failed to evoke at an early stage (Chen et al., 2021). With aging, hair cells at the basal turn first start to damage and then gradually expand to the middle and apic turns (Fetoni et al., 2018). This pathological change pattern is like the pattern of noise-induced deafness and age-related deafness (Zhou et al., 2016). This kind of mice model further proves that Cx26 plays an essential role in maintaining hearing function, especially in maintaining the active amplification of the cochlea. The rest of the cochlear blood supply depends on two vascular networks, one serving the spiral limbus, and another serving the spiral ligaments and SVs (**Figure 2**).

Pathological mechanisms of connexin26-related hearing loss

Cx26 mutation leads to disruption of potassium recycling in cochlear lymph

In 1983, Santos-Sacchi and Dallos proposed the hypothesis of the GJ function in potassium recycling (Santos-Sacchi and Dallos, 1983). The cochlear GJ is a specific potassium ion channel. By GJ, expelled potassium ions from hair cells are sunken into supporting cells and are eventually transported back to the endolymph.

Potassium recycling is such a process that potassium flows through ion channels in the cochlear GJ system from the perilymph into the endolymph, participating in the formation of hair cell receptor potentials and stable endocochlear potential (EP), finally returning to the perilymph (Lv et al., 2021; **Figure 1**). Potassium recycling is thought to be critical for maintaining high endolymphatic potassium concentrations and EP (Chen et al., 2021).

The cochlea is filled with endolymph and perilymph of unique and different ionic environments. The ionic composition of endolymph is different from that of perilymph. Such as, the potassium concentration in the endolymph is 30 times higher than that of the perilymph, in contrast, Na^+ concentration in the perilymph is 10 times higher than that in the endolymph. This leads to the potential difference between different parts of the cochlea in the resting state. EP is the positive voltage (+80 mV) of cochlear endolymph in scale media at the resting state. Once acoustic stimulation, the positively charged EP becomes the driving force to promote potassium ions of endolymph in the scala media to pass through the mechano-transduction channel in the top of hair cells and generates auditory receptor current and potential. Thus, the positive EP is necessary for hearing maintenance (Chen and Zhao, 2014; Chen et al., 2021). Gap junction coupling is required to produce positive EP. Loss of Cx26 expression in the cochlea can lead to decreased EP (Chen et al., 2014). Compared with WT mice, Cx26 KO mice had about a 50% reduction in EP (Cohen-Salmon et al., 2002).

The EP reduction attenuates the potassium inflow driving force into hair cell stereocilia and weakens outer hair cell (OHC) electromotility. OHC electromotility serves as a major source of active cochlear amplification in mammals (Ashmore, 2008; Liu et al., 2019). Active cochlear amplification can increase hearing sensitivity and frequency selectivity (Dallos, 2008; Zheng et al., 2021). Therefore, Cx26 deficiency in the cochlear supporting cells can impair active cochlear amplification with DPOAE reduction (Lin et al., 2019).

Based on GJ functions in the cochlea, researchers have hypothesized that the pathological mechanism of deafness caused by Cx26 mutations may be due to dysfunction of

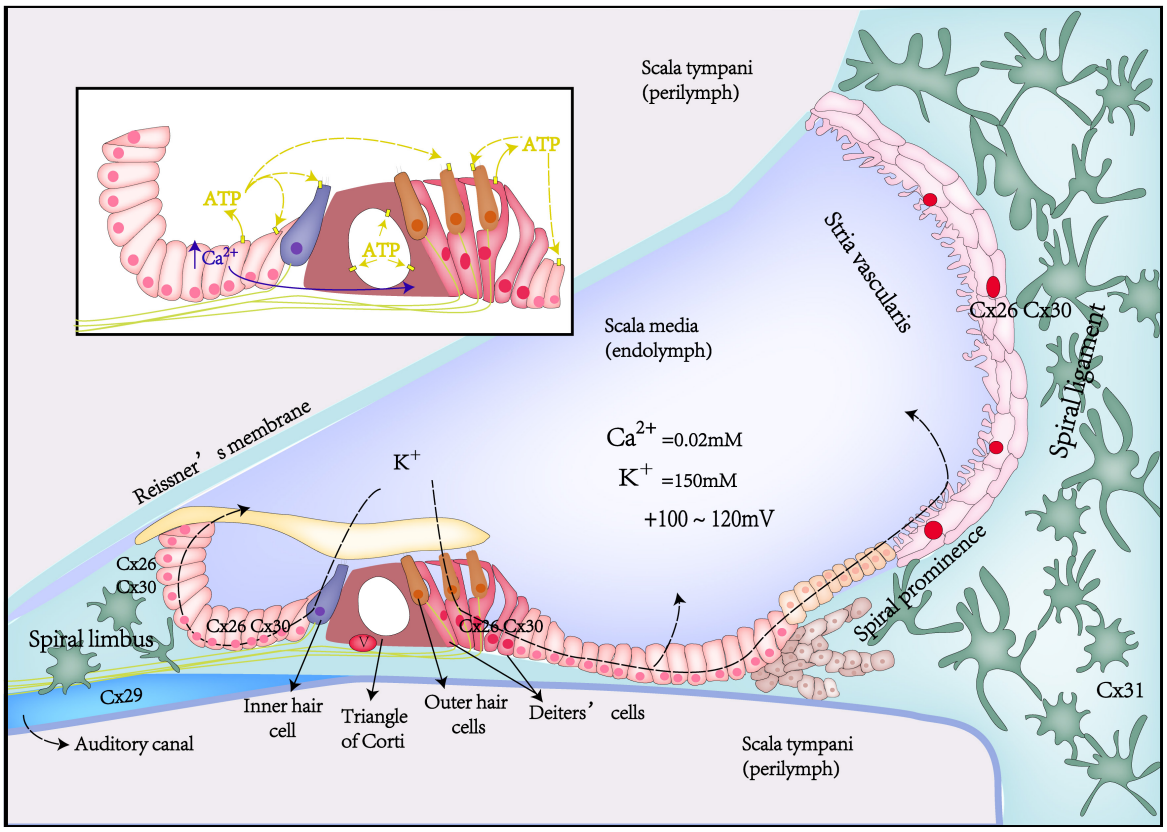

FIGURE 1
Schematic diagrams of Cx expression, potassium recycling, and ATP-Ca^{2+} signaling in the inner ear.

GJ, leading to impair potassium recycling in the cochlea. They hypothesized that *GJB2* mutations produce functionally defective or non-functional Cx26 proteins that affect the permeability of the cochlear GJ, impairing GJ coupling and disrupting potassium recycling, and also (1) leading to potassium excessive accumulation in extracellular space near hair cell, generating cell toxicity and eventually damaging the hair cells (Salt and Ohyama, 1993; Teubner et al., 2003; Wangemann, 2006; Zhao, 2017); (2) leading to EP reduction; and (3) leading to impair active cochlear amplification (Kamiya et al., 2014; Chang et al., 2015).

The potassium recycling dysfunction hypothesis can explain the pathogenesis of most of the GJ-related hearing loss including profound congenital hearing loss and late-onset progressive hearing loss. However, there has been no direct evidence found to support this hypothesis so far. Moreover, more and more model mice have been studied, and the theory of potassium recycling has been challenged and questioned in many ways (Zhu et al., 2015). For example, many mutations do not affect the ion permeability of the GJ but still cause deafness (Beltramello et al., 2005); R75W mutant mice exhibit severe deafness but have normal EP (Inoshita et al., 2008), and so on. Therefore, in our opinion, the Cx26 mutation causing impaired potassium recycling may not be its main pathogenic mechanism. The hypothesis of potassium recycling defect cannot explain that Cx26 deficiency can lead to congenital deafness and delayed deafness. The congenital deafness caused by Cx26 mutation is not due to the degeneration of cells and the reduction of cochlear potential but may be due to the developmental disorder of the cochlea itself.

Critical role of ATP triggered intercellular Ca^{2+} signaling in cochlear development

As an intercellular channel, GJ also plays an important role in intercellular Ca^{2+} signaling transduction (Sirko et al., 2019). Calcium signaling is involved in a variety of cell pathophysiological processes, which is not only the main driving force of cell proliferation and growth but also closely related to cell death (Sirko et al., 2019).

The spread of intercellular Ca^{2+} waves can be realized through transmitting second messengers (Ca^{2+} and IP_3 by GJ channels, or ATP and IP_3 by hemichannels). During

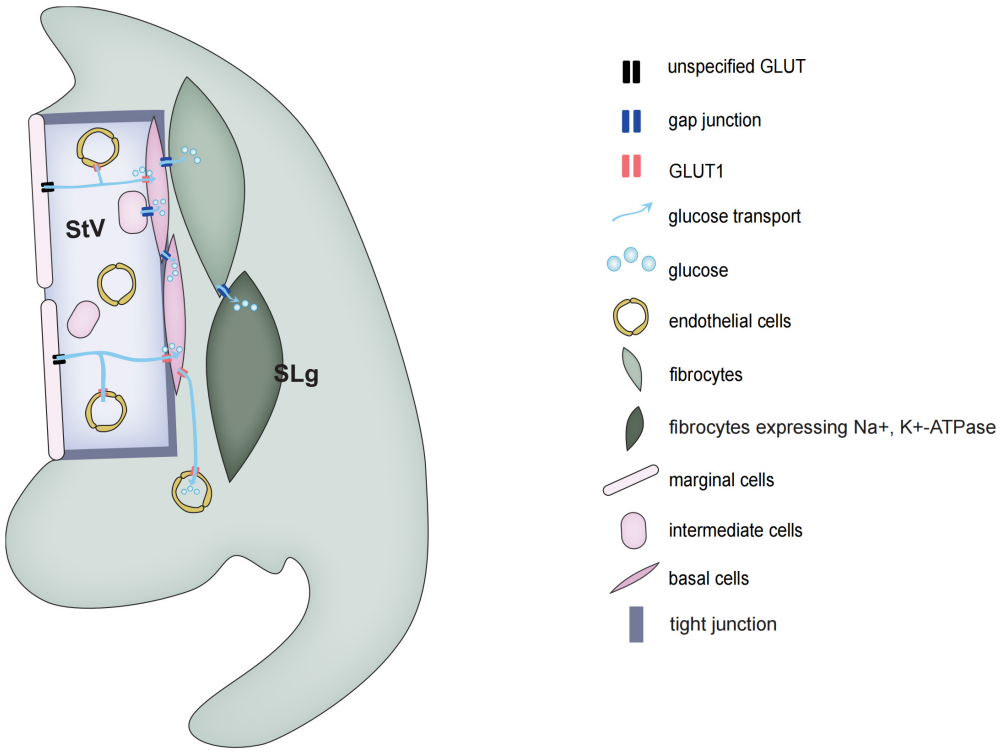

FIGURE 2
Schematic diagrams of glucose transport in the stria vascularis and spiral ligament of the cochlea.

cochlear development, supporting cells of the Kölliker's organ can spontaneously and rhythmically release ATP to the endolymphatic surface *via* hemichannels, as well as to adjacent supporting cells *via* GJ channels (Mese et al., 2011; Sellitto et al., 2021). Then, ATP can activate the G protein-coupled P2 purinergic receptor (P2R) of the adjacent cells, producing phospholipase C (PLC)-dependent IP_3, which activates the endoplasmic reticulum IP_3 receptor and promotes endoplasmic reticulum calcium release, thereby inducing Ca^{2+} signaling (Piazza et al., 2007). Initially, intracellular Ca^{2+} release from supporting cells usually starts from a small group of cells (2–4) and then passes rapidly through gap junction channels, synchronizing the entire Kölliker'so rgan syncytium, causing cumulative ATP release, and eventually activating the P2Rs on adjacent inner hair cells (IHC), which again leads to causing depolarization of IHCs and the release of calcium-dependent glutamate from ribbon synapses, activating spiral ganglion neurons (SGNs) to generate action potentials(Ceriani et al., 2016). This process is called as the ATP-triggered intercellular Ca^{2+} signaling pathway or sound-independent spontaneous electrical activity, which is a key transient physiological activity during auditory development (Ceriani et al., 2016). With the disappearance of Kölliker's organ, mature synapses of hair cells start to be established for chemical-electrical connection with postsynaptic afferent nerves, and the abovementioned transient physiological activity ends. Thus, ATP triggered intercellular Ca^{2+} signaling pathway plays a critical role in promoting the maturation of hair cells and SGNs and the refinement of synapses and nerve fibers.

In addition, the propagation of the intercellular Ca^{2+} wave activates and opens TMEM16A (a Ca^{2+}-activated chloride channel), causing osmotic cell contraction and wrinkle movement of tall columnar cells of Kölliker's organ (Tritsch et al., 2007). TMEM16A is highly expressed in columnar supporting cells near IHC. The wrinkle movement of columnar cells will also depolarize IHC and increase the frequency of spontaneous Ca^{2+} action potentials (APs) of IHC at the prehearing stage, thus triggering synaptic vesicle exocytosis and promoting the development and maturation of IHC and SGN at prehearing stage (Wang et al., 2015).

Connexin, as the core of ATP-triggered intercellular Ca^{2+} signaling pathway, and its defect will lead to the disruption of calcium signal transmission. Both $Gjb2^{loxP/loxP}$; Sox10-Cre mice and $Gjb6^{-/-}$ mice showed that Ca^{2+} waves failed to propagate in the Kölliker's organ (Ortolano et al., 2008; Crispino et al., 2011), and consequently failed to acquire normal hearing (Sun et al., 2022). On the contrary, P2rx7 and Panx1, as alternative parts for ATP-triggered intercellular Ca^{2+} signaling, $P2rx7^{-/-}$ (MGI:3606250) and $Panx1^{-/-}$ (MGI:3606250) mice, showed that normal Ca^{2+} waves spread in Kölliker's organ and

normal hearing phenotype (Suadicani et al., 2006). Moreover, overexpression of Cx30 by transduction *in vivo* with BAAV (bovine adeno-associated virus) vectors encoding Cx30 *via* canalostomy at P4 not only restored calcium wave transmission in Gjb6$^{-/-}$ mice but also partially and significantly improved hearing threshold around P30 (Crispino et al., 2011).

Although IHCs and OHCs do not express GJs, the Ribbon synapse of IHC retained immature morphology in Gjb2$^{loxP/loxP}$; Sox10-Cre mice and Gjb6$^{-/-}$ mice under transmission electron microscopy observation (Johnson et al., 2017). And patch clamp experiments also showed membrane currents and exocytosis capability of IHC retained at the prehearing stage (Johnson et al., 2017). The impaired synapse and nerve innervation of OHC also have been found in Cx26 deficiency mice (Johnson et al., 2017).

In conclusion, these results demonstrated that Cx-dependent ATP-triggered intercellular Ca^{2+} signaling pathway plays a key role in postnatal auditory development. Some scholars proposed the hypothesis that the disrupted Ca^{2+} signaling of developing cochlear epithelium prevents hearing acquisition in Cx26 deficiency mice (Ceriani et al., 2016; Johnson et al., 2017; Sun et al., 2022). However, the disrupted Ca^{2+} signaling hypothesis cannot explain the abnormal development of cochlear support cells, such as the failure of the tunnel of Corti to open and the failure of inner and outer column cells to differentiate and mature.

Energy supply of the cochlear supporting cell *via* gap junction-mediated glucose transport pathway

The mammalian cochlear sensory epithelium is basically an avascular structure. With one exception, there is only one capillary, the spiral vessel, that traverses the sensory epithelium beneath the tunnel of Corti. The rest of the cochlear blood supply depends on two vascular networks, one serving the spiral limbus and another serving the spiral ligaments and SVs. The spiral ligament vessel, which is embedded in the fibrocytes forming part of the C-sys, crosses SVs and divides into many fine capillaries in the SVs.

Glucose transport is divided into two types, the family of glucose transporters (GLUT) that promote glucose diffusion along concentration gradient and sodium-dependent glucose transporters (SGLTs) that transport glucose against a concentration gradient (Mueckler and Thorens, 2013; Deng and Yan, 2016). Blood glucose is mainly transported along a concentration gradient, which does not require energy, but requires a carrier. In rats, the concentration of glucose in the perilymph of vestibular scala and media scala is only about 50% of that in blood plasma, while the glucose concentration in the endolymph is less than 10%. In 1983, Santos-Sacchi and Dallos discovered that GJs can help transport glucose and other metabolic substances to adjacent cells of the sensory epithelium (Santos-Sacchi and Dallos, 1983). Using a fluorescent glucose tracer (2-NBDG) which can monitor the ability of glucose uptake in living cells, it has been shown that glucose transport is through the intercellular GJs network system (Zou et al., 2005). Also in astrocytes, the network of GJs can transport energy and nutrients from the vascular zone to distant neurons in the avascular zone.

During cochlear development, both hair cells and supporting cells require a large amount of energy for differentiation and maturation. The insufficient energy supply will disturb normal development. Autophagy provides important energy for early development, and the deletion of autophagy-related molecules can be lethal to mouse embryos (He et al., 2017; Liu et al., 2021). Similarly, complete knockout of Cx26 mice has embryonic lethality, which is related to impaired transplacental glucose uptake (Bakirtzis et al., 2003). Interference with autophagy in early development also disrupts cochlear sensory epithelial development (Bu et al., 2022). In adult mice, the normal OHC electromotility activity also requires a large amount of energy, and the concertina movements of OHCs can reach 10,000 Hz frequency, and such a high frequency of cellular concertina movements must be accompanied by a large consumption of energy (Zhu et al., 2013). However, OHC electromotility does not depend on ATP but probably on the constant uptake of glucose from the cortilymph by the glucose transporters in the lateral walls of OHCs. Glucose of cortilymph may come from the hemichannel secretion of supporting cells.

Mutations in Cx26 reduce the coupling of CJs, which limits the transport of nutrients, especially glucose from distal vessels to avascular sensory epithelium. The glucose transport pathway mediated by GJs is critical for the differentiation and maturation of supporting cells, especially the inner and outer column cells of the tunnel of Corti during early development (Xie et al., 2019). Limited energy supply may hinder the formation of microtubules of inner and outer column cells, leading to failure to open the tunnel of Corti, which can explain the developmental disorder in congenitally profound deafness model mice (Lin et al., 2013; Xie et al., 2019). The lack of nutrients such as glucose affects ATP production, leading to reactive oxygen species (ROS) overload and cell apoptosis (Wang et al., 2016; Fetoni et al., 2018). This provides a mechanism to explain the massive loss of OHCs due to their high elevated levels of mitochondrial metabolism, making them more susceptible to intracellular ATP deprivation (Wang et al., 2022). Considering that OHCs in the high-frequency region require more energy, it could not only explain that Cx26 defect model mice with delayed progressive hearing loss that usually start to

hearing impairment at the high frequencies but also explain that Cx26-related delayed hearing loss has noise susceptibility and age-related characteristics (Fetoni et al., 2018; Lin et al., 2019).

Summary and outlook

Cx26 plays a critical role for hearing acquisition and maintenance. Cx26 mutations can induce congenital deafness and late-onset hearing loss. Cx26 is responsible for intercellular substance transfer and signal communication. GJ channels and hemichannels generally allow the passage of potassium, ATP-calcium signaling, and glucose. Potassium recycling is critical for maintaining EP and OHC electromotility. Therefore, Cx26 mutation can disrupt potassium recycling in cochlea lymph, leading to EP reduction and active cochlear amplification impairment. ATP-triggered intercellular Ca2+ signaling is critical for cochlear development. Cx26 mutation can lead to cochlear IHC development disorder. Cochlear development for hearing acquisition and OHC electromotility for hearing maintenance require sufficient energy supply, which depends on the cochlear supporting cell by GJ-mediated glucose transport pathway. Thus, energy deprivation at different periods due to Cx26 deficiency can cause cochlear non-sensory and sensory epithelial cell development arrest or OHC electromotility impairment with aging or noise.

Cx26 function has been studied for decades, most of which focus on downstream function changes. Nowadays, there are some advances in the treatment of *GJB2* mutation-related deafness. Yu et al. (2014) and Iizuka et al. (2015) used virally mediated gene therapy to restore Cx26 expression in a mouse model of Gjb2 deletion and improved the auditory responses or development of the cochlear structure. Xu et al. (2022) found that systemic administration of dexamethasone could prevent OHCs loss and improve auditory responses at some frequencies. Monoclonal antibodies developed in the last three decades have become the most important class of therapeutic biologicals (Buratto et al., 2021). Ziraldo et al. (2019) found that a human-derived monoclonal antibody named abEC1.1 can selectively modulate hemichannel function and efficiently inhibit hyperactive mutant Cx26 hemichannels implicated in autosomal dominant non-syndromic hearing impairment accompanied by keratitis and hystrix-like ichthyosis-deafness (KID/HID) syndrome (Xu et al., 2017). So far, there is no drug to prevent or treat Cx26 mutation-related hearing loss. Post-translational modifications of proteins can regulate the Cx26 protein life cycle and/or channel selective permeability by the covalent addition of functional groups or proteins, changing the hydrophilicity and spatial structure of Cx26. The upstream molecular regulation mechanism of Cx26 deserves further study to find more information for novel protective or therapeutic strategies to prevent or treat hereditary deafness caused by GJB2 mutation.

Author contributions

PC: study conception and write the manuscript. WW and JZ: study conception and draft the manuscript and figures. JC, YL, and LS: study conception and screening. SH: quality control and write the manuscript. JY: study conception, quality control, and write the manuscript. All authors contributed to the article and approved the submitted version.

Funding

This work was supported by grants from the National Science Foundation of China (82000989 to PC, 82000977 to SH, and 81873698 to JY) and the Shanghai Sailing Program (20YF1428800 to PC and 20YF1428900 to SH).

Conflict of interest

The authors declare that the research was conducted in the absence of any commercial or financial relationships that could be construed as a potential conflict of interest.

Publisher's note

References

Aasen, T., Johnstone, S., Vidal-Brime, L., Lynn, K. S., and Koval, M. (2018). Connexins: synthesis, post-translational modifications, and trafficking in health and disease. *Int. J. Mol. Sci.* 19;1296. doi: 10.3390/ijms19051296

Ahmad, S., Chen, S., Sun, J., and Lin, X. (2003). Connexins 26 and 30 are co-assembled to form gap junctions in the cochlea of mice. *Biochem. Biophys. Res. Commun.* 307, 362–368. doi: 10.1016/s0006-291x(03)01166-5

Ashmore, J. (2008). Cochlear outer hair cell motility. *Physiol. Rev.* 88, 173–210. doi: 10.1152/physrev.00044.2006

Bakirtzis, G., Jamieson, S., Aasen, T., Bryson, S., Forrow, S., Tetley, L., et al. (2003). The effects of a mutant connexin 26 on epidermal differentiation. *Cell Commun. Adhes.* 10, 359–364. doi: 10.1080/cac.10.4-6.359.364

Bedner, P., Niessen, H., Odermatt, B., Kretz, M., Willecke, K., and Harz, H. (2006). Selective permeability of different connexin channels to the second messenger cyclic AMP. *J. Biol. Chem.* 281, 6673–6681. doi: 10.1074/jbc.M511235200

Beltramello, M., Piazza, V., Bukauskas, F. F., Pozzan, T., and Mammano, F. (2005). Impaired permeability to Ins(1,4,5)P3 in a mutant connexin underlies recessive hereditary deafness. *Nat. Cell Biol.* 7, 63–69. doi: 10.1038/ncb1205

Bennett, B. C., Purdy, M. D., Baker, K. A., Acharya, C., McIntire, W. E., Stevens, R. C., et al. (2016). An electrostatic mechanism for Ca(2+)-mediated regulation of gap junction channels. *Nat. Commun.* 7:8770. doi: 10.1038/ncomms9770

Beyer, E. C., and Berthoud, V. M. (2018). Gap junction gene and protein families: connexins, innexins, and pannexins. *Biochim. Biophys. Acta Biomembr.* 1860, 5–8. doi: 10.1016/j.bbamem.2017.05.016

Bu, C., Xu, L., Han, Y., Wang, M., Wang, X., Liu, W., et al. (2022). c-Myb protects cochlear hair cells from cisplatin-induced damage *via* the PI3K/Akt signaling pathway. *Cell Death Discov.* 8:78. doi: 10.1038/s41420-022-00879-9

Buniello, A., Montanaro, D., Volinia, S., Gasparini, P., and Marigo, V. (2004). An expression atlas of connexin genes in the mouse. *Genomics* 83, 812–820. doi: 10.1016/j.ygeno.2003.10.011

Buratto, D., Donati, V., Zonta, F., and Mammano, F. (2021). Harnessing the therapeutic potential of antibodies targeting connexin hemichannels. *Biochim. Biophys. Acta Mol. Basis Dis.* 1867:166047. doi: 10.1016/j.bbadis.2020.166047

Ceriani, F., Pozzan, T., and Mammano, F. (2016). Critical role of ATP-induced ATP release for Ca2+ signaling in nonsensory cell networks of the developing cochlea. *Proc. Natl. Acad. Sci. U.S.A.* 113, E7194–E7201. doi: 10.1073/pnas.1616061113

Chang, Q., Tang, W., Ahmad, S., Zhou, B., and Lin, X. (2008). Gap junction mediated intercellular metabolite transfer in the cochlea is compromised in connexin30 null mice. *PLoS One* 3:e4088. doi: 10.1371/journal.pone.0004088

Chang, Q., Tang, W., Kim, Y., and Lin, X. (2015). Timed conditional null of connexin26 in mice reveals temporary requirements of connexin26 in key cochlear developmental events before the onset of hearing. *Neurobiol. Dis.* 73, 418–427. doi: 10.1016/j.nbd.2014.09.005

Chen, J., Chen, J., Zhu, Y., Liang, C., and Zhao, H. B. (2014). Deafness induced by Connexin 26 (GJB2) deficiency is not determined by endocochlear potential (EP) reduction but is associated with cochlear developmental disorders. *Biochem. Biophys. Res. Commun.* 448, 28–32. doi: 10.1016/j.bbrc.2014.04.016

Chen, J., Chen, P., He, B., Gong, T., Li, Y., Zhang, J., et al. (2021). Connexin30-deficiency causes mild hearing loss with the reduction of endocochlear potential and ATP release. *Front. Cell Neurosci.* 15:819194. doi: 10.3389/fncel.2021.819194

Chen, J., and Zhao, H. B. (2014). The role of an inwardly rectifying K(+) channel (Kir4.1) in the inner ear and hearing loss. *Neuroscience* 265, 137–146. doi: 10.1016/j.neuroscience.2014.01.036

Chen, Y., Hu, L., Wang, X., Sun, C., Lin, X., Li, L., et al. (2016). Characterization of a knock-in mouse model of the homozygous p.V37I variant in Gjb2. *Sci. Rep.* 6:33279. doi: 10.1038/srep33279

Cohen-Salmon, M., Ott, T., Michel, V., Hardelin, J. P., Perfettini, I., Eybalin, M., et al. (2002). Targeted ablation of connexin26 in the inner ear epithelial gap junction network causes hearing impairment and cell death. *Curr. Biol.* 12, 1106–1111. doi: 10.1016/s0960-9822(02)00904-1

Crispino, G., Di Pasquale, G., Scimemi, P., Rodriguez, L., Galindo Ramirez, F., De Siati, R. D., et al. (2011). BAAV mediated GJB2 gene transfer restores gap junction coupling in cochlear organotypic cultures from deaf Cx26Sox10Cre mice. *PLoS One* 6:e23279. doi: 10.1371/journal.pone.0023279

Dallos, P. (2008). Cochlear amplification, outer hair cells and prestin. *Curr. Opin. Neurobiol.* 18, 370–376. doi: 10.1016/j.conb.2008.08.016

Deng, D., and Yan, N. (2016). GLUT, SGLT, and SWEET: structural and mechanistic investigations of the glucose transporters. *Protein Sci.* 25, 546–558. doi: 10.1002/pro.2858

Fetoni, A. R., Zorzi, V., Paciello, F., Ziraldo, G., Peres, C., Raspa, M., et al. (2018). Cx26 partial loss causes accelerated presbycusis by redox imbalance and dysregulation of Nfr2 pathway. *Redox Biol.* 19, 301–317. doi: 10.1016/j.redox.2018.08.002

Forge, A. (1984). Gap junctions in the stria vascularis and effects of ethacrynic acid. *Hear. Res.* 13, 189–200. doi: 10.1016/0378-5955(84)90108-4

Gerido, D. A., DeRosa, A. M., Richard, G., and White, T. W. (2007). Aberrant hemichannel properties of Cx26 mutations causing skin disease and deafness. *Am. J. Physiol. Cell Physiol.* 293, C337–C345. doi: 10.1152/ajpcell.00626.2006

Gridley, T., and Murray, S. A. (2022). Mouse mutagenesis and phenotyping to generate models of development and disease. *Curr. Top. Dev. Biol.* 148, 1–12. doi: 10.1016/bs.ctdb.2022.02.012

He, Z., Guo, L., Shu, Y., Fang, Q., Zhou, H., Liu, Y., et al. (2017). Autophagy protects auditory hair cells against neomycin-induced damage. *Autophagy* 13, 1884–1904. doi: 10.1080/15548627.2017.1359449

Hernandez, V. H., Bortolozzi, M., Pertegato, V., Beltramello, M., Giarin, M., Zaccolo, M., et al. (2007). Unitary permeability of gap junction channels to second messengers measured by FRET microscopy. *Nat. Methods* 4, 353–358. doi: 10.1038/nmeth1031

Iizuka, T., Kamiya, K., Gotoh, S., Sugitani, Y., Suzuki, M., Noda, T., et al. (2015). Perinatal Gjb2 gene transfer rescues hearing in a mouse model of hereditary deafness. *Hum. Mol. Genet.* 24, 3651–3661. doi: 10.1093/hmg/ddv109

Inoshita, A., Iizuka, T., Okamura, H. O., Minekawa, A., Kojima, K., Furukawa, M., et al. (2008). Postnatal development of the organ of Corti in dominant-negative Gjb2 transgenic mice. *Neuroscience* 156, 1039–1047. doi: 10.1016/j.neuroscience.2008.08.027

Jagger, D. J., and Forge, A. (2013). The enigmatic root cell - emerging roles contributing to fluid homeostasis within the cochlear outer sulcus. *Hear. Res.* 303, 1–11. doi: 10.1016/j.heares.2012.10.010

Johnson, S. L., Ceriani, F., Houston, O., Polishchuk, R., Polishchuk, E., Crispino, G., et al. (2017). Connexin-mediated signaling in nonsensory cells is crucial for the development of sensory inner hair cells in the mouse cochlea. *J. Neurosci.* 37, 258–268. doi: 10.1523/JNEUROSCI.2251-16.2016

Kamiya, K., Yum, S. W., Kurebayashi, N., Muraki, M., Ogawa, K., Karasawa, K., et al. (2014). Assembly of the cochlear gap junction macromolecular complex requires connexin 26. *J. Clin. Invest.* 124, 1598–1607. doi: 10.1172/JCI67621

Kanaporis, G., Mese, G., Valiuniene, L., White, T. W., Brink, P. R., and Valiunas, V. (2008). Gap junction channels exhibit connexin-specific permeability to cyclic nucleotides. *J. Gen. Physiol.* 131, 293–305. doi: 10.1085/jgp.200709934

Kikuchi, T., Kimura, R. S., Paul, D. L., and Adams, J. C. (1995). Gap junctions in the rat cochlea: immunohistochemical and ultrastructural analysis. *Anat. Embryol.* 191, 101–118. doi: 10.1007/BF00186783

Kikuchi, T., Kimura, R. S., Paul, D. L., Takasaka, T., and Adams, J. C. (2000). Gap junction systems in the mammalian cochlea. *Brain Res. Brain Res. Rev.* 32, 163–166. doi: 10.1016/s0165-0173(99)00076-4

Kumar, N. M., and Gilula, N. B. (1996). The gap junction communication channel. *Cell* 84, 381–388. doi: 10.1016/s0092-8674(00)81282-9

Lautermann, J., ten Cate, W. J., Altenhoff, P., Grümmer, R., Traub, O., Frank, H., et al. (1998). Expression of the gap-junction connexins 26 and 30 in the rat cochlea. *Cell Tissue Res.* 294, 415–420. doi: 10.1007/s004410051192

Leibovici, M., Safieddine, S., and Petit, C. (2008). Mouse models for human hereditary deafness. *Curr. Top. Dev. Biol.* 84, 385–429. doi: 10.1016/S0070-2153(08)00608-X

Leybaert, L., Lampe, P. D., Dhein, S., Kwak, B. R., Ferdinandy, P., Beyer, E. C., et al. (2017). Connexins in cardiovascular and neurovascular health and disease: pharmacological implications. *Pharmacol. Rev.* 69, 396–478. doi: 10.1124/pr.115.012062

Lin, L., Wang, Y. F., Wang, S. Y., Liu, S. F., Yu, Z., Xi, L., et al. (2013). Ultrastructural pathological changes in the cochlear cells of connexin 26 conditional knockout mice. *Mol. Med. Rep.* 8, 1029–1036. doi: 10.3892/mmr.2013.1614

Lin, X., Li, G., Zhang, Y., Zhao, J., Lu, J., Gao, Y., et al. (2019). Hearing consequences in Gjb2 knock-in mice: implications for human p.V37I mutation. *Aging* 11, 7416–7441. doi: 10.18632/aging.102246

Liu, W., Xu, L., Wang, X., Zhang, D., Sun, G., Wang, M., et al. (2021). PRDX1 activates autophagy *via* the PTEN-AKT signaling pathway to protect against cisplatin-induced spiral ganglion neuron damage. *Autophagy* 17, 4159–4181. doi: 10.1080/15548627.2021.1905466

Liu, Y., Qi, J., Chen, X., Tang, M., Chu, C., Zhu, W., et al. (2019). Critical role of spectrin in hearing development and deafness. *Sci. Adv.* 5:eaav7803. doi: 10.1126/sciadv.aav7803

Lv, J., Fu, X., Li, Y., Hong, G., Li, P., Lin, J., et al. (2021). Deletion of Kcnj16 in mice does not alter auditory function. *Front. Cell Dev. Biol.* 9:630361. doi: 10.3389/fcell.2021.630361

Mammano, F. (2019). Inner ear connexin channels: roles in development and maintenance of cochlear function. *Cold Spring Harb. Perspect. Med.* 9:a033233. doi: 10.1101/cshperspect.a033233

Mese, G., Sellitto, C., Li, L., Wang, H. Z., Valiunas, V., Richard, G., et al. (2011). The Cx26-G45E mutation displays increased hemichannel activity in a mouse model of the lethal form of keratitis-ichthyosis-deafness syndrome. *Mol. Biol. Cell.* 22, 4776–4786. doi: 10.1091/mbc.E11-09-0778

Moreno, A. P. (2005). Connexin phosphorylation as a regulatory event linked to channel gating. *Biochim. Biophys. Acta* 1711, 164–171. doi: 10.1016/j.bbamem.2005.02.016

Mueckler, M., and Thorens, B. (2013). The SLC2 (GLUT) family of membrane transporters. *Mol. Aspects Med.* 34, 121–138. doi: 10.1016/j.mam.2012.07.001

Niessen, H., Harz, H., Bedner, P., Krämer, K., and Willecke, K. (2000). Selective permeability of different connexin channels to the second messenger inositol 1,4,5-trisphosphate. *J. Cell Sci.* 113(Pt 8), 1365–1372. doi: 10.1242/jcs.113.8.1365

Ortolano, S., Di Pasquale, G., Crispino, G., Anselmi, F., Mammano, F., and Chiorini, J. A. (2008). Coordinated control of connexin 26 and connexin 30 at the regulatory and functional level in the inner ear. *Proc. Natl. Acad. Sci. U.S.A.* 105, 18776–18781. doi: 10.1073/pnas.0800831105

Piazza, V., Ciubotaru, C. D., Gale, J. E., and Mammano, F. (2007). Purinergic signalling and intercellular Ca2+ wave propagation in the organ of Corti. *Cell Calcium* 41, 77–86. doi: 10.1016/j.ceca.2006.05.005

Sáez, J. C., and Leybaert, L. (2014). Hunting for connexin hemichannels. *FEBS Lett.* 588, 1205–1211. doi: 10.1016/j.febslet.2014.03.004

Salt, A. N., and Ohyama, K. (1993). Accumulation of potassium in scala vestibuli perilymph of the mammalian cochlea. *Ann. Otol. Rhinol. Laryngol.* 102, 64–70. doi: 10.1177/000348949310200112

Santos-Sacchi, J., and Dallos, P. (1983). Intercellular communication in the supporting cells of the organ of Corti. *Hear. Res.* 9, 317–326. doi: 10.1016/0378-5955(83)90034-5

Sellitto, C., Li, L., and White, T. W. (2021). Connexin hemichannel inhibition ameliorates epidermal pathology in a mouse model of keratitis ichthyosis deafness syndrome. *Sci. Rep.* 11:24118. doi: 10.1038/s41598-021-03627-8

Sirko, P., Gale, J. E., and Ashmore, J. F. (2019). Intercellular Ca(2+) signalling in the adult mouse cochlea. *J. Physiol.* 597, 303–317. doi: 10.1113/JP276400

Söhl, G., and Willecke, K. (2003). An update on connexin genes and their nomenclature in mouse and man. *Cell Commun. Adhes.* 10, 173–180. doi: 10.1080/cac.10.4-6.173.180

Suadicani, S. O., Brosnan, C. F., and Scemes, E. (2006). P2X7 receptors mediate ATP release and amplification of astrocytic intercellular Ca2+ signaling. *J. Neurosci.* 26, 1378–1385. doi: 10.1523/JNEUROSCI.3902-05.2006

Sun, L., Gao, D., Chen, J., Hou, S., Li, Y., Huang, Y., et al. (2022). Failure of hearing acquisition in mice with reduced expression of connexin 26 correlates with the abnormal phasing of apoptosis relative to autophagy and defective ATP-dependent Ca(2+) signaling in Kölliker's organ. *Front. Cell Neurosci.* 16:816079. doi: 10.3389/fncel.2022.816079

Sun, Y., Tang, W., Chang, Q., Wang, Y., Kong, W., and Lin, X. (2009). Connexin30 null and conditional connexin26 null mice display distinct pattern and time course of cellular degeneration in the cochlea. *J. Comp. Neurol.* 516, 569–579. doi: 10.1002/cne.22117

Teubner, B., Michel, V., Pesch, J., Lautermann, J., Cohen-Salmon, M., Söhl, G., et al. (2003). Connexin30 (Gjb6)-deficiency causes severe hearing impairment and lack of endocochlear potential. *Hum. Mol. Genet.* 12, 13–21. doi: 10.1093/hmg/ddg001

Thönnissen, E., Rabionet, R., Arbonès, M. L., Estivill, X., Willecke, K., and Ott, T. (2002). Human connexin26 (GJB2) deafness mutations affect the function of gap junction channels at different levels of protein expression. *Hum. Genet.* 111, 190–197. doi: 10.1007/s00439-002-0750-2

Tritsch, N. X., Yi, E., Gale, J. E., Glowatzki, E., and Bergles, D. E. (2007). The origin of spontaneous activity in the developing auditory system. *Nature* 450, 50–55. doi: 10.1038/nature06233

Tsutsui, K., Kumon, H., Ichikawa, H., and Tawara, J. (1976). Preparative method for suspended biological materials for SEM by using of polycationic substance layer. *J. Electron. Microsc.* 25, 163–168.

Verselis, V. K., Ginter, C. S., and Bargiello, T. A. (1994). Opposite voltage gating polarities of two closely related connexins. *Nature* 368, 348–351. doi: 10.1038/368348a0

Verselis, V. K., and Srinivas, M. (2008). Divalent cations regulate connexin hemichannels by modulating intrinsic voltage-dependent gating. *J. Gen. Physiol.* 132, 315–327. doi: 10.1085/jgp.200810029

Wang, H. C., Lin, C. C., Cheung, R., Zhang-Hooks, Y., Agarwal, A., Ellis-Davies, G., et al. (2015). Spontaneous activity of cochlear hair cells triggered by fluid secretion mechanism in adjacent support cells. *Cell* 163, 1348–1359. doi: 10.1016/j.cell.2015.10.070

Wang, M., Dong, Y., Gao, S., Zhong, Z., Cheng, C., Qiang, R., et al. (2022). Hippo/YAP signaling pathway protects against neomycin-induced hair cell damage in the mouse cochlea. *Cell Mol. Life Sci.* 79:79. doi: 10.1007/s00018-021-04029-9

Wang, Y., Chang, Q., Tang, W., Sun, Y., Zhou, B., Li, H., et al. (2009). Targeted connexin26 ablation arrests postnatal development of the organ of Corti. *Biochem. Biophys. Res. Commun.* 385, 33–37. doi: 10.1016/j.bbrc.2009.05.023

Wang, Y., Lin, C., He, Y., Li, A., Ni, W., Sun, S., et al. (2016). Mir-27a promotes apoptosis of cochlear sensory epithelium in Cx26 knockout mice. *Front. Biosci.* 21, 364–373. doi: 10.2741/4393

Wangemann, P. (2006). Supporting sensory transduction: cochlear fluid homeostasis and the endocochlear potential. *J. Physiol.* 576, 11–21. doi: 10.1113/jphysiol.2006.112888

Xie, L., Chen, S., Xu, K., Cao, H. Y., Du, A. N., Bai, X., et al. (2019). Reduced postnatal expression of cochlear Connexin26 induces hearing loss and affects the developmental status of pillar cells in a dose-dependent manner. *Neurochem. Int.* 128, 196–205. doi: 10.1016/j.neuint.2019.04.012

Xu, K., Chen, S., Xie, L., Qiu, Y., Liu, X. Z., Bai, X., et al. (2022). The protective effects of systemic dexamethasone on sensory epithelial damage and hearing loss in targeted Cx26-null mice. *Cell Death Dis.* 13:545. doi: 10.1038/s41419-022-04987-3

Xu, L., Carrer, A., Zonta, F., Qu, Z., Ma, P., Li, S., et al. (2017). Design and characterization of a human monoclonal antibody that modulates mutant connexin 26 hemichannels implicated in deafness and skin disorders. *Front. Mol. Neurosci.* 10:298. doi: 10.3389/fnmol.2017.00298

Yu, Q., Wang, Y., Chang, Q., Wang, J., Gong, S., Li, H., et al. (2014). Virally expressed connexin26 restores gap junction function in the cochlea of conditional Gjb2 knockout mice. *Gene Ther.* 21, 71–80. doi: 10.1038/gt.2013.59

Zhao, H. B. (2017). Hypothesis of K(+)-recycling defect is not a primary deafness mechanism for Cx26 (GJB2) deficiency. *Front. Mol. Neurosci.* 10:162. doi: 10.3389/fnmol.2017.00162

Zhao, H. B., and Yu, N. (2006). Distinct and gradient distributions of connexin26 and connexin30 in the cochlear sensory epithelium of guinea pigs. *J. Comp. Neurol.* 499, 506–518. doi: 10.1002/cne.21113

Zheng, J., Takahashi, S., Zhou, Y., and Cheatham, M. A. (2021). Prestin and electromotility may serve multiple roles in cochlear outer hair cells. *Hear. Res.* 423, 108428. doi: 10.1016/j.heares.2021.108428

Zhou, X. X., Chen, S., Xie, L., Ji, Y. Z., Wu, X., Wang, W. W., et al. (2016). Reduced connexin26 in the mature cochlea increases susceptibility to noise-induced hearing lossin mice. *Int. J. Mol. Sci.* 17:301. doi: 10.3390/ijms17030301

Zhu, Y., Chen, J., Liang, C., Zong, L., Chen, J., Jones, R. O., et al. (2015). Connexin26 (GJB2) deficiency reduces active cochlear amplification leading to late-onset hearing loss. *Neuroscience* 284, 719–729. doi: 10.1016/j.neuroscience.2014.10.061

Zhu, Y., Liang, C., Chen, J., Zong, L., Chen, G. D., and Zhao, H. B. (2013). Active cochlear amplification is dependent on supporting cell gap junctions. *Nat. Commun.* 4:1786. doi: 10.1038/ncomms2806

Ziraldo, G., Buratto, D., Kuang, Y., Xu, L., Carrer, A., Nardin, C., et al. (2019). A human-derived monoclonal antibody targeting extracellular connexin domain selectively modulates hemichannel function. *Front. Physiol.* 10:392. doi: 10.3389/fphys.2019.00392

Zou, C., Wang, Y., and Shen, Z. (2005). 2-NBDG as a fluorescent indicator for direct glucose uptake measurement. *J. Biochem. Biophys. Methods* 64, 207–215. doi: 10.1016/j.jbbm.2005.08.001

frontiers | Frontiers in Molecular Neuroscience

TYPE Review
PUBLISHED 11 October 2022
DOI 10.3389/fnmol.2022.1031989

OPEN ACCESS

EDITED BY
Zuhong He,
Department of Otolaryngology,
Zhongnan Hospital, Wuhan University,
China

REVIEWED BY
Zheng-De Du,
Department of Otolaryngology,
Affiliated Beijing Friendship Hospital,
Capital Medical University, China
Jean Defourny,
Fonds National de la Recherche
Scientifique (FNRS), Belgium

*CORRESPONDENCE
Lianhua Sun
sunlianhua@xinhuamed.com.cn
Jun Yang
yangjun@xinhuamed.com.cn

†These authors have contributed
equally to this work

SPECIALTY SECTION
This article was submitted to
Methods and Model Organisms,
a section of the journal
Frontiers in Molecular Neuroscience

RECEIVED 30 August 2022
ACCEPTED 23 September 2022
PUBLISHED 11 October 2022

CITATION
Chen J, Gao D, Sun L and Yang J
(2022) Kölliker's organ-supporting cells
and cochlear auditory development.
Front. Mol. Neurosci. 15:1031989.
doi: 10.3389/fnmol.2022.1031989

Kölliker's organ-supporting cells and cochlear auditory development

Jianyong Chen[1,2,3†], Dekun Gao[1,2,3†], Lianhua Sun[1,2,3*] and Jun Yang[1,2,3*]

[1]Department of Otorhinolaryngology-Head and Neck Surgery, Xinhua Hospital, Shanghai Jiaotong University School of Medicine, Shanghai, China, [2]Institute of Ear Science, School of Medicine, Shanghai Jiao Tong University, Shanghai, China, [3]Shanghai Key Laboratory of Otolaryngology and Translational Medicine, Shanghai, China

The Kölliker's organ is a transient cellular cluster structure in the development of the mammalian cochlea. It gradually degenerates from embryonic columnar cells to cuboidal cells in the internal sulcus at postnatal day 12 (P12)–P14, with the cochlea maturing when the degeneration of supporting cells in the Kölliker's organ is complete, which is distinct from humans because it disappears at birth already. The supporting cells in the Kölliker's organ play a key role during this critical period of auditory development. Spontaneous release of ATP induces an increase in intracellular Ca^{2+} levels in inner hair cells in a paracrine form *via* intercellular gap junction protein hemichannels. The Ca^{2+} further induces the release of the neurotransmitter glutamate from the synaptic vesicles of the inner hair cells, which subsequently excite afferent nerve fibers. In this way, the supporting cells in the Kölliker's organ transmit temporal and spatial information relevant to cochlear development to the hair cells, promoting fine-tuned connections at the synapses in the auditory pathway, thus facilitating cochlear maturation and auditory acquisition. The Kölliker's organ plays a crucial role in such a scenario. In this article, we review the morphological changes, biological functions, degeneration, possible trans-differentiation of cochlear hair cells, and potential molecular mechanisms of supporting cells in the Kölliker's organ during the auditory development in mammals, as well as future research perspectives.

KEYWORDS

Kölliker's organ supporting cells, cochlear auditory development, degeneration, trans-differentiation, hair cells

Introduction

Mammals are not born with a sense of hearing, which gradually matures during the 12th to 14th day of life (Geal-Dor et al., 1993). During the development of hearing, the Kölliker's organ supporting cells play a key regulatory role (Tritsch et al., 2007; Dayaratne et al., 2014), changing cell morphology and numbers during the embryonic and postnatal periods, eventually degenerating and disappearing after the external auditory canal opens, the endocochlear potential is established,

and the cochlea can receive external acoustic stimuli, and then eventually diffuse into internal sulcus cells, at which point the cochlear hearing becomes mature (Lim and Anniko, 1985). Delayed degeneration or dysfunction of Kölliker's organ-supporting cells can lead to abnormal cochlear hearing development (Lim, 1986). In addition, Kölliker's organ-supporting cells can be induced to differentiate into new hair cells as inner ear progenitors for hair cell regeneration, which in turn can repair damaged hearing (Chai et al., 2011, 2012; Wang et al., 2015; Cheng et al., 2017; Zhang et al., 2017, 2018; You et al., 2018). Although the Kölliker's organ was described more than a century ago, the molecular mechanisms regulating cochlear auditory development are still far beyond understanding. In this article, we review the morphological changes, biological functions, degeneration, possible trans-differentiation into hair cells, and potential molecular mechanisms of Kölliker's organ-supporting cells during development, as well as future research perspectives to gain insight and understanding of the role of Kölliker's organ-supporting cells in cochlear auditory development.

Morphological changes in Kölliker's organ-supporting cells during auditory development and possible mechanisms

The organ of Corti consists of a chimera of hair cells and supporting cells connected in a highly ordered manner, and is an important component of the inner ear auditory receptors (Lim, 1986). At the base of the inner spiral sulcus is a single layer of cuboidal epithelium, which is derived from the degenerated Kölliker's organ-supporting cells (Lim and Anniko, 1985).

The Kölliker's organ is the earliest visible epithelial structure, present in the late embryonic and early postnatal periods (P0–P14), which is a marker of cochlear immaturity (Dayaratne et al., 2014). The differentiated Kölliker's organ consists mainly of closely spaced columnar cells, and due to the dense distribution, the nucleus can appear in different areas of the cell (mostly at the base of the Kölliker's organ), thus appearing stratified in cross-section (Hinojosa, 1977). Kölliker's organ-supporting cells have elongated cytosomes, usually separated by an extracellular space of about 200 Å, with some extracellular gaps down to 30 Å, with bipolar or unipolar protrusions at the top of the cell and microvilli visible at the end, which were shown to be about 3–4 μm long in mice and appeared within 10 days after birth (Hinojosa, 1977). Some of these cells can be mitotically active in late embryonic and early postnatal stages and have the potential to trans-differentiate into hair cells (Wu and Kelley, 2012; Dayaratne et al., 2014).

The morphology and structure of Kölliker's organ-supporting cells undergo programmed changes and alterations during the embryonic period and after birth: the cytoplasm moves away from the cell membrane, the cells develop folds, and the cell gaps increase in size. After this critical period, the columnar cells gradually degenerate and their number decreases dramatically to about 12% of the original number of cells in the adult cochlea, and are eventually replaced by cuboidal-like cells that form a mature internal sulcus before degenerating and disappearing (**Figure 1**), at which point the cochlea matures in hearing (Tritsch et al., 2007). The origin of the cuboidal-like epithelial cells that replace the columnar

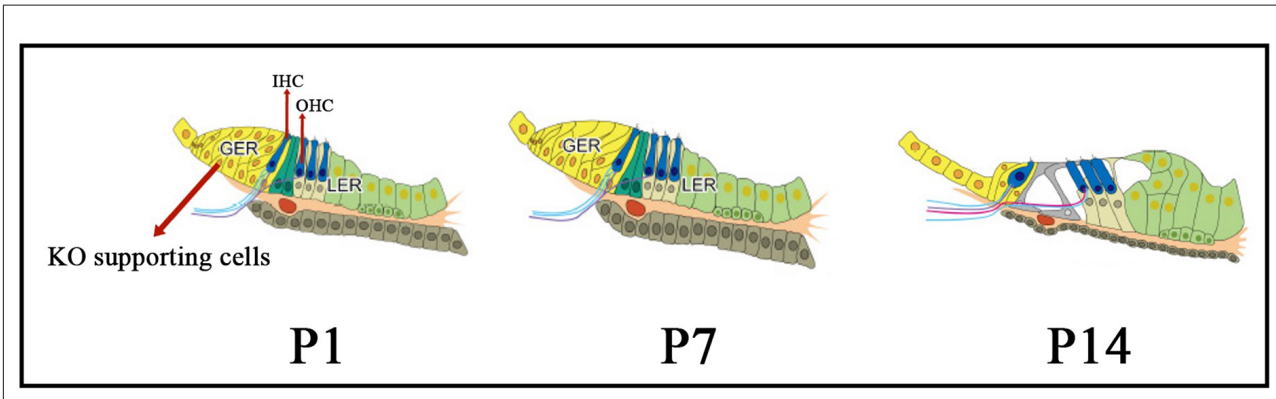

FIGURE 1
The morphology and structure of Kölliker's organ-supporting cells from immature to mature stages. From P1 to P14, the cytoplasm moves away from the cell membrane, the cells develop folds, and the cell gaps increase in size. Also, during this critical period, the columnar cells gradually degenerate and their number decreases dramatically, and are eventually replaced by cuboidal-like cells which form a mature internal sulcus, at which point the cochlea matures in hearing. KO, Kölliker's organ; GER, Greater epithelial ridge; LER, Lesser epithelial ridge; OHC, Outer hair cells; IHC, inner hair cells.

supporting cells of the Kölliker's organ during cochlear developmental maturation and remodeling of the Kölliker's organ is unclear.

The role of ATP in initiating spontaneous morphological changes in Kölliker's organ-supporting cells was first described by Tritsch et al. (2007). After ATP is released into the extracellular space through gap-linked hemichannels on the surface of Kölliker's organ-supporting cells, it in turn, acts on the purine P2X and P2Y receptors on the surface of the cells themselves receptors on the cell surface, causing intracellular Ca^{2+} elevation and inward current generation (Tritsch et al., 2007; Liang et al., 2009). Using real-time imaging, the study found that these rhythmic structural changes first start in a small group of cells within the Kölliker's organ and then radially spread to neighboring cells through gap junctions (Tritsch and Bergles, 2010). Much like inward currents, the frequency of these morphological events was significantly increased in border cells adjacent to the hair cells within the Kölliker's organ region, suggesting that border cells around the hair cells first initiate this spontaneous activity and play a key regulatory role (Nishani Dayaratne et al., 2015).

This spontaneous morphological change in the rodent Kölliker's organ does not occur at birth, and studies suggest that cellular morphological changes need to be initiated when the cochlea develops to a certain extent. The low level of purinergic receptor expression on the surface of Kölliker's organ-supporting cells in the early postnatal period results in ATP-induced inward currents and calcium waves at low levels, which are insufficient to initiate this process (Tritsch and Bergles, 2010). It was found that neither strong current stimulation nor elevated extracellular K^+ ion concentrations induced spontaneous morphological changes; whereas when the increased intracellular Ca^{2+} concentrations, cells underwent depolarization, activated Kölliker's organ-supporting cells, and further promoted changes in cell diameter in neighboring cells (Tritsch et al., 2007; Tritsch and Bergles, 2010). These results suggest that the intracellular Ca^{2+} concentration is a key factor in triggering rhythmic morphological changes in cells that diffuse into adjacent cells within the Kölliker's organ (Tritsch et al., 2007; Peng et al., 2012).

It is now believed that one of the key factors initiating this morphological change is the Ca^{2+}-activated Cl^- channel, leading to Cl^- efflux, which decreases the cell membrane threshold potential level and further causes an efflux of intracellular fluid due to the osmotic gradient, resulting in sawtooth morphological changes in Kölliker's organ-supporting cells (Tritsch et al., 2010). Furthermore, this outflow of intracellular fluid may be influenced by the distribution of water channel proteins (especially AQP4) within the Kölliker's organ-supporting cells (Nishani Dayaratne et al., 2015), and additionally, the activation of intracellular contractile proteins may also be responsible for the altered morphology of the supporting cells (Tritsch et al., 2010; Liu Y. et al., 2019).

Biological functions of Kölliker's organ-supporting cells in the regulation of cochlear hearing development

Intracellular spontaneous electrical activity in Kölliker's organ-supporting cells promotes auditory maturation

Studies have shown that afferent nerve fibers are not in a silent state before the onset of hearing and that the hair cells continuously release low levels of glutamate, triggering spontaneous electrical activity that plays an important role in promoting the survival and maturation of auditory neurons, the development of synapses, and the refinement of audio localization (Lelli et al., 2009; Blankenship and Feller, 2010; Wang and Bergles, 2015). Rodents are not auditory at birth and do not respond to external sounds until 2 weeks after birth, and Kölliker's organ-supporting cells play a key role in this auditory maturation process (Forsythe, 2007; He and Yang, 2011).

The inner and outer hair cells generate spontaneous calcium action potentials in the first week of life. Spontaneous calcium action potentials begin to guide cochlear development before the appearance of hearing (Beurg et al., 2008; Marcotti, 2012; Sendin et al., 2014). While this spontaneous calcium action potential of immature inner and outer hair cells is certainly important in cochlear development, the developmental maturation process of hearing also relies on the cellular communication network formed by Kölliker's organ-supporting cells through gap junctions. In the second week of life, Kölliker's organ-supporting cells begin to release adenosine triphosphate (ATP) spontaneously and release ATP to the endolymphatic surface *via* gap junction hemichannels composed of Cx26 and Cx30 between Kölliker's organ-supporting cells and act as paracrine receptors on the surface of neighboring hair cells to produce phospholipase C (PLC)-dependent diacylglycerol and inositol triphosphate (IP3; Rodriguez et al., 2012; Giorgi et al., 2018). The intracellular diffusion of IP3 and subsequent binding to IP3 receptors in hair cells triggers the release of Ca^{2+} from the endoplasmic reticulum (ER) calcium pool and an increase in cytoplasmic Ca^{2+} concentration, which further induces the release of the neurotransmitter glutamate from synaptic vesicles in inner hair cells, excites hair cells and their afferent nerve fibers, activates type I spiral neurons (SGNs) to generate action potentials and in this way transmits cochlear development to the upstream auditory pathway. This transmits temporal and spatial information about cochlear development to the upstream auditory pathway and refines synaptic connections in the auditory pathway, thus promoting cochlear maturation and auditory acquisition (Tritsch and Bergles, 2010; Rodriguez et al., 2012; Johnson et al., 2017). It has been suggested that ATP released by Kölliker's organ-supporting cells primarily

coordinates spontaneous electrical activity with its neighboring inner hair cells, with little association with the more distant inner hair cells, and it is hypothesized that this mechanism may be critical for the establishment of audio localization in the cochlear nucleus before the emergence of hearing (Tritsch et al., 2007).

Ca^{2+} release from Kölliker's organ-supporting cells promotes cochlear development

Ca^{2+} is the primary messenger for intercellular messaging in the cochlea and is involved in the transduction of a large number of signaling pathways (Tritsch et al., 2010). ATP in the cochlea triggers changes in intracellular Ca^{2+} concentration in Kölliker's organ-supporting cells and intercellular calcium wave transmission, which in turn transmits important biological information to the cochlear sensory epithelium. Organ-on-chip model studies have shown that developing cochlear Kölliker's organ-supporting cells release ATP to drive spontaneous Ca^{2+} signals *via* gap junction protein hemichannels (Mazzarda et al., 2020). Before the appearance of hearing, the spontaneous release of ATP from the Kölliker's organ further mediates the release of Ca^{2+} within Kölliker's organ-supporting cells after release into the extracellular compartment *via* hemichannels, initially inducing the release of Ca^{2+} from only a small group of Kölliker's organ-supporting cells, which subsequently propagate rapidly through the intercellular gap junction channels, further initiating the release of Ca^{2+} from the calcium pool in neighboring Kölliker's organ-supporting cells. The release of large amounts of Ca^{2+} promotes the synchronization of neighboring cells, which further causes the release of ATP (Zhao et al., 2005). In this way, the P2 purinoceptor/phospholipase C/IP3/Ca^{2+} signaling cascade is maintained in an orderly and positive feedback manner, causing sustained spontaneous electrical activity, and promoting cochlear development.

Kölliker's organ-supporting cells form a functional syncytium through extensive intercellular gap junctions (Goodenough and Paul, 2009), through which intercellular Ca^{2+} propagation and ATP release occur, providing a Kölliker's organ cell-to-cell signaling metabolic basis, i.e., facilitating intercellular signaling when the gap junctions are open and closing them under some specific physiological conditions (Goodenough and Paul, 2009; Mammano, 2013). GJB2 mutations are mainly characterized by degeneration of outer hair cells and hypoplasia of the vascular stripe and are the main cause of deafness in 50% of pre-speech deafness (Hochman et al., 2010). In addition, GJB6 mutation in rodents was found to reduce Ca^{2+} in Kölliker's organ-supporting cells, leading to an increased hearing threshold (Rodriguez et al., 2012; Chen et al., 2021a); while Cx26 cKD mice also showed reduced ATP release, downregulation of ATP-dependent calcium signaling, the disappearance of calcium waves and increased hearing threshold in Kölliker's organ-supporting cells (Sun et al., 2022).

Kölliker's organ-supporting cells promote the formation of tectorial membrane in the organ of corti

Studies have shown that glycoproteins secreted by Kölliker's organ-supporting cells, such as otocollagen and capsid protein, are involved in the formation of the tectorial membrane (Hinojosa, 1977; Lim and Anniko, 1985; Zine and Romand, 1996). During early developmental stages, the tectorial membrane is attached to the Kölliker's organ-supporting cells by a network of thin filaments, which gradually separate as the cochlea matures, and about 2 weeks after birth, the tectorial membrane is completely separated from the Kölliker's organ and eventually extends to the out hair cells. Thyroid hormone is a key factor in regulating this process, and thyroid hormone deficiency prolongs the survival of Kölliker's organ-supporting cells and causes tectorial membrane malformations (Uziel et al., 1981).

PR-domain-containing 16 (PRDM16) is a key transcriptional regulator in craniofacial, adipose, and neural tissue development (Fumasoni et al., 2007; Shull et al., 2020). It was found that PRDM16 is highly expressed in the nuclei of Kölliker's organ-supporting cells in the bottom and middle cochlear apex by embryonic day 13.5 and decreases rapidly at birth. Its expression in the Kölliker's organ continued throughout development until postnatal day 7, and PRDM16 was thus suggested as a possible specific marker for Kölliker's organ-supporting cells (Ebeid et al., 2022). Further, by studying the model with Prdm16cGT double allele deletion mice, it was found that the cochlear Kölliker's organ of Prdm16 gene-deficient mice at day P0 had poor development, shortened cochlear ducts, reduced proliferation of Kölliker's organ-supporting cells, increased density of hair cells and supporting cells in the parietal ring, and loss of anchoring ability of the lid membrane to the Kölliker's organ, indicating that Prdm16 is a regulatory gene necessary for Kölliker's organ-supporting cells' proliferation (Ebeid et al., 2022). Cochlear duct development requires the proliferation of these cells for convergent extension and to achieve normal hair cells and supporting cell densities within the organ of Corti (Chen et al., 2002; Driver et al., 2017). In addition, gene expression analysis revealed that α-tectorin (TECTA) expression was downregulated and β-tectorin (TECTB) appeared upregulated in the cochlea of Prdm16cGT-deficient mice. α-TECTA and TECTB are essential proteins in the tectorial membrane (Richardson et al., 2008), and mutant mice with α-tectorin exhibit abnormal tectorial membrane and hearing loss (Legan et al., 2014; Kim et al., 2019), and the study hypothesized that deletion

of the Prdm16cGT gene leads to dysregulation of tectorin subunit expression, resulting in abnormal tectorial membrane morphology.

Kölliker's organ-supporting cells subtypes

Single-cell RNA transcriptome sequencing-based studies have revealed that Kölliker's organ-supporting cells also have different cellular subtypes (Chen et al., 2021b). The study, based on clustering analysis of cells with similar gene expression patterns, revealed the existence of four different cell subtypes in Kölliker's organ-supporting cells (Kolla et al., 2020; Chen et al., 2021b; Kubota et al., 2021). The Kubota et al. (2021) study of organoid development classified Kölliker's organ-supporting cells into three different cell subtypes. Gene expression localization showed that specific overexpressed genes were displayed in different regions of the Kölliker's organ and gradually degenerated and disappeared as the cochlea matured (Kubota et al., 2021). Chen et al. (2021b) identified four cell subsets from P1 to P14, of which the number of cells decreased gradually, while the other four cell subsets proliferated at P1 to P7 and completely disappeared at P14. These eight cell subpopulations were found to be closely linked on the t-SEN cell space map and had very similar gene expression patterns and biological properties (Kolla et al., 2020; Chen et al., 2021b; Kubota et al., 2021). Kamiya et al. (2001) also found that apoptosis and mitosis co-exist in Kölliker's organ-supporting cells at P7 postnatally and that the cells not only degenerate but also regenerate before disappearing around P12, demonstrating that mitotic proliferation of Kölliker's organ-supporting cells occurs not only in embryonic development but also in the development of the normal auditory system after birth.

Molecular mechanisms of Kölliker's organ-supporting cell degeneration

Impaired or delayed degeneration of the Kölliker's organ can lead to structural deformities of the organ of Corti, especially the organ of Corti lid (Uziel, 1986). However, the molecular mechanisms of Kölliker's organ-supporting cell degeneration are not clear.

Apoptosis induces programmed degeneration of Kölliker's organ-supporting cell

He and Yang (2015b) found that the morphology of Kölliker's organ-supporting cells in the neonatal P1, P3, P5, P10, P12, and P14 rat cochlea gradually changed from short columnar to tall columnar cell morphology from the basal turn to the apical turn and the number of cells also gradually decreased in addition to the change in cell morphology, presuming that apoptosis of Kölliker's organ-supporting cells exists during the development of the neonatal rat cochlea (He and Yang, 2015b). He and Yang (2015a,b) showed that Kölliker's organ-supporting cells exhibited a programmed apoptotic process from basal turn to the apical turn, but *in vitro* tests showed proliferation, suggesting that the initiating factor of apoptosis may come from outside the Kölliker's organ-supporting cells rather than from intrinsic cellular factors. On this basis, Hou et al. (2019, 2020) further found that the expression levels of caspase-3, caspase-8, caspase-9, and BCL-gene mRNA and protein in the cochlear basement membrane of rats at different days of age after birth were significantly time-dependent, and the study concluded that *in vivo* Kölliker's organ-supporting cells not only existed in apoptosis but also in proliferation. The number of proliferating cells is much less than the number of apoptotic cells, which eventually manifests in the tissue structure as the disappearance of Kölliker's organ-supporting cells (Hou et al., 2019, 2020).

Liu et al. (2017) investigated the morphological changes of Kölliker's organ-supporting cells and the expression of apoptosis-related factors during early postnatal development. It was found that on day P5, the Kölliker's organ in the basal turn of the cochlea became significantly smaller, while the Kölliker's organ in the middle and apical turn became smaller. On day P12 the cochlea showed the disappearance of the Kölliker's organ in the basal turn and middle turn, and at this stage, the Kölliker's organ in the apical turn was still present, but the number of cells was significantly reduced and its morphology changed from a high columnar to a short columnar shape. The results of immunohistochemistry and TUNEL staining showed the presence of necrotic cytomorphological changes in some TUNEL-positive Kölliker's organ-supporting cells at day P7, showing chromatin condensation and vacuole-like changes (Liu et al., 2017).

It was concluded that exogenous and endogenous apoptotic pathways exist during the apoptosis of supporting cells as the rat cochlear Kölliker's organ develops *in vivo*. After birth, the Kölliker's organ in the cochlea degenerates in a time-dependent pattern in which cysteine proteases are involved in apoptotic cell death during postnatal development, suggesting the involvement of endogenous factors (Adrain and Martin, 2001).

Apoptosis and proliferation co-exist during the degeneration of the Kölliker's organ, and the degenerative disappearance of the Kölliker's organ is thought to be a disturbance of the balance between apoptosis and mitosis (Kamiya et al., 2001). It is still unclear why such cell proliferation exists in Kölliker's organ-supporting cells at a later stage of their degenerative disappearance.

The regulatory role of thyroid hormone (T3) in the degeneration of the Kölliker's organ-supporting cells

The thyroid hormone is a key factor in guiding the orderly degeneration of the Kölliker's organ during cochlear development (Mustapha et al., 2009; Peeters et al., 2015; Sundaresan et al., 2016). Hypothyroidism and mutations in the thyroid hormone receptor beta gene cause delayed degeneration of the Kölliker's organ, while ectopic treatment with T3 (3,5-triiodo-L-thyroxine) on days P0 and P1 leads to earlier degeneration of the Kölliker's organ and hearing loss (Rusch et al., 2001; Peeters et al., 2015; Borse et al., 2021). Peeters et al. (2015) investigated the time course of apoptosis support by the Kölliker's organ and the effect of ectopic T3 on apoptosis. Furthermore, in methimazole-treated hypothyroid rat cochlea studies showed that Kölliker's organ-supporting cells lacked TUNEL-stained positive apoptotic cells at day P7. It has been reported that apoptosis in Kölliker's organ-supporting cells may be regulated by some unknown mechanism regulating the expression of the thyroid hormone receptor β gene in Kölliker's supporting cells and thus regulating this programmed apoptosis (Ng et al., 2013).

Studies have reported that immunoreactivity for the neurotrophin receptor p75NTR, a mediator of neuronal survival or differentiation, is detected in the Kölliker's organ of P5 rats and that this immunoreactivity changes in response to thyroxine (T4; Knipper et al., 1999). It is unclear whether p75NTR contributes to Kölliker's organ-supporting cell apoptosis (Sato et al., 2006). T3-induced Kölliker's organ-supporting cells' apoptosis is a unique cell- and time-specific form of apoptosis in the late mitotic phase of tissue maturation and may involve a series of pre-apoptotic events, including cellular reorganization and cellular translocation before the cell death phase, in addition to how this process is coordinated with other unknown signals together with other unknown signals, still need to be investigated in depth (Coen et al., 2007). Although it is not clear how premature remodeling leads to deafness, these studies suggest that cochlear development is a precisely ordered regulatory process and that T3 provides an important molecular signaling role in the orderly regulation of these remodeling events.

Autophagy regulates the programmed degeneration of Kölliker's organ-supporting cells

Several studies have reported the relationship between autophagy and hearing loss, and activation of autophagy can reduce noisiness (Guo et al., 2021), drug resistance (He et al., 2017; Liu et al., 2021; Zhang et al., 2022), and the degree of inner ear damage and hearing loss in the elderly (He et al., 2020, 2021). It was found that autophagy is closely related to the occurrence and development of sensorineural deafness (Zhou et al., 2020) and that autophagy activators can effectively reduce the level of oxidative stress in hair cells and decrease hair cell death, thus attenuating high-intensity noise-induced damage to hair cells (Li et al., 2018). In addition, autophagy also plays an important regulatory role during inner ear development and is essential for maintaining the morphology and function of auditory hair cells (Zhou et al., 2020).

The existence of autophagy during Kölliker's organ-supporting cell degeneration was investigated and a large number of autophagic vacuoles containing organelles was first detected by Hinojosa (Hinojosa, 1977). Autophagy markers, including LC3-II, SQSTM1/p62, and Beclin1, were detected in Kölliker's organ-supporting cells by immunohistochemical staining. In addition, it showed that during early postnatal cochlear development, the expression of LC3-II gradually decreased and the expression of p62 increased, compared with that between P7 and P10. Compared to apoptotic markers that peak at P1, autophagic flux peaks earlier at P1, and activated autophagic flux gradually decreases with the degeneration of Kölliker's organ-supporting cells from P1 until P14 (Hou et al., 2019).

Apoptosis and autophagy in Kölliker's organ-supporting cells show different time-dependent and sophisticated expression patterns, with the peak of autophagic activity during postnatal maturation of cochlear hearing development located on postnatal day 1 (P1) or earlier, while the expression of apoptotic markers (Bcl-2, caspase-3, caspase-8, and caspase-9) follows a bell-shaped curve, with peak expression at P3 (Qu et al., 2007). Organelles are digested by autophagy before apoptosis, and autophagy can provide a source of energy for the removal of aggregated proteins and damaged organelles, both of which play different roles at different stages of cochlear development (Aburto et al., 2012; Liu et al., 2017). These results suggest that autophagy plays an important early role in the pre-apoptotic transformation and degeneration of the Kölliker's organ during early postnatal development and that any disturbance in autophagy or apoptosis of Kölliker's organ-supporting cells during development will lead to impaired cochlear development and eventually cause hearing loss (He et al., 2017). Therefore, the dynamic balance between autophagy and apoptosis regulates the normal differentiation and orderly organization of developing cochlear supporting cells, but the regulatory mechanism of the dynamic balance between autophagy and apoptosis is currently unknown (He et al., 2017; Zhou et al., 2020). Abnormal intracellular calcium signaling mediated by Gjb2 may be a key regulator of abnormal alterations in the autophagy-apoptosis signaling pathway and still requires in-depth study (Inoshita et al., 2014; Sun et al., 2022).

Molecular signaling pathways of Kölliker's organ-supporting cells degeneration

Studies have confirmed that some important genes and signaling pathways play an important role in cochlear hearing development, such as Sox2 (Cheng et al., 2019), Pou4f3, and Atoh1 genes (Chen et al., 2021c); FGF (Tang et al., 2016), Notch (Ni et al., 2016; Waqas et al., 2016), FoxG1 (He et al., 2020, 2021), Strip1 (Zhang et al., 2021), mTOR (Fu et al., 2018, 2022) and Wnt signaling pathway (Chai et al., 2012; Liu et al., 2016). However, the molecular mechanisms of signaling pathways associated with the degenerative disappearance of Kölliker's organ-supporting cells early in postnatal cochlear hearing development are not clear. It has been proposed that Hedgehog signaling inhibits the sensory differentiation ability of Kölliker's organ-supporting cells, regulates the fate of Kölliker's organ-supporting cells, and induces cochlear developmental maturation (Driver et al., 2008).

Chen et al. (2021b) performed KEGG signaling pathway analysis in different subtypes of Kölliker's organ-supporting cells by scRNA-seq and found that genes in different subtypes of Kölliker's organ-supporting cells were significantly enriched in the Ribosome signaling pathway; however, in the Cluster 3, a large number of genes were enriched in the Ribosome signaling pathway and Protein digestion and absorption signaling pathway. The Ribosome signaling pathway is an important signaling pathway that regulates cell proliferation and development (Pelletier et al., 2018). The results of scRNA-seq showed that from P1 to P7, there was a significant proliferation of cell numbers, but cell numbers showed a decrease throughout Kölliker's organ-supporting cells development, presumably mainly associated with the PI3K-Akt signaling pathway, a negative regulatory pathway of gene expression in the Cluster 3. The PI3K-Akt signaling pathway is an important signaling pathway that regulates cell proliferation, differentiation, apoptosis, and migration (Jia et al., 2019; Bu et al., 2022). It has also been shown to regulate cochlear hair cell regeneration (Mullen et al., 2012; Xia W. et al., 2019). A large number of Col family genes on Cluster 3 are enriched in the PI3K-Akt signaling pathway, including Col4a1, Col4a2, Col6a1, Col6a2, and Col1a1, which are presumed to regulate the dynamic balance of proliferation and apoptosis in Kölliker's organ-supporting cells. The Col family genes Col3a1, Col5a1, Col5a2, Col6a1, and Col1a1 in the Cluster 0 regulate the autophagy of these apoptotic proteins and cellular debris and provide the energy required to promote the apoptotic process through autophagic catabolism (Komatsu et al., 2005), which in turn directs the Kölliker's organ-supporting cells under the sequential degeneration or trans-differentiation of Kölliker's organ-supporting cells. The role of this signaling pathway and related genes in regulating Kölliker's organ-supporting cell degeneration and auditory development needs to be further investigated. The proposed signal pathway diagram of the molecular mechanism of degeneration and trans-differentiation of Kölliker's organ-supporting cells has been shown in **Figure 2**.

Kölliker's organ-supporting cells have the potential to trans-differentiate into hair cells

Adult mammalian cochlear hair cells have no regenerative capacity, but studies have shown that newborn rodent cochlear basement membrane cells have a limited but transient regenerative potential, which is mainly derived from non-sensory cells in the cochlea (Chai et al., 2018). Under normal conditions, mitotic cells in the neonatal mouse cochlea are relatively quiescent, and early damage caused by various factors will indirectly activate these non-sensory cells to exert their limited regenerative potential to restore the damaged hair cell population and thus repair hearing (Gao et al., 2019; Liu W. et al., 2019; Chai et al., 2022). Kölliker's organ-supporting cells normally exist in the late mid-embryonic and early postnatal stages as a transient neonatal cell population, and it was found that some cell populations located in the Kölliker's organ region retain the properties of precursor cells, which can regenerate and transform and are the precursor cell pool for hair cell regeneration (Chai et al., 2011, 2012; Bramhall et al., 2014).

Math1 overexpression induces the trans-differentiation of Kölliker's organ-supporting cells into hair cells

Math1 is a homolog of the Drosophila gene, the deletion of which leads to failure of inner ear hair cell differentiation (Chen et al., 2002). It was found that induction of Math1 overexpression in Kölliker's organ-supporting cells led to the generation of a large number of ectopic hair cells, and these newborn ectopic hair cells were positive for myosin VIIa (a hair cell-specific marker) and could form keratin plates and stereocilia bundles (Zheng and Gao, 2000; Zhang et al., 2007).

Overexpression of Math1 resulted in the interdental cells of the organ of Corti and its adjacent organ of Corti, the internal sulcus, and the Hensen's cells regions, and axonal extension from the auditory nerve bundle to some of the new hair cells regions, suggesting that the new hair cells attract the guided regeneration of auditory spiral neurons (Gubbels et al., 2008).

The Kölliker's organ does not express the Math1 gene after birth and is normally expressed only in the embryonic sensory epithelium starting at E12.5, suggesting that the reason why Kölliker's organ-supporting cells do not continue to differentiate into hair cells after birth but gradually transform into internal sulci, most likely because of the absence of Math1 expression (Bermingham et al., 1999). Math1 is expressed in differentiated

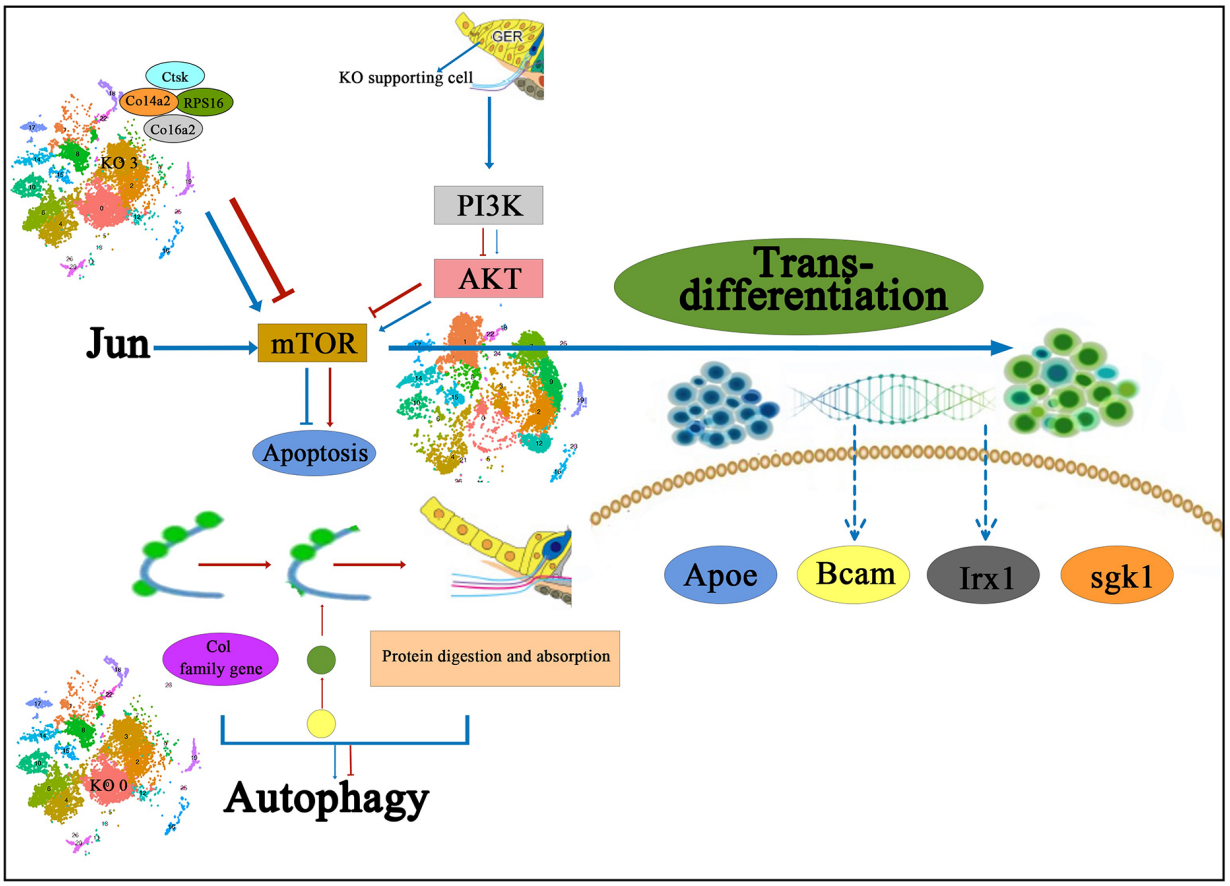

FIGURE 2
The proposed signal pathway diagram of the molecular mechanism of Kölliker's organ-supporting cells degeneration and trans-differentiation. It is shown that Col family genes on KO 3 and the PI3K-Akt signaling pathway are presumed to regulate the dynamic balance of proliferation and apoptosis in Kölliker's organ-supporting cells, and also the Col family genes in the KO 0 regulate the autophagy of these apoptotic proteins and cellular debris and provide the energy required to promote the apoptotic process. In addition, it has been proposed that the PI3K-Akt-mTOR signaling pathway may be one of the underlying mechanisms to induce the differentiation process of Kölliker's organ-supporting cells to hair cells. IHC, inner hair cells; KO 0, Cluster 0 of Kölliker's organ-supporting cells; KO 3, Cluster 3 of Kolliker's organ-supporting cells.

hair cells in the early embryonic stage but is downregulated in supporting cells in the late embryonic stage and is absent in cells outside the sensory epithelium (Chen et al., 2002; Woods et al., 2004). In addition, it was found that when cochlear organ cultures overexpressing Math1 caused the production of ectopic hair cells within the large and small epithelial crest regions, while knockdown of Hes1 also resulted in the production of ectopic hair cells and these hair cells showed elevated levels of Math1 expression (Zheng and Gao, 2000). The Hes1 gene is normally expressed only in the Kölliker's organ of P0–P3, suggesting that Hes1 may repress Math1 expression to some extent early in life, consistent with the idea that Hes5 is primarily involved in the precise regulation of ectopic hair cells (Zine et al., 2001; McGovern et al., 2018). Math1 is an essential gene for hair cell differentiation and plays a positive regulatory role, while Hes1 and Hes5 are negative regulators of hair cell differentiation (Zine et al., 2001; Su et al., 2015). Future attempts might be made to continue the differentiation of postnatal Kölliker's organ-supporting cells to hair cells by upregulating the expression levels of Math1 and or downregulating Hes1 in Kölliker's organ-supporting cells.

Atoh1 overexpression induced trans-differentiation of Kölliker's organ-supporting cells into hair cells

It was found that after induction of Atoh1 overexpression, ectopic hair cell regeneration occurred in different subtypes of Corti organelle supporting cells (Liu et al., 2012; Richardson and Atkinson, 2015; Walters et al., 2017; Yamashita et al., 2018). Kelly et al. (2012) identified a large number of isolated ectopic hair cells in the non-sensory Kölliker's organ region by constructing a triple allele TGATOH1 mouse model. These

ectopic hair cells displayed a stereocilia structure similar to that of mature hair cells, but exhibited different maturation and were scattered within the Kölliker's organ (Kelly et al., 2012). Ectopic hair cells regeneration occurs most vigorously in the Kölliker's organ region, but the efficiency of induced transformed hair cells remains low, compared to ectopic expression of Atoh1 alone, and it was shown that co-activation of Atoh1 with other transcription factors, such as Pou4f3, Gfi1, Gata3, and Nymc, induces more stem cells to trans-differentiate into hair cell-like cells, and the newly generated cells are more mature in both neonatal and mature mouse cochlea (Liu et al., 2012; Walters et al., 2017; Chen et al., 2021c). Xu et al. (2021) induced Atoh1 in Sox2-overexpressing positive progenitor cells in Kölliker's organ and found that ectopic expression of Atoh1 promoted the trans-differentiation of progenitor cells to hair cells regeneration while demonstrating the importance of the Isl1/Tub/Znf532 pathway in promoting Atoh1-mediated hair cells regeneration. All these studies suggest that the supporting cells in the lateral of the Kölliker's organ can serve as a source of progenitor cells for hair cell regeneration in the early postnatal period.

Lgr5-positive progenitor cells in the Kölliker's organ have the potential to generate cochlear hair cells

In the neonatal mouse cochlea, Wnt-responsive Lgr5-expressing cells are progenitors of regenerative hair cells, and upregulation of Wnt signaling stimulates the proliferation of Lgr5-positive progenitors (Chai et al., 2011, 2012). Lgr5 expression decreases gradually during cochlear development and maturation, mainly in IPs, and IPCs. In the adult cochlea, Lgr5 is only expressed in D3 s (Chai et al., 2012). Several studies have shown that Lgr5-labeled cochlear progenitor cells, following hair cell injury, can regenerate by mitosis and/or directly differentiate to generate new cochlear hair cells in the early postnatal period (Shi et al., 2012, 2013; Cox et al., 2014).

Recent studies have shown that multiple signaling pathways play an important role in hair cell regeneration by inducing proliferation and differentiation of Lg5 progenitor cells (Chen et al., 2021d). Activation of Wnt/β-linked protein signaling and inhibition of Notch signaling can induce Lgr5 progenitor cells to regenerate Myo7a-positive hair cells (Chai et al., 2012; Korrapati et al., 2013; Mizutari et al., 2013). Lgr5 progenitor cells can be regulated by many other factors and signaling pathways such as Shh, Foxg1, and Hippo (Gregorieff et al., 2015; Chen et al., 2017; Cheng et al., 2017; Zhang et al., 2020). The efficiency of regenerating hair cells from inner ear Lgr5 progenitor cells remains very limited, suggesting that hair cells regeneration involves other factors or signaling pathways (Wu et al., 2016; Lu et al., 2017; Fang et al., 2019; Xia L. et al., 2019). A previous study of hair cell regeneration and differentiation in the presence of SEC inhibitor flavopiridol showed that flavopiridol decreased the proliferative capacity of Lgr5 progenitor cells, but with no effect on the differentiation ability (Chen et al., 2021d). These results suggest that SEC plays an important role in regulating inner ear progenitor cells and thus influencing hair cells regeneration, and further *in vivo* studies are needed to elucidate the role of SEC in the inner ear, which will lay the experimental foundation for using cochlear progenitor cells to regenerate functional cochlea for the treatment of patients with sensorineural deafness.

Zhang et al. (2020) studied using $Sox2^{CreER/Foxg1loxp/loxp}$ mice and $Lgr5^{EGFPCreER/Foxg1loxp/loxp}$ mice to conditionally and specifically knock down Foxg1 in Sox2supporting cells and Lgr5 progenitor cells of neonatal mice, respectively and found that conditional knockdown of Foxg1 in both Sox2 supporting cells and Lgr5 progenitor cells at postnatal day 1 (P; cKD) resulted in the appearance of a large number of additional hair cells that In particular, more additional internal hair cells were generated at day P7, and these nascent hair cells with normal cilia bundles and synapses survived until at least P30. In addition, sphere formation assays showed that Foxg1 cKD in Lgr5 progenitor cells did not significantly alter their sphere formation capacity, and the findings suggest that Foxg1 cKD may directly trans-differentiate supporting cells and progenitor cells by inducing This study provides new evidence for the role of Foxg1 in regulating hair cell regeneration from supporting cells and progenitor cells in the neonatal mouse cochlea (Zhang et al., 2020).

BMI1 and cochlear hair cell regeneration

It was shown that Bmi1 regulates redox homeostasis and reactive oxygen species (ROS) levels and is expressed in hair cells and supporting cells in addition to spiral ligament and spiral ganglion cells, thus playing an important role in the survival of auditory hair cells (Chen et al., 2015). It was found that Bmi1 knockdown significantly reduced the sphere formation ability of neonatal mouse Corti organ-supporting cells and Lgr5-positive progenitor cells, suggesting that Bmi1 is required to initiate the proliferation of neonatal mouse supporting cells and progenitor cells (Lu et al., 2017). It was also found that in Bmi1 knockout neonatal mice, DKK1 expression was significantly upregulated, while β-linked protein and Lgr5 expression were significantly downregulated, suggesting that Bmi1 indirectly exercises its role as an activator of the Wnt signaling pathway by inhibiting the DKK family of Wnt inhibitors (Cho et al., 2013). Bmi1 plays an important role in regulating the proliferation of neonatal mouse cochlear supporting cells and Lgr5-positive progenitor cells through the Wnt signaling pathway, suggesting that Bmi1 may be a new therapeutic target for hair cell regeneration.

Downregulation of Ephrin-B2 signaling induced trans-differentiation of Kölliker's organ-supporting cells into hair cells

Ephrins and their Eph receptors are the large Eph family genes that control tissue morphogenesis and are divided into two subclasses, EphB and EphA, based on their affinity for transmembrane EphB ligands or the glycosylphosphatidylinositol-anchored ephrin-A (Gale et al., 1996). EphB and EphA play an important role in the boundary formation between adjacent cell types by interacting with specific EphB or EphA4 receptors (Dahmann et al., 2011). The previous study found that EphA4 receptors interacting with Ephrin-B2 (EphBs at the end of EphA4), is the only receptor to be exclusively expressed in the inner and outer hair cells (Bianchi and Liu, 1999; Miko et al., 2008). While Ephrin-B2 specifically restricted expression in the Kölliker's organ-supporting cells located medially to the inner hair cell layer from embryonic day (E) 16 and formed a gene-specific expression boundary. Such expression profile can distinguish adjacent supporting cells from hair cells and persists in the post-hearing onset (Defourny et al., 2015). Ephrin-B2 and EphA4 show complementary expression patterns in the developing organ of Corti, participate in sorting at the hair cell/support cell layer and play a key regulatory role in inducing the formation of different cell types in the organ of Corti. It has been hypothesized that cells migrating across non-lineage boundaries transfer their phenotype to fit the identity of their local neighbors, and thus manipulating these boundaries may be an unexpected strategy for generating additional hair cells (Defourny et al., 2011).

Defourny et al. (2015) showed that hair cells could arise directly from Kölliker's organ-supporting cells located at the medial border with inner hair cell layers by inhibiting Ephrin-B2 signaling. Through using soluble inhibitors, short hairpin RNA (shRNA)-mediated gene silencing, and Ephrin-B2 conditional knockout mice, it was found that at late embryonic stages (the normal hair cell generation phase), downregulation of Ephrin-B2 signaling resulted in translocation of supporting cells to the hair cells layers and subsequent switch in cell identity from supporting cell to hair cell fate. This study demonstrates that manipulation of Ephrin-B2 gene expression in the Kölliker's organ-supporting cells located at the medial border of the inner hair cell layer at the early stage can serve as a novel hair cell regeneration strategy to directly convert support cells to trans-differentiation hair cells.

Nevertheless, the exact mechanism of this cell fate change precisely occurs remains unclear. One possible explanation is that specific expression of the Sox2 transcription factor in supporting cells induces the differentiation process of supporting cells to hair cells (Millimaki et al., 2010). Furthermore, throughout cochlear development, ephrin-B2 and Notch have similar expression patterns in supporting cell types (Lanford et al., 1999), similar to the vascular regeneration model (Swift and Weinstein, 2009), and Ephrin-B2 may be a downstream target of Notch signaling involved in Notch signaling to couple cell separation and differentiation (Cheng et al., 2004; Tossell et al., 2011). Thus, the downregulation of Ephrin-B2 expression resulting in the absence of Notch signaling pathway components may weaken the fate of supporting cells and make them more susceptible to transition to the hair cell phenotype (Defourny et al., 2015). Further studies are still needed to reveal the underlying mechanisms of this trans-differentiation process.

Single-cell transcriptome sequencing reveals that Kölliker's organ-supporting cells have the potential to trans-differentiate into hair cells

Kolla et al. (2020) based on scRNA sequencing technology in E14 and E16 day mouse cochlea found two types of precursor cells expressing Cdkn1b and Sox2 marker genes, which these two groups of cells are located in the medial and lateral regions of the Kölliker' organ structure, respectively (Kolla et al., 2020). Furthermore, Kubota et al. (2021) used P2 day mice and similarly found that Kölliker's organ-supporting cell subtypes located in the lateral and medial regions can regenerate into hair cells and supporting cells.

Chen et al. (2021b) also showed that four cell subtypes gradually developed into two different trajectory directions, with one part towards the outer hair cells subtype, and the other part eventually shifting toward the fate of the inner hair cells. The analysis of cell developmental trajectories suggests that these four cell subtypes have the potential to trans-differentiate into inner and outer hair cells, two of which may have the potential to trans-differentiate into outer hair cells, and the other two subtypes have the potential to trans-differentiate into inner hair cells (Chen et al., 2021b).

Future research perspectives and prospects

Differentiation of Kölliker's organ-supporting cells to the hair cell phenotype can be induced by overexpression of Math1 and Atoh1 genes, such cells with differentiation potential are fewer and the cell transformation rate is lower (Zheng and Gao, 2000; Shou et al., 2003; Kelly et al., 2012). Therefore, future research should be devoted to improving the efficiency of Kölliker's organ-supporting cell trans-differentiation into hair cells, and establishing an

efficient and safe induction system. Meanwhile, how to induce the transformed neonatal hair cells to form functional mature cilia bundles and establish normal and durable synaptic connections with spiral ganglia (Chai et al., 2017; Li et al., 2019; Xia et al., 2020), to truly achieve functional recovery of neonatal hair cells, needs further study, and immortalized cell lines of hair cell progenitors need to be established.

In the future, there is still a need to optimize the conditions of mouse inner ear stem cell isolated culture and proliferation, to establish a safe and efficient technology system for differentiation of inner ear stem cells into mature hair cells (Wei et al., 2021; Guo et al., 2022; Hu et al., 2022; Tao et al., 2022), to screen mouse stem cell lines that can be used for stem cell therapy (Liu et al., 2018; Tang et al., 2019); discovering new molecular markers specific for inner ear hair cells and their precursor cells (Qi et al., 2019), thus providing conditions for the establishment of rapid and non-destructive cell identification and sorting techniques, and thus laying a solid theoretical foundation and providing technical support for stem cell therapy for sensorineural deafness technical support.

Author contributions

JC and DG drafted the manuscript. JY and LS revised the manuscript. All authors contributed to the article and approved the submitted version.

Funding

This study was funded by the National Natural Science Foundation of China (81873689, 82271179, and 82230035).

Acknowledgments

We are grateful to the National Natural Science Foundation for supporting this study, and to LC Sciences for their support and guidance.

Conflict of interest

The authors declare that the research was conducted in the absence of any commercial or financial relationships that could be construed as a potential conflict of interest.

Publisher's note

References

Aburto, M. R., Sánchez-Calderón, H., Hurlé, J. M., Varela-Nieto, I., and Magariños, M. (2012). Early otic development depends on autophagy for apoptotic cell clearance and neural differentiation. *Cell Death Dis.* 3:e394. doi: 10.1038/cddis.2012.132

Adrain, C., and Martin, S. J. (2001). The mitochondrial apoptosome: a killer unleashed by the cytochrome seas. *Trends Biochem. Sci.* 26, 390–397. doi: 10.1016/s0968-0004(01)01844-8

Bermingham, N. A., Hassan, B. A., Price, S. D., Vollrath, M. A., Ben-Arie, N., Eatock, R. A., et al. (1999). Math1: an essential gene for the generation of inner ear hair cells. *Science* 284, 1837–1841. doi: 10.1126/science.284.5421.1837

Beurg, M., Safieddine, S., Roux, I., Bouleau, Y., Petit, C., Dulon, D., et al. (2008). Calcium- and otoferlin-dependent exocytosis by immature outer hair cells. *J. Neurosci.* 28, 1798–1803. doi: 10.1523/JNEUROSCI.4653-07.2008

Bianchi, L. M., and Liu, H. (1999). Comparison of ephrin-A ligand EphA receptor distribution in the developing inner ear. *Anat. Rec.* 254, 127–134. doi: 10.1002/(SICI)1097-0185(19990101)254:1<127::AID-AR16>3.0.CO;2-Q

Blankenship, A. G., and Feller, M. B. (2010). Mechanisms underlying spontaneous patterned activity in developing neural circuits. *Nat. Rev. Neurosci.* 11, 18–29. doi: 10.1038/nrn2759

Borse, V., Kaur, T., Hinton, A., Ohlemiller, K., and Warchol, M. E. (2021). Programmed cell death recruits macrophages into the developing mouse cochlea. *Front. Cell. Dev. Biol.* 9:777836. doi: 10.3389/fcell.2021.777836

Bramhall, N. F., Shi, F., Arnold, K., Hochedlinger, K., and Edge, A. S. (2014). Lgr5-positive supporting cells generate new hair cells in the postnatal cochlea. *Stem Cell Rep.* 2, 311–322. doi: 10.1016/j.stemcr.2014.01.008

Bu, C., Xu, L., Han, Y., Wang, M., Wang, X., Liu, W., et al. (2022). c-Myb protects cochlear hair cells from cisplatin-induced damage via the PI3K/Akt signaling pathway. *Cell Death Discov.* 8:78. doi: 10.1038/s41420-022-00879-9

Chai, R., Kuo, B., Wang, T., Liaw, E. J., Xia, A., Jan, T. A., et al. (2012). Wnt signaling induces proliferation of sensory precursors in the postnatal mouse cochlea. *Proc. Natl. Acad. Sci. U S A* 109, 8167–8172. doi: 10.1073/pnas.1202774109

Chai, R., Li, G. L., Wang, J., and Huang, H. (2018). Hearing loss: reestablish the neural plasticity in regenerated spiral ganglion neurons and sensory hair cells 2018. *Neural Plast.* 2018:4759135. doi: 10.1155/2018/4759135

Chai, R., Li, G. L., Wang, J., and Zou, J. (2017). Hearing loss: reestablish the neural plasticity in regenerated spiral ganglion neurons and sensory hair cells. *Neural Plast.* 2017:1807581. doi: 10.1155/2017/1807581

Chai, R., Li, H., Yang, T., Sun, S., and Yuan, Y. (2022). Editorial: hearing loss: mechanisms and prevention. *Front. Cell. Dev. Biol.* 10:838271. doi: 10.3389/fcell.2022.838271

Chai, R., Xia, A., Wang, T., Jan, T. A., Hayashi, T., Bermingham-McDonogh, O., et al. (2011). Dynamic expression of Lgr5, a Wnt target gene, in the developing and mature mouse cochlea. *J. Assoc. Res. Otolaryngol.* 12, 455–469. doi: 10.1007/s10162-011-0267-2

Chen, J., Chen, P., He, B., Gong, T., Li, Y., Zhang, J., et al. (2021a). Connexin30-deficiency causes mild hearing loss with the reduction of endocochlear potential and ATP release. *Front. Cell. Neurosci.* 15:819194. doi: 10.3389/fncel.2021.819194

Chen, J., Gao, D., Chen, J., Hou, S., He, B., Li, Y., et al. (2021b). Single-Cell RNA sequencing analysis reveals greater epithelial ridge cells degeneration during postnatal development of cochlea in rats. *Front. Cell. Dev. Biol.* 9:719491. doi: 10.3389/fcell.2021.719491

Chen, P., Johnson, J. E., Zoghbi, H. Y., and Segil, N. (2002). The role of Math1 in inner ear development: uncoupling the establishment of the sensory primordium from hair cell fate determination. *Development* 129, 2495–2505. doi: 10.1242/dev.129.10.2495

Chen, Y., Li, L., Ni, W., Zhang, Y., Sun, S., Miao, D., et al. (2015). Bmi1 regulates auditory hair cell survival by maintaining redox balance. *Cell Death Dis.* 6:e1605. doi: 10.1038/cddis.2014.549

Chen, Y., Gu, Y., Li, Y., Li, G. L., Chai, R., Li, W., et al. (2021c). Generation of mature and functional hair cells by co-expression of Gfi1, Pou4f3 and Atoh1 in the postnatal mouse cochlea. *Cell Rep.* 35:109016. doi: 10.1016/j.celrep.2021.109016

Chen, Y., Qiang, R., Zhang, Y., Cao, W., Wu, L., Jiang, P., et al. (2021d). The expression and roles of the super elongation complex in mouse cochlear Lgr5+ progenitor cells. *Front. Cell. Neurosci.* 15:735723. doi: 10.3389/fncel.2021.735723

Chen, Y., Lu, X., Guo, L., Ni, W., Zhang, Y., Zhao, L., et al. (2017). Hedgehog signaling promotes the proliferation and subsequent hair cell formation of progenitor cells in the neonatal mouse cochlea. *Front. Mol. Neurosci.* 10:426. doi: 10.3389/fnmol.2017.00426

Cheng, C., Guo, L., Lu, L., Xu, X., Zhang, S., Gao, J., et al. (2017). Characterization of the transcriptomes of Lgr5+ hair cell progenitors and Lgr5- supporting cells in the mouse cochlea. *Front. Mol. Neurosci.* 10:122. doi: 10.3389/fnmol.2017.00122

Cheng, C., Wang, Y., Guo, L., Lu, X., Zhu, W., Muhammad, W., et al. (2019). Age-related transcriptome changes in Sox2+ supporting cells in the mouse cochlea. *Stem Cell Res. Ther.* 10:365. doi: 10.1186/s13287-019-1437-0

Cheng, Y. C., Amoyel, M., Qiu, X., Jiang, Y. J., Xu, Q., Wilkinson, D. G., et al. (2004). Notch activation regulates the segregation and differentiation of rhombomere boundary cells in the zebrafish hindbrain. *Dev. Cell* 6, 539–550. doi: 10.1016/s1534-5807(04)00097-8

Cho, J. H., Dimri, M., and Dimri, G. P. (2013). A positive feedback loop regulates the expression of polycomb group protein BMI1 via WNT signaling pathway. *J. Biol. Chem.* 288, 3406–3418. doi: 10.1074/jbc.M112.422931

Coen, L., Le Blay, K., Rowe, I., and Demeneix, B. A. (2007). Caspase-9 regulates apoptosis/proliferation balance during metamorphic brain remodeling in Xenopus. *Proc. Natl. Acad. Sci. U S A* 104, 8502–8507. doi: 10.1073/pnas.0608877104

Cox, B. C., Chai, R., Lenoir, A., Liu, Z., Zhang, L., Nguyen, D. H., et al. (2014). Spontaneous hair cell regeneration in the neonatal mouse cochlea *in vivo*. *Development* 141, 816–829. doi: 10.1242/dev.103036

Dahmann, C., Oates, A. C., and Brand, M. (2011). Boundary formation and maintenance in tissue development. *Nat. Rev. Genet.* 12, 43–55. doi: 10.1038/nrg2902

Dayaratne, M. W., Vlajkovic, S. M., Lipski, J., and Thorne, P. R. (2014). Kölliker's organ and the development of spontaneous activity in the auditory system: implications for hearing dysfunction. *Biomed. Res. Int.* 2014:367939. doi: 10.1155/2014/367939

Defourny, J., Lallemend, F., and Malgrange, B. (2011). Structure and development of cochlear afferent innervation in mammals. *Am. J. Physiol. Cell Physiol.* 301, C750–C761. doi: 10.1152/ajpcell.00516.2010

Defourny, J., Mateo Sánchez, S., Schoonaert, L., Robberecht, W., Davy, A., Nguyen, L., et al. (2015). Cochlear supporting cell transdifferentiation and integration into hair cell layers by inhibition of ephrin-B2 signalling. *Nat. Commun.* 6:7017. doi: 10.1038/ncomms8017

Driver, E. C., Northrop, A., and Kelley, M. W. (2017). Cell migration, intercalation and growth regulate mammalian cochlear extension. *Development* 144, 3766–3776. doi: 10.1242/dev.151761

Driver, E. C., Pryor, S. P., Hill, P., Turner, J., Rüther, U., Biesecker, L. G., et al. (2008). Hedgehog signaling regulates sensory cell formation and auditory function in mice and humans. *J. Neurosci.* 28, 7350–7358. doi: 10.1523/JNEUROSCI.0312-08.2008

Ebeid, M., Barnas, K., Zhang, H., Yaghmour, A., Noreikaite, G., and Bjork, B. C. (2022). PRDM16 expression and function in mammalian cochlear development. *Dev. Dyn.* doi: 10.1002/dvdy.480. [Online ahead of print].

Fang, Q., Zhang, Y., Chen, X., Li, H., Cheng, L., Zhu, W., et al. (2019). Three-dimensional graphene enhances neural stem cell proliferation through metabolic regulation. *Front. Bioeng. Biotechnol.* 7:436. doi: 10.3389/fbioe.2019.00436

Forsythe, I. D. (2007). Hearing: a fantasia on Kölliker's organ. *Nature* 450, 43–44. doi: 10.1038/450043a

Fu, X., Li, P., Zhang, L., Song, Y., An, Y., Zhang, A., et al. (2022). Activation of Rictor/mTORC2 signaling acts as a pivotal strategy to protect against sensorineural hearing loss. *Proc. Natl. Acad. Sci. U S A* 119:e2107357119. doi: 10.1073/pnas.2107357119

Fu, X., Sun, X., Zhang, L., Jin, Y., Chai, R., Yang, L., et al. (2018). Tuberous sclerosis complex-mediated mTORC1 overactivation promotes age-related hearing loss. *J. Clin. Invest.* 128, 4938–4955. doi: 10.1172/JCI98058

Fumasoni, I., Meani, N., Rambaldi, D., Scafetta, G., Alcalay, M., Ciccarelli, F. D., et al. (2007). Family expansion and gene rearrangements contributed to the functional specialization of PRDM genes in vertebrates. *BMC Evol. Biol.* 7:187. doi: 10.1186/1471-2148-7-187

Gale, N. W., Holland, S. J., Valenzuela, D. M., Flenniken, A., Pan, L., Ryan, T. E., et al. (1996). Eph receptors and ligands comprise two major specificity subclasses and are reciprocally compartmentalized during embryogenesis. *Neuron* 17, 9–19. doi: 10.1016/s0896-6273(00)80276-7

Gao, S., Cheng, C., Wang, M., Jiang, P., Zhang, L., Wang, Y., et al. (2019). Blebbistatin inhibits neomycin-induced apoptosis in hair cell-like HEI-OC-1 cells and in cochlear hair cells. *Front. Cell. Neurosci.* 13:590. doi: 10.3389/fncel.2019.00590

Geal-Dor, M., Freeman, S., Li, G., and Sohmer, H. (1993). Development of hearing in neonatal rats: air and bone conducted ABR thresholds. *Hear. Res.* 69, :236–242. doi: 10.1016/0378-5955(93)90113-f

Giorgi, C., Danese, A., Missiroli, S., Patergnani, S., and Pinton, P. (2018). Calcium dynamics as a machine for decoding signals. *Trends Cell Biol.* 28, 258–273. doi: 10.1016/j.tcb.2018.01.002

Goodenough, D. A., and Paul, D. L. (2009). Gap junctions. *Cold. Spring. Harb. Perspect. Biol.* 1:a002576. doi: 10.1101/cshperspect.a002576

Gregorieff, A., Liu, Y., Inanlou, M. R., Khomchuk, Y., and Wrana, J. L. (2015). Yap-dependent reprogramming of $Lgr5^{+}$ stem cells drives intestinal regeneration and cancer. *Nature* 526, 715–718. doi: 10.1038/nature15382

Gubbels, S. P., Woessner, D. W., Mitchell, J. C., Ricci, A. J., and Brigande, J. V. (2008). Functional auditory hair cells produced in the mammalian cochlea by in utero gene transfer. *Nature* 455, 537–541. doi: 10.1038/nature07265

Guo, L., Cao, W., Niu, Y., He, S., Chai, R., Yang, J., et al. (2021). Autophagy regulates the survival of hair cells and spiral ganglion neurons in cases of noise, ototoxic drug and age-induced sensorineural hearing loss. *Front. Cell. Neurosci.* 15:760422. doi: 10.3389/fncel.2021.760422

Guo, R., Xiao, M., Zhao, W., Zhou, S., Hu, Y., Liao, M., et al. (2022). 2D Ti(3)C(2)T(x)MXene couples electrical stimulation to promote proliferation and neural differentiation of neural stem cells. *Acta Biomater.* 139, 105–117. doi: 10.1016/j.actbio.2020.12.035

He, S., and Yang, J. (2011). Maturation of neurotransmission in the developing rat cochlea: immunohistochemical evidence from differential expression of synaptophysin and synaptobrevin 2. *Eur. J. Histochem.* 55:e2. doi: 10.4081/ejh.2011.e2

He, Y., and Yang, J. (2015a). ATP release mechanism from the supporting cells in the Kölliker organ in vitro in the cochlea of newborn rat. *Zhonghua Er Bi Yan Hou Tou Jing Wai Ke Za Zhi* 50, 43–49. doi: 10.3760/cma.j.issn.1673-0860.2015.01.010

He, Y., and Yang, J. (2015b). The study on the proliferation and the apoptosis factors in vitro of Kölliker organ supporting cells in the cochlea of newborn rat. *Lin Chung Er Bi Yan Hou Tou Jing Wai Ke Za Zhi* 29, 152–159. doi: 10.13201/j.issn.1001-1781.2015.02.015

He, Z., Guo, L., Shu, Y., Fang, Q., Zhou, H., Liu, Y., et al. (2017). Autophagy protects auditory hair cells against neomycin-induced damage. *Autophagy* 13, 1884–1904. doi: 10.1080/15548627.2017.1359449

He, Z. H., Li, M., Fang, Q. J., Liao, F. L., Zou, S. Y., Wu, X., et al. (2021). FOXG1 promotes aging inner ear hair cell survival through activation of the autophagy pathway. *Autophagy* 17, 4341–4362. doi: 10.1080/15548627.2021.1916194

He, Z. H., Zou, S. Y., Li, M., Liao, F. L., Wu, X., Sun, H. Y., et al. (2020). The nuclear transcription factor FoxG1 affects the sensitivity of mimetic aging hair cells to inflammation by regulating autophagy pathways. *Redox. Biol.* 28:101364. doi: 10.1016/j.redox.2019.101364

Hinojosa, R. (1977). A note on development of Corti's organ. *Acta Otolaryngol.* 84, 238–251. doi: 10.3109/00016487709123963

Hochman, J. B., Stockley, T. L., Shipp, D., Lin, V. Y., Chen, J. M., Nedzelski, J. M., et al. (2010). Prevalence of Connexin 26 (GJB2) and Pendred (SLC26A4) mutations in a population of adult cochlear implant candidates. *Otol. Neurotol.* 31, 919–922. doi: 10.1097/MAO.0b013e3181e3d324

Hou, S., Chen, P., Chen, J., Chen, J., Sun, L., Chen, J., et al. (2020). Distinct expression patterns of apoptosis and autophagy-associated proteins and genes during postnatal development of spiral ganglion neurons in rat. *Neural Plast.* 2020:9387560. doi: 10.1155/2020/9387560

Hou, S., Chen, J., and Yang, J. (2019). Autophagy precedes apoptosis during degeneration of the Kölliker's organ in the development of rat cochlea. *Eur. J. Histochem.* 63:3025. doi: 10.4081/ejh.2019.3025

Hu, Y., Chen, Z., Wang, H., Guo, J., Cai, J., Chen, X., et al. (2022). Conductive nerve guidance conduits based on morpho butterfly wings for peripheral nerve repair. *ACS Nano* 16, 1868–1879. doi: 10.1021/acsnano.1c11627

Inoshita, A., Karasawa, K., Funakubo, M., Miwa, A., Ikeda, K., and Kamiya, K. (2014). Dominant negative connexin26 mutation R75W causing severe hearing loss influences normal programmed cell death in postnatal organ of Corti. *BMC Genet.* 15:1. doi: 10.1186/1471-2156-15-1

Jia, X., Wen, Z., Sun, Q., Zhao, X., Yang, H., Shi, X., et al. (2019). Apatinib suppresses the proliferation and apoptosis of gastric cancer cells via the PI3K/Akt signaling pathway. *J. BUON* 24, 1985–1991.

Johnson, S. L., Ceriani, F., Houston, O., Polishchuk, R., Polishchuk, E., Crispino, G., et al. (2017). Connexin-mediated signaling in nonsensory cells is crucial for the development of sensory inner hair cells in the mouse cochlea. *J. Neurosci.* 37, 258–268. doi: 10.1523/JNEUROSCI.2251-16.2016

Kamiya, K., Takahashi, K., Kitamura, K., Momoi, T., and Yoshikawa, Y. (2001). Mitosis and apoptosis in postnatal auditory system of the C3H/He strain. *Brain Res.* 901, 296–302. doi: 10.1016/s0006-8993(01)02300-9

Kelly, M. C., Chang, Q., Pan, A., Lin, X., and Chen, P. (2012). Atoh1 directs the formation of sensory mosaics and induces cell proliferation in the postnatal mammalian cochlea *in vivo*. *J. Neurosci.* 32, 6699–6710. doi: 10.1523/JNEUROSCI.5420-11.2012

Kim, D. K., Kim, J. A., Park, J., Niazi, A., Almishaal, A., and Park, S. (2019). The release of surface-anchored α-tectorin, an apical extracellular matrix protein, mediates tectorial membrane organization. *Sci. Adv.* 5:eaay6300. doi: 10.1126/sciadv.aay6300

Knipper, M., Gestwa, L., Ten Cate, W. J., Lautermann, J., Brugger, H., Maier, H., et al. (1999). Distinct thyroid hormone-dependent expression of TrKB and p75NGFR in nonneuronal cells during the critical TH-dependent period of the cochlea. *J. Neurobiol.* 38, 338–356.

Kolla, L., Kelly, M. C., Mann, Z. F., Anaya-Rocha, A., Ellis, K., Lemons, A., et al. (2020). Characterization of the development of the mouse cochlear epithelium at the single cell level. *Nat. Commun.* 11:2389. doi: 10.1038/s41467-020-16113-y

Komatsu, M., Waguri, S., Ueno, T., Iwata, J., Murata, S., Tanida, I., et al. (2005). Impairment of starvation-induced and constitutive autophagy in Atg7-deficient mice. *J. Cell. Biol.* 169, 425–434. doi: 10.1083/jcb.200412022

Korrapati, S., Roux, I., Glowatzki, E., and Doetzlhofer, A. (2013). Notch signaling limits supporting cell plasticity in the hair cell-damaged early postnatal murine cochlea. *PLoS One* 8:e73276. doi: 10.1371/journal.pone.0073276

Kubota, M., Scheibinger, M., Jan, T. A., and Heller, S. (2021). Greater epithelial ridge cells are the principal organoid-forming progenitors of the mouse cochlea. *Cell Rep.* 34:108646. doi: 10.1016/j.celrep.2020.108646

Lanford, P. J., Lan, Y., Jiang, R., Lindsell, C., Weinmaster, G., Gridley, T., et al. (1999). Notch signalling pathway mediates hair cell development in mammalian cochlea. *Nat. Genet.* 21, 289–292. doi: 10.1038/6804

Legan, P. K., Goodyear, R. J., Morín, M., Mencia, A., Pollard, H., Olavarrieta, L., et al. (2014). Three deaf mice: mouse models for TECTA-based human hereditary deafness reveal domain-specific structural phenotypes in the tectorial membrane. *Hum. Mol. Genet.* 23, 2551–2568. doi: 10.1093/hmg/ddt646

Lelli, A., Asai, Y., Forge, A., Holt, J. R., and Géléoc, G. S. (2009). Tonotopic gradient in the developmental acquisition of sensory transduction in outer hair cells of the mouse cochlea. *J. Neurophysiol.* 101, 2961–2973. doi: 10.1152/jn.00136.2009

Li, G., Chen, K., You, D., Xia, M., Li, W., Fan, S., et al. (2019). Laminin-coated electrospun regenerated silk fibroin mats promote neural progenitor cell proliferation, differentiation and survival *in vitro*. *Front. Bioeng. Biotechnol.* 7:190. doi: 10.3389/fbioe.2019.00190

Li, H., Song, Y., He, Z., Chen, X., Wu, X., Li, X., et al. (2018). Meclofenamic acid reduces reactive oxygen species accumulation and apoptosis, inhibits excessive autophagy and protects hair cell-like HEI-OC1 cells from cisplatin-induced damage. *Front. Cell. Neurosci.* 12:139. doi: 10.3389/fncel.2018.00139

Liang, Y., Huang, L., and Yang, J. (2009). Differential expression of ryanodine receptor in the developing rat cochlea. *Eur. J. Histochem.* 53:e30. doi: 10.4081/ejh.2009.e30

Lim, D. J. (1986). Functional structure of the organ of Corti: a review. *Hear. Res.* 22, 117–146. doi: 10.1016/0378-5955(86)90089-4

Lim, D. J., and Anniko, M. (1985). Developmental morphology of the mouse inner ear. A scanning electron microscopic observation. *Acta Otolaryngol. Suppl.* 422, 1–69.

Liu, J., Cai, L., He, Y., and Yang, J. (2017). Apoptosis pattern and alterations of expression of apoptosis-related factors of supporting cells in Kölliker's organ *in vivo* in early stage after birth in rats. *Eur. J. Histochem.* 61:2706. doi: 10.4081/ejh.2017.2706

Liu, L., Chen, Y., Qi, J., Zhang, Y., He, Y., Ni, W., et al. (2016). Wnt activation protects against neomycin-induced hair cell damage in the mouse cochlea. *Cell Death Dis.* 7:e2136. doi: 10.1038/cddis.2016.35

Liu, Z., Dearman, J. A., Cox, B. C., Walters, B. J., Zhang, L., Ayrault, O., et al. (2012). Age-dependent in vivo conversion of mouse cochlear pillar and Deiters' cells to immature hair cells by Atoh1 ectopic expression. *J. Neurosci.* 32, 6600–6610. doi: 10.1523/JNEUROSCI.0818-12.2012

Liu, Y., Qi, J., Chen, X., Tang, M., Chu, C., Zhu, W., et al. (2019). Critical role of spectrin in hearing development and deafness. *Sci. Adv.* 5:eaav7803. doi: 10.1126/sciadv.aav7803

Liu, Z., Tang, M., Zhao, J., Chai, R., and Kang, J. (2018). Looking into the future: toward advanced 3D biomaterials for stem-cell-based regenerative medicine. *Adv. Mater.* 30:e1705388. doi: 10.1002/adma.201705388

Liu, W., Xu, X., Fan, Z., Sun, G., Han, Y., Zhang, D., et al. (2019). Wnt signaling activates TP53-induced glycolysis and apoptosis regulator and protects against cisplatin-induced spiral ganglion neuron damage in the mouse cochlea. *Antioxid. Redox Signal.* 30, 1389–1410. doi: 10.1089/ars.2017.7288

Liu, W., Xu, L., Wang, X., Zhang, D., Sun, G., Wang, M., et al. (2021). PRDX1 activates autophagy via the PTEN-AKT signaling pathway to protect against cisplatin-induced spiral ganglion neuron damage. *Autophagy* 17, 4159–4181. doi: 10.1080/15548627.2021.1905466

Lu, X., Sun, S., Qi, J., Li, W., Liu, L., Zhang, Y., et al. (2017). Bmi1 regulates the proliferation of cochlear supporting cells via the canonical Wnt signaling pathway. *Mol. Neurobiol.* 54, 1326–1339. doi: 10.1007/s12035-016-9686-8

Mammano, F. (2013). ATP-dependent intercellular Ca^{2+} signaling in the developing cochlea: facts, fantasies and perspectives. *Semin. Cell Dev. Biol.* 24, 31–39. doi: 10.1016/j.semcdb.2012.09.004

Marcotti, W. (2012). Functional assembly of mammalian cochlear hair cells. *Exp. Physiol.* 97, 438–451. doi: 10.1113/expphysiol.2011.059303

Mazzarda, F., D'Elia, A., Massari, R., De Ninno, A., Bertani, F. R., Businaro, L., et al. (2020). Organ-on-chip model shows that ATP release through connexin hemichannels drives spontaneous Ca^{2+} signaling in non-sensory cells of the greater epithelial ridge in the developing cochlea. *Lab Chip* 20, 3011–3023. doi: 10.1039/d0lc00427h

McGovern, M. M., Zhou, L., Randle, M. R., and Cox, B. C. (2018). Spontaneous hair cell regeneration is prevented by increased notch signaling in supporting cells. *Front. Cell Neurosci.* 12:120. doi: 10.3389/fncel.2018.00120

Miko, I. J., Henkemeyer, M., and Cramer, K. S. (2008). Auditory brainstem responses are impaired in EphA4 and ephrin-B2 deficient mice. *Hear. Res.* 235, 39–46. doi: 10.1016/j.heares.2007.09.003

Millimaki, B. B., Sweet, E. M., and Riley, B. B. (2010). Sox2 is required for maintenance and regeneration, but not initial development, of hair cells in the zebrafish inner ear. *Dev. Biol.* 338, 262–269. doi: 10.1016/j.ydbio.2009.12.011

Mizutari, K., Fujioka, M., Hosoya, M., Bramhall, N., Okano, H. J., Okano, H., et al. (2013). Notch inhibition induces cochlear hair cell regeneration and recovery of hearing after acoustic trauma. *Neuron* 77, 58–69. doi: 10.1016/j.neuron.2012.10.032

Mullen, L. M., Pak, K. K., Chavez, E., Kondo, K., Brand, Y., and Ryan, A. F. (2012). Ras/p38 and PI3K/Akt but not Mek/Erk signaling mediate BDNF-induced neurite formation on neonatal cochlear spiral ganglion explants. *Brain Res.* 1430, 25–34. doi: 10.1016/j.brainres.2011.10.054

Mustapha, M., Fang, Q., Gong, T. W., Dolan, D. F., Raphael, Y., Camper, S. A., et al. (2009). Deafness and permanently reduced potassium channel gene expression and function in hypothyroid Pit1dw mutants. *J. Neurosci.* 29, 1212–1223. doi: 10.1523/JNEUROSCI.4957-08.2009

Ng, L., Kelley, M. W., and Forrest, D. (2013). Making sense with thyroid hormone–the role of T_3 in auditory development. *Nat. Rev. Endocrinol.* 9, 296–307. doi: 10.1038/nrendo.2013.58

Ni, W., Zeng, S., Li, W., Chen, Y., Zhang, S., Tang, M., et al. (2016). Wnt activation followed by Notch inhibition promotes mitotic hair cell regeneration in the postnatal mouse cochlea. *Oncotarget* 7, 66754–66768. doi: 10.18632/oncotarget.11479

Nishani Dayaratne, M. W., Vlajkovic, S. M., Lipski, J., and Thorne, P. R. (2015). Putative role of border cells in generating spontaneous morphological activity within Kölliker's organ. *Hear. Res.* 330, 90–97. doi: 10.1016/j.heares.2015.06.017

Peeters, R. P., Ng, L., Ma, M., and Forrest, D. (2015). The timecourse of apoptotic cell death during postnatal remodeling of the mouse cochlea and its premature

onset by triiodothyronine (T3). *Mol. Cell. Endocrinol.* 407, 1–8. doi: 10.1016/j.mce.2015.02.025

Pelletier, J., Thomas, G., and Volarević, S. (2018). Ribosome biogenesis in cancer: new players and therapeutic avenues. *Nat. Rev. Cancer* 18, 51–63. doi: 10.1038/nrc.2017.104

Peng, Y., Chen, J., He, S., Yang, J., and Wu, H. (2012). Release of ATP from marginal cells in the cochlea of neonatal rats can be induced by changes in extracellular and intracellular ion concentrations. *PLoS One* 7:e47124. doi: 10.1371/journal.pone.0047124

Qi, J., Liu, Y., Chu, C., Chen, X., Zhu, W., Shu, Y., et al. (2019). A cytoskeleton structure revealed by super-resolution fluorescence imaging in inner ear hair cells. *Cell Discov.* 5:12. doi: 10.1038/s41421-018-0076-4

Qu, X., Zou, Z., Sun, Q., Luby-Phelps, K., Cheng, P., Hogan, R. N., et al. (2007). Autophagy gene-dependent clearance of apoptotic cells during embryonic development. *Cell* 128, 931–946. doi: 10.1016/j.cell.2006.12.044

Richardson, R. T., and Atkinson, P. J. (2015). Atoh1 gene therapy in the cochlea for hair cell regeneration. *Expert Opin. Biol. Ther.* 15, 417–430. doi: 10.1517/14712598.2015.1009889

Richardson, G. P., Lukashkin, A. N., and Russell, I. J. (2008). The tectorial membrane: one slice of a complex cochlear sandwich. *Curr. Opin. Otolaryngol. Head Neck Surg.* 16, 458–464. doi: 10.1097/MOO.0b013e32830e20c4

Rodriguez, L., Simeonato, E., Scimemi, P., Anselmi, F., Calì, B., Crispino, G., et al. (2012). Reduced phosphatidylinositol 4,5-bisphosphate synthesis impairs inner ear $Ca2^{+}$ signaling and high-frequency hearing acquisition. *Proc. Natl. Acad. Sci. U S A* 109, 14013–14018. doi: 10.1073/pnas.1211869109

Rusch, A., Ng, L., Goodyear, R., Oliver, D., Lisoukov, I., Vennstrom, B., et al. (2001). Retardation of cochlear maturation and impaired hair cell function caused by deletion of all known thyroid hormone receptors. *J. Neurosci.* 21, 9792–9800. doi: 10.1523/JNEUROSCI.21-24-09792.2001

Sato, T., Doi, K., Taniguchi, M., Yamashita, T., Kubo, T., and Tohyama, M. (2006). Progressive hearing loss in mice carrying a mutation in the p75 gene. *Brain Res.* 1091, 224–234. doi: 10.1016/j.brainres.2005.12.104

Sendin, G., Bourien, J., Rassendren, F., Puel, J. L., and Nouvian, R. (2014). Spatiotemporal pattern of action potential firing in developing inner hair cells of the mouse cochlea. *Proc. Natl. Acad. Sci. U S A* 111, 1999–2004. doi: 10.1073/pnas.1319615111

Shi, F., Hu, L., and Edge, A. S. (2013). Generation of hair cells in neonatal mice by β-catenin overexpression in Lgr5-positive cochlear progenitors. *Proc. Natl. Acad. Sci. U S A* 110, 13851–13856. doi: 10.1073/pnas.1219952110

Shi, F., Kempfle, J. S., and Edge, A. S. (2012). Wnt-responsive Lgr5-expressing stem cells are hair cell progenitors in the cochlea. *J. Neurosci.* 32, 9639–9648. doi: 10.1523/JNEUROSCI.1064-12.2012

Shou, J., Zheng, J. L., and Gao, W. Q. (2003). Robust generation of new hair cells in the mature mammalian inner ear by adenoviral expression of Hath1. *Mol. Cell. Neurosci.* 23, 169–179. doi: 10.1016/s1044-7431(03)00066-6

Shull, L. C., Sen, R., Menzel, J., Goyama, S., Kurokawa, M., and Artinger, K. B. (2020). The conserved and divergent roles of Prdm3 and Prdm16 in zebrafish and mouse craniofacial development. *Dev. Biol.* 461, 132–144. doi: 10.1016/j.ydbio.2020.02.006

Su, Y. X., Hou, C. C., and Yang, W. X. (2015). Control of hair cell development by molecular pathways involving Atoh1, Hes1 and Hes5. *Gene* 558, 6–24. doi: 10.1016/j.gene.2014.12.054

Sun, L., Gao, D., Chen, J., Hou, S., Li, Y., Huang, Y., et al. (2022). Failure Of hearing acquisition in mice with reduced expression of connexin 26 correlates with the abnormal phasing of apoptosis relative to autophagy and defective ATP-dependent Ca^{2+} signaling in Kölliker's Organ. *Front. Cell. Neurosci.* 16:816079. doi: 10.3389/fncel.2022.816079

Sundaresan, S., Kong, J. H., Fang, Q., Salles, F. T., Wangsawihardja, F., Ricci, A. J., et al. (2016). Thyroid hormone is required for pruning, functioning and long-term maintenance of afferent inner hair cell synapses. *Eur. J. Neurosci.* 43, 148–161. doi: 10.1111/ejn.13081

Swift, M. R., and Weinstein, B. M. (2009). Arterial-venous specification during development. *Circ. Res.* 104, 576–588. doi: 10.1161/CIRCRESAHA.108.188805

Tang, M., Li, J., He, L., Guo, R., Yan, X., Li, D., et al. (2019). Transcriptomic profiling of neural stem cell differentiation on graphene substrates. *Colloids Surf. B Biointerfaces* 182:110324. doi: 10.1016/j.colsurfb.2019.06.054

Tang, D., Lin, Q., He, Y., Chai, R., and Li, H. (2016). Inhibition of H3K9me2 reduces hair cell regeneration after hair cell loss in the zebrafish lateral line by down-regulating the Wnt and Fgf signaling pathways. *Front. Mol. Neurosci.* 9:39. doi: 10.3389/fnmol.2016.00039

Tao, Y., Liu, X., Yang, L., Chu, C., Tan, F., Yu, Z., et al. (2022). AAV-ie-K558R mediated cochlear gene therapy and hair cell regeneration. *Signal Transduct. Target. Ther.* 7:109. doi: 10.1038/s41392-022-00938-8

Tossell, K., Kiecker, C., Wizenmann, A., Lang, E., and Irving, C. (2011). Notch signalling stabilises boundary formation at the midbrain-hindbrain organiser. *Development* 138, 3745–3757. doi: 10.1242/dev.070318

Tritsch, N. X., and Bergles, D. E. (2010). Developmental regulation of spontaneous activity in the Mammalian cochlea. *J. Neurosci.* 30, 1539–1550. doi: 10.1523/JNEUROSCI.3875-09.2010

Tritsch, N. X., Yi, E., Gale, J. E., Glowatzki, E., and Bergles, D. E. (2007). The origin of spontaneous activity in the developing auditory system. *Nature* 450, 50–55. doi: 10.1038/nature06233

Tritsch, N. X., Zhang, Y. X., Ellis-Davies, G., and Bergles, D. E. (2010). ATP-induced morphological changes in supporting cells of the developing cochlea. *Purinergic Signal.* 6, 155–166. doi: 10.1007/s11302-010-9189-4

Uziel, A. (1986). Periods of sensitivity to thyroid hormone during the development of the organ of Corti. *Acta Otolaryngol. Suppl.* 429, 23–27. doi: 10.3109/00016488609122726

Uziel, A., Gabrion, J., Ohresser, M., and Legrand, C. (1981). Effects of hypothyroidism on the structural development of the organ of Corti in the rat. *Acta Otolaryngol.* 92, 469–480. doi: 10.3109/00016488109133286

Walters, B. J., Coak, E., Dearman, J., Bailey, G., Yamashita, T., Kuo, B., et al. (2017). *In* vivo interplay between $p27^{Kip1}$, GATA3, ATOH1 and POU4F3 converts non-sensory cells to hair cells in adult mice. *Cell Rep.* 19, 307–320. doi: 10.1016/j.celrep.2017.03.044

Wang, H. C., and Bergles, D. E. (2015). Spontaneous activity in the developing auditory system. *Cell Tissue Res.* 361, 65–75. doi: 10.1007/s00441-014-2007-5

Wang, T., Chai, R., Kim, G. S., Pham, N., Jansson, L., Nguyen, D. H., et al. (2015). $Lgr5^{+}$ cells regenerate hair cells via proliferation and direct transdifferentiation in damaged neonatal mouse utricle. *Nat. Commun.* 6:6613. doi: 10.1038/ncomms7613

Waqas, M., Zhang, S., He, Z., Tang, M., and Chai, R. (2016). Role of Wnt and Notch signaling in regulating hair cell regeneration in the cochlea. *Front. Med.* 10, 237–249. doi: 10.1007/s11684-016-0464-9

Wei, H., Chen, Z., Hu, Y., Cao, W., Ma, X., Zhang, C., et al. (2021). Topographically conductive butterfly wing substrates for directed spiral ganglion neuron growth. *Small* 17:e2102062. doi: 10.1002/smll.202102062

Woods, C., Montcouquiol, M., and Kelley, M. W. (2004). Math1 regulates development of the sensory epithelium in the mammalian cochlea. *Nat. Neurosci.* 7, 1310–1318. doi: 10.1038/nn1349

Wu, D. K., and Kelley, M. W. (2012). Molecular mechanisms of inner ear development. *Cold Spring Harb. Perspect. Biol.* 4:a008409. doi: 10.1101/cshperspect.a008409

Wu, J., Li, W., Lin, C., Chen, Y., Cheng, C., Sun, S., et al. (2016). Co-regulation of the Notch and Wnt signaling pathways promotes supporting cell proliferation and hair cell regeneration in mouse utricles. *Sci. Rep.* 6:29418. doi: 10.1038/srep29418

Xia, W., Hu, J., Ma, J., Huang, J., Jing, T., Deng, L., et al. (2019). Mutations in TOP2B cause autosomal-dominant hereditary hearing loss via inhibition of the PI3K-Akt signalling pathway. *FEBS Lett.* 593, 2008–2018. doi: 10.1002/1873-3468.13482

Xia, L., Shang, Y., Chen, X., Li, H., Xu, X., Liu, W., et al. (2020). Oriented neural spheroid formation and differentiation of neural stem cells guided by anisotropic inverse opals. *Front. Bioeng. Biotechnol.* 8:848. doi: 10.3389/fbioe.2020.00848

Xia, L., Zhu, W., Wang, Y., He, S., and Chai, R. (2019). Regulation of neural stem cell proliferation and differentiation by graphene-based biomaterials. *Neural Plast.* 2019:3608386. doi: 10.1155/2019/3608386

Xu, Z., Rai, V., and Zuo, J. (2021). TUB and ZNF532 promote the Atoh1-mediated hair cell regeneration in mouse cochleae. *Front. Cell. Neurosci.* 15:759223. doi: 10.3389/fncel.2021.759223

Yamashita, T., Zheng, F., Finkelstein, D., Kellard, Z., Carter, R., Rosencrance, C. D., et al. (2018). High-resolution transcriptional dissection of *in vivo* Atoh1-mediated hair cell conversion in mature cochleae identifies Isl1 as a co-reprogramming factor. *PLoS Genet.* 14:e1007552. doi: 10.1371/journal.pgen.1007552

You, D., Guo, L., Li, W., Sun, S., Chen, Y., Chai, R., et al. (2018). Characterization of Wnt and Notch-responsive $Lgr5^{+}$ hair cell progenitors in the striolar region of the neonatal mouse utricle. *Front. Mol. Neurosci.* 11:137. doi: 10.3389/fnmol.2018.00137

Zhang, S., Dong, Y., Qiang, R., Zhang, Y., Zhang, X., Chen, Y., et al. (2021). Characterization of *Strip1* expression in mouse cochlear hair cells. *Front. Genet.* 12:625867. doi: 10.3389/fgene.2021.625867

Zhang, Y., Fang, Q., Wang, H., Qi, J., Sun, S., Liao, M., et al. (2022). Increased mitophagy protects cochlear hair cells from aminoglycoside-induced damage. *Autophagy* 1–17. doi: 10.1080/15548627.2022.2062872. [Online ahead of print].

Zhang, Y., Guo, L., Lu, X., Cheng, C., Sun, S., Li, W., et al. (2018). Characterization of $Lgr6^{+}$ cells as an enriched population of hair cell progenitors compared to $Lgr5^{+}$ cells for hair cell generation in the neonatal mouse cochlea. *Front. Mol. Neurosci.* 11:147. doi: 10.3389/fnmol.2018.00147

Zhang, Y., Zhai, S. Q., Shou, J., Song, W., Sun, J. H., Guo, W., et al. (2007). Isolation, growth and differentiation of hair cell progenitors from the newborn rat cochlear greater epithelial ridge. *J. Neurosci. Methods* 164, 271–279. doi: 10.1016/j.jneumeth.2007.05.009

Zhang, S., Zhang, Y., Dong, Y., Guo, L., Zhang, Z., Shao, B., et al. (2020). Knockdown of Foxg1 in supporting cells increases the trans-differentiation of supporting cells into hair cells in the neonatal mouse cochlea. *Cell. Mol. Life Sci.* 77, 1401–1419. doi: 10.1007/s00018-019-03291-2

Zhang, S., Zhang, Y., Yu, P., Hu, Y., Zhou, H., Guo, L., et al. (2017). Characterization of $Lgr5^{+}$ progenitor cell transcriptomes after neomycin injury in the neonatal mouse cochlea. *Front. Mol. Neurosci.* 10:213. doi: 10.3389/fnmol.2017.00213

Zhao, H. B., Yu, N., and Fleming, C. R. (2005). Gap junctional hemichannel-mediated ATP release and hearing controls in the inner ear. *Proc. Natl. Acad. Sci. U S A* 102, 18724–18729. doi: 10.1073/pnas.0506481102

Zheng, J. L., and Gao, W. Q. (2000). Overexpression of Math1 induces robust production of extra hair cells in postnatal rat inner ears. *Nat. Neurosci.* 3, 580–586. doi: 10.1038/75753

Zhou, H., Qian, X., Xu, N., Zhang, S., Zhu, G., Zhang, Y., et al. (2020). Disruption of Atg7-dependent autophagy causes electromotility disturbances, outer hair cell loss and deafness in mice. *Cell Death Dis.* 11:913. doi: 10.1038/s41419-020-03110-8

Zine, A., Aubert, A., Qiu, J., Therianos, S., Guillemot, F., Kageyama, R., et al. (2001). Hes1 and Hes5 activities are required for the normal development of the hair cells in the mammalian inner ear. *J. Neurosci.* 21, 4712–4720. doi: 10.1523/JNEUROSCI.21-13-04712.2001

Zine, A., and Romand, R. (1996). Development of the auditory receptors of the rat: a SEM study. *Brain Res.* 721, 49–58. doi: 10.1016/0006-8993(96)00147-3

frontiers | Frontiers in Molecular Neuroscience

TYPE Review
PUBLISHED 12 October 2022
DOI 10.3389/fnmol.2022.1028125

OPEN ACCESS

EDITED BY
Qingyin Zheng,
Case Western Reserve University,
United States

REVIEWED BY
Yan Chen,
Fudan University, China
Fangyi Chen,
Southern University of Science
and Technology, China

*CORRESPONDENCE
Yafeng Yu
yfyu1024@163.com
Jiangang Fan
entscfjg@163.com
Renjie Chai
renjiec@seu.edu.cn

†These authors have contributed equally to this work and share first authorship

SPECIALTY SECTION
This article was submitted to Methods and Model Organisms, a section of the journal Frontiers in Molecular Neuroscience

RECEIVED 25 August 2022
ACCEPTED 21 September 2022
PUBLISHED 12 October 2022

CITATION
Ma X, Guo J, Fu Y, Shen C, Jiang P, Zhang Y, Zhang L, Yu Y, Fan J and Chai R (2022) G protein-coupled receptors in cochlea: Potential therapeutic targets for hearing loss. *Front. Mol. Neurosci.* 15:1028125. doi: 10.3389/fnmol.2022.1028125

G protein-coupled receptors in cochlea: Potential therapeutic targets for hearing loss

Xiangyu Ma[1†], Jiamin Guo[1†], Yaoyang Fu[2], Cangsong Shen[3], Pei Jiang[1], Yuan Zhang[4,5], Lei Zhang[6], Yafeng Yu[7*], Jiangang Fan[8*] and Renjie Chai[1,8,9,10,11*]

[1]State Key Laboratory of Bioelectronics, Jiangsu Province High-Tech Key Laboratory for Bio-Medical Research, Department of Otolaryngology Head and Neck Surgery, Zhongda Hospital, School of Life Sciences and Technology, Advanced Institute for Life and Health, Southeast University, Nanjing, China, [2]Department of Psychiatry, The First Affiliated Hospital, Zhejiang University School of Medicine, Hangzhou, China, [3]College of Life Science and Technology, Huazhong University of Science and Technology, Wuhan, China, [4]Jiangsu Provincial Key Medical Discipline (Laboratory), Department of Otolaryngology Head and Neck Surgery, Affiliated Drum Tower Hospital of Nanjing University Medical School, Nanjing, China, [5]Research Institute of Otolaryngology, Nanjing, China, [6]Department of Otorhinolaryngology, Head and Neck Surgery, The Second Hospital of Anhui Medical University, Hefei, China, [7]First Affiliated Hospital of Soochow University, Soochow, China, [8]Department of Otolaryngology Head and Neck Surgery, Sichuan Provincial People's Hospital, University of Electronic Science and Technology of China, Chengdu, China, [9]Co-Innovation Center of Neuroregeneration, Nantong University, Nantong, China, [10]Institute for Stem Cell and Regeneration, Chinese Academy of Sciences, Beijing, China, [11]Beijing Key Laboratory of Neural Regeneration and Repair, Capital Medical University, Beijing, China

The prevalence of hearing loss-related diseases caused by different factors is increasing worldwide year by year. Currently, however, the patient's hearing loss has not been effectively improved. Therefore, there is an urgent need to adopt new treatment measures and treatment techniques to help improve the therapeutic effect of hearing loss. G protein-coupled receptors (GPCRs), as crucial cell surface receptors, can widely participate in different physiological and pathological processes, particularly play an essential role in many disease occurrences and be served as promising therapeutic targets. However, no specific drugs on the market have been found to target the GPCRs of the cochlea. Interestingly, many recent studies have demonstrated that GPCRs can participate in various pathogenic process related to hearing loss in the cochlea including heredity, noise, ototoxic drugs, cochlear structure, and so on. In this review, we comprehensively summarize the functions of 53 GPCRs known in the cochlea and their relationships with hearing loss, and highlight the recent advances of new techniques used in cochlear study including cryo-EM, AI, GPCR drug screening, gene therapy vectors, and CRISPR editing technology, as well as discuss in depth the future direction of novel GPCR-based drug development and gene therapy for cochlear hearing loss. Collectively, this review is to facilitate basic and (pre-) clinical research in this area, and provide beneficial help for emerging GPCR-based cochlear therapies.

KEYWORDS

hearing loss, G protein-coupled receptors, cochlea, drug therapy, gene therapy

Introduction

Hearing disease currently affects nearly 1.5 billion people worldwide.[1] Most hearing loss is mainly occurred in the cochlea of the inner ear. The cochlea can be divided into five parts: Organ of Corti (OC), Stria Vascularis (SV), Reissner's Membrane (RM), Mesenchymal Cell (MC), Bony Labyrinth (BL), and Spiral Ganglion Neurons (SGNs) (**Figure 1A**; van der Valk et al., 2021; Kelley, 2022). Among them, the OC is the main organ of sound perception in the cochlea, particularly the hair cells (HCs) and various supporting cells (SCs) of the OC are essential for hearing (Wagner and Shin, 2019; Driver and Kelley, 2020), but cell abnormalities in other areas of the cochlea can also cause hearing damage (Jang et al., 2022). Hearing damage can be caused by a variety of factors, including heredity, noise, ototoxic drugs, damage to the cochlear environment and structure. However, current treatment options (cochlear implants and hearing aids) mainly depend on the capacity of residual HCs and SGNs to improve the patient's hearing level to a certain extent (Wolf et al., 2022).

G protein-coupled receptors (GPCRs) with seven transmembrane domains are the largest superfamily of mammalian cell surface receptors, which have more than 800 members (Foord et al., 2005; Wingler and Lefkowitz, 2020). GPCRs govern a wide range of physiological processes, such as hormone release, neurotransmitter transmission, and immune responses, mainly through the recognition and activation of heterotrimeric G proteins (Gα, Gβ, and Gγ) by binding to a variety of ligands (proteins, peptides, and lipids, etc.), as well as GPCRs phosphorylated by G protein-coupled receptor kinases (GRKs) to recruit β-arrestins and internalize and inactivate GPCRs (Wang et al., 2018; Insel et al., 2019). Based on structural similarity, GPCRs in humans are divided into five major families: Rhodopsin receptors (Class A), Secretin receptors (Class B1), Adhesion receptors (Class B2), Glutamate receptors (Class C), and Frizz/Taste 2 (Class F) (Kochman, 2014; Hauser et al., 2017). Currently, more than 100 GPCRs could be regarded as therapeutic targets, especially more than 30% of marketed drugs have been designed for GPCRs (Hauser et al., 2017).

Compared with extensive studies on GPCRs in mental illness (Pasquini et al., 2022) and cancer (Chaudhary and Kim, 2021), the function studies of GPCRs in the cochlea are very limited, scattered, and unsystematic. In particular, there are still no specific drugs on the market targeting the GPCR of the cochlea. With the in-depth study of GPCRs in the cochlea, we believe that more GPCR functions in the cochlea will be revealed, and more drugs and treatment programs targeting cochlear GPCRs will be discovered. In this review, we therefore characterized the distribution and function of 53 GPCRs expressed in the cochlea, as well as their relationships with hearing loss. Notably, five GPCRs (V2R, EDNRB, S1PR, VLGR1, and mGluR7) of them in the cochlea have been reported to be directly associated with human hearing disorders (**Figure 1B**). We also summarize the new advances in cochlear research techniques, and suggest the future direction of novel GPCR-based drug development and gene therapy for cochlear hearing loss.

1 www.who.int/publications-detail-redirect/world-report-on-hearing

Roles of class A G protein-coupled receptors in cochlea

Vasopressin and oxytocin receptors

Vasopressin type 2 receptor (V2R) is primarily expressed in the kidney and participates in controlling water homeostasis (Kim et al., 2021; Zhou et al., 2021). V2R is activated by arginine vasopressin (AVP), which in turn induces the buildup of downstream cAMP (Wang et al., 2021). Numerous V2R-related human diseases have been identified, including nephrotic syndrome of inappropriate diuresis (NSIAD), X-linked congenital nephrogenic diabetes insipidus (NDI), and hyponatremia (Makita et al., 2020). V2R-related antagonists have also been extensively studied, such as Tolvaptan (de la Nuez Veulens et al., 2022).

In the cochlea, V2R is mainly expressed in HCs, SGNs, and SVs (Takumida et al., 2012). V2R is thought to play a role in endolymphatic hydrops (EH). EH is caused by an imbalance in the volume of endolymph and is thought to be associated with the pathology of Menière's disease (MD) that is a kind of hearing loss's inner ear disease (Zou et al., 2019; Wang et al., 2022). EH can be also inhibited *via* reducing the expression of V2R. The degree of cochlear hydrops can be alleviated by applying the V2R antagonist (OPC-41061/Tolvaptan) (Egami et al., 2016). Additionally, the expression level of V2R in the cochlea can be significantly inhibited by vincamine, thereby reducing EH and regulating hearing (Li et al., 2018). However, studies found that EH is significantly attenuated by electroacupuncture (EA), but V2R is up-regulated (Jiang L. et al., 2019; Jiang L. Y. et al., 2019). Therefore, it is still needed to validate the function of V2R in the regulation of EH.

Endothelin receptors

Endothelin receptor B (EDNRB) is activated by endothelins (ETs), and three ETs (ET-1, ET-2, and ET-3) have equal affinity for EDNRB (Shihoya et al., 2016; Izume et al., 2020). EDNRB is widely expressed in circulatory organs including vascular endothelium, brain, and intestine, especially endothelin receptor antagonists have been used to treat circulatory system diseases (Bondurand et al., 2018; Shihoya et al., 2018). Heterozygous

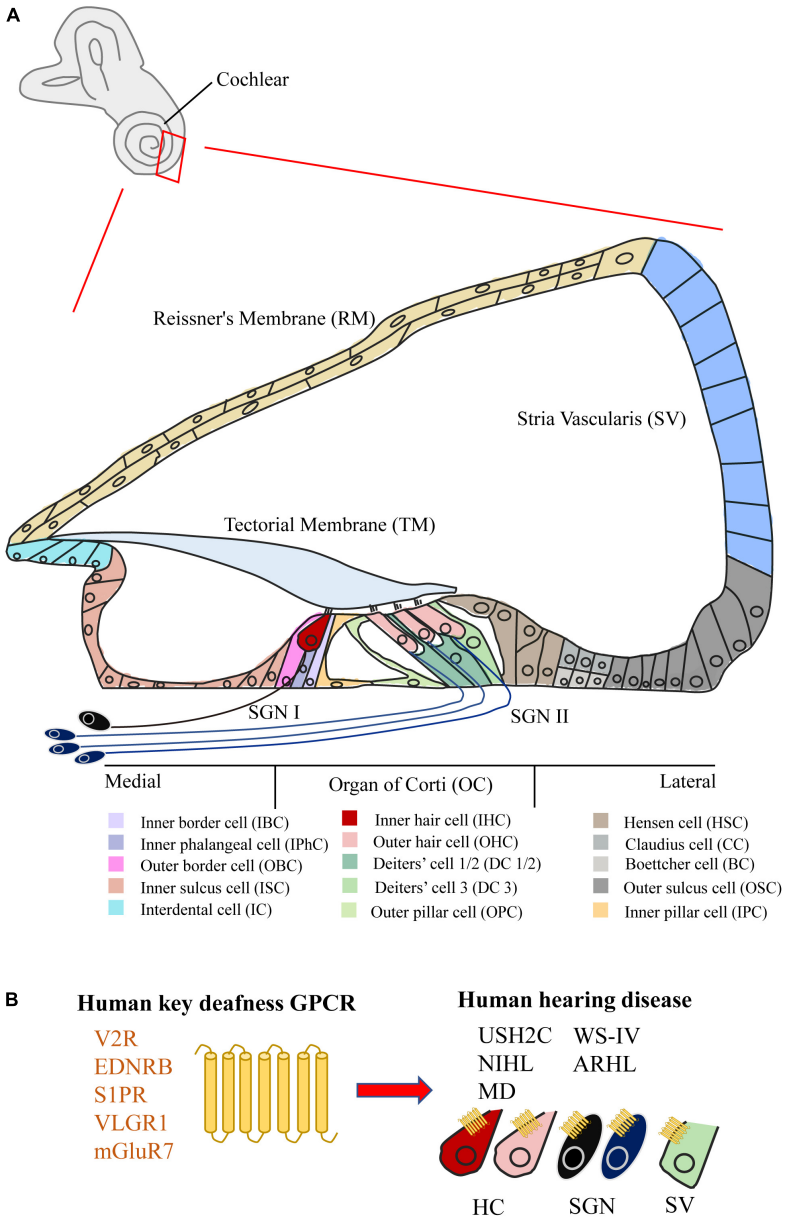

FIGURE 1
Structure of the cochlea and the GPCR related to human hearing disease. **(A)** Schematic of the mammalian mature cochlea (cross-section). The cochlea can be divided into five parts, including Organ of Corti (OC), Stria Vascularis (SV), Reissner's Membrane (RM), Spiral Ganglion Neurons (SGNs), Bony Labyrinth (BL) (not shown), and Mesenchymal Cell (MC) (not shown). Among them, two kinds of hair cell (HC) and various kinds of supporting cell (SC) can be subdivided in OC. **(B)** The summary of five key GPCRs (V2R, EDNRB, S1PR, VLGR1, and mGluR7) in cochlea related to human hearing disease (USH2C, WS-IV, NIHL, ARHL, and MD).

and homozygous mutations in EDNRB and ET-3 are found in patients of Waardenburg-Shah syndrome (WS-IV) that is one kind of syndromes with genetic hearing loss (GHL) (Huang et al., 2021). Homozygous mutations of the *EDNRB* gene can be also identified in Moroccan deaf patients (AitRaise et al., 2022).

EDNRB is expressed in SV's melanocytes and the SGN of the cochlea, which is important for postnatal hearing development (Ida-Eto et al., 2011; Renauld et al., 2021). In mouse models, both *EDNRB* spontaneously mutated and *EDNRB* homozygous knockout ($EDNRB^{-/-}$) mice developed severe congenital deafness (Gariepy et al., 1996; Matsushima et al., 2002). In the case of $EDNRB^{-/-}$, melanocytes in the SV of the cochlea are defective and the SGN undergoes postnatal degeneration (Ida-Eto et al., 2011). The introduction of human *DBH-EDNRB* transgene can restore the SGN of $EDNRB^{-/-}$ mice to a certain extent and improve the hearing levels, but the

defect of melanocytes does not change (Ida-Eto et al., 2011). Therefore, targeted modulation of EDNRB expression in SGN might be a new strategy to treat congenital hearing loss patients with WS-IV.

Glycoprotein hormone receptors

Thyrotropin receptor (TSHR) can be activated by thyrotropin (TSH), which then stimulates thyroid hormone production through the G_s and G_q signaling pathways (Tuncel, 2017; Vieira et al., 2022). Abnormalities in TSHR can lead to autoimmune diseases such as hypothyroidism and hyperthyroidism. Recent studies have elucidated the structures of the activated and inactivated states of TSHR with different types of antibodies, which provides a structural basis for subsequent antibody drug and small molecule drug discovery (Duan et al., 2022; Faust et al., 2022).

In a mouse model, $TSHR^{hyt/hyt}$ mutant mice express the gene encoding the *TSHR* with a point mutation in the highly conserved transmembrane structure, rendering TSHR unable to bind with TSH (Gu et al., 1995). The autosomal recessive $TSHR^{hyt/hyt}$ mutant mice develop severe hearing loss, and outer hair cells (OHCs) of the cochlea exhibit developmental defects and loss of functional integrity (O'Malley et al., 1995; Li et al., 1999; Song et al., 2006). Of note, the exact role of TSHR in the cochlea remains currently in a stagnant state.

Lysophospholipid (S1P) receptors

Sphingosine-1-phosphate receptors (S1PR1 to S1PR5) can be involved in the regulation of immune and vascular systems after activation by sphingosine-1-phosphate (S1P) (Cartier and Hla, 2019). Three inherited missense mutations (R108P, R108Q, and Y140C) in S1PR2 are found in patients with deaf (Santos-Cortez et al., 2016; Hofrichter et al., 2018). A recent protein structure study revealed that three mutation sites associated with human autosomal recessive hearing loss (ARHL) lead to changes of the protein structure of S1PR2 (Chen et al., 2022). These structural changes affect the binding of S1PR2 to the ligand S1P, to G_{13}, suggesting that the S1PR2-G_{13} signaling complex plays a role in maintaining normal hearing function of the cochlea.

S1PR1-3 was also found to be expressed in the mouse cochlea (Nakayama et al., 2014). Among them, S1PR2 can be specifically expressed in HCs, SCs, SGNs, and SVs (Ingham et al., 2016). In mouse models, both mutation ($S1PR2^{stdf/stdf}$) and knockout of S1PR2 ($S1PR2^{-/-}$) result in progressive hearing loss, essentially starting at 2–4 weeks postnatally with varying degrees of hearing impairment to complete deafness, which is characterized by the defect of SV at the onset and followed by decreased intracochlear potential (EP) and subsequent loss of HCs and SGNs (Herr et al., 2007, 2016; Kono et al., 2007; Ingham et al., 2016). Remarkably, mice lacking the *S1PR3* did not develop a hearing impairment phenotype (Kono et al., 2007). S1PR2 is also a potential target to protect hearing loss by preventing the ototoxic drugs induced apoptosis of HC and SGN. Administration of an S1PR2 antagonist (JTE013) resulted in the increase of gentamicin ototoxicity (Nakayama et al., 2014), whereas administration of an S1PR2 agonist (CYM-5478) reduced the cisplatin ototoxicity by reducing ROS accumulation (Wang et al., 2020). Of note, antagonists of S1PR1 and S1PR3 failed to increase gentamicin ototoxicity (Nakayama et al., 2014). Overall, S1PR2 plays a key role in maintaining hearing function and inhibiting damage caused by ototoxicity, particularly it is worthy of in-depth study as an ear protection therapeutic drug target.

P2Y receptors (purinergic receptors)

P2Y receptor (P2YR), as a GPCR subfamily of eight subunits (P2YR1, 2, 4, 6, 11–14) known, can respond to extracellular nucleotides (Cabou and Martinez, 2022). Among them, P2YR1, 11–13 are activated by ATP/ADP, P2YR4, 6, 14 are activated by UTP/UDP, and P2YR2 receptors are activated by ATP/UTP (Abbracchio et al., 2006; Koles et al., 2019). The expression of six P2YRs (P2YR1, 2, 4, 6, 12, 14) could be detected in the cochlea (Parker et al., 2003; Huang et al., 2010; O'Keeffe et al., 2010; Koles et al., 2019). Before hearing maturation (<P15), five P2YRs except P2YR1 could be detected in both sensory and non-sensory cells in the cochlea. After hearing maturation (>P15), only P2YR12 and P2YR14 could not be detected in HCs. The specific expressions of six P2YRs in the cochlea are shown in **Table 1**.

P2YR1, 2, 4 have been functionally studied to some extent in the cochlea. Among them, P2YR1 plays an important role in the burst firing before hearing onset. The maturation of emerging neural circuits is facilitated by spontaneous bursts of electrical activity in the developing nervous system (Blankenship and Feller, 2010). K^+ release can be triggered when P2RY1 is activated in SCs, thereby activating inner hair cells (IHCs) and SGNs (Babola et al., 2020, 2021). Both pharmacological (MRS2500) inhibition of P2RY1 or *P2RY1* deletion significantly reduced burst firing in SGNs (Babola et al., 2020, 2021). Moreover, P2YR4 mediated the inhibition of Na^+ uptake in cochlear RMs, possibly in response to noise exposure (Kim et al., 2010). In particular, P2YR2 and P2YR4 in the cochlea can also induce the propagation of Ca^{2+} waves (Piazza et al., 2007).

Dopamine receptors

G protein-coupled dopamine receptors execute almost all the physiological functions of catecholaminergic neurotransmitter dopamine. This dopamine receptor family

TABLE 1 Class A GPCRs relevant to cochlea.

GPCR family	Subtypes	Roles in cochlea	Localization	Genetic modulation	References
Class A GPCRs					
Vasopressin and oxytocin receptors	V2R	Play a role in endolymphatic hydrops (EH)	HC, SGN, SV	-	Zou et al., 2019; Wang et al., 2022
		Associated with human Menière's disease (MD) with hearing loss			
Endothelin receptors	EDNRB	Associated with human Waardenburg–Shah syndrome (WS-IV) [a kind of genetic hearing loss (GHL)]	SV's melanocytes, SGN	*EDNAB*$^{-/-}$ mice	Ida-Eto et al., 2011
		Affect hearing function: severe congenital deafness when knockout		*DBH-EDNAB* mice	
		SV's melanocytes are defective and the SGN undergoes postnatal degeneration when knockout		WS4 mice	Matsushima et al., 2002
Glycoprotein hormone receptors	TSHR	TSHR hyt/hyt mutant mice (autosomal recessive) develop severe hearing loss	-	*TSHR*$^{hyt/hyt}$ mice	Gu et al., 1995
		Affect OHC development and function			
Lysophospholipid (S1P) receptors	S1PR1	-	Cochlea	-	Nakayama et al., 2014
	S1PR2	Associated with human autosomal recessive hearing loss (ARHL)	HC, SC, SGN, SV	*S1PR2*$^{stdf/stdf}$	Ingham et al., 2016
		Lead to progressive hearing loss when knockout or mutated		*S1PR2*$^{-/-}$	Herr et al., 2007
		Affect the development of SV at the onset			
		Inhibit damage caused by ototoxicity			
	S1PR3	No hearing impairment phenotype when knockout	Cochlea	*S1PR3*$^{-/-}$ mice	Kono et al., 2007
P2Y receptors (Purinergic receptors)	P2YR1	Play an important role in the burst firing before hearing onset	RM, SC (<P15)	*P2RY1*$^{-/-}$ mice	Babola et al., 2020
			OHC, OSC, RM (>P15)	*P2RY1-LacZ* mice	
	P2YR2	Induce the propagation of Ca2+ waves	OHC, IHC, PC, DC, HSC, OSC, SV, RM (<P15)	-	Koles et al., 2019
			OHC, PC, OSC (>P15)		
	P2YR4	Mediate to inhibit Na+ uptake in cochlear RMs	OHC, IHC, SGN, HSC, OSC, SV, RM (<P15)	-	Koles et al., 2019
		Induce the propagation of Ca2+ waves	OHC, IHC, SGN, PC, DC, HSC, OSC, SV, RM (>P15)		
	P2YR6	-	OHC, IHC, SGN, PC, SV, RM (<P15)	-	Koles et al., 2019
			OHC, SGN, PC, SV, RM (>P15)		
	P2YR12	-	OHC, SGN, PC, RM (<P15)	-	Koles et al., 2019
			SGN, RM (>P15)		

(Continued)

10.3389/fnmol.2022.1028125

TABLE 1 (Continued)

GPCR family	Subtypes	Roles in cochlea	Localization	Genetic modulation	References
	P2YR14	-	OHC, IHC, SGN, OSC (<P15) SGN, OSC (>P15)	-	Koles et al., 2019
Dopamine receptors	DRD1	Activate adenylyl cyclase	OHC, SGN	*DRD1*$^{-/-}$ mice	Maison et al., 2012
Chemokine receptors	DRD2	Inhibit adenylyl cyclase	OHC, SGN	*DRD2*$^{-/-}$ mice	Maison et al., 2012
	DRD4	Inhibit adenylyl cyclase	SGN	*DRD4*$^{-/-}$ mice	Maison et al., 2012
	DRD5	Activate adenylyl cyclase	OHC, SGN	*DRD5*$^{-/-}$ mice	Maison et al., 2012
	CXCR4	Regulates cochlear development and stem cell homing	SGN	-	Zhang et al., 2015
	CX3CR1	Regulation of inflammatory response	Macrophages, monocytes	*CX3CR1*$^{-/-}$ mice	Zhang et al., 2021
Dopamine receptors	CCR2	Regulating inflammatory response to noise–and drug-induced hearing impairment	Monocytes	*CCR2*$^{-/-}$ mice	Hirose and Li, 2019
Cannabinoid receptors	CCR7	Protects against noise-induced auditory cell damage	Monocytes	-	Maeda et al., 2018
Apelin receptors	CB2R	Ototoxicity induced by cisplatin treatment was inhibited, and inflammation and oxidative stress were reduced	OC, SLF, SGN	-	Ghosh et al., 2018
	APJ	Anti-oxidation, prevent cell apoptosis	OHC, IHC	-	Yin et al., 2020
Adenosine receptors	AA1R	Protects the mouse cochlea from noise damage, cisplatin induced ototoxicity, and age-related hearing loss, and reduces the death of auditory cells	SGN, SC, IHC	*AA1R*$^{-/-}$ mice	Vlajkovic et al., 2009
	AA2AR	Coupled with G_s proteins that promote adenylate cyclase	SGN, OC	*AA2AR*$^{-/-}$ mice	Vlajkovic et al., 2017
	AA2BR	Coupled with G_s proteins that promote adenylate cyclase	SGN, OC	-	Manalo et al., 2020
	AA3R	Coupled with $G_{i/o}$ proteins inhibit adenylate cyclase activity	SC, IHC	-	Vlajkovic et al., 2007
Class A orphan receptors	GPR26	Deleted as part of a recessive mouse mutant (hb/hb) that exhibits severe hearing impairment	SLF, SGN	*hb/hb* mice	Buniello et al., 2013
				GPR26$^{-/-}$ mice	Zhang et al., 2011
	LGR4	Involved in the regulation of Wnt/β-catenin activity by playing a permissive role in the Wnt/β-catenin signaling pathway	HC, PC, DC	*LGR4-LacZ* mice	Zak et al., 2016
	LGR5	Regulate cochlear development and promote hair cell regeneration	IPC, SC, DC	*LGR5-eGFP* mice	Cheng et al., 2017
				LGR5-EGFP-IRES-CreERT2 mice	Zak et al., 2016
	LGR6	Regulation of progenitor cell proliferation	IPC, SC	*LGR6-EGFP-IRES-CreERT2* mice	Zhang Y. et al., 2018

HC, hair cell; SGN, Spiral Ganglion Neuron; SV, Stria Vascularis; SC, supporting cell; RM, Reissner's Membrane; OHC, outer hair cell; OSC, outer sulcus cell; IHC, inner hair cell; PC, Pillar cell; DC, Deiters' cell; HSC, Hensen cell; OC, Organ of Corti; IPC, inner Pillar cell; SLF, spiral ligament fibrocytes.

10.3389/fnmol.2022.1028125

includes five GPCR subtypes, and can be divided into two categories: DRD1 (dopamine receptor D1) and DRD5 binding to G proteins and activating adenylyl cyclase; DRD2, DRD3, and DRD4 binding to G proteins and inhibiting adenylyl cyclase (Beaulieu and Gainetdinov, 2011). Transcriptome sequencing of whole cochlear samples from adult mice revealed the presence of DRD1, DRD2, DRD4, and DRD5 transcripts, but not DRD3 mRNA. DRD1, DRD5, and DRD2 receptors were expressed in OHCs and SGNs, but DRD4 receptors were expressed only in SGNs (Maison et al., 2012).

There is no consensus on which receptors can mediate the hearing (Meredith and Rennie, 2021), but it is widely accepted that activated dopamine receptors can decrease the excitotoxicity of IHC synapses through the effect of dopamine on afferents (Oestreicher et al., 1997). Current biochemical and pharmacological evidence suggests that dopamine release from lateral cochlear efferent neurons can inhibit the cochlear nerve fiber activity (Gaborjan et al., 1999; Ruel et al., 2001). Studies have also shown that the administration of dopamine and dopaminergic agonists may reduce the action potentials' firing rate in frog semicircular canal afferents (Andrianov et al., 2009). In guinea pigs and rats, dopamine reduced the rate of action potential firing from cochlear auditory afferents (Oestreicher et al., 1997; Wu et al., 2020). Exposure to sound also raise dopamine in mouse efferent neurons, revealing that dopamine has very vital neuroprotective effect (Maison et al., 2012; Wu et al., 2020). When the DRD1, DRD2, DRD4, and DRD5 dopamine receptor knockout mice were respectively exposed to noise, all four mutants demonstrated increased vulnerability (Maison et al., 2012). These studies not also support the role of dopaminergic signaling in the HC system of different species, but reveal its potential application value in hearing protection.

Chemokine receptors

Chemokines regulate cell migration and proliferation, as well as immune and inflammatory responses. Twenty chemokine receptors have been identified, including four subfamilies (Sanchez et al., 2019). Chemokine receptors and chemokines can participate in various physiological and pathological processes, including cancer cell growth (Smith et al., 2004) and metastasis (Zlotnik et al., 2011), angiogenesis (Keeley et al., 2010; Lin et al., 2015), and immune responses of patient prognosis (He et al., 2022). Chemokine receptors reported in the cochlea include CXCR4, CX3CR1, CCR2, and CCR7.

CXCR4 and its ligand CXC chemokine ligand 12 (CXCL12, also called as stromal cell-derived factor-1) involve in regulating neural stem cell migration, differentiation and maturation (Zhang et al., 2015), vertebrate embryogenesis (Peyvandi et al., 2018b). In the cochlea, CXCR4 protein is mainly expressed in SGNs. CXCR4/CXCL12 participates in cochlear development in neonatal mice and rats (Zhang et al., 2015, 2016), and stem cell homing in noise-induced injury areas in adult rats (Zhang et al., 2014; Peyvandi et al., 2018a). CX3CR1, as a receptor for the chemokine Fractalkine, is found to express in NK cells, macrophages, monocytes, microglia, and partly T cells (Jung et al., 2000). CX3CR1 is also expressed in macrophages and monocytes of the mouse cochlea (Claussen et al., 2022). In response to the transformation of monocytes and migration of macrophages in hearing damage caused by noise stimulation (Shin et al., 2022a,b), CX3CR1 regulates the inflammatory response caused by cochlear injury (Zhang et al., 2021). CX3CR1-deficient cochlear macrophages can also aggravate the ototoxicity of kanamycin (Sato et al., 2010). Remarkably, CCR2 and CCR7 may be also involved in regulating inflammatory response in hearing impairment induced by noise and drugs (Sautter et al., 2006; Maeda et al., 2018; Hirose and Li, 2019). Therefore, chemokine receptors and chemokines play important roles in cochlear development, stem cell homing and immune response after hearing damage, suggesting them with a potential to repair hearing damage and protect nerves.

Cannabinoid receptors

Cannabinoid 2 receptors (CB2Rs), one type of cannabinoid receptor, are found in peripheral tissues of immunological origin (Munro et al., 1993; Brown et al., 2002) and are distributed in different brain regions (Ishiguro et al., 2022). CB2Rs are post-synaptically expressed and up-regulated in response to injury and inflammation (Ishiguro et al., 2022). CB2Rs are mainly distributed in OC, spiral ligament and SGN cells in the cochlea of rats and mice (Kim et al., 2014; Kaur et al., 2016; Ghosh et al., 2018). CB2Rs can protect the cochlea and reduce ototoxicity, inflammation and oxidative stress with cisplatin treatment in rats (Vlajkovic et al., 2006; Dhukhwa et al., 2021). The effect of CB2Rs on preventing cisplatin induced hearing loss was blocked by injection of the antagonist AM630, but HC loss was reduced by injection of JWH105 (one agonist of CB2R). Of note, after knock-down of CB2Rs by siRNA, the cochlea is more sensitive to cisplatin induced hearing loss (Ghosh et al., 2018). Therefore, CB2Rs may be an important therapeutic target against ototoxicity.

Apelin receptors

Apelin receptor (APJ) and its ligand Apelin are key participators involved in the regulation of oxidative stress. Among various subtypes of Apelin, Apelin-13 has the strongest

biological activity (Niknazar et al., 2019). APJ/Apelin is widely expressed in the heart, brain, kidney, stomach and intestines (Fournel et al., 2017; Lv et al., 2017), and has antioxidant and apoptotic effects in distinct cell types (Bircan et al., 2016; Aminyavari et al., 2019). Apelin attenuates DNA damage caused by ROS accumulation in cisplatin-induced myocardial toxicity (Zhang P. et al., 2017). Apelin-13 protects cardiomyocytes by reducing oxidative damage in a rat model of myocardial infarction (Azizi et al., 2013).

Both APJ and Apelin are expressed in mouse cochlear HCs and HEI-OC1 cells, and the expression of APJ in OHCs is significantly higher than that in IHCs (Yin et al., 2020). Cisplatin can down-regulate the expression of Apelin in HCs and HEI-OC1 cells, and treatment with Apelin in advance can improve the survival rate of HEI-OC1 cells under cischloride ototoxicity and alleviate the damage of cochlear mitochondrial membrane potential by ROS (Yin et al., 2020). In addition, noise-induced oxidative stress and DPOAE response were significantly altered and inhibited by Apelin-13 pretreatment (Khoshsirat et al., 2021).

Adenosine receptors

This adenosine receptor family includes four GPCRs, designated as A1, A2A, A2B, and A3. Adenosine A1 receptor (AA1R) and adenosine A3 receptor (AA3R) coupled with $G_{i/o}$ proteins to inhibit adenylate cyclase activity, whereas adenosine A2A receptor (AA2AR) and adenosine A2B receptor (AA2BR) coupled with G_s proteins to activate adenylate cyclase (Vlajkovic et al., 2007). Together, the adenosine receptor family and its signaling molecules regulate cellular activity in peripheral organs.

The distribution of four adenosine receptors in the cochlea is diverse (Vlajkovic et al., 2009; Manalo et al., 2020). AA1R is distributed in SGNs, and in SCs and IHCs of the OC, but AA2AR and AA2BR localize to SGNs, OC, and cochlear vessels. AA3R is mainly expressed in SCs and inner HCs of the OC. The balance between AA1R and AA2AR determines the cochlear response to oxidative stress. AA1R can protect the cochlea of mice from noise injury, cisplatin-induced ototoxicity and age-related hearing loss (Vlajkovic et al., 2011, 2017; Sheth et al., 2019). Similar results have been reported in rat, chinchilla and guinea pig (Ramkumar et al., 1994, 2004; Tabuchi et al., 2012). Administration of AA1R probiotics R-PIA and ADAC was more significant in inhibiting cisplatin-induced ototoxicity (Vlajkovic et al., 2010; Kaur et al., 2016), and the protective effect of R-PIA was inhibited by combined use of AA1R antagonist DPCPX (Whitworth et al., 2004). In contrast, AA2AR and AA2BR play a negative regulatory role in hearing loss, with cochlear protection achieved by the use of the inhibitor (istradefylline) (Han et al., 2019; Manalo et al., 2020; Shin et al., 2021).

Class A orphan receptors

GPR26, one class of orphan receptors for Class A, is mainly expressed in the brain and attracted attention due to its role in central nervous system diseases (Alavi et al., 2018; Watkins and Orlandi, 2020). *GPR26* is deleted along with two other genes (*CPMX2* and *CHST15*) in recessive mouse mutant mice (*hb/hb*) that exhibit severe hearing impairment (Buniello et al., 2013). Symptoms of anxiety and depression were presented in *GPR26* knockout mice, but no hearing function was reported (Zhang et al., 2011). In the mouse cochlea, GPR26 expression was detected in spiral ligament fibrocytes (SLF) and SGNs (Buniello et al., 2013), but *hb/hb* mutant mice in the cochlea without GPR26 expression, indicating that it is worth using the $GPR26^{-/-}$ mice to examine the role of GPR26 in the cochlea.

Another class of orphan receptors for Class A is one member of the leucine-rich repeat-containing G-protein-coupled receptors (LGRs) family. LGR4, LGR5, and LGR6 could be expressed in the cochlea (Zak et al., 2016; Zhang Y. et al., 2018; Smith-Cortinez et al., 2021). LGR5 is considered as a marker of cochlear stem cells and participates in the development of auditory HCs (Smith-Cortinez et al., 2021). LGR5 regulates cochlear development by enhancing the Wnt/β-catenin signaling pathway (Cheng et al., 2017; McLean et al., 2017), especially LGR5-positive SCs have the potential to transdifferentiate into HCs, suggesting that it may be acted as a therapeutic target for hearing loss (Cox et al., 2014; Zhang S. et al., 2017; Smith-Cortinez et al., 2021; Ma et al., 2022). LGR5-deficient mice produce additional HCs, and LGR4-deficient mice show similar results (Zak et al., 2016). $LGR6^{+}$ cells, a subtype of $LGR5^{+}$ progenitor cells, also regulate progenitor cell proliferation and HC production (Zhang Y. et al., 2018).

Roles of class B1 G protein-coupled receptors in cochlea

Vasoactive intestinal peptide and pituitary adenylate cyclase-activating peptide receptors

Vasoactive intestinal peptide (VIP) and pituitary adenylate cyclase-activating peptide (PACAP) receptors include VPAC1R, VPAC2R, and PAC1R, which are activated by VIP and PACAP (Hollenstein et al., 2014; Langer et al., 2022). Among them, unlike VPAC1R and VPAC2R, PAC1R can specifically binds to PACAP but has a lower affinity toward VIP (Vaudry et al., 2009). These two neuropeptides are widely distributed and involved in development, anti-apoptosis, and neuroprotection together with their receptors (Langer et al., 2022). In the cochlea, VIP and VIP receptors are mainly expressed in SGNs (Kitanishi et al., 1998).

In addition, the levels of VIP and VPAC1R were down-regulated in the cochlea of chronic alcoholic rats, implying that they might act as neurotransmitters (Feng and Liu, 2015). However, there are still few studies on VIP and VIP receptors, and their specific mechanisms of action in the cochlea need to be further studied.

PACAP and PAC1R are expressed in HCs, SCs, SGNs, afferent, and efferent nerve fibers, and stria vascularis of the cochlea (Abu-Hamdan et al., 2006; Drescher et al., 2006; Ruel et al., 2021). Endogenous PACAP plays important roles in protection against noise-induced hearing loss (NIHL) (Ruel et al., 2021), maintenance of hearing during aging in mice (Fulop et al., 2019) and against oxidative stress-induced apoptosis (Racz et al., 2010). Current functional studies focused on the role of PACAP in the cochlea as well as the PAC1R in the protection of NIHL (Ruel et al., 2021). After noise injury, the *PAC1R*$^{-/-}$ knockout mice exhibited a significant increase in hearing threshold, but the humanized mice expressing human PAC1R (TgHPAC1R) showed a relatively small increase in hearing threshold. Taken together, with the establishment of a mouse model corresponding to the PAC1R, other roles of the PAC1R in the cochlea will be gradually uncovered.

Corticotropin-releasing factor receptors

Corticotropin-releasing factor receptors (CRFRs) in mammals only express CRFR1 and CRFR2, which are activated by corticotropin-releasing factor (CRF). As the main regulator of stress response, they participate in neuroendocrine, metabolism and response to stress (Vetter, 2015; Dedic et al., 2018). Among them, CRFR1 has a higher affinity for CRF than CRFR2 does.

CRFR1 is mainly localized in inner sulcus cells (ISCs), Hensen cells (HSCs), Deiters' cells (DCs), and border cells (BCs) in the cochlea (Graham and Vetter, 2011), but no expression in HCs and SGNs. CRFR1 plays an important role in maintaining normal auditory function, IHC and HC innervation development. In *CRFR1*$^{-/-}$ mice, both ABR thresholds and DP thresholds were elevated, suggesting that elimination of CRFR1 might result in decreased cochlear sensitivity and impaired OHC motility (Graham and Vetter, 2011), as well as defects in IHC, afferent and efferent innervation (Graham and Vetter, 2011).

Likewise, the effects of CRFR2 on the cochlea are diverse. CRFR2 is mainly expressed in ISCs, DCs, inner border cells (IBCs), SGNs, Claudius cells (CCs), and Boettcher cells (BoCs) (Graham et al., 2010), but not in HCs. CRFR2 constitutively modulates hearing sensitivity under normal conditions and performs an important protective function in noise-induced hearing loss. Mice lacking *CRFR2* exhibited significantly lower hearing thresholds under normal conditions, but more severe hearing impairment when exposed to noise (Graham et al., 2010). Interestingly, there was no loss of IHCs or OHCs in the cochlea of *CRFR2*$^{-/-}$ mice exposed to moderate ambient noise (Graham et al., 2010). CRFR2 affects cochlear hearing function by acting on glutamatergic transmission, purinergic signaling and activation of Akt/PKB signaling in the cochlea (Graham et al., 2010). Currently CRFR1 and CRFR2 have been considered as promising targets for the treatment of asthma and alcoholism drug therapy (Tantisira et al., 2004; Lowery and Thiele, 2010).

Calcitonin receptors

Calcitonin Gene-Related Peptide Receptor (CGRPR) is a heterodimeric membrane protein complex composed of receptor activity-modifying protein 1 (RAMP1) and calcitonin receptor-like receptor (CLR) with the ability to bind to CGRP (Liang et al., 2018). As an important sensory neuropeptide, CGRP is widely expressed in the nervous system and exists in two forms, i.e., α-CGRP and β-CGRP (Lv et al., 2022). CGRP plays important roles in migraine pathophysiology, inflammatory response, and blood pressure (Mehkri et al., 2022). At present, good progress has been made in the drug research of GCRP and CGRPR, and four related monoclonal antibodies have been developed (Deganutti et al., 2021). In addition, GCRP plays an important role in the cochlea. GCRP is expressed in the lateral olivocochlear (LOC), medial olivocochlear (MOC) efferent neurons and type II SGNs (SGN IIs) and up-regulates excitatory of auditory nerve (AN) activity (Schrott-Fischer et al., 2007; Vyas et al., 2019; Le Prell et al., 2021). In α*CGRP* knockout mice, ABR thresholds were reduced and hearing impairment was presented (Maison et al., 2003). Additionally, the CGRPR complex in the cochlea exhibits maturation during the first 3 months, which corresponds to an increase in cochlear nerve activity (Dickerson et al., 2016). However, research on CGRPR in the cochlea is relatively lagging, particularly the location and specific function of CGRPR in the cochlea are currently unknown.

Roles of class B2 G protein-coupled receptors in cochlea

Adhesion G protein-coupled receptor C

Cadherin EGF LAG Seven-pass G-type Receptor 1 (CELSR1), also named as Adhesion G-protein Receptor C1 (ADGRC1), is mainly distributed in the nervous system. In

humans and mice, mutations in *CELSR1* strongly affect neural tube development (Ravni et al., 2009; Allache et al., 2012).

CELSR1 is expressed in both inner ear HCs and SCs, and is considered as a key Planar cell polarity (PCP) protein in the cochlea to be involved in cellular communication and coordination between HCs and SCs (Shima et al., 2002; Curtin et al., 2003; Davies et al., 2005). In two *CELSR1* mutant mice (*Scy* and *Crsh*), the OHCs were massively misoriented, most severely at the apex of the cochlea (Curtin et al., 2003). Interestingly, no significant auditory HC dislocation and hearing impairment were observed in *CELSR1* knockout mice but not in mutant strains, which may be due to compensatory effects from other *CELSR* genes (e.g., *CELSR2, 3*) (Tissir and Goffinet, 2006; Duncan et al., 2017). In addition, there are some PCP proteins in cochlear HCs, but whether and how CELSR1 cooperates with other PCP proteins to effect on the plane polarity of HCs, which is largely unknown and needs to further study.

Adhesion G protein-coupled receptor V

Very large G protein-coupled receptor 1 (VLGR1), known as MASS1, Adhesion G-protein Receptor V1 (ADGRV1), Neurepin and G protein-coupled receptor 98 (GPR98), is to date the largest known protein in GPCR super-families including about 6,300 amino acid residues (Sun et al., 2013). Several *VLGR1* mutations have been reported to cause Usher syndrome type IIC (USH2C) in humans, a genetically heterogeneous autosomal recessive disorder characterized by hearing impairment and epileptic seizures (Kimberling et al., 1995; Ebermann et al., 2007; Bonnet and El-Amraoui, 2012).

In the inner ear, VLGR1 is expressed in the ankle region of HCs stereocilia, which can form the ankle-link complex with Usherin, Vezatin, and Whirlin (Michalski et al., 2007). VLGR1 was identified to form a complex with Clarin-1, CDH23, and PCDH15 at the ribbon synapses of HCs (Zallocchi et al., 2012b), and can also interact with various proteins including Harmony (Verpy et al., 2000), PDZ7 (Colcombet-Cazenave et al., 2022), MyosinVIIa (Michalski et al., 2007), and SNAP25 (Zallocchi et al., 2012a). In various *VLGR1* mutant or knockout mouse models, the stereociliary development of auditory HCs is impaired, the ankle-links are absent, and hearing impairment of varying degrees occurs (Skradski et al., 2001; McMillan and White, 2004; Yagi et al., 2005). Collectively, VLGR1 can carry out the stereociliary development and hearing function.

Adhesion G protein-coupled receptor A

G protein-coupled receptor 125 (GPR125) is also named as adhesion G protein-coupled receptor A3 (ADGRA3), and involve in regulating planar cell polarity signaling (Li et al., 2013). GPR125 is widely expressed in the cochlea, especially in OHCs, SGNs, and interdental cells (ICs) (Sun et al., 2021). However, in GP125-deficient mice, various types of cells developed normally, and hearing function was not impaired (Sun et al., 2021), implying that GPR125 may not regulate the planar cell polarity in the cochlea.

Roles of class C G protein-coupled receptors in cochlea

Metabotropic glutamate receptors

The metabotropic glutamate receptor (mGluR) family includes eight known subtypes (mGluR1∼8) that are subdivided into three groups (group I-III) (Niswender and Conn, 2010; Reiner and Levitz, 2018; Ge and Wang, 2022). In general, group I (mGluR1 and mGluR5) mainly positively regulate the activity of glutamatergic synapses. In contrast, both group II (mGluR2 and mGluR3) and III mGluR (mGluR4, mGluR6∼8) function in limiting the release of neurotransmitters. In addition, most mGluRs can be alternatively spliced at the intracellular C-terminus to generate isoforms such as mGluR7a and mGluR7b, and then form homo- and heterodimers for dynamic regulation (Seebahn et al., 2011; Habrian et al., 2019).

Among all mGluRs, mGluR1 is present both in the SGNs and HCs (Ye et al., 2017). mGluR4, mGluR7a, mGluR7b, and mGluR8b were found at the pre-synaptic ribbons of IHCs, while mGluR2 is localized at post-synaptic type I SGNs (SGN Is) and efferent lateral olivocochlear GABAergic fibers (Doleviczenyi et al., 2005; Klotz et al., 2019; Klotz and Enz, 2021). Moreover, mGluR7 and mGluR8 can be detected at the OHCs (Friedman et al., 2009; Girotto et al., 2014). Especially, mGluR1 can enhance efferent inhibition of developing IHCs and promote excitatory neurotransmission in SGN Is (Peng et al., 2004; Ye et al., 2017). In contrast, mGluR2 can protect cochlea from damage by inhibiting efferent dopamine release onto IHCs (Doleviczenyi et al., 2005). Interestingly, mGluR7 is also associated with ARHL and NIHL in humans (Friedman et al., 2009; Newman et al., 2012; Chang et al., 2018; Yu et al., 2018; Matyas et al., 2019), and mGluR7 knockout mice exhibited hearing deficits (Fisher et al., 2020). These studies suggest that mGluRs, especially group II and III mGluRs, can play a key role in preventing excitotoxicity induced by excessive glutamate release from IHCs. However, mGluR4 and mGluR8b, which co-localize with the mGluR7, warrant further investigation of their specific functions in IHCs. In addition, whether mGluR4, mGluR7a, mGluR7b, and mGluR8b can form different homologous and/or heterodimeric receptors to execute diverse roles in IHCs deserves further investigation.

γ-Aminobutyric acid B receptors

The γ-aminobutyric acid receptor type B (GABA B receptor), as a metabotropic receptor, can be activated by γ-aminobutyric acid (GABA) and mediate long-term, slow signaling responses mainly in the form of heterodimers (Mao et al., 2020; Fritzius et al., 2022; Vlachou, 2022). GABAB receptors are composed of two distinct subunits, GB1 and GB2. Due to the alternative splicing of GB1 subunit mRNA, 14 different GB1 isoforms can be generated, of which GB1a and GB1b are most widely studied (Bowery and Enna, 2000; Shaye et al., 2021; Shen et al., 2021). What's more, GABA B receptors were found to be localized at all mature or nascent cochlear SGNs, including SGN I and SGN II, but not in HCs (Lin et al., 2000; Reijntjes and Pyott, 2016). GABA B receptors affect OHC function in the cochlea. In mice knocked out of GABA B1, hearing thresholds increased by about 10 dB (Maison et al., 2009). In addition, GABA B(1a,2) on the SGN modulates the strength of the SGN-HC synapse by inhibiting the release of acetylcholine (Ach) following GABA activation (Wedemeyer et al., 2013). In contrast to the few studies that work in the cochlea, research on GABA B receptors in the auditory domain is currently focused on the cochlear nuclear complex (CNC) of the brain (Kou et al., 2013; Qu et al., 2015). Whether there is a potential correlation between the GABA B receptors of the cochlea and CNC is worthy of follow-up study.

Calcium-sensing receptors

The calcium-sensing receptor (CaSR) works as a key regulator by sensing extracellular Ca^{2+} fluctuations to affect downstream intracellular signaling pathways (Tuffour et al., 2021). Thus, CaSR plays a key role in maintaining cellular Ca^{2+} homeostasis. In cochlea, Ca^{2+} homeostasis is also essential for acoustic transduction and proper development of cochlea, including synaptic transmission, mechanoelectrical transduction and the network of SCs (Ceriani and Mammano, 2012; Sirko et al., 2019). CaSR expression is detected in fibrocytes of the spiral ligament and spiral limbus, smooth muscle cells (SMCs) of the spiral modiolar arteries and epithelia of the osseous spiral lamina (Wonneberger et al., 2000; Minakata et al., 2019). Only one work has reported the role of CaSR in cochlear fibrocytes, where CaSR can regulate Ca^{2+} concentration (Minakata et al., 2019). When the CaSR inhibitor (NPS2143 and Calhex231) was used, the hearing threshold increased by 20–30 dB, indicating that the Ca^{2+} signal mediated by CaSR is required for hearing. Therefore, the study of the complete regulatory pathway of CaSR to maintain cochlear Ca^{2+} homeostasis will help to treat hearing loss.

Class C orphans receptors

GPR156, as an orphan GPCR of class C, has a significant sequence homology with GABA B receptor (Calver et al., 2003), and has a high $G_{i/o}$ constitutive activity (Watkins and Orlandi, 2021). GPR156 is currently only reported as a key regulator of orientation in sensory HCs (Kindt et al., 2021). GPR156 is expressed in all HCs of the cochlea, and knockout of GPR156 causes hearing loss but not HC death (Kindt et al., 2021). GPR156 distribution can be polarized by the transcription factor EMX2, which is then signaled by $G\alpha_i$ to trigger a 180° reversal of HC orientation (Kindt et al., 2021). The EMX2 > GPR156 > $G\alpha_i$ signaling cascade is therefore required for HC orientation (especially OHC1 and OHC2) and hearing function. In this signaling cascade, how EMX2 affects GPR156 and whether there are agonists combined with GPR156 to participate in the reversal of HCs worth further research.

Roles of class F G protein-coupled receptors in cochlea

Frizzled receptors

Class F of GPCR or frizzled GPCR family includes ten Frizzleds (FZD1-10) and Smoothened (SMO), all of them have this cysteine-rich domain (CRD) in their extracellular region (Schulte and Wright, 2018; Zhang X. et al., 2018; Kozielewicz et al., 2020; Schulte and Kozielewicz, 2020). These receptors play key roles in embryonic development, cellular polarity, proliferation, differentiation, and maintenance of stem cells.

The 10 FZDs coordinate the Wnt signaling in two ways: through disheveled (DVL1-3)–dependent pathway (Clevers and Nusse, 2012; Grainger and Willert, 2018) and through heterotrimeric G-protein-mediated pathway (Dijksterhuis et al., 2014; Kilander et al., 2014). In addition to FZD5 and FZD8, the other eight FZDs have been reported to couple to various types of G proteins (Schulte and Wright, 2018). Most of these *FZD*s were detected by RT-PCR in the rat cochlea (Daudet et al., 2002) and RNA *in situ* hybridization in the chicken cochlea (Sienknecht and Fekete, 2008). In the mammalian cochlea, *FZD1* and *FZD2* were both expressed at lower levels in sensory HCs, but at higher levels in SCs (Yu et al., 2010). And the expression of *FZD4* can be detected in auditory and vestibular HCs (Wang et al., 2001). Furthermore, both FZD3 and FZD6 are expressed in cochlear SCs (Ghimire and Deans, 2019) and the medial side of HCs (Montcouquiol et al., 2006; Chang et al., 2016), but FZD3 is expressed in SGNs (Duncan et al., 2019; Stoner et al., 2021). While the expression of FZD9 can be detected in early cochlear inner phalangeal cells (IPhCs), IBCs, and the third-row DCs (Zhang et al., 2019).

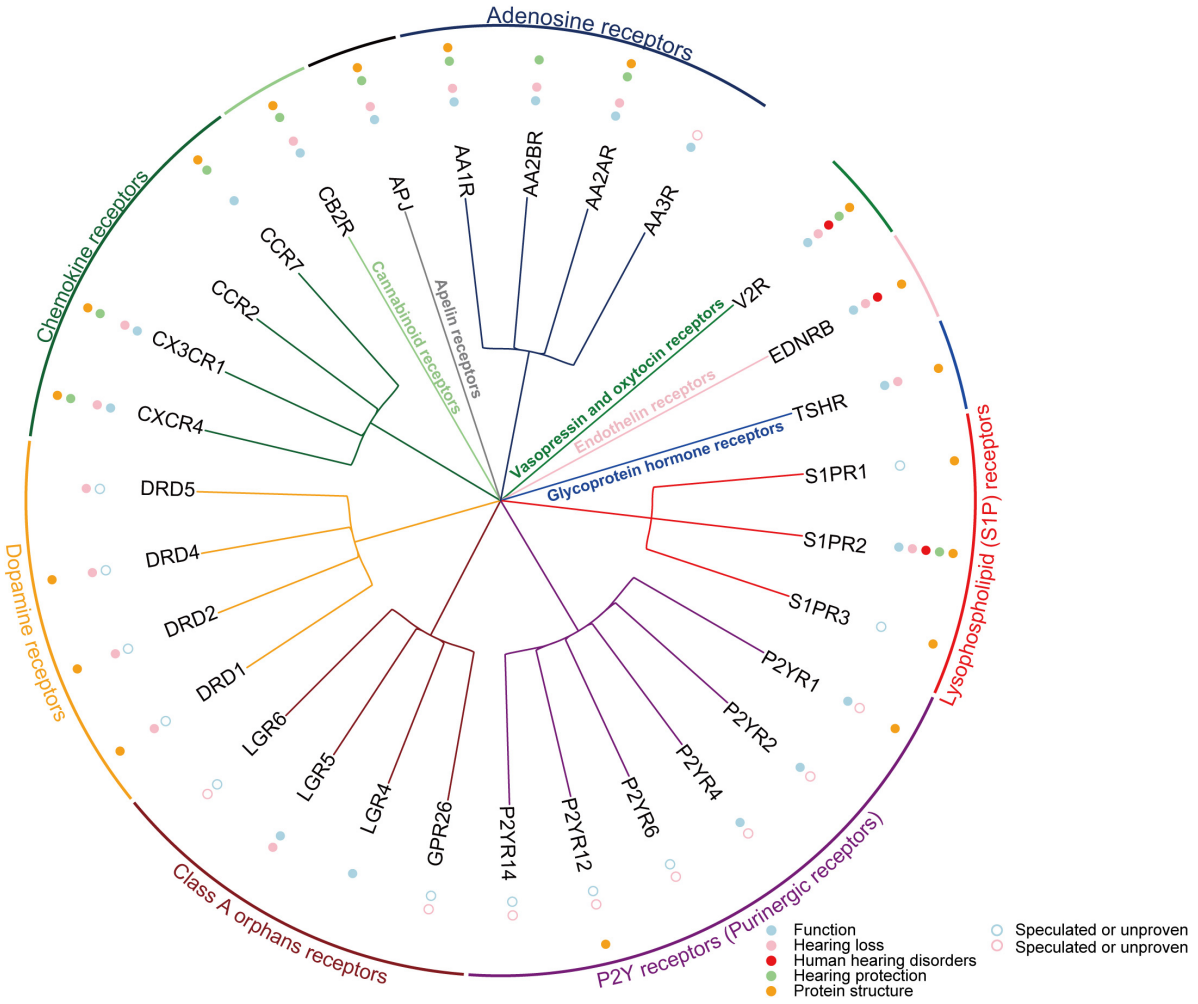

FIGURE 2
The summary of reported 30 Class A GPCRs in cochlea. The blue circle indicates that GPCR are functional in the cochlea. Pink circle indicates GPCR associated with hearing loss. Red circle indicates GPCR associated with human hearing disorders. Green circle indicates GPCR involved in hearing protection. The orange circle indicates that the GPCR has resolved the protein structure. Open circles indicate conjectures or confirmed conclusions.

Among the 10 FZDs, FZD 2, 3, 4, 6, and 9 play different important roles in the cochlea. Knockout of *FZD2* in the mouse cochlea results in defects in OHC number and orientation, which are most severe in the apical region. In addition, a recent study identified *FZD2* as a signature gene in one of three distinct SGN I populations by using single-cell transcriptome (Grandi et al., 2020). In the mouse cochlea, planar polarity is guided by the PCP proteins FZD3 and FZD6. However, FZD3 and FZD6 are functionally redundant, and the orientation of HCs is severely affected only in *FZD3/6* double knockout mice (Wang et al., 2006). Moreover, FZD3 and FZD6 play a key role in guiding SGN II peripheral axons turning (Ghimire and Deans, 2019). A recent study uncovered SPAG6 as a regulator of FZD6, because FZD6 lost its normal polarized distribution in *SPAG6*$^{-/-}$ mice (Li et al., 2021). Furthermore, a novel non-canonical Wnt pathway was identified in cochlear HCs that signals through PI3K, Rac1 and Gsk3β to regulate the PCP pathway by promoting the junctional localization of core PCP proteins such as FZD6 (Landin Malt et al., 2021). Compared with the above-mentioned FZDs, FZD4 does not affect HC survival but only affects HC function, so only the late onset hearing loss can be found in *FZD4*$^{-/-}$ mice (Wang et al., 2001). The main role of FZD9 in cochlea is HC regeneration, and *FZD9*$^{+}$ cells have strong ability of proliferation, differentiation and HC generation. It still has HC-generating capacity at 6 days after treatment *in vivo* lineage tracing, especially it can act as an effective marker for HC progenitors (Zhang et al., 2019). Therefore, FZD9 has clinical translational value for the regeneration of HCs.

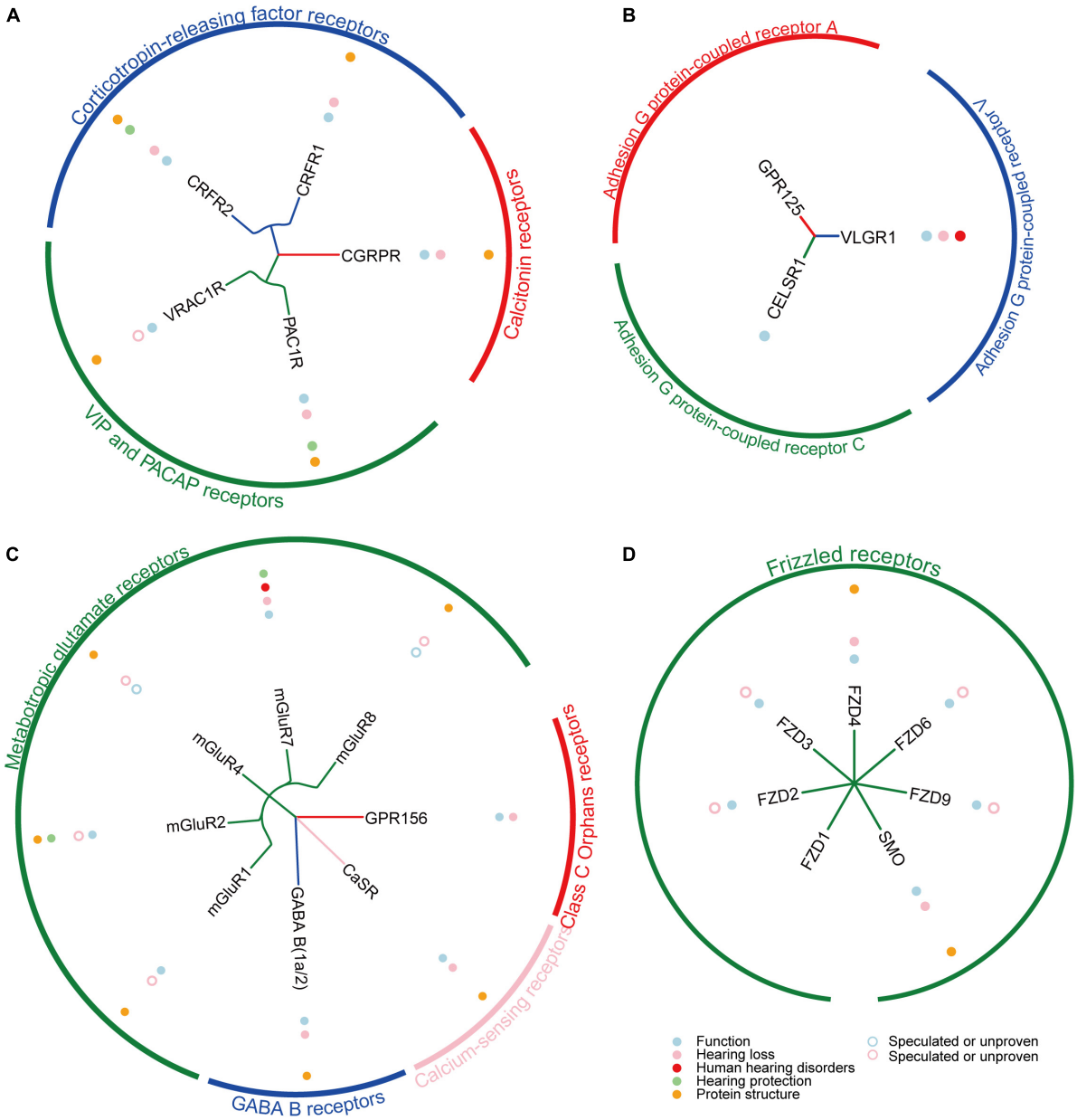

FIGURE 3
The summary of reported Class B1/B2/C/F GPCRs in cochlea. **(A)** The summary of reported 5 Class B1 GPCRs in cochlea. **(B)** The summary of reported 3 Class B2 GPCRs in cochlea. **(C)** The summary of reported 8 Class C GPCRs in cochlea. **(D)** The summary of reported 7 Class F GPCRs in cochlea.

SMO mediates the Hedgehog (Hh) signaling pathway, activated SMO lead Gli to translocate into the nucleus to activate target genes, in which SMO can couple to $G_{i/o}$ and $G_{12/13}$ (Gorojankina, 2016; Qi et al., 2019; Okashah et al., 2020). In the auditory field, SMO is found to participate in cochlear development, HC differentiation and hearing function. In mouse embryos carried inner ear conditional knockout of *Smoothened* (*SMO*^{ecko}), the cochlea exhibited hypoplasia, in which the cochlear duct and saccule were completely absent in *SMO*^{ecko} embryos (Brown and Epstein, 2011; Muthu et al., 2019). What's more, in *SMO*^{cko} mouse (similar to *SMO*^{ecko} mouse) early cochlea, apex HCs preferentially accelerate differentiation (Tateya et al., 2013). Although *SMO*^{cko} mice survive after birth, HCs in the apical region appear disorganized and reduced in number, causing hearing loss which predominantly at low frequencies. And *SMO*^{ecko} has also been used to identify key genes that are activated and repressed by Shh signaling

TABLE 2 Class B1 GPCRs relevant to cochlea.

GPCR family	Subtypes	Roles in cochlea	Localization	Genetic modulation	References
Class B1 GPCRs					
VIP and PACAP receptors	VPAC1R	Possibly acting as neurotransmitters	SGN	-	Feng and Liu, 2015
	PAC1R	Protection of NIHL	HC, SC, SGN, ANF, ENF, SV	*PAC1R*$^{-/-}$ mice	Ruel et al., 2021
				TgHPAC1R mice	
Corticotropin-releasing factor receptors	CRFR1	Maintaining normal auditory function	ISC, HSC, DC, BC	*CRFR1*$^{-/-}$ mice	Graham and Vetter, 2011
		Involved IHC and HC innervation development		*CRFR1-GFP* mice	
	CRFR2	Constitutively modulates hearing sensitivity	ISC, HSC, DC, IBC, SGNs, CC, BoC	*CRFR2*$^{-/-}$ mice	Graham et al., 2010
		Protection of NIHL			
Calcitonin receptors	CGRPR	Associated with increased cochlear nerve activity	-	-	Dickerson et al., 2016

SGN, Spiral Ganglion Neuron; HC, hair cell; SC, supporting cell; ANF, afferent nerve fiber; ENF, efferent nerve fiber; SV, Stria Vascularis; ISC, inner sulcus cell; HSC, Hensen cell; DC, Deiters' cell; BC, border cell; IBC, inner border cell; CC, Claudius cell; BoC, Boettcher cell.

in the cochlea during the initial stages of growth (Muthu et al., 2019). In addition, SMO may be associated with otosclerosis (Brown and Epstein, 2011) and cochlear neural stem cell (NSC) transplantation (Huang et al., 2018). The use of taurine during transplantation can up-regulate Hh pathway proteins such as SMO, thereby stimulating the cell proliferation and differentiation of NSCs into SGNs. These results suggest that SMO has potential applications in the treatment of hearing impairment and cochlear NSC transplantation.

Emerging G protein-coupled receptor-based treatment

G protein-coupled receptor-based drug development

G protein-coupled receptors are keeping great advantages as drug targets, thanks to the rapid development of single-particle cryo-electron microscopy (cryo-EM) technology and artificial intelligence (AI) technology in recent years. Since the first use of cryo-EM to resolve the complex structure of GPCR and G protein in 2017, the number of GPCR structures resolved every year has grown exponentially (Liang et al., 2017; Kooistra et al., 2021). Compared with previous X-ray crystallography studies required higher thermal stability, cryo-EM can obtain different conformations of stable GPCRs and structures of complexes with G proteins that are closer to the native state, which greatly improves the efficiency of ligand screening or drug design (Renaud et al., 2018). So far, the structures of 30 GPCRs functioning in the cochlea have been successfully resolved (**Figures 2**, **3**; **Supplementary Table 1**). In recent years, the application of AI in structural biology has also greatly promoted the elucidation of GPCRs and the corresponding drug design. For example, AlphaFold2 and RosettaFold are the most typical applications at present (Baek et al., 2021; Jumper et al., 2021) with high accuracy, high speed, and convenience for GPCR structure-oriented drug design. In addition, according to statistics, GPCRs remain one of the most important drug targets (Hauser et al., 2017).

There are many types of GPCRs targeting drugs in clinical trials, including peptides, monoclonal antibodies, recombinant proteins, small molecules, and nanobodies (Saikia et al., 2019). According to the mode of action, it can be divided into agonists, antagonists, positive allosteric modulators (PAM), negative allosteric modulators (NAM) and so on (Hauser et al., 2017; Odoemelam et al., 2020). When a ligand binds to a GPCR, the receptor undergoes a conformational change in which agonists can activate and antagonists can inhibit signal

TABLE 3 Class B2 GPCRs relevant to cochlea.

GPCR family	Subtypes	Roles in cochlea	Localization	Genetic modulation	References
Class B2 GPCRs					
Adhesion G protein-coupled receptor C	CELSR1	Guide OHC orientation	HC, SC	*CELSR1*$^{-/-}$ mice	Duncan et al., 2017
				CELSR1$^{Crsh/Crsh}$ mouse	Curtin et al., 2003
				CELSR1$^{Scy/Scy}$ mice	
Adhesion G protein-coupled receptor V	VLGR1	Involved in the stereociliary development of hair cells	HC	*VLGR1*$^{-/-}$ mice	Yagi et al., 2005
		Cause Usher syndrome type IIC (USH2C) in humans		*VLGR1/delTM7* mice	McMillan and White, 2004
				VLGR1$^{BUB/BnJ}$ mice	Skradski et al., 2001
				VLGR1^{Frings} mice	
Adhesion G protein-coupled receptor A	GPR125	No effect on cochlear development and hearing	OHC, SGNS, IC	*GPR125*$^{-/-}$ mice	Sun et al., 2021
				Gpr125$^{lacZ/lacZ}$ mice	

HC, hair cell; SC, supporting cell; OHC, outer hair cell; SGN, Spiral Ganglion Neuron; IC, interdental cell.

transduction pathways. In contrast to orthosteric ligands such as agonists and antagonists, allosteric modulators (PAM or NAM) as promising therapeutic agents can infiltrate into a pocket that is different in space than the orthotopic site, and modulate signaling only in the presence of the natural ligand to prevent adverse side effects (Massink et al., 2020; Yang et al., 2022).

In cochlear research and treatment, GPCR-targeted drugs have also been used to some extent. For example, S1PR2 agonist (CYM-5478) (Wang et al., 2020), CaSR inhibitors (NPS2143 and Calhex231) (Minakata et al., 2019), V2R antagonist (OPC-41061/Tolvaptan) (Egami et al., 2016), CB2R agonist (JWH105) (Vlajkovic et al., 2006; Dhukhwa et al., 2021), AA1R agonists (R-PIA and ADAC) (Vlajkovic et al., 2010; Kaur et al., 2016), AA2AR antagonist (istradefylline) (Han et al., 2019; Manalo et al., 2020; Shin et al., 2021) all have a therapeutic and protective effect on the cochlea. Among these GPCR-targeted drugs, V2R antagonist (OPC-41061/Tolvaptan) and AA2AR antagonist (istradefylline) have been approved by the US Food and Drug Administration (FDA) (NDA022075, NDA022275). V2R antagonist (OPC-41061/Tolvaptan) is approved for the treatment of autosomal dominant polycystic kidney disease, fibrosis, hyponatremia, heart failure, and the syndrome of dysregulated antidiuretic hormone secretion in humans (Cao et al., 2022; Martin-Grace et al., 2022). AA2AR antagonist (istradefylline) is widely used to treat Parkinson's disease in humans (Merighi et al., 2022). However, many GPCRs extensively developed in the cochlea, such as CRFR1 (Graham and Vetter, 2011), CRFR2 (Graham et al., 2010), and CGRPR (Maison et al., 2003) mentioned above, also have great potential in the future of cochlear therapy to treat or prevent of noise- and pharmaceutical-induced auditory toxicity (Lowery and Thiele, 2010; Hauser et al., 2017; Deganutti et al., 2021). Therefore, besides existing drugs targeting GPCRs that can be further tried to be applied to the treatment of the cochlea, more structures of potential GPCRs targets are helpful to design drugs in cochlear therapy.

G protein-coupled receptor-based gene therapy

The use of drugs generally only works when the target protein exists and expresses. Considering that one out of every 1,000 births in the world is hereditary deafness (Ajay et al., 2022), and mutations or deletions of 124 genes have been found to cause hearing loss,[2] so these hereditary hearing impairments are difficult to treat with

2 https://hereditaryhearingloss.org/

TABLE 4 Class C GPCRs relevant to cochlea.

GPCR family	Subtypes	Roles in cochlea	Localization	Genetic modulation	References
Class C GPCRs					
Metabotropic glutamate receptors	mGluR1	Enhance efferent inhibition of IHCs	SGN, HC	-	Ye et al., 2017
		Promote excitatory neurotransmission in SGN I			Peng et al., 2004
	mGluR2	Inhibit efferent dopamine release onto IHCs	SGN I, efferent lateral olivocochlear GABAergic fiber	-	Doleviczenyi et al., 2005
	mGluR4	-	IHC	-	Klotz et al., 2019
	mGluR7	Associated with ARHL and NIHL	HC	*mGluR7*$^{-/-}$ mice	Chang et al., 2018
		Knockout results in hearing deficits			Fisher et al., 2020
	mGluR8	-	HC	-	Klotz et al., 2019
GABA B receptors	GABA B(1a,2)	Affect OHC function	SGN	*GABA B1-GFP reporter* mouse	Maison et al., 2009
		Modulate the strength of the SGN-HC synapse		*GABA B1a*$^{-/-}$ mice	Wedemeyer et al., 2013
				GABA B1b$^{-/-}$ mice	
Calcium-sensing receptors	CaSR	Maintain cochlear Ca^{2+} homeostasis	Fibrocytes of the spiral ligament and spiral limbus, SMC of the spiral modiolar arteries and epithelia of the osseous spiral lamina	-	Minakata et al., 2019
Class C Orphans receptors	GPR156	EMX2 > GPR156 > $G\alpha_i$ signaling cascade is required for HC orientation	HC	*GPR156*$^{-/-}$ mice	Kindt et al., 2021
				GPR156^{exon2} zebrafish	
				GPR156^{sa34566} zebrafish	

SGN, Spiral Ganglion Neuron; HC, hair cell; IHC, inner hair cell; SMC, smooth muscle cell.

10.3389/fnmol.2022.1028125

TABLE 5 Class F GPCRs relevant to cochlea.

GPCR family	Subtypes	Roles in cochlea	Localization	Genetic modulation	References
Class F GPCRs					
Frizzled receptors	FZD1	-	HC, SC	*FZD1*$^{-/-}$ mice	Yu et al., 2010
	FZD2	Guide OHC orientation	HC, SC, SGN I	*FZD2*$^{-/-}$ mice	Yu et al., 2010
		A marker as one distinct type I SGN			Grandi et al., 2020
	FZD3	Guide planar polarity of HC with FZD6	HC, SC, SGN	*ATOH1*-Cre: *FZD3*$^{-/-}$ mice	Stoner et al., 2021
		Guide Type II SGN peripheral axons turning with FZD6		*NEUROD1*-cre: *FZD3*$^{-/-}$ mice	Wang et al., 2006
				FZD3$^{-/-}$ mice	Ghimire and Deans, 2019
				FZD3$^{-/-}$; *FZD6*$^{-/-}$ mice	
	FZD4	Knockout results in the late onset hearing loss	HC	*FZD4*$^{-/-}$ mice	Wang et al., 2001
	FZD6	Guide planar polarity of HC with FZD3	HC, SC	*FZD6*$^{-/-}$ mice	Wang et al., 2006
		Guide Type II SGN peripheral axons turning with FZD3		*FZD3*$^{-/-}$; *FZD6*$^{-/-}$ mice	Ghimire and Deans, 2019
	FZD9	Promote hair cell regeneration	IPhC, IBC, DC	*FZD9-CreER; ROSA26-tdTomato* Mice	Zhang et al., 2019
	SMO	Affect cochlear development: cochlear duct and saccule were absent when knockout	HC, NSC	*FOXG1-Cre; SMO*$^{loxp/-}$ (*SMO*^{ecko}) mice	Muthu et al., 2019
		Affect hair cell differentiation: apical HCs appear disorganized and reduced when knockout		*EMX2-Cre; SMO*$^{-/-}$ (*SMO*^{cko}) mice	Brown and Epstein, 2011
		Affect hearing function: hearing loss at low frequencies when knockout			Tateya et al., 2013
		Promote cochlear NSC transplantation			Huang et al., 2018

HC, hair cell; SC, supporting cell; SGN, Spiral Ganglion Neuron; IPhC, inner phalangeal cell; IBC, inner border cell; DC, Deiters' cell; NSC, neural stem cell.

10.3389/fnmol.2022.1028125

drugs. Therefore, gene therapy provides a therapeutic direction for hearing loss caused by gene mutation or deletion (Lee et al., 2020; Maguire and Corey, 2020). Briefly, the introducing a normal gene into the target cell through a delivery vector to replace or enhance the defective gene, can restore a normal level to avoid loss of function. In the field of cochlear therapy, gene therapy was first used to rescue hearing loss in the *VGLUT3* knockout mouse, a model of congenital deafness, as early as 2012 (Akil et al., 2012). Subsequently, many deafness caused by gene mutation or deletion were studied by similar gene therapy approaches, including *TMC1* (Nist-Lund et al., 2019), *GJB2* (Iizuka et al., 2015), *USH1C* (Pan et al., 2017), and so on.

In recent years, the CRISPR (clustered regularly interspaced short palindromic repeats) based gene editing methods have opened up new avenues for gene therapy in the field of hearing (Zuris et al., 2015). It can target gene disruption or repair mutations to restore gene function, no need to consider how to produce adequate levels of exogenous transgene expression. At present, the exploration of gene editing methods for cochlear gene therapy is mainly based on CRISPR-Cas9 and CRISPR-Cas13 (Geleoc and El-Amraoui, 2020; Botto et al., 2021). The CRISPR-Cas9 system edits DNA, and the cure may be permanent after the correction of disease-causing mutation *in vivo*. It has been studied in a series of hearing treatments, for example, the dominant mutation of the *TMC1* gene in a Beethoven mouse model of hearing loss has been successfully corrected. Hearing was significantly restored in the treated mice, and this effect was stable for up to a year (Gao et al., 2018; Gyorgy et al., 2019). Unlike the CRISPR-Cas9 system targeting DNA, CRISPR-Cas13 system edits disease-associated RNA transcripts, which is transient and potentially reversible, thus also offering improved safety. Two recent studies have revealed the potential of the CRISPR-Cas13 system in gene therapy for the repair of hearing loss caused by mutations, including CRISPR-Cas13X (Xiao et al., 2022) and CRISPR-CasRx (Guo et al., 2022).

The good news is that the first gene therapy for a disease caused by a specific genetic mutation has been approved by the FDA at 2017 (Maguire et al., 2021), supporting the huge clinical potential of gene therapy. In the field of GPCR-related gene therapy, considerable progress has been made in the study of rhodopsin (RHO) in the retina (Athanasiou et al., 2018). Multiple works rescue retinal degeneration in *RHO* mutant mice for up to 6–9 months by supplementing exogenous *RHO* (O'Reilly et al., 2007; Chadderton et al., 2009; Mao et al., 2011). In addition, there is some work to correct *RHO* mutations by CRISPR/Cas9 gene editing for the treatment of inherited retinal degeneration (Bakondi et al., 2016; Burnight et al., 2017). Among the nine genes with mutations or deletions of GPCR-encoding genes that cause hearing loss, including *GABA B1* (Maison et al., 2009), *GPR156* (Kindt et al., 2021), *mGluR7* (Friedman et al., 2009), *VLGR1* (Kimberling et al., 1995), *PAC1R* (Ruel et al., 2021), *EDNRB* (Huang et al., 2021), *S1PR2* (Santos-Cortez et al., 2016), *TSHR* (Li et al., 1999), and *CRFR1* (Graham and Vetter, 2011), five of them *mGluR7* (Friedman et al., 2009), *VLGR1* (Kimberling et al., 1995), *EDNRB* (Huang et al., 2021), *V2R* (Zou et al., 2019; Wang et al., 2022), and *S1PR2* (Santos-Cortez et al., 2016) are directly related to human deafness, which are especially worth developing for gene therapy.

Conclusion

In this review, we mainly summarize the expression of five subfamilies of GPCRs in the cochlea, their functions, their relationship with hearing loss, and their potential therapeutic directions (**Tables 1–5**). A total of 53 GPCRs have been reported to be expressed in the cochlea, of which 38 have been shown to function in the cochlea (**Figures 2**, **3**; **Supplementary Table 1**). Most importantly, 27 GPCRs were found to be associated with hearing loss, 5 of which were directly associated with human hearing disorders (VLGR1, mGluR7, V2R, EDNRB, and S1PR2). In addition, 13 GPCRs (CXCR4, CX3CR1, CCR2, CCR7, CB2R, APJ, AA1R, AA2AR, AA2BR, PAC1R, CRFR2, mGluR7, and S1PR2) were confirmed to play a hearing protective role in noise and ototoxicity. We also prospect the GPCR-targeted drug development and gene therapies in the future. In conclusion, GPCRs have great potential in the treatment of hearing loss, so more GPCR functions in the cochlea, more GPCRs related to hearing loss, and more GPCR-based treatment regimens remain to be further explored.

Author contributions

YY, JF, and RC conceived this review. XM and JG wrote the manuscript. YF, CS, PJ, YZ, LZ, YY, JF, and RC revised the manuscript. All authors have read and approved the final manuscript.

Funding

This work was supported by grants from National Key R&D Program of China (No. 2017YFA0103903), Strategic Priority Research Program of the Chinese Academy of Sciences (XDA16010303), National Natural Science Foundation of China (No. 81970882 and 81970892), Natural

Science Foundation from Jiangsu Province (BE2019711 and BK20190062), Shenzhen Fundamental Research Program (JCYJ20190814093401920), Open Research Fund of State Key Laboratory of Genetic Engineering, Fudan University (No. SKLGE1809), and Postdoctoral Innovative Talent Support Program (BX20220122).

Conflict of interest

The authors declare that the research was conducted in the absence of any commercial or financial relationships that could be construed as a potential conflict of interest.

The reviewers FC and YC declared a past co-authorship with the authors XM, YZ, and RC to the handling editor.

Publisher's note

Supplementary material

The Supplementary Material for this article can be found online at: https://www.frontiersin.org/articles/10.3389/fnmol.2022.1028125/full#supplementary-material

References

Abbracchio, M. P., Burnstock, G., Boeynaems, J. M., Barnard, E. A., Boyer, J. L., Kennedy, C., et al. (2006). International Union of Pharmacology LVIII: Update on the P2Y G protein-coupled nucleotide receptors: From molecular mechanisms and pathophysiology to therapy. *Pharmacol. Rev.* 58, 281–341. doi: 10.1124/pr.58.3.3

Abu-Hamdan, M. D., Drescher, M. J., Ramakrishnan, N. A., Khan, K. M., Toma, V. S., Hatfield, J. S., et al. (2006). Pituitary adenylyl cyclase-activating polypeptide (PACAP) and its receptor (PAC1-R) in the cochlea: Evidence for specific transcript expression of PAC1-R splice variants in rat microdissected cochlear subfractions. *Neuroscience* 140, 147–161. doi: 10.1016/j.neuroscience.2006.01.019

AitRaise, I., Amalou, G., Bousfiha, A., Charoute, H., Rouba, H., Abdelghaffar, H., et al. (2022). Genetic heterogeneity in GJB2, COL4A3, ATP6V1B1 and EDNRB variants detected among hearing impaired families in Morocco. *Mol. Biol. Rep.* 49, 3949–3954. doi: 10.1007/s11033-022-07245-z

Ajay, E., Gunewardene, N., and Richardson, R. (2022). Emerging therapies for human hearing loss. *Expert Opin. Biol. Ther.* 22, 689–705. doi: 10.1080/14712598.2022.2072208

Akil, O., Seal, R. P., Burke, K., Wang, C., Alemi, A., During, M., et al. (2012). Restoration of hearing in the VGLUT3 knockout mouse using virally mediated gene therapy. *Neuron* 75, 283–293. doi: 10.1016/j.neuron.2012.05.019

Alavi, M. S., Shamsizadeh, A., Azhdari-Zarmehri, H., and Roohbakhsh, A. (2018). Orphan G protein-coupled receptors: The role in CNS disorders. *Biomed. Pharmacother.* 98, 222–232. doi: 10.1016/j.biopha.2017.12.056

Allache, R., De Marco, P., Merello, E., Capra, V., and Kibar, Z. (2012). Role of the planar cell polarity gene CELSR1 in neural tube defects and caudal agenesis. *Birth Defects Res. A Clin. Mol. Teratol.* 94, 176–181. doi: 10.1002/bdra.23002

Aminyavari, S., Zahmatkesh, M., Farahmandfar, M., Khodagholi, F., Dargahi, L., and Zarrindast, M. R. (2019). Protective role of Apelin-13 on amyloid beta25-35-induced memory deficit; involvement of autophagy and apoptosis process. *Prog. Neuropsychopharmacol. Biol. Psychiatry* 89, 322–334. doi: 10.1016/j.pnpbp.2018.10.005

Andrianov, G. N., Ryzhova, I. V., and Tobias, T. V. (2009). Dopaminergic modulation of afferent synaptic transmission in the semicircular canals of frogs. *Neurosignals* 17, 222–228. doi: 10.1159/000224632

Athanasiou, D., Aguila, M., Bellingham, J., Li, W., McCulley, C., Reeves, P. J., et al. (2018). The molecular and cellular basis of rhodopsin retinitis pigmentosa reveals potential strategies for therapy. *Prog. Retin. Eye Res.* 62, 1–23. doi: 10.1016/j.preteyeres.2017.10.002

Azizi, Y., Faghihi, M., Imani, A., Roghani, M., and Nazari, A. (2013). Post-infarct treatment with [Pyr1]-apelin-13 reduces myocardial damage through reduction of oxidative injury and nitric oxide enhancement in the rat model of myocardial infarction. *Peptides* 46, 76–82. doi: 10.1016/j.peptides.2013.05.006

Babola, T. A., Kersbergen, C. J., Wang, H. C., and Bergles, D. E. (2020). Purinergic signaling in cochlear supporting cells reduces hair cell excitability by increasing the extracellular space. *Elife* 9:e52160. doi: 10.7554/eLife.52160

Babola, T. A., Li, S., Wang, Z., Kersbergen, C. J., Elgoyhen, A. B., Coate, T. M., et al. (2021). Purinergic signaling controls spontaneous activity in the auditory system throughout early development. *J. Neurosci.* 41, 594–612. doi: 10.1523/JNEUROSCI.2178-20.2020

Baek, M., DiMaio, F., Anishchenko, I., Dauparas, J., Ovchinnikov, S., Lee, G. R., et al. (2021). Accurate prediction of protein structures and interactions using a three-track neural network. *Science* 373, 871–876. doi: 10.1126/science.abj8754

Bakondi, B., Lv, W., Lu, B., Jones, M. K., Tsai, Y., Kim, K. J., et al. (2016). In vivo CRISPR/Cas9 gene editing corrects retinal dystrophy in the S334ter-3 rat model of autosomal dominant retinitis pigmentosa. *Mol. Ther.* 24, 556–563. doi: 10.1038/mt.2015.220

Beaulieu, J. M., and Gainetdinov, R. R. (2011). The physiology, signaling, and pharmacology of dopamine receptors. *Pharmacol. Rev.* 63, 182–217. doi: 10.1124/pr.110.002642

Bircan, B., Cakir, M., Kirbag, S., and Gul, H. F. (2016). Effect of apelin hormone on renal ischemia/reperfusion induced oxidative damage in rats. *Ren. Fail.* 38, 1122–1128. doi: 10.1080/0886022X.2016.1184957

Blankenship, A. G., and Feller, M. B. (2010). Mechanisms underlying spontaneous patterned activity in developing neural circuits. *Nat. Rev. Neurosci.* 11, 18–29. doi: 10.1038/nrn2759

Bondurand, N., Dufour, S., and Pingault, V. (2018). News from the endothelin-3/EDNRB signaling pathway: Role during enteric nervous system development and involvement in neural crest-associated disorders. *Dev. Biol.* 4, S156–S169. doi: 10.1016/j.ydbio.2018.08.014

Bonnet, C., and El-Amraoui, A. (2012). Usher syndrome (sensorineural deafness and retinitis pigmentosa): Pathogenesis, molecular diagnosis and therapeutic approaches. *Curr. Opin. Neurol.* 25, 42–49. doi: 10.1097/WCO.0b013e32834ef8b2

Botto, C., Dalkara, D., and El-Amraoui, A. (2021). Progress in gene editing tools and their potential for correcting mutations underlying hearing and vision loss. *Front. Genome Ed.* 3:737632. doi: 10.3389/fgeed.2021.737632

Bowery, N. G., and Enna, S. J. (2000). gamma-aminobutyric acid(B) receptors: First of the functional metabotropic heterodimers. *J. Pharmacol. Exp. Ther.* 292, 2–7.

Brown, A. S., and Epstein, D. J. (2011). Otic ablation of smoothened reveals direct and indirect requirements for Hedgehog signaling in inner ear development. *Development* 138, 3967–3976. doi: 10.1242/dev.066126

Brown, S. M., Wager-Miller, J., and Mackie, K. (2002). Cloning and molecular characterization of the rat CB2 cannabinoid receptor. *Biochim. Biophys. Acta* 1576, 255–264. doi: 10.1016/s0167-4781(02)00341-x

Buniello, A., Hardisty-Hughes, R. E., Pass, J. C., Bober, E., Smith, R. J., and Steel, K. P. (2013). Headbobber: A combined morphogenetic and cochleosaccular mouse model to study 10qter deletions in human deafness. *PLoS One* 8:e56274. doi: 10.1371/journal.pone.0056274

Burnight, E. R., Gupta, M., Wiley, L. A., Anfinson, K. R., Tran, A., Triboulet, R., et al. (2017). Using CRISPR-Cas9 to generate gene-corrected autologous iPSCs for the treatment of inherited retinal degeneration. *Mol. Ther.* 25, 1999–2013. doi: 10.1016/j.ymthe.2017.05.015

Cabou, C., and Martinez, L. O. (2022). The interplay of endothelial P2Y receptors in cardiovascular health: From vascular physiology to pathology. *Int. J. Mol. Sci.* 23:5883. doi: 10.3390/ijms23115883

Calver, A. R., Michalovich, D., Testa, T. T., Robbins, M. J., Jaillard, C., Hill, J., et al. (2003). Molecular cloning and characterisation of a novel GABAB-related G-protein coupled receptor. *Brain Res. Mol. Brain Res.* 110, 305–317. doi: 10.1016/s0169-328x(02)00662-9

Cao, X., Wang, P., Yuan, H., Zhang, H., He, Y., Fu, K., et al. (2022). Benzodiazepine derivatives as potent vasopressin V2 receptor antagonists for the treatment of autosomal dominant kidney disease. *J. Med. Chem.* 65, 9295–9311. doi: 10.1021/acs.jmedchem.2c00567

Cartier, A., and Hla, T. (2019). Sphingosine 1-phosphate: Lipid signaling in pathology and therapy. *Science* 366:eaar5551. doi: 10.1126/science.aar5551

Ceriani, F., and Mammano, F. (2012). Calcium signaling in the cochlea–molecular mechanisms and physiopathological implications. *Cell Commun. Signal.* 10:20. doi: 10.1186/1478-811X-10-20

Chadderton, N., Millington-Ward, S., Palfi, A., O'Reilly, M., Tuohy, G., Humphries, M. M., et al. (2009). Improved retinal function in a mouse model of dominant retinitis pigmentosa following AAV-delivered gene therapy. *Mol. Ther.* 17, 593–599. doi: 10.1038/mt.2008.301

Chang, H., Smallwood, P. M., Williams, J., and Nathans, J. (2016). The spatio-temporal domains of Frizzled6 action in planar polarity control of hair follicle orientation. *Dev. Biol.* 409, 181–193. doi: 10.1016/j.ydbio.2015.10.027

Chang, N. C., Dai, C. Y., Lin, W. Y., Yang, H. L., Wang, H. M., Chien, C. Y., et al. (2018). The association of GRM7 single nucleotide polymorphisms with age-related hearing impairment in a Taiwanese population. *J. Int. Adv. Otol.* 14, 170–175. doi: 10.5152/iao.2018.5109

Chaudhary, P. K., and Kim, S. (2021). An insight into GPCR and G-proteins as cancer drivers. *Cells* 10:3288. doi: 10.3390/cells10123288

Chen, H., Chen, K., Huang, W., Staudt, L. M., Cyster, J. G., and Li, X. (2022). Structure of S1PR2-heterotrimeric G13 signaling complex. *Sci. Adv.* 8:eabn0067. doi: 10.1126/sciadv.abn0067

Cheng, C., Guo, L., Lu, L., Xu, X., Zhang, S., Gao, J., et al. (2017). Characterization of the transcriptomes of Lgr5+ hair cell progenitors and Lgr5-supporting cells in the mouse cochlea. *Front. Mol. Neurosci.* 10:122. doi: 10.3389/fnmol.2017.00122

Claussen, A. D., Quevedo, R. V., Kirk, J. R., Higgins, T., Mostaert, B., Rahman, M. T., et al. (2022). Chronic cochlear implantation with and without electric stimulation in a mouse model induces robust cochlear influx of CX3CR1$^{+/GFP}$ macrophages. *Hear. Res.* 108510. doi: 10.1016/j.heares.2022.108510

Clevers, H., and Nusse, R. (2012). Wnt/beta-catenin signaling and disease. *Cell* 149, 1192–1205. doi: 10.1016/j.cell.2012.05.012

Colcombet-Cazenave, B., Cordier, F., Zhu, Y., Bouvier, G., Litsardaki, E., Laserre, L., et al. (2022). Deciphering the molecular interaction between the adhesion G protein-coupled receptor ADGRV1 and its PDZ-containing regulator PDZD7. *Front. Mol. Biosci.* 9:923740. doi: 10.3389/fmolb.2022.923740

Cox, B. C., Chai, R., Lenoir, A., Liu, Z., Zhang, L., Nguyen, D. H., et al. (2014). Spontaneous hair cell regeneration in the neonatal mouse cochlea in vivo. *Development* 141, 816–829. doi: 10.1242/dev.103036

Curtin, J. A., Quint, E., Tsipouri, V., Arkell, R. M., Cattanach, B., Copp, A. J., et al. (2003). Mutation of Celsr1 disrupts planar polarity of inner ear hair cells and causes severe neural tube defects in the mouse. *Curr. Biol.* 13, 1129–1133. doi: 10.1016/s0960-9822(03)00374-9

Daudet, N., Ripoll, C., Moles, J. P., and Rebillard, G. (2002). Expression of members of Wnt and Frizzled gene families in the postnatal rat cochlea. *Brain Res. Mol. Brain Res.* 105, 98–107. doi: 10.1016/s0169-328x(02)00397-2

Davies, A., Formstone, C., Mason, I., and Lewis, J. (2005). Planar polarity of hair cells in the chick inner ear is correlated with polarized distribution of c-flamingo-1 protein. *Dev. Dyn.* 233, 998–1005. doi: 10.1002/dvdy.20376

de la Nuez Veulens, A., Ginarte, Y. M. A., Fernandez, R. E. R., Leclerc, F., and Cabrera, L. A. M. (2022). Prediction of molecular interactions and physicochemical properties relevant for vasopressin V2 receptor antagonism. *J. Mol. Model.* 28:31. doi: 10.1007/s00894-021-05022-6

Dedic, N., Chen, A., and Deussing, J. M. (2018). The CRF family of neuropeptides and their receptors–mediators of the central stress response. *Curr. Mol. Pharmacol.* 11, 4–31. doi: 10.2174/1874467210666170302104053

Deganutti, G., Atanasio, S., Rujan, R. M., Sexton, P. M., Wootten, D., and Reynolds, C. A. (2021). Exploring ligand binding to calcitonin gene-related peptide receptors. *Front. Mol. Biosci.* 8:720561. doi: 10.3389/fmolb.2021.720561

Dhukhwa, A., Al Aameri, R. F. H., Sheth, S., Mukherjea, D., Rybak, L., and Ramkumar, V. (2021). Regulator of G protein signaling 17 represents a novel target for treating cisplatin induced hearing loss. *Sci. Rep.* 11:8116. doi: 10.1038/s41598-021-87387-5

Dickerson, I. M., Bussey-Gaborski, R., Holt, J. C., Jordan, P. M., and Luebke, A. E. (2016). Maturation of suprathreshold auditory nerve activity involves cochlear CGRP-receptor complex formation. *Physiol. Rep.* 4:e12869. doi: 10.14814/phy2.12869

Dijksterhuis, J. P., Petersen, J., and Schulte, G. (2014). WNT/Frizzled signalling: Receptor-ligand selectivity with focus on FZD-G protein signalling and its physiological relevance: IUPHAR Review 3. *Br. J. Pharmacol.* 171, 1195–1209. doi: 10.1111/bph.12364

Doleviczenyi, Z., Halmos, G., Repassy, G., Vizi, E. S., Zelles, T., and Lendvai, B. (2005). Cochlear dopamine release is modulated by group II metabotropic glutamate receptors via GABAergic neurotransmission. *Neurosci. Lett.* 385, 93–98. doi: 10.1016/j.neulet.2005.05.017

Drescher, M. J., Drescher, D. G., Khan, K. M., Hatfield, J. S., Ramakrishnan, N. A., Abu-Hamdan, M. D., et al. (2006). Pituitary adenylyl cyclase-activating polypeptide (PACAP) and its receptor (PAC1-R) are positioned to modulate afferent signaling in the cochlea. *Neuroscience* 142, 139–164. doi: 10.1016/j.neuroscience.2006.05.065

Driver, E. C., and Kelley, M. W. (2020). Development of the cochlea. *Development* 147:dev162263. doi: 10.1242/dev.162263

Duan, J., Xu, P., Luan, X., Ji, Y., He, X., Song, N., et al. (2022). Hormone- and antibody-mediated activation of the thyrotropin receptor. *Nature* 609, 854–859. doi: 10.1038/s41586-022-05173-3

Duncan, J. S., Fritzsch, B., Houston, D. W., Ketchum, E. M., Kersigo, J., Deans, M. R., et al. (2019). Topologically correct central projections of tetrapod inner ear afferents require Fzd3. *Sci. Rep.* 9:10298. doi: 10.1038/s41598-019-46553-6

Duncan, J. S., Stoller, M. L., Francl, A. F., Tissir, F., Devenport, D., and Deans, M. R. (2017). Celsr1 coordinates the planar polarity of vestibular hair cells during inner ear development. *Dev. Biol.* 423, 126–137. doi: 10.1016/j.ydbio.2017.01.020

Ebermann, I., Scholl, H. P., Charbel Issa, P., Becirovic, E., Lamprecht, J., Jurklies, B., et al. (2007). A novel gene for Usher syndrome type 2: Mutations in the long isoform of whirlin are associated with retinitis pigmentosa and sensorineural hearing loss. *Hum. Genet.* 121, 203–211. doi: 10.1007/s00439-006-0304-0

Egami, N., Kakigi, A., Takeda, T., and Yamasoba, T. (2016). Dehydration effects of a V2 antagonist on endolymphatic hydrops in guinea pigs. *Hear. Res.* 332, 151–159. doi: 10.1016/j.heares.2015.12.017

Faust, B., Billesbolle, C. B., Suomivuori, C. M., Singh, I., Zhang, K., Hoppe, N., et al. (2022). Autoantibody mimicry of hormone action at the thyrotropin receptor. *Nature* 609, 846–853. doi: 10.1038/s41586-022-05159-1

Feng, J., and Liu, H. (2015). [The expression and significance of VIP and its receptor in the cochlea of different degrees of chronic alcoholism rats]. *Lin Chung Er Bi Yan Hou Tou Jing Wai Ke Za Zhi* 29, 1295–1298.

Fisher, N. M., Gould, R. W., Gogliotti, R. G., McDonald, A. J., Badivuku, H., Chennareddy, S., et al. (2020). Phenotypic profiling of mGlu7 knockout mice reveals new implications for neurodevelopmental disorders. *Genes Brain Behav.* 19:e12654. doi: 10.1111/gbb.12654

Foord, S. M., Bonner, T. I., Neubig, R. R., Rosser, E. M., Pin, J. P., Davenport, A. P., et al. (2005). International Union of Pharmacology. XLVI. G protein-coupled receptor list. *Pharmacol. Rev.* 57, 279–288. doi: 10.1124/pr.57.2.5

Fournel, A., Drougard, A., Duparc, T., Marlin, A., Brierley, S. M., Castro, J., et al. (2017). Apelin targets gut contraction to control glucose metabolism via the brain. *Gut* 66, 258–269. doi: 10.1136/gutjnl-2015-310230

Friedman, R. A., Van Laer, L., Huentelman, M. J., Sheth, S. S., Van Eyken, E., Corneveaux, J. J., et al. (2009). GRM7 variants confer susceptibility to age-related hearing impairment. *Hum. Mol. Genet.* 18, 785–796. doi: 10.1093/hmg/ddn402

Fritzius, T., Stawarski, M., Isogai, S., and Bettler, B. (2022). Structural basis of GABAB receptor regulation and signaling. *Curr. Top. Behav. Neurosci.* 52, 19–37. doi: 10.1007/7854_2020_147

Fulop, D. B., Humli, V., Szepesy, J., Ott, V., Reglodi, D., Gaszner, B., et al. (2019). Hearing impairment and associated morphological changes in pituitary adenylate cyclase activating polypeptide (PACAP)-deficient mice. *Sci. Rep.* 9:14598. doi: 10.1038/s41598-019-50775-z

Gaborjan, A., Lendvai, B., and Vizi, E. S. (1999). Neurochemical evidence of dopamine release by lateral olivocochlear efferents and its presynaptic modulation in guinea-pig cochlea. *Neuroscience* 90, 131–138. doi: 10.1016/s0306-4522(98)00461-8

Gao, X., Tao, Y., Lamas, V., Huang, M., Yeh, W. H., Pan, B., et al. (2018). Treatment of autosomal dominant hearing loss by in vivo delivery of genome editing agents. *Nature* 553, 217–221. doi: 10.1038/nature25164

Gariepy, C. E., Cass, D. T., and Yanagisawa, M. (1996). Null mutation of endothelin receptor type B gene in spotting lethal rats causes aganglionic megacolon and white coat color. *Proc. Natl. Acad. Sci. U.S.A.* 93, 867–872. doi: 10.1073/pnas.93.2.867

Ge, Y., and Wang, Y. T. (2022). Postsynaptic signaling at glutamatergic synapses as therapeutic targets. *Curr. Opin. Neurobiol.* 75:102585. doi: 10.1016/j.conb.2022.102585

Geleoc, G. G. S., and El-Amraoui, A. (2020). Disease mechanisms and gene therapy for Usher syndrome. *Hear. Res.* 394:107932. doi: 10.1016/j.heares.2020.107932

Ghimire, S. R., and Deans, M. R. (2019). Frizzled3 and Frizzled6 cooperate with Vangl2 to direct cochlear innervation by type II spiral ganglion neurons. *J. Neurosci.* 39, 8013–8023. doi: 10.1523/JNEUROSCI.1740-19.2019

Ghosh, S., Sheth, S., Sheehan, K., Mukherjea, D., Dhukhwa, A., Borse, V., et al. (2018). The endocannabinoid/cannabinoid receptor 2 system protects against cisplatin-induced hearing loss. *Front. Cell. Neurosci.* 12:271. doi: 10.3389/fncel.2018.00271

Girotto, G., Vuckovic, D., Buniello, A., Lorente-Canovas, B., Lewis, M., Gasparini, P., et al. (2014). Expression and replication studies to identify new candidate genes involved in normal hearing function. *PLoS One* 9:e85352. doi: 10.1371/journal.pone.0085352

Gorojankina, T. (2016). Hedgehog signaling pathway: A novel model and molecular mechanisms of signal transduction. *Cell. Mol. Life Sci.* 73, 1317–1332. doi: 10.1007/s00018-015-2127-4

Graham, C. E., Basappa, J., and Vetter, D. E. (2010). A corticotropin-releasing factor system expressed in the cochlea modulates hearing sensitivity and protects against noise-induced hearing loss. *Neurobiol. Dis.* 38, 246–258. doi: 10.1016/j.nbd.2010.01.014

Graham, C. E., and Vetter, D. E. (2011). The mouse cochlea expresses a local hypothalamic-pituitary-adrenal equivalent signaling system and requires corticotropin-releasing factor receptor 1 to establish normal hair cell innervation and cochlear sensitivity. *J. Neurosci.* 31, 1267–1278. doi: 10.1523/JNEUROSCI.4545-10.2011

Grainger, S., and Willert, K. (2018). Mechanisms of Wnt signaling and control. *Wiley Interdiscip. Rev. Syst. Biol. Med.* 10:e1422. doi: 10.1002/wsbm.1422

Grandi, F. C., De Tomasi, L., and Mustapha, M. (2020). Single-cell RNA analysis of type I spiral ganglion neurons reveals a Lmx1a population in the cochlea. *Front. Mol. Neurosci.* 13:83. doi: 10.3389/fnmol.2020.00083

Gu, W. X., Du, G. G., Kopp, P., Rentoumis, A., Albanese, C., Kohn, L. D., et al. (1995). The thyrotropin (TSH) receptor transmembrane domain mutation (Pro556-Leu) in the hypothyroid hyt/hyt mouse results in plasma membrane targeting but defective TSH binding. *Endocrinology* 136, 3146–3153. doi: 10.1210/endo.136.7.7789342

Guo, Y., Han, L., Han, S., Tang, H., Wang, S., Cui, C., et al. (2022). Specific knockdown of Htra2 by CRISPR-CasRx prevents acquired sensorineural hearing loss in mice. *Mol. Ther. Nucleic Acids* 28, 643–655. doi: 10.1016/j.omtn.2022.04.014

Gyorgy, B., Nist-Lund, C., Pan, B., Asai, Y., Karavitaki, K. D., Kleinstiver, B. P., et al. (2019). Allele-specific gene editing prevents deafness in a model of dominant progressive hearing loss. *Nat. Med.* 25, 1123–1130. doi: 10.1038/s41591-019-0500-9

Habrian, C. H., Levitz, J., Vyklicky, V., Fu, Z., Hoagland, A., McCort-Tranchepain, I., et al. (2019). Conformational pathway provides unique sensitivity to a synaptic mGluR. *Nat. Commun.* 10:5572. doi: 10.1038/s41467-019-13407-8

Han, B. R., Lin, S. C., Espinosa, K., Thorne, P. R., and Vlajkovic, S. M. (2019). Inhibition of the adenosine A2A receptor mitigates excitotoxic injury in organotypic tissue cultures of the rat cochlea. *Cells* 8:877. doi: 10.3390/cells8080877

Hauser, A. S., Attwood, M. M., Rask-Andersen, M., Schioth, H. B., and Gloriam, D. E. (2017). Trends in GPCR drug discovery: New agents, targets and indications. *Nat. Rev. Drug Discov.* 16, 829–842. doi: 10.1038/nrd.2017.178

He, C., He, L., Lu, Q., Xiao, J., and Dong, W. (2022). The functions and prognostic values of chemokine and chemokine receptors in gastric cancer. *Am. J. Cancer Res.* 12, 3034–3050.

Herr, D. R., Grillet, N., Schwander, M., Rivera, R., Muller, U., and Chun, J. (2007). Sphingosine 1-phosphate (S1P) signaling is required for maintenance of hair cells mainly via activation of S1P2. *J. Neurosci.* 27, 1474–1478. doi: 10.1523/JNEUROSCI.4245-06.2007

Herr, D. R., Reolo, M. J., Peh, Y. X., Wang, W., Lee, C. W., Rivera, R., et al. (2016). Sphingosine 1-phosphate receptor 2 (S1P2) attenuates reactive oxygen species formation and inhibits cell death: Implications for otoprotective therapy. *Sci. Rep.* 6:24541. doi: 10.1038/srep24541

Hirose, K., and Li, S. Z. (2019). The role of monocytes and macrophages in the dynamic permeability of the blood-perilymph barrier. *Hear. Res.* 374, 49–57. doi: 10.1016/j.heares.2019.01.006

Hofrichter, M. A. H., Mojarad, M., Doll, J., Grimm, C., Eslahi, A., Hosseini, N. S., et al. (2018). The conserved p.Arg108 residue in S1PR2 (DFNB68) is fundamental for proper hearing: Evidence from a consanguineous Iranian family. *BMC Med. Genet.* 19:81. doi: 10.1186/s12881-018-0598-5

Hollenstein, K., de Graaf, C., Bortolato, A., Wang, M. W., Marshall, F. H., and Stevens, R. C. (2014). Insights into the structure of class B GPCRs. *Trends Pharmacol. Sci.* 35, 12–22. doi: 10.1016/j.tips.2013.11.001

Huang, L. C., Thorne, P. R., Vlajkovic, S. M., and Housley, G. D. (2010). Differential expression of P2Y receptors in the rat cochlea during development. *Purinergic Signal.* 6, 231–248. doi: 10.1007/s11302-010-9191-x

Huang, S., Song, J., He, C., Cai, X., Yuan, K., Mei, L., et al. (2021). Genetic insights, disease mechanisms, and biological therapeutics for Waardenburg syndrome. *Gene Ther.* 29, 479–497. doi: 10.1038/s41434-021-00240-2

Huang, X., Wu, W., Hu, P., and Wang, Q. (2018). Taurine enhances mouse cochlear neural stem cells proliferation and differentiation to sprial gangli through activating sonic hedgehog signaling pathway. *Organogenesis* 14, 147–157. doi: 10.1080/15476278.2018.1477462

Ida-Eto, M., Ohgami, N., Iida, M., Yajima, I., Kumasaka, M. Y., Takaiwa, K., et al. (2011). Partial requirement of endothelin receptor B in spiral ganglion neurons for postnatal development of hearing. *J. Biol. Chem.* 286, 29621–29626. doi: 10.1074/jbc.M111.236802

Iizuka, T., Kamiya, K., Gotoh, S., Sugitani, Y., Suzuki, M., Noda, T., et al. (2015). Perinatal Gjb2 gene transfer rescues hearing in a mouse model of hereditary deafness. *Hum. Mol. Genet.* 24, 3651–3661. doi: 10.1093/hmg/ddv109

Ingham, N. J., Carlisle, F., Pearson, S., Lewis, M. A., Buniello, A., Chen, J., et al. (2016). S1PR2 variants associated with auditory function in humans and endocochlear potential decline in mouse. *Sci. Rep.* 6:28964. doi: 10.1038/srep28964

Insel, P. A., Sriram, K., Gorr, M. W., Wiley, S. Z., Michkov, A., Salmeron, C., et al. (2019). GPCRomics: An approach to discover GPCR drug targets. *Trends Pharmacol. Sci.* 40, 378–387. doi: 10.1016/j.tips.2019.04.001

Ishiguro, H., Kibret, B. G., Horiuchi, Y., and Onaivi, E. S. (2022). Potential role of cannabinoid type 2 receptors in neuropsychiatric and neurodegenerative disorders. *Front. Psychiatry* 13:828895. doi: 10.3389/fpsyt.2022.828895

Izume, T., Miyauchi, H., Shihoya, W., and Nureki, O. (2020). Crystal structure of human endothelin ETB receptor in complex with sarafotoxin S6b. *Biochem. Biophys. Res. Commun.* 528, 383–388. doi: 10.1016/j.bbrc.2019.12.091

Jang, M. W., Lim, J., Park, M. G., Lee, J. H., and Lee, C. J. (2022). Active role of glia-like supporting cells in the organ of Corti: Membrane proteins and their roles in hearing. *Glia* 70, 1799–1825. doi: 10.1002/glia.24229

Jiang, L., He, J., Chen, X., and Chen, H. (2019). Effect of electroacupuncture on arginine vasopressin-induced endolymphatic hydrops. *J. Tradit. Chin. Med.* 39, 221–228.

Jiang, L. Y., He, J. J., Chen, X. X., Sun, X. J., Wang, X. Z., Zhong, S., et al. (2019). Arginine vasopressin-aquaporin-2 pathway-mediated dehydration effects of electroacupuncture in guinea pig model of AVP-induced eendolymphatic hydrops. *Chin. J. Integr. Med.* 25, 763–769. doi: 10.1007/s11655-017-2411-2

Jumper, J., Evans, R., Pritzel, A., Green, T., Figurnov, M., Ronneberger, O., et al. (2021). Highly accurate protein structure prediction with AlphaFold. *Nature* 596, 583–589. doi: 10.1038/s41586-021-03819-2

Jung, S., Aliberti, J., Graemmel, P., Sunshine, M. J., Kreutzberg, G. W., Sher, A., et al. (2000). Analysis of fractalkine receptor CX(3)CR1 function by targeted deletion and green fluorescent protein reporter gene insertion. *Mol. Cell. Biol.* 20, 4106–4114. doi: 10.1128/MCB.20.11.4106-4114.2000

Kaur, T., Borse, V., Sheth, S., Sheehan, K., Ghosh, S., Tupal, S., et al. (2016). Adenosine A1 receptor protects against cisplatin ototoxicity by suppressing the NOX3/STAT1 inflammatory pathway in the cochlea. *J. Neurosci.* 36, 3962–3977. doi: 10.1523/JNEUROSCI.3111-15.2016

Keeley, E. C., Mehrad, B., and Strieter, R. M. (2010). CXC chemokines in cancer angiogenesis and metastases. *Adv. Cancer Res.* 106, 91–111. doi: 10.1016/S0065-230X(10)06003-3

Kelley, M. W. (2022). Cochlear development; new tools and approaches. *Front. Cell Dev. Biol.* 10:884240. doi: 10.3389/fcell.2022.884240

Khoshsirat, S., Abbaszadeh, H. A., Peyvandi, A. A., Heidari, F., Peyvandi, M., Simani, L., et al. (2021). Apelin-13 prevents apoptosis in the cochlear tissue of

noise-exposed rat via Sirt-1 regulation. *J. Chem. Neuroanat.* 114:101956. doi: 10.1016/j.jchemneu.2021.101956

Kilander, M. B., Petersen, J., Andressen, K. W., Ganji, R. S., Levy, F. O., Schuster, J., et al. (2014). Disheveled regulates precoupling of heterotrimeric G proteins to Frizzled 6. *FASEB J.* 28, 2293–2305. doi: 10.1096/fj.13-246363

Kim, C. H., Kim, H. Y., Lee, H. S., Chang, S. O., Oh, S. H., and Lee, J. H. (2010). P2Y4-mediated regulation of Na^+ absorption in the Reissner's membrane of the cochlea. *J. Neurosci.* 30, 3762–3769. doi: 10.1523/JNEUROSCI.3300-09.2010

Kim, H. J., Ryu, J., Woo, H. M., Cho, S. S., Sung, M. K., Kim, S. C., et al. (2014). Patterns of gene expression associated with Pten deficiency in the developing inner ear. *PLoS One* 9:e97544. doi: 10.1371/journal.pone.0097544

Kim, S., Jo, C. H., and Kim, G. H. (2021). The role of vasopressin V2 receptor in drug-induced hyponatremia. *Front. Physiol.* 12:797039. doi: 10.3389/fphys.2021.797039

Kimberling, W. J., Weston, M. D., Moller, C., van Aarem, A., Cremers, C. W., Sumegi, J., et al. (1995). Gene mapping of Usher syndrome type IIa: Localization of the gene to a 2.1-cM segment on chromosome 1q41. *Am. J. Hum. Genet.* 56, 216–223.

Kindt, K. S., Akturk, A., Jarysta, A., Day, M., Beirl, A., Flonard, M., et al. (2021). EMX2-GPR156-Galphai reverses hair cell orientation in mechanosensory epithelia. *Nat. Commun.* 12:2861. doi: 10.1038/s41467-021-22997-1

Kitanishi, T., Suzuki, M., Kitano, H., Yazawa, Y., Yamada, H., and Kitajima, K. (1998). Immunohistochemical detection of vasoactive intestinal polypeptide (VIP) and the VIP receptor in the rat inner ear. *Acta Otolaryngol. Suppl.* 539, 52–56.

Klotz, L., and Enz, R. (2021). MGluR7 is a presynaptic metabotropic glutamate receptor at ribbon synapses of inner hair cells. *FASEB J.* 35:e21855. doi: 10.1096/fj.202100672R

Klotz, L., Wendler, O., Frischknecht, R., Shigemoto, R., Schulze, H., and Enz, R. (2019). Localization of group II and III metabotropic glutamate receptors at pre- and postsynaptic sites of inner hair cell ribbon synapses. *FASEB J.* 33, 13734–13746. doi: 10.1096/fj.201901543R

Kochman, K. (2014). Superfamily of G-protein coupled receptors (GPCRs)–extraordinary and outstanding success of evolution. *Postepy Hig. Med. Dosw.* 68, 1225–1237. doi: 10.5604/17322693.1127326

Koles, L., Szepesy, J., Berekmeri, E., and Zelles, T. (2019). Purinergic signaling and cochlear injury-targeting the immune system? *Int. J. Mol. Sci.* 20:2979. doi: 10.3390/ijms20122979

Kono, M., Belyantseva, I. A., Skoura, A., Frolenkov, G. I., Starost, M. F., Dreier, J. L., et al. (2007). Deafness and stria vascularis defects in S1P2 receptor-null mice. *J. Biol. Chem.* 282, 10690–10696. doi: 10.1074/jbc.M700370200

Kooistra, A. J., Mordalski, S., Pandy-Szekeres, G., Esguerra, M., Mamyrbekov, A., Munk, C., et al. (2021). GPCRdb in 2021: Integrating GPCR sequence, structure and function. *Nucleic Acids Res.* 49, D335–D343. doi: 10.1093/nar/gkaa1080

Kou, Z. Z., Qu, J., Zhang, D. L., Li, H., and Li, Y. Q. (2013). Noise-induced hearing loss is correlated with alterations in the expression of GABAB receptors and PKC gamma in the murine cochlear nucleus complex. *Front. Neuroanat.* 7:25. doi: 10.3389/fnana.2013.00025

Kozielewicz, P., Turku, A., and Schulte, G. (2020). Molecular pharmacology of class F receptor activation. *Mol. Pharmacol.* 97, 62–71. doi: 10.1124/mol.119.117986

Landin Malt, A., Clancy, S., Hwang, D., Liu, A., Smith, C., Smith, M., et al. (2021). Non-canonical Wnt signaling regulates cochlear outgrowth and planar cell polarity via Gsk3beta inhibition. *Front. Cell Dev. Biol.* 9:649830. doi: 10.3389/fcell.2021.649830

Langer, I., Jeandriens, J., Couvineau, A., Sanmukh, S., and Latek, D. (2022). Signal transduction by VIP and PACAP receptors. *Biomedicines* 10:406. doi: 10.3390/biomedicines10020406

Le Prell, C. G., Hughes, L. F., Dolan, D. F., and Bledsoe, S. C. Jr. (2021). Effects of calcitonin-gene-related-peptide on auditory nerve activity. *Front. Cell Dev. Biol.* 9:752963. doi: 10.3389/fcell.2021.752963

Lee, S., Dondzillo, A., Gubbels, S. P., and Raphael, Y. (2020). Practical aspects of inner ear gene delivery for research and clinical applications. *Hear. Res.* 394:107934. doi: 10.1016/j.heares.2020.107934

Li, D., Henley, C. M., and O'Malley, B. W. Jr. (1999). Distortion product otoacoustic emissions and outer hair cell defects in the hyt/hyt mutant mouse. *Hear. Res.* 138, 65–72. doi: 10.1016/s0378-5955(99)00150-1

Li, X., Roszko, I., Sepich, D. S., Ni, M., Hamm, H. E., Marlow, F. L., et al. (2013). Gpr125 modulates Dishevelled distribution and planar cell polarity signaling. *Development* 140, 3028–3039. doi: 10.1242/dev.094839

Li, X., Zhang, D., Xu, L., Han, Y., Liu, W., Li, W., et al. (2021). Planar cell polarity defects and hearing loss in sperm-associated antigen 6 (Spag6)-deficient mice. *Am. J. Physiol. Cell Physiol.* 320, C132–C141. doi: 10.1152/ajpcell.00166.2020

Li, Y., Zou, Q., and Zhang, J. (2018). Vincamine exerts protective effect on spiral ganglion neurons in endolymphatic hydrops guinea pig models. *Am. J. Transl. Res.* 10, 3650–3663.

Liang, Y. L., Khoshouei, M., Deganutti, G., Glukhova, A., Koole, C., Peat, T. S., et al. (2018). Cryo-EM structure of the active, Gs-protein complexed, human CGRP receptor. *Nature* 561, 492–497. doi: 10.1038/s41586-018-0535-y

Liang, Y. L., Khoshouei, M., Radjainia, M., Zhang, Y., Glukhova, A., Tarrasch, J., et al. (2017). Phase-plate cryo-EM structure of a class B GPCR-G-protein complex. *Nature* 546, 118–123. doi: 10.1038/nature22327

Lin, L., Chen, Y. S., Yao, Y. D., Chen, J. Q., Chen, J. N., Huang, S. Y., et al. (2015). CCL18 from tumor-associated macrophages promotes angiogenesis in breast cancer. *Oncotarget* 6, 34758–34773. doi: 10.18632/oncotarget.5325

Lin, X., Chen, S., and Chen, P. (2000). Activation of metabotropic GABAB receptors inhibited glutamate responses in spiral ganglion neurons of mice. *Neuroreport* 11, 957–961. doi: 10.1097/00001756-200004070-00012

Lowery, E. G., and Thiele, T. E. (2010). Pre-clinical evidence that corticotropin-releasing factor (CRF) receptor antagonists are promising targets for pharmacological treatment of alcoholism. *CNS Neurol. Disord. Drug Targets* 9, 77–86. doi: 10.2174/187152710790966605

Lv, X., Chen, Q., Zhang, S., Gao, F., and Liu, Q. (2022). CGRP: A new endogenous cell stemness maintenance molecule. *Oxid. Med. Cell. Longev.* 2022:4107433. doi: 10.1155/2022/4107433

Lv, X., Kong, J., Chen, W. D., and Wang, Y. D. (2017). The role of the Apelin/APJ system in the regulation of liver disease. *Front. Pharmacol.* 8:221. doi: 10.3389/fphar.2017.00221

Ma, X., Zhang, S., Qin, S., Guo, J., Yuan, J., Qiang, R., et al. (2022). Transcriptomic and epigenomic analyses explore the potential role of H3K4me3 in neomycin-induced cochlear Lgr5+ progenitor cell regeneration of hair cells. *Hum. Cell* 35, 1030–1044. doi: 10.1007/s13577-022-00727-z

Maeda, Y., Kariya, S., Omichi, R., Noda, Y., Sugaya, A., Fujimoto, S., et al. (2018). Targeted PCR array analysis of genes in innate immunity and glucocorticoid signaling pathways in mice cochleae following acoustic trauma. *Otol. Neurotol.* 39, e593–e600. doi: 10.1097/MAO.0000000000001874

Maguire, A. M., Bennett, J., Aleman, E. M., Leroy, B. P., and Aleman, T. S. (2021). Clinical perspective: Treating RPE65-associated retinal dystrophy. *Mol. Ther.* 29, 442–463. doi: 10.1016/j.ymthe.2020.11.029

Maguire, C. A., and Corey, D. P. (2020). Viral vectors for gene delivery to the inner ear. *Hear. Res.* 394:107927. doi: 10.1016/j.heares.2020.107927

Maison, S. F., Casanova, E., Holstein, G. R., Bettler, B., and Liberman, M. C. (2009). Loss of GABAB receptors in cochlear neurons: Threshold elevation suggests modulation of outer hair cell function by type II afferent fibers. *J. Assoc. Res. Otolaryngol.* 10, 50–63. doi: 10.1007/s10162-008-0138-7

Maison, S. F., Emeson, R. B., Adams, J. C., Luebke, A. E., and Liberman, M. C. (2003). Loss of alpha CGRP reduces sound-evoked activity in the cochlear nerve. *J. Neurophysiol.* 90, 2941–2949. doi: 10.1152/jn.00596.2003

Maison, S. F., Liu, X. P., Eatock, R. A., Sibley, D. R., Grandy, D. K., and Liberman, M. C. (2012). Dopaminergic signaling in the cochlea: Receptor expression patterns and deletion phenotypes. *J. Neurosci.* 32, 344–355. doi: 10.1523/JNEUROSCI.4720-11.2012

Makita, N., Manaka, K., Sato, J., and Iiri, T. (2020). V2 vasopressin receptor mutations. *Vitam. Horm.* 113, 79–99. doi: 10.1016/bs.vh.2019.08.012

Manalo, J. M., Liu, H., Ding, D., Hicks, J., Sun, H., Salvi, R., et al. (2020). Adenosine A2B receptor: A pathogenic factor and a therapeutic target for sensorineural hearing loss. *FASEB J.* 34, 15771–15787. doi: 10.1096/fj.202000939R

Mao, C., Shen, C., Li, C., Shen, D. D., Xu, C., Zhang, S., et al. (2020). Cryo-EM structures of inactive and active GABAB receptor. *Cell Res.* 30, 564–573. doi: 10.1038/s41422-020-0350-5

Mao, H., James, T. Jr., Schwein, A., Shabashvili, A. E., Hauswirth, W. W., Gorbatyuk, M. S., et al. (2011). AAV delivery of wild-type rhodopsin preserves retinal function in a mouse model of autosomal dominant retinitis pigmentosa. *Hum. Gene Ther.* 22, 567–575. doi: 10.1089/hum.2010.140

Martin-Grace, J., Tomkins, M., O'Reilly, M. W., Thompson, C. J., and Sherlock, M. (2022). Approach to the patient: Hyponatremia and the syndrome of inappropriate antidiuresis (SIAD). *J. Clin. Endocrinol. Metab.* 107, 2362–2376. doi: 10.1210/clinem/dgac245

Massink, A., Amelia, T., Karamychev, A., and Ap, I. J. (2020). Allosteric modulation of G protein-coupled receptors by amiloride and its derivatives. Perspectives for drug discovery? *Med. Res. Rev.* 40, 683–708. doi: 10.1002/med.21633

Matsushima, Y., Shinkai, Y., Kobayashi, Y., Sakamoto, M., Kunieda, T., and Tachibana, M. (2002). A mouse model of Waardenburg syndrome type 4 with a new spontaneous mutation of the endothelin-B receptor gene. *Mamm. Genome* 13, 30–35. doi: 10.1007/s00335-001-3038-2

Matyas, P., Postyeni, E., Komlosi, K., Szalai, R., Bene, J., Magyari, L., et al. (2019). Age-related hearing impairment associated NAT2, GRM7, GRHL2 susceptibility gene polymorphisms and haplotypes in roma and Hungarian populations. *Pathol. Oncol. Res.* 25, 1349–1355. doi: 10.1007/s12253-018-0388-6

McLean, W. J., Yin, X., Lu, L., Lenz, D. R., McLean, D., Langer, R., et al. (2017). Clonal expansion of Lgr5-positive cells from mammalian cochlea and high-purity generation of sensory hair cells. *Cell Rep.* 18, 1917–1929. doi: 10.1016/j.celrep.2017.01.066

McMillan, D. R., and White, P. C. (2004). Loss of the transmembrane and cytoplasmic domains of the very large G-protein-coupled receptor-1 (VLGR1 or Mass1) causes audiogenic seizures in mice. *Mol. Cell. Neurosci.* 26, 322–329. doi: 10.1016/j.mcn.2004.02.005

Mehkri, Y., Hanna, C., Sriram, S., Lucke-Wold, B., Johnson, R. D., and Busl, K. (2022). Calcitonin gene-related peptide and neurologic injury: An emerging target for headache management. *Clin. Neurol. Neurosurg.* 220:107355. doi: 10.1016/j.clineuro.2022.107355

Meredith, F. L., and Rennie, K. J. (2021). Dopaminergic inhibition of Na^+ currents in vestibular inner ear afferents. *Front. Neurosci.* 15:710321. doi: 10.3389/fnins.2021.710321

Merighi, S., Borea, P. A., Varani, K., Vincenzi, F., Travagli, A., Nigro, M., et al. (2022). Pathophysiological role and medicinal chemistry of A2A adenosine receptor antagonists in Alzheimer's disease. *Molecules* 27:2680. doi: 10.3390/molecules27092680

Michalski, N., Michel, V., Bahloul, A., Lefevre, G., Barral, J., Yagi, H., et al. (2007). Molecular characterization of the ankle-link complex in cochlear hair cells and its role in the hair bundle functioning. *J. Neurosci.* 27, 6478–6488. doi: 10.1523/JNEUROSCI.0342-07.2007

Minakata, T., Inagaki, A., Yamamura, A., Yamamura, H., Sekiya, S., and Murakami, S. (2019). Calcium-sensing receptor is functionally expressed in the cochlear perilymphatic compartment and essential for hearing. *Front. Mol. Neurosci.* 12:175. doi: 10.3389/fnmol.2019.00175

Montcouquiol, M., Sans, N., Huss, D., Kach, J., Dickman, J. D., Forge, A., et al. (2006). Asymmetric localization of Vangl2 and Fz3 indicate novel mechanisms for planar cell polarity in mammals. *J. Neurosci.* 26, 5265–5275. doi: 10.1523/JNEUROSCI.4680-05.2006

Munro, S., Thomas, K. L., and Abu-Shaar, M. (1993). Molecular characterization of a peripheral receptor for cannabinoids. *Nature* 365, 61–65. doi: 10.1038/365061a0

Muthu, V., Rohacek, A. M., Yao, Y., Rakowiecki, S. M., Brown, A. S., Zhao, Y. T., et al. (2019). Genomic architecture of Shh-dependent cochlear morphogenesis. *Development* 146:dev181339. doi: 10.1242/dev.181339

Nakayama, M., Tabuchi, K., Hoshino, T., Nakamagoe, M., Nishimura, B., and Hara, A. (2014). The influence of sphingosine-1-phosphate receptor antagonists on gentamicin-induced hair cell loss of the rat cochlea. *Neurosci. Lett.* 561, 91–95. doi: 10.1016/j.neulet.2013.12.063

Newman, D. L., Fisher, L. M., Ohmen, J., Parody, R., Fong, C. T., Frisina, S. T., et al. (2012). GRM7 variants associated with age-related hearing loss based on auditory perception. *Hear. Res.* 294, 125–132. doi: 10.1016/j.heares.2012.08.016

Niknazar, S., Abbaszadeh, H. A., Peyvandi, H., Rezaei, O., Forooghirad, H., Khoshsirat, S., et al. (2019). Protective effect of [Pyr1]-apelin-13 on oxidative stress-induced apoptosis in hair cell-like cells derived from bone marrow mesenchymal stem cells. *Eur. J. Pharmacol.* 853, 25–32. doi: 10.1016/j.ejphar.2019.03.012

Nist-Lund, C. A., Pan, B., Patterson, A., Asai, Y., Chen, T., Zhou, W., et al. (2019). Improved TMC1 gene therapy restores hearing and balance in mice with genetic inner ear disorders. *Nat. Commun.* 10:236. doi: 10.1038/s41467-018-08264-w

Niswender, C. M., and Conn, P. J. (2010). Metabotropic glutamate receptors: Physiology, pharmacology, and disease. *Annu. Rev. Pharmacol. Toxicol.* 50, 295–322. doi: 10.1146/annurev.pharmtox.011008.145533

Odoemelam, C. S., Percival, B., Wallis, H., Chang, M. W., Ahmad, Z., Scholey, D., et al. (2020). G-Protein coupled receptors: Structure and function in drug discovery. *RSC Adv.* 10, 36337–36348. doi: 10.1039/d0ra08003a

Oestreicher, E., Arnold, W., Ehrenberger, K., and Felix, D. (1997). Dopamine regulates the glutamatergic inner hair cell activity in guinea pigs. *Hear. Res.* 107, 46–52. doi: 10.1016/s0378-5955(97)00023-3

Okashah, N., Wright, S. C., Kawakami, K., Mathiasen, S., Zhou, J., Lu, S., et al. (2020). Agonist-induced formation of unproductive receptor-G12 complexes. *Proc. Natl. Acad. Sci. U.S.A.* 117, 21723–21730. doi: 10.1073/pnas.2003787117

O'Keeffe, M. G., Thorne, P. R., Housley, G. D., Robson, S. C., and Vlajkovic, S. M. (2010). Developmentally regulated expression of ectonucleotidases NTPDase5 and NTPDase6 and UDP-responsive P2Y receptors in the rat cochlea. *Histochem. Cell Biol.* 133, 425–436. doi: 10.1007/s00418-010-0682-1

O'Malley, B. W. Jr., Li, D., and Turner, D. S. (1995). Hearing loss and cochlear abnormalities in the congenital hypothyroid (hyt/hyt) mouse. *Hear. Res.* 88, 181–189. doi: 10.1016/0378-5955(95)00111-g

O'Reilly, M., Palfi, A., Chadderton, N., Millington-Ward, S., Ader, M., Cronin, T., et al. (2007). RNA interference-mediated suppression and replacement of human rhodopsin in vivo. *Am. J. Hum. Genet.* 81, 127–135. doi: 10.1086/519025

Pan, B., Askew, C., Galvin, A., Heman-Ackah, S., Asai, Y., Indzhykulian, A. A., et al. (2017). Gene therapy restores auditory and vestibular function in a mouse model of Usher syndrome type 1c. *Nat. Biotechnol.* 35, 264–272. doi: 10.1038/nbt.3801

Parker, M. S., Onyenekwu, N. N., and Bobbin, R. P. (2003). Localization of the P2Y4 receptor in the guinea pig organ of Corti. *J. Am. Acad. Audiol.* 14, 286–295.

Pasquini, S., Contri, C., Merighi, S., Gessi, S., Borea, P. A., Varani, K., et al. (2022). Adenosine receptors in neuropsychiatric disorders: Fine regulators of neurotransmission and potential therapeutic targets. *Int. J. Mol. Sci.* 23:1219. doi: 10.3390/ijms23031219

Peng, B. G., Li, Q. X., Ren, T. Y., Ahmad, S., Chen, S. P., Chen, P., et al. (2004). Group I metabotropic glutamate receptors in spiral ganglion neurons contribute to excitatory neurotransmissions in the cochlea. *Neuroscience* 123, 221–230. doi: 10.1016/j.neuroscience.2003.09.010

Peyvandi, A. A., Roozbahany, N. A., Peyvandi, H., Abbaszadeh, H. A., Majdinasab, N., Faridan, M., et al. (2018b). Critical role of SDF-1/CXCR4 signaling pathway in stem cell homing in the deafened rat cochlea after acoustic trauma. *Neural Regen. Res.* 13, 154–160. doi: 10.4103/1673-5374.224382

Peyvandi, A. A., Abbaszadeh, H. A., Roozbahany, N. A., Pourbakht, A., Khoshsirat, S., Niri, H. H., et al. (2018a). Deferoxamine promotes mesenchymal stem cell homing in noise-induced injured cochlea through PI3K/AKT pathway. *Cell Prolif.* 51:e12434. doi: 10.1111/cpr.12434

Piazza, V., Ciubotaru, C. D., Gale, J. E., and Mammano, F. (2007). Purinergic signalling and intercellular Ca^{2+} wave propagation in the organ of Corti. *Cell Calcium* 41, 77–86. doi: 10.1016/j.ceca.2006.05.005

Qi, X., Liu, H., Thompson, B., McDonald, J., Zhang, C., and Li, X. (2019). Cryo-EM structure of oxysterol-bound human smoothened coupled to a heterotrimeric Gi. *Nature* 571, 279–283. doi: 10.1038/s41586-019-1286-0

Qu, J., Liao, Y. H., Kou, Z. Z., Wei, Y. Y., Huang, J., Chen, J., et al. (2015). Puerarin alleviates noise-induced hearing loss via affecting PKCgamma and GABAB receptor expression. *J. Neurol. Sci.* 349, 110–116. doi: 10.1016/j.jns.2014.12.038

Racz, B., Horvath, G., Reglodi, D., Gasz, B., Kiss, P., Gallyas, F. Jr., et al. (2010). PACAP ameliorates oxidative stress in the chicken inner ear: An in vitro study. *Regul. Pept.* 160, 91–98. doi: 10.1016/j.regpep.2009.12.003

Ramkumar, V., Ravi, R., Wilson, M. C., Gettys, T. W., Whitworth, C., and Rybak, L. P. (1994). Identification of A1 adenosine receptors in rat cochlea coupled to inhibition of adenylyl cyclase. *Am. J. Physiol.* 267(3 Pt 1), C731–C737. doi: 10.1152/ajpcell.1994.267.3.C731

Ramkumar, V., Whitworth, C. A., Pingle, S. C., Hughes, L. F., and Rybak, L. P. (2004). Noise induces A1 adenosine receptor expression in the chinchilla cochlea. *Hear. Res.* 188, 47–56. doi: 10.1016/S0378-5955(03)00344-7

Ravni, A., Qu, Y., Goffinet, A. M., and Tissir, F. (2009). Planar cell polarity cadherin Celsr1 regulates skin hair patterning in the mouse. *J. Invest. Dermatol.* 129, 2507–2509. doi: 10.1038/jid.2009.84

Reijntjes, D. O. J., and Pyott, S. J. (2016). The afferent signaling complex: Regulation of type I spiral ganglion neuron responses in the auditory periphery. *Hear. Res.* 336, 1–16. doi: 10.1016/j.heares.2016.03.011

Reiner, A., and Levitz, J. (2018). Glutamatergic signaling in the central nervous system: Ionotropic and metabotropic receptors in concert. *Neuron* 98, 1080–1098. doi: 10.1016/j.neuron.2018.05.018

Renaud, J. P., Chari, A., Ciferri, C., Liu, W. T., Remigy, H. W., Stark, H., et al. (2018). Cryo-EM in drug discovery: Achievements, limitations and prospects. *Nat. Rev. Drug Discov.* 17, 471–492. doi: 10.1038/nrd.2018.77

Renauld, J. M., Davis, W., Cai, T., Cabrera, C., and Basch, M. L. (2021). Transcriptomic analysis and ednrb expression in cochlear intermediate cells reveal developmental differences between inner ear and skin melanocytes. *Pigment Cell Melanoma Res.* 34, 585–597. doi: 10.1111/pcmr.12961

Ruel, J., Guitton, M. J., Gratias, P., Lenoir, M., Shen, S., Puel, J. L., et al. (2021). Endogenous pituitary adenylate cyclase-activating polypeptide (PACAP) plays a protective effect against noise-induced hearing loss. *Front. Cell Neurosci.* 15:658990. doi: 10.3389/fncel.2021.658990

Ruel, J., Nouvian, R., Gervais d'Aldin, C., Pujol, R., Eybalin, M., and Puel, J. L. (2001). Dopamine inhibition of auditory nerve activity in the adult mammalian cochlea. *Eur. J. Neurosci.* 14, 977–986. doi: 10.1046/j.0953-816x.2001.01721.x

Saikia, S., Bordoloi, M., and Sarmah, R. (2019). Established and in-trial GPCR families in clinical trials: A review for target selection. *Curr. Drug Targets* 20, 522–539. doi: 10.2174/1389450120666181105152439

Sanchez, J., Lane, J. R., Canals, M., and Stone, M. J. (2019). Influence of chemokine N-terminal modification on biased agonism at the chemokine receptor CCR1. *Int. J. Mol. Sci.* 20:2417. doi: 10.3390/ijms20102417

Santos-Cortez, R. L., Faridi, R., Rehman, A. U., Lee, K., Ansar, M., Wang, X., et al. (2016). Autosomal-recessive hearing impairment due to rare missense variants within S1PR2. *Am. J. Hum. Genet.* 98, 331–338. doi: 10.1016/j.ajhg.2015.12.004

Sato, E., Shick, H. E., Ransohoff, R. M., and Hirose, K. (2010). Expression of fractalkine receptor CX3CR1 on cochlear macrophages influences survival of hair cells following ototoxic injury. *J. Assoc. Res. Otolaryngol.* 11, 223–234. doi: 10.1007/s10162-009-0198-3

Sautter, N. B., Shick, E. H., Ransohoff, R. M., Charo, I. F., and Hirose, K. (2006). CC chemokine receptor 2 is protective against noise-induced hair cell death: Studies in CX3CR1$^{+/GFP}$ mice. *J. Assoc. Res. Otolaryngol.* 7, 361–372. doi: 10.1007/s10162-006-0051-x

Schrott-Fischer, A., Kammen-Jolly, K., Scholtz, A., Rask-Andersen, H., Glueckert, R., and Eybalin, M. (2007). Efferent neurotransmitters in the human cochlea and vestibule. *Acta Otolaryngol.* 127, 13–19. doi: 10.1080/00016480600652123

Schulte, G., and Kozielewicz, P. (2020). Structural insight into Class F receptors–what have we learnt regarding agonist-induced activation? *Basic Clin. Pharmacol. Toxicol.* 126(Suppl. 6), 17–24. doi: 10.1111/bcpt.13235

Schulte, G., and Wright, S. C. (2018). Frizzleds as GPCRs–more conventional than we thought! *Trends Pharmacol. Sci.* 39, 828–842. doi: 10.1016/j.tips.2018.07.001

Seebahn, A., Dinkel, H., Mohrluder, J., Hartmann, R., Vogel, N., Becker, C. M., et al. (2011). Structural characterization of intracellular C-terminal domains of group III metabotropic glutamate receptors. *FEBS Lett.* 585, 511–516. doi: 10.1016/j.febslet.2010.12.042

Shaye, H., Stauch, B., Gati, C., and Cherezov, V. (2021). Molecular mechanisms of metabotropic GABAB receptor function. *Sci. Adv.* 7:eabg3362. doi: 10.1126/sciadv.abg3362

Shen, C., Mao, C., Xu, C., Jin, N., Zhang, H., Shen, D. D., et al. (2021). Structural basis of GABAB receptor-Gi protein coupling. *Nature* 594, 594–598. doi: 10.1038/s41586-021-03507-1

Sheth, S., Sheehan, K., Dhukhwa, A., Al Aameri, R. F. H., Mamillapalli, C., Mukherjea, D., et al. (2019). Oral administration of caffeine exacerbates cisplatin-induced hearing loss. *Sci. Rep.* 9:9571. doi: 10.1038/s41598-019-45964-9

Shihoya, W., Izume, T., Inoue, A., Yamashita, K., Kadji, F. M. N., Hirata, K., et al. (2018). Crystal structures of human ETB receptor provide mechanistic insight into receptor activation and partial activation. *Nat. Commun.* 9:4711. doi: 10.1038/s41467-018-07094-0

Shihoya, W., Nishizawa, T., Okuta, A., Tani, K., Dohmae, N., Fujiyoshi, Y., et al. (2016). Activation mechanism of endothelin ETB receptor by endothelin-1. *Nature* 537, 363–368. doi: 10.1038/nature19319

Shima, Y., Copeland, N. G., Gilbert, D. J., Jenkins, N. A., Chisaka, O., Takeichi, M., et al. (2002). Differential expression of the seven-pass transmembrane cadherin genes Celsr1-3 and distribution of the Celsr2 protein during mouse development. *Dev. Dyn.* 223, 321–332. doi: 10.1002/dvdy.10054

Shin, M., Pandya, M., Espinosa, K., Telang, R., Boix, J., Thorne, P. R., et al. (2021). Istradefylline mitigates age-related hearing loss in C57BL/6J mice. *Int. J. Mol. Sci.* 22:8000. doi: 10.3390/ijms22158000

Shin, S. H., Jung, J., Park, H. R., Sim, N. S., Choi, J. Y., and Bae, S. H. (2022a). The Time course of monocytes infiltration after acoustic overstimulation. *Front. Cell. Neurosci.* 16:844480. doi: 10.3389/fncel.2022.844480

Shin, S. H., Yoo, J. E., Jung, J., Choi, J. Y., and Bae, S. H. (2022b). Inflammatory monocytes infiltrate the spiral ligament and migrate to the basilar membrane after noise exposure. *Clin. Exp. Otorhinolaryngol.* 15, 153–159. doi: 10.21053/ceo.2021.00857

Sienknecht, U. J., and Fekete, D. M. (2008). Comprehensive Wnt-related gene expression during cochlear duct development in chicken. *J. Comp. Neurol.* 510, 378–395. doi: 10.1002/cne.21791

Sirko, P., Gale, J. E., and Ashmore, J. F. (2019). Intercellular Ca^{2+} signalling in the adult mouse cochlea. *J. Physiol.* 597, 303–317. doi: 10.1113/JP276400

Skradski, S. L., Clark, A. M., Jiang, H., White, H. S., Fu, Y. H., and Ptacek, L. J. (2001). A novel gene causing a mendelian audiogenic mouse epilepsy. *Neuron* 31, 537–544. doi: 10.1016/s0896-6273(01)00397-x

Smith, M. C., Luker, K. E., Garbow, J. R., Prior, J. L., Jackson, E., Piwnica-Worms, D., et al. (2004). CXCR4 regulates growth of both primary and metastatic breast cancer. *Cancer Res.* 64, 8604–8612. doi: 10.1158/0008-5472.CAN-04-1844

Smith-Cortinez, N., Yadak, R., Hendriksen, F. G. J., Sanders, E., Ramekers, D., Stokroos, R. J., et al. (2021). LGR5-positive supporting cells survive ototoxic trauma in the adult mouse cochlea. *Front. Mol. Neurosci.* 14:729625. doi: 10.3389/fnmol.2021.729625

Song, L., McGee, J. A., and Walsh, E. J. (2006). Consequences of combined maternal, fetal and persistent postnatal hypothyroidism on the development of auditory function in Tshrhyt mutant mice. *Brain Res.* 1101, 59–72. doi: 10.1016/j.brainres.2006.05.027

Stoner, Z. A., Ketchum, E. M., Sheltz-Kempf, S., Blinkiewicz, P. V., Elliott, K. L., and Duncan, J. S. (2021). Fzd3 expression within inner ear afferent neurons is necessary for central pathfinding. *Front. Neurosci.* 15:779871. doi: 10.3389/fnins.2021.779871

Sun, H., Wang, T., Atkinson, P. J., Billings, S. E., Dong, W., and Cheng, A. G. (2021). Gpr125 marks distinct cochlear cell types and is dispensable for cochlear development and hearing. *Front. Cell Dev. Biol.* 9:690955. doi: 10.3389/fcell.2021.690955

Sun, J. P., Li, R., Ren, H. Z., Xu, A. T., Yu, X., and Xu, Z. G. (2013). The very large G protein coupled receptor (Vlgr1) in hair cells. *J. Mol. Neurosci.* 50, 204–214. doi: 10.1007/s12031-012-9911-5

Tabuchi, K., Sakai, S., Nakayama, M., Nishimura, B., Hayashi, K., Hirose, Y., et al. (2012). The effects of A1 and A2A adenosine receptor agonists on kainic acid excitotoxicity in the guinea pig cochlea. *Neurosci. Lett.* 518, 60–63. doi: 10.1016/j.neulet.2012.04.057

Takumida, M., Kakigi, A., Egami, N., Nishioka, R., and Anniko, M. (2012). Localization of aquaporins 1, 2, and 3 and vasopressin type 2 receptor in the mouse inner ear. *Acta Otolaryngol.* 132, 807–813. doi: 10.3109/00016489.2012.662718

Tantisira, K. G., Lake, S., Silverman, E. S., Palmer, L. J., Lazarus, R., Silverman, E. K., et al. (2004). Corticosteroid pharmacogenetics: Association of sequence variants in CRHR1 with improved lung function in asthmatics treated with inhaled corticosteroids. *Hum. Mol. Genet.* 13, 1353–1359. doi: 10.1093/hmg/ddh149

Tateya, T., Imayoshi, I., Tateya, I., Hamaguchi, K., Torii, H., Ito, J., et al. (2013). Hedgehog signaling regulates prosensory cell properties during the basal-to-apical wave of hair cell differentiation in the mammalian cochlea. *Development* 140, 3848–3857. doi: 10.1242/dev.095398

Tissir, F., and Goffinet, A. M. (2006). Expression of planar cell polarity genes during development of the mouse CNS. *Eur. J. Neurosci.* 23, 597–607. doi: 10.1111/j.1460-9568.2006.04596.x

Tuffour, A., Kosiba, A. A., Zhang, Y., Peprah, F. A., Gu, J., and Shi, H. (2021). Role of the calcium-sensing receptor (CaSR) in cancer metastasis to bone: Identifying a potential therapeutic target. *Biochim. Biophys. Acta Rev. Cancer* 1875:188528. doi: 10.1016/j.bbcan.2021.188528

Tuncel, M. (2017). Thyroid stimulating hormone receptor. *Mol. Imaging Radionucl. Ther.* 26(Suppl. 1), 87–91. doi: 10.4274/2017.26.suppl.10

van der Valk, W. H., Steinhart, M. R., Zhang, J., and Koehler, K. R. (2021). Building inner ears: Recent advances and future challenges for in vitro organoid systems. *Cell Death Differ.* 28, 24–34. doi: 10.1038/s41418-020-00678-8

Vaudry, D., Falluel-Morel, A., Bourgault, S., Basille, M., Burel, D., Wurtz, O., et al. (2009). Pituitary adenylate cyclase-activating polypeptide and its receptors: 20 years after the discovery. *Pharmacol. Rev.* 61, 283–357. doi: 10.1124/pr.109.001370

Verpy, E., Leibovici, M., Zwaenepoel, I., Liu, X. Z., Gal, A., Salem, N., et al. (2000). A defect in harmonin, a PDZ domain-containing protein expressed in the inner ear sensory hair cells, underlies Usher syndrome type 1C. *Nat. Genet.* 26, 51–55. doi: 10.1038/79171

Vetter, D. E. (2015). Cellular signaling protective against noise-induced hearing loss–a role for novel intrinsic cochlear signaling involving corticotropin-releasing factor? *Biochem. Pharmacol.* 97, 1–15. doi: 10.1016/j.bcp.2015.06.011

Vieira, I. H., Rodrigues, D., and Paiva, I. (2022). The mysterious universe of the TSH receptor. *Front. Endocrinol.* 13:944715. doi: 10.3389/fendo.2022.944715

Vlachou, S. (2022). A brief history and the significance of the GABAB receptor. *Curr. Top. Behav. Neurosci.* 52, 1–17. doi: 10.1007/7854_2021_264

Vlajkovic, S. M., Abi, S., Wang, C. J., Housley, G. D., and Thorne, P. R. (2007). Differential distribution of adenosine receptors in rat cochlea. *Cell Tissue Res.* 328, 461–471. doi: 10.1007/s00441-006-0374-2

Vlajkovic, S. M., Ambepitiya, K., Barclay, M., Boison, D., Housley, G. D., and Thorne, P. R. (2017). Adenosine receptors regulate susceptibility to noise-induced neural injury in the mouse cochlea and hearing loss. *Hear. Res.* 345, 43–51. doi: 10.1016/j.heares.2016.12.015

Vlajkovic, S. M., Guo, C. X., Telang, R., Wong, A. C., Paramananthasivam, V., Boison, D., et al. (2011). Adenosine kinase inhibition in the cochlea delays the onset of age-related hearing loss. *Exp. Gerontol.* 46, 905–914. doi: 10.1016/j.exger.2011.08.001

Vlajkovic, S. M., Housley, G. D., and Thorne, P. R. (2009). Adenosine and the auditory system. *Curr. Neuropharmacol.* 7, 246–256. doi: 10.2174/157015909789152155

Vlajkovic, S. M., Lee, K. H., Wong, A. C., Guo, C. X., Gupta, R., Housley, G. D., et al. (2010). Adenosine amine congener mitigates noise-induced cochlear injury. *Purinergic Signal.* 6, 273–281. doi: 10.1007/s11302-010-9188-5

Vlajkovic, S. M., Vinayagamoorthy, A., Thorne, P. R., Robson, S. C., Wang, C. J., and Housley, G. D. (2006). Noise-induced up-regulation of NTPDase3 expression in the rat cochlea: Implications for auditory transmission and cochlear protection. *Brain Res.* 1104, 55–63. doi: 10.1016/j.brainres.2006.05.094

Vyas, P., Wu, J. S., Jimenez, A., Glowatzki, E., and Fuchs, P. A. (2019). Characterization of transgenic mouse lines for labeling type I and type II afferent neurons in the cochlea. *Sci. Rep.* 9:5549. doi: 10.1038/s41598-019-41770-5

Wagner, E. L., and Shin, J. B. (2019). Mechanisms of hair cell damage and repair. *Trends Neurosci.* 42, 414–424. doi: 10.1016/j.tins.2019.03.006

Wang, L., Xu, J., Cao, S., Sun, D., Liu, H., Lu, Q., et al. (2021). Cryo-EM structure of the AVP-vasopressin receptor 2-Gs signaling complex. *Cell Res.* 31, 932–934. doi: 10.1038/s41422-021-00483-z

Wang, S. Q., Li, C. L., Xu, J. Q., Chen, L. L., Xie, Y. Z., Dai, P. D., et al. (2022). The effect of endolymphatic hydrops and mannitol dehydration treatment on guinea pigs. *Front. Cell. Neurosci.* 16:836093. doi: 10.3389/fncel.2022.836093

Wang, W., Qiao, Y., and Li, Z. (2018). New insights into modes of GPCR activation. *Trends Pharmacol. Sci.* 39, 367–386. doi: 10.1016/j.tips.2018.01.001

Wang, W., Shanmugam, M. K., Xiang, P., Yam, T. Y. A., Kumar, V., Chew, W. S., et al. (2020). Sphingosine 1-phosphate receptor 2 induces otoprotective responses to cisplatin treatment. *Cancers* 12:211. doi: 10.3390/cancers12010211

Wang, Y., Guo, N., and Nathans, J. (2006). The role of Frizzled3 and Frizzled6 in neural tube closure and in the planar polarity of inner-ear sensory hair cells. *J. Neurosci.* 26, 2147–2156. doi: 10.1523/JNEUROSCI.4698-05.2005

Wang, Y., Huso, D., Cahill, H., Ryugo, D., and Nathans, J. (2001). Progressive cerebellar, auditory, and esophageal dysfunction caused by targeted disruption of the frizzled-4 gene. *J. Neurosci.* 21, 4761–4771. doi: 10.1523/JNEUROSCI.21-13-04761.2001

Watkins, L. R., and Orlandi, C. (2020). Orphan G protein coupled receptors in affective disorders. *Genes* 11:694. doi: 10.3390/genes11060694

Watkins, L. R., and Orlandi, C. (2021). In vitro profiling of orphan G protein coupled receptor (GPCR) constitutive activity. *Br. J. Pharmacol.* 178, 2963–2975. doi: 10.1111/bph.15468

Wedemeyer, C., Zorrilla de San Martin, J., Ballestero, J., Gomez-Casati, M. E., Torbidoni, A. V., Fuchs, P. A., et al. (2013). Activation of presynaptic GABA(B(1a,2)) receptors inhibits synaptic transmission at mammalian inhibitory cholinergic olivocochlear-hair cell synapses. *J. Neurosci.* 33, 15477–15487. doi: 10.1523/JNEUROSCI.2554-13.2013

Whitworth, C. A., Ramkumar, V., Jones, B., Tsukasaki, N., and Rybak, L. P. (2004). Protection against cisplatin ototoxicity by adenosine agonists. *Biochem. Pharmacol.* 67, 1801–1807. doi: 10.1016/j.bcp.2004.01.010

Wingler, L. M., and Lefkowitz, R. J. (2020). Conformational basis of G protein-coupled receptor signaling versatility. *Trends Cell Biol.* 30, 736–747. doi: 10.1016/j.tcb.2020.06.002

Wolf, B. J., Kusch, K., Hunniford, V., Vona, B., Kuhler, R., Keppeler, D., et al. (2022). Is there an unmet medical need for improved hearing restoration? *EMBO Mol. Med.* 14, e15798. doi: 10.15252/emmm.202215798

Wonneberger, K., Scofield, M. A., and Wangemann, P. (2000). Evidence for a calcium-sensing receptor in the vascular smooth muscle cells of the spiral modiolar artery. *J. Membr. Biol.* 175, 203–212. doi: 10.1007/s002321001068

Wu, J. S., Yi, E., Manca, M., Javaid, H., Lauer, A. M., and Glowatzki, E. (2020). Sound exposure dynamically induces dopamine synthesis in cholinergic LOC efferents for feedback to auditory nerve fibers. *Elife* 9:e52419. doi: 10.7554/eLife.52419

Xiao, Q., Xu, Z., Xue, Y., Xu, C., Han, L., Liu, Y., et al. (2022). Rescue of autosomal dominant hearing loss by in vivo delivery of mini dCas13X-derived RNA base editor. *Sci. Transl. Med.* 14:eabn0449. doi: 10.1126/scitranslmed.abn0449

Yagi, H., Takamura, Y., Yoneda, T., Konno, D., Akagi, Y., Yoshida, K., et al. (2005). Vlgr1 knockout mice show audiogenic seizure susceptibility. *J. Neurochem.* 92, 191–202. doi: 10.1111/j.1471-4159.2004.02875.x

Yang, X., Wang, X., Xu, Z., Wu, C., Zhou, Y., Wang, Y., et al. (2022). Molecular mechanism of allosteric modulation for the cannabinoid receptor CB1. *Nat. Chem. Biol.* 18, 831–840. doi: 10.1038/s41589-022-01038-y

Ye, Z., Goutman, J. D., Pyott, S. J., and Glowatzki, E. (2017). mGluR1 enhances efferent inhibition of inner hair cells in the developing rat cochlea. *J. Physiol.* 595, 3483–3495. doi: 10.1113/JP272604

Yin, H., Zhang, H., Kong, Y., Wang, C., Guo, Y., Gao, Y., et al. (2020). Apelin protects auditory cells from cisplatin-induced toxicity in vitro by inhibiting ROS and apoptosis. *Neurosci. Lett.* 728:134948. doi: 10.1016/j.neulet.2020.134948

Yu, H., Smallwood, P. M., Wang, Y., Vidaltamayo, R., Reed, R., and Nathans, J. (2010). Frizzled 1 and Frizzled 2 genes function in palate, ventricular septum and neural tube closure: General implications for tissue fusion processes. *Development* 137, 3707–3717. doi: 10.1242/dev.052001

Yu, P., Jiao, J., Chen, G., Zhou, W., Zhang, H., Wu, H., et al. (2018). Effect of GRM7 polymorphisms on the development of noise-induced hearing loss in Chinese Han workers: A nested case-control study. *BMC Med. Genet.* 19:4. doi: 10.1186/s12881-017-0515-3

Zak, M., van Oort, T., Hendriksen, F. G., Garcia, M. I., Vassart, G., and Grolman, W. (2016). LGR4 and LGR5 regulate hair cell differentiation in the sensory epithelium of the developing mouse cochlea. *Front. Cell. Neurosci.* 10:186. doi: 10.3389/fncel.2016.00186

Zallocchi, M., Meehan, D. T., Delimont, D., Rutledge, J., Gratton, M. A., Flannery, J., et al. (2012b). Role for a novel Usher protein complex in hair cell synaptic maturation. *PLoS One* 7:e30573. doi: 10.1371/journal.pone.0030573

Zallocchi, M., Delimont, D., Meehan, D. T., and Cosgrove, D. (2012a). Regulated vesicular trafficking of specific PCDH15 and VLGR1 variants in auditory hair cells. *J. Neurosci.* 32, 13841–13859. doi: 10.1523/JNEUROSCI.1242-12.2012

Zhang, C., Frye, M. D., Riordan, J., Sharma, A., Manohar, S., Salvi, R., et al. (2021). Loss of CX3CR1 augments neutrophil infiltration into cochlear tissues after acoustic overstimulation. *J. Neurosci. Res.* 99, 2999–3020. doi: 10.1002/jnr.24925

Zhang, L. L., Wang, J. J., Liu, Y., Lu, X. B., Kuang, Y., Wan, Y. H., et al. (2011). GPR26-deficient mice display increased anxiety- and depression-like behaviors accompanied by reduced phosphorylated cyclic AMP responsive element-binding protein level in central amygdala. *Neuroscience* 196, 203–214. doi: 10.1016/j.neuroscience.2011.08.069

Zhang, P., Yi, L. H., Meng, G. Y., Zhang, H. Y., Sun, H. H., and Cui, L. Q. (2017). Apelin-13 attenuates cisplatin-induced cardiotoxicity through inhibition of ROS-mediated DNA damage and regulation of MAPKs and AKT pathways. *Free Radic. Res.* 51, 449–459. doi: 10.1080/10715762.2017.1313414

Zhang, P. Z., Cao, X. S., Jiang, X. W., Wang, J., Liang, P. F., Wang, S. J., et al. (2014). Acoustical stimulus changes the expression of stromal cell-derived factor-1 in the spiral ganglion neurons of the rat cochlea. *Neurosci. Lett.* 561, 140–145. doi: 10.1016/j.neulet.2013.12.061

Zhang, S., Liu, D., Dong, Y., Zhang, Z., Zhang, Y., Zhou, H., et al. (2019). Frizzled-9+ supporting cells are progenitors for the generation of hair cells in the postnatal mouse cochlea. *Front. Mol. Neurosci.* 12:184. doi: 10.3389/fnmol.2019.00184

Zhang, S., Zhang, Y., Yu, P., Hu, Y., Zhou, H., Guo, L., et al. (2017). Characterization of Lgr5+ progenitor cell transcriptomes after neomycin injury in the neonatal mouse cochlea. *Front. Mol. Neurosci.* 10:213. doi: 10.3389/fnmol.2017.00213

Zhang, W., Sun, J. Z., Han, Y., Chen, J., Liu, H., Wang, Y., et al. (2016). CXCL12/CXCR4 signaling pathway regulates cochlear development in neonatal mice. *Mol. Med. Rep.* 13, 4357–4364. doi: 10.3892/mmr.2016.5085

Zhang, W., Zhang, F., Han, Y., Liu, H., Wang, Y., Yue, B., et al. (2015). Auditory stimulation modulates CXCL12/CXCR4 expression in postnatal development of the newborn rat cochlea. *Neuroreport* 26, 681–687. doi: 10.1097/WNR.0000000000000408

Zhang, X., Dong, S., and Xu, F. (2018). Structural and druggability landscape of Frizzled G protein-coupled receptors. *Trends Biochem. Sci.* 43, 1033–1046. doi: 10.1016/j.tibs.2018.09.002

Zhang, Y., Guo, L., Lu, X., Cheng, C., Sun, S., Li, W., et al. (2018). Characterization of Lgr6+ cells as an enriched population of hair cell progenitors compared to Lgr5+ cells for hair cell generation in the neonatal mouse cochlea. *Front. Mol. Neurosci.* 11:147. doi: 10.3389/fnmol.2018.00147

Zhou, F., Ye, C., Ma, X., Yin, W., Croll, T. I., Zhou, Q., et al. (2021). Molecular basis of ligand recognition and activation of human V2 vasopressin receptor. *Cell Res.* 31, 929–931. doi: 10.1038/s41422-021-00480-2

Zlotnik, A., Burkhardt, A. M., and Homey, B. (2011). Homeostatic chemokine receptors and organ-specific metastasis. *Nat. Rev. Immunol.* 11, 597–606. doi: 10.1038/nri3049

Zou, J., Wang, Z., Chen, Y., Zhang, G., Chen, L., and Lu, J. (2019). MRI detection of endolymphatic hydrops in Meniere's disease in 8 minutes using MIIRMR and a 20-channel coil after targeted gadolinium delivery. *World J. Otorhinolaryngol. Head Neck Surg.* 5, 180–187. doi: 10.1016/j.wjorl.2019.04.001

Zuris, J. A., Thompson, D. B., Shu, Y., Guilinger, J. P., Bessen, J. L., Hu, J. H., et al. (2015). Cationic lipid-mediated delivery of proteins enables efficient protein-based genome editing in vitro and in vivo. *Nat. Biotechnol.* 33, 73–80. doi: 10.1038/nbt.3081

frontiers | Frontiers in Molecular Neuroscience

TYPE Original Research
PUBLISHED 19 October 2022
DOI 10.3389/fnmol.2022.1020803

OPEN ACCESS

EDITED BY
Yu Sun,
Huazhong University of Science and Technology, China

REVIEWED BY
Hao Xiong,
Sun Yat-sen Memorial Hospital, China
Renjie Chai,
Southeast University, China

*CORRESPONDENCE
Shu-Sheng Gong
gongss1962@163.com
Guo-Peng Wang
guopengwang@ccmu.edu.cn

†These authors have contributed equally to this work

SPECIALTY SECTION
This article was submitted to Methods and Model Organisms, a section of the journal Frontiers in Molecular Neuroscience

RECEIVED 16 August 2022
ACCEPTED 23 September 2022
PUBLISHED 19 October 2022

CITATION
Chen Z-R, Guo J-Y, He L, Liu S, Xu J-Y, Yang Z-J, Su W, Liu K, Gong S-S and Wang G-P (2022) Co-transduction of dual-adeno-associated virus vectors in the neonatal and adult mouse utricles.
Front. Mol. Neurosci. 15:1020803.
doi: 10.3389/fnmol.2022.1020803

Co-transduction of dual-adeno-associated virus vectors in the neonatal and adult mouse utricles

Zhong-Rui Chen[1,2†], Jing-Ying Guo[1,2†], Lu He[1,2], Shan Liu[1,2], Jun-Yi Xu[1,2], Zi-Jing Yang[1,2], Wei Su[1,2], Ke Liu[1,2], Shu-Sheng Gong[1,2*] and Guo-Peng Wang[1,2*]

[1]Department of Otolaryngology-Head and Neck Surgery, Beijing Friendship Hospital, Capital Medical University, Beijing, China, [2]Clinical Center for Hearing Loss, Capital Medical University, Beijing, China

Adeno-associated virus (AAV)-mediated gene transfer is an efficient method of gene over-expression in the vestibular end organs. However, AAV has limited usefulness for delivering a large gene, or multiple genes, due to its small packaging capacity (< 5 kb). Co-transduction of dual-AAV vectors can be used to increase the packaging capacity for gene delivery to various organs and tissues. However, its usefulness has not been well validated in the vestibular sensory epithelium. In the present study, we characterized the co-transduction of dual-AAV vectors in mouse utricles following inoculation of two AAV-serotype inner ear (AAV-ie) vectors via canalostomy. Firstly, co-transduction efficiencies were compared between dual-AAV-ie vectors using two different promoters: cytomegalovirus (CMV) and CMV early enhancer/chicken β-actin (CAG). In the group of dual AAV-ie-CAG vectors, the co-transduction rates for striolar hair cells (HCs), extrastriolar HCs, striolar supporting cells (SCs), and extrastriolar SCs were 23.14 ± 2.25%, 27.05 ± 2.10%, 57.65 ± 7.21%, and 60.33 ± 5.69%, respectively. The co-transduction rates in the group of dual AAV-ie-CMV vectors were comparable to those in the dual AAV-ie-CAG group. Next, we examined the co-transduction of dual-AAV-ie-CAG vectors in the utricles of neonatal mice and damaged adult mice. In the neonatal mice, co-transduction rates were 52.88 ± 3.11% and 44.93 ± 2.06% in the striolar and extrastriolar HCs, respectively, which were significantly higher than those in adult mice. In the *Pou4f3*$^{+/DTR}$ mice, following diphtheria toxin administration, which eliminated most HCs and spared the SCs, the co-transduction rate of SCs was not significantly different to that of normal utricles. Transgene expression persisted for up to 3 months in the adult mice. Furthermore, sequential administration of two AAV-ie-CAG vectors at an interval of 1 week resulted in a higher co-transduction rate in HCs than concurrent delivery. The auditory brainstem responses and swim tests did not

reveal any disruption of auditory or vestibular function after co-transduction with dual-AAV-ie vectors. In conclusion, dual-AAV-ie vectors allow efficient co-transduction in the vestibular sensory epithelium and facilitate the delivery of large or multiple genes for vestibular gene therapy.

KEYWORDS

adeno-associated virus, gene transfer, utricle, mice, hair cell, transduction

Introduction

Peripheral vestibular dysfunction is a significant cause of imbalance and dizziness. Lesions of the sensory epithelium of vestibular end organs, such as Meniere's disease (Tsuji et al., 2000b), aminoglycoside ototoxicity (Tsuji et al., 2000a), and syndromic inherited diseases (Jones and Jones, 2014), are common causes of peripheral vestibular dysfunction. Currently, drugs and the vestibular rehabilitation are clinically available treatments for those patients; However, the functional recovery is largely insufficient in some cases, particularly in those of bilateral vestibular hypofunction (Chow et al., 2021).

Gene therapy is a promising strategy for functional recovery and repair of the inner ear sensory epithelium. Adeno-associated virus (AAV) is a commonly used gene transfer vector and proved safe and effective in clinical trials (Nathwani et al., 2011; Yla-Herttuala, 2012; MacLaren et al., 2014). AAV is lowly immunogenic, non-integrating, and efficient in transducing dividing and non-dividing cells (Kay, 2011). Furthermore, single local administration is suitable for long-term treatment (Kay, 2011). However, AAV has limited packaging capacity (<5 kb), which limits its clinical usefulness (Reisinger, 2020). Gene therapy for certain inner ear diseases requires delivery of target genes larger than 5 kb, such as *Myo VIIa* for Usher syndrome type 1B and *Otof* for DFNB9 (Jones and Jones, 2014). Recent studies have reported that the delivery of a single therapeutic gene is inadequate to induce functional HC regeneration. Manipulation of multiple transcription factors is required for HC regeneration and functional recovery of the inner ear (Costa et al., 2015; Wu et al., 2016; You et al., 2018; Menendez et al., 2020). Therefore, increasing the packaging capacity of AAV would enable the delivery of large or multiple genes, thereby increasing the clinical usefulness of the system.

Substantial efforts have been made to circumvent the packaging limit of AAV vectors (Reisinger, 2020). Several studies have attempted to express protein fragments using AAV vectors loaded with truncated cDNAs, to provide partial gene function (Liu et al., 2005; Ostedgaard et al., 2005). In the inner ear of zebrafish, C-terminal C2F domain of otoferlin, but not the N-terminal C2A domain, can restore hearing and balance (Chatterjee et al., 2015). However, AAV-mediated expression of otoferlin fragments in mammals failed to improve hearing in an otoferlin knockout (Otof-/-) model (Tertrais et al., 2019). Thus, protein fragments differ in terms of their capacity to induce functional recovery. This heterogeneity is a major barrier to the application of protein fragments.

Based on the intrinsic ability of AAV genomes to achieve intermolecular concatemerization (Duan et al., 1998), co-transduction of dual-AAVs in a single cell has been used. Different strategies are used to split a large gene expression cassette into halves, which are independently packaged in two AAV vectors (Trapani et al., 2014). Co-transduction by dual-AAV vectors partially rescued the auditory function in otoferlin knockout mice and *Tmc*1 mutant mice (Akil et al., 2019; Al-Moyed et al., 2019; Wu et al., 2021). This method rescued the vestibular function after co-injection of dual-AAV vectors into a neonatal mouse model of Usher syndrome type 1c (Pan et al., 2017). However, it is not clear whether co-transduction of dual-AAV vectors is effective for the vestibular end organs of normal or damaged adult mice. It is also unknown whether sequential administration of dual-AAV vectors leads to favorable co-transduction, which is necessary for the overexpression of multiple genes in a sequential manner. Furthermore, the long-term performance of dual-AAV vectors needs to be explored.

In this study, we evaluated the efficiency and safety of dual-AAV vectors for the vestibular end organs of mice. For this purpose, we used AAV-serotype inner ear (AAV-ie), which is an efficient vector for inner ear gene transfer (Tan et al., 2019). We assessed the co-transduction efficiency of dual-AAV-ie vectors after concurrent or sequential administration under different circumstances, including normal and damaged adult and neonatal mouse utricles, which has not yet been explored in detail. We found that dual-AAV-ie vectors provided satisfactory co-transduction efficiency with minimum damage to the inner ear.

Materials and methods

Adeno-associated virus vectors

We used purified AAV-ie viral vectors driven by the promoters of cytomegalovirus (CMV) or CMV early

enhancer/chicken β-actin (CAG). AAV-ie with reporter genes of enhanced green fluorescent protein (EGFP) or mCherry were used for the experiments. The vectors were purchased from PackGene Biotech Co., Ltd. (Guangzhou, Guangdong, China) at a titer of 1×10^{13} vg/mL. The vectors were generated by triple plasmid transfection into HEK293T cells. The titers of the vectors were determined using Droplet Digital PCR. Vector aliquots were stored in phosphate-buffered saline (PBS) with 0.001% pluronic F-68 at -80°C.

Animals and diphtheria toxin treatments

The animal experiments were conducted according to the guidelines of the Animal Care and Use Committee of Capital Medical University of China. Wild-type C57BL/6J (6–8-week-old) and CD-1 (postnatal day 1, P1) mice were purchased from SPF Biotechnology Co., Ltd. (Beijing, China). *Pou4f3*$^{+/DTR}$ mice were purchased from the Jackson Laboratory (Bar Harbor, ME, US) and bred in the Laboratory Animal Department at Capital Medical University of China. *Pou4f3*$^{+/DTR}$ mice (8–10 weeks old) received two intramuscular injections of 100 ng/g DT (List Biological Laboratories, Campbell, CA, USA) 1 day apart. The surgeries were performed 10 days later.

Surgeries

Adult mice were anesthetized via intraperitoneal injection of xylazine (7 mg/kg; Sigma-Aldrich, St Louis, MO, USA) and ketamine (120 mg/kg; Gutian Pharmaceutical Co., Gutian, Fujian, China). Ketoprofen (10 mg/kg; Sigma-Aldrich) was subcutaneously injected immediately before the operation. Sedation was induced and maintained in neonatal mice using hypothermic anesthesia. The surgeries were performed only on the left ears. After shaving and sterilization of the overlying skin, an incision was made in the left post-auricular region. The posterior or lateral semicircular canal was exposed after separation of the overlying muscles. The surgeries were performed as previously described (Wang et al., 2014; Guo et al., 2017, 2018). For concurrent injection of dual-AAV-ie vectors, two AAV-ie vectors (1 μl for each) were mixed prior to the surgery. Mixed vector suspensions were inoculated via the posterior semicircular canal at a rate of 0.5 μl/min using a micro-injection pump. For the sequential administration of dual vectors, 1 μl of AAV-ie-CAG-EGFP vector was injected through the lateral semicircular canal, followed 1 week later by a second injection of 1 μl of AAV-ie-CAG-mCherry through the posterior semicircular canal. Animals were euthanized 2 weeks or 3 months after the surgery.

Auditory brainstem response and swim tests

ABR and swim tests were performed 2 weeks or 3 months after the surgery. For the ABR test, anesthetized animals were placed on a heating mat in an electrically and acoustically shielded chamber. Subdermal needle electrodes were placed at the vertex (active), and beneath the pinna of the test ear (reference) and contralateral ear (ground). Acoustic stimuli (5-ms tone bursts) were generated by the Tucker Davis Technologies (TDT) System III hardware and SigGenRZ software (TDT, Alachua, FL, USA). The responses evoked at octave frequencies of 4, 8, 16, and 32 kHz were recorded. A total of 1,024 responses were averaged for each stimulus level at 5-dB intervals. The threshold was defined as the lowest stimulus level at which ABR waves could be reliably detected. To evaluate vestibular function, the swim tests were performed as previously described (Hardisty-Hughes et al., 2010).

Immunofluorescence staining

Following deep anesthesia and euthanasia, the temporal bones of the mice were harvested and fixed in 4% paraformaldehyde and PBS overnight at 4°C. After rinsing with PBS, utricles were collected, permeabilized in 0.3% Triton X-100 (Sigma-Aldrich) for 20 min, and blocked with 5% normal goat serum (ZSGB-BIO, Beijing, China) for 1 h at room temperature. The samples were incubated overnight at 4°C with the following primary antibodies: rabbit anti-myosin VIIa antibody (1:300; Proteus BioSciences Inc., Ramona, CA, USA), mouse anti-GFP antibody tagged with Alexa Fluor 488 (1:100; Santa Cruz Biotechnology Inc., Dallas, TX, USA), and rat anti-mCherry antibody (1:100; Invitrogen, Carlsbad, CA, USA). After rinsing with PBS, samples were incubated with fluorescence-labeled secondary antibodies tagged with Alexa Fluor 594 or 647 (1:300; Invitrogen) for 1 h at room temperature. The nuclei were stained with 4',6-diamidino-2-phenylindole (DAPI; 1:1,000; AppliChem, Darmstadt, Germany) for 5 min at room temperature. After rinsing with PBS, samples were mounted on glass slides with Fluoromount-G (Southern Biotech, Birmingham, AL, USA). Confocal images were obtained using a scanning confocal microscope (TCS SP8, Leica Camera AG, Wetzlar, Germany). Pictures were cropped, labeled, and spaced using WPS Office software (Kingsoft Office Software, Inc., Beijing, China).

Cell counts and co-transduction efficiency analysis

The cells were counted using confocal images obtained with a 63 × objective lens and an additional 2 × digital zoom.

The images were processed using ImageJ software (National Institutes of Health, Bethesda, MD, USA). Three views of the striolar and extrastriolar regions each (~90 × 90 μm per view) were randomly captured at the level of the cuticular plate of HCs for HC counting, and at the level of supporting cell (SC) nuclei for SC counting. At the level of the cuticular plate of HCs, the numbers of GFP-positive/mCherry-positive/myosin VIIa-positive cells (co-transduced HCs) and all myosin VIIa-positive cells (HCs) were recorded and divided to obtain the co-transduction rate of HCs. Similarly, at the level of SC nuclei, the numbers of GFP-positive/mCherry-positive cells (co-transduced SCs) and all DAPI-positive cells (SCs) were recorded and divided to obtain the co-transduction rate of SCs. Each group included 5–6 samples.

Statistical analyses

Data are presented as mean ± standard error of mean (SEM). Statistical analyses were performed using GraphPad Prism 9 software (GraphPad Software, Inc., San Diego, CA, USA). Statistical differences in co-transduction efficiency were determined using Student's *t*-test. Differences were considered statistically significant when the *P*-value was < 0.05.

Results

Co-transduction of dual-adeno-associated virus-ie vectors was efficient in normal adult mouse utricle

The transduction profile of dual-AAV-ie was investigated using AAV-ie vectors driven by CAG or CMV promoters. Dual-AAV-ie vector mixtures, AAV-ie-CAG-EGFP and AAV-ie-CAG-mCherry, or AAV-ie-CMV-EGFP and AAV-ie-CMV-mCherry, were, respectively, inoculated into the adult mouse inner ear. The utricles were sampled 2 weeks after the surgery.

The whole mounts of utricles revealed robust GFP and mCherry expression throughout the utricles after dual-AAV-ie transduction in both groups (**Figures 1A–F'''**). Co-localization of GFP and mCherry was extensively found in the vestibular HCs and SCs of both dual-AAV-ie groups, indicating co-transduction by dual-AAV-ie vectors. The HCs stained by the myosin VIIa antibody exhibited minimal morphological damage after dual-AAV-ie transduction.

The co-transduction rates of HCs and SCs from the striolar and extrastriolar regions were quantitatively analyzed (**Table 1**). The co-transduction rates of HCs (**Figure 1G**) and SCs (**Figure 1H**) were not significantly different between the dual-AAV-ie-CAG and dual-AAV-ie-CMV groups (striolar HCs: 23.14 ± 2.25% *vs.* 31.14 ± 4.02%, $P = 0.1206$; extrastriolar HCs: 27.05 ± 2.10% *vs.* 27.31 ± 3.05%, $P = 0.9454$; striolar SCs: 57.65 ± 7.21% *vs.* 49.27 ± 10.05%, $P = 0.5171$; extrastriolar SCs: 60.33 ± 5.69% *vs.* 55.17 ± 8.29%, $P = 0.6217$, respectively). There was no significant difference in co-transduction rates of HCs or SCs between the striolar and the extrastriolar regions in each dual-AAV-ie group.

Dual adeno-associated virus-ie vectors allowed co-transduction in the normal neonatal mouse utricle and damaged adult mouse utricle

The transduction profiles of dual-AAV-ie were assessed in normal neonatal mice. A mixture of AAV-ie-CAG-EGFP and AAV-ie-CAG-mCherry vectors was injected at P1. The co-transductions were evaluated 2 weeks later. Intense co-expression of GFP and mCherry was seen throughout the sensory epithelium (**Figure 2**) and transitional epithelium of the utricle (**Supplementary Figure 1**). The co-transduction rates were 52.88 ± 3.11%, 44.93 ± 2.06%, 71.92 ± 5.47%, and 72.11 ± 3.61% in striolar HCs, extrastriolar HCs, striolar SCs, and extrastriolar SCs, respectively (**Table 1**). Compared to the co-transduction rate of dual AAV-ie-CAG vectors in normal adult mice (**Table 1**), that of HCs in neonatal mice was significantly higher in both the striolar and extrastriolar regions (**Figure 2D**; striolar HCs: 52.88 ± 3.11% *vs.* 23.14 ± 2.25%, $P < 0.01$; extrastriolar HCs: 44.93 ± 2.06% *vs.* 27.05 ± 2.10%, $P < 0.01$, respectively), although the co-transduction rates of SCs were comparable (**Figure 2E**; striolar SCs: 71.92 ± 5.47% *vs.* 57.65 ± 7.21%, $P = 0.1535$; extrastriolar SCs: 72.11 ± 3.61% *vs.* 60.33 ± 5.69%, $P = 0.1190$, respectively).

In the damaged group, most utricular HCs were experimentally ablated by two intramuscular injections of DT in adult *Pou4f3*$^{+/DTR}$ mice. The mixture of AAV-ie-CAG-EGFP and AAV-ie-CAG-mCherry vectors was injected 10 days after DT administration. Immunofluorescence staining of utricles was performed 2 weeks later. As indicated by the myosin VIIa staining, scattered HCs were present in the extrastriolar region of the utricle (**Figures 3A–A'''**). Intense over-expression of GFP and mCherry was present in HCs (**Figures 3B–B'''**) and SCs (**Figures 3C–C'''**). As shown in **Table 1**, the co-transduction rates of HCs in the striolar and extrastriolar regions were significantly higher than normal adult mice (**Figure 3D**; striolar HCs: 56.78 ± 8.15% *vs.* 23.14 ± 2.25%, $P < 0.01$; extrastriolar HCs: 59.28 ± 7.81% *vs.* 27.05 ± 2.10%, $P < 0.01$, respectively). No significant difference was observed in the co-transduction rate of SCs between the damaged and normal utricles in the striolar and extrastriolar regions (**Figure 3E**; striolar SCs: 66.18 ± 6.02% *vs.* 57.65 ± 7.21%, $P = 0.3832$; extrastriolar SCs: 65.11 ± 6.45% *vs.* 60.33 ± 5.69%, $P = 0.6000$, respectively). In

10.3389/fnmol.2022.1020803

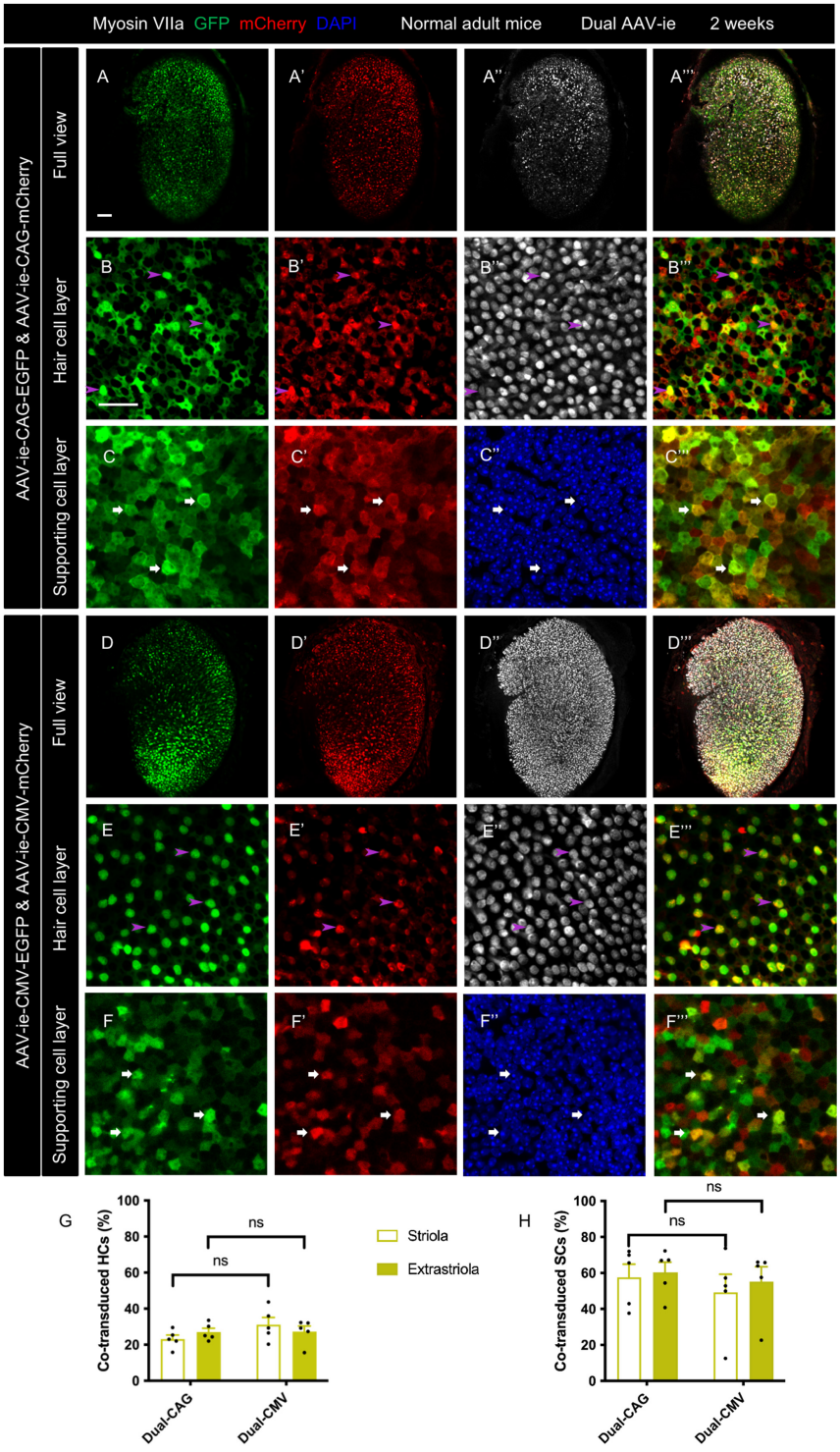

FIGURE 1
Co-transduction of dual-AAV-ie vectors in the normal adult mouse utricle. Dual AAV-ie-CAG vectors (AAV-ie-CAG-EGFP and AAV-ie-CAG-mCherry) or dual AAV-ie-CMV vectors (AAV-ie-CMV-EGFP and AAV-ie-CMV-mCherry) were inoculated into the inner ear of adult mice. Utricles were harvested 2 weeks after the surgery. **(A–C‴)** Low- **(A–A‴)** and high- **(B–C‴)** magnification images show extensive co-expression of GFP and mCherry in both HCs (arrowheads in **B–B‴**; representative images of the extrastriolar region) and SCs (arrows in **C–C‴**; representative images of the striolar region) after transduction by dual AAV-ie-CAG vectors. **(D–F‴)** Abundant HCs (arrowheads in **E–E‴**; representative images of the extrastriolar region) and SCs (arrows in **F–F‴**; representative images of the extrastriolar region) express both GFP and mCherry after transduction by dual-AAV-ie-CMV vectors. Scale bars, 50 μm in A for **(A–A‴)** and **(D–D‴)**; 20 μm in B for the remaining images. **(G,H)** Quantitative analysis showing that dual-AAV-ie-CAG and dual-AAV-ie-CMV vectors achieve comparable co-transduction rates in HCs **(G)** and SCs **(H)**. Data are mean ± SEM. *P*-values were calculated by Student's *t*-test. "ns", not significant.

TABLE 1 Summary of the co-transduction rate of each group.

Groups	Striolar HCs%	Extrastriolar HCs%	Striolar SCs%	Extrastriolar SCs%
Dual AAV-CAG-2w ($N = 5$)	23.14 ± 2.25	27.05 ± 2.10	57.65 ± 7.21	60.33 ± 5.69
Dual AAV-CMV-2w ($N = 5$)	31.14 ± 4.02	27.31 ± 3.05	49.27 ± 10.05	55.17 ± 8.29
Neonatal-2w ($N = 5$)	52.88 ± 3.11	44.93 ± 2.06	71.92 ± 5.47	72.11 ± 3.61
Damaged-2w ($N = 6$)	56.78 ± 8.15	59.28 ± 7.81	66.18 ± 6.02	65.11 ± 6.45
Adult-3m ($N = 5$)	27.96 ± 4.32	33.11 ± 1.40	64.96 ± 5.13	74.71 ± 3.64
Neonatal-3m ($N = 5$)	35.60 ± 5.60	31.43 ± 4.38	44.41 ± 8.72	45.68 ± 9.32
Damaged-3m ($N = 5$)	36.13 ± 3.60	39.15 ± 4.03	66.57 ± 4.52	65.88 ± 4.36
Sequential-2w ($N = 6$)	38.87 ± 1.25	37.59 ± 0.55	75.46 ± 2.99	71.96 ± 3.51

addition, no significant difference was found in co-transduction rates of HCs or SCs between the striolar and the extrastriolar regions in neonatal or *Pou4f3*$^{+/DTR}$ mouse utricle.

Co-transduction of dual-adeno-associated virus-ie vectors was maintained for up to 3 months in adult mice

To assess long-term transduction by dual-AAV-ie vectors, co-transduction efficiency was evaluated at 3 months after delivery of AAV-ie-CAG-EGFP and AAV-ie-CAG-mCherry to normal adult mice, normal neonatal mice, and damaged adult mice. Immunofluorescence staining revealed extensive and robust co-expression of GFP and mCherry in the utricular sensory epithelium of all three groups (**Figures 4A–I**"'). In normal adult mice, the co-transduction rate in striolar HCs showed no significant difference at 3 months and 2 weeks, but it was slightly increased in extrastriolar HCs at 3 months (striolar HCs: 27.96 ± 4.32% *vs.* 23.14 ± 2.25%, $P = 0.3509$; extrastriolar HCs: 33.11 ± 1.40% *vs.* 27.05 ± 2.10%, $P < 0.05$, respectively). The co-transduction rates of SCs were comparable at 3 months and 2 weeks (striolar SCs: 64.96 ± 5.13% *vs.* 57.65 ± 7.21%, $P = 0.4325$; extrastriolar SCs: 74.71 ± 3.64% *vs.* 60.33 ± 5.69%, $P = 0.0661$, respectively).

The co-transduction rates in the normal neonatal mice were lower at 3 months than 2 weeks in both HCs and SCs (**Figures 4J,K**; striolar HCs: 35.60 ± 5.60% *vs.* 52.88 ± 3.11%, $P < 0.05$; extrastriolar HCs: 31.43 ± 4.38% *vs.* 44.93 ± 2.06%, $P < 0.05$; striolar SCs: 44.41 ± 8.72% *vs.* 71.92 ± 5.47%, $P < 0.05$; extrastriolar SCs: 45.68 ± 9.32% *vs.* 72.11 ± 3.61%, $P < 0.05$, respectively).

The damaged adult mice exhibited no significant difference in co-transduction rates between 3 months and 2 weeks (striolar HCs: 36.13 ± 3.60% *vs.* 56.78 ± 8.15%, $P = 0.0594$; extrastriolar HCs: 39.15 ± 4.03% *vs.* 59.28 ± 7.81%, $P = 0.0601$; striolar SCs: 66.57 ± 4.52% *vs.* 66.18 ± 6.02%, $P = 0.9620$; extrastriolar SCs: 65.88 ± 4.36% *vs.* 65.11 ± 6.45%, $P = 0.9267$, respectively).

Sequential delivery of dual-adeno-associated virus-ie vectors resulted in a higher co-transduction rate in HCs than concurrent delivery

Sequential delivery of dual vectors is sometimes required for the sequential over-expression of target genes in the sensory epithelium (Yao et al., 2018). After sequential administration of dual-AAV-ie-CAG vectors with an interval of 1 week, extensive co-expression of GFP and mCherry was found throughout the sensory epithelium (**Figures 5A–C**"'). The co-transduction rates of HCs after sequential administration of dual AAV-ie-CAG vectors were significantly higher than those after the concurrent injection of dual AAV-ie-CAG vectors (**Figure 5D** and **Table 1**; striolar HCs: 38.87 ± 1.25% *vs.* 23.14 ± 2.25%, $P < 0.01$; extrastriolar HCs: 37.59 ± 0.55% *vs.* 27.05 ± 2.10%, $P < 0.01$, respectively). The co-transduction rate of striolar SCs was higher after sequential administration than concurrent injection (**Figure 5E** and **Table 1**; 75.46 ± 2.99% *vs.* 57.65 ± 7.21%, respectively, $P < 0.05$), whereas the co-transduction rate of extrastriolar SCs after sequential administration was comparable to that after concurrent delivery (**Figure 5E** and **Table 1**; 71.96 ± 3.51% *vs.* 60.33 ± 5.69%, respectively, $P = 0.1048$).

Concurrent delivery of dual-adeno-associated virus-ie vectors had minimal impact on the auditory and vestibular functions

ABR and swim tests were performed 2 weeks and 3 months after the concurrent delivery of AAV-ie-CAG-EGFP and AAV-ie-CAG-mCherry in normal adult mice. Age-matched mice of the same background served as normal controls. As shown in **Figure 6**, no significant difference was found between the groups in terms of the ABR thresholds at 4, 8, 16, and 32 kHz frequencies, or the swim test scores, demonstrating that co-transduction of dual-AAV-ie vectors had minimal impact on the auditory and vestibular functions.

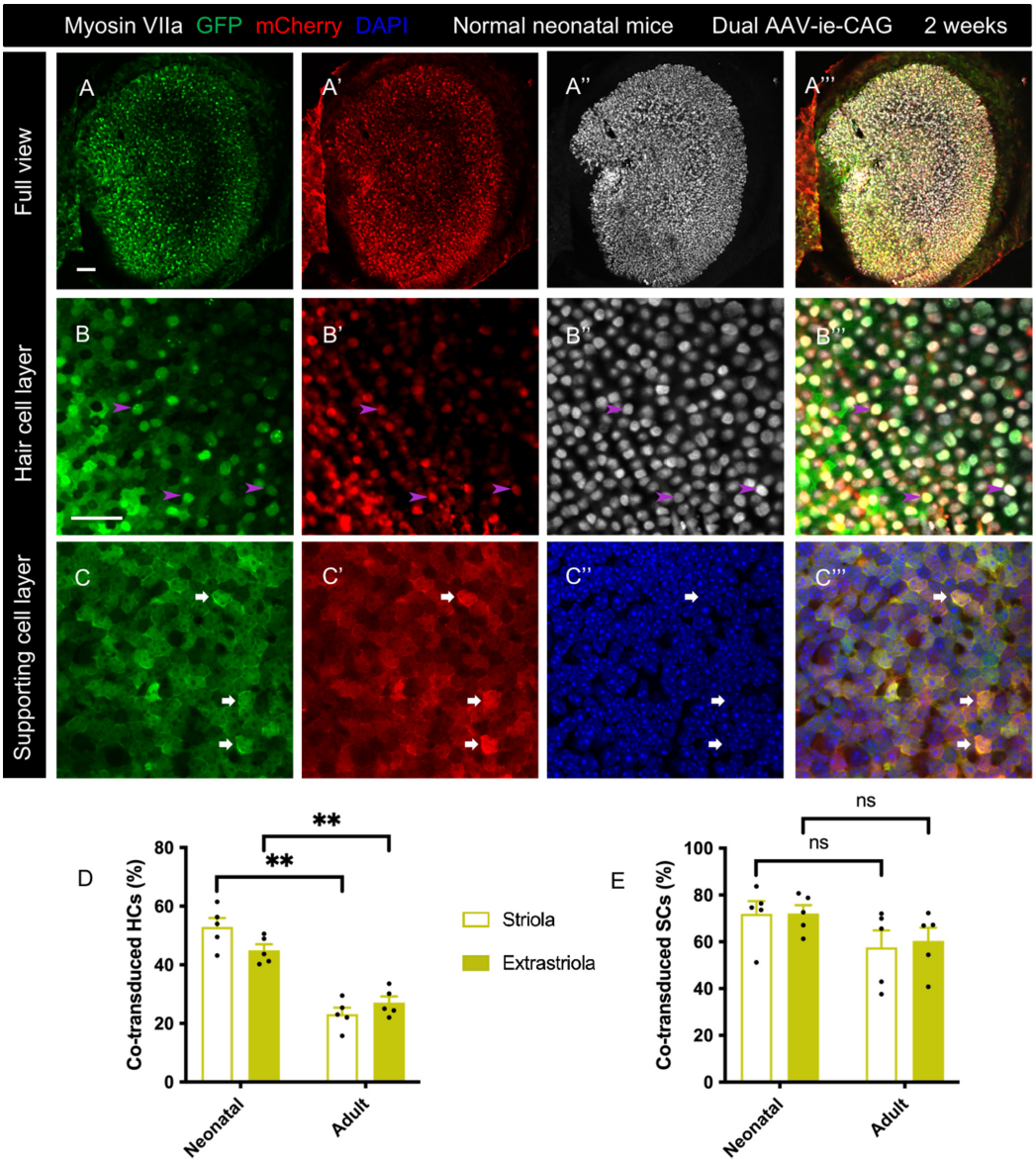

FIGURE 2
Co-transduction of dual AAV-ie vectors in the normal utricle of neonatal mice. AAV-ie-CAG-EGFP and AAV-ie-CAG-mCherry were injected into the neonatal mice at postnatal day 1 (P1). The utricles were sampled at P15. **(A–A'')** Low-magnification images. **(B–C'')** Numerous hair cells (HCs) (**B–B''**; arrowheads; representative images of the extrastriolar region) and supporting cells (SCs) (**C–C''**; arrows; representative images of the striolar region) express both GFP and mCherry. Scale bars, 50 μm in A for **(A–A'')**; 20 μm in B for **(B–C'')**. **(D,E)** Comparative analysis of the co-transduction rates of HCs **(D)** and SCs **(F)** between normal neonatal and adult mice. The co-transduction rates of HCs in neonatal mice are significantly higher than in adult mice in striolar and extrastriolar regions, whereas the co-transduction rates of SCs are comparable between the groups. Data are mean ± SEM. *P*-values were calculated using Student's *t*-test. "ns", not significant. $^{**}P < 0.01$.

Discussion

Dual-AAV-ie vectors achieved efficient co-transduction in the normal and damaged vestibular sensory epithelium of mice. The transduction was maintained for up to 3 months after co-transduction in adult mice. Sequential administration of dual-AAV-ie vectors was associated with a higher co-transduction rate in HCs than after concurrent delivery. Moreover, ABR and swim tests showed that co-transduction by dual-AAV-ie vectors minimally affected the inner ear function of normal mice. Taken together, the results showed that co-transduction by dual-AAV-ie vectors served as an efficient and safe approach for gene delivery to the mouse vestibular end organs.

Co-transduction of AAV vectors has been used *in vivo* in various tissues, such as the retina and cochlea (Colella et al., 2014; Carvalho et al., 2017; Al-Moyed et al., 2019;

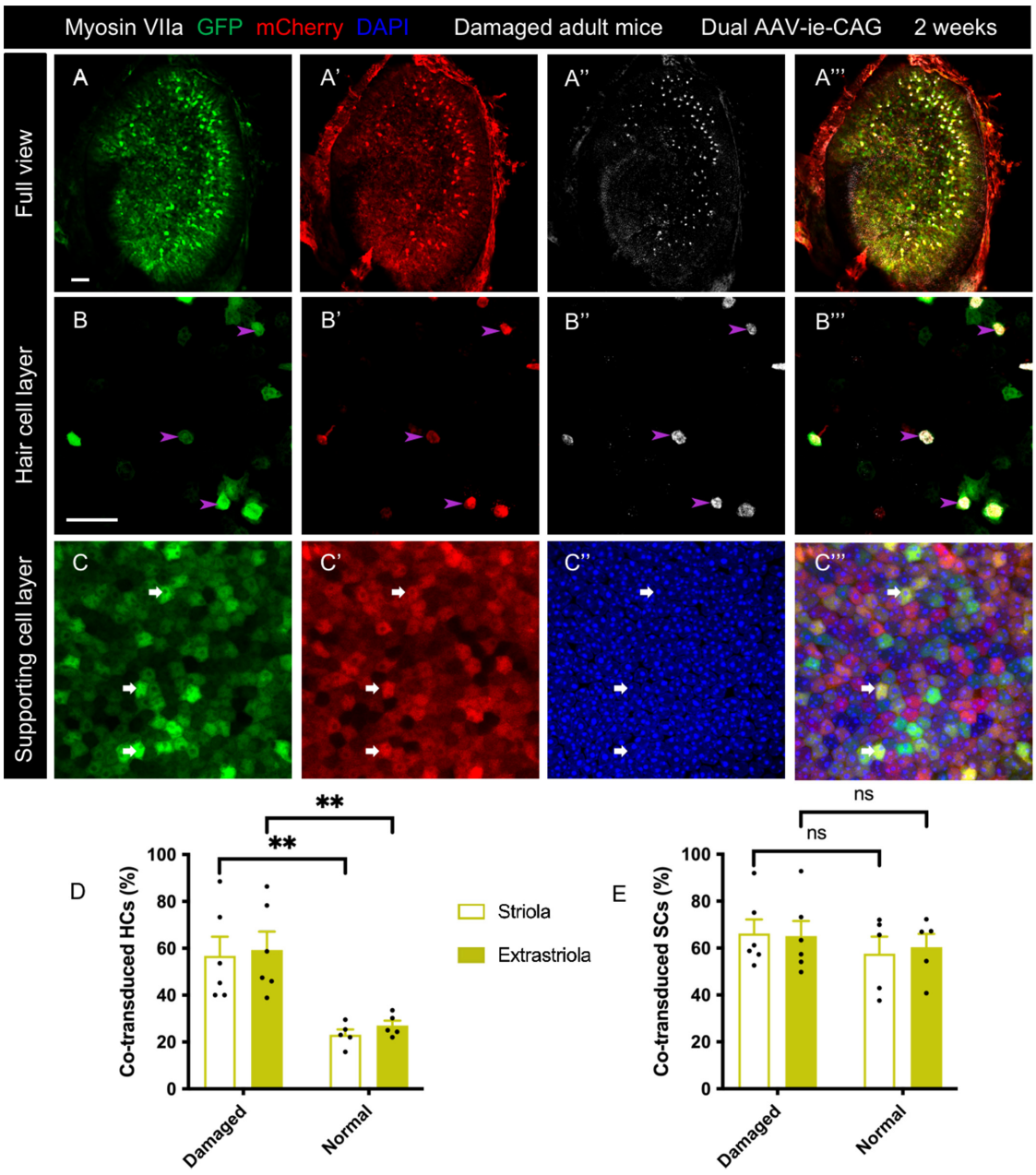

FIGURE 3
Co-transduction of dual-AAV-ie vectors in the damaged adult mouse utricle. AAV-ie-CAG-EGFP and AAV-ie-CAG-mCherry were injected into the inner ear of adult *Pou4f3*$^{+/DTR}$ mice 10 days following diphtheria toxin administration. Utricles were sampled 2 weeks after the surgery. **(A–A'')** Low-magnification images show extensive expression of GFP and mCherry throughout the utricle, with the loss of most hair cells (HCs). **(B–C'')** High-magnification images show co-transduction of dual-AAV-ie-CAG vectors in residual HCs (**B–B''**; arrowheads; representative images of the extrastriolar region) and abundant supporting cells (SCs) (**C–C''**; arrows; representative images of the extrastriolar region). Scale bars, 50 μm in A for **(A–A'')**; 20 μm in B for **(B–C'')**. **(D,E)** Comparative analysis of the co-transduction rates of HCs **(D)** and SCs **(E)** in damaged and normal adult mice. The co-transduction rates of HCs in damaged adult mice are significantly higher than those of normal mice in striolar and extrastriolar regions, whereas the co-transduction rates of SCs are comparable. Data are mean ± SEM. *P*-values were calculated using Student's *t*-test. "ns," not significant. $^{**}P < 0.01$.

Omichi et al., 2020; Wu et al., 2021). Dual-AAV6 vectors allowed otoferlin overexpression in 19–30% of inner HCs of deaf Otof-/- mice and improved the deafness (Al-Moyed et al., 2019). Perinatal injection of a mixture of AAV-Anc80L65-harmonin-a1 and AAV-Anc80L65-harmonin-b1 improved deafness and vestibular dysfunction in Ush1c mice (Pan et al., 2017), demonstrating a possible role of dual-AAV method for gene delivery to the vestibular system. In the current study, we

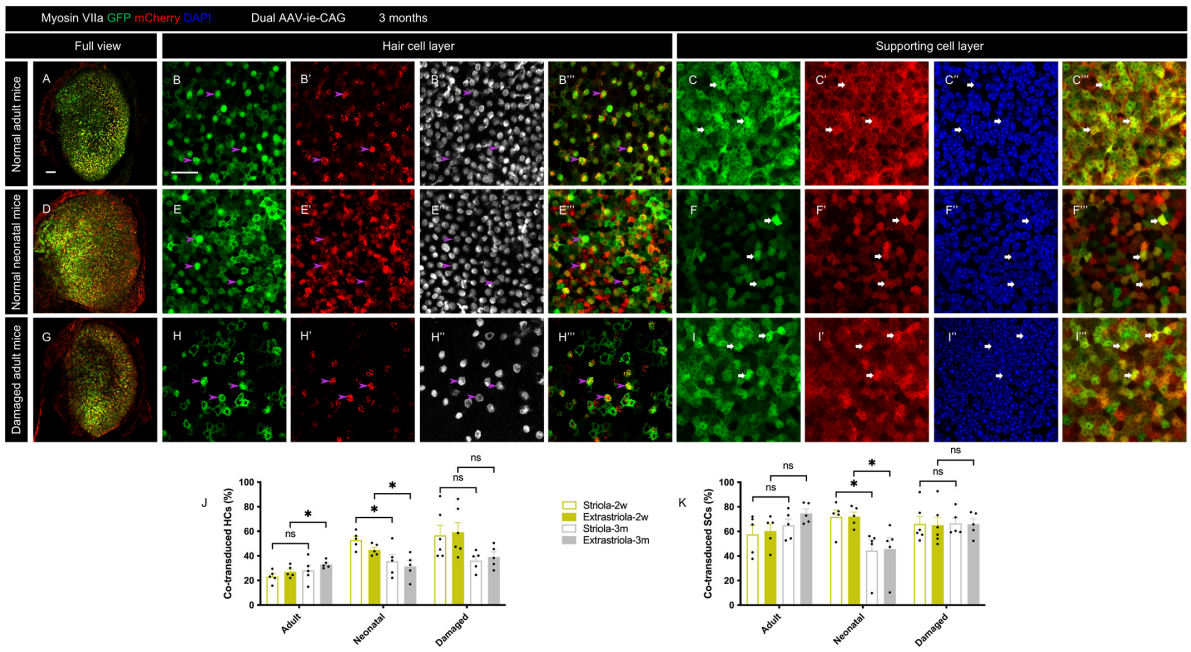

FIGURE 4
Long-term co-transduction of dual-AAV-ie vectors in the mouse utricle. Utricles were sampled 3 months after the injection of AAV-ie-CAG-EGFP and AAV-ie-CAG-mCherry. **(A–C‴)** Normal adult mice (**B–B‴** representative images of the extrastriolar region; (**C–C‴** representative images of the striolar region). **(D–F‴)** Normal neonatal mice (**E–E‴** representative images of the extrastriolar region; **F–F‴** representative images of the extrastriolar region). **(G–I‴)** Adult *Pou4f3*$^{+/DTR}$ mice following diphtheria toxin administration (**H-H‴**, representative images of the extrastriolar region; **I–I‴** representative images of the extrastriolar region). Scale bars, 50 μm in A for A, D and G; 20 μm in B for the remaining images. **(J,K)** Comparative analysis of the co-transduction rates of hair cells (HCs) **(J)** and supporting cells (SCs) **(K)** at 2 weeks and 3 months after dual-AAV-ie injection. In the normal adult mice, the co-transduction rate of extrastriolar HCs slightly increases at 3 months, while the co-transduction rates of striolar HCs and both regions of SCs are not significantly different at 3 months than 2 weeks. In the normal neonatal mice, the co-transduction rates of HCs and SCs decreases at 3 months. In addition, the co-transduction rates of HCs and SCs in the damaged adult mice are not significantly different at 3 months than 2 weeks. Data are mean ± SEM. *P*-values were calculated using Student's *t*-test. "ns," not significant. $^{*}P < 0.05$.

explored the possible applications of dual-AAV for normal and damaged vestibular end organs of adult mice. We demonstrated that sequential administration of dual-AAV vectors allows efficient co-transduction. The performance of dual-AAV vectors persisted for up to 3 months. Our results should aid the future application of dual-AAV vectors in the vestibular system.

Co-transduction efficiency might be affected by several processes. First, cellular entry largely depends on the multi-step interaction of viral capsids with receptors on the targeted cells (Zengel and Carette, 2020). However, the expression of AAV receptors in the mouse utricle has not been explored. Our data revealed that the co-transduction of dual-AAV-ie was significantly lower than that of single-AAV-ie injection (Tan et al., 2019). It might be because different age of mice and injection approach were used in Tan's study, or due to the receptor competition when dual AAV-ie vectors were injected. Second, the intracellular events underlying the endomembranous cross and nuclear translocation remain largely unknown (Zengel and Carette, 2020). Finally, interaction between the promoters and RNA polymerase II (Domenger and Grimm, 2019) is important for transcription initiation. In the present study, dual-AAV-ie-CAG vectors and dual-AAV-ie-CMV vectors had comparable efficiency. Nevertheless, the cellular process of dual-AAV vectors remains unknown.

The postnatal stage provides a significant opportunity for the treatment of certain inherited inner ear diseases (Al-Moyed et al., 2019; Guo J. et al., 2021). Otoferlin overexpression at the end of the first postnatal week in the cochlea of Otof-/- mice is too late to prevent synapse degeneration (Al-Moyed et al., 2019). The capability of programmed cell cycle reactivity of the mouse inner ear declines sharply after birth (White et al., 2006), implying that gene therapy based on cell cycle manipulation should target the perinatal period. The present study showed that dual-AAV-ie-CAG was capable of efficient co-transduction in the utricle of neonatal mice (**Figure 2**), suggesting its potential usefulness for the aforementioned purposes. The co-transduction efficiencies of HCs and SCs were reduced at 3 months compared to 2 weeks (**Figure 4**), which might be explained by the active mitosis and differentiation of the utricular sensory epithelium during the neonatal period (Burns et al., 2012).

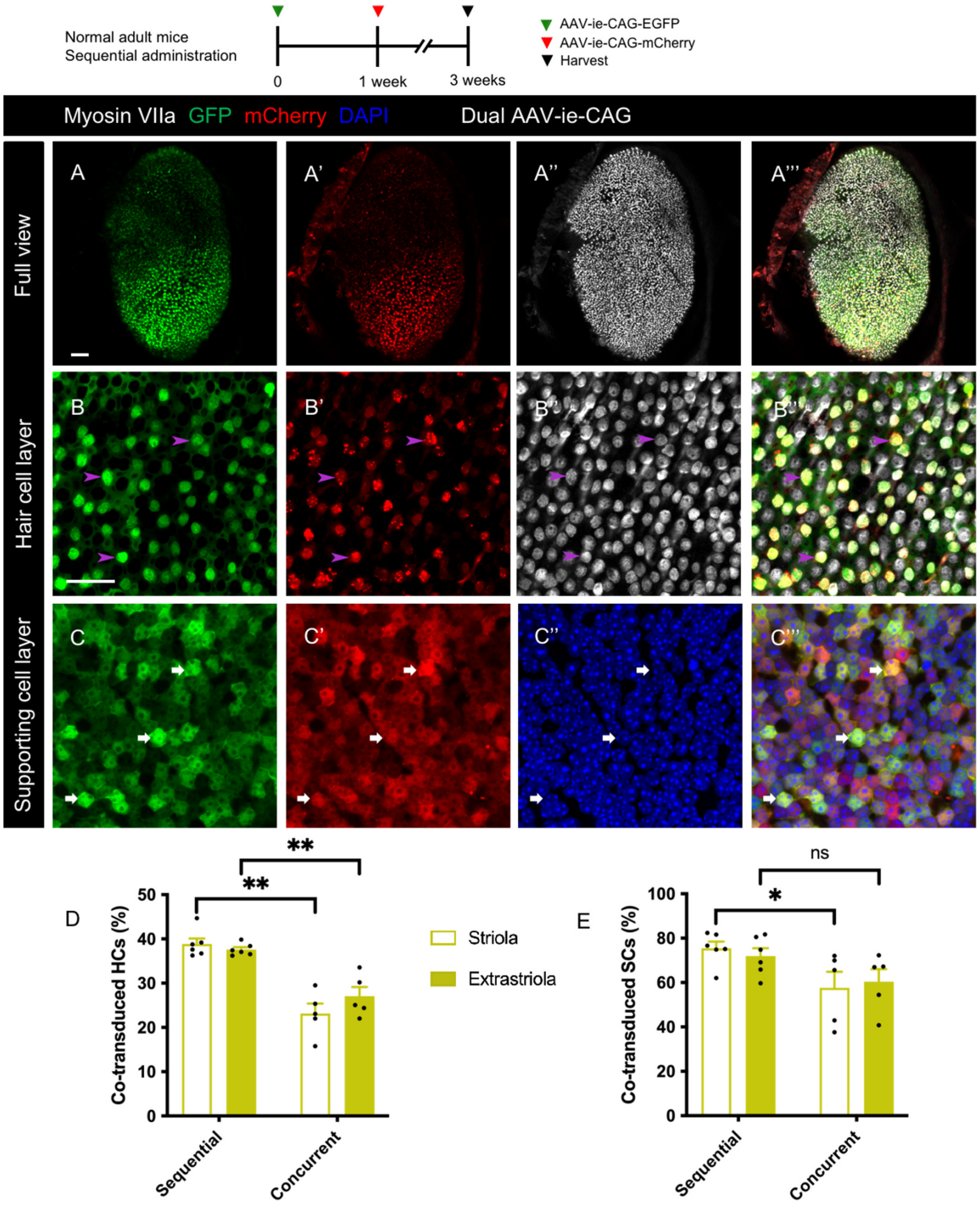

FIGURE 5
Co-transduction of dual-AAV-ie vectors in the normal adult mouse utricle after sequential administration. AAV-ie-CAG-EGFP was injected through the lateral semicircular canal, and AAV-ie-CAG-mCherry was injected through the posterior semicircular canal after 1 week. Utricles were sampled 2 weeks after the second injection. **(A–A‴)** Low-magnification images show extensive GFP and mCherry expression throughout the utricle. **(B–C‴)** Co-localization of GFP and mCherry expression is determined at the level of the cuticular plate of hair cells (HCs) (**B–B‴**; arrowheads; representative images of the striolar region) and the layer of supporting cell (SC) nuclei (**C–C‴**; arrows; representative images of the striolar region). Scale bars, 50 μm in A for **(A–A‴)**; 20 μm in B for **(B–C‴)**. **(D,E)** Comparative analysis of the co-transduction rates of HCs **(D)** and SCs **(E)** after sequential and concurrent injections. The co-transduction rates of striolar and extrastriolar HCs in the sequential group are significantly higher than those of the concurrent injection group. The co-transduction rate of striolar SCs show higher than that of the concurrent injection group, whereas the co-transduction rates of extrastriolar SCs is comparable between the groups. Data are mean ± SEM. *P*-values were calculated using Student's *t*-test. "ns," not significant. $^{*}P < 0.05$, $^{**}P < 0.01$.

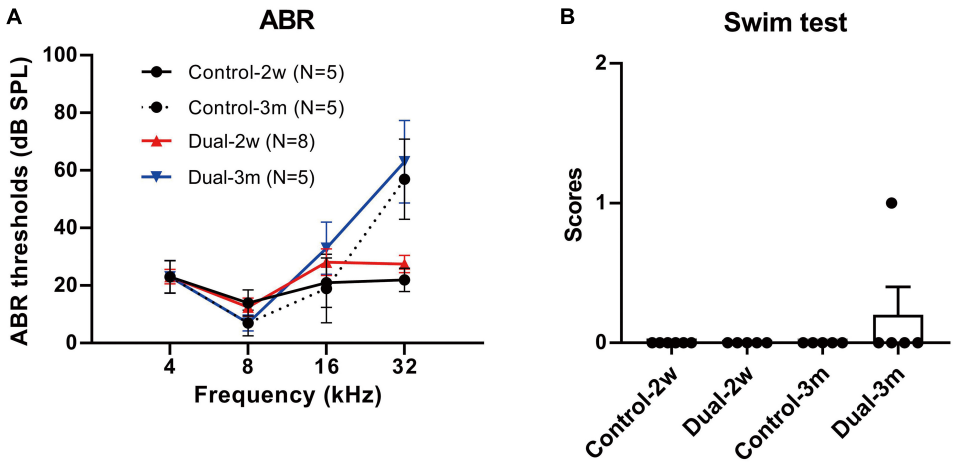

FIGURE 6
ABR thresholds and swim test scores 2 weeks and 3 months after co-transduction of dual-AAV-ie vectors in normal adult mice. **(A)** There is no significant difference in ABR thresholds between mice 2 weeks or 3 months after the injection of dual-AAV-ie vectors and control animals (i.e., age-matched mice without surgery) according to Student's *t*-test at each frequency. **(B)** Swim test scores show no significant difference between the groups according to Student's *t*-test. Data are mean ± SEM.

Genetic manipulation is a promising technique for HC regeneration and functional recruitment of damaged vestibular sensory epithelium (Li et al., 2016; Zhang et al., 2020); therefore, it has received significant attention. However, the induced HCs are insufficient in number, and in terms of maturation, which leads to variable functional outcomes (Schlecker et al., 2011; Guo J. Y. et al., 2021). There is a consensus that a single factor might not lead to sufficient regeneration of mature HCs (Shibata et al., 2020). Certain strategies have been used to manipulate multiple transcription factors or signaling pathways, and have achieved superior HC regeneration in transgenic mouse models (Costa et al., 2015; Kuo et al., 2015; Menendez et al., 2020; Chen et al., 2021; Iyer and Groves, 2021). However, transgenic mice cannot be used for clinical treatments; as an alternative, dual-AAV vectors with multiple target genes may be used. Therefore, the tropism of dual-AAV-ie-CAG vectors was tested herein in the damaged utricles of mice with experimental depletion of most HCs. The results showed that the co-transduction had higher efficiency in residual HCs, while it remained equivalent to normal mice in SCs, implying that it would be an efficient way to simultaneously overexpress multiple genes for HC regeneration.

Sufficient HC regeneration in the lesioned vestibular sensory epithelium may be achieved using a two-step reprogramming method: proliferation of SCs is stimulated, followed by the manipulation of essential transcription factors in SCs. Therefore, sequential over-expression of two target genes may be required. Sequential administration of dual-AAV vectors with different genes has been used for retinal diseases and successfully restored the vision of mice with congenital blindness (Yao et al., 2018), suggesting that this strategy might induce regeneration of the inner ear. Our data showed that sequential administration of dual-AAV-ie vectors resulted in satisfactory co-transduction in the mouse utricle (**Figure 5**), suggesting its potential usefulness for HC regeneration of vestibular sensory epithelium.

In summary, we comprehensively evaluated the co-transduction efficiency of dual-AAV vectors in the vestibular sensory epithelium under various conditions. Although the present study did not include therapeutic genes, understanding the co-transduction characteristics and safety profile of dual-AAV vectors may aid the delivery of large or multiple genes for vestibular gene therapy in the future.

Data availability statement

The raw data supporting the conclusions of this article will be made available by the authors, upon reasonable request.

Ethics statement

The animal study was reviewed and approved by Animal Care and Use Committee of Capital Medical University of China.

Author contributions

Z-RC contributed to the conceptualization and methodology of the study and wrote the original draft.

J-YG contributed to the conceptualization and methodology of the study, manuscript writing, reviewing, and editing. LH completed the data curation. SL, J-YX, and Z-JY conducted the surgeries. WS and KL were responsible for the software and validation. G-PW and S-SG provided the conceptualization, writing, reviewing, and supervision. All authors contributed to the article and approved the submitted version.

Funding

This work was supported by the National Natural Science Foundation of China (grant numbers 82171131, 81900929, and 82101210), Beijing Natural Science Foundation (grant numbers 7194256 and 7212022), Beijing Hospital Authority Youth Program (grant number QML20180101), and Beijing Talents Fund (grant number 2018000021469G206).

Conflict of interest

The authors declare that the research was conducted in the absence of any commercial or financial relationships that could be construed as a potential conflict of interest.

Publisher's note

Supplementary material

The Supplementary Material for this article can be found online at: https://www.frontiersin.org/articles/10.3389/fnmol.2022.1020803/full#supplementary-material

SUPPLEMENTARY FIGURE 1
Co-transduction of dual-AAV-ie vectors in the transitional epithelium of the neonatal mouse utricle. AAV-ie-CAG-EGFP and AAV-ie-CAG-mCherry were injected at postnatal day 1. The utricles were sampled 2 weeks **(A–B″)** or 3 months **(C–D″)** following injection. Robust co-expression of GFP (arrows in **B–B″**) and mCherry (arrows in **D–D″**) are present in the transitional epithelium. The dashed lines **(B″,D″)** delineate the boundary of the sensory and transitional epithelium. Scale bars, 50 μm in A for **(A,C)**; 10 μm in B for the remaining images.

References

Akil, O., Dyka, F., Calvet, C., Emptoz, A., Lahlou, G., Nouaille, S., et al. (2019). Dual AAV-mediated gene therapy restores hearing in a DFNB9 mouse model. *Proc. Natl. Acad. Sci. U.S.A.* 116, 4496–4501. doi: 10.1073/pnas.1817537116

Al-Moyed, H., Cepeda, A. P., Jung, S., Moser, T., Kugler, S., and Reisinger, E. (2019). A dual-AAV approach restores fast exocytosis and partially rescues auditory function in deaf otoferlin knock-out mice. *EMBO Mol. Med.* 11:e9396. doi: 10.15252/emmm.201809396

Burns, J. C., On, D., Baker, W., Collado, M. S., and Corwin, J. T. (2012). Over half the hair cells in the mouse utricle first appear after birth, with significant numbers originating from early postnatal mitotic production in peripheral and striolar growth zones. *J. Assoc. Res. Otolaryngol.* 13, 609–627. doi: 10.1007/s10162-012-0337-0

Carvalho, L. S., Turunen, H. T., Wassmer, S. J., Luna-Velez, M. V., Xiao, R., Bennett, J., et al. (2017). Evaluating efficiencies of dual AAV approaches for retinal targeting. *Front. Neurosci.* 11:503. doi: 10.3389/fnins.2017.00503

Chatterjee, P., Padmanarayana, M., Abdullah, N., Holman, C. L., LaDu, J., Tanguay, R. L., et al. (2015). Otoferlin deficiency in zebrafish results in defects in balance and hearing: Rescue of the balance and hearing phenotype with full-length and truncated forms of mouse otoferlin. *Mol. Cell Biol.* 35, 1043–1054. doi: 10.1128/MCB.01439-14

Chen, Y., Gu, Y., Li, Y., Li, G. L., Chai, R., Li, W., et al. (2021). Generation of mature and functional hair cells by co-expression of Gfi1, Pou4f3, and Atoh1 in the postnatal mouse cochlea. *Cell Rep.* 35:109016. doi: 10.1016/j.celrep.2021.109016

Chow, M. R., Ayiotis, A. I., Schoo, D. P., Gimmon, Y., Lane, K. E., Morris, B. J., et al. (2021). Posture, gait, quality of life, and hearing with a vestibular implant. *N. Engl. J. Med.* 384, 521–532. doi: 10.1056/NEJMoa2020457

Colella, P., Trapani, I., Cesi, G., Sommella, A., Manfredi, A., Puppo, A., et al. (2014). Efficient gene delivery to the cone-enriched pig retina by dual AAV vectors. *Gene Ther.* 21, 450–456. doi: 10.1038/gt.2014.8

Costa, A., Sanchez-Guardado, L., Juniat, S., Gale, J. E., Daudet, N., and Henrique, D. (2015). Generation of sensory hair cells by genetic programming with a combination of transcription factors. *Development* 142, 1948–1959. doi: 10.1242/dev.119149

Domenger, C., and Grimm, D. (2019). Next-generation AAV vectors-do not judge a virus (only) by its cover. *Hum. Mol. Genet.* 28, R3–R14. doi: 10.1093/hmg/ddz148

Duan, D., Sharma, P., Yang, J., Yue, Y., Dudus, L., Zhang, Y., et al. (1998). Circular intermediates of recombinant adeno-associated virus have defined structural characteristics responsible for long-term episomal persistence in muscle tissue. *J. Virol.* 72, 8568–8577. doi: 10.1128/JVI.72.11.8568-8577.1998

Guo, J. Y., He, L., Chen, Z. R., Liu, K., Gong, S. S., and Wang, G. P. (2021). AAV8-mediated Atoh1 overexpression induces dose-dependent regeneration of vestibular hair cells in adult mice. *Neurosci. Lett.* 747:135679. doi: 10.1016/j.neulet.2021.135679

Guo, J. Y., He, L., Qu, T.-F., Liu, Y. Y., Liu, K., Wang, G. P., et al. (2018). Canalostomy as a surgical approach to local drug delivery into the inner ears of adult and neonatal mice. *J. Vis. Exp.* 135:57351. doi: 10.3791/57351

Guo, J. Y., Liu, Y. Y., Qu, T. F., Peng, Z., Xie, J., Wang, G. P., et al. (2017). Cochleovestibular gene transfer in neonatal mice by canalostomy. *Neuroreport* 28, 682–688. doi: 10.1097/WNR.0000000000000827

Guo, J., Ma, X., Skidmore, J. M., Cimerman, J., Prieskorn, D. M., Beyer, L. A., et al. (2021). GJB2 gene therapy and conditional deletion reveal developmental stage-dependent effects on inner ear structure and function. *Mol. Ther. Methods Clin. Dev.* 23, 319–333. doi: 10.1016/j.omtm.2021.09.009

Hardisty-Hughes, R. E., Parker, A., and Brown, S. D. (2010). A hearing and vestibular phenotyping pipeline to identify mouse mutants with hearing impairment. *Nat. Protoc.* 5, 177–190. doi: 10.1038/nprot.2009.204

Iyer, A. A., and Groves, A. K. (2021). Transcription factor reprogramming in the inner ear: Turning on cell fate switches to regenerate sensory hair cells. *Front. Cell Neurosci.* 15:660748. doi: 10.3389/fncel.2021.660748

Jones, S. M., and Jones, T. A. (2014). Genetics of peripheral vestibular dysfunction: Lessons from mutant mouse strains. *J. Am. Acad. Audiol.* 25, 289–301. doi: 10.3766/jaaa.25.3.8

Kay, M. A. (2011). State-of-the-art gene-based therapies: The road ahead. *Nat. Rev. Genet.* 12, 316–328. doi: 10.1038/nrg2971

Kuo, B. R., Baldwin, E. M., Layman, W. S., Taketo, M. M., and Zuo, J. (2015). In vivo cochlear hair cell generation and survival by coactivation of beta-catenin and Atoh1. *J. Neurosci.* 35, 10786–10798. doi: 10.1523/JNEUROSCI.0967-15.2015

Li, W., You, D., Chen, Y., Chai, R., and Li, H. (2016). Regeneration of hair cells in the mammalian vestibular system. *Front. Med.* 10:143–151. doi: 10.1007/s11684-016-0451-1

Liu, M., Yue, Y., Harper, S. Q., Grange, R. W., Chamberlain, J. S., and Duan, D. (2005). Adeno-associated virus-mediated microdystrophin expression protects young mdx muscle from contraction-induced injury. *Mol. Ther.* 11, 245–256. doi: 10.1016/j.ymthe.2004.09.013

MacLaren, R. E., Groppe, M., Barnard, A. R., Cottriall, C. L., Tolmachova, T., Seymour, L., et al. (2014). Retinal gene therapy in patients with choroideremia: Initial findings from a phase 1/2 clinical trial. *Lancet* 383, 1129–1137. doi: 10.1016/S0140-6736(13)62117-0

Menendez, L., Trecek, T., Gopalakrishnan, S., Tao, L., Markowitz, A. L., Yu, H. V., et al. (2020). Generation of inner ear hair cells by direct lineage conversion of primary somatic cells. *Elife* 9:e55249. doi: 10.7554/eLife.55249

Nathwani, A. C., Tuddenham, E. G., Rangarajan, S., Rosales, C., McIntosh, J., Linch, D. C., et al. (2011). Adenovirus-associated virus vector-mediated gene transfer in hemophilia B. *N. Engl. J. Med.* 365, 2357–2365. doi: 10.1056/NEJMoa1108046

Omichi, R., Yoshimura, H., Shibata, S. B., Vandenberghe, L. H., and Smith, R. J. H. (2020). Hair cell transduction efficiency of single- and dual-AAV serotypes in adult murine cochleae. *Mol. Ther. Methods Clin. Dev.* 17, 1167–1177. doi: 10.1016/j.omtm.2020.05.007

Ostedgaard, L. S., Rokhlina, T., Karp, P. H., Lashmit, P., Afione, S., Schmidt, M., et al. (2005). A shortened adeno-associated virus expression cassette for CFTR gene transfer to cystic fibrosis airway epithelia. *Proc. Natl. Acad. Sci. U.S.A.* 102, 2952–2957. doi: 10.1073/pnas.0409845102

Pan, B., Askew, C., Galvin, A., Heman-Ackah, S., Asai, Y., Indzhykulian, A. A., et al. (2017). Gene therapy restores auditory and vestibular function in a mouse model of Usher syndrome type 1c. *Nat. Biotechnol.* 35, 264–272. doi: 10.1038/nbt.3801

Reisinger, E. (2020). Dual-AAV delivery of large gene sequences to the inner ear. *Hear Res.* 394, 107857. doi: 10.1016/j.heares.2019.107857

Schlecker, C., Praetorius, M., Brough, D. E., Presler, R. G. Jr., Hsu, C., Plinkert, P. K., et al. (2011). Selective atonal gene delivery improves balance function in a mouse model of vestibular disease. *Gene Ther.* 18, 884–890. doi: 10.1038/gt.2011.33

Shibata, S. B., West, M. B., Du, X., Iwasa, Y., Raphael, Y., and Kopke, R. D. (2020). Gene therapy for hair cell regeneration: Review and new data. *Hear Res.* 394, 107981. doi: 10.1016/j.heares.2020.107981

Tan, F., Chu, C., Qi, J., Li, W., You, D., Li, K., et al. (2019). AAV-ie enables safe and efficient gene transfer to inner ear cells. *Nat. Commun.* 10:3733. doi: 10.1038/s41467-019-11687-8

Tertrais, M., Bouleau, Y., Emptoz, A., Belleudy, S., Sutton, R. B., Petit, C., et al. (2019). Viral transfer of mini-otoferlins partially restores the fast component of exocytosis and uncovers ultrafast endocytosis in auditory hair cells of Otoferlin knock-out mice. *J. Neurosci.* 39, 3394–3411. doi: 10.1523/JNEUROSCI.1550-18.2018

Trapani, I., Colella, P., Sommella, A., Iodice, C., Cesi, G., de Simone, S., et al. (2014). Effective delivery of large genes to the retina by dual AAV vectors. *EMBO Mol. Med.* 6, 194–211. doi: 10.1002/emmm.201302948

Tsuji, K., Velazquez-Villasenor, L., Rauch, S. D., Glynn, R. J., Wall, C. III, and Merchant, S. N. (2000b). Temporal bone studies of the human peripheral vestibular system. Meniere's disease. *Ann. Otol. Rhinol. Laryngol. Suppl.* 181, 26–31. doi: 10.1177/00034894001090s505

Tsuji, K., Velazquez-Villasenor, L., Rauch, S. D., Glynn, R. J., Wall, C. III, and Merchant, S. N. (2000a). Temporal bone studies of the human peripheral vestibular system. Aminoglycoside ototoxicity. *Ann. Otol. Rhinol. Laryngol. Suppl.* 181, 20–25. doi: 10.1177/00034894001090s504

Wang, G. P., Guo, J. Y., Peng, Z., Liu, Y. Y., Xie, J., and Gong, S. S. (2014). Adeno-associated virus-mediated gene transfer targeting normal and traumatized mouse utricle. *Gene Ther.* 21, 958–966. doi: 10.1038/gt.2014.73

White, P. M., Doetzlhofer, A., Lee, Y. S., Groves, A. K., and Segil, N. (2006). Mammalian cochlear supporting cells can divide and trans-differentiate into hair cells. *Nature* 441, 984–987. doi: 10.1038/nature04849

Wu, J., Li, W., Lin, C., Chen, Y., Cheng, C., Sun, S., et al. (2016). Co-regulation of the Notch and Wnt signaling pathways promotes supporting cell proliferation and hair cell regeneration in mouse utricles. *Sci. Rep.* 6:29418. doi: 10.1038/srep29418

Wu, J., Solanes, P., Nist-Lund, C., Spataro, S., Shubina-Oleinik, O., Marcovich, I., et al. (2021). Single and dual vector gene therapy withf AAV9-PHP.B rescues hearing in Tmc1 mutant mice. *Mol. Ther.* 29, 973–988. doi: 10.1016/j.ymthe.2020.11.016

Yao, K., Qiu, S., Wang, Y. V., Park, S. J. H., Mohns, E. J., Mehta, B., et al. (2018). Restoration of vision after de novo genesis of rod photoreceptors in mammalian retinas. *Nature* 560, 484–488. doi: 10.1038/s41586-018-0425-3

Yla-Herttuala, S. (2012). Endgame: Glybera finally recommended for approval as the first gene therapy drug in the European union. *Mol. Ther.* 20, 1831–1832. doi: 10.1038/mt.2012.194

You, D., Guo, L., Li, W., Sun, S., Chen, Y., Chai, R., et al. (2018). Characterization of Wnt and Notch-responsive Lgr5+ hair cell progenitors in the striolar region of the neonatal mouse utricle. *Front. Mol. Neurosci.* 11:137. doi: 10.3389/fnmol.2018.00137

Zengel, J., and Carette, J. E. (2020). Structural and cellular biology of adeno-associated virus attachment and entry. *Adv. Virus Res.* 106, 39–84. doi: 10.1016/bs.aivir.2020.01.002

Zhang, Y., Zhang, S., Zhang, Z., Dong, Y., Ma, X., Qiang, R., et al. (2020). Knockdown of Foxg1 in Sox9+ supporting cells increases the trans-differentiation of supporting cells into hair cells in the neonatal mouse utricle. *Aging* 12, 19834–19851. doi: 10.18632/aging.104009

frontiers | Frontiers in Neuroscience

TYPE Original Research
PUBLISHED 03 November 2022
DOI 10.3389/fnins.2022.1032087

OPEN ACCESS

EDITED BY
Zuhong He,
Department of Otolaryngology, Zhongnan Hospital, Wuhan University, China

REVIEWED BY
Haiying Sun,
Huazhong University of Science and Technology, China
Qiaojun Fang,
Second Hospital of Anhui Medical University, China

*CORRESPONDENCE
Shuangba He
hesb@njtrh.org

†These authors have contributed equally to this work and share first authorship

SPECIALTY SECTION
This article was submitted to Auditory Cognitive Neuroscience, a section of the journal Frontiers in Neuroscience

RECEIVED 30 August 2022
ACCEPTED 18 October 2022
PUBLISHED 03 November 2022

CITATION
Meng W, Cai M, Gao Y, Ji H, Sun C, Li G, Wei Y, Chen Y, Ni H, Yan M and He S (2022) Analysis of postoperative effects of different semicircular canal surgical technique in patients with labyrinthine fistulas.
Front. Neurosci. 16:1032087.
doi: 10.3389/fnins.2022.1032087

Analysis of postoperative effects of different semicircular canal surgical technique in patients with labyrinthine fistulas

Wei Meng[1†], Mingjing Cai[1†], Yanhui Gao[1†], Hongbo Ji[2], Chuan Sun[1], Guangfei Li[1], Yanyan Wei[1], Yan Chen[1], Hui Ni[3], Min Yan[3] and Shuangba He[1*]

[1]Department of Otorhinolaryngology Head and Neck Surgery, Nanjing Tongren Hospital, School of Medicine, Southeast University, Nanjing, China, [2]Department of Imaging, Nanjing Tongren Hospital, School of Medicine, Southeast University, Nanjing, China, [3]Department of Operating Room, Nanjing Tongren Hospital, School of Medicine, Southeast University, Nanjing, China

Objective: Different semicircular canal surgery techniques have been used to treat patients with labyrinthine fistulas caused by middle ear cholesteatoma. This study evaluated postoperative hearing and vestibular function after various semicircular canal surgeries.

Materials and methods: In group 1, from January 2008 to December 2014, 29 patients with middle ear cholesteatoma complicated by labyrinthine fistulas were treated with surgery involving covering the fistulas with simple fascia. In group 2, from January 2015 to October 2021, 36 patients with middle ear cholesteatoma complicated by labyrinthine fistulas were included. Cholesteatomas on the surface of type I labyrinthine fistulas were cleaned using the "under water technique" and capped with a "sandwich" composed of fascia, bone meal, and fascia. Cholesteatomas on the surface of type II and III fistulas were cleaned using the "under water technique," and the labyrinthine fistula was plugged with a "pie" composed of fascia, bone meal, and fascia, and then covered with bone wax.

Results: Some patients with labyrinthine fistulas in group 1 exhibited symptoms of vertigo after surgery. In group 2 Patients with type II labyrinthine fistulas experienced short-term vertigo after semicircular canal occlusion, but no cases of vertigo were reported during long-term follow-up. "sandwich." In patients with type II labyrinthine fistulas, the semicircular canal occlusion influenced postoperative hearing improvement. However, postoperative patient hearing was still superior to preoperative hearing.

Conclusion: The surface of type I labyrinthine fistulas should be capped by a "sandwich" composed of fascia, bone meal, and fascia. Type II and III labyrinthine fistulas should be plugged with a "pie" composed of fascia, bone meal, and fascia, covered with bone wax.

KEYWORDS

middle ear cholesteatoma, labyrinthine fistula, semicircular canal occlusion, analysis, hearing

Introduction

Labyrinthine fistulas, also known as localized labyrinthitis or perilabyrinthitis, are a complication of chronic suppurative otitis media that is usually caused by cholesteatoma invading the osseous labyrinth and account for 4.9–12.7% of middle ear cholesteatomas (Rosito et al., 2019). The classification and intraoperative management of labyrinthine fistulas vary, and a clear standard is lacking. Whether the effect on inner ear function in labyrinthine fistulas with serious clinical lesions can be reduced when the cholesteatoma epithelium is completely removed remains controversial (Geerse et al., 2017; Lim et al., 2017). This controversy is due to the intraoperative opening of the labyrinth, which may lead to neurological hearing loss and the risk of further development of the remaining fistula, leading to suppurative labyrinthitis or cholesteatoma recurrence.

Among the various proposed classification criteria for labyrinthine fistulas, the widely used Dornhofer method divides fistulas, which are considered to be an erosion of the bony labyrinth with an intact endosteum, into three types (Dornhoffer and Milewski, 1995). A type I fistula is defined as an erosion of the bony labyrinth with an intact endosteum. A type II fistula is a true fistula consisting of an open perilymphatic space. A type III fistula consists of an open perilymphatic space with concomitant involvement or destruction of the underlying membranous labyrinth. This system is schematically represented in **Figures 1A**, **2A**, **3F**.

The latest classification, described by Quaranta et al. (2009), divides fistulas into six stages based on computed tomography and intraoperative findings. This staging system considers fistula size and depth.

Based on the convenience of the proposed analysis, we applied Dornhoffer and Milewski (1995) classification method in the present study.

According to the summary of surgical treatment techniques for superior semicircular canal dehiscence syndrome by previous scholars, the most commonly used surgical techniques for local bone defects in the superior semicircular canal involve application of various materials (such as bone, fascia, fat, and bone wax) (Mikulec et al., 2005; Ossen et al., 2017; Nguyen et al., 2018). The techniques were the plugging, resurfacing or capping. Studies showed that the success rate of occlusion was high (Mikulec et al., 2005). However, the occlusion technique is invasive and increases the risk of sensorineural hearing loss (Ziylan et al., 2017). Moreover, the type of reconstruction material may also affect the long-term results. Previous reports showed that autologous bone produced optimal results with less tissue inflammation. Conversely, fat, fascia, and muscle resulted in the lowest success rate (Kwok et al., 2019). In this study, we used some of the techniques described above to treat patients with labyrinthine fistulas caused by middle ear cholesteatoma. Our analysis included various combinations of autologous bone meal and fascia that were applied to repair bone defects in patients with different types of labyrinthine fistulas. In addition, postsurgical hearing and vestibular function were monitored.

Materials and methods

We retrospectively analyzed the clinical data of group 1 and group 2 patients with middle ear cholesteatoma complicated by a labyrinthine fistula (**Table 1**).

Grouping

Group 1 included 29 patients with middle ear cholesteatoma complicated by labyrinthine fistulas that were treated between January 2008 and December 2014 (type I, $n = 21$; type II, $n = 8$; type III, $n = 0$).

Group 2 included 36 patients with middle ear cholesteatoma complicated by labyrinthine fistulas that were treated between January 2015 and October 2021 (type I, $n = 23$; type II, $n = 12$; and type III, $n = 1$).

Surgical methods

Open radical mastoidectomy was performed to remove the cholesteatoma and expose the external semicircular canal, facial nerve, and auditory ossicle for all patients. The cholesteatoma at the labyrinthine fistula was temporarily retained and the entire

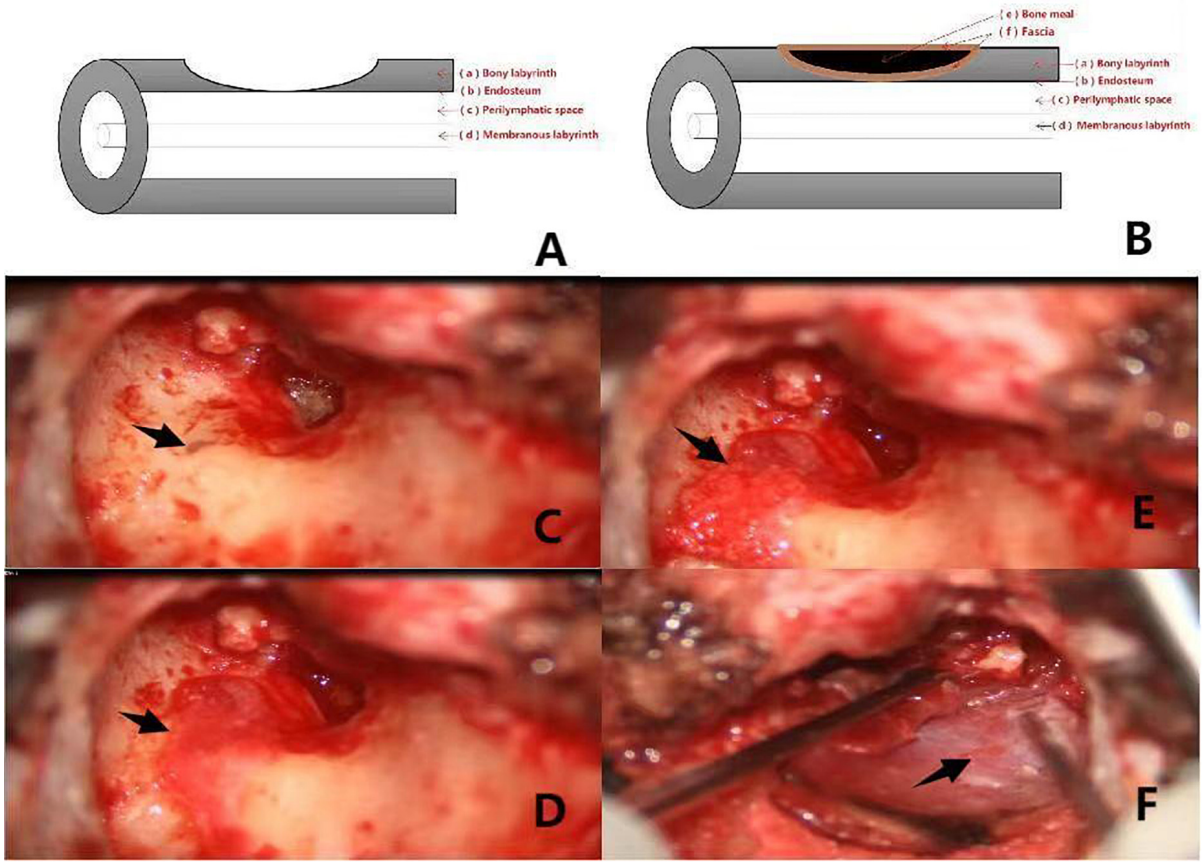

FIGURE 1
(A,B) Shows the preoperative and postoperative pattern diagram of a patient with type I labyrinteric fistula. The red arrows (a–f) respectively, represent the bony labyrinth, endosteum, perilymphatic space, membranous labyrinth, bone meal, fascia. Pictures **(C–F)** are intraoperative of a patient with type I labyrinthine fistula. **(C)**: Type I labyrinthine fistula with endosteum and cholesteatoma epithelium covered with surface (the black arrow). **(D)**: Fascia placed on the surface of the fistula (the black arrow). **(E)**: Surface of the fascia with clean bone meal (the black arrow). **(F)**: Fascia placed on the surface of the bone meal (the black arrow).

intraoperative cavity was repeatedly rinsed with 1% adrenaline and dexamethasone saline. Dexamethasone was then injected into the operative cavity and the cholesteatoma epithelium at the labyrinthine fistula was removed "under water." "under water" technology is throughout this step, saline containing corticosteroids was continuously superfused on to the area of surgery, creating a complete protective cover over the fistula and avoiding leakage of the perilymph, so that the removal of matrix and perimatrix was performed "under water" (Thangavelu et al., 2022).

Group 1

Surgical methods included open mastoidectomy, tympanoplasty, and facial nerve exploration. Intraoperatively, the researchers covered the labyrinthine fistula with simple fascia only, administered a dexamethasone injection, and proceeded with the operation.

Group 2

Type I fistulas were treated using open mastoidectomy + tympanoplasty + facial nerve exploration. Cholesteatomas on the surface of the labyrinthine fistula were cleaned using the "under water technique" and capped with a "sandwich" composed of fascia, bone meal, and fascia. Type II and III fistulas were treated with open mastoidectomy + tympanoplasty + facial nerve decompression + semicircular canal occlusion. Cholesteatomas on the surface of the labyrinthine fistula were cleaned using the "under water technique" and the fistula was plugged with a "pie" composed of fascia, bone meal, and fascia and then covered with bone wax. Hearing reconstruction was subsequently performed.

In one patient with a type III labyrinthine fistula and extremely severe preoperative mixed hearing loss, auditory ossicular chain reconstruction was not performed simultaneously.

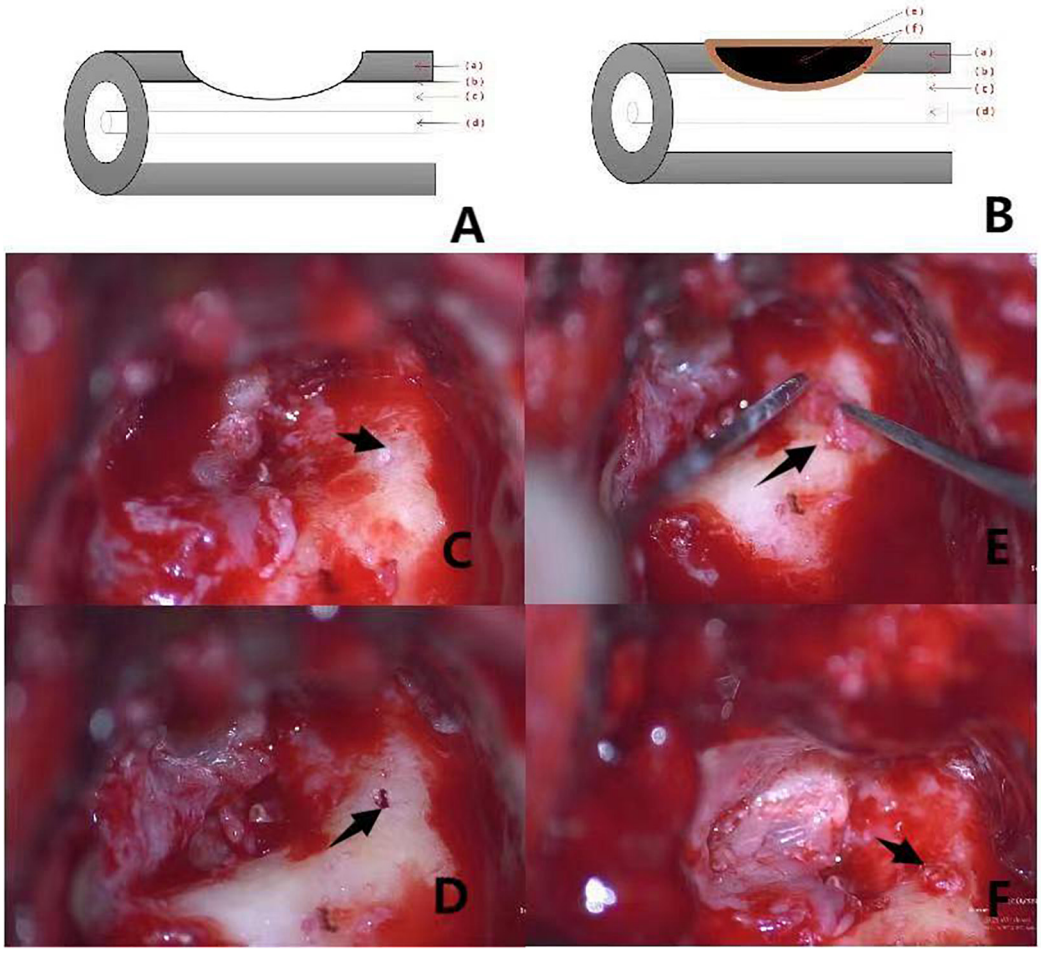

FIGURE 2
(A,B) Shows the preoperative and postoperative pattern diagram of a patient with type II labyrinteric fistula. The red arrows (a–f) respectively, represent the bony labyrinth, endosteum, perilymphatic space, membranous labyrinth, bone meal, fascia. Pictures **(C–F)** are intraoperative of a patient with type II labyrinthine fistula. **(C)**: Labyrinthine type II fistula with superficial cholesteatoma epithelium showing deep invagination within the external semicircular canals (the black arrow). **(D)**: Destruction of the endosteum is visible after "under water" cleaning of the cholesteatoma epithelium on the surface of the fistula (the black arrow). **(E)**: Placement of clean bone meal inside the fascia with a "pie" filling of the external semicircular canal (the black arrow). **(F)**: Filling the posterior surface of the semicircular canal by application of fascia is observed (the black arrow).

All labyrinthine fistulas were located in the external semicircular canal.

Images

Surgical images and pattern diagram of type I, II, and III labyrinthine fistulas in group 2 are shown in Figures 1–3.

Postoperative treatment (7 days)

Anti-inflammatory therapy

Third-generation cephalosporins were administered intravenously for 7 days.

Anti-vertigo therapy

Betahistine tablets (1–2 tablets three times daily) were administered to patients with postoperative vertigo symptoms.

Hormone therapy

Daily hormone use was prescribed.

Nutritional neurotherapy

Ginaton (intravenous infusion) and mecobalamin (intravenous injection) were prescribed.

Daily observation

General patient conditions were observed, and bedside examinations for nystagmus were performed.

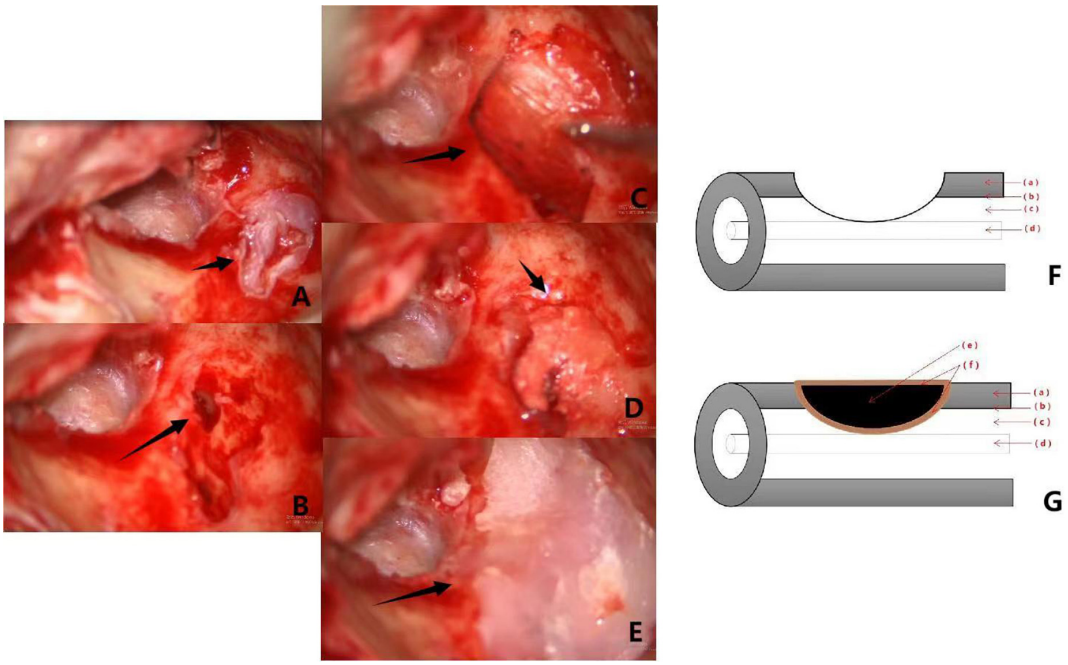

FIGURE 3
Pictures **(A–E)** are intraoperative of a patient with type III labyrinthine fistula. **(A)**: Type III labyrinth fistula with the superficial cholesteatoma epithelium located deep in the external semicircular canal (the black arrow). **(B)**: Cholesteatoma epithelium on the surface of the fistula (the black arrow). After the cholesteatoma epithelium is cleaned "under water," the membrane labyrinth is destroyed. **(C)**: The fascia is placed on the surface of the fistula (the black arrow). **(D)**: Clean bone powder is placed on the fascia and the external semicircular canal is filled with a "pie" shape (the black arrow). **(E)**: The surface of the semicircular canal is covered with bone wax (the black arrow). **(F,G)** Show the preoperative and postoperative pattern diagram of a patient with type III labyrinteric fistula. The red arrows (a–f) respectively, represent the bony labyrinth, endosteum, perilymphatic space, membranous labyrinth, bone meal, fascia.

TABLE 1 Characteristics of participants in groups 1 and 2.

Variable	Group	
	Group 1	Group 2
Number	29	36
Age (years)	51 ± 17.0	49 ± 1.33
Sex		
	Male 15	Male 19
	Female 14	Female 17
Side	Right 19	Right 20
	Left 10	Left 16
Type (Dornhoffer)	I 21	I 23
	II 8	II 12
	III 0	III 1
Presentation		
	With vertigo 5	With vertigo 9
	Without vertigo 24	Without vertigo 27

Postoperative checks

The bandage, the auricular and the incision of postauricular were observed at 3 days postoperatively, and once patients were able to sit independently, vestibular rehabilitation training was initiated.

Statistical methods

Statistical analysis was performed using SPSS software (SPSS version 19.0; Wilcoxon signed-rank test). Differences were considered significant at $P \leq 0.05$.

Results

Postoperative follow-up of middle-ear cholesteatoma patients with labyrinthine fistulas

A total of 65 patients with middle ear cholesteatoma and labyrinthine fistulas were followed up between January 2008 and October 2021, including 29 and 36 patients in groups 1 and 2, respectively. The patients were continuously followed up postoperatively. In group 1, middle ear cholesteatoma recurred in 2 of the 21 patients with type I labyrinthine fistulas.

Comparisons of pre- and postoperative examinations

Pre- and postoperative hearing comparisons

Preoperative hearing comparisons

Bone conduction (BC) and air conduction (AC) thresholds were measured at frequencies of 250, 500, 1000, 2000, 4000, and 8000 Hz in the pure tone audiogram.

The average preoperative BC in patients with type I labyrinthine fistulas in groups 1 and 2 were 32.33 ± 0.48dB and 33.25 ± 0.72dB ($t = 0.419$, $P \geq 0.05$) (Table 2).

The average preoperative BC in patients with type II labyrinthine fistulas in groups 1 and 2 were 38.45 ± 0.35dB and 37.75 ± 0.35dB, ($t = 0.207$, $P \geq 0.05$) (Table 3).

The average preoperative differences in air-bone (A-B) gap of patients with type I labyrinthine fistulas in groups 1 and 2 were 27.45 ± 0.72dB and 28.50 ± 0.45dB ($t = 0.341$, $P \geq 0.05$) (Table 4).

The average preoperative differences in A-B gap of patients with type II labyrinthine fistulas in groups 1 and 2 were 37.75 ± 0.24dB and 38.33 ± 0.35dB ($t = 0.576$, $P \geq 0.05$) (Table 5).

The average preoperative A-B gap of patients with type I and type II labyrinthine fistulas was not significantly different between groups 1 and 2.

Postoperative hearing comparison

In patients with type I labyrinthine fistulas, the average postoperative A-B gap of group 1 was not significantly different from that of group 2 (17.04 ± 0.65dB and 16.54 ± 0.38dB, $t = 0.421$, $P \geq 0.05$) (Table 6).

The average A-B gap of patients with type I labyrinthine fistulas was not significantly different between groups 1 and 2.

The average postoperative A-B gap of patients with type II labyrinthine fistulas was significantly different between groups 1 and 2 (22.25 ± 1.59dB and 28.33 ± 1.10dB, respectively, $t = 3.772$, $P \leq 0.05$) (Table 7).

The average A-B gap of patients with type II labyrinthine fistulas was significantly different between groups 1 and 2.

Patients with type III fistulas showed extremely severe sensorineural deafness on the affected side preoperatively that did not significantly improve postoperatively.

Pre- and postoperative vestibular function examinations (caloric test, video head impulse test)

Caloric testing (at 30°C and 44°C) was performed in a completely dark room. The video head impulse test (vHIT) was performed while the patient sat on a chair and focused their eyes on a dot 1.5 m away on the opposite wall. After calibration, the examiner performed fast angular head movements in the planes of the semicircular canals (right horizontal–left horizontal, right superior–left posterior, and left superior–right posterior). This yielded the mean vestibular-oculo reflex (VOR) gains of all semicircular canals, calculated by the vHIT system as the ratio of the area under the curve of eye velocity to head velocity (from 60 ms before peak head acceleration to the last value of 0°/s as the head returns to rest). The diagnostic criteria for normal vestibular function are as follows: (1) caloric test: normal summation of caloric summed maximum slow-phase eye velocity (sMSPV) (°/s) is higher than 12°/s; (2) vHIT test: gain is normal when the VOR gain is between 0.8 and 1.2.

In patients with occasional preoperative vertigo, vestibular function was examined preoperatively, and at 1 week and 3 months postoperatively, and symptoms were followed up simultaneously.

Type I labyrinthine fistula patients

Type I patients in groups 1 and 2 showed no preoperative symptoms of vertigo.

Type II and III labyrinthine fistula patients

Group 1: Five of eight patients reported vertigo with attractors during outpatient treatment, whereas, Two of the five patients reported experiencing sudden vertigo preoperatively without an obvious cause. Postoperatively, eight of erght patients experienced vertigo with an attractor during outpatient treatment. A vestibular function examination (caloric test) was performed preoperatively in two of eight patients and the vestibular predominance of one of two patients was partial to the healthy side, whereas the vestibular function of the affected side was weak. The vestibular function of the other patient was normal. In addition, the vestibular function of the two patients did not change significantly at 1 week or 3 months postoperatively (Table 8).

Group 2: Eight of the twelve patients experienced preoperative episodes of sudden vertigo without obvious causes. Obvious symptoms of vertigo occurred during the first 1 weeks postoperatively. Symptoms resolved after drug treatment and vestibular rehabilitation training, even with attractors, during outpatient treatment. The patients' daily activity levels returned to normal, and no episodes of vertigo occurred during long-term follow-up.

Preoperative vestibular function examinations (caloric test) revealed that the vestibular predominance of six of eight patients was partial to the healthy side, whereas the vestibular function of the affected side was weakened. The vHIT test on the affected side was positive, the gain was reduced, compensatory saccade waves appeared, and vestibular function was normal. Vestibular function examinations performed at 1 week and 3 months postoperatively revealed that the affected side was weakened in all eight patients (Figure 4 and Table 9).

TABLE 2 The average preoperative BC in patients with type I labyrinthine fistulas in group 1 and 2.

Frequencies	0.25 KHz	0.5 KHz	1 KHz	2 KHz	4 KHz	8 KHz
Group1 (dB)	35.29 ± 0.56	35.37 ± 0.52	30.33 ± 0.47	25.33 ± 0.72	30.29 ± 0.38	37.37 ± 0.23
Group 2 (dB)	35.00 ± 1.20	30.50 ± 0.39	30.75 ± 0.55	30.50 ± 0.84	35.25 ± 0.46	37.50 ± 0.88

The average preoperative BC: group 1 (dB) 32.33 ± 0.48; group 2 (dB) 33.25 ± 0.72. $t = 0.419$, $P \geq 0.05$.

TABLE 3 The average preoperative BC in patients with type II labyrinthine fistulas in group 1 and 2.

Frequencies	0.25 KHz	0.5 KHz	1 KHz	2 KHz	4 KHz	8 KHz
Group 1 (dB)	40.66 ± 0.21	40.25 ± 0.10	40.55 ± 0.75	33.64 ± 0.62	35.25 ± 0.31	40.35 ± 0.11
Group 2 (dB)	40.51 ± 0.31	40.00 ± 0.11	40 ± 0.85	35.50 ± 0.52	35.50 ± 0.10	35.00 ± 0.21

The average preoperative BC: group 1 (dB) 38.45 ± 0.35; group 2 (dB) 37.75 ± 0.35. $t = 0.207$, $P \geq 0.05$.

TABLE 4 The average preoperative differences in A-B gap of patients with type I labyrinthine fistulas in groups 1 and 2.

Frequencies	0.25 KHz	0.5 KHz	1 KHz	2 KHz	4 KHz	8 KHz
Group 1 (dB)	30.55 ± 1.1	35.25 ± 0.91	20.66 ± 0.81	20.66 ± 0.51	22.33 ± 0.32	35.25 ± 0.67
Group 2 (dB)	35.25 ± 0.55	35.25 ± 0.67	20.65 ± 0.25	20.55 ± 0.45	24.05 ± 0.13	35.25 ± 0.65

The average preoperative differences in A-B gap: group 1 (dB) 27.45 ± 0.72; group 2 (dB) 28.50 ± 0.45. $t = 0.341$, $P \geq 0.05$.

TABLE 5 The average preoperative differences in A-B gap of patients with type II labyrinthine fistulas in groups 1 and 2.

Frequencies	0.25 KHz	0.5 KHz	1 KHz	2 KHz	4 KHz	8 KHz
Group 1 (dB)	40.50 ± 0.11	40.50 ± 0.21	30.25 ± 0.35	35.75 ± 0.55	35.5 ± 0.10	44.00 ± 0.12
Group 2 (dB)	40.29 ± 0.41	40.37 ± 0.32	35.33 ± 0.21	35.33 ± 0.55	35.29 ± 0.51	43.37 ± 0.10

The average preoperative differences in A-B gap: group 1 (dB) 37.75 ± 0.24; group 2 (dB) 38.33 ± 0.35. $t = 0.576$, $P \geq 0.05$.

TABLE 6 The average postoperative differences in A-B gap of patients with type I labyrinthine fistulas in group 1 and group 2.

Frequencies	0.25 KHz	0.5 KHz	1 KHz	2 KHz	4 KHz	8 KHz
Group 1 (dB)	15.25 ± 0.78	15.33 ± 0.55	15.75 ± 0.25	15.33 ± 0.97	20.29 ± 0.25	20.29 ± 1.1
Group 2 (dB)	15.25 ± 0.41	15.75 ± 0.21	14.75 ± 0.32	14.66 ± 0.75	18.83 ± 0.11	20 ± 0.48

The average postoperative differences in A-B gap: group 1 (dB) 17.04 ± 0.65; group 2 (dB) 16.54 ± 0.38. $t = 0.421$, $P \geq 0.05$.

TABLE 7 The average postoperative differences in A-B gap of patients with type II labyrinthine fistulas in group 1 and group 2.

Frequencies	0.25 KHz	0.5 KHz	1 KHz	2 KHz	4 KHz	8 KHz
Group 1 (dB)	15.75 ± 3.2	20.50 ± 1.10	20.50 ± 2.50	20.75 ± 0.90	20.25 ± 1.21	35.75 ± 0.63
Group 2 (dB)	25.29 ± 2.50	25.29 ± 0.87	20.37 ± 1.20	25.33 ± 0.75	35.33 ± 0.2	38.37 ± 1.50

The average postoperative differences in A-B gap: group 1 (dB) 22.25 ± 1.59; group 2 (dB) 28.33 ± 1.10. $t = 3.772$, $P \leq 0.05$.

TABLE 8 Pre- and postoperative vestibular function examinations of type II labyrinthine fistula patients in group 1.

	1	2
Pre-operative caloric sMSPV (°/s)	26	9
1 week postoperative caloric sMSPV (°/s)	25	10
3 months postoperative caloric sMSPV (°/s)	27	12

One patient with a type III labyrinthine fistula experienced dizziness for 4 years. Six months preoperatively, the vertigo worsened with occasional gait instability. Preoperative vestibular function examination (caloric test) revealed weakened vestibular function of the affected side and horizontal semicircular canal paresis, caloric sMSPV (°/s):

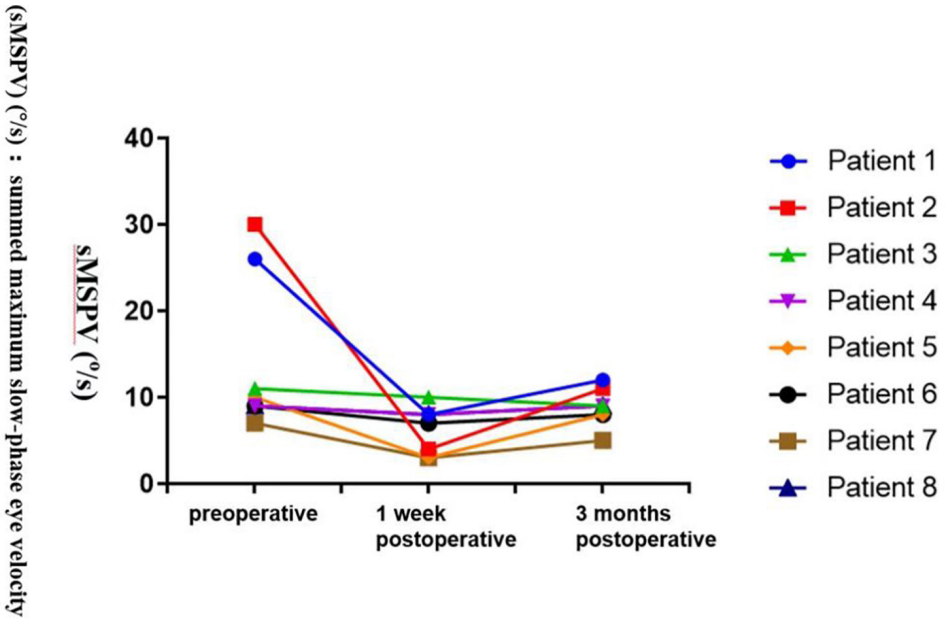

FIGURE 4
Caloric test results [summed maximum slow phase velocity of the eye, caloric sMSPV (°/s)] of the operated side of 8 patients with vertigo in group 2 before and after surgical plugging of external semicircular canal. Each patient is color coded. Vestibular function examinations performed at 1 week and 3 months postoperatively revealed that the affected side was weakened in all eight patients. The vestibular function of the patient was the worst one week after the operation, and gradually recovered in the later period, but it was not normal.

TABLE 9 Pre- and postoperative vestibular function examinations of type II labyrinthine fistula patients in group 2.

	1	2	3	4	5	6	7	8
Preoperative ESCCVOR gain	0.85	1.0	0.35	0.42	0.51	0.36	0.30	0.56
1 weekpostoperative ESCC VOR gain	0.30	0.51	0.2	0.31	0.26	0.12	0.12	0.40
3 months postoperative LSCC VOR gain	0.56	0.62	0.33	0.40	0.46	0.39	0.29	0.50
Preoperative PSCCVOR gain	0.84	0.88	0.44	0.39	0.54	0.68	0.69	0.50
1 weekpostoperative PSCC VOR gain	0.87	0.78	0.30	0.5	0.55	0.58	0.70	0.49
3 months postoperative PSCC VOR gain	0.82	0.86	0.38	0.42	0.56	0.70	0.82	0.45
Preoperative ASCCVOR gain	0.83	0.84	0.57	0.68	0.50	0.68	0.54	0.67
1 weekpostoperative ASCC VOR gain	0.78	0.90	0.42	0.60	0.43	0.32	0.40	0.70
3 months postoperative ASCC VOR gain	0.85	0.87	0.50	0.56	0.58	0.70	0.36	0.70
Preoperative caloric sMSPV (°/s)	26	30	11	9	10	9	7	9
1 weekpostoperative caloric sMSPV (°/s)	8	4	10	8	3	7	3	8
3 months postoperative caloric sMSPV (°/s)	12	11	9	9	8	8	5	9

2, vHIT: The test on the affected side was positive, ESCC VOR gine was 0.35. Although the unstable gait and vertigo persisted, they gradually disappeared after the vestibular rehabilitation training after surgery. The vestibular function (caloric test) of the affected side was eased at 3 months compared to one week after surgery, caloric sMSPV (°/s): 4,vHIT: The test on the affected side was positive, ESCC VOR gine was 0.59.

Imaging examinations: Pre- versus postoperative

Pre- and postoperative imaging examinations of patients with type I fistulas in the group 2 are shown in Figure 5.

Comparisons of preoperative and postoperative imaging examinations of patients in group 2 with type II fistulas are shown in Figure 6.

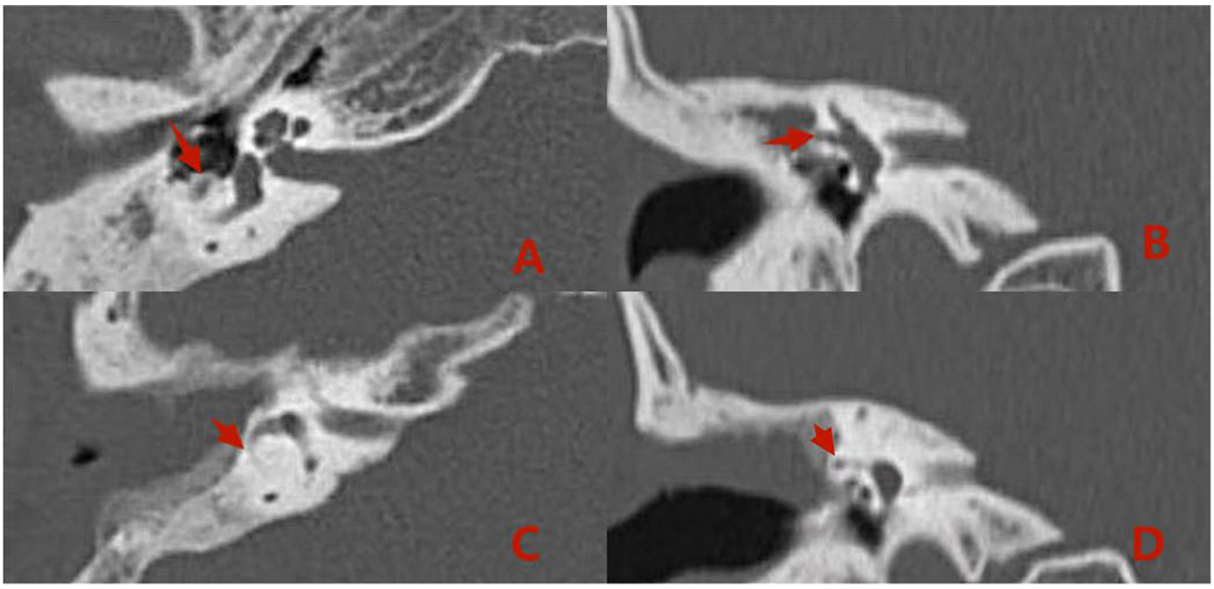

FIGURE 5
Computed tomography (CT) images acquired **(A,B)** preoperatively from a patient with type I labyrinthine fistula. Preoperative **(A,B)**: The right cholesteatoma is adjacent to bone resorption, the boundary with the external semicircular canal is unclear, and the shape of the external semicircular canal is acceptable (the red arrows). Postoperative **(C,D)**: The cholesteatoma has been removed, the shape of the lateral semicircular canal is acceptable, and intraoperative fillers are applied to fill the external semicircular canal (the red arrows).

Comparisons of preoperative and postoperative imaging findings in group 2 patients with type III fistulas are shown in Figure 7.

Discussion

Labyrinthine fistulas are a common complication of middle ear cholesteatoma. Typically, treatment is difficult and several related factors influence the postoperative effects. For example, the rate of preoperative vertigo, degree of damage to the external semicircular canal, preoperative hearing, and vestibular function affect repeat operations and recovery of postoperative ear symptoms. Management of labyrinthine fistulas secondary to middle ear cholesteatoma remains controversial. Two methods have been described in the literature. One method advocates leaving the cholesteatoma epithelium to temporarily cover the fistula to avoid inducing further damage to the labyrinthine structure, as the opening of the labyrinth might further damage cochlear function. Another technique advocates the complete removal of cholesteatoma in the fistula area and sealing through the bone or cartilage, as residual cholesteatoma can progress with further bone resorption and destruction, causing further hearing loss; however, there is also a risk of intracranial complications (Djalilian et al., 2021). This study applied Dornhoffer and Milewski (1995) fistula classification and reviewed follow-ups of patients previously treated for labyrinthine fistulas caused by middle ear cholesteatoma to determine the ideal surgical treatment.

Analysis of postoperative vertigo symptoms and vestibular function

Postoperative follow-up revealed that patients with type I or II labyrinthine fistulas in group 1 experienced vertigo after exposure to attractive stimulation. The researchers suspected that this was due to a lack of cortical bone protection for the labyrinthine fistulas after surgery. Patients with type I labyrinthine fistulas in group 2 had no symptoms of vertigo because the surface of the labyrinthine fistula had been capped intraoperatively with a "sandwich" of fascia, bone meal, and fascia.

In patients with type II labyrinthine fistulas that were plugged with fascia, bone meal, and bone wax, obvious vestibular symptoms occurred 1 week postoperatively due to intraoperative stimulation of the semicircular canal. In those cases, we observed a significant decrease in the patient's vestibular functions 1 week after the operation due to provision of postoperative anti-vertigo drug therapy that was intended to effectively alleviate postoperative vestibular symptoms. Subsequently, no vertigo occurred during the long-term follow-up.

The follow-up of vestibular symptoms in type III patients showed that the vestibular symptoms persisted after the surgery,

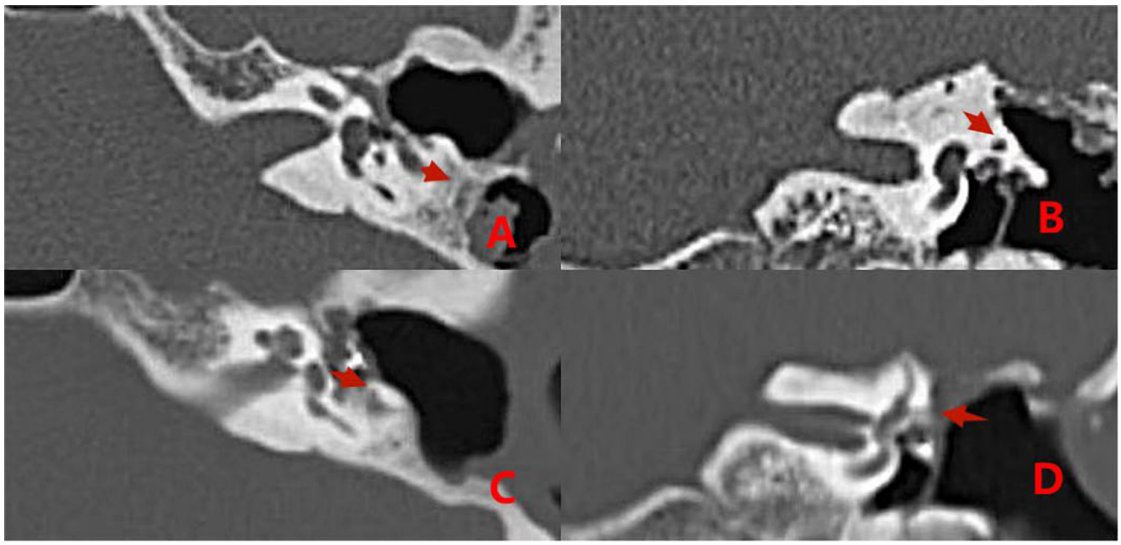

FIGURE 6
CT images acquired before and after surgery from a patient with type II labyrinthine fistula undergoing a second surgery. Preoperative **(A,B)**: The left cholesteatoma is adjacent to the bone resorption with a normal external semicircular canal shape (the red arrows). Postoperative **(C,D)**: The removal of cholesteatoma, the abnormal shape of the external semicircular canal, and the intraoperative fillers inside and adjacent to it (the red arrows).

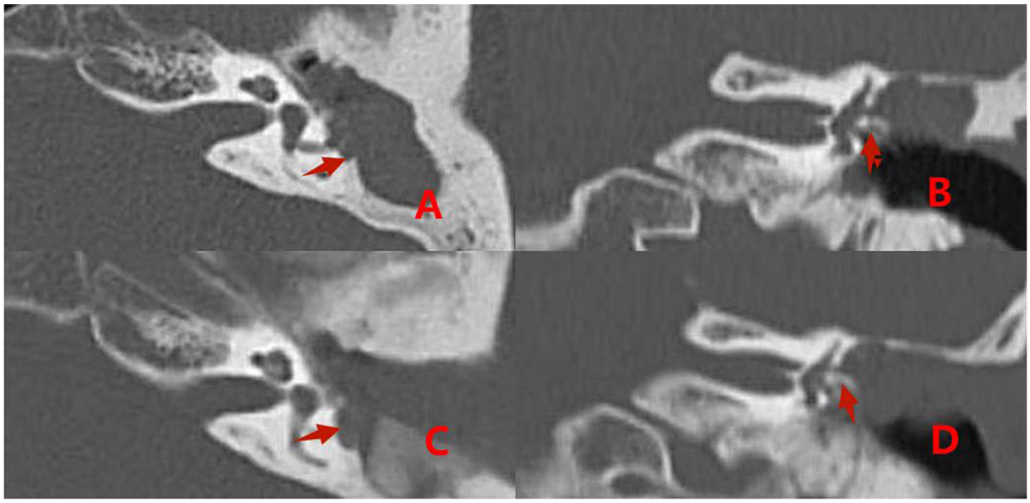

FIGURE 7
Pre- and postoperative CT images acquired from a patient with a type III labyrinthine fistula. Preoperative **(A,B)**: The left cholesteatoma is adjacent to the bone destruction (the red arrows). Postoperative **(C,D)**: The removal of the cholesteatoma, the abnormal shape of the external semicircular canal, and intraoperative fillers inside and adjacent to it (the red arrows).

and they were relieved by drugs and vestibular rehabilitation training. No cases of vertigo occurred during the long-term follow-up.

Similar to results from previous studies, plugging of a semicircular canal could affect both vestibular function and hearing. After the initial deterioration, most patients recovered during the follow-up period. However, vestibular function loss can persist (Geerse et al., 2017; Misale et al., 2019).

Analysis of postoperative hearing changes

The preoperative BC did not differ significantly between groups 1 and 2.

The average A-B gap did not differ significantly between groups 1 and 2. Specifically, in patients with type I labyrinthine fistulas, the removal of cholesteatoma on the labyrinthine

surface of the fistula and the "sandwich" capping of two layers of fascia and bone meal did not affect the postoperative hearing improvement.

We found a significant difference in the average A-B gap between groups 1 and 2 due to the destruction of the membrane labyrinth caused by plugging the semicircular canal with fascia and bone meal during the operation of type II labyrinthine fistulas. This approach influenced postoperative hearing improvement. However, postoperative patient hearing was still superior to preoperative hearing.

Patients with type III fistulas showed extremely severe sensorineural deafness preoperatively with no significant postoperative changes.

Similar to previous studies, we found that hearing loss could persist after surgery (Jiang et al., 2022; Kontorinis and Thachil, 2022; Stultiens et al., 2022).

Importance of complete intraoperative cholesteatoma removal

Complete cholesteatoma removal is the main purpose of surgery in patients with middle ear cholesteatomas. In particular, cholesteatoma scurf on the fistula surface requires complete removal to prevent postoperative recurrence or further spread of the inner ear infection. Previous studies (Wiatr et al., 2015; Bo et al., 2016; Rah et al., 2018) showed no significant effects on the preservation of BC hearing in the three types of labyrinthine fistulas; thus, removal of the cholesteatoma matrix had no significant effect on postoperative BC hearing in patients with middle ear cholesteatoma accompanied by labyrinthine fistulas. The follow-up of patients with labyrinthine fistulas in the present study showed that the use of appropriate surgical methods could preserve partial hearing in patients who underwent complete cholesteatoma removal. In patients with type I labyrinthine fistulas, the endosteum was not destroyed by the cholesteatoma; therefore, after removal of the epithelium of cholesteatoma on the surface of the labyrinthine fistula, the surface was capped by the "sandwich" method and the hearing was reconstructed simultaneously. In patients with type II labyrinthine fistulas, due to bone labyrinth destruction, we operated cautiously and simultaneously plugged the semicircular canal with a "pie" when removing the cholesteatoma epithelium. In this study, after the reconstruction, postoperative hearing was affected by operation of the semicircular canal. However, hearing examinations showed that postoperative patient hearing was still superior to preoperative hearing. Consequently, the researchers chose surgery involving complete cholesteatoma removal for middle ear cholesteatoma patients with labyrinthine fistulas.

Significance of pre- and postoperative hormone use

In this study, the surgeon used the "under water" surgical method after clearing the cholesteatoma (Yamauchi et al., 2014; Hassannia et al., 2019; Creighton et al., 2021; Thangavelu et al., 2022). Specifically, before operating on the labyrinthine fistula, the researchers injected dexamethasone into the operation area. The epithelium of the cholesteatoma on the surface of the labyrinthine fistula was cleaned, and the corresponding semicircular canal operation was performed according to the labyrinthine fistula classification. This approach provided the following two advantages: protecting the inner ear from accidental gas interference at the liquid level, and preventing accidental perilymph inhalation and membrane labyrinth destruction (Zhang et al., 2021; Kawamura et al., 2022). Postoperatively, intravenous corticosteroids were continued to stabilize inner ear function and relieve possible symptoms of vertigo.

Conclusion

Our analysis of the various management methods for semicircular canals in patients with different labyrinthine fistulas caused by middle ear cholesteatoma led to the following conclusions:

In patients with type I labyrinthine fistulas, the surface of the fistula should be capped with a "sandwich" composed of fascia, bone meal, and fascia. Our results showed that hearing improved postoperatively, and no vertigo occurred during the long-term follow-up.

In patients with type II and III labyrinthine fistulas, the fistulas should be plugged with a "pie" composed of fascia, bone meal, and fascia and then covered with bone wax. The semicircular canal occlusion influenced postoperative hearing improvement. However, postoperative patient hearing was still superior to preoperative hearing. No vertigo episodes occurred during long-term follow-up.

Data availability statement

The original contributions presented in this study are included in the article/supplementary material, further inquiries can be directed to the corresponding author.

Ethics statement

The studies involving human participants were reviewed and approved by Ethics Committee of Nanjing Tongren

Hospital. The patients/participants provided their written informed consent to participate in this study. Written informed consent was obtained from the individual(s) for the publication of any potentially identifiable images or data included in this article.

Author contributions

WM and MC: writing—original draft preparation. YG, HJ, and YW: methodology and data curation. CS and GL: find the relevant knowledge. YC, HN, and MY: provide the clinical data. SH: writing—review and editing. All authors contributed to the article and approved the submitted version.

Funding

This work was supported by the grants from National Natural Science Foundation of China (No. 82171153), the Natural Science Foundation of Jiangsu Province (No. BK20211012), and Nanjing Medical Science and Technique Development Foundation (No. QRX17033).

Conflict of interest

The authors declare that the research was conducted in the absence of any commercial or financial relationships that could be construed as a potential conflict of interest.

Publisher's note

All claims expressed in this article are solely those of the authors and do not necessarily represent those of their affiliated organizations, or those of the publisher, the editors and the reviewers. Any product that may be evaluated in this article, or claim that may be made by its manufacturer, is not guaranteed or endorsed by the publisher.

References

Bo, Y., Yang, Y., Xiaodong, C., Xi, W., Keyong, T., Yu, Z., et al. (2016). A retrospective study on post-operative hearing of middle ear cholesteatoma patients with labyrinthine fistula. *Acta Otolaryngol.* 136, 8–11. doi: 10.3109/00016489.2015.1087650

Creighton, F. X. Jr., Zhang, L., Ward, B., and Carey, J. P. (2021). Hearing outcomes for an underwater endoscopic technique for transmastoid repair of superior semicircular canal dehiscence. *Otol. Neurotol.* 42, e1691–e1697. doi: 10.1097/mao.0000000000003238

Djalilian, H., Borrelli, M., and Desales, A. (2021). Cholesteatoma causing a horizontal semicircular canal fistula. *Ear Nose Throat J.* 100, 888s–891s. doi: 10.1177/01455613211040580

Dornhoffer, J. L., and Milewski, C. (1995). Management of the open labyrinth. *Otolaryngol. Head Neck Surg.* 112, 410–414. doi: 10.1016/s0194-5998(95)70275-x

Geerse, S., de Wolf, M. J. F., Ebbens, F. A., and van Spronsen, E. (2017). Management of labyrinthine fistula: Hearing preservation versus prevention of residual disease. *Eur. Arch. Otorhinolaryngol.* 274, 3605–3612. doi: 10.1007/s00405-017-4697-2

Hassannia, F., Douglas-Jones, P., and Rutka, J. A. (2019). Gauging the effectiveness of canal occlusion surgery: How I do it. *J. Laryngol. Otol.* 133, 1012–1016. doi: 10.1017/s0022215119002032

Jiang, Y., Xu, M., Yao, Q., Li, Z., Wu, Y., Chen, Z., et al. (2022). Changes of vestibular symptoms in menière's disease after triple semicircular canal occlusion: A long-term follow-up study. *Front. Neurol.* 13:797699. doi: 10.3389/fneur.2022.797699

Kawamura, Y., Yamauchi, D., Kobayashi, T., Ikeda, R., Kawase, T., and Katori, Y. (2022). Hearing outcomes of transmastoid plugging for superior canal dehiscence syndrome by underwater endoscopic surgery: With special reference to transient bone conduction increase in early postoperative period. *Otol. Neurotol.* 43, 368–375. doi: 10.1097/mao.0000000000003461

Kontorinis, G., and Thachil, G. (2022). Triple semicircular canal occlusion: A surgical perspective with short- and long-term outcomes. *J. Laryngol. Otol.* 136, 125–128. doi: 10.1017/S002221512100387X

Kwok, P., Gleich, O., Spruss, T., and Strutz, J. (2019). Different materials for plugging a dehiscent superior semicircular canal: A comparative histologic study using a gerbil model. *Otol. Neurotol.* 40, e532–e541. doi: 10.1097/mao.0000000000002205

Lim, J., Gangal, A., and Gluth, M. B. (2017). Surgery for cholesteatomatous labyrinthine fistula. *Ann. Otol. Rhinol. Laryngol.* 126, 205–215. doi: 10.1177/0003489416683193

Mikulec, A. A., Poe, D. S., and McKenna, M. J. (2005). Operative management of superior semicircular canal dehiscence. *Laryngoscope* 115, 501–507. doi: 10.1097/01.mlg.0000157844.48036.e7

Misale, P., Lepcha, A., Chandrasekharan, R., and Manusrut, M. (2019). Labyrinthine fistulae in squamosal type of chronic otitis media: Therapeutic outcome. *Iran. J. Otorhinolaryngol.* 31, 167–172.

Nguyen, T., Lagman, C., Sheppard, J. P., Romiyo, P., Duong, C., Prashant, G. N., et al. (2018). Middle cranial fossa approach for the repair of superior semicircular canal dehiscence is associated with greater symptom resolution compared to transmastoid approach. *Acta Neurochir. (Wien)* 160, 1219–1224. doi: 10.1007/s00701-017-3346-2

Ossen, M. E., Stokroos, R., Kingma, H., van Tongeren, J., Van Rompaey, V., Temel, Y., et al. (2017). Heterogeneity in reported outcome measures after surgery in superior canal dehiscence syndrome-a systematic literature review. *Front. Neurol.* 8:347. doi: 10.3389/fneur.2017.00347

Quaranta, N., Liuzzi, C., Zizzi, S., Dicorato, A., and Quaranta, A. (2009). Surgical treatment of labyrinthine fistula in cholesteatoma surgery. *Otolaryngol. Head Neck Surg.* 140, 406–411. doi: 10.1016/j.otohns.2008.11.028

Rah, Y. C., Han, W. G., Joo, J. W., Nam, K. J., Rhee, J., Song, J. J., et al. (2018). One-stage complete resection of cholesteatoma with labyrinthine fistula: Hearing changes and clinical outcomes. *Ann. Otol. Rhinol. Laryngol.* 127, 241–248. doi: 10.1177/0003489418755407

Rosito, L. P. S., Canali, I., Teixeira, A., Silva, M. N., Selaimen, F., and Costa, S. S. D. (2019). Cholesteatoma labyrinthine fistula: Prevalence and impact. *Braz. J. Otorhinolaryngol.* 85, 222–227. doi: 10.1016/j.bjorl.2018.01.005

Stultiens, J. J. A., Guinand, N., Van Rompaey, V., érez Fornos, A. P., Kunst, H. P. M., Kingma, H., et al. (2022). The resilience of the inner ear-vestibular and audiometric impact of transmastoid semicircular canal plugging. *J. Neurol.* 269, 5229–5238. doi: 10.1007/s00415-021-10693-5

Thangavelu, K., Weiß, R., Mueller-Mazzotta, J., Schulze, M., Stuck, B. A., and Reimann, K. (2022). Post-operative hearing among patients with labyrinthine fistula as a complication of cholesteatoma using "under water technique".

Eur. Arch. Otorhinolaryngol. 279, 3355–3362. doi: 10.1007/s00405-021-07058-z

Wiatr, M., Składzień, J., Wiatr, A., Tomik, J., Strêk, P., and Medoń, D. (2015). Postoperative bone conduction threshold changes in patients operated on for chronic otitis media–analysis. *Otolaryngol. Pol.* 69, 1–6.

Yamauchi, D., Yamazaki, M., Ohta, J., Kadowaki, S., Nomura, K., Hidaka, H., et al. (2014). Closure technique for labyrinthine fistula by "underwater" endoscopic ear surgery. *Laryngoscope* 124, 2616–2618. doi: 10.1002/lary.24785

Zhang, Y., Cheng, Y., Chen, Z., Chen, F., and Zhang, Q. (2021). Case report: Preservation of otolithic function after triple semicircular canal occlusion in a patient with intractable ménière disease. *Front. Neurol.* 12:713275. doi: 10.3389/fneur.2021.713275

Ziylan, F., Kinaci, A., Beynon, A. J., and Kunst, H. P. (2017). A comparison of surgical treatments for superior semicircular canal dehiscence: A systematic review. *Otol. Neurotol.* 38, 1–10. doi: 10.1097/mao.0000000000001277

frontiers | Frontiers in Molecular Neuroscience

TYPE Original Research
PUBLISHED 28 November 2022
DOI 10.3389/fnmol.2022.1031278

OPEN ACCESS

EDITED BY
Yu Sun,
Huazhong University of Science and Technology, China

REVIEWED BY
Yilai Shu,
Fudan University,
China
Jun Yang,
Shanghai Jiaotong University School of Medicine, China
Dongdong Ren,
Fudan University,
China

*CORRESPONDENCE
Shusheng Gong
gongss@ccmu.edu.cn
Ke Liu
liuke@ccmu.edu.cn

†These authors have contributed equally to this work and share first authorship

SPECIALTY SECTION
This article was submitted to Methods and Model Organisms, a section of the journal Frontiers in Molecular Neuroscience

RECEIVED 29 August 2022
ACCEPTED 31 October 2022
PUBLISHED 28 November 2022

CITATION
Song X, Li Y, Guo R, Yu Q, Liu S, Teng Q, Chen Z-R, Xie J, Gong S and Liu K (2022) Cochlear resident macrophage mediates development of ribbon synapses *via* CX3CR1/CX3CL1 axis.
Front. Mol. Neurosci. 15:1031278.
doi: 10.3389/fnmol.2022.1031278

Cochlear resident macrophage mediates development of ribbon synapses *via* CX3CR1/CX3CL1 axis

Xinyu Song[1,2†], Yang Li[1,2†], Rui Guo[1,2], Qianru Yu[1,2], Shan Liu[1,2], Qi Teng[1,2], Zhong-Rui Chen[1,2], Jing Xie[1,2], Shusheng Gong[1,2*] and Ke Liu[1,2*]

[1]Department of Otolaryngology Head and Neck Surgery, Beijing Friendship Hospital, Capital Medical University, Beijing, China, [2]Clinical Center for Hearing Loss, Capital Medical University, Beijing, China

Cochlear ribbon synapses formed between spiral ganglion neurons and inner hair cells in postnatal mice must undergo significant morphological and functional development to reach auditory maturation. However, the mechanisms underlying cochlear ribbon synapse remodeling remain unclear. This study found that cochlear resident macrophages are essential for cochlear ribbon synapse development and maturation in mice *via* the CX3CR1/CX3CL1 axis. CX3CR1 expression (a macrophage surface-specific receptor) and macrophage count in the cochlea were significantly increased from postnatal day 7 then decreased from days 14 to 28. Seven-day treatment with CX3CR1 inhibitors and artificial upregulation of CX3CL1 levels in the inner ear environment using the semicircular canal injection technique were initiated on day 7, and this resulted in a significant increase in hearing threshold on day 28. Additionally, abnormalities in the morphology and number of cochlear ribbon synapses were detected on day P14, which may be associated with hearing impairment. In conclusion, macrophage regulation of cochlear ribbon synapse remodeling *via* the CX3CR1/CX3CL1 axis is required during hearing development and offers a new perspective on immune-related hearing loss throughout auditory development. Importantly, it could be a new treatment target for sensorineural hearing loss.

KEYWORDS

cochlear macrophage, ribbon synapses, CX3CR1/CX3CL1, development, hearing Loss

Introduction

The ribbon synapse of the inner hair cells is the first excitatory afferent synapse in the auditory pathway and is critical for sound encoding and transmission from the cochlea to the brain (Lu et al., 2016; Coate et al., 2019). The number of cochlear ribbon synapses continuously decreases after peaking at P7-P10. This process, known as synaptic pruning, involves axonal fine-tuning and contraction of immature spiral ganglion neurons terminals

(Yu et al., 2021). We previously found that autophagy may be necessary for the remodeling of ribbon synapses in cochlear inner hair cells (IHCs) before the onset of hearing. Autophagy serves as one of the primary mechanisms of hearing development and maturation in the postnatal cochlea. In this study, autophagy in IHCs was regulated by rapamycin and 3-methyladenine, autophagy activators and inhibitors, respectively. We found that normal hearing function could not be established in treated mice, coupled with immature ribbon synapses in cochlear IHC (Xiong et al., 2020). However, the mechanism is yet to be fully elucidated owing to the complexity of the molecular mechanism of ribbon synapse pruning and maturation.

Current research indicates that microglia, the resident macrophages of the brain, play a direct role in synaptic pruning in the central nervous system (CNS) (Kempf and Schwab, 2013; Brites and Fernandes, 2015; Kim et al., 2017). The role of microglia in the CNS has been extensively studied. In the adult brain, microglia interact with the neurons and synapses. (Favuzzi et al., 2021; Basilico et al., 2022) Microglia engulf and eliminate dying cells as part of their well-known phagocytosis, but it has also been demonstrated that they eliminate weakly active synapses. Several chemokine signaling pathways, especially the fractalkine (CX3CL1) signaling system, regulate these interactions (Korbecki et al., 2020; Pawelec et al., 2020). CX3CR1 is a leukocyte surface protein that is most abundant in monocytes and macrophages in various organs (Leonardi et al., 2018). CX3CL1 is secreted mainly by endothelial cells and neurons, and CX3CR1 is its specific receptor (Cormican and Griffin, 2021).

Macrophages and mononuclear phagocytes are major players in the cochlear innate immune system and are responsible for mediating pathogen detection and elimination, tissue homeostasis, and injury response (Hu et al., 2018). The immune defense function of cochlear macrophages in the inflammatory environment following various pathological injuries have been extensively studied. These injuries include auditory damage, ototoxicity, immune attack, and mechanical damage caused by cochlear implantation, which all cause an inflammatory response in the cochlea. The development of new genetic and functional analysis tools has revealed the presence of cochlear-resident immune cells. It was found that approximately 62% of cochlear resident macrophages are located in the neural tissue and approximately 36% are located at the edges of the spiral ligament and bone spiral plate. Macrophages are evenly distributed along a gradient from the apex to the base of the cochlea, with few aggregates or gaps in macrophage distribution. This spatial configuration ensures that each cell has an immune examination area and that all cochlear regions are under immune surveillance (Okano et al., 2008). However, the function of cochlea resident macrophages has not yet been clarified.

This study hypothesized that macrophages are involved in synaptic pruning *via* the CX3CL1-CX3CR1 axis. Phagocytosis of macrophages during synaptogenesis may be necessary for IHC synaptic remodeling in the cochlea before the onset of hearing. We found that the increasing and decreasing trends in the number of macrophages residing in the cochlea matched with the trends in synaptic pruning, with macrophages residing in the cochlea mainly clustered near the auditory nerve and ribbon synapses during the peak abundance of synapses. To control macrophage pruning in cochlear synapses, CX3CR1 receptor inhibitors were injected, and CX3CL1 levels were artificially increased in the inner ear environment. CX3CR1 inhibitor treatment increased the number of synapses remaining after cochlear synaptic pruning. In contrast, CX3CL1 upregulation reduced the number of synapses in the cochlea. Neither treatment resulted in normal hearing.

Materials and method

Animals

C57BL/6J pregnant mice were obtained from Beijing Vital River Laboratory Animal Technology Co. Ltd. 87 postnatal mice were included in this experiment. All animal experiments were approved by the Animal Ethics Committee of Capital Medical University and were performed strictly by the standards of the Animal Ethics Committee.

Drug administration

AZD8797 (MCE, KAND567), an inhibitor of CX3CR1, was dissolved in DMSO as a stock solution (10 mM/ml) and stored at-20°C. Before use, AZD8797 was diluted with Corn oil. Animals in each group received intraperitoneal injections of AZD8797 at a dose of 1 mM/kg daily from P7 to P14 consecutively, the controls were administered with the same amount of DMSO with Corn oil. CX3CL1 (peprotech, 300-31) was dissolved in pure water as a stock solution (1 mg/ml) and stored at −20°C. For P7 mice, 0.6ul of concentrated storage solution was diluted with water to 2 μl of working solution before injecting the drug into the semicircular canal.

Auditory brainstem response

Intraperitoneal injection of ketamine and xylazine (100 mg/kg of ketamine and 10 mg/kg of xylazine) was used to anesthetize the animals. A warming blanket was used to keep the body temperature at 37.5°C. Subdermally applied stainless steel needle electrodes were positioned posterior to the animal's stimulated and unstimulated ears (inverting input and ground) and above the vertex (noninverting input). The amplitude was detected at 90 dB SPL for each stimulus frequency during an ABR test using System 3 hardware and SigGen/BioSig software (TDT, United States). The threshold was determined by the lowest stimulus intensity that produced a repeatable ABR wave.

Immunofluorescence

The cochleae were extracted and fixed with 4% paraformaldehyde in phosphate-buffered saline (PBS) for 1 h before the audiological examinations. After that, the basilar membranes were meticulously cut apart. Samples were cleaned with PBS before being incubated at room temperature with 0.3% TritonX-100 for 30 min and 10% goat serum (ZSGB-BIO) for 1 h. The preparation were incubated overnight at 4°Cwith primary antibodies including: rat anti-F480 (1:50, Abcam, MAB386), rabbit anti-CX3CR1 (1:50, Santa, sc-377227),mouse anti-GluA2 (1:400, Millipore, MAB397), mouse anti-CtBP2 (1:500, Abcam, ab204663). The next day, samples were carefully washed three times with PBS for 10 min each and incubated with Alexa FluorTM 488, 568, or 647 (1:300) conjugated secondary antibodies for 2 h at room temperature, followed by three washes with PBS for 10 min each and mounted on a glass coverslip with DAPI (ZSGB-BIO, ZLI-9557).

Laser confocal microscopy

Images were scanned with a × 60 oil-immersion confocal microscope (TCS SP8 II; Leica, Wetzlar, Germany). All Scanning was performed from top to bottom with an interval of 0.5 μm/layer, and a series of z-stack images were acquired.

Quantification of the immunofluorescence signals

In order to calculate the average number of ribbon synapses for each IHC, the total numbers of GluA2- and CtBP2-stained puncta were added together and divided by the total number of IHC nuclei.

Quantitative analysis of macrophage morphology and distribution

The size and morphology of macrophages are determined by distinctive F4-80 expressions. Greater in size than other types of leukocytes and having uncommon shapes like dendritic, amoeboid-curved, or aberrant morphologies with protrusions. We employed a well-known specialized surface stain called F4-80 to positively stain the critical cells in order to determine their distribution. A subset of cochlear macrophages includes macrophages in the neural tissue, basement membrane macrophages (BM-macrophages), and extravascular lateral wall macrophages. Using bright-field illumination and a fluorescence microscope, each macrophage was distinguished as a subset of the cochlear macrophage population. The osseous spiral layer, the basal membrane, and the lateral wall of the vasculature can all be distinguished visually as parts of the cochlea. By counting the number of cells present in a sample of 0.1 mm^2 in each of the three anatomical cochlear turns (apical, middle, and basal) per specimen, distribution analyses for macrophages at neural tissue, basement membrane macrophages (BM-macrophages), and extravascular lateral wall were carried out. After computing the mean for these counts, an average value per unit area in each cochlea was generated. Cell counts per unit area across specimens for each group were averaged to obtain group means.

Western blot analysis

Hank's balanced salt solution was used to newly dissect the cochlea after it was quickly removed (Gibco, 1491037). The cochlea was homogenized in ice-cold RIPA lysis solution (G2002, Servicebio) with phosphatase inhibitor cocktails and RIPA lysis buffer base (G2007, Servicebio), After 30 min on ice, tissue fragments were separated by centrifugation at 12,000 *g* for 10 min at 4°C, with the supernatants being kept as the total protein fractions. The BCA Protein Assay Kit was used to measure the protein concentrations (G2026, Servicebio). For every sample, two cochleas from the same mouse were combined. Primary antibody concentrations were anti-CX3CR1 (1:500; Abcam, ab8020) and anti-GAPDH (1:1000; AF5009, Beyotime). Protein samples (10 ll) were separated using SDS-PAGE (G2003, Servicebio). The proteins were then transferred onto nitrocellulose after electrophoresis. The membrane that was blocked using a 5% nonfat dry milk solution in 0.5% TBST. The membranes were exposed to primary antibodies against CX3CR1 (1:500) or anti-GAPDH (1:1000) for overnight incubation at 4°C, followed by three TBST washes lasting 10 min each. Secondary antibodies were applied to the membranes and incubated for 1 h at a concentration of 1:6000. The membrane was thoroughly washed before the immunoreactive bands could be seen using ECL. Using AlphaEase FC software, X-ray films of Western blots were scanned and examined. Using the optical density ratio of the CX3CR1 band within the GAPDH bands, the relative expression rates of several samples were examined.

Result

Inner hair cells undergo synaptic pruning before auditory maturation

To determine the trends in the number of cochlear ribbons during synaptic pruning, presynaptic proteins were labeled with an anti-RIBEYE/CtBP2 antibody and postsynaptic proteins with an anti-GluA2 antibody. In the initial state (p1-p7) of ribbon synapse formation in the cochlea, the presynaptic dots were in the vicinity of the subnuclear or perinuclear region then gradually decreased to the basal level of the IHC cytoplasm at P14. Fewer presynaptic ribbons appeared at P1, and a higher number of presynaptic ribbons appeared around P7. The number of

presynaptic ribbons gradually decreased from P14, after which the number remained stable (Figures 1A,B). Additionally, postsynaptic proteins were expressed at P14.

Synaptic pruning is accompanied by a high degree of macrophage activation

To confirm the timing of the presence of cochlear resident macrophages, they were labeled with an anti-F4-80 antibody. The number of cochlear macrophages peaked at P7, were distributed near the cochlear basilar membrane and auditory nerve, and were clustered near the cochlear ribbon synapses of the inner hair cells. Macrophages were usually circular and amoeboid in shape at the newborn stage, which was associated with phagocytosis. As the cochlear ribbon synapse and auditory nerve developed and matured, the number of macrophages decreased from P14, and the distribution migrated from the basilar membrane to the lateral wall of the blood vessels and auditory nerve. The number of macrophages stabilized within a certain range (Figures 2A,B).

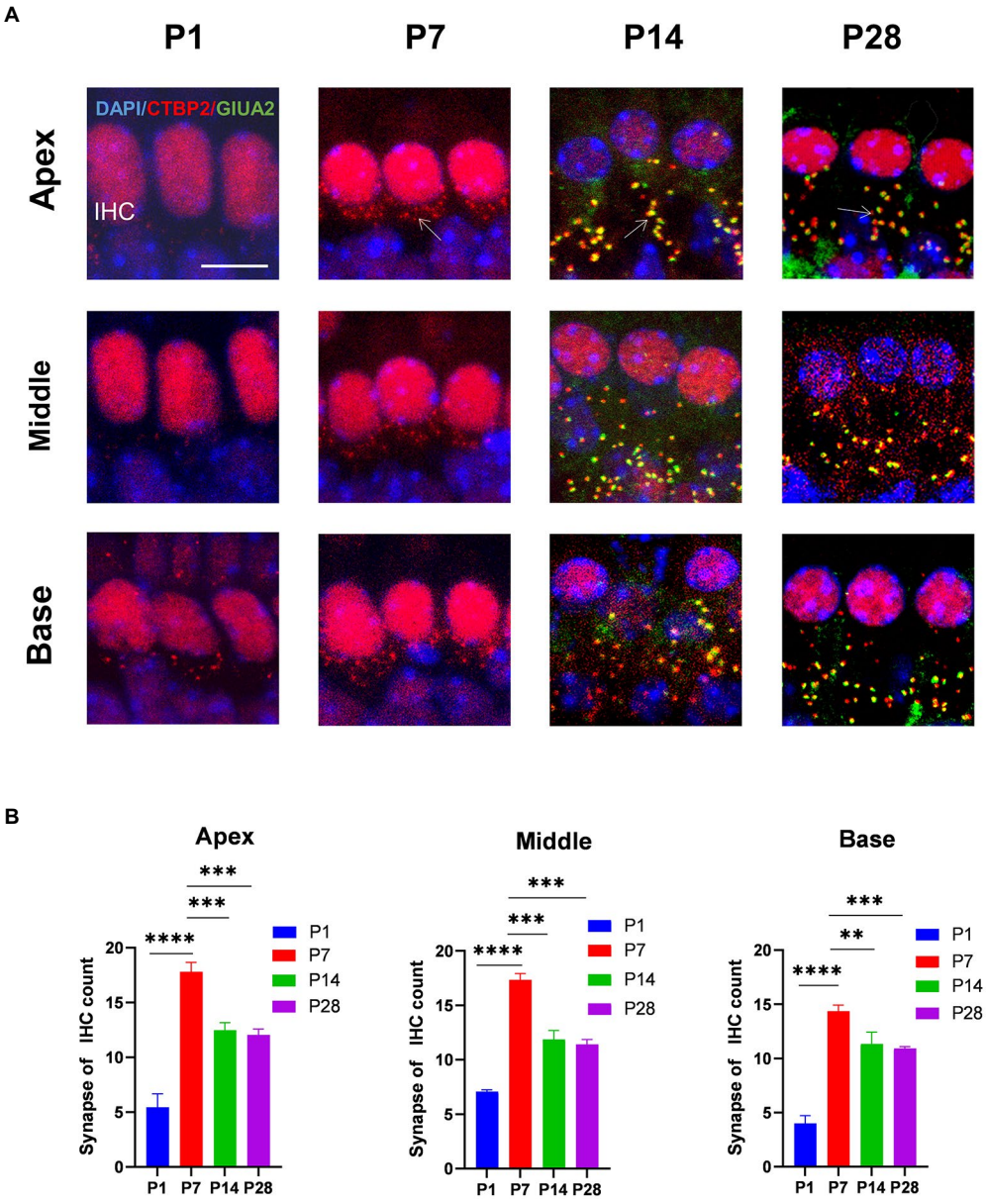

FIGURE 1
The number of synapses during postnatal mouse cochlear development is detected from P1 to P28. **(A)**: ctbp2 dots (red) and glua2 dots (green) on immunofluorescence staining show the dynamic changes in presynaptic and postsynaptic proteins on P1, P7, P14, and p28. Scale bar=5 μm, n=3. The image at the bottom is an enlarged image of macrophages. **(B)** The number of synapses per IHCs is increased from birth to P7 until P14, after which the number of synapses are stabilized. **p<0.01, ***p<0.001, ****p<0.0001.

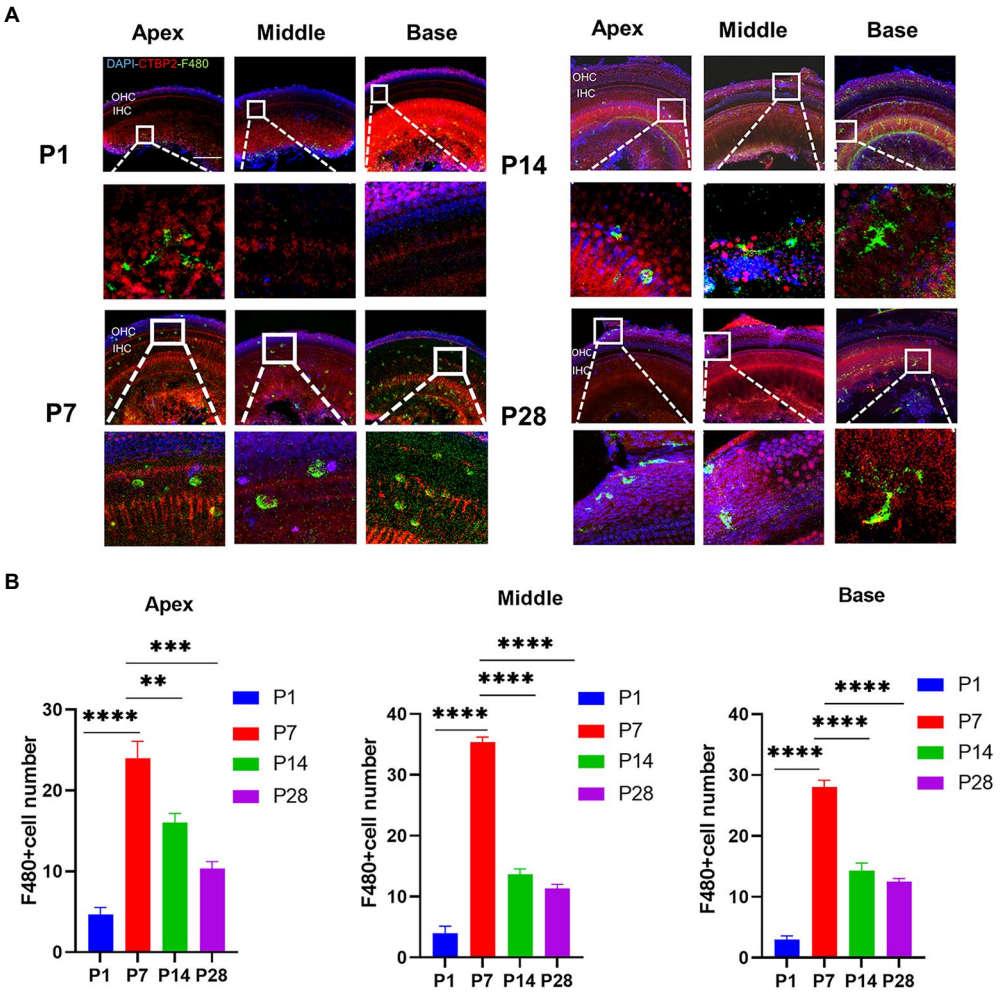

FIGURE 2
The number of macrophages during cochlear development in postnatal mice is detected from P1 to P28. **(A)** Immunofluorescence staining (green) is used to detect the dynamic changes in the number of macrophages on P1, P7, P14, and p28. Scale bar=50 μm, *n*=3. At P7, macrophages have a round shape, while they have a dendritic shape after P14. **(B)** The number of macrophages is increased from birth to P7 and then decreased until P14. ***p*<0.01, ****p*<0.001, *****p*<0.0001.

CX3CR1 plays a key role in the activation and recruitment of macrophages during the development

To investigate the key role of CX3CR1 in cochlear macrophage activation, migration, and phagocytosis, cochlear macrophages were labeled with anti-CX3CR1 and anti-F4-80 antibodies. The results showed that macrophages almost completely expressed CX3CR1 receptors at P7. Quantification of the double-positive cells showed that the number of CX3CR1+ and F4-80+ double-positive cells was markedly higher at P7 than that at other periods before hearing maturation (Figures 3A–G). This indicated that the trend of CX3CR1-positive macrophages was consistent with the trend of the number of synapses. Correspondingly, when whole cochlear tissue was used for quantitative western blotting analysis, CX3CR1 expression was also observed to be much higher at P7 than that at other periods before hearing development (Figures 4A,B). This suggested that CX3CR1 was highly expressed in activated and migratory active macrophages and was involved in the critical process of synaptic pruning.

Absence of CX3CR1 blocks synaptic pruning and increases the number of synapses

To determine whether CX3CR1 receptors play a key role in synaptic pruning before the maturation of cochlear IHC hearing function. The CX3CR1 inhibitor was injected continuously for 7 days since P7 (Figure 5A). At P14, mice injected with the CX3CR1 inhibitor showed decreased expression of CX3CR1 protein (Supplementary Figure 1). In addition, the treatment group showed a significant increase in pre-synaptic and post-synaptic signals in the apical, middle, and basal turns (Figure 5B).

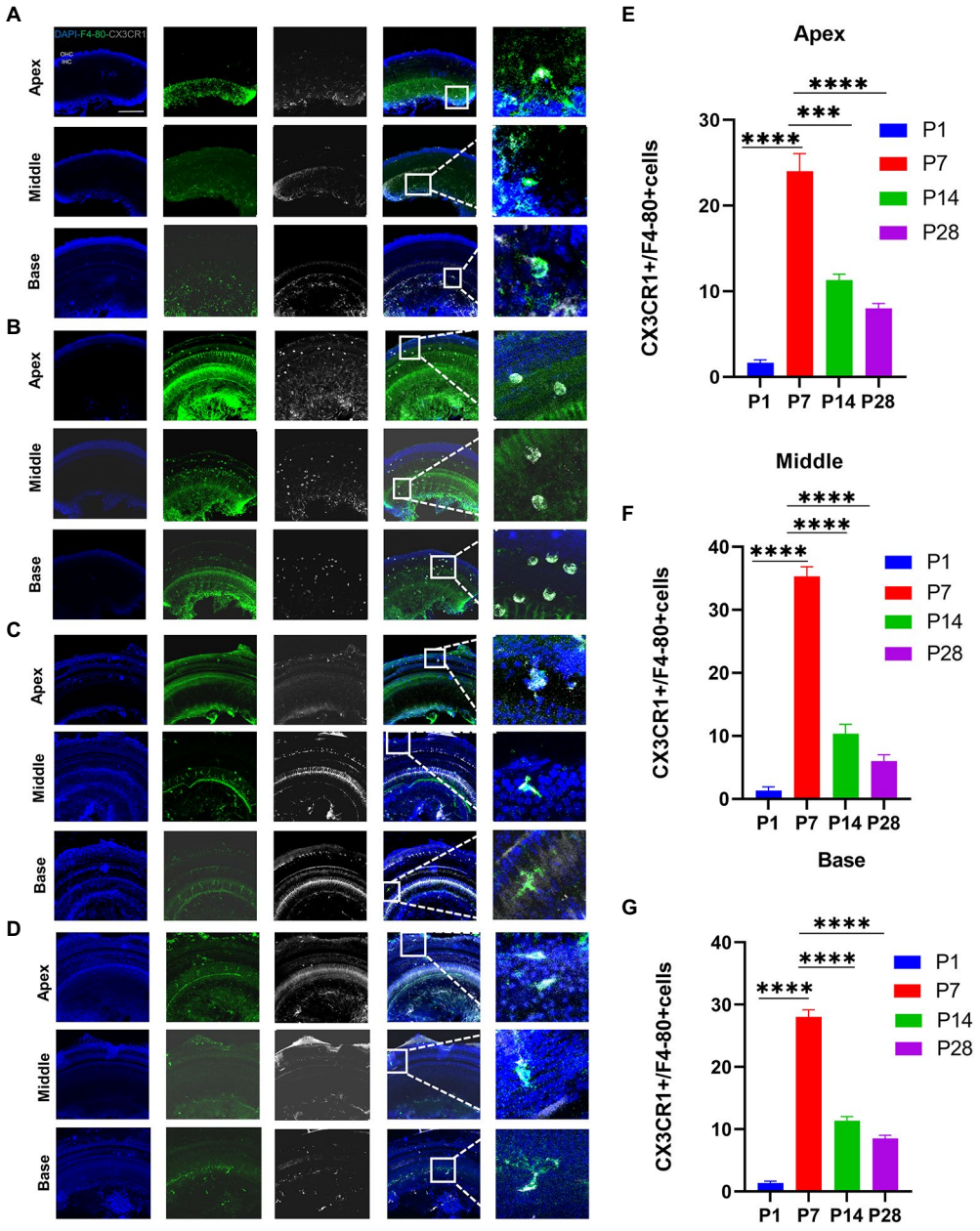

FIGURE 3
Detection of the number of CX3CR1+macrophages during cochlear development from P1 to P28 in postnatal mice. **(A)** Immunofluorescence staining is used to detect the number of CX3CR1+macrophages and identify the dynamic changes in the number of macrophages in P1. CX3CR1 (grey) colocalized with f4-80 (green). The nuclei are stained with DAPI. **(B)** Immunofluorescence staining is used to detect the number of CX3CR1+macrophages and identify the dynamic changes in the number of macrophages at P7. **(C)** Immunofluorescence staining is used to detect the number of CX3CR1+macrophages and identify the dynamic changes in the number of macrophages at P14. **(D)** Immunofluorescence staining is used to detect the number of CX3CR1+macrophages and identify the dynamic changes in the number of macrophages at P28. Scale bar=50 μm, *n*=3. The image on the right is an enlarged image on the left. **(E–G)** Quantitative analysis of the number of CX3CR1+macrophages from P1 to P28 showing that the number of CX3CR1+macrophages from the apical to the middle to the basal turn of the cochlea is significantly higher on P7 than on P1, P14, and P28. ***p*<0.01, ****p*<0.001, *****p*<0.0001.

These results showed that in resident macrophages in the cochlea, injection of the CX3CR1 receptor inhibitor led to a large amount of synaptic signal accumulation (Figure 5C). These findings showed that ribbon synaptic pruning and remodeling of cochlear IHC were impaired after deletion of CX3CR1 expression. Next, we investigated whether the inhibition of CX3CR1 expression could significantly affect the development and maturation of hearing. Auditory brainstem response (ABR) tests were performed in treated mice and control mice at 28 days postnatally. It was found that the ABR thresholds were significantly higher, the ABR

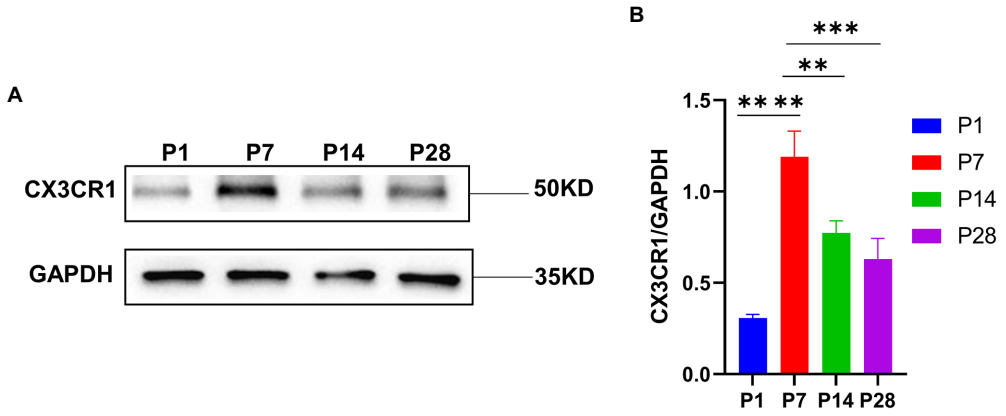

FIGURE 4
(A) CX3CR1 expression in the cochlea of postnatal mice is determined by western blotting. A significantly stronger band is identified around P7 than in P1, P14, and P28 (n=3). **(B)** Quantitative analysis of CX3CR1 expression from P1 to P28 showing that the ratio of CX3CR1 to GAPDH is significantly higher in P7 than in P1, P14, and P28. ****p<0.0001,**p=0.0019, ***p=0.0003. GAPDH is used as the loading control (n=3).

I-wave amplitude was decreased, and the ABR I-wave latency period was extended in the treatment group (Figures 5D–F). This suggested that the inhibition of CX3CR1 expression before hearing onset may severely affect the development of hearing and lead to hearing loss.

CX3CL1 upregulation promotes synaptic pruning

We investigated whether CX3CL1 upregulation in mice at 7 days postnatal interferes with the synaptic pruning function of cochlear resident macrophages. CX3CL1 is secreted by neurons and has an association with spiral neurons and macrophages. Macrophages were labeled in frozen sections, and on P28, macrophages were mainly distributed near the spiral ganglion and the lateral wall of the blood vessels in the cochlear sections of mice (Supplementary Figure 2). Thus, with respect to spatial effects, CX3CL1 secreted by spiral neurons is more likely to bind to receptors on the surface of cochlear-resident macrophages. We exogenously administered CX3CL1 to P7 mice by posterior semicircular canal surgery (Figure 6A). At P14, the number of sub-IHC band synapses was significantly lower in CX3CL1-treated mice than in control mice (Figures 6B,C). There was also no difference in the number of cochlear synapses at P14 between the treatment and control groups when pure water was introduced through the semicircular canal (Supplementary Figure 3). Overall, our results suggest that CX3CL1 upregulation enhanced synaptic pruning, resulting in a significant reduction in the number of synapses.

Next, it was investigated whether the exogenous administration of CX3CL1 could significantly affect the development and maturation of hearing. At P28, the ABR threshold was significantly higher, the ABR I-wave amplitude was decreased, and the ABR I-wave latency period was extended in the treatment group (Figures 6D–F). This suggested that CX3CL1 upregulation before hearing onset may severely affect hearing development and maturation, leading to hearing loss. The first week after birth is a critical period for auditory development in mice, and the most important feature of this period is synaptic remodeling, which occurs as synaptic pruning and refinement of redundant synapses, as demonstrated in our study. Within a month of birth, the modification of cochlear ribbon synapses is completed. In adult mice, synaptic pruning activity is reduced or absent, as shown by the maintenance of synaptic quantity at a steady level, which denotes the completion of auditory development.

Discussion

Wong et al. reported that in the initial state of ribbon synapse formation in the cochlea, the presynaptic dots around the subnuclear or perinuclear region are also replaced by a "floating" ribbon. By the second week of life, these presynaptic dots gradually descend to the basal level of the IHC cytoplasm, providing a plausible explanation for the majority of synaptic signals in the basal region of the IHC. Furthermore, the number of presynaptic signals peak 1 week postnatally and then decrease until they stabilize (Wong et al., 2014). Our study also confirmed the changes in cochlear ribbon synapse morphology and number before hearing maturation. Macrophages are one of the key elements of the intrinsic immune system in mature organs, and they primarily function as an immunological defense to keep the internal environment at homeostasis (Wynn and Vannella, 2016; Duan, 2018), and macrophages are resident immune cells in the cochlea (Liu et al., 2018; He et al., 2020). They play a continuous monitoring role in the homeostatic environment, thus helping maintain tissue homeostasis under pathological and physiological conditions (Ito et al., 2022).

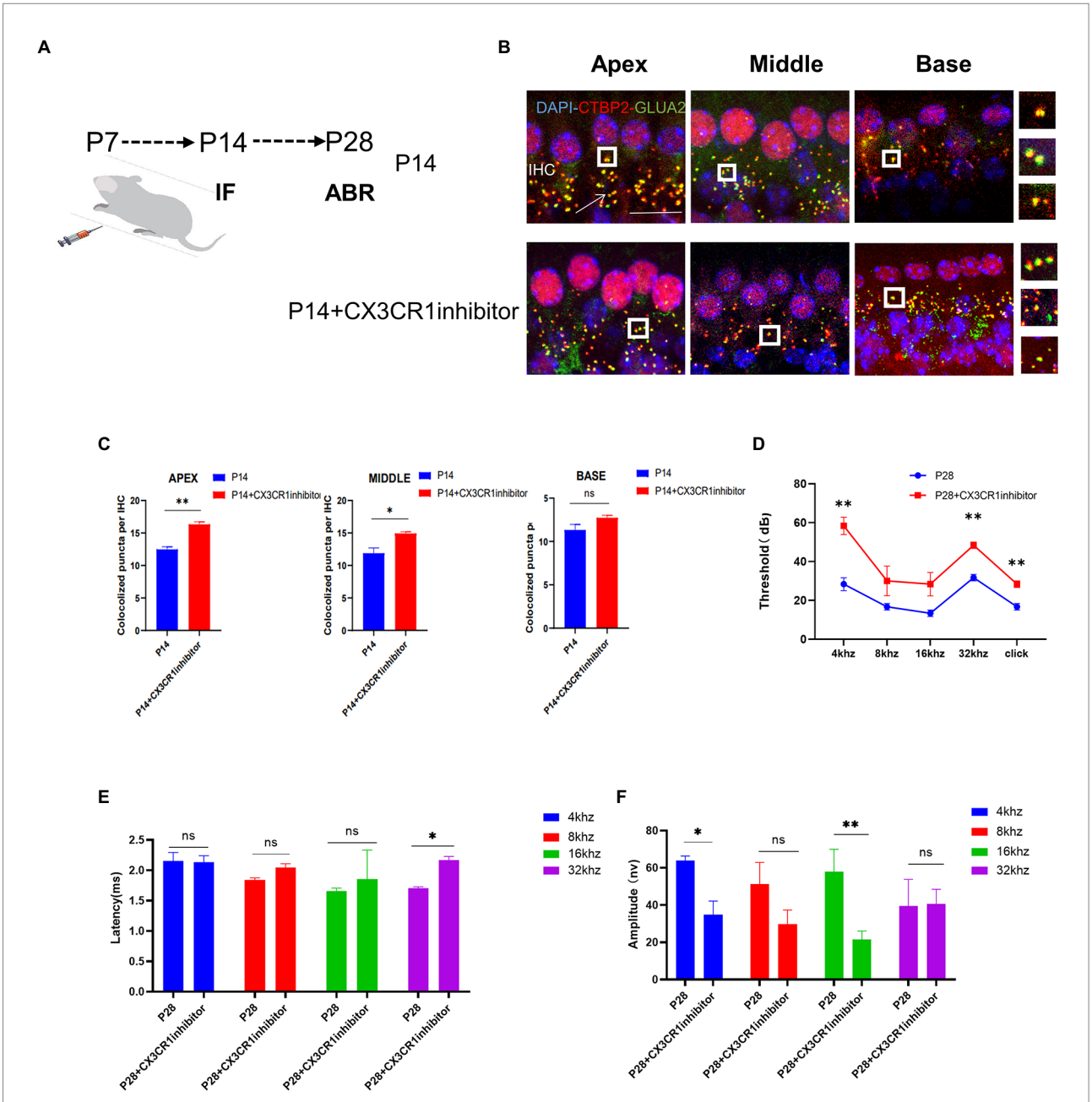

FIGURE 5
Inhibition of CX3CR1 activation in postnatal mice significantly impairs the morphological features of the ribbon synapses in cochlear IHC. **(A)** Mice were intraperitoneally injected with CX3CR1 inhibitor or normal saline daily starting from 7 days after birth. **(B)** Immunofluorescence staining of IHC ribbon synapses at P14 in each group. Presynaptic and postsynaptic proteins are co-stained; the nucleus is stained with DAPI. A magnified view of the synaptic sites is shown on the right. **(C)** Quantitative analysis showing that the number of synapses in the apex to the middle and bottom synapses in the cochlea is significantly higher in the CX3CR1 inhibitor-treated group than in the control group (*p<0.05, **p<0.01). Scale bar=10 μm, n=3. **(D–F)** Quantification of ABR threshold, amplitude, and latency of ABR wave I on P14 in control mice and CX3CR1 inhibitor mice. Significant increases in ABR thresholds at 4 and 32 kHz and click frequencies are detected in treated mice and controls. The latency of ABR wave I across frequencies (32 kHz) at P14 is longer in the treated mice than in controls. The amplitude of ABR wave I across frequencies (4 and 16 kHz) at P14 is lower in treated mice than in control mice (treatment group: n=4, control group: n=4; *p<0.05, **p<0.01).

Cochlear resident macrophages exhibit remarkable plasticity, allowing them to rapidly switch between active phenotypes and adapt to changing neuronal and environmental conditions. (Hough et al., 2022) In the CNS, microglia protruding as resident macrophages appear near presynaptic neurons, where they remain for about 5 min and then retract (Wake et al., 2009). A recent study (Tremblay et al., 2010) found specific attachments of microglia protrusions to presynaptic and postsynaptic regions in the visual cortex of young mice. In the current study, cochlear resident macrophages were heavily

10.3389/fnmol.2022.1031278

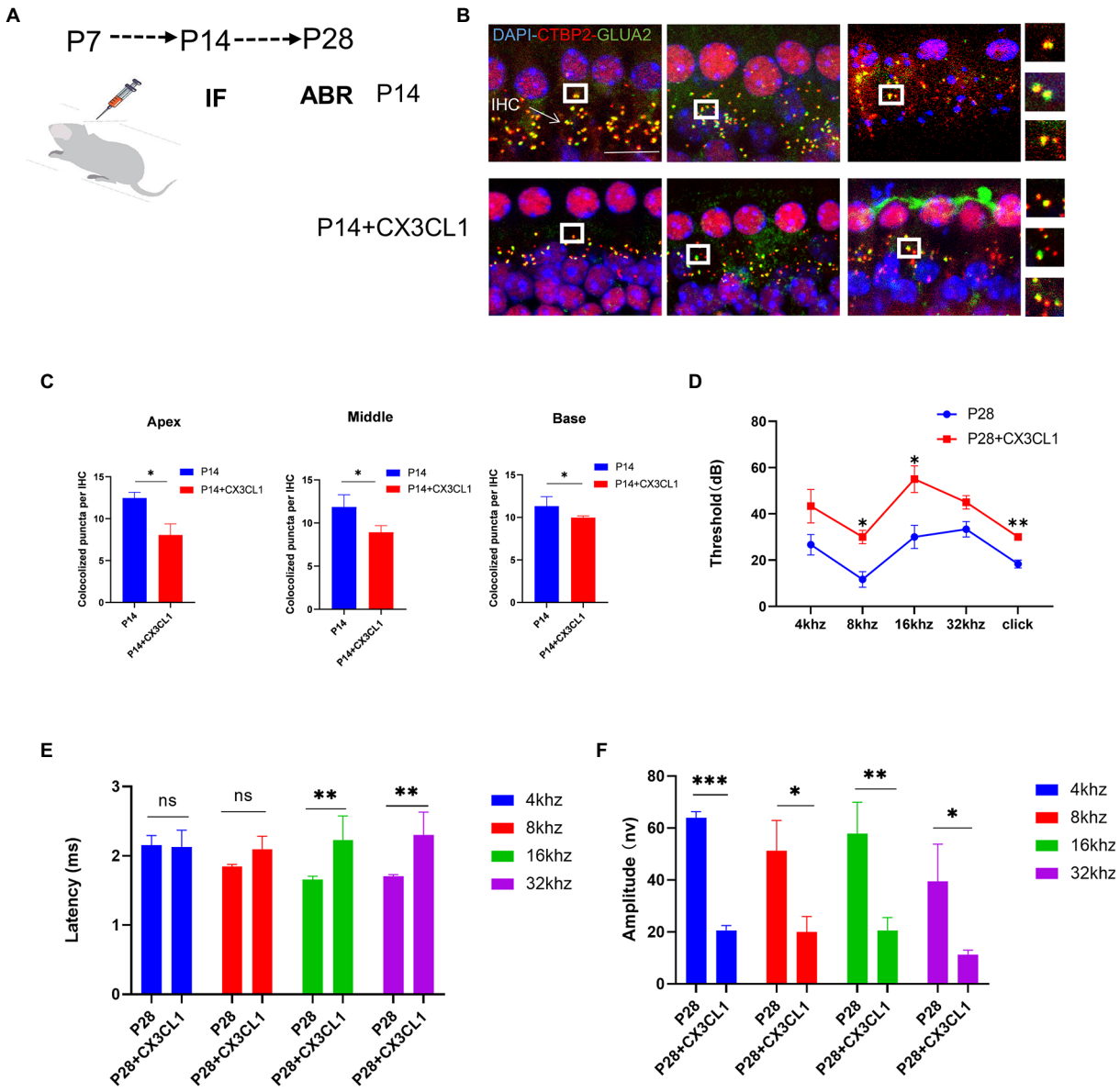

FIGURE 6
CX3CL1 overexpression in postnatal mice significantly impairs the morphological features of ribbon synapses in cochlear IHC. **(A)** CX3CL1 is injected into the semicircular canal of mice 7 days after birth **(B)**. IHC ribbon synapses in each group are subjected to immunofluorescence staining at P14. Presynaptic protein and postsynaptic protein are co-stained; the nucleus is stained with DAPI. The right side is the enlarged image of the synaptic point. **(C)** Quantitative analysis of synapse numbers showing that the number of synapses in the apex to the middle and bottom synapses in the cochlea is significantly higher in the CX3CL1 treatment group than in the control group (*p<0.05, **p<0.01). Scale bar=10 μm, n=3. **(D–F)** Quantification of ABR threshold, amplitude, and latency of ABR wave I in control mice and CX3CL1 mice on P14. Significant increases in ABR thresholds at 8 and 16 kHz and click frequencies are detected in both treated mice and control mice. The latency of ABR wave I across frequencies (16 and 32 kHz) at P14 is longer in treated mice than in control mice. The amplitude of ABR wave I across frequencies (4, 8, 16, and 32 kHz) at P14 is lower in treated mice than in control mice (treatment group: n=4, control group: n=4; *p<0.05, **p<0.01).

activated and highly migratory 1 week after birth, and they clustered near the inner hair cell ribbon synapses, making frequent but transient contacts with the synapses. The resident macrophages in the cochlea moved back to the region around the ganglion and spiral ligament once the ribbon synapse pruning activity was completed and the ribbon synapses and hearing matured. Additionally, the form changed from amoeboid-like to dendritic. This may be related to the potency of macrophage phagocytosis.

To our best knowledge, this study is the first to verify the role of the CX3CL1/CX3CR1 axis in regulating cochlear resident macrophages in synaptic remodeling and hearing maturation. Our findings are consistent with previous research that CX3CL1 is almost completely produced by neurons (Harry, 2013; Madrigal

et al., 2017) and that the CX3CR1 receptor is almost completely expressed on the surface of resident macrophages (Parkhurst et al., 2013). In general, it is thought that the binding of soluble CX3CL1 to its receptor CX3CR1 maintains microglia in a "quiescent" or "off" state (Boche et al., 2013), thus pruning and refining cochlear banded synapses at different stages of auditory development. In the CNS, fractalkine receptor-driven EGFP expression has emerged as a reliable marker for microglial recognition during development (Hsu et al., 2006; Meghraoui-Kheddar et al., 2020).

The synaptic density increases during development in animals lacking this receptor, indicating a deficiency in synaptic pruning. In addition to the chemokine receptor route, the classical activation pathway of complement cascade receptors also contributes to synaptic clearance by microglia (Hong et al., 2016). c1q is thought to be important in the developing nervous system by controlling synaptic pruning (Werneburg et al., 2020). These signals not only control synaptic remodeling in early neurodevelopment, but also play a crucial role in several neurological diseases. Thus, our findings confirm that mice lacking CX3CR1-expressing cochlear macrophages have an increased number of synapses with reduced synaptic pruning during development. CX3CL1, which is locally secreted, may be essential for synapse identification by macrophages and may play a role in macrophage migration to the brain or proliferation during development. The findings demonstrated that CX3CL1 upregulation promoted synaptic pruning and reduced synaptic density and can result in irreversible hearing loss in mice.

Conclusion

In conclusion, inhibition of CX3CR1 expression on the surface receptors of resident macrophages in the cochlea leads to impaired pruning and refinement of cochlear ribbon synapses, resulting in severe hearing loss, as confirmed in mice in the CX3CR1 inhibition group. Abnormal ABR test results were still observed at P28, providing further evidence that this hearing loss was long-lasting. CX3CL1 neuronal secretion similarly affected cochlear ribbon synapses and hearing function in adult mice. These findings provide evidence that prior to the start of hearing in postnatal mice, macrophages are involved in ribbon synapse remodeling *via* the CX3CL1/CX3CR1 axis, which is necessary for the development of hearing (Figure 7). Collectively, these findings demonstrate that macrophages play a key role in auditory development and maturation. This study suggests that developing ribbon synapses may be potential therapeutic targets for hearing protection in some forms of hearing impairment linked to cochlear macrophages (Bhuskute and Page, 2021; Noulaheu, 2021).

Data availability statement

The raw data supporting the conclusions of this article will be made available by the authors, without undue reservation.

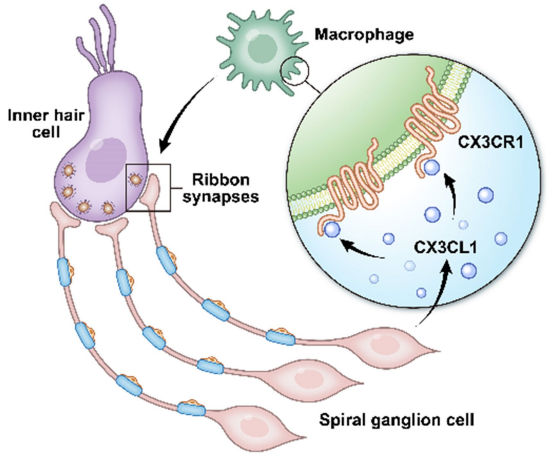

FIGURE 7
In the cochlea, inner hair cells convert mechanical vibrations into electrical signals *via* ribbon synapses at the base of cells to the auditory nerve, thereby allowing sound information to travel up the auditory pathway to the brain for processing. Cochlear spiral neurons secrete CX3CL1, which binds to CX3CR1, a specific receptor on the surface of macrophages, to phagocytose the excess weak ribbon synapses around inner hair cells during hearing development, participating in ribbon synaptic pruning.

Ethics statement

The animal study was reviewed and approved by Animal Ethics Committee of Capital Medical University.

Author contributions

KL contributed to the design of the study, and analyzed and interpreted the result. SG contributed to the design of the study. XS, YL, RG, QY, SL, QT, Z-RC, and JX conducted the experiments and analyzed the generated data. XS and YL participated in the design and completion of supplementary experiments and wrote the manuscript. All authors contributed to the article and approved the submitted version.

Funding

This work was supported by the National Natural Science Foundation of China (82071037, 81770997, 81830030, and 82071054); The Joint Funding Project of Beijing Natural Science Foundation and Beijing Education Committee (KZ201810025040).

Acknowledgments

We thank Jingjing Wang as well as Ke Song for providing the public laboratory platform for immunofluorescence experiments.

Conflict of interest

The authors declare that the research was conducted in the absence of any commercial or financial relationships that could be construed as a potential conflict of interest.

Publisher's note

All claims expressed in this article are solely those of the authors and do not necessarily represent those of their affiliated organizations, or those of the publisher, the editors and the reviewers. Any product that may be evaluated in this article, or claim that may be made by its manufacturer, is not guaranteed or endorsed by the publisher.

Supplementary material

The Supplementary material for this article can be found online at: https://www.frontiersin.org/articles/10.3389/fnmol.2022.1031278/full#supplementary-material

References

Basilico, B., Ferrucci, L., Ratano, P., Golia, M. T., Grimaldi, A., Rosito, M., et al. (2022). Microglia control glutamatergic synapses in the adult mouse hippocampus. *Glia* 70, 173–195. doi: 10.1002/glia.24101

Bhuskute, A., and Page, N. (2021). Congenital and Neonatally acquired Sensorineural hearing loss. *Pediatr. Ann.* 50, e292–e296. doi: 10.3928/19382359-20210629-01

Boche, D., Perry, V. H., and Nicoll, J. A. R. (2013). Activation patterns of microglia and their identification in the human brain. *Neuropathol. Appl. Neurobiol.* 39, 3–18. doi: 10.1111/nan.12011

Brites, D., and Fernandes, A. (2015). Neuroinflammation and depression: microglia activation, extracellular microvesicles and microRNA dysregulation. *Front. Cell. Neurosci.* 9:476. doi: 10.3389/fncel.2015.00476

Coate, T. M., Scott, M. K., and Gurjar, M. (2019). Current concepts in cochlear ribbon synapse formation. *Synapse* 73:e22087. doi: 10.1002/syn.22087

Cormican, S., and Griffin, M. D. (2021). Fractalkine (CX3CL1) and its receptor CX3CR1: a promising therapeutic target in chronic kidney disease? *Front. Immunol.* 12:664202. doi: 10.3389/fimmu.2021.664202

Duan, H. (2018). Novel therapeutic strategies for solid tumor based on body's intrinsic antitumor immune system. *Cell. Physiol. Biochem.* 47, 441–457. doi: 10.1159/000489979

Favuzzi, E., Huang, S., Saldi, G. A., Binan, L., Ibrahim, L. A., Fernández-Otero, M., et al. (2021). GABA-receptive microglia selectively sculpt developing inhibitory circuits. *Cells* 184, 4048–4063.e32. doi: 10.1016/j.cell.2021.06.018

Harry, G. J. (2013). Microglia during development and aging. *Pharmacol. Ther.* 139, 313–326. doi: 10.1016/j.pharmthera.2013.04.013

He, W., Yu, J., Sun, Y., and Kong, W. (2020). Macrophages in noise-exposed cochlea: changes, regulation and the potential role. *Aging Dis.* 11, 191–199. doi: 10.14336/AD.2019.0723

Hong, S., Beja-Glasser, V. F., Nfonoyim, B. M., Frouin, A., Li, S., Ramakrishnan, S., et al. (2016). Complement and microglia mediate early synapse loss in Alzheimer mouse models. *Science* 352, 712–716. doi: 10.1126/science.aad8373

Hough, K., Verschuur, C. A., Cunningham, C., and Newman, T. A. (2022). Macrophages in the cochlea; an immunological link between risk factors and progressive hearing loss. *Glia* 70, 219–238. doi: 10.1002/glia.24095

Hsu, T. C., Tzang, B. S., Huang, C. N., Lee, Y. J., Liu, G. Y., Chen, M. C., et al. (2006). Increased expression and secretion of interleukin-6 in human parvovirus B19 non-structural protein (NS1) transfected COS-7 epithelial cells. *Clin. Exp. Immunol.* 144, 152–157. doi: 10.1111/j.1365-2249.2006.03023.x

Hu, B. H., Zhang, C., and Frye, M. D. (2018). Immune cells and non-immune cells with immune function in mammalian cochleae. *Hear. Res.* 362, 14–24. doi: 10.1016/j.heares.2017.12.009

Ito, T., Kurata, N., and Fukunaga, Y. (2022). Tissue-resident macrophages in the Stria Vascularis. *Front. Neurol.* 13:818395. doi: 10.3389/fneur.2022.818395

Kempf, A., and Schwab, M. E. (2013). Nogo-a represses anatomical and synaptic plasticity in the central nervous system. *Physiology* 28, 151–163. doi: 10.1152/physiol.00052.2012

Kim, H. J., Cho, M. H., Shim, W. H., Kim, J. K., Jeon, E. Y., Kim, D. H., et al. (2017). Deficient autophagy in microglia impairs synaptic pruning and causes social behavioral defects. *Mol. Psychiatry* 22, 1576–1584. doi: 10.1038/mp.2016.103

Korbecki, J., Simińska, D., Kojder, K., Grochans, S., Gutowska, I., Chlubek, D., et al. (2020). Fractalkine/CX3CL1 in neoplastic processes. *Int. J. Mol. Sci.* 21:3723. doi: 10.3390/ijms21103723

Leonardi, I., Li, X., Semon, A., Li, D., Doron, I., Putzel, G., et al. (2018). CX3CR1(+) mononuclear phagocytes control immunity to intestinal fungi. *Science* 359, 232–236. doi: 10.1126/science.aao1503

Liu, W., Molnar, M., Garnham, C., Benav, H., and Rask-Andersen, H. (2018). Macrophages in the human cochlea: saviors or predators—a study using super-resolution immunohistochemistry. *Front. Immunol.* 9:223. doi: 10.3389/fimmu.2018.00223

Lu, X., Shu, Y., Tang, M., and Li, H. (2016). Mammalian cochlear hair cell regeneration and ribbon synapse reformation. *Neural Plast.* 2016, 1–9. doi: 10.1155/2016/2523458

Madrigal, J. L., Caso, J. R., García-Bueno, B., Gutiérrez, I. L., and Leza, J. C. (2017). Noradrenaline induces CX3CL1 production and release by neurons. *Neuropharmacology* 114, 146–155. doi: 10.1016/j.neuropharm.2016.12.001

Meghraoui-Kheddar, A., Barthelemy, S., Boissonnas, A., and Combadière, C. (2020). Revising CX3CR1 expression on murine classical and non-classical monocytes. *Front. Immunol.* 11:1117. doi: 10.3389/fimmu.2020.01117

Noulaheu, S. F. (2021). Reducing the emergency department revolving door syndrome for the poor, uninsured, and chronically ill patient in Los Angeles: process improvement recommendations from a county health program evaluation. *Popul. Health Manag.* 24, 376–384. doi: 10.1089/pop.2020.0036

Okano, T., Nakagawa, T., Kita, T., Kada, S., Yoshimoto, M., Nakahata, T., et al. (2008). Bone marrow-derived cells expressing Iba1 are constitutively present as resident tissue macrophages in the mouse cochlea. *J. Neurosci. Res.* 86, 1758–1767. doi: 10.1002/jnr.21625

Parkhurst, C. N., Yang, G., Ninan, I., Savas, J. N., Yates, J. R. III, Lafaille, J. J., et al. (2013). Microglia promote learning-dependent synapse formation through brain-derived neurotrophic factor. *Cells* 155, 1596–1609. doi: 10.1016/j.cell.2013.11.030

Pawelec, P., Ziemka-Nalecz, M., Sypecka, J., and Zalewska, T. (2020). The impact of the CX3CL1/CX3CR1 axis in neurological disorders. *Cells* 9:2277. doi: 10.3390/cells9102277

Tremblay, M. È., Lowery, R. L., and Majewska, A. K. (2010). Microglial interactions with synapses are modulated by visual experience. *PLoS Biol.* 8:e1000527. doi: 10.1371/journal.pbio.1000527

Wake, H., Moorhouse, A. J., Jinno, S., Kohsaka, S., and Nabekura, J. (2009). Resting microglia directly monitor the functional state of synapses in vivo and determine the fate of ischemic terminals. *J. Neurosci.* 29, 3974–3980. doi: 10.1523/JNEUROSCI.4363-08.2009

Werneburg, S., Jung, J., Kunjamma, R. B., Ha, S. K., Luciano, N. J., Willis, C. M., et al. (2020). Targeted complement inhibition at synapses prevents microglial synaptic engulfment and synapse loss in demyelinating disease. *Immunity* 52, 167–182.e7. doi: 10.1016/j.immuni.2019.12.004

Wong, A. B., Rutherford, M. A., Gabrielaitis, M., Pangršič, T., Göttfert, F., Frank, T., et al. (2014). Developmental refinement of hair cell synapses tightens the coupling of Ca^{2+} influx to exocytosis. *EMBO J.* 33, 247–264. doi: 10.1002/embj.201387110

Wynn, T. A., and Vannella, K. M. (2016). Macrophages in tissue repair, regeneration, and fibrosis. *Immunity* 44, 450–462. doi: 10.1016/j.immuni.2016.02.015

Xiong, W., Wei, W., Qi, Y., Du, Z., Qu, T., Liu, K., et al. (2020). Autophagy is required for remodeling in postnatal developing ribbon synapses of cochlear inner hair cells. *Neuroscience* 431, 1–16. doi: 10.1016/j.neuroscience.2020.01.032

Yu, C., Gao, H. M., and Wan, G. (2021). Macrophages are dispensable for postnatal pruning of the Cochlear ribbon synapses. *Front. Cell. Neurosci.* 15:736120. doi: 10.3389/fncel.2021.736120

frontiers | Frontiers in Neuroscience

TYPE Review
PUBLISHED 12 December 2022
DOI 10.3389/fnins.2022.1068611

OPEN ACCESS

EDITED BY
Peter Thorne,
The University of Auckland,
New Zealand

REVIEWED BY
Yingzi He,
Eye and ENT Hospital of Fudan University, China
Wei Cao,
The Second Hospital of Anhui Medical University, China

*CORRESPONDENCE
Zuhong He
hezuhong@163.com
Xiong Chen
zn_chenxiong@whu.edu.cn

†These authors have contributed equally to this work

SPECIALTY SECTION
This article was submitted to Auditory Cognitive Neuroscience, a section of the journal Frontiers in Neuroscience

RECEIVED 14 October 2022
ACCEPTED 17 November 2022
PUBLISHED 12 December 2022

CITATION
Sun Y, Zou S, He Z and Chen X (2022) The role of autophagy and ferroptosis in sensorineural hearing loss. *Front. Neurosci.* 16:1068611. doi: 10.3389/fnins.2022.1068611

The role of autophagy and ferroptosis in sensorineural hearing loss

Ying Sun†, Shengyu Zou†, Zuhong He* and Xiong Chen*

Department of Otorhinolaryngology-Head and Neck Surgery, Zhongnan Hospital of Wuhan University, Wuhan, China

Hearing loss has become a common sensory defect in humans. Because of the limited regenerative ability of mammalian cochlear hair cells (HCs), HC damage (caused by ototoxic drugs, aging, and noise) is the main risk factor of hearing loss. However, how HCs can be protected from these risk factors remains to be investigated. Autophagy is a process by which damaged cytoplasmic components are sequestered into lysosomes for degradation. Ferroptosis is a novel form of non-apoptotic regulated cell death involving intracellular iron overloading and iron-dependent lipid peroxide accumulation. Recent studies have confirmed that autophagy is associated with ferroptosis, and their crosstalk may be the potential therapeutic target for hearing loss. In this review, we provide an overview of the mechanisms of ferroptosis and autophagy as well as their relationship with HC damage, which may provide insights for a new future in the protection of HCs.

KEYWORDS

autophagy, ferroptosis, ferritinophagy, sensorineural hearing loss, hair cell

Introduction

As a common sensory disorder in humans, hearing loss affects 1.5 billion people around the world (WHO, 2021). Sensorineural hearing loss (SNHL), an important type of hearing loss, refers to pathological changes in the cochlear hair cells (HCs), auditory nerves, or central auditory system. Ototoxic drugs, aging, and noise are common pathogenic factors of hearing loss that can cause damage or loss of HCs (Mills and Going, 1982). Unfortunately, adult mammalian cochlear HCs are not capable of regeneration; consequently, irreversible damage to HCs can result in permanent deafness (Zine et al., 2021). Protecting HCs is, therefore, a key focus of auditory research. However, the detailed mechanism underlying cochlear HC damage remains largely unknown.

In recent years, autophagy and ferroptosis have attracted much attention, and the modulation of autophagy and ferroptosis is a very attractive potential approach for the future treatment of SNHL. Autophagy is a highly conserved degradation system in eukaryotic cells that can remove damaged organelles and macromolecular proteins

and be induced by reactive oxygen species (ROS) accumulation (Boya et al., 2018). In the auditory system, especially in HCs, previous studies reported the relationship between autophagy and hearing loss (Guo et al., 2021; Zhao et al., 2021), specifically, that moderately activating autophagy can reduce HC damage in both cochlear HCs and HEI-OC1 cells (a mouse auditory cell line) after neomycin or gentamicin injury (He et al., 2017). Ferroptosis is a non-apoptotic mechanism of cell death that mainly relies on the iron-mediated production of ROS and follows plasma membrane damage (Dixon and Stockwell, 2014). Generally, ferroptosis accompanies lipid peroxidase, impaired antioxidant capacity, and increased intracellular iron accumulation (Tang et al., 2021). New research has found that the development and progression of many diseases are related to ferroptosis (Lin et al., 2022; Wang K. et al., 2022). Recently, several studies have revealed the link between ferroptosis and hearing loss and proved that the inhibition of ferroptosis may alleviate HC damage (Hu et al., 2020; Zheng et al., 2020; Jian et al., 2021).

In this paper, we review recent studies about the role of autophagy and ferroptosis in HC damage. We also focus on the molecular regulatory mechanism of autophagy and ferroptosis *in vitro* and *in vivo*. Additionally, in this review, we discuss the regulatory impact of autophagy on ferroptosis and further discuss whether regulating ferroptosis through autophagy could be a potential measure for the protection of HCs.

The role of autophagy in hair cell damage

Autophagy is not only a physiological process of degradation for long-lived proteins and damaged organelles in eukaryotic cells but also an important adaptive mechanism in the response to cellular stress (e.g., infection, poisoning, and hypoxia) (Chen et al., 2017). Under normal physiological conditions, autophagy is essential for the maintenance of cell homeostasis, while under some stress conditions, autophagy will be activated and promoted. Autophagy is divided into macroautophagy, microautophagy, and chaperone-mediated autophagy (Morel et al., 2017). Generally speaking, macroautophagy, as the main process for cells to remove damaged organelles and other related fragments, is referred to as "autophagy" (Feng et al., 2014). Autophagy takes place throughout the dynamic development of cells and plays the function of a "double-edged sword" (Wei et al., 2012). In other words, while autophagy confers a pro-survival effect, allowing cells to fight against cellular stressors such as excess ROS (Chen et al., 2017), under certain circumstances, excessive autophagy can also cause autophagic cell death (Clarke and Puyal, 2012).

The role of autophagy in age-related hearing loss

Age-related hearing loss (ARHL) is the most common form of aging in the auditory system and clinically manifests as progressive bilateral symmetrical hearing loss (Bowl and Dawson, 2019). As a major cause of sensory disturbances, ARHL limits social interaction among older individuals and thus leads to cognitive function decline, depression, anxiety, and loneliness (Jafari et al., 2021). Oxidative stress theory is the most common hypothesis regarding aging (Martin et al., 1996). With increasing age, the production of ROS increases, while body antioxidant capacity gradually decreases (Fu et al., 2018). The level of autophagy decreases with age (Youn et al., 2020), and moderate upregulation of autophagy can promote the survival of aging HCs by scavenging damaged mitochondria, which may suggest that autophagy impairment is a key factor in ARHL (Dong et al., 2021; Gumeni et al., 2021). Moderately promoting autophagic activity may, therefore, advance the viability of aging HCs.

Recently, some molecules have been reported to regulate the level of autophagy in ARHL. MicroRNAs (miRNAs) are a kind of short, endogenous, and highly evolutionarily conserved single-stranded RNAs. miRNAs can regulate the expression of target genes by inducing the degradation and inhibiting the translation of target mRNA. miR-34a blocks autophagy flux by inhibiting the expression of the autophagy-related gene 9A (ATG9A) and promotes the death of senescent HEI-OC1 cells (Pang et al., 2017). Additionally, miR-34a mediates autophagy through more than one target. In HEI-OC1 cells, siRNA was used to downregulate the expression of Sirtuin 1 (SIRT1), which can impair autophagy by significantly decreasing the conversion of microtubule- associated protein 1 light chain 3 (LC3) I to LC3 II and influencing the deacetylation of ATG9A, inducing the accumulation of p62 and HEI-OC1 cell death (Pang et al., 2019). One study suggested that miR-34a targeted SIRT1, protected cochlear HCs, and delayed ARHL by regulating mitochondria-specific autophagy (mitophagy) (Xiong et al., 2019). In addition, Forkhead box G1(FOXG1) protects HCs from oxidative damage by activating autophagy during cell senescence (He et al., 2021).

As a selective kind of autophagy, mitophagy plays an important role in ARHL pathological changes. Mitophagy refers to the process of selectively degrading damaged mitochondria and maintaining mitochondrial homeostasis. Since mitochondria are the "energy factories" and free radical metabolic centers in cells, dysfunction caused by mitochondrial damage leads to metabolic disorders of ROS. Excessive ROS can cause oxidative damage to mitochondrial lipids, DNA, and proteins, making mitochondria produce more ROS and eventually triggering apoptosis (Ashrafi and Schwarz, 2013). However, to prevent cellular damage, mitophagy will be activated to preserve a population of healthy mitochondria. Researchers found that mitophagy is involved in aging HCs.

Prohibitin 2 (PHB2), a protein receptor on the intima of mitochondria, is exposed when the mitochondrial outer membrane is ruptured and then interacts with the autophagy protein LC3 II to activate mitophagy. Yu et al. (2021) found that PHB2 expression was increased along with mitophagy activation in mice with ARHL, indicating that PHB2 may be involved in mitophagy. However, the exact mechanism underlying the role of PHB2 in ARHL is unclear and thus needs to be explored further (Yu et al., 2021). BCL2 interacting protein 3 like/Nip3-like protein X (BNIP3L/NIX) is a protein located in the outer mitochondrial membrane that participates in mitophagy by promoting the formation of autophagosomes to engulf target mitochondria (Li et al., 2021). BNIP3L/NIX was significantly downregulated in both *in vivo* and *in vitro* models of aging, while overexpression of BNIP3L/NIX alleviated HC senescence by promoting mitophagy (Kim et al., 2021).

The role of autophagy in drug-induced hearing loss

Chemotherapeutic agents (e.g., cisplatin) and aminoglycosides (e.g., neomycin and gentamicin) are two major classes of ototoxic drugs. These drugs can cause bilateral and irreversible SNHL. Because of their side effects, the application of ototoxic drugs is limited, and hearing loss prevention following ototoxic drug treatment has long attracted researchers' attention. ROS have been identified as one of the classical causes of SNHL mediated by cisplatin and aminoglycosides (Gentilin et al., 2019; Fang et al., 2022) and can be generated after ototoxic drug treatment (Liu et al., 2016; Li et al., 2018). If ROS are generated in excess, they will damage the antioxidant defense capacity of HCs and induce cell apoptosis (Gentilin et al., 2019).

Autophagy is a common cellular response when cells are exposed to stress stimuli such as ototoxic drugs. Previous studies showed that ROS can induce autophagy in auditory cells after cisplatin and aminoglycoside injury (Hirose et al., 1997; Liu et al., 2021). Autophagic activity increases significantly in HCs following treatment with neomycin or cisplatin (Levano and Bodmer, 2015; He et al., 2017). The activation of autophagy has been observed to promote HC survival after neomycin treatment, and blocking the activation of autophagy can increase ROS levels and induce HC apoptosis (He et al., 2017). Therefore, exploring the effect of autophagy on HC protection along with the underlying mechanism may have therapeutic implications for the prevention and treatment of ototoxic drug-induced hearing loss.

Autophagy is regulated by many factors during ototoxic drug damage. The overexpression of YTHDF1 (the YT521-B homology N6-methyladenosine RNA binding protein) could enhance the activation of autophagy by promoting the translation of the autophagy-related gene ATG14 (autophagy-related gene 14), while a deficiency thereof suppressed autophagy and increased the loss of HCs after cisplatin damage (Huang et al., 2022). Overexpression of TFEB (transcription factor EB), a transcription factor, activated autophagy in cochlear HCs and HEI-OC1 cells and subsequently alleviated cisplatin-induced apoptosis (Li et al., 2022). Upregulation of autophagy by phosphorylation of the Ser9 site of GSK-3β(glycogen synthase kinase-3β), a multifunctional serine/threonine protein kinase, could attenuate cisplatin-induced ototoxicity, which may be related to the activation of the WNT/β-catenin signaling pathway (Liu et al., 2019). PINK1 (phosphatase and tensin homolog induced putative kinase 1)/Parkin-mediated mitophagy can inhibit mitochondrial proteotoxicity and maintain mitochondrial protein homeostasis. Research reported that in HEI-OC1 cells, neomycin attenuated PINK1/Parkin-mediated mitophagy by promoting ATF3 (activating transcription factor 3) expression, and damaged cochlear HCs could be partially rescued when mitophagy was induced (Zhang et al., 2022). After cisplatin treatment, ROS aggravates the damage and promotes the activation of PINK1/Parkin-related mitophagy to clear dysfunctional mitochondria and inhibit the activation of JNK (c-Jun N-terminal kinase)-related apoptotic pathways to protect HEI-OC1 cells against cisplatin-induced damage (Yang et al., 2018).

The role of autophagy in noise-induced hearing loss

Noise is one of the main causes of SNHL. Following noise exposure, the accumulation of ROS contributing to the pathogenesis of noise-induced loss of sensory HCs is well accepted. Noise-induced stress increases the level of ROS in outer HCs and then leads to HC damage, which is the key to metabolic injury (Hill et al., 2016). In addition, ROS induce inflammation by producing cytokines and damage cochlear HCs (Wakabayashi et al., 2010). However, ROS can also induce autophagy to perform cellular defense functions (Vernon and Tang, 2013).

Following noise exposure, autophagy is triggered to limit pathological changes to HCs. Miao et al. (2021) found that two autophagy metabolites, phosphatidylethanolamine (PE) and phosphatidylcholine, were significantly decreased in the plasma samples of patients suffering from noise-induced hearing loss (NIHL). They confirmed that PI3K (phosphatidylinositide 3-kinase), AKT (protein kinase B), and ATG5 (autophagy-related gene 5) were significantly downregulated in NIHL patients by using real-time quantitative PCR (Miao et al., 2021). Yuan et al. (2015) found that increasing autophagy activity by using rapamycin can inhibit ROS accumulation and reduce noise-induced HC loss (Yuan et al., 2015). In contrast, treatment with either the autophagy

inhibitor 3-methyladenine or LC3 II siRNA can exacerbate noise-induced HC loss and NIHL (Fang et al., 2022). Recently, pejvakin has been reported to regulate autophagy in NIHL. Pejvakin is a peroxisome-associated protein from the gasdermin family that helps to maintain the normal three-dimensional ciliated ladder structure and mechanical transduction of HCs (Kazmierczak et al., 2017). In response to sound overstimulation, pejvakin promotes pexophagy (the autophagic degradation of peroxisomes) by recruiting LC3 II directly and protects the auditory HCs against oxidative stress (Defourny et al., 2019). Based on the above studies, the importance of autophagy in NIHL is worthy of further exploration.

The role of ferroptosis in hair cell damage

Dixon et al. (2012) identified a novel form of regulated cell death, denoted "ferroptosis." The morphology and biochemistry of ferroptosis differ from other forms of cell death. Morphologically, mitochondrial cristae loss and outer membrane rupture are characteristic signatures of ferroptotic cells (Xie et al., 2016). Biochemically, ferroptosis is characterized by its association with the accumulation of iron and the subsequent production of ROS, as well as lipid peroxidation (Xie et al., 2016). Once the ability of the antioxidant system to scavenge overexpressed ROS is exceeded, oxidative stress will occur, resulting in lipid peroxidation, which damages cellular structures and leads to cell death. The labile iron pool, moreover, can facilitate a Fenton reaction and peroxidize polyunsaturated fatty acids (PUFAs) to generate lipid peroxides, resulting in plasma membrane rupture and eventually, cell death (Stockwell, 2022). In brief, iron-dependent ROS production results in lipid peroxidation and ultimately leads to membrane damage, which is the core mechanism of ferroptosis. ROS produced by the Fenton reaction, PUFAs, and lipid peroxidation can promote ferroptosis, but the system Xc^-/glutathione(GSH)/glutathione peroxidase 4(GPX4) axis can inhibit ferroptosis by influencing the redox status of cells (Liang et al., 2022).

Since ferroptosis was discovered, some evidence has shown the close relationship between ferroptosis and many pathologies. For example, ferroptosis is widely believed to function as a tumor-suppression mechanism. Phosphoglycerol dehydrogenase, by binding and regulating PCBP2 [Poly(rC) binding protein 2] protein expression to promote the mRNA stability of SLC7A11 (the catalytic subunit of system Xc^-), can inhibit cell ferroptosis and ultimately promote the malignant progression of bladder cancer (Shen et al., 2022). The ferroptosis inducer dihydroartemisinin intensively strengthens the cytotoxicity of cisplatin for pancreatic ductal adenocarcinoma cells, which may act as a promising therapeutic strategy for drug-resistant tumors (Du et al., 2021).

Similarly, ferroptosis also plays an important role in HC injury. Neomycin induced intracellular Fe^{2+} increases and lipid peroxidation in the HEI-OC1 cell line and cochlear HCs (Zheng et al., 2020). After cisplatin treatment, the mitochondria in HEI-OC1 cells showed mitochondrial shrinkage and loss of mitochondrial crests—typical characteristics of ferroptotic cells (Hu et al., 2020). Moreover, ferroptosis may be a cause of auditory cortex degeneration, leading to central presbycusis. Levels of acyl-CoA synthetase long-chain family member 4 (ACSL4) and transferrin receptor 1 were increased in the auditory cortex of rat models that mimic aging induced by D-galactose, and removing excess iron from cells by deferoxamine treatment inhibited ferroptosis and delayed cellular senescence (Chen et al., 2020). However, the role of ferroptosis in aging HCs has not been reported.

As mentioned above, ferroptosis occurs when lipid ROS production exceeds the antioxidant capability. Glutathione peroxidase 4 (GPX4) can convert lipid hydroperoxides to lipid alcohols by using reduced GSH as a cofactor, reducing ROS-induced damage to cells (Loscalzo, 2008). GPX4 is regarded as the robust central regulator and lethal signal of ferroptotic cell death, and the inactivation or absence of GPX4 can cause the accumulation of lipid peroxides. Inhibiting GPX4 will lead to a redox homeostasis imbalance, eventually resulting in ferroptotic cell death. Neomycin significantly decreased the expression of GPX4 in cochlear HCs (Zheng et al., 2020). Hu et al. (2020) found that the expression of GPX4 was inhibited by cisplatin, and ROS accumulated in HEI-OC1 cells. These findings may suggest that the balance of redox homeostasis in ototoxic drug-damaged HCs is disrupted, which could promote ferroptotic cell death. Nuclear factor erythroid 2-related factor 2 (Nrf2) is a key transcription factor in the antioxidant response. When the organism is under oxidative stress, Nrf2 dissociates from Keap1 (Kelch-like ECH-associated protein 1) and binds to the antioxidant response elements of target genes such as GPX4, activating the transcription of antioxidant genes. Positively regulating the Nrf2-GPX4 axis can prevent ferroptosis in carbon tetrachloride-induced acute liver injury in mice (Zhao et al., 2022). Knockdown of Nrf2 facilitated erastin-induced cell destruction in HepG2 cells, implying a pivotal role of Nrf2 against ferroptosis (Dai et al., 2021). However, knockout of Nrf2 substantially inhibited cisplatin-induced HEI-OC1 cell death by decreasing transferrin receptor 1 protein levels and increasing GPX4 protein levels (Wang W. et al., 2022). These results suggest that the role of Nrf2 in ferroptosis regulation may be tissue-specific.

Excessive lipid peroxidation can induce ferroptosis in cells. How lipid peroxidation is generated during ferroptosis depends on the enzyme system that promotes phospholipid

peroxidation. For example, ACSL4 catalyzes PUFAs in the membrane structure to produce corresponding coenzyme A, which then forms lipid peroxides through a series of downstream reactions and eventually leads to cell disintegration (Doll et al., 2017). ACSL4 was a key enzyme in arachidonic acid-induced ferroptosis. He et al. (2022) found that cisplatin-treated HCs showed significant enrichment in the arachidonic acid metabolic pathway by metabolomics assays. Researchers found that inhibiting the expression of ACSL4 could reduce the content of lipid peroxides and protect HCs (He et al., 2022). These findings indicate that HCs treated with cisplatin experience lipid metabolism disorders, which, if prevented by intervention, can resist ferroptosis and reduce the destructive effect of cisplatin on HCs. Thus, ACSL4 may be a key factor contributing to cisplatin sensitivity in HCs and a potential therapeutic target for SNHL.

Several ferroptosis inhibitors may allow for potent and selective therapeutic measures for preventing HC damage. Liproxstatin-1 and ferrostatin-1, which are aromatic amine antioxidants, inhibit lipid peroxidation directly by free radical capture (Zilka et al., 2017). A study demonstrated that liproxstatin-1 protected HCs from aminoglycoside-induced ototoxicity by inhibiting ferroptosis in HEI-OC1 cells and neonatal mouse cochlear HCs (Zheng et al., 2020). Similar effects were also observed for ferrostatin-1 in damaged HCs (Hu et al., 2020). Regarding their mitigating effect on ototoxicity, ferroptosis inhibitors may be expected to be used to protect HCs from ototoxic drugs. In addition, from the perspective of HCs damage, ferroptosis has only been reported in ototoxic drug-induced hearing loss, and whether this pathway is involved in ARHL and NIHL needs to be further explored.

The relationship between autophagy and ferroptosis

The relationship between autophagy and ferroptosis has attracted much attention. As universally acknowledged, autophagy is often involved in ferroptosis. Increasing evidence indicates that ferroptosis requires autophagy machinery for its execution. For example, erastin, a ferroptosis inducer, can activate autophagy, while knockout of some autophagy-related genes significantly inhibited ferroptosis induced by erastin (Hou et al., 2016). Autophagy can lead to the accumulation of iron ions and lipid peroxidation, eventually promoting ferroptosis.

Ferritinophagy refers to a selective autophagy process that manifests as the movement of ferritin to lysosomes and its degradation, releasing free iron. Through quantitative proteomics pair analysis of all the proteins in autophagosomes, Mancias et al. (2015) discovered a specific protein, the nuclear receptor coactivator 4 (NCOA4), that is closely related to ferritin and so were the first to discover and name the process of ferritinophagy. Highly enriched in autolysosomes, NCOA4 mediates the targeted recognition of ferritin by autophagosomes by binding to ferritin (Gao et al., 2016). Ferritinophagy plays an important regulatory role in organism pathology. When ferritinophagy is over-induced, Fe^{2+} overload in the cytoplasmic matrix promotes lipid peroxidation, resulting in cell membrane damage and ferroptosis (Ajoolabady et al., 2021). However, blocking autophagy or knocking out NCOA4 can inhibit the accumulation of lipid ROS, so preventing the eventual occurrence of ferroptosis (Gao et al., 2016).

Therefore, studying the mechanism of NCOA4-mediated ferritinophagy and its pathophysiological role in different diseases may provide avenues for treatment. Ito et al. (2021) established a mouse model of heart failure by using the method of transverse aortic constriction. Their results showed that, compared with the control group, the accumulation of free iron and lipid peroxidation were inhibited in the hearts of mice with knockout of NCOA4. Further, the degree of left ventricular dilatation was reduced and cardiac function was improved, indicating that activating ferritinophagy can lead to the development of heart failure. Compound 9a was used to block the interaction between NCOA4 and ferritin heavy chain 1 to inhibit ferritinophagy and block ferroptosis, thus significantly improving the brain damage of rats with ischemic stroke (Fang et al., 2021). Similarly, cisplatin treatment promoted ROS-induced lipid peroxidation and caused iron accumulation by activating NCOA4-medicated ferritinophagy (Jian et al., 2021). In summary, most studies have shown that the upregulation of ferritinophagy can promote the occurrence of ferroptosis, while the downregulation of ferritinophagy can inhibit ferroptosis (**Figure 1**). Currently, ferritinophagy is less studied in the field of auditory diseases, and targeting ferritinophagy may be a promising therapeutic strategy for the treatment of SNHL. In addition, selective autophagy processes such as lipophagy (Bai et al., 2019), clockophagy (Yang et al., 2019), and chaperone-mediated autophagy (Wu et al., 2019) also cause lipid peroxidation and subsequent ferroptotic cell death and may be potential targets of SNHL.

The relationship between autophagy and ferroptosis, however, is controversial. Subjecting cells to oxidative stress and injury can activate their self-protection mechanism. Autophagy may protect cells against ferroptotic cell death. Sorafenib could induce both apoptosis and ferroptosis in Desmoid-type fibromatosis cells. Furthermore, using the autophagy inhibitor hydroxychloroquine could enhance sorafenib-induced cytotoxicity. These results show that autophagy may have a pro-survival function through the inhibition of ferroptosis and apoptosis (Schut et al., 2022). Similarly, Zhao et al. (2020) reported that 15-lipoxygenase binds to PE to produce

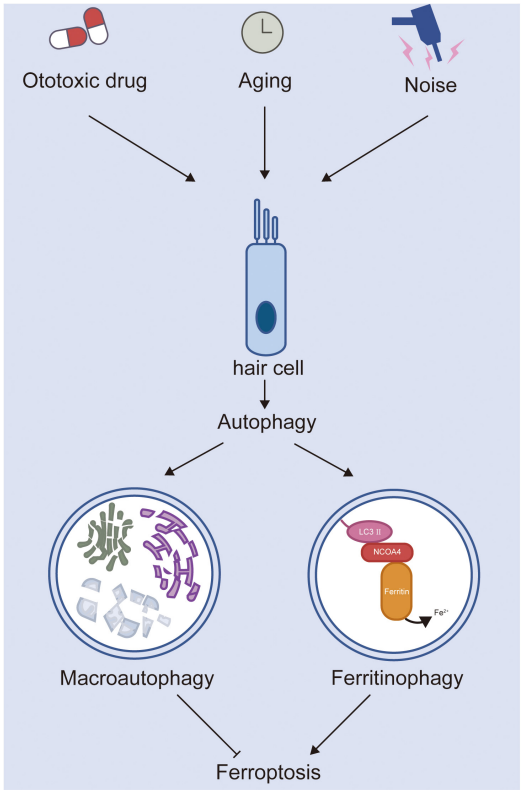

FIGURE 1
The roles of autophagy and ferroptosis in hair cell injury.

an oxidation product, 15-hydroperoxyeicosatetraenoic acid, which can lead to pro-ferroptotic cell damage and activate the pro-survival autophagy pathway to limit cell damage. Therefore, it seems to be a closely regulated mechanism between autophagy and ferroptosis. More research is needed to reveal the molecular mechanism between autophagy and ferroptosis and provide new potential therapeutic targets for hearing loss.

Conclusion

Generally, autophagy plays a dual role in HC damage. Moderately increased autophagy can help maintain intracellular homeostasis by reducing oxidative stress, while autophagic cell death can occur under other conditions. Although many molecules that can regulate autophagy have been reported, research has been limited to external and animal experiments, and few clinical trials have examined the impact of autophagy on HCs.

Ferroptosis is widely investigated in both physiologic and pathogenic processes but has not been extensively studied in the auditory field. At present, it is reported that ototoxic drugs (e.g., neomycin and cisplatin) can induce ferroptosis in HCs, but it remains unclear whether ferroptosis engages in aging and noise-induced HC damage. Regulating ferroptosis may, therefore, be a promising strategy in SNHL therapy. However, additional studies on ferroptosis and its involvement in SNHL are needed to identify the corresponding therapeutic targets.

Increasingly, the relationship between autophagy and ferroptosis has appealed to researchers. An increasing number of studies have revealed that ferritinophagy-mediated ferroptosis is involved in the occurrence and development of neurodegenerative disease, reperfusion injury, and cancers (Santana-Codina and Mancias, 2018). While ferritinophagy is a worthy target for the treatment of SNHL, its complete molecular mechanism and pathophysiological process in SNHL still call for further study. Clarification of the crosstalk between autophagy and ferroptosis would not only favor a comprehensive understanding of cell death pathways but also provide us with new ideas for the future treatment of SNHL.

Author contributions

XC and ZH conceived and designed the study and reviewed and edited the manuscript. YS and SZ wrote the manuscript. All authors have read and approved the submitted version of the manuscript.

Funding

This study was supported by grants from the National Natural Science Foundation of China (No. 81800915), the Fundamental Research Funds for the Central Universities (2042022kf0059), and the Key Research and Development Program of Hubei Province (2022BCA046).

Conflict of interest

The authors declare that the research was conducted in the absence of any commercial or financial relationships that could be construed as a potential conflict of interest.

Publisher's note

All claims expressed in this article are solely those of the authors and do not necessarily represent those of their affiliated organizations, or those of the publisher, the editors and the reviewers. Any product that may be evaluated in this article, or claim that may be made by its manufacturer, is not guaranteed or endorsed by the publisher.

References

Ajoolabady, A., Aslkhodapasandhokmabad, H., Libby, P., Tuomilehto, J., Lip, G. Y. H., Penninger, J. M., et al. (2021). Ferritinophagy and ferroptosis in the management of metabolic diseases. *Trends Endocrinol. Metab.* 32, 444–462. doi: 10.1016/j.tem.2021.04.010

Ashrafi, G., and Schwarz, T. L. (2013). The pathways of mitophagy for quality control and clearance of mitochondria. *Cell Death Differ.* 20, 31–42. doi: 10.1038/cdd.2012.81

Bai, Y., Meng, L., Han, L., Jia, Y., Zhao, Y., Gao, H., et al. (2019). Lipid storage and lipophagy regulates ferroptosis. *Biochem. Biophys. Res. Commun.* 508, 997–1003. doi: 10.1016/j.bbrc.2018.12.039

Bowl, M. R., and Dawson, S. J. (2019). Age-related hearing loss. *Cold Spring Harb. Perspect. Med.* 9:a033217. doi: 10.1101/cshperspect.a033217

Boya, P., Codogno, P., and Rodriguez-Muela, N. (2018). Autophagy in stem cells: repair, remodelling and metabolic reprogramming. *Development* 145:dev146506. doi: 10.1242/dev.146506

Chen, X., Li, D., Sun, H., Wang, W., Wu, H., Kong, W., et al. (2020). Relieving ferroptosis may partially reverse neurodegeneration of the auditory cortex. *FEBS J.* 287, 4747–4766. doi: 10.1111/febs.15266

Chen, Y. F., Liu, H., Luo, X. J., Zhao, Z., Zou, Z. Y., Li, J., et al. (2017). The roles of reactive oxygen species (ROS) and autophagy in the survival and death of leukemia cells. *Crit. Rev. Oncol. Hematol.* 112, 21–30. doi: 10.1016/j.critrevonc.2017.02.004

Clarke, P. G., and Puyal, J. (2012). Autophagic cell death exists. *Autophagy* 8, 867–869. doi: 10.4161/auto.20380

Dai, C., Li, H., Wang, Y., Tang, S., Velkov, T., and Shen, J. (2021). Inhibition of oxidative stress and ALOX12 and NF-κB pathways contribute to the protective effect of baicalein on carbon tetrachloride-induced acute liver injury. *Antioxidants* 10:976. doi: 10.3390/antiox10060976

Defourny, J., Aghaie, A., Perfettini, I., Avan, P., Delmaghani, S., and Petit, C. (2019). Pejvakin-mediated pexophagy protects auditory hair cells against noise-induced damage. *Proc. Natl. Acad. Sci. U.S.A.* 116, 8010–8017. doi: 10.1073/pnas.1821844116

Dixon, S. J., Lemberg, K. M., Lamprecht, M. R., Skouta, R., Zaitsev, E. M., Gleason, C. E., et al. (2012). Ferroptosis: an iron-dependent form of nonapoptotic cell death. *Cell* 149, 1060–1072. doi: 10.1016/j.cell.2012.03.042

Dixon, S. J., and Stockwell, B. R. (2014). The role of iron and reactive oxygen species in cell death. *Nat. Chem. Biol.* 10, 9–17. doi: 10.1038/nchembio.1416

Doll, S., Proneth, B., Tyurina, Y. Y., Panzilius, E., Kobayashi, S., Ingold, I., et al. (2017). ACSL4 dictates ferroptosis sensitivity by shaping cellular lipid composition. *Nat. Chem. Biol.* 13, 91–98. doi: 10.1038/nchembio.2239

Dong, J., Zhang, K. J., Li, G. C., Chen, X. R., Lin, J. J., Li, J. W., et al. (2021). CDDO-Im ameliorates osteoarthritis and inhibits chondrocyte apoptosis in mice via enhancing Nrf2-dependent autophagy. *Acta Pharmacol. Sin.* 43, 1793–1802. doi: 10.1038/s41401-021-00782-6

Du, J., Wang, X., Li, Y., Ren, X., Zhou, Y., Hu, W., et al. (2021). DHA exhibits synergistic therapeutic efficacy with cisplatin to induce ferroptosis in pancreatic ductal adenocarcinoma via modulation of iron metabolism. *Cell Death Dis.* 12:705. doi: 10.1038/s41419-021-03996-y

Fang, J., Wu, H., Zhang, J., Mao, S., Shi, H., Yu, D., et al. (2022). A reduced form of nicotinamide riboside protects the cochlea against aminoglycoside-induced ototoxicity by SIRT1 activation. *Biomed. Pharmacother.* 150:113071. doi: 10.1016/j.biopha.2022.113071

Fang, Y., Chen, X., Tan, Q., Zhou, H., Xu, J., and Gu, Q. (2021). Inhibiting ferroptosis through disrupting the NCOA4-FTH1 interaction: a new mechanism of action. *ACS Central Sci.* 7, 980–989. doi: 10.1021/acscentsci.0c01592

Feng, Y., He, D., Yao, Z., and Klionsky, D. J. (2014). The machinery of macroautophagy. *Cell Res.* 24, 24–41. doi: 10.1038/cr.2013.168

Fu, X., Sun, X., Zhang, L., Jin, Y., Chai, R., Yang, L., et al. (2018). Tuberous sclerosis complex-mediated mTORC1 overactivation promotes age-related hearing loss. *J. Clin. Investig.* 128, 4938–4955. doi: 10.1172/jci98058

Gao, M., Monian, P., Pan, Q., Zhang, W., Xiang, J., and Jiang, X. (2016). Ferroptosis is an autophagic cell death process. *Cell Res.* 26, 1021–1032. doi: 10.1038/cr.2016.95

Gentilin, E., Simoni, E., Candito, M., Cazzador, D., and Astolfi, L. (2019). Cisplatin-induced ototoxicity: updates on molecular targets. *Trends Mol. Med.* 25, 1123–1132. doi: 10.1016/j.molmed.2019.08.002

Gumeni, S., Papanagnou, E. D., Manola, M. S., and Trougakos, I. P. (2021). Nrf2 activation induces mitophagy and reverses Parkin/Pink1 knock down-mediated neuronal and muscle degeneration phenotypes. *Cell Death Dis.* 12:671. doi: 10.1038/s41419-021-03952-w

Guo, L., Cao, W., Niu, Y., He, S., Chai, R., and Yang, J. (2021). Autophagy regulates the survival of hair cells and spiral ganglion neurons in cases of noise, ototoxic drug, and age-induced sensorineural hearing loss. *Front. Cell Neurosci.* 15:760422. doi: 10.3389/fncel.2021.760422

He, F., Huang, X., Wei, G., Lin, X., Zhang, W., Zhuang, W., et al. (2022). Regulation of ACSL4-catalyzed lipid peroxidation process resists cisplatin ototoxicity. *Oxid. Med. Cell Longev.* 2022:3080263. doi: 10.1155/2022/3080263

He, Z., Guo, L., Shu, Y., Fang, Q., Zhou, H., Liu, Y., et al. (2017). Autophagy protects auditory hair cells against neomycin-induced damage. *Autophagy* 13, 1884–1904. doi: 10.1080/15548627.2017.1359449

He, Z. H., Li, M., Fang, Q. J., Liao, F. L., Zou, S. Y., Wu, X., et al. (2021). FOXG1 promotes aging inner ear hair cell survival through activation of the autophagy pathway. *Autophagy* 17, 4341–4362. doi: 10.1080/15548627.2021.1916194

Hill, K., Yuan, H., Wang, X., and Sha, S. H. (2016). Noise-induced loss of hair cells and cochlear synaptopathy are mediated by the activation of AMPK. *J. Neurosci.* 36, 7497–7510. doi: 10.1523/jneurosci.0782-16.2016

Hirose, K., Hockenbery, D. M., and Rubel, E. W. (1997). Reactive oxygen species in chick hair cells after gentamicin exposure in vitro. *Hear. Res.* 104, 1–14. doi: 10.1016/s0378-5955(96)00169-4

Hou, W., Xie, Y., Song, X., Sun, X., Lotze, M. T., Zeh, H. J., et al. (2016). Autophagy promotes ferroptosis by degradation of ferritin. *Autophagy* 12, 1425–1428. doi: 10.1080/15548627.2016.1187366

Hu, B., Liu, Y., Chen, X., Zhao, J., Han, J., Dong, H., et al. (2020). Ferrostatin-1 protects auditory hair cells from cisplatin-induced ototoxicity in vitro and in vivo. *Biochem. Biophys. Res. Commun.* 533, 1442–1448. doi: 10.1016/j.bbrc.2020.10.019

Huang, Y., Gao, D., Wu, Y., Sun, L., Chen, J., Chen, J., et al. (2022). YTHDF1 protects auditory hair cells from cisplatin-induced damage by activating autophagy via the promotion of ATG14 Translation. *Mol. Neurobiol.* 59, 7134–7151. doi: 10.1007/s12035-022-03021-z

Ito, J., Omiya, S., Rusu, M. C., Ueda, H., Murakawa, T., Tanada, Y., et al. (2021). Iron derived from autophagy-mediated ferritin degradation induces cardiomyocyte death and heart failure in mice. *eLife* 10:e62174. doi: 10.7554/eLife.62174

Jafari, Z., Kolb, B. E., and Mohajerani, M. H. (2021). Age-related hearing loss and cognitive decline: MRI and cellular evidence. *Ann. N. Y. Acad. Sci.* 1500, 17–33. doi: 10.1111/nyas.14617

Jian, B., Pang, J., Xiong, H., Zhang, W., Zhan, T., Su, Z., et al. (2021). Autophagy-dependent ferroptosis contributes to cisplatin-induced hearing loss. *Toxicol. Lett.* 350, 249–260. doi: 10.1016/j.toxlet.2021.07.010

Kazmierczak, M., Kazmierczak, P., Peng, A. W., Harris, S. L., Shah, P., Puel, J. L., et al. (2017). Pejvakin, a candidate stereociliary rootlet protein, regulates hair cell function in a cell-autonomous manner. *J. Neurosci.* 37, 3447–3464. doi: 10.1523/jneurosci.2711-16.2017

Kim, Y. J., Choo, O. S., Lee, J. S., Jang, J. H., Woo, H. G., Choung, Y. H., et al. (2021). BCL2 Interacting Protein 3-like/NIX-mediated mitophagy plays an important role in the process of age-related hearing loss. *Neuroscience* 455, 39–51. doi: 10.1016/j.neuroscience.2020.12.005

Levano, S., and Bodmer, D. (2015). Loss of STAT1 protects hair cells from ototoxicity through modulation of STAT3, c-Jun, Akt, and autophagy factors. *Cell Death Dis.* 6:e2019. doi: 10.1038/cddis.2015.362

Li, H., Song, Y., He, Z., Chen, X., Wu, X., Li, X., et al. (2018). Meclofenamic acid reduces reactive oxygen species accumulation and apoptosis, inhibits excessive autophagy, and protects hair cell-like HEI-OC1 cells from cisplatin-induced damage. *Front. Cell. Neurosci.* 12:139. doi: 10.3389/fncel.2018.00139

Li, Y., Zheng, W., Lu, Y., Zheng, Y., Pan, L., Wu, X., et al. (2021). BNIP3L/NIX-mediated mitophagy: molecular mechanisms and implications for human disease. *Cell Death Dis.* 13:14. doi: 10.1038/s41419-021-04469-y

Li, Z., Yao, Q., Tian, Y., Jiang, Y., Xu, M., Wang, H., et al. (2022). Trehalose protects against cisplatin-induced cochlear hair cell damage by activating TFEB-mediated autophagy. *Biochem. Pharmacol.* 197:114904. doi: 10.1016/j.bcp.2021.114904

Liang, D., Minikes, A. M., and Jiang, X. (2022). Ferroptosis at the intersection of lipid metabolism and cellular signaling. *Mol. Cell* 82, 2215–2227. doi: 10.1016/j.molcel.2022.03.022

Lin, Y., Xu, W., Hou, Y., Wang, S., Zhang, H., Ran, M., et al. (2022). The multifaceted role of ferroptosis in kidney diseases. *Chemicobiol. Interact.* 365:110107. doi: 10.1016/j.cbi.2022.110107

Liu, L., Chen, Y., Qi, J., Zhang, Y., He, Y., Ni, W., et al. (2016). Wnt activation protects against neomycin-induced hair cell damage in the mouse cochlea. *Cell Death Dis.* 7:e2136. doi: 10.1038/cddis.2016.35

Liu, T., Zong, S., Luo, P., Qu, Y., Wen, Y., Du, P., et al. (2019). Enhancing autophagy by down-regulating GSK-3β alleviates cisplatin-induced ototoxicity *in vivo* and *in vitro*. *Toxicol. Lett.* 313, 11–18. doi: 10.1016/j.toxlet.2019.05.025

Liu, W., Xu, L., Wang, X., Zhang, D., Sun, G., Wang, M., et al. (2021). PRDX1 activates autophagy via the PTEN-AKT signaling pathway to protect against cisplatin-induced spiral ganglion neuron damage. *Autophagy* 17, 4159–4181. doi: 10.1080/15548627.2021.1905466

Loscalzo, J. (2008). Membrane redox state and apoptosis: death by peroxide. *Cell Metab.* 8, 182–183. doi: 10.1016/j.cmet.2008.08.004

Mancias, J. D., Pontano Vaites, L., Nissim, S., Biancur, D. E., Kim, A. J., Wang, X., et al. (2015). Ferritinophagy via NCOA4 is required for erythropoiesis and is regulated by iron dependent HERC2-mediated proteolysis. *eLife* 4:e10308. doi: 10.7554/eLife.10308

Martin, G. M., Austad, S. N., and Johnson, T. E. (1996). Genetic analysis of ageing: role of oxidative damage and environmental stresses. *Nat. Genet.* 13, 25–34. doi: 10.1038/ng0596-25

Miao, L., Wang, B., Zhang, J., Yin, L., and Pu, Y. (2021). Plasma metabolomic profiling in workers with noise-induced hearing loss: a pilot study. *Environ. Sci. Pollut. Res. Int.* 28, 68539–68550. doi: 10.1007/s11356-021-15468-z

Mills, J. H., and Going, J. A. (1982). Review of environmental factors affecting hearing. *Environ. Health Perspect.* 44, 119–127. doi: 10.1289/ehp.8244119

Morel, E., Mehrpour, M., Botti, J., Dupont, N., Hamaï, A., Nascimbeni, A. C., et al. (2017). Autophagy: a Druggable Process. *Annu. Rev. Pharmacol. Toxicol.* 57, 375–398. doi: 10.1146/annurev-pharmtox-010716-104936

Pang, J., Xiong, H., Lin, P., Lai, L., Yang, H., Liu, Y., et al. (2017). Activation of miR-34a impairs autophagic flux and promotes cochlear cell death via repressing ATG9A: implications for age-related hearing loss. *Cell Death Dis.* 8:e3079. doi: 10.1038/cddis.2017.462

Pang, J., Xiong, H., Ou, Y., Yang, H., Xu, Y., Chen, S., et al. (2019). SIRT1 protects cochlear hair cell and delays age-related hearing loss via autophagy. *Neurobiol. Aging* 80, 127–137. doi: 10.1016/j.neurobiolaging.2019.04.003

Santana-Codina, N., and Mancias, J. D. (2018). The Role of NCOA4-Mediated Ferritinophagy in Health and Disease. *Pharmaceuticals* 11:114. doi: 10.3390/ph11040114

Schut, A. W., Vriends, A. L. M., Sacchetti, A., Timbergen, M. J. M., Alman, B. A., Al-Jazrawe, M., et al. (2022). In desmoid-type fibromatosis cells sorafenib induces ferroptosis and apoptosis, which are enhanced by autophagy inhibition. *Eur. J. Surg. Oncol.* 48, 1527–1535. doi: 10.1016/j.ejso.2022.02.020

Shen, L., Zhang, J., Zheng, Z., Yang, F., Liu, S., Wu, Y., et al. (2022). PHGDH inhibits ferroptosis and promotes malignant progression by upregulating SLC7A11 in bladder cancer. *Int. J. Biol. Sci.* 18, 5459–5474. doi: 10.7150/ijbs.74546

Stockwell, B. R. (2022). Ferroptosis turns 10: emerging mechanisms, physiological functions, and therapeutic applications. *Cell* 185, 2401–2421. doi: 10.1016/j.cell.2022.06.003

Tang, D., Chen, X., Kang, R., and Kroemer, G. (2021). Ferroptosis: molecular mechanisms and health implications. *Cell Res.* 31, 107–125. doi: 10.1038/s41422-020-00441-1

Vernon, P. J., and Tang, D. (2013). Eat-me: autophagy, phagocytosis, and reactive oxygen species signaling. *Antioxid. Redox Signal.* 18, 677–691. doi: 10.1089/ars.2012.4810

Wakabayashi, K., Fujioka, M., Kanzaki, S., Okano, H. J., Shibata, S., Yamashita, D., et al. (2010). Blockade of interleukin-6 signaling suppressed cochlear inflammatory response and improved hearing impairment in noise-damaged mice cochlea. *Neurosci. Res.* 66, 345–352. doi: 10.1016/j.neures.2009.12.008

Wang, K., Chen, X. Z., Wang, Y. H., Cheng, X. L., Zhao, Y., Zhou, L. Y., et al. (2022). Emerging roles of ferroptosis in cardiovascular diseases. *Cell Death Discov.* 8:394. doi: 10.1038/s41420-022-01183-2

Wang, W., Ma, P., Gao, W., Lu, P., Ding, X., Chen, J., et al. (2022). Nrf2 knockout affected the ferroptosis signaling pathway against cisplatin-induced hair cell-like HEI-OC1 cell death. *Oxid. Med. Cell Longev.* 2022:2210733. doi: 10.1155/2022/2210733

Wei, K., Wang, P., and Miao, C. Y. (2012). A double-edged sword with therapeutic potential: an updated role of autophagy in ischemic cerebral injury. *CNS Neurosci. Therap.* 18, 879–886. doi: 10.1111/cns.12005

WHO (2021). *Deafness and Hearing Loss*. Geneva: WHO.

Wu, Z., Geng, Y., Lu, X., Shi, Y., Wu, G., Zhang, M., et al. (2019). Chaperone-mediated autophagy is involved in the execution of ferroptosis. *Proc. Natl. Acad. Sci. U.S.A.* 116, 2996–3005. doi: 10.1073/pnas.1819728116

Xie, Y., Hou, W., Song, X., Yu, Y., Huang, J., Sun, X., et al. (2016). Ferroptosis: process and function. *Cell Death Differ.* 23, 369–379. doi: 10.1038/cdd.2015.158

Xiong, H., Chen, S., Lai, L., Yang, H., Xu, Y., Pang, J., et al. (2019). Modulation of miR-34a/SIRT1 signaling protects cochlear hair cells against oxidative stress and delays age-related hearing loss through coordinated regulation of mitophagy and mitochondrial biogenesis. *Neurobiol. Aging* 79, 30–42. doi: 10.1016/j.neurobiolaging.2019.03.013

Yang, M., Chen, P., Liu, J., Zhu, S., Kroemer, G., Klionsky, D. J., et al. (2019). Clockophagy is a novel selective autophagy process favoring ferroptosis. *Sci. Adv.* 5:eaaw2238. doi: 10.1126/sciadv.aaw2238

Yang, Q., Sun, G., Yin, H., Li, H., Cao, Z., Wang, J., et al. (2018). PINK1 Protects Auditory Hair Cells and Spiral Ganglion Neurons from Cisplatin-induced Ototoxicity via Inducing Autophagy and Inhibiting JNK Signaling Pathway. *Free Rad. Biol. Med.* 120, 342–355. doi: 10.1016/j.freeradbiomed.2018.02.025

Youn, C. K., Jun, Y., Jo, E. R., and Cho, S. I. (2020). Age-Related Hearing Loss in C57BL/6J Mice Is Associated with Mitophagy Impairment in the Central Auditory System. *Int. J. Mol. Sci.* 21:7202. doi: 10.3390/ijms21197202

Yu, X., Guan, M., Shang, H., Teng, Y., Teng, Y., Wang, B., et al. (2021). The expression of PHB2 in the cochlea: Possible relation to age-related hearing loss. *Cell Biol. Int.* 45, 2490–2498. doi: 10.1002/cbin.11693

Yuan, H., Wang, X., Hill, K., Chen, J., Lemasters, J., Yang, S. M., et al. (2015). Autophagy attenuates noise-induced hearing loss by reducing oxidative stress. *Antioxid. Redox Signal.* 22, 1308–1324. doi: 10.1089/ars.2014.6004

Zhang, Y., Fang, Q., Wang, H., Qi, J., Sun, S., Liao, M., et al. (2022). Increased mitophagy protects cochlear hair cells from aminoglycoside-induced damage. *Autophagy* [Epub ahead of print]. doi: 10.1080/15548627.2022.2062872

Zhao, J., Dar, H. H., Deng, Y., St Croix, C. M., Li, Z., Minami, Y., et al. (2020). PEBP1 acts as a rheostat between prosurvival autophagy and ferroptotic death in asthmatic epithelial cells. *Proc. Natl. Acad. Sci. U.S.A.* 117, 14376–14385. doi: 10.1073/pnas.1921618117

Zhao, T., Yu, Z., Zhou, L., Wang, X., Hui, Y., Mao, L., et al. (2022). Regulating Nrf2-GPx4 axis by bicyclol can prevent ferroptosis in carbon tetrachloride-induced acute liver injury in mice. *Cell Death Discov.* 8:380. doi: 10.1038/s41420-022-01173-4

Zhao, T., Zheng, T., Yu, H., Hu, B. H., Hu, B., Ma, P., et al. (2021). Autophagy impairment as a key feature for acetaminophen-induced ototoxicity. *Cell Death Dis.* 12:3. doi: 10.1038/s41419-020-03328-6

Zheng, Z., Tang, D., Zhao, L., Li, W., Han, J., Hu, B., et al. (2020). Liproxstatin-1 Protects Hair Cell-Like HEI-OC1 Cells and Cochlear Hair Cells against Neomycin Ototoxicity. *Oxid. Med. Cell. Long.* 2020:1782659. doi: 10.1155/2020/1782659

Zilka, O., Shah, R., Li, B., Friedmann Angeli, J. P., Griesser, M., Conrad, M., et al. (2017). On the Mechanism of Cytoprotection by Ferrostatin-1 and Liproxstatin-1 and the Role of Lipid Peroxidation in Ferroptotic Cell Death. *ACS Central Sci.* 3, 232–243. doi: 10.1021/acscentsci.7b00028

Zine, A., Messat, Y., and Fritzsch, B. (2021). A human induced pluripotent stem cell-based modular platform to challenge sensorineural hearing loss. *Stem Cells* 39, 697–706. doi: 10.1002/stem.3346

frontiers | Frontiers in Molecular Neuroscience

TYPE Original Research
PUBLISHED 26 April 2023
DOI 10.3389/fnmol.2023.1064579

OPEN ACCESS

EDITED BY
Stefan Liebau,
University of Tübingen, Germany

REVIEWED BY
Francoise Helmbacher,
UMR7288 Institut de Biologie du Développement de Marseille (IBDM), France
Hongzhe Li,
United States Department of Veterans Affairs, United States

*CORRESPONDENCE
Zu-hong He
✉ hezuhong@163.com
Wei-jia Kong
✉ entwjkong@hust.edu.cn

†These authors have contributed equally to this work

RECEIVED 08 October 2022
ACCEPTED 11 April 2023
PUBLISHED 26 April 2023

CITATION
Mu Y-r, Zou S-y, Li M, Ding Y-y, Huang X, He Z-h and Kong W-j (2023) Role and mechanism of FOXG1-related epigenetic modifications in cisplatin-induced hair cell damage. *Front. Mol. Neurosci.* 16:1064579. doi: 10.3389/fnmol.2023.1064579

Role and mechanism of FOXG1-related epigenetic modifications in cisplatin-induced hair cell damage

Yu-rong Mu[1†], Sheng-yu Zou[2†], Ming Li[1], Yan-yan Ding[1], Xiang Huang[1], Zu-hong He[2*] and Wei-jia Kong[1*]

[1]Department of Otorhinolaryngology, Union Hospital, Tongji Medical College, Huazhong University of Science and Technology, Wuhan, China, [2]Department of Otorhinolaryngology-Head and Neck Surgery, Zhongnan Hospital of Wuhan University, Wuhan, China

Cisplatin is widely used in clinical tumor chemotherapy but has severe ototoxic side effects, including tinnitus and hearing damage. This study aimed to determine the molecular mechanism underlying cisplatin-induced ototoxicity. In this study, we used CBA/CaJ mice to establish an ototoxicity model of cisplatin-induced hair cell loss, and our results showed that cisplatin treatment could reduce FOXG1 expression and autophagy levels. Additionally, H3K9me2 levels increased in cochlear hair cells after cisplatin administration. Reduced FOXG1 expression caused decreased microRNA (miRNA) expression and autophagy levels, leading to reactive oxygen species (ROS) accumulation and cochlear hair cell death. Inhibiting miRNA expression decreased the autophagy levels of OC-1 cells and significantly increased cellular ROS levels and the apoptosis ratio *in vitro*. *In vitro*, overexpression of FOXG1 and its target miRNAs could rescue the cisplatin-induced decrease in autophagy, thereby reducing apoptosis. BIX01294 is an inhibitor of G9a, the enzyme in charge of H3K9me2, and can reduce hair cell damage and rescue the hearing loss caused by cisplatin *in vivo*. This study demonstrates that FOXG1-related epigenetics plays a role in cisplatin-induced ototoxicity through the autophagy pathway, providing new ideas and intervention targets for treating ototoxicity.

KEYWORDS

cisplatin, ototoxicity, hair cells, FOXG1, epigenetics, autophagy

Introduction

Cisplatin is widely used to treat tumors but frequently causes ototoxicity, including tinnitus and hearing loss (Lanvers-Kaminsky et al., 2017). Cisplatin-related ototoxicity is cumulative with dose and time (Keilty et al., 2021) and may be related to various factors, such as DNA damage, oxidative stress, and cellular inflammatory factors (Wu et al., 2021). Cisplatin is widely used in clinical practice despite the risk of ototoxicity (Kros and Steyger, 2019). While numerous studies have been conducted, the mechanism underlying cisplatin-induced ototoxicity remains elusive.

Forkhead box G1 (FOXG1) plays an important role in the development of hair cells (HCs) and supporting cells and the innervation of cochlear and vestibular neuron (Pauley et al., 2006; Zhang et al., 2020). However, the exact role of FOXG1 in cisplatin-induced ototoxic injury remains unclear. In this study, we use a cisplatin-induced HC damage model to determine the underlying mechanism of FOXG1 in ototoxicity.

Autophagy is an essential intracellular process that transports cytoplasmic substances to lysosomes for degradation (Klionsky et al., 2021). Previous studies have shown that FOXG1 plays an important role in the process of hearing degradation by regulating autophagy (He et al., 2021). BIX01294 is an inhibitor of G9a, the enzyme in charge of Histone H3 lysine 9 dimethylation (H3K9me2), and can induce autophagy in various cell types, including neuroblastoma (Ke et al., 2014), glioma stem-like (Ciechomska et al., 2016), oral squamous cell carcinoma (Ren et al., 2015), breast and colon cancer (Kim et al., 2013), and osteosarcoma (Fan et al., 2015) cells. Many microRNAs (miRNAs) regulate the autophagy pathway and influence body processes (Mao et al., 2018; Yuan et al., 2018; Chen et al., 2019; Xie et al., 2019; Khodakarimi et al., 2021). In addition, BIX01294 can reduce HCs loss in organ of Corti explant under cisplatin treatment (Yu et al., 2013). The roles of FOXG1, autophagy, and H3K9me2 in mammalian hair cells and their interrelationships in cisplatin ototoxicity require further exploration.

H3K9me2 modifications and miRNA activities are epigenetic processes. Epigenetics is the regulation of gene expression programs in conjunction with DNA templates including DNA modification, histone modification, and noncoding RNA regulation (Han and He, 2016). H3K9me2 levels increase after neomycin and cisplatin is applied to the cochlea; however, this increase disappears after prolonged neomycin action, indicating that changes in H3K9me2 levels after HC injuries are dynamic (Yu et al., 2013). Epigenetic modifications play an important role in development, protection, and regeneration of inner ear (Layman and Zuo, 2014).

In the present study, we analyzed the roles and mechanisms of FoxG1 and epigenetics in cisplatin-induced hair cell loss in CBA/CaJ mouse model. Our data show that FOXG1 regulates autophagy levels under cisplatin-induced HC injury and that FOXG1 overexpression activates autophagy after cisplatin treatment. We also evaluated H3K9me2 levels in OC-1 cells and cochlea after cisplatin treatment and found that H3K9me2 affects autophagy through FOXG1, affecting the ability of autophagy-related miRNAs to regulate autophagy. Inhibition of H3K9me2 helps reduce hearing and hair cell loss induced by cisplatin *in vivo*. This study demonstrates the important roles of FOXG1 and epigenetics in cisplatin-induced ototoxicity through the autophagy pathway, providing a new target for investigating cisplatin-associated ototoxicity.

Results

Construction of a cisplatin-induced ototoxicity animal model

Furosemide transiently decreases the red blood cell count in the stria vascularis on the cochlear lateral wall, allowing cisplatin to easily pass through the blood–ear barrier into the cochlea (Li et al., 2011). We administered furosemide at 200 mg/kg (intraperitoneal) and cisplatin at different concentrations (0.5, 1, 1.5, and 2 mg/kg, subcutaneous) daily for three consecutive days to CBA/CaJ mice to create the model, followed by 3 days of post-treatment recovery. Mouse hearing was evaluated based on the auditory brainstem response (ABR). The threshold of click ABR in the treatment groups (mice treated with different cisplatin concentrations) was higher than that in the control group to different degrees (Figure 1A, $p < 0.05$). In the treatment groups, the tone burst ABR showed varying degrees of loss at 8, 16, 24, 32, and 40 kHz, and the tone burst ABR loss increased as cisplatin concentrations increased (Figure 1B, $p < 0.05$). After modeling, the cochlea was dissected, and cochlear HC loss was assessed via immunofluorescence staining with phalloidin and DAPI. Outer HCs loss in the cochlea worsened with increasing cisplatin concentrations (Figures 1C, D, $p < 0.05$, $n = 3$). The loss of outer HCs began from the base turn and spread toward the apex of the sensory epithelium of Corti as the cisplatin concentration increased.

OC-1 cell viability decreases with increasing cisplatin concentrations and treatment times

HEI-OC1 is one of the most commonly used mouse auditory cell lines suitable for exploring ototoxic drug models (Kalinec et al., 2016). We treated OC-1 cells with cisplatin at different concentrations and times to construct the cisplatin-induced OC-1 cell cytotoxicity model. First, we treated OC-1 cells with 5, 10, 30, 50, and 100 μM cisplatin for 24 h and detected their viability with CCK-8. Viable OC-1 cell numbers gradually decreased with increasing cisplatin concentrations. Approximately 50% of the OC-1 cells were viable 24 h after 30 μM cisplatin treatment (Figure 2A, $p < 0.001$, $n = 6$).

Then, we treated OC-1 cells with 5 μM cisplatin for 12, 24, 48, and 72 h and assessed cell viability with CCK-8. Viable OC-1 cell numbers gradually decreased as the treatment time increased, significantly decreasing at 72 h (Figure 2B, $p < 0.05$, $n = 3$). Subsequently, we treated OC-1 cells with 30 μM cisplatin for 12, 24, 48, and 72 h and assessed cell viability with CCK-8. Viable OC-1 cell numbers decreased significantly over time with this higher cisplatin concentration (Figure 2C, $p < 0.05$, $n = 3$).

Next, we treated OC-1 cells with 5, 10, 30, 50, and 100 μM cisplatin for 24 h and labeled apoptotic cells with annexin V and dead cells with propidium iodide (PI) to assess the apoptotic and dead cell ratio by flow cytometry. The apoptotic and dead cell ratios of OC-1 cells gradually increased as the cisplatin concentration increased (Figures 2D–F, $p < 0.01$, $n = 3$). Additionally, OC-1 cells were treated with low (5 μM) or high (30 μM) cisplatin concentrations for 12, 24, 48, and 72 h before flow cytometry. The apoptotic and dead cell ratios of OC-1 cells gradually increased as the cisplatin treatment time increased (Figures 2G–K, $p < 0.05$, $n = 3$).

The accumulation of mitochondrial superoxide in cells can induce DNA damage and ultimately lead to cell damage (Srinivas et al., 2019). We detected the level of oxidative stress in OC-1 cells by Mito-SOX flow cytometry. After treatment with 5, 10, 30, 50, and 100 μM cisplatin for 24 h, the flow cytometry results showed that ROS levels in OC-1 cells gradually increased as the cisplatin concentration increased (Figures 3A, B, $p < 0.01$, $n = 3$). Next, OC-1 cells were treated with low (5 μM) or high (30 μM) cisplatin concentrations for 12, 24, 48, and 72 h before

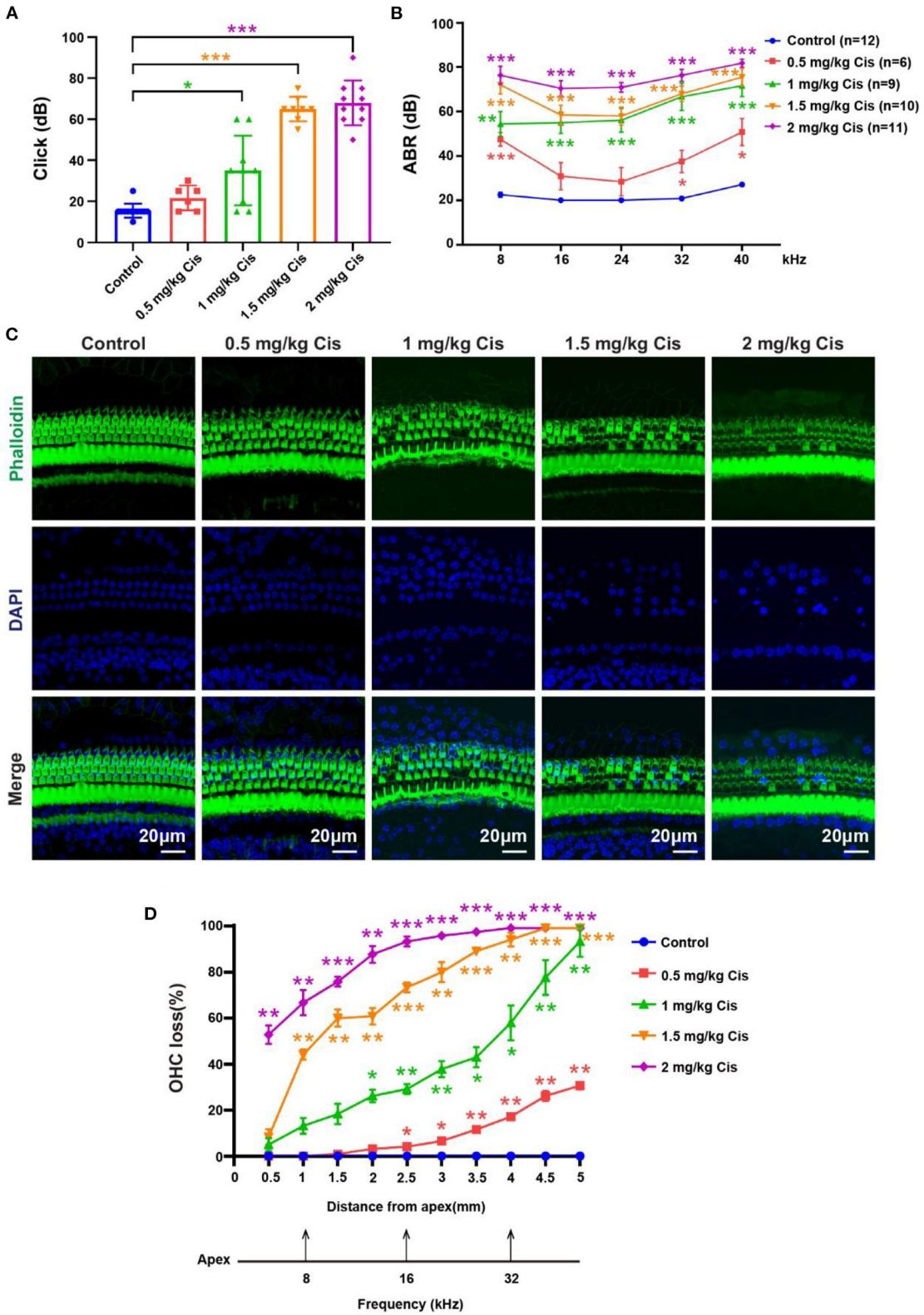

FIGURE 1
Results of the hearing loss model treated with different cisplatin concentrations. **(A)** Statistical scatter plot of the click ABR. **(B)** Statistical line chart of the tone burst ABR. **(C)** Immunofluorescence staining with phalloidin and DAPI in the cochlea. **(D)** Quantification of the immunofluorescence staining in the cochlea. *p <0.05, **p <0.01, ***p< 0.001.

10.3389/fnmol.2023.1064579

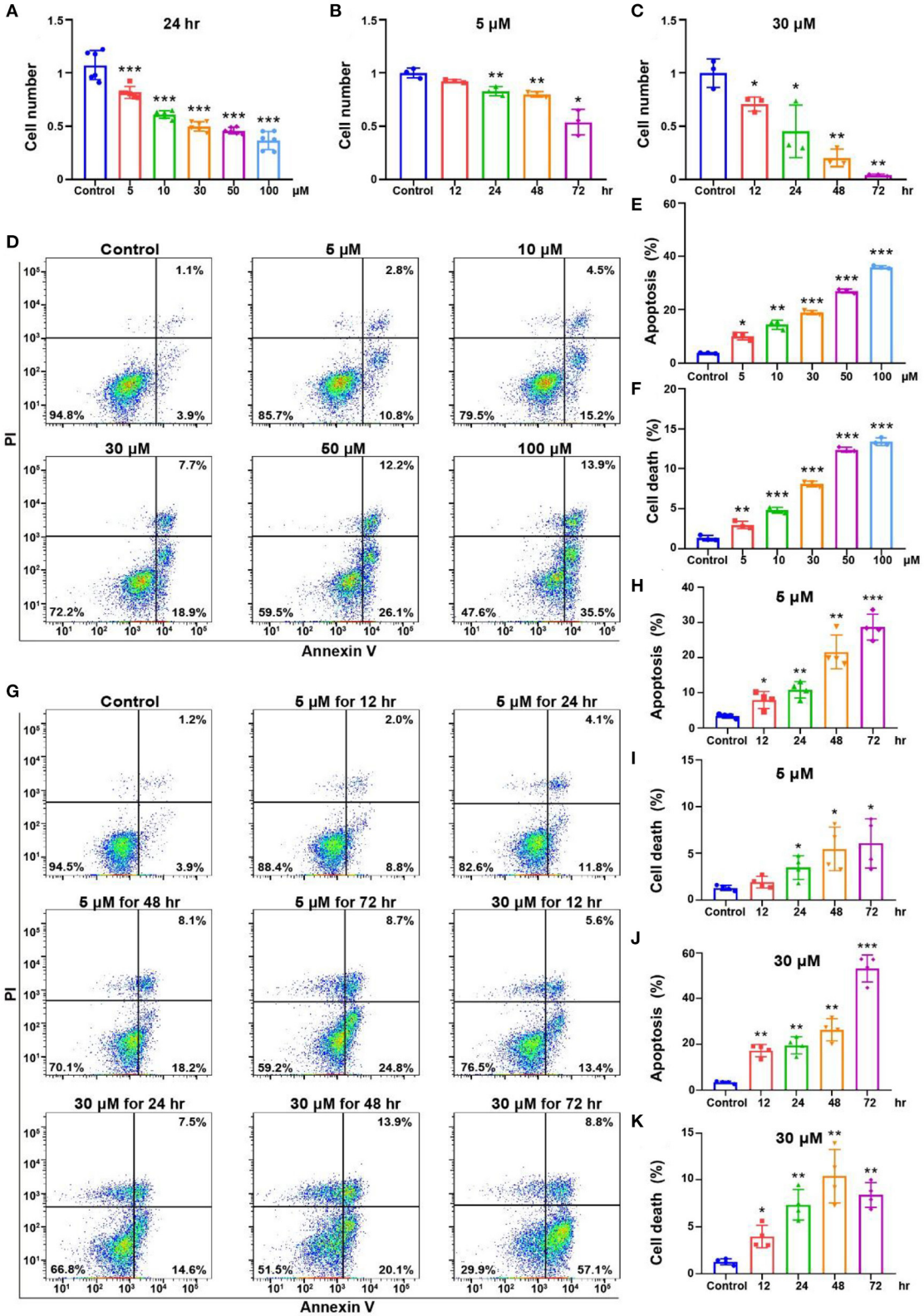

FIGURE 2
Cell viability and apoptosis flow cytometry results for the OC-1 cells treated with different concentrations of cisplatin. **(A)** CCK-8 cell viability changes after different concentrations of cisplatin treatment for 24 h. **(B)** CCK-8 cell viability changes after 5 μM cisplatin treatment for different times. **(C)** CCK-8 cell viability changes after 30 μM cisplatin treatment for different times. **(D)** Flow cytometry of apoptosis in cells treated with different cisplatin concentrations for 24 h. **(E)** Quantification of the apoptosis ratio in **(D)**. **(F)** Quantification of the cell death ratio in **(D)**. **(G)** Flow cytometry of cells treated with 5 or 30 μM cisplatin for different times. **(H)** Quantification of the apoptosis ratio in **(G)**. **(I)** Quantification of the cell death in **(G)**. **(J)** Quantification of the apoptosis ratio in **(G)**. **(K)** Quantification of the cell death ratio in **(G)**. $^{*}p < 0.05$, $^{**}p < 0.01$, $^{***}p < 0.001$.

Mito-SOX flow cytometry. The low cisplatin concentration (5 μM) slightly increased ROS levels in OC-1 cells over time, becoming significant after a longer period (Figures 3C, D, $p < 0.05$, $n = 3$). The high cisplatin concentration (30 μM) significantly increased ROS levels in OC-1 cells over time (Figures 3C, E, $p < 0.05$, $n = 3$). After cisplatin treatment, the level of ROS in OC-1 cells increased, indicating that ROS accumulates in OC-1 cells as cisplatin concentrations and treatment times increase.

FOXG1 expression and autophagy level are altered by cisplatin treatment

FOXG1 is a nuclear transcription factor that participates in morphogenesis, cell fate determination, and proliferation and is required for mammalian inner ear morphogenesis (Zhang et al., 2020). FOXG1 is related to the survival of HCs; however, the specific downstream pathways and mechanisms are unclear. FOXG1 is related to mitochondrial function and metabolism, as is autophagy (He et al., 2020). Autophagy is an essential intracellular process that transports cytoplasmic substances to lysosomes for degradation (Klionsky et al., 2021). It plays a crucial role in adaptive responses to starvation and other forms of stress (Jiang and Mizushima, 2014). Autophagy is involved in multiple signaling pathways and contributes to HC development and protection. With autophagy pathway activation, autophagosomes can envelop the damaged mitochondria and fuse with lysosomes to form autolysosomes, degrading the damaged mitochondria and promoting HC survival (He et al., 2017).

To investigate changes in FOXG1 and autophagy levels after cisplatin treatment in a mouse model, we administered furosemide and different cisplatin concentrations. We dissected the cochlea 3 days post-cisplatin treatment and extracted proteins for western blotting. FOXG1 and LC3B levels in the cochlea increased relative to the control after treatment with low cisplatin concentrations but decreased with high cisplatin concentrations (Figures 4A–C, $p < 0.05$, $n = 3$). Immunofluorescence staining showed similar LC3B levels in the cochlea after cisplatin treatment to those observed by western blotting. LC3B fluorescence intensity increased after treatment with 0.5 mg/kg cisplatin but decreased with 1.5 mg/kg cisplatin (Figure 4D, $p < 0.05$, $n = 3$).

We next treated in OC-1 cells with 5 and 30 μM cisplatin for 24 h and performed transmission electron microscopy (TEM) to confirm the changes in autophagy after cisplatin treatment. The 5 μM cisplatin group demonstrated a significantly higher number of autophagic vacuoles and autolysosomes than the control group. In contrast, the 30 μM cisplatin treatment group showed a significantly lower number of autophagic vacuoles and autolysosomes than the control group (Figures 4E–G, $p < 0.05$, $n = 3$).

Next, we treated OC-1 cells with 5, 10, 30, 50, and 100 μM cisplatin for 24 h and detected changes in FOXG1 and LC3B levels. Western blotting showed that FOXG1 levels increased with 5 μM cisplatin relative to the control but decreased when the cisplatin concentrations exceeded 30 μM. Similarly, LC3B levels increased with 5 and 10 μM cisplatin treatment before gradually decreasing when the cisplatin concentrations exceeded 30 μM. These findings indicate that autophagy levels initially increase and then decrease as cisplatin concentration increases (Figures 4H–J, $p < 0.05$, $n = 3$).

Then, we treated OC-1 cells with 5 μM cisplatin for 12, 24, 48, and 72 h and detected changes in FOXG1 and LC3B levels. Western blotting showed that FOXG1 and LC3B levels were increased relative to the control in the treatment group at 48 h; however, no significant differences were observed between the treatment and control groups at 72 h (Figures 4K–M, $p < 0.05$, $n = 3$). Finally, we repeated this experiment with 30 μM cisplatin. Western blotting showed that FOXG1 and LC3B levels gradually decreased after cisplatin treatment (Figures 4N–P, $p < 0.05$, $n = 3$). These results suggest that FOXG1 plays an important protective role against cisplatin-induced ototoxic damage in OC-1 cells. However, FOXG1 and autophagy levels are significantly reduced after the cell damage exceeds its repair capacity.

We found that cisplatin treatment could affect FOXG1 expression and autophagy pathway. Our previous study showed that FOXG1 could regulate the autophagy pathway in presbycusis (He et al., 2021). Here, low cisplatin doses activated FOXG1 expression and the autophagy pathway. As the cisplatin concentration gradually increased, FOXG1 and LC3B expression levels decreased. Therefore, we speculate that low concentrations of cisplatin activate the cells' self-defense mechanism, increasing FOXG1 expression and activating the autophagy pathway to eliminate ROS in OC-1 cells. With high concentrations of cisplatin, cells gradually lose their self-defense ability, significantly reducing FOXG1 expression and autophagy levels.

H3K9me2 changes in HCs after cisplatin treatment

Epigenetic modifications have recently been found to contribute to inner ear development and HC regeneration (Taiber et al., 2022). Histone methylation and demethylation are implicated in transcriptional regulation, genome integrity, and epigenetics (Klose and Zhang, 2007). H3K9 methylation is critical for early embryogenesis and is involved in the transcriptional repression of developmental genes (Tachibana et al., 2002).

We treated the mouse model with different cisplatin concentrations. At 3 days post-cisplatin treatment, we detected changes in H3K9me2 levels in the cochlea, which were decreased relative to the control at low cisplatin concentrations (0.5 and 1 mg/kg) but increased at high cisplatin concentrations (1.5 and 2 mg/kg; Figures 5A, B, $p < 0.05$, $n = 3$). Immunofluorescence staining showed similar H3K9me2 levels in the cochlea after cisplatin treatment to those observed by western blotting. H3K9me2 fluorescence intensity was decreased with 0.5 mg/kg cisplatin but increased with 1.5 mg/kg cisplatin (Figure 5C, $p < 0.05$, $n = 3$). We then treated OC-1 cells with 5, 10, 30, 50, and 100 μM cisplatin for 24 h and detected H3K9me2 levels. H3K9me2 levels decreased with 0.5 μM cisplatin relative to control but increased when cisplatin concentrations exceeded 10 μM (Figures 5D, E, $p < 0.05$, $n = 3$). H3K9me2 levels decreased relative to control after low-concentration cisplatin treatment *in vivo* and *in vitro*. When the concentration of cisplatin increased, the level

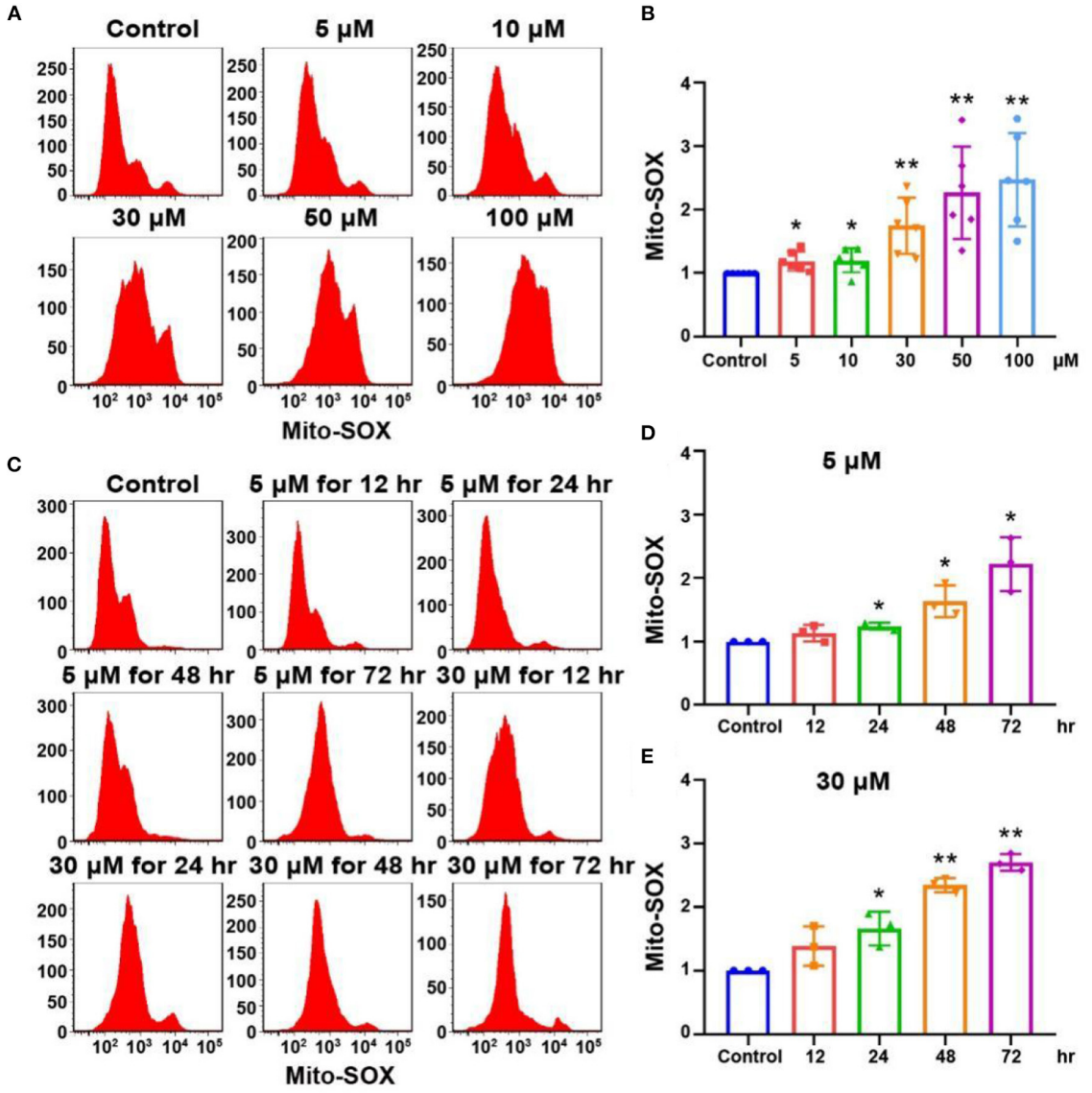

FIGURE 3
Mito-SOX flow cytometry of OC-1 cells treated with different cisplatin concentrations and times. **(A)** ROS levels in cells treated with different cisplatin concentrations for 24 h. **(B)** Quantification of the data in A. **(C)** ROS levels in cells treated with 5 or 30 μM cisplatin for different times. **(D)** Quantification of the data in **(C)**. **(E)** Quantification of the data in **(C)**. *$p < 0.05$, **$p < 0.01$.

of H3K9me2 increased, and the expression of FOXG1 and the autophagy pathway were inhibited.

BIX01294 is an inhibitor of euchromatic histone methyltransferase G9a that can transiently and reversibly inhibit H3K9me2 activity by competing with G9a for substrates (Kubicek et al., 2007; Kondengaden et al., 2016; Milite et al., 2019). H3K9me2 inhibition by BIX01294 can induce autophagy in various cell types, including glioblastoma cells (Ciechomska et al., 2016). Previous studies have shown that BIX01294 can reduce HC loss in organ of Corti explant under cisplatin treatment (Yu et al., 2013).

We treated OC-1 cells with different concentrations (0.5, 1, 2, 3, and 5 μM) of the G9a inhibitor BIX01294 for 24 h to inhibit H3K9me2 levels and detected their viability with CCK-8. Viable OC-1 cell numbers gradually decreased as the BIX01294 concentration increased (Supplementary Figure 1A, $p < 0.05$, $n = 6$). We performed flow cytometry on the BIX01294-treated OC-1 cells to detect changes in the ratios of apoptotic and dead cells. The apoptotic and dead cell ratios of OC-1 cells increased significantly as BIX01294 concentrations increased (Supplementary Figures 1B–D, $p < 0.05$, $n = 3$). We also performed Mito-SOX flow cytometry to detect mitochondrial ROS in the OC-1 cells treated with BIX01294. ROS levels in OC-1 cells increased significantly as BIX01294 concentrations increased (Supplementary Figures 2A, B, $p < 0.05$, $n = 3$).

Next, we treated OC-1 cells with different BIX01294 concentrations (0.5, 1, 2, 3, and 5 μM) for 24 h and detected G9a

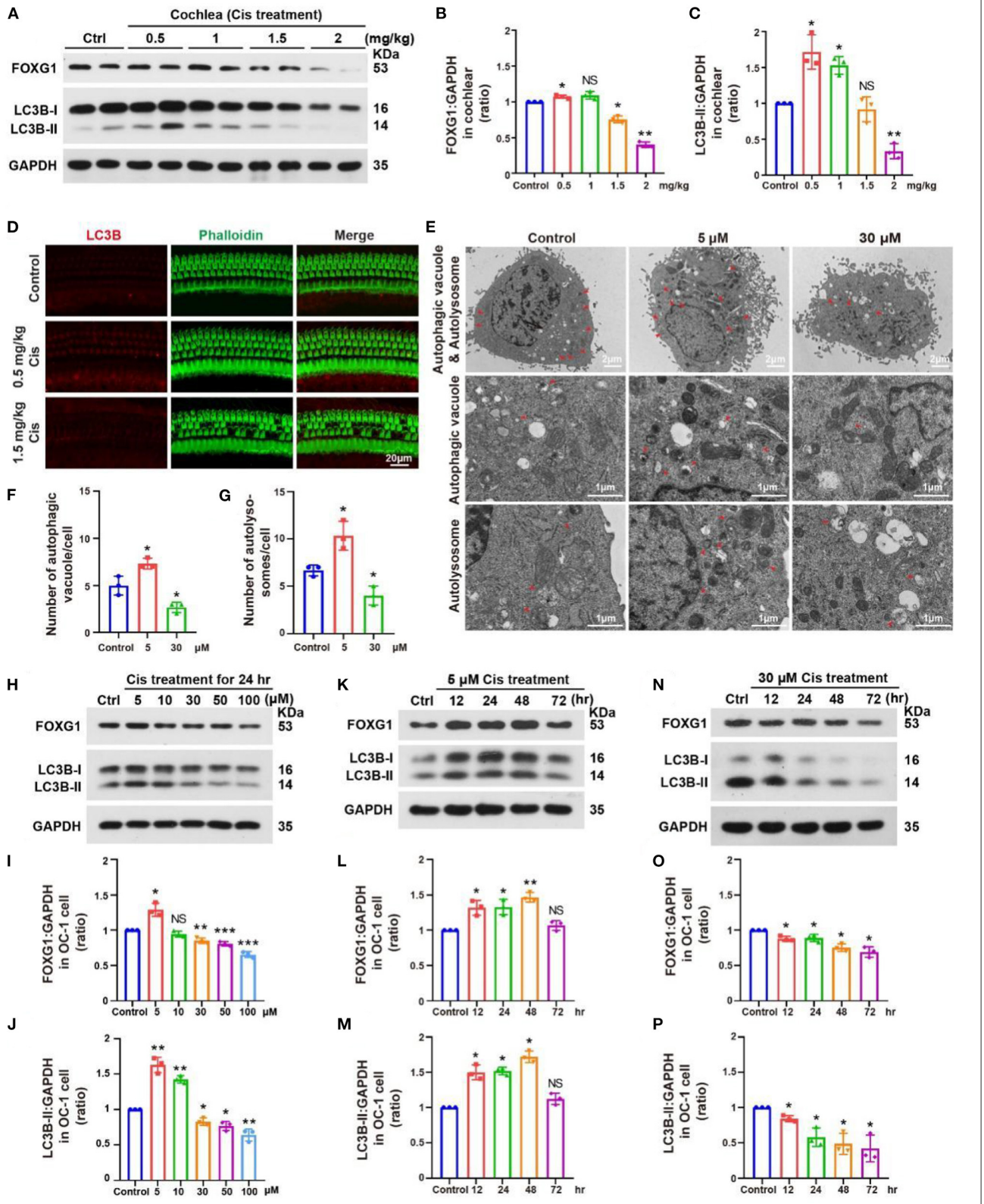

FIGURE 4
Changes in FOXG1 and autophagy levels in the cochlea and OC-1 cells after cisplatin treatment. **(A)** Western blotting of changes in FOXG1 and LC3B levels in the cochlea after treatment with different cisplatin concentrations. **(B, C)** Quantification of the western blotting in **(A)**. **(D)** Immunofluorescence staining for LC3B and phalloidin in the cochlea after cisplatin treatment. **(E)** TEM of changes in autophagic vacuoles and autolysosomes after treatment with 5 or 30 μM cisplatin for 24 h. **(F)** Quantification of the autophagic vacuoles changes in **(E)**. **(G)** Quantification of the autolysosomes changes in **(E)**. **(H)** Western blotting of changes in FOXG1 and LC3B levels after treatment with different cisplatin concentrations for 24 h. **(I, J)** Quantification of the western blotting in **(H)**. **(K)** Western blotting of changes in FOXG1 and LC3B levels after treatment with 5 μM cisplatin for different times. **(L, M)** Quantification of the western blotting in **(K)**. **(N)** Western blotting of changes in FOXG1 and LC3B levels after treatment with 30 μM cisplatin for different times. **(O, P)** Quantification of the western blotting in **(N)**. $*p < 0.05$, $**p < 0.01$, $***p < 0.001$.

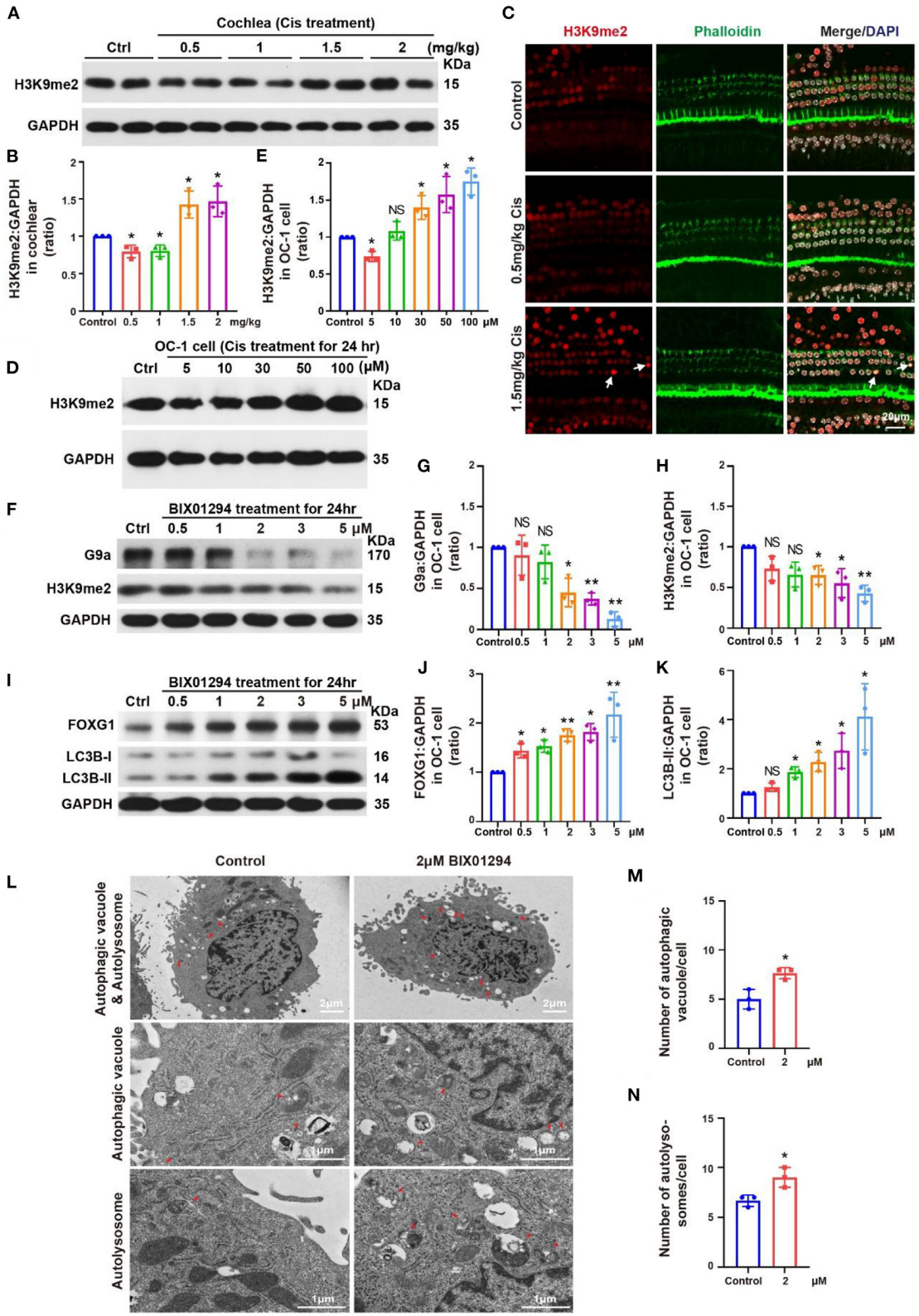

FIGURE 5
Changes in H3K9me2 levels in the cochlea and OC-1 cells after treatment with different cisplatin concentrations. **(A)** Western blotting of changes in H3K9me2 levels in the cochlea after treatment with different cisplatin concentrations. **(B)** Quantification of the western blotting in **(A)**. **(C)** Immunofluorescence staining for H3K9me2, phalloidin, and DAPI in the cochlea after cisplatin treatment. **(D)** Western blotting of changes in H3K9me2 levels after treatment with different cisplatin concentrations for 24 h. **(E)** Quantification of the western blotting in **(D)**. **(F)** Western blotting of changes in H3K9me2 levels with different BIX01294 concentrations for 24 h. **(G, H)** Quantification of the western blotting in **(F)**. **(I)** Western blotting of changes in FOXG1 and LC3B levels after treatment with different BIX01294 concentrations for 24 h. **(J, K)** Quantification of the western blotting in **(I)**. **(L)** TEM of the changes in autophagic vacuoles and autolysosomes after treatment with 2 μM BIX01294 for 24 h. **(M)** Quantification of the autophagic vacuoles changes in **(L)**. **(N)** Quantification of the autolysosomes changes in **(L)**. *$p < 0.05$, **$p < 0.01$.

and H3K9me2 levels. G9a and H3K9me2 levels gradually decreased as BIX01294 concentrations increased (Figures 5F–H, $p < 0.05$, $n = 3$). We then detected FOXG1 and LC3B levels, which gradually increased as BIX01294 concentrations increased (Figures 5I–K, $p < 0.05$, $n = 3$). To confirm the changes in autophagy after BIX01294 treatment, we treated OC-1 cells with 2 μM BIX01294 for 24 h and performed TEM. The 2 μM BIX01294 treatment group showed significantly increased autophagic vacuoles and autolysosomes compared to the control group (Figures 5L–N, $p < 0.05$, $n = 3$). FOXG1 and LC3B levels significantly increased after BIX01294 treatment, indicating that H3K9me2 may be an upstream regulator of FOXG1 and autophagy. After treating OC-1 cells with BIX01294, the H3K9me2 level decreased significantly, and the expressions of FOXG1 and LC3B increased significantly. Overall, FOXG1 and autophagy levels increased and H3K9me2 levels decreased in response to low-concentration cisplatin. At high concentrations of cisplatin, the levels of FOXG1 and autophagy decreased, while the level of H3K9me2 increased. These findings suggest that H3K9me2 may be the upstream regulator of FOXG1 and autophagy.

H3K9me2 may regulate autophagy pathway activation through FOXG1

We used small interfering RNAs (siRNAs) to knock down *Foxg1* expression in OC-1 cells and quantified FOXG1 and LC3B levels. LC3B levels decreased significantly after FOXG1 knockdown (Figures 6A–C, $p < 0.05$, $n = 3$). Next, we constructed a plasmid to overexpress FOXG1 in OC-1 cells and found that FOXG1 expression increased after plasmid transfection (Figures 6D, E, $p < 0.05$, $n = 3$). Then, we treated OC-1 cells transfected with the *Foxg1*-overpressing plasmid with cisplatin; this overexpression rescued the decrease in autophagy levels caused by cisplatin (Figures 6F, G, $p < 0.05$, $n = 3$). These results indicate that FOXG1 might upregulate autophagy during cisplatin injury.

We further explored whether FOXG1 silencing inhibited BIX01294-induced LC3B activation and found that FOXG1 was required for BIX01294-induced autophagy activation (Figures 6H, I, $p < 0.05$, $n = 3$). Finally, we treated OC-1 cells with BIX01294 followed by cisplatin and found that BIX01294 prevented the decreases in FOXG1 and autophagy levels caused by cisplatin (Figures 6J–L, $p < 0.05$, $n = 3$). These results indicate that H3K9me2 may regulateg autophagy through a FOXG1-dependent pathway.

FOXG1 and H3K9me2 regulate autophagy pathway activation through autophagy-related miRNAs

Many microRNAs (miRNAs) regulate the autophagy pathway and influence various body processes (Khodakarimi et al., 2021), including miR-34a, miR-96, miR-182, and miR-183, which are associated with apoptosis and autophagy. For example, miR-34 overexpression significantly decreased ovarian cancer cell proliferation by activating apoptosis and autophagy (Jia et al., 2019). miR-96 overexpression inhibits autophagosome formation in the hippocampus by inhibiting Atg7 and Atg16L1 expression (Gan et al., 2017). Reduced miR-182 expression inhibits RAB10 expression, reducing cell viability and autophagy and promoting apoptosis in gastric cancer cells (Duan et al., 2022). miR-183 knockdown in medullary thyroid carcinoma increases LC3B expression, reducing cell proliferation (Abraham et al., 2011). Therefore, we studied the relationships among FOXG1, H3K9me2, and autophagy-related miRNAs.

We extracted RNA from OC-1 cells after siRNA-*Foxg1* treatment and detected changes in several autophagy-related miRNAs with rt-PCR. miR-34a, miR-96, miR-182, and miR-183 expression levels decreased FOXG1 expression decreased. In contrast, miR-15a and miR-124 levels did not change significantly (Figure 7A, $p < 0.05$, $n = 3$). We treated OC-1 cells pretreated with BIX01294 or overexpressing FOXG1 with 30 μM cisplatin for 24 h and extracted RNA to detect miR-34a, miR-96, miR-182, and miR-183 expression levels. miR-34a, miR-96, miR-182, and miR-183 levels decreased after cisplatin treatment, and pre-treatment with BIX01294 or FOXG1 overexpression prevented this decrease (Figure 7B, $p < 0.05$, $n = 3$).

Next, we studied the regulatory effect of miRNAs on the autophagy pathway. We used an miRNA inhibitor to inhibit target miRNA expression in OC-1 cells and determined the inhibition efficiency of miR-34a, miR-96, miR-182, and miR-183 by rt-PCR, revealing significantly inhibited expression (Figure 7C, $p < 0.001$, $n = 3$). Then, we quantified LC3B levels with miR-34a, miR-96, miR-182, and miR-183 inhibition, revealing significantly decreased expression (Figures 7D, E, $p < 0.05$, $n = 3$). Furthermore, we examined BIX01294's regulatory effect on autophagy with miR-34a, miR-96, miR-182, and miR-183 inhibition. LC3B levels were decreased after BIX01294 treatment when these four miRNAs were inhibited (Figures 7F, G, $p < 0.05$, $n = 3$).

miRNA mimics are commonly used to overexpress target miRNAs. We used miRNA mimics to overexpress miR-34a, miR-96, miR-182, and miR-183 in OC-1 cells and assessed their overexpression efficiency with rt-PCR, revealing that they were all significantly overexpressed (Figure 7H, $p < 0.001$). Next, we quantified LC3B levels with miR-34a, miR-96, miR-182, and miR-183 overexpression after cisplatin treatment and found that they were increased (Figures 7I, J, $p < 0.05$, $n = 3$), indicating that overexpressing these miRNAs facilitates autophagy activation under cisplatin treatment.

FOXG1 knockdown decreased the levels of miR-34a, miR-96, miR-182, and miR-183 and inhibited the autophagy pathway. Our results showed that the level of autophagy significantly decreased when the expression of the above miRNAs was inhibited. The expression levels of these miRNAs were inhibited after high-dose cisplatin treatment, and this inhibition could be recovered by BIX01294 treatment or overexpressing FOXG1. BIX01294 could not activate the autophagy pathway when these miRNAs were inhibited. However, the overexpression of the above miRNAs could restore autophagy under cisplatin treatment. Our results showed that miR-34a, miR-96, miR-182, and miR-183 were related to the activation of the autophagy pathway, and FOXG1 autophagy regulation is miRNA-dependent.

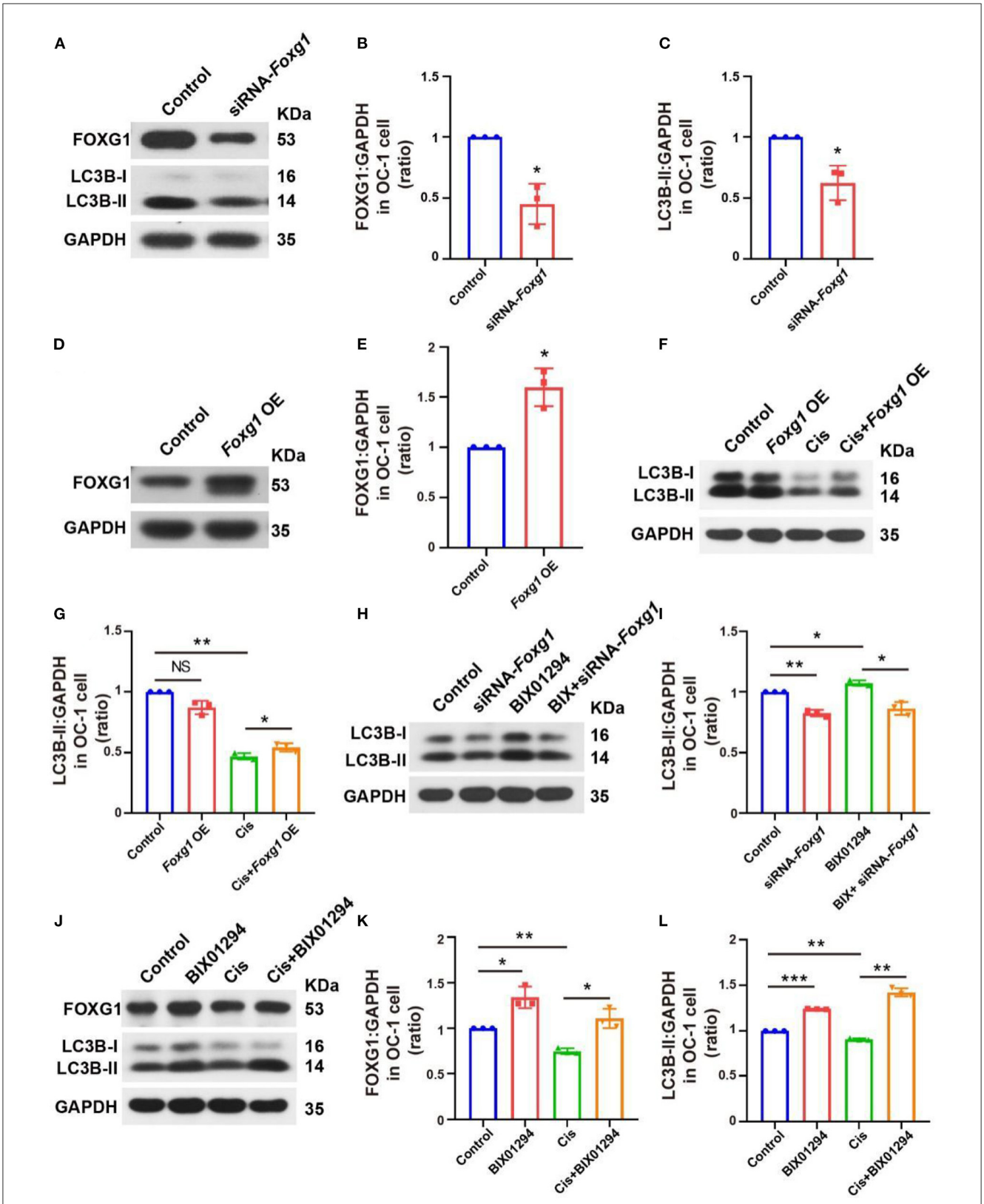

FIGURE 6
FOXG1 and BIX01294 may regulate autophagy pathway activation, and the BIX01294-induced autophagy activation pathway may be FoxG1-dependent. **(A)** Western blotting of FOXG1 and LC3B levels after *Foxg1* knock down. **(B, C)** Quantification of the western blotting in **(A)**. **(D)** Western blotting of the *Foxg1* overexpression plasmid's transfection efficiency. **(E)** Quantification of the western blotting in **(D)**. **(F)** Western blotting LC3B levels with *Foxg1* overexpression and cisplatin treatment. **(G)** Quantification of the western blotting in **(F)**. **(H)** Western blotting of LC3B levels with *Foxg1* knockdown and BIX01294 treatment. **(I)** Quantification of the western blotting in **(H)**. **(J)** Western blotting of FOXG1 and LC3B levels after cisplatin and BIX01294 treatment. **(K, L)** Quantification of the western blotting in **(J)**. $^{*}p < 0.05$, $^{**}p < 0.01$, $^{***}p < 0.001$.

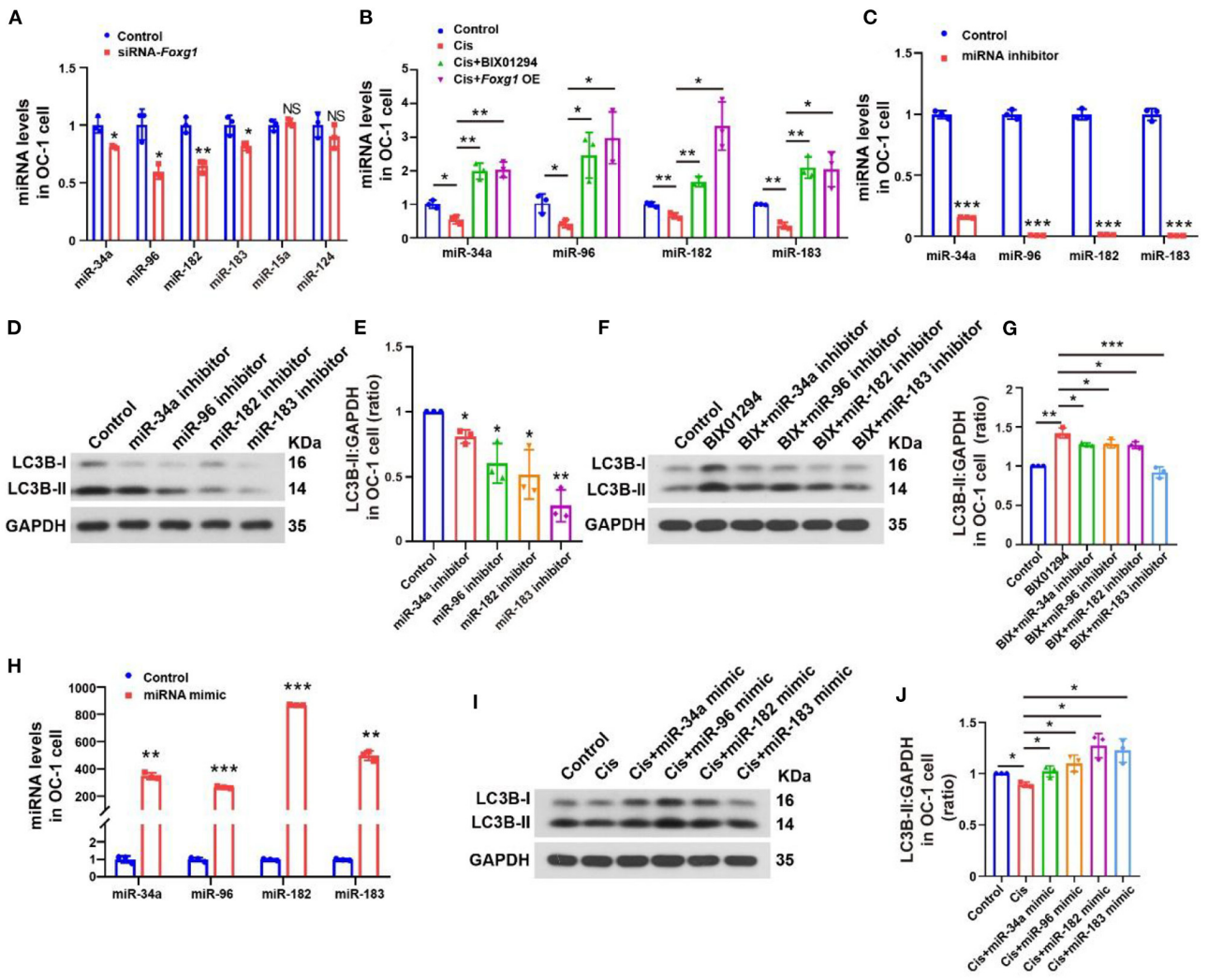

FIGURE 7
Autophagy levels of OC-1 cells change through the regulation of miR-34a, miR-96, miR-182, and miR-183 expression. **(A)** rt-PCR of changes in miR-34a, miR-96, miR-182, and miR-183 expression with *Foxg1* knockdown **(B)** rt-PCR of the expression in miR-34a, miR-96, miR-182, and miR-183 changes after cisplatin treatment with BIX01294 pre-treatment or *Foxg1* overexpression. **(C)** rt-PCR of miR-34a, miR-96, miR-182, and miR-183 expression inhibition efficiency. **(D)** Western blotting of changes in LC3B levels after miR-34a, miR-96, miR-182, and miR-183 inhibition. **(E)** Quantification of the western blotting in **(F)**. **(F)** Western blotting of changes in LC3B levels after BIX01294 treatment with miR-34a, miR-96, miR-182, and miR-183 inhibition. **(G)** Quantification of the western blotting in **(F)**. **(H)** rt-PCR of miRNA mimic efficiency for enhancing miR-34a, miR-96, miR-182, and miR-183 expression. **(I)** Western blotting of changes in LC3B levels after cisplatin treatment with miR-34a, miR-96, miR-182, and miR-183 mimics. **(J)** Quantification of the western blotting in **(F)**. $*p < 0.05$, $**p < 0.01$, $***p < 0.001$.

MiRNA levels are associated with apoptosis ratios and ROS levels in OC-1 cells

We performed flow cytometry on OC-1 cells with inhibited miR-34a, miR-96, miR-182, and miR-183 expression to detect changes in the ratios of apoptotic and dead cells and found that these ratios were significantly increased (Figures 8A–C, $p < 0.05$, $n = 3$). We also performed Mito-SOX flow cytometry to detect mitochondrial ROS levels in these cells and found that they were significantly increased (Figures 8D, E, $p < 0.05$, $n = 3$). The apoptosis and death ratios and the ROS levels of the OC-1 cells, significantly increased as the miRNA levels decreased, suggesting that these miRNAs play an important protective role in OC-1 cell survival.

We also found that BIX01294 treatment induced OC-1 apoptosis with miR-34a, miR-96, miR-182 and miR-183 inhibition (Figures 8F–H, $p < 0.05$, $n = 4$). Furthermore, miR-34a, miR-96, miR-182, and miR-183 overexpression reduced cisplatin-induced apoptosis in OC-1 cells, indicating that overexpression of autophagy-related miRNAs protects OC-1 cells from cisplatin-induced injury (Figures 8I–K, $p < 0.05$, $n = 4$). These results indicate that these miRNAs could rescue OC-1 cell damage during cisplatin injury.

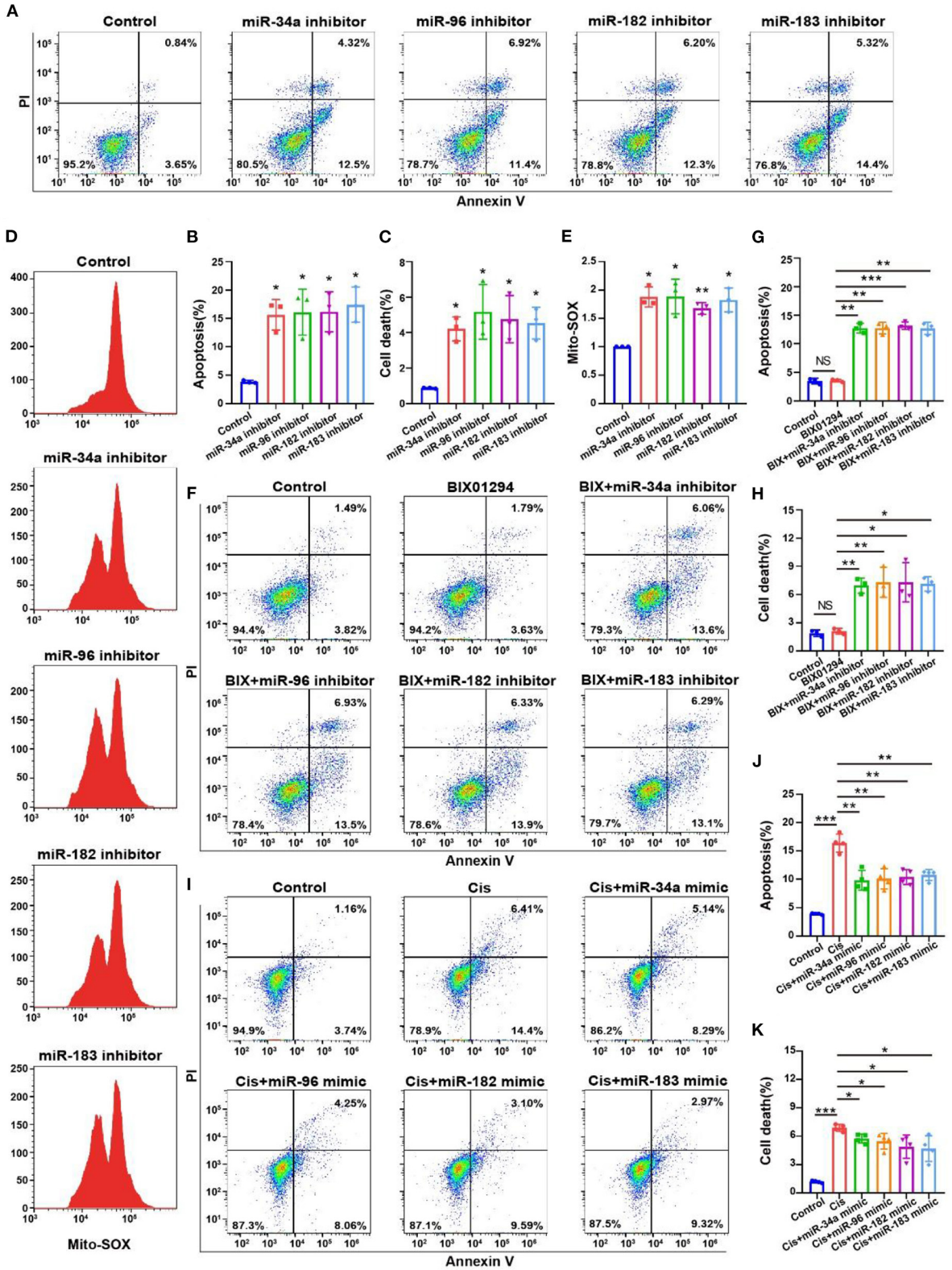

FIGURE 8
Flow cytometry of apoptosis and ROS levels with miR-34a, miR-96, miR-182, and miR-183 regulation in the OC-1 cells. **(A)** Annexin V flow cytometry of apoptosis with miR-34a, miR-96, miR-182, and miR-183 inhibition. **(B)** Quantification of the apoptosis ratio in **(A)**. **(C)** Quantification of the cell death ratio in **(A)**. **(D)** Mito-SOX flow cytometry of cellular ROS level with miR-34a, miR-96, miR-182, and miR-183 inhibition. **(E)** Quantification of the data in **(D)**. **(F)** Annexin V flow cytometry of apoptosis after BIX01294 treatment with inhibiting miR-34a, miR-96, miR-182, and miR-183. **(G)** Quantification of the apoptosis ratio in **(A)**. **(H)** Quantification of the cell death ratio in **(F)**. **(I)** Annexin V flow cytometry of apoptosis after cisplatin treatment with miR-34a, miR-96, miR-182, and miR-183 mimics. **(J)** Quantification of the apoptosis ratio in **(I)**. **(K)** Quantification of the cell death ratio in **(I)**. $*p < 0.05$, $**p < 0.01$, $***p < 0.001$.

BIX01294 can protect against cisplatin-induced ototoxicity *in vivo*

To investigate the role of H3K9me2 in hearing during cisplatin-induced injury, we administrated BIX01294 via intraperitoneal injection before and during cisplatin administration *in vivo*. The groups were treated as follows: 2 mg/kg cisplatin, 2 mg/kg cisplatin +20 mg/kg BIX01294, and 2 mg/kg cisplatin +40 mg/kg BIX01294. We administrated BIX01294 via intraperitoneal injection to CBA/CaJ mice on the day before the initiation of cisplatin injections and half an hour before each furosemide injection. The ABR results showed that 40 mg/kg BIX01294 intraperitoneal injection could rescue cisplatin-induced hearing loss, while the hearing changes in the 20 mg/kg BIX01294 group were not significant compared to the cisplatin-only group (Figures 9A, B). The protective effect of BIX01294 on cisplatin-induced hearing loss was more obvious at low-frequencies. BIX01294 rescued the ABR threshold shift at 16 kHz (Figure 9C). We sacrificed the mice after the ABR test, and the cochlea was dissected after fixation and decalcification. We used Myosin 7a and phalloidin to label HCs and quantify HC loss. We observed that the loss of outer HCs in mice in the cisplatin +40 mg/kg BIX01294 group was significantly reduced compared to that in the cisplatin-only group, especially in the apical and middle turns (Figures 9D, E, $p < 0.05$). These results suggest that BIX01294 reduced the ototoxicity caused by cisplatin and protected hearing in CBA/CaJ mice.

Discussion

Cisplatin is clinically used to treat tumors but has ototoxic side effects. Studying the mechanism of cisplatin-induced ototoxicity is crucial in hearing research. In this study, we conducted related mechanistic experiments since FOXG1-related epigenetics appeared to play a role in cisplatin-induced HC damage.

Auditory system studies have revealed hundreds of miRNAs that are differentially expressed during mammalian inner ear development and aging (Weston et al., 2006; Rudnicki et al., 2014). miRNAs participate in proliferation, apoptosis, and transcription factor regulation, thus playing important roles in organ development and maturation (Harfe, 2005), including sensory organs and systems (e.g., the inner ear and auditory system) (Conte et al., 2013). Transcription factors control miRNA expression at the transcriptional level (Nenna et al., 2022). In an animal acute LPS-induced hearing loss model, the histone deacetylase 2 Hdac2/transcription factor Sp1/miR-204-5p/apoptosis suppressor gene Bcl-2 regulatory axis mediated apoptosis in the cochlea (Xie et al., 2021). FOXG1 is a nuclear transcription factor that participates in morphogenesis and cell fate determination and proliferation and is required for mammalian inner ear morphogenesis (Zhang et al., 2020). In this study, we knocked down FOXG1 expression in OC-1 cells and observed decreased autophagy levels and altered levels of autophagy-related miRNAs, including miR-34, miR-96, miR-182, and miR-183. Autophagy levels also decreased when these miRNAs were inhibited. We demonstrated that reducing FOXG1 expression decreases the autophagy level by reducing miR-34a, miR-96, miR-182, and miR-183 expression levels, leading to cisplatin-induced ototoxicity.

H3K9me2 modification is one of the most abundant and dynamic histone modifications and its levels are highly variable in disease development and pathogenesis (Bhaumik et al., 2007). Studies have shown that BIX01294 can reduce the resistance of tumors to cisplatin by inhibiting H3H9me2 and increase the tumor chemosensitivity by enhancing autophagy (Li et al., 2020; Fu et al., 2023). Herein, we found that cisplatin-induced injury increased H3K9me2 levels, and H3K9me2 inhibition increased FOXG1 expression and autophagy levels in OC-1 cells.

This study demonstrated that inhibition of H3H9me2 by BIX01294 *in vivo* can reduce the damage to the inner ear hair cells caused by cisplatin, indicating that the regulation of epigenetics can reduce the ototoxicity of cisplatin *in vivo*. Therefore, whether overexpression of FOXG1 and miRNA *in vivo* can also reduce the ototoxicity of cisplatin will become a new research goal in ototoxicity prevention and treatment. Many inner ear gene therapy methods exist for cochlear hair cells and supporting cells, such as synthetic adeno-associated virus approaches (Zhu et al., 2019). Because of the low transduction rate of adeno-associated virus in the cochlea, researchers have designed AAV-inner ear for gene delivery in the mouse cochlea and achieved a good therapeutic effect (Tan et al., 2019). RNase readily degrades miRNA in the plasma; thus, researchers have used exosomes produced by lentiviral overexpression of miR-21 as a carrier to deliver miR-21 to the inner ear, preventing hearing loss from ischemia-reperfusion (Hao et al., 2022). Injecting miR-375 agomir can alleviate nasal mucosa inflammation in allergic rhinitis mice (Wang et al., 2018). However, the ability to overexpress FOXG1 and miRNA efficiently in the inner ear remains limited. Preventing and treating hair cell damage and hearing loss caused by cisplatin through gene therapy is a new focus of inner ear research.

We used the cisplatin ototoxic OC-1 cell line and the CBA/CaJ mouse model to determine FoxG1's role and mechanism in cisplatin-induced ototoxic HC degeneration. We found that cisplatin decreased FOXG1 expression and autophagy levels, and that H3K9me2 played a role in cisplatin-induced ototoxicity. Reduced FOXG1 expression resulted in a series of miRNA changes that reduced autophagy activity and led to ROS accumulation and subsequent cochlear HC death. Following miRNA inhibition, autophagy levels decreased, but ROS levels and the apoptosis ratio increased, leading to HC death (Figure 10). By epigenetic regulation, we found that combining G9a inhibition with cisplatin has the potential to rescue hearing trauma and sensory hair cells loss. This protocol might represent an improvement for patients to limit chemotherapy-induced hearing loss. Our study has identified a potential target for future auditory HC protection against cisplatin injury.

Materials and methods

Animals

Six-week-old male SPF-grade CBA/CaJ mice (RRID: IMSR_JAX:000654) were obtained from SPF (Beijing) Biotechnology Co. They were kept for 1 week after purchase

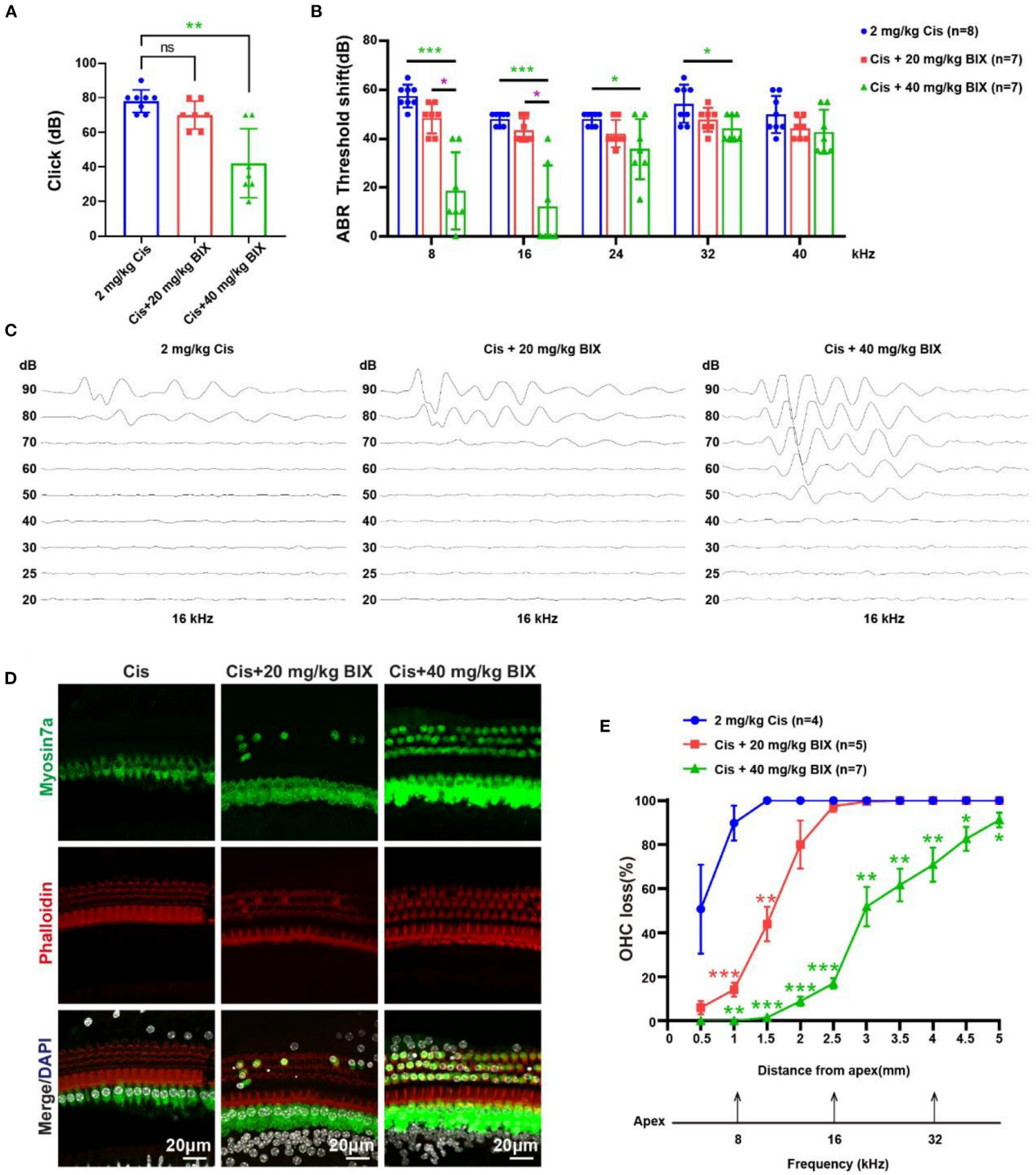

FIGURE 9
Results of the mouse hearing loss treated with cisplatin and BIX01294. **(A)** Statistical scatter plot of the click ABR. **(B)** Statistical line chart of the tone burst ABR threshold shifts. **(C)** Tone burst ABR at 16 kHz. **(D)** Immunofluorescence staining with myosin7a, phalloidin and DAPI of middle turn in the cochlea. **(E)** Quantification of the immunofluorescence staining in the cochlea. *$p < 0.05$, **$p < 0.01$, ***$p < 0.001$.

to allow them to adapt to the environment before the experiments began. All experimental work passed the ethical review for animal experiments and was conducted according to Committee on Animal Research policies at Tongji Medical College, Huazhong University of Science and Technology.

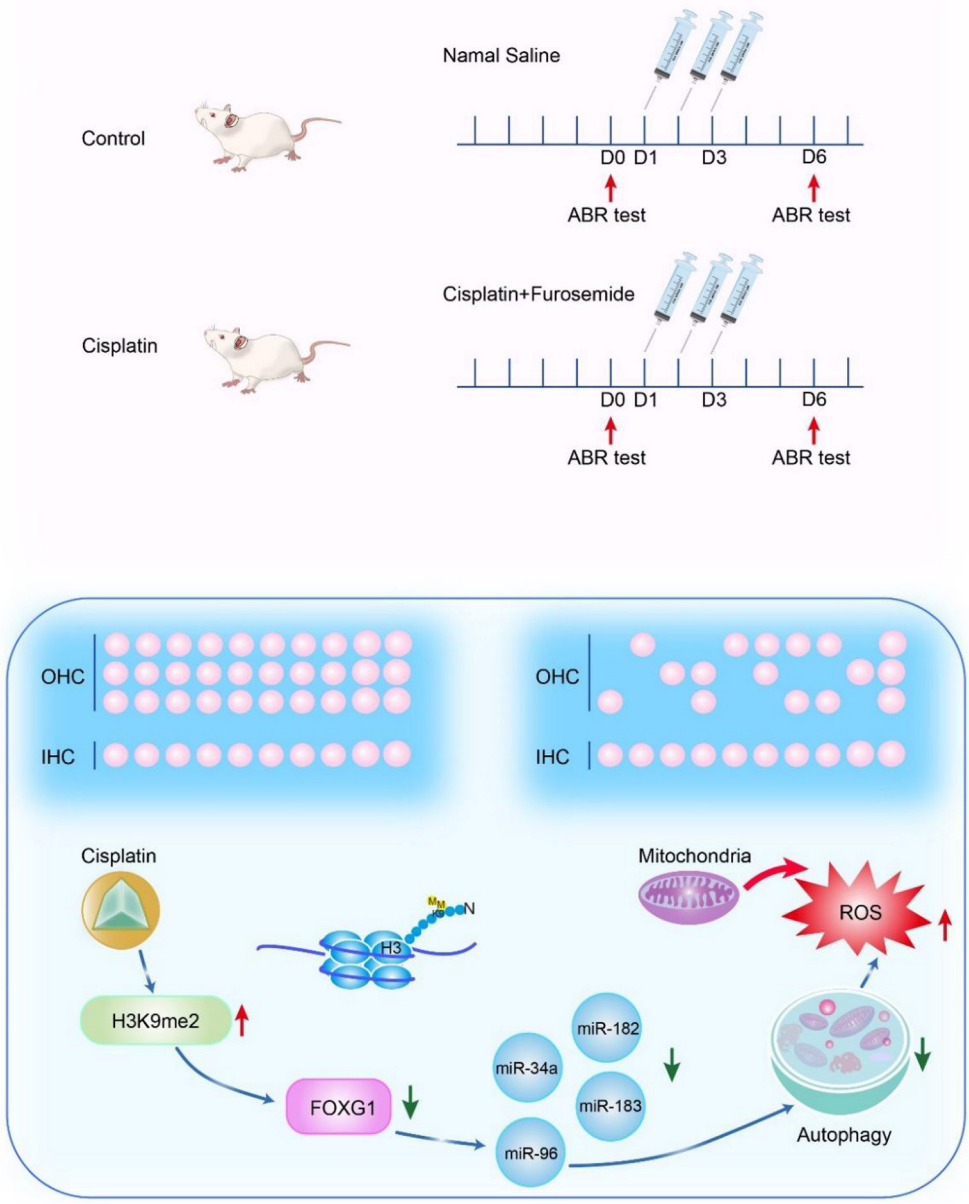

FIGURE 10
Mechanism of FOXG1-related epigenetic modifications in cisplatin-induced HC damage.

Drugs

Cisplatin was obtained from Yunnan Botanical Pharmaceutical Co., furosemide from Henan Runhong Pharmaceutical Co., and BIX01294 from APExBIO (cat no. A1909).

In vivo drug treatment

The *in vivo* experiments used male SPF-grade CBA/CaJ mice. The cisplatin group were given furosemide and cisplatin to create the animal model. First, furosemide at 200 mg/kg was injected intraperitoneally. Next, half an hour later, cisplatin at 0.5, 1, 1.5, or 2 mg/kg was given subcutaneously. Then, 1 h later, 0.5 ml isotonic sodium chloride solution was given intraperitoneally. The control group was injected with isotonic sodium chloride solution. All injections were performed for three consecutive days. In the cisplatin +BIX01294 group, BIX01294 at 20 mg/kg or 40 mg/kg was injected intraperitoneally. BIX01294 was injected on the day before the start of cisplatin injection and half an hour before each furosemide injection.

ABR

The ABR was measured before and 3 days after treatment. After anesthesia induction, the mice were placed in a soundproof room and kept warm with a warm water bag. Electrodes were inserted

into the ear to be tested, the contralateral ear, and subcutaneously in the middle of the head. A TDT device measured the click ABR and tone burst ABR at 8, 16, 24, 32, and 40 kHz. Each frequency was measured from 90 dB and lowered by 10 dB each time until there was no response to determine the threshold for each frequency.

Cell culture

The OC-1 cells were cultured in a 37°C incubator with 5% CO_2 in a complete culture medium of high-glucose DMEM (Hyclone) supplemented with 10% fetal bovine serum (Gibco) and 50 units/ml penicillin. Cultured cells were passaged when they reached 80%−90% confluence. Cells were digested with 0.25% trypsin, and the digestion was terminated with the complete medium. The cells were collected in a 5 ml EP tube, centrifuged at 1,500 rpm for 5 min at room temperature, and the supernatant was discarded. Thereafter, 2 ml of the complete culture medium was added to resuspend and inoculate an appropriate amount in a 10 cm Petri dish.

CCK-8

The cells were seeded in 96-well plates at the appropriate density and treated with the appropriate drugs 24 h after inoculation. Each group comprised six sub-wells. After treatment, the drugs were removed, and 100 μl DMEM containing 10% CCK-8 reagent was added to each well. Each well's absorbance at 450 nm was measured after 30 min and 1 h in the 37°C incubator.

Transfection

siRNA-*Foxg1* was designed and synthesized by Tsingke Biotechnology Co. to knock down *Foxg1* expression in OC-1 cells, *Foxg1* overexpressing plasmid was designed and synthesized by Shanghai GenePharma Co. to upregulate *Foxg1* expression. The miRNA inhibitors and miRNA mimics were designed and synthesized by Guangzhou RiboBio Co. to inhibit or increase target miRNA expression. The OC-1 cells were passaged, seeded in six-well plates for 24 h, cultured to 50%−60% confluence, and transfected in Opti-MEM using lipo3000 reagent. At 6–8 h after transfection, the Opti-MEM was replaced with the complete culture medium.

Rt-PCR

Total RNA was extracted from cells using TRIzol reagents. A miRNA rt-PCR reagent (Guangzhou RiboBio Co.) and a reverse transcription kit (Takara) to perform miRNA reverse transcription and rt-PCR.

Protein extraction

Cells were digested using 0.25% trypsin, which was stopped using a complete culture medium. Briefly, cells were collected in a 1.5 ml EP tube, centrifuged at 1,500 rpm for 5 min at room temperature, and the supernatant was discarded. Next, cells were resuspended in a RIPA buffer containing phosphatase inhibitors, protease inhibitors, and PMSF and left to lyse on ice for 20 min. Then, a 5× loading buffer was added to the lysed mixture, which was boiled at 95°C for 15 min and stored at −20°C.

The cochlea was dissected, removed, and soaked in phosphate-buffered saline (PBS). Next, a pre-chilled RIPA buffer containing phosphatase inhibitors, protease inhibitors, and PMSF was added. Then, the cochlea was crushed and sonicated at 20% energy for 5 s before centrifugation at 12,000 rpm and 4°C for 10 min in a low-temperature high-speed centrifuge. Finally, the supernatant was aspirated, and a 5× loading buffer was added to the mixture, which was boiled at 95°C for 15 min and stored at −20°C.

Western blotting

SDS-PAGE gel electrophoresis was performed to separate the proteins. The proteins on the gel were transferred to PVDF membranes, which were blocked with 5% nonfat milk in TBST for 1 h at room temperature on a shaker. The membrane was placed in the primary antibody, incubated overnight using a refrigerator shaker, washed three times with TBST for 5 min each, and then incubated with a 1:5,000 secondary antibody for 1 h at room temperature. Washing with TBST was performed thrice for 5 min each, and exposure to film was achieved using an ECL solution in a dark room. The films were developed, fixed, and air dried. After scanning the films, we analyzed the immunoblot bands using Image J. The primary antibodies used were anti-FOXG1 antibody (Abcam, ab18259), anti-LC3B antibody (Sigma-Aldrich, L7543), anti-G9a antibody (Abcam, ab185050), and anti-H3K9me2 antibody (Abcam, ab176882).

Flow cytometry

Mito-SOX Red (Thermo Fisher Scientific) was used to analyze mitochondrial ROS production. After trypsinization, the OC-1 cells were collected via centrifugation and washed with PBS. The cell pellets were then resuspended in a solution containing Mito-SOX Red for 15 min at 37°C in the dark and analyzed via flow cytometry (FACSCalibur, BD Biosciences,).

FITC/annexin V (BD Biosciences) was used to analyze apoptosis and PI to differentiate between live and dead cells. The OC-1 cells were trypsinized and collected via centrifugation at 1,000 rpm for 5 min, washed with PBS, resuspended in binding buffer, and aliquoted at 1×10^5 cells (100 μl) into a 5 ml flow tube. FITC/annexin V and PI were added to the tube, and the mixture was vortexed gently, incubated at room temperature for 15 min in the dark, and analyzed via flow cytometry within 1 h.

TEM

The OC-1 cells were fixed in 2.5% glutaraldehyde (Sigma-Aldrich) for 24 h and 1% osmic acid (Sigma-Aldrich) for 1–2 h, dehydrated with acetone (Sinopharm Chemical Reagent), and embedded with Araldite CY212 (TAAB). Ultrathin sections were stained with alcohol uranyl acetate (Polysciences) and alkaline lead citrate (Sigma-Aldrich). The sections were gently washed with distilled water and observed under a JEM 1230 transmission electron microscope (JEOL Ltd.).

Immunofluorescence staining

Anti-FOXG1 antibody (Abcam, ab18259), anti-LC3B antibody (Sigma-Aldrich, L7543), anti-H3K9me2 antibody (Abcam, ab176882), Moysin7a (Proteus Biosciences, 25-6790), rhodamine phalloidin (Yeasen), and DAPI (Solarbio) were used to analyze the FOXG1 expression and detect autophagy, H3K9me2, HCs, and microfilament structure and nucleus, respectively.

The samples were incubated in 4% paraformaldehyde (Sigma-Aldrich) for 1 h and then blocked with 0.5% Triton X-100 (blocking medium) for 1 h. The primary antibodies were then added at a 1:400–1:1,000 dilution and incubated overnight at 4°C. The samples were washed thrice with PBST, incubated with fluorescent secondary antibodies for 1 h at room temperature in the dark, rewashed thrice with PBST, and reincubated with rhodamine phalloidin and DAPI for 30 min in the dark. After sealing the slides with clear nail polish, we imaged them using a confocal microscope.

Data analysis

All data were presented as means ± SDs. All experiments were repeated at least thrice. Statistical analysis was performed using Microsoft Excel and GraphPad Prism 8. Statistical significance was determined using a two-tailed unpaired *t*-test when comparing two groups and using one-way ANOVA and Dunnett's multiple comparison test when comparing more than two groups. *p*-values of <0.05 were considered statistically significant.

Data availability statement

The original contributions presented in the study are included in the article/Supplementary material, further inquiries can be directed to the corresponding author/s. The raw data from the figures presented in the study are publicly available. This data can be found here: https://www.jianguoyun.com/p/DSZBQ_EQmd-ECxjv094EIAA.

Ethics statement

The animal study was reviewed and approved by the Committee on Animal Research of Tongji Medical College, Huazhong University of Science and Technology.

Author contributions

W-jK and Z-hH conceived and designed the study and reviewed and edited the manuscript. Y-rM, S-yZ, ML, Y-yD, and XH performed the experiments. Z-hH, Y-rM, and S-yZ analyzed the data and wrote the manuscript. All authors have read and approved the published version of the manuscript.

Funding

This work was financially supported by the National Natural Science Foundation of China (Nos. 81873700, 82222017, and 82271183), Hubei Province's Key Research and Development Program (No. 2022BCA046), the Fundamental Research Funds for the Central Universities (2042022kf0059), and the Knowledge Innovation Program of Wuhan-Shuguang (2022020801020493).

Conflict of interest

The authors declare that the research was conducted in the absence of any commercial or financial relationships that could be construed as a potential conflict of interest.

Publisher's note

Supplementary material

The Supplementary Material for this article can be found online at: https://www.frontiersin.org/articles/10.3389/fnmol.2023.1064579/full#supplementary-material

SUPPLEMENTARY FIGURE 1
Cell viability and apoptosis flow cytometry results for the OC-1 cells treated with different BIX01294 concentrations. **(A)** CCK-8 cell viability after treatment with different BIX01294 concentrations for 24 h. **(B)** Annexin V flow cytometry of apoptosis in cells treated with different BIX01294 concentrations for 24 h. **(C)** Quantification of the apoptosis ratio in **(B)**. **(D)** Quantification of the cell death ratio in B. $*p < 0.05$, $**p < 0.01$, $***p < 0.001$.

SUPPLEMENTARY FIGURE 2
Mito-SOX flow cytometry of OC-1 cells treated with BIX01294. **(A)** ROS level of treated with different BIX01294 concentrations for 24 h. **(B)** Quantification of the data in A. $*p < 0.05$.

References

Abraham, D., Jackson, N., Gundara, J. S., Zhao, J., Gill, A. J., Delbridge, L., et al. (2011). MicroRNA profiling of sporadic and hereditary medullary thyroid cancer identifies predictors of nodal metastasis, prognosis, and potential therapeutic targets. *Clin. Cancer Res.* 17, 4772–4781. doi: 10.1158/1078-0432.CCR-11-0242

Bhaumik, S. R., Smith, E., and Shilatifard, A. (2007). Covalent modifications of histones during development and disease pathogenesis. *Nat. Struct. Mol. Biol.* 14, 1008–1016. doi: 10.1038/nsmb1337

Chen, P., Chen, F., Lei, J., Li, Q., and Zhou, B. (2019). Activation of the miR-34a-mediated SIRT1/mTOR signaling pathway by urolithin a attenuates d-galactose-induced brain aging in mice. *Neurotherapeutics* 16, 1269–1282. doi: 10.1007/s13311-019-00753-0

Ciechomska, I. A., Przanowski, P., Jackl, J., Wojtas, B., and Kaminska, B. (2016). BIX01294, an inhibitor of histone methyltransferase, induces autophagy-dependent differentiation of glioma stem-like cells. *Sci. Rep.* 6, 38723. doi: 10.1038/srep38723

Conte, I., Banfi, S., and Bovolenta, P. (2013). Non-coding RNAs in the development of sensory organs and related diseases. *Cell. Mol. Life Sci.* 70, 4141–4155. doi: 10.1007/s00018-013-1335-z

Duan, X., Yu, X., and Li, Z. (2022). Circular RNA hsa_circ_0001658 regulates apoptosis and autophagy in gastric cancer through microRNA-182/Ras-related protein Rab-10 signaling axis. *Bioengineered* 13, 2387–2397. doi: 10.1080/21655979.2021.2024637

Fan, J.-D., Lei, P.-J., Zheng, J.-Y., Wang, X., Li, S., Liu, H., et al. (2015). The selective activation of p53 target genes regulated by SMYD2 in BIX-01294 induced autophagy-related cell death. *PLoS ONE* 10, e0116782. doi: 10.1371/journal.pone.0116782

Fu, J., Yu, M., Xu, W., and Yu, S. (2023). High expression of G9a induces cisplatin resistance in hepatocellular carcinoma. *Cell J.* 25, 118–125. doi: 10.22074/cellj.2022.557564.1077

Gan, J., Cai, Q., Qu, Y., Zhao, F., Wan, C., Luo, R., et al. (2017). miR-96 attenuates status epilepticus-induced brain injury by directly targeting Atg7 and Atg16L1. *Sci. Rep.* 7, 10270. doi: 10.1038/s41598-017-10619-0

Han, Y., and He, X. (2016). Integrating epigenomics into the understanding of biomedical insight. *Bioinform. Biol. Insights* 10, 267–289. doi: 10.4137/BBI.S38427

Hao, F., Shan, C., Zhang, Y., Zhang, Y., and Jia, Z. (2022). Exosomes derived from microRNA-21 overexpressing neural progenitor cells prevent hearing loss from ischemia-reperfusion injury in mice via inhibiting the inflammatory process in the cochlea. *ACS Chem. Neurosci.* 13, 2464–2472. doi: 10.1021/acschemneuro.2c00234

Harfe, B. D. (2005). MicroRNAs in vertebrate development. *Curr. Opin. Genet. Dev.* 15, 410–415. doi: 10.1016/j.gde.2005.06.012

He, Z., Guo, L., Shu, Y., Fang, Q., Zhou, H., Liu, Y., et al. (2017). Autophagy protects auditory hair cells against neomycin-induced damage. *Autophagy* 13, 1884–1904. doi: 10.1080/15548627.2017.1359449

He, Z.-H., Li, M., Fang, Q.-J., Liao, F.-L., Zou, S.-Y., Wu, X., et al. (2021). FOXG1 promotes aging inner ear hair cell survival through activation of the autophagy pathway. *Autophagy* 17, 4341–4362. doi: 10.1080/15548627.2021.1916194

He, Z.-H., Zou, S.-Y., Li, M., Liao, F.-L., Wu, X., Sun, H.-Y., et al. (2020). The nuclear transcription factor FoxG1 affects the sensitivity of mimetic aging hair cells to inflammation by regulating autophagy pathways. *Redox Biol.* 28, 101364. doi: 10.1016/j.redox.2019.101364

Jia, Y., Lin, R., Jin, H., Si, L., Jian, W., Yu, Q., et al. (2019). MicroRNA-34 suppresses proliferation of human ovarian cancer cells by triggering autophagy and apoptosis and inhibits cell invasion by targeting Notch 1. *Biochimie* 160, 193–199. doi: 10.1016/j.biochi.2019.03.011

Jiang, P., and Mizushima, N. (2014). Autophagy and human diseases. *Cell Res.* 24, 69–79. doi: 10.1038/cr.2013.161

Kalinec, G., Thein, P., Park, C., and Kalinec, F. (2016). HEI-OC1 cells as a model for investigating drug cytotoxicity. *Hear. Res.* 335, 105–117. doi: 10.1016/j.heares.2016.02.019

Ke, X. X., Zhang, D., Zhu, S., Xia, Q., Xiang, Z., Cui, H., et al. (2014). Inhibition of H3K9 methyltransferase G9a repressed cell proliferation and induced autophagy in neuroblastoma cells. *PLoS ONE* 9, e106962. doi: 10.1371/journal.pone.0106962

Keilty, D., Khandwala, M., Liu, Z. A., Papaioannou, V., Bouffet, E., Hodgson, D., et al. (2021). Hearing loss after radiation and chemotherapy for CNS and head-and-neck tumors in children. *J. Clin. Oncol.* 39, 3813–3821. doi: 10.1200/JCO.21.00899

Khodakarimi, S., Zarebkohan, A., Kahroba, H., Omrani, M., Sepasi, T., Mohaddes, G., et al. (2021). The role of miRNAs in the regulation of autophagy in autoimmune diseases. *Life Sci.* 287, 119726. doi: 10.1016/j.lfs.2021.119726

Kim, Y., Kim, Y.-S., Kim, D. E., Lee, J. S., Song, J. H., Kim, H.-G., et al. (2013). BIX-01294 induces autophagy-associated cell death via EHMT2/G9a dysfunction and intracellular reactive oxygen species production. *Autophagy* 9, 2126–2139. doi: 10.4161/auto.26308

Klionsky, D. J., Abdel-Aziz, A. K., Abdelfatah, S., Abdellatif, M., Abdoli, A., Abel, A., et al. (2021). Guidelines for the use and interpretation of assays for monitoring autophagy (4th edition) (1). *Autophagy* 17, 1–382. doi: 10.1080/15548627.2020.1797280

Klose, R. J., and Zhang, Y. (2007). Regulation of histone methylation by demethylimination and demethylation. *Nat. Rev. Mol. Cell Biol.* 8, 307–318. doi: 10.1038/nrm2143

Kondengaden, S. M., Luo, L.-F., Huang, K., Zhu, M., Zang, L., Bataba, E., et al. (2016). Discovery of novel small molecule inhibitors of lysine methyltransferase G9a and their mechanism in leukemia cell lines. *Eur. J. Med. Chem.* 122, 382–393. doi: 10.1016/j.ejmech.2016.06.028

Kros, C. J., and Steyger, P. S. (2019). Aminoglycoside- and cisplatin-induced ototoxicity: mechanisms and otoprotective strategies. *Cold Spring Harb. Perspect. Med.* 9. doi: 10.1101/cshperspect.a033548

Kubicek, S., O'Sullivan, R. J., August, E. M., Hickey, E. R., Zhang, Q., Teodoro, M. L., et al. (2007). Reversal of H3K9me2 by a small-molecule inhibitor for the G9a histone methyltransferase. *Mol. Cell* 25, 473–481. doi: 10.1016/j.molcel.2007.01.017

Lanvers-Kaminsky, C., Zehnhoff-Dinnesen, A. A., Parfitt, R., and Ciarimboli, G. (2017). Drug-induced ototoxicity: mechanisms, pharmacogenetics, and protective strategies. *Clin. Pharmacol. Ther.* 101, 491–500. doi: 10.1002/cpt.603

Layman, W. S., and Zuo, J. (2014). Epigenetic regulation in the inner ear and its potential roles in development, protection, and regeneration. *Front. Cell. Neurosci.* 8, 446. doi: 10.3389/fncel.2014.00446

Li, Q., Wang, M., Zhang, Y., Wang, L., Yu, W., Bao, X., et al. (2020). BIX-01294-enhanced chemosensitivity in nasopharyngeal carcinoma depends on autophagy-induced pyroptosis. *Acta Biochim. Biophys. Sin.*52, 1131–1139. doi: 10.1093/abbs/gmaa097

Li, Y., Ding, D., Jiang, H., Fu, Y., and Salvi, R. (2011). Co-administration of cisplatin and furosemide causes rapid and massive loss of cochlear hair cells in mice. *Neurotox. Res.* 20, 307–319. doi: 10.1007/s12640-011-9244-0

Mao, Z., Yao, M., Li, Y., Fu, Z., Li, S., Zhang, L., et al. (2018). miR-96-5p and miR-101-3p as potential intervention targets to rescue TiO2 NP-induced autophagy and migration impairment of human trophoblastic cells. *Biomater. Sci.* 6, 3273–3283. doi: 10.1039/C8BM00856F

Milite, C., Feoli, A., Horton, J. R., Rescigno, D., Cipriano, A., Pisapia, V., et al. (2019). Discovery of a novel chemotype of histone lysine methyltransferase EHMT1/2 (GLP/G9a) inhibitors: rational design, synthesis, biological evaluation, and co-crystal structure. *J. Med. Chem.* 62, 2666–2689. doi: 10.1021/acs.jmedchem.8b02008

Nenna, A., Loreni, F., Giacinto, O., Chello, C., Nappi, P., Chello, M., et al. (2022). miRNAs in cardiac myxoma: new pathologic findings for potential therapeutic opportunities. *Int. J. Mol. Sci.* 23, 3309. doi: 10.3390/ijms23063309

Pauley, S., Lai, E., and Fritzsch, B. (2006). Foxg1 is required for morphogenesis and histogenesis of the mammalian inner ear. *Dev. Dyn.* 235, 2470–2482. doi: 10.1002/dvdy.20839

Ren, A., Qiu, Y., Cui, H., and Fu, G. (2015). Inhibition of H3K9 methyltransferase G9a induces autophagy and apoptosis in oral squamous cell carcinoma. *Biochem. Biophys. Res. Commun.* 459, 10–17. doi: 10.1016/j.bbrc.2015.01.068

Rudnicki, A., Isakov, O., Ushakov, K., Shivatzki, S., Weiss, I., Friedman, L. M., et al. (2014). Next-generation sequencing of small RNAs from inner ear sensory epithelium identifies microRNAs and defines regulatory pathways. *BMC Genomics* 15, 484. doi: 10.1186/1471-2164-15-484

Srinivas, U. S., Tan, B. W. Q., Vellayappan, B. A., and Jeyasekharan, A. D. (2019). ROS and the DNA damage response in cancer. *Redox Biol.* 25, 101084. doi: 10.1016/j.redox.2018.101084

Tachibana, M., Sugimoto, K., Nozaki, M., Ueda, J., Ohta, T., Ohki, M., et al. (2002). G9a histone methyltransferase plays a dominant role in euchromatic histone H3 lysine 9 methylation and is essential for early embryogenesis. *Genes Dev.* 16, 1779–1791. doi: 10.1101/gad.989402

Taiber, S., Gwilliam, K., Hertzano, R., and Avraham, K. B. (2022). The genomics of auditory function and disease. *Annu. Rev. Genomics Hum. Genet.* 23, 275–299. doi: 10.1146/annurev-genom-121321-094136

Tan, F., Chu, C., Qi, J., Li, W., You, D., Li, K., et al. (2019). AAV-ie enables safe and efficient gene transfer to inner ear cells. *Nat. Commun.* 10, 3733. doi: 10.1038/s41467-019-11687-8

Wang, T., Chen, D., Wang, P., Xu, Z., and Li, Y. (2018). miR-375 prevents nasal mucosa cells from apoptosis and ameliorates allergic rhinitis via inhibiting JAK2/STAT3 pathway. *Biomed. Pharmacother.* 103, 621–627. doi: 10.1016/j.biopha.2018.04.050

Weston, M. D., Pierce, M. L., Rocha-Sanchez, S., Beisel, K. W., and Soukup, G. A. (2006). MicroRNA gene expression in the mouse inner ear. *Brain Res.* 1111, 95–104. doi: 10.1016/j.brainres.2006.07.006

Wu, P., Wu, X., Zhang, C., Chen, X., Huang, Y., Li, H., et al. (2021). Hair cell protection from ototoxic drugs. *Neural Plast.* 2021, 4909237. doi: 10.1155/2021/4909237

Xie, L., Huang, W., Fang, Z., Ding, F., Zou, F., Ma, X., et al. (2019). CircERCC2 ameliorated intervertebral disc degeneration by regulating mitophagy and apoptosis through miR-182-5p/SIRT1 axis. *Cell Death Dis.* 10, 751. doi: 10.1038/s41419-019-1978-2

Xie, L., Zhou, Q., Chen, X., Du, X., Liu, Z., Fei, B., et al. (2021). Elucidation of the Hdac2/Sp1/miR-204-5p/Bcl-2 axis as a modulator of cochlear apoptosis via in vivo/in vitro models of acute hearing loss. *Mol. Ther. Nucleic Acids* 23, 1093–1109. doi: 10.1016/j.omtn.2021.01.017

Yu, H., Lin, Q., Wang, Y., He, Y., Fu, S., Jiang, H., et al. (2013). Inhibition of H3K9 methyltransferases G9a/GLP prevents ototoxicity and ongoing hair cell death. *Cell Death Dis.* 4, e506. doi: 10.1038/cddis.2013.28

Yuan, Y., Zhang, Y., Han, L., Sun, S., and Shu, Y. (2018). miR-183 inhibits autophagy and apoptosis in gastric cancer cells by targeting ultraviolet radiation resistance-associated gene. *Int. J. Mol. Med.* 42, 3562–3570. doi: 10.3892/ijmm.2018.3871

Zhang, S., Zhang, Y., Dong, Y., Guo, L., Zhang, Z., Shao, B., et al. (2020). Knockdown of Foxg1 in supporting cells increases the trans-differentiation of supporting cells into hair cells in the neonatal mouse cochlea. *Cell. Mol. Life Sci.* 77, 1401–1419. doi: 10.1007/s00018-019-03291-2

Zhu, S., Ying, Y., Ye, J., Chen, M., Wu, Q., Dou, H., et al. (2019). AAV2.7m8 is a powerful viral vector for inner ear gene therapy. *Nat. Commun.* 10, 427. doi: 10.1038/s41467-018-08243-1

Frontiers in
Molecular Neuroscience

Leading research into the brain's molecular structure, design and function

Part of the most cited neuroscience series, this journal explores and identifies key molecules underlying the structure, design and function of the brain across all levels.

Discover the latest Research Topics

See more →

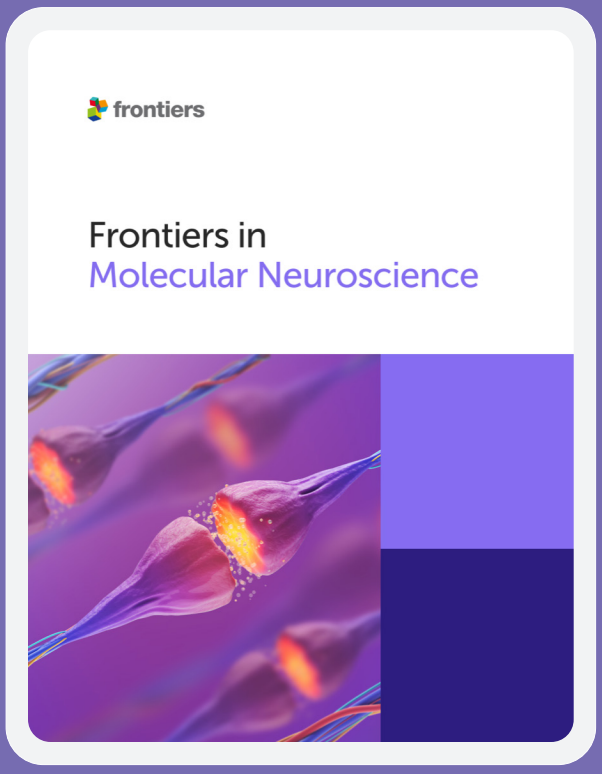

Frontiers

Avenue du Tribunal-Fédéral 34
1005 Lausanne, Switzerland
frontiersin.org

Contact us

+41 (0)21 510 17 00
frontiersin.org/about/contact